april 1961
the institute of radio engineers

Proceedings of the IRE

in this issue

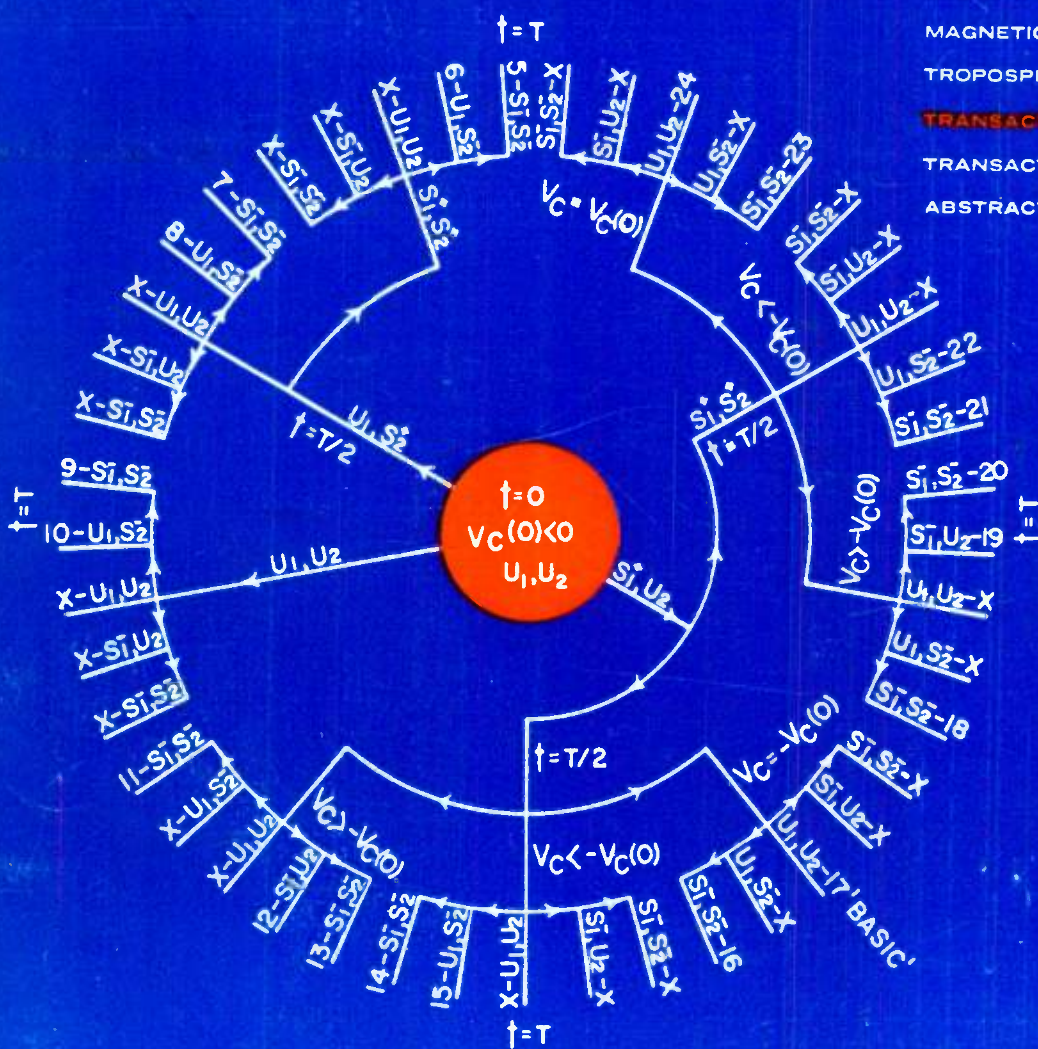

SUBHARMONIC OSCILLATOR ANALYSIS: Page 779

NEW*

Revolutionary† DO-T and DI-T TRANSISTOR TRANSFORMERS

FROM STOCK—Hermetically Sealed to MIL-T-27A Specs.

There is no transformer even twice the size of the DO-T and DI-T series which has as much as 1/10th the power handling ability . . . which can equal the efficiency . . . or equal the response range. And none to approach the reliability of the DO-T and DI-T units (proved to, but exceeding MIL-T-27A grade 4).

- **High Power Rating** .... up to 10 times greater.
- **Excellent Response** .... twice as good at low end.
- **Low Distortion** .... reduced 80%.
- **High Efficiency** .... up to 30% better . . . compare DCR.
- **Moisture Proof** .... hermetically sealed to MIL-T-27A.
- **Rugged** .... completely metal cased.
- **Anchored Leads** .... will withstand 10 pound pull test.
- **Printed Circuit Use** .... (solder melting) plastic insulated leads.
- **Suited to Clip Mounting** .... use Augat #6009-8A clip.

TRANSFORMERS PICTURED ACTUAL SIZE
DO-T: 5/16 Dia. x 13/32", 1/10 Oz.; DI-T: 5/16 Dia. x 1/4", 1/20 Oz.

Typical Printed Circuit Positioning

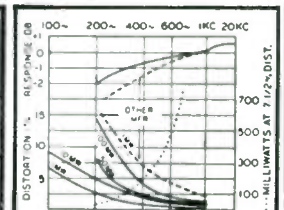

TYPICAL DO-T PERFORMANCE
SOURCE RATED PRI. IMP. AND D.C.
LOAD RATED SEC. IMP.

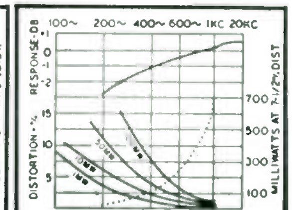

TYPICAL DI-T PERFORMANCE
SOURCE RATED PRI. IMP. AND D.C.
LOAD RATED SEC. IMP.

DO-T No.	Pri. Imp.	D.C. Ma.‡ in Pri.	Sec. Imp.	Pri. Res. DO-T	Pri. Res. DI-T	Mw. Level	DI-T No.
DO-T1	20,000 30,000	.5 .5	800 1200	850	815	50	DI-T1
DO-T2	500 600	3 3	50 60	60	65	100	DI-T2
DO-T3	1000 1200	3 3	50 60	115	110	100	DI-T3
DO-T4	600	3	3.2	60		100	
DO-T5	1200	2	3.2	115	110	100	DI-T5
DO-T6	10,000	1	3.2	790		100	
DO-T7	200,000 500	0 0	1000 100,000	8500 —		25	
	Reactor 2.5 Hys./2 Ma., .9 Hy /4 Ma				630		DI-T8
DO-T8	" 3.5 Hys./2 Ma., 1 Hy./5 Ma.			630			
DO-T9	10,000 12,000	1 1	500 CT 600 CT	800	870	100	DI-T9
DO-T10	10,000 12,500	1 1	1200 CT 1500 CT	800	870	100	DI-T10
DO-T11	10,000 12,500	1 1	2000 CT 2500 CT	800	870	100	DI-T11
DO-T12	150 CT 200 CT	10 10	12 16	11		500	
DO-T13	300 CT 400 CT	7 7	12 16	20		500	
DO-T14	600 CT 800 CT	5 5	12 16	43		500	
DO-T15	800 CT 1070 CT	4 4	12 16	51		500	
DO-T16	1000 CT 1330 CT	3.5 3.5	12 16	71		500	
DO-T17	1500 CT 2000 CT	3 3	12 16	108		500	
DO-T18	7500 CT 10,000 CT	1 1	12 16	505		500	
DO-T19	300 CT	7	600	19	20	500	DI-T19
DO-T20	500 CT	5.5	600	31	32	500	DI-T20
DO-T21	900 CT	4	600	53	53	500	DI-T21
DO-T22	1500 CT 600	3 5	600 1500 CT	86 —	87	500	DI-T22
DO-T23	20,000 CT 30,000 CT	.5 .5	800 CT 1200 CT	850	815	100	DI-T23
DO-T24	200,000 CT 500 CT	0 0	1000 CT 100,000 CT	8500 —		25	
DO-T25	10,000 CT 12,000 CT	1 1	1500 CT 1800 CT	800	870	100	DI-T25

DO-T No.	Pri. Imp.	D.C. Ma.‡ in Pri.	Sec. Imp.	Pri. Res. DO-T	Pri. Res. DI-T	Mw. Level	DI-T No.
	Reactor 4.5 Hys./2 Ma., 1.2 Hys./4 Ma.				2300		DI-T26
DO-T26	' 6 Hys./2 Ma., 1.5 Hys./5 Ma.			2100			
	Reactor .9 Hy./2 Ma., .5 Hy./6 Ma.				105		DI-T27
DO-T27	" 1.25 Hys./2 Ma., .5 Hy./11 Ma.			100			
	Reactor .1 Hy./4 Ma., .08 Hy./10 Ma.				25		DI-T28
DO-T28	" .3 Hy./4 Ma., .15 Hys./20 Ma.			25			
DO-T29	120 CT 150 CT	10 10	3.2 4	10		500	
DO-T30	320 CT 400 CT	7 7	3.2 4	20		500	
DO-T31	640 CT 800 CT	5 5	3.2 4	43		500	
DO-T32	800 CT 1000 CT	4 4	3.2 4	51		500	
DO-T33	1060 CT 1330 CT	3.5 3.5	3.2 4	71		500	
DO-T34	1600 CT 2000 CT	3 3	3.2 4	109		500	
DO-T35	8000 CT 10,000 CT	1 1	3.2 4	505		100	
DO-T36	10,000 CT 12,000 CT	1 1.	10,000 CT 12,000 CT	950	970	100	DI-T36
*DO-T37	2000 CT 2500 CT	3 3	8000 Split 10,000 Split	195		100	
*DO-T38	10,000 CT 12,000 CT	1 1	2000 Split 2400 Split	560		100	
*DO-T39	20,000 CT 30,000 CT	.5 .5	1000 Split 1500 Split	800		100	
*DO-T40	40,000 CT 50,000 CT	.25 .25	400 Split 500 Split	1700		50	
*DO-T41	400 CT 500 CT	8 6	400 Split 500 Split	46		500	
*DO-T42	400 CT 500 CT	8 6	120 Split 150 Split	46		500	
*DOT-43	400 CT 500 CT	8 6	40 Split 50 Split	46		500	
*DO-T44	80 CT 100 CT	12 10	32 Split 40 Split	9.8		500	
DO-TSH	Drawn Hipermalloy shield and cover 20/30 db						DI-TSH

‡ DCMA shown is for single ended useage (under 5% distortion—100MW—1KC) . . . for push pull, DCMA can be any balanced value taken by .5W transistors (under 5% distortion—500MW—1KC)

† DO-T & DI-T units designed for transistor application only. Pats. Pend.

* DO-T37 thru DO-T44 newly added to series.

ial Units to
ifications

UNITED TRANSFORMER CORPORATION
150 Varick Street, New York 13, N. Y.
PACIFIC MFG. DIVISION: 4008 W. JEFFERSON BLVD., LOS ANGELES 16, CALIF.
EXPORT DIVISION: 13 EAST 40th STREET, NEW YORK 16, N. Y. CABLES: "ARLAB"

VOLUME 49, NUMBER 4

April, 1961

published monthly by The Institute of Radio Engineers, Inc.

Proceedings of the IRE®

contents

COVER

The unusual flow diagram on the cover indicates various combinations of saturated (S) and unsaturated (U) states of two magnetic cores in a subharmonic oscillator and shows the many possible sequences of states through which the cores could go during one cycle of operation. The diagram makes it readily possible to determine which sequences satisfy the conditions necessary for parametric operation, as discussed on page 779.

APRIL

published monthly by The Institute of Radio Engineers, Inc.

Proceedings of the IRE

continued

APRIL

PROCEEDINGS OF THE IRE, published monthly by The Institute of Radio Engineers, Inc., at 1 East 79 Street, New York 21, N. Y. Manuscripts should be submitted in triplicate to the Editorial Department. Correspondence column items should not exceed four double-spaced pages (illustrations count as one-half page each). Responsibility for contents of papers published rests upon the authors, and not the IRE or its members. All republication rights, including translations, are reserved by the IRE and granted only on request. Abstracting is permitted with mention of source.

Thirty days advance notice is required for change of address. Price per copy: members of the Institute of Radio Engineers, one additional copy $1.25; non-members $2.25. Yearly subscription price: to members $9.00, one additional subscription $13.50; to non-members in United States, Canada, and U. S. Possessions $18.00; to non-members in foreign countries $19.00. Second-class postage paid at Menasha, Wisconsin, under the act of March 3, 1879. Acceptance for mailing at a special rate of postage is provided for in the act of Febuary 28, 1925, embodied in Paragraph 4, Section 412. P. L. and R., authorized October 26, 1927. Printed in U.S.A.

Here is the first of two reports on work we recently completed to help improve our nation's airports. This report (prepared by M. A. Warskow and E. N. Hooton of our Department of Aviation Systems Research) describes the operations research phase. The second report, to appear in May, will describe some of the mathematical concepts and considerations.

Analyzing Airport Design

PART I

Creating airport capacity adequate to cope with the ever-increasing volume of air traffic requires improved runway designs, more runways, and often more airports. These improvements in some cases will include new electronic devices to control airport aircraft traffic. For example, TRACE (Taxi Routing and Coordination Equipment) may be used to ease taxi and runway crossing problems to increase capacity. Since these improvements cost a great deal, airport planners must have a reliable yardstick to measure the capacity of their airports. They must be able to measure the improvement in service—the most important being the reduction in delays—against the cost of new installations.

Recently, on behalf of the FAA Bureau of Research and Development, we studied airport operations in great detail with the object of devising a technique that would enable planners to predict airport capacity for any given design and stage of development. The technique developed utilizes mathematical models to predict the average delay caused by aircraft using any given runway system.

Since we were to forecast the results of actual, rather than theoretical, operations, the inputs to the models were based on the results of time and motion studies of actual operations at 11 airports around the country. Some of these data were also used to verify the suitability of our mathematical models. The results from testing the models over a wide range of operating rates are considered satisfactory.

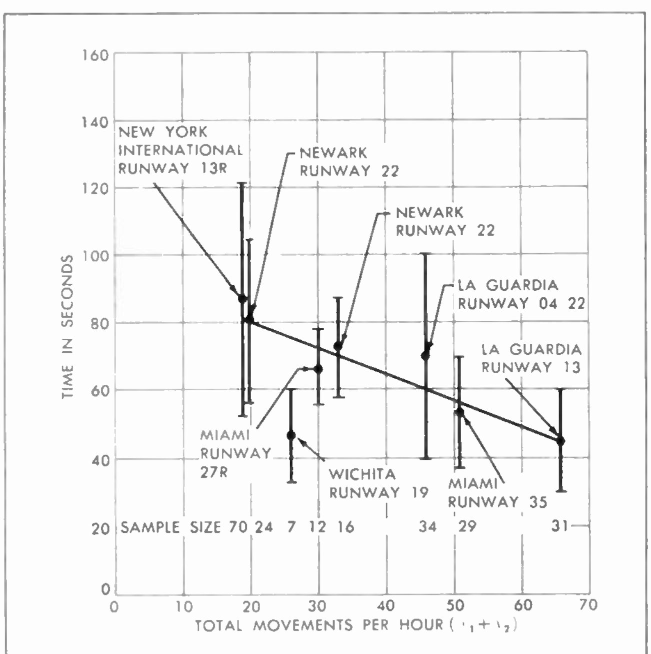

Figure 1. VFR Spacing for Departure Followed by Departure

As part of our studies, we documented the actual spacings between aircraft using a common runway/taxiway system. It was soon apparent that the pilots and controllers at the airports become more efficient as the number of operations increases until the runway is completely loaded. An example of this "pressure factor," as we call it, is shown in Figure 1, which shows the decrease in time intervals between successive departures with increasing movement rates at various airports.

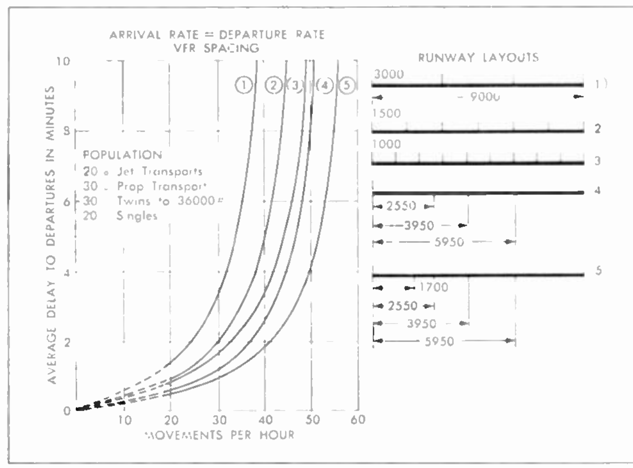

Figure 2. Effect of Runway Turn-Off Layout

At all these airports except one (Wichita), the mixture of aircraft was predominantly four-engine airliners. At Wichita, the traffic consisted mainly of small, light aircraft. Figure 1 illustrates the fact that these light aircraft can space themselves much closer and can therefore directly affect capacity (in this case, giving an increase in capacity). Other combinations of aircraft (for example, a jet following a jet) have their own distinctive spacing factors, which have been determined for realistic inputs into the airport capacity calculation. Similar data were obtained for other spacings: (1) successive arrivals, (2) departures followed by arrivals, and (3) arrivals followed by departures. Data analysis and model development (based on queueing theory) went hand in hand until the most realistic model was obtained.

By the use of the models developed, it is possible to show, for example, in Figure 2, the increase in capacity resulting from the use of improved high-speed turnoffs on any given runway. Note that at an average steady-state delay of 6 minutes, the operating rate varies from 35 to 53 movements per hour, depending on the runway layout. To determine model inputs, we must specify (as in Figure 2) the aircraft population, the runway layout, the operating rates, the ratio of arrivals to departures, and the weather.

In Figure 2, the reduction of delay resulting from the addition of better turnoffs can be related to cost. The reduction of cost is obtained by placing a dollar value on the cost of delays to the aircraft awaiting arrival or departure. This is an appreciable cost—about $15 per minute for jet 707-type aircraft.

Thus, for the first time, the airport planner has a yardstick for measuring airport capacity in terms that we can all understand.

A complete bound set of our fifth series of articles is available on request. Write to Harold Hechtman at AIL for your set.

AIRBORNE INSTRUMENTS LABORATORY
DEER PARK, LONG ISLAND, NEW YORK
A DIVISION OF CUTLER-HAMMER, INC.

150,000 µF

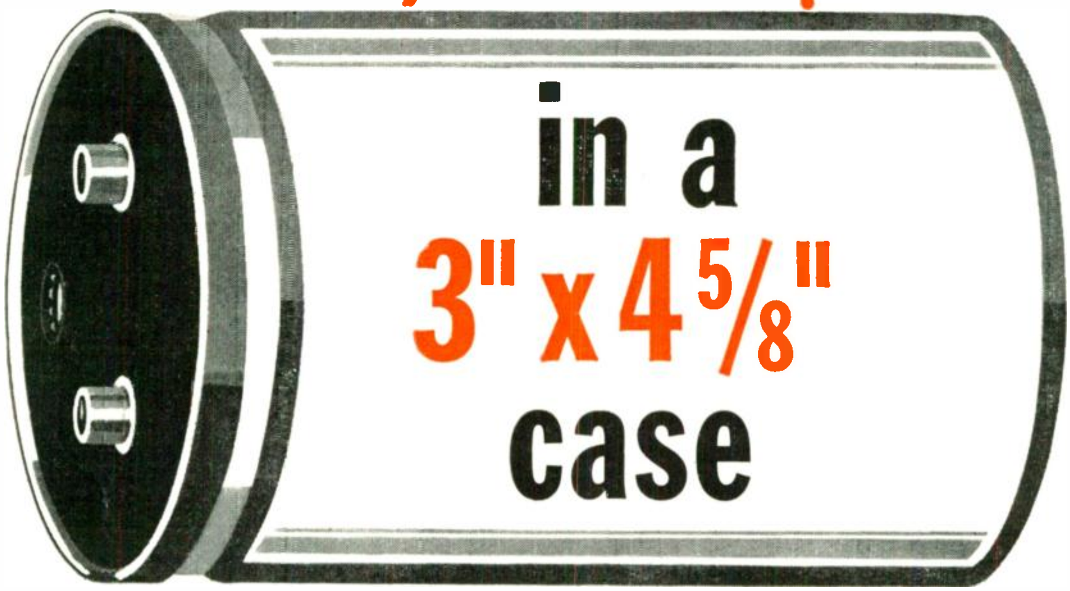

Powerlytic* Capacitors are packed with capacitance!

Designed specifically for applications requiring maximum capacitance in small physical size, Sprague Type 36D Aluminum Electrolytics find wide use in power supplies for digital computers, industrial controls, high-gain amplifiers, and allied equipment. Furnished in case sizes ranging from 1⅜" dia. x 2⅛" long to 3" dia. x 4⅝" long, Powerlytic Capacitors are available with capacitances which were previously impossible to obtain in the various case sizes.

Engineered for 65 C Operation

In Powerlytics, Sprague's many years of research, design, and production experience have produced a capacitor which allows the equipment designer maximum space economy for operating temperatures up to 65 C. This encompasses the great majority of applications in transistorized digital equipment and similar apparatus.

Outstanding Performance Characteristics

Powerlytic Capacitors have not only low ESR and low leakage currents but offer extremely long shelf life as well. Furthermore, they have the ability to withstand unusually high ripple currents.

Superior Seal and Safety Vents

Type 36D Powerlytics use the most reliable seal that Sprague has developed for aluminum electrolytic capacitors. This consists of crimping a beaded aluminum can onto a rubber gasket recessed in a rigid molded cover. Pressure-type safety vents employing silicone rubber are used on all case covers.

Choice of Terminal and Insulating Tube Styles

Tapped terminal inserts, often preferred for strap or bus bar connections, are available as well as solder lug terminals for use with permanently wired connections. In addition to the standard bare case, Powerlytic Capacitors may also be obtained with a new clear skin-tight plastic tube which adds very little to the bare case dimensions. They are also available with a Kraftboard tube.

Broad Range of Standard Ratings

Sprague's standard line of Powerlytic Capacitors includes 183 ratings covering capacitance values from 45 to 150,000 μF, in voltages from 3 to 450 WVDC. Each rating is the maximum capacitance available for a given case size.

• • •

For complete technical data on Type 36D Powerlytic Capacitors, write for Engineering Bulletin 3431 to Technical Literature Section, Sprague Electric Company, 235 Marshall Street, North Adams, Massachusetts.

*trademark

SPRAGUE COMPONENTS

CAPACITORS
TRANSISTORS
MAGNETIC COMPONENTS
RESISTORS

INTERFERENCE FILTERS
PULSE TRANSFORMERS
PIEZOELECTRIC CERAMICS
PULSE-FORMING NETWORKS

HIGH TEMPERATURE MAGNET WIRE
CERAMIC-BASE PRINTED NETWORKS
PACKAGED COMPONENT ASSEMBLIES
FUNCTIONAL DIGITAL CIRCUITS

SPRAGUE®
THE MARK OF RELIABILITY

NEW BELL LABORATORIES RESEARCH FORESHADOWS COMMUNICATIONS AT OPTICAL FREQUENCIES

A revolutionary new device, the continuously operating Optical Gas Maser, now under investigation at Bell Telephone Laboratories, foreshadows a whole new medium for communications: light.

Light waves vibrate at frequencies tens of millions of times higher than broadcast radio waves. Because of these high frequencies, a beam of light has exciting potentialities for handling enormous amounts of information.

Now for the first time, Bell Laboratories' new Optical Gas Maser continuously generates light waves that are "coherent." That is, the light waves move in phase as seen looking across the beam.

With further research, it is expected that such beams can be made to carry large amounts of information. The beams can be transmitted through long pipes. They can be projected very precisely through space, and might be used for communications between space vehicles.

Research with coherent light is another example of how Bell Laboratories prepares ahead for communications needs.

The Optical Gas Maser (above) was first demonstrated at Bell Telephone Laboratories. Heart of unit is a 40-inch tube containing helium and neon. Interaction between gas atoms produces a continuous, coherent beam of infrared light that may one day be used in communications.

BELL TELEPHONE LABORATORIES

WORLD CENTER OF COMMUNICATIONS RESEARCH AND DEVELOPMENT

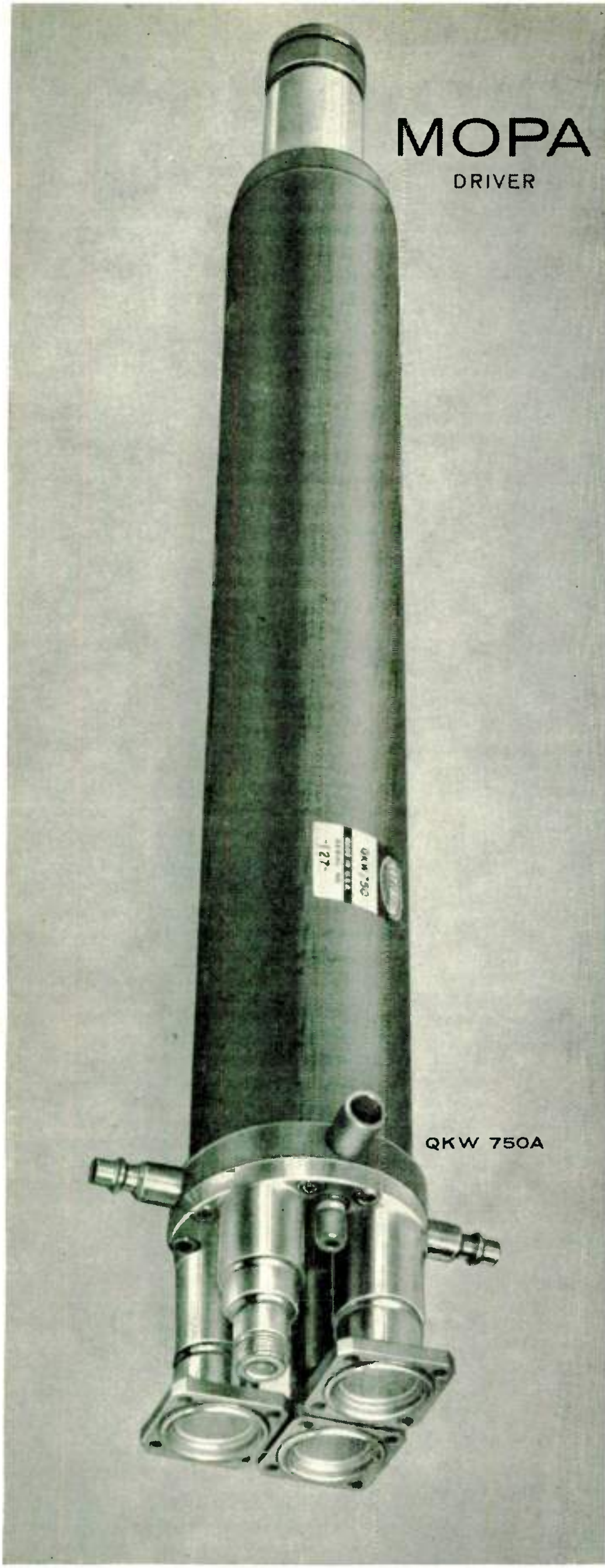

MOPA chain at S-band.

New Raytheon broadband TWT drives Amplitron* in high-duty-cycle frequency-diversity applications

QKW 750A has 60 kw minimum peak power, 18 db minimum gain, and more than sufficient bandwidth to drive the QKS 622 Amplitron in S-band MOPA chain.

A new traveling wave tube—Raytheon's QKW 750A—now makes possible a complete broadband, high-power MOPA chain at S-band.

The tube has a duty cycle of .015 and is designed for pulsed operation over the full 2,900 to 3,100 Mc range. It provides a minimum of 18 db gain and 60 kw peak power to drive a Raytheon QKS 622 Amplitron. Output of the amplifier chain is in the megawatt range. A companion tube—the QKW 782—covers the 2,700 to 2,900 Mc range.

Microwave systems designers should note that the bandwidth, peak and average power capability, and gain characteristics of the new TWT are well above the specified values as shown in the accompanying curve. This fact lends a high degree of conservatism and reliability to system design.

Write for detailed information and application service to Microwave and Power Tube Division, Raytheon Company, Waltham 54, Massachusetts. In Canada: Waterloo, Ontario.

*Raytheon Trademark

RAYTHEON COMPANY

MICROWAVE AND POWER TUBE DIVISION

RAYTHEON

BOSTON, MASS., BRowning 2-9600 • ENGLEWOOD CLIFFS, N. J., LOwell 7-4911 • BALTIMORE, MD., SOuthfield 1-0450 • CHICAGO, ILL., NAtional 5-4000
DAYTON, OHIO, BAldwin 3-8128 • LOS ANGELES, CALIF., PLymouth 7-3151 • CANADA: Waterloo, Ont., SHerwood 5-6831

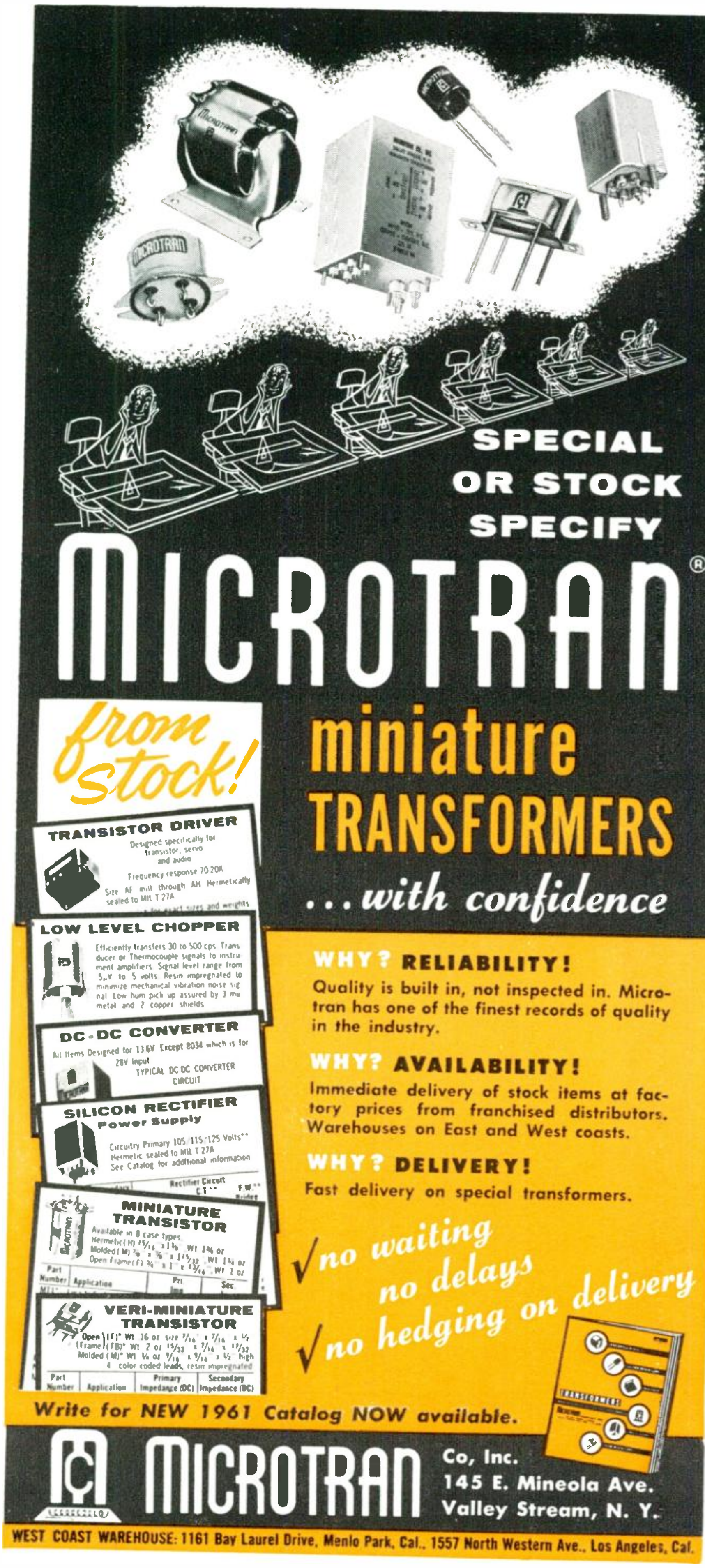

Meetings with Exhibits

● As a service both to Members and the industry, we will endeavor to record in this column each month those meetings of IRE, its sections and professional groups which include exhibits.

April 12-13, 1961

15th Annual Spring Technical Conference—"Electronic Data Processing." Hotel Alms, Cincinnati, Ohio.

Exhibits: Mr. J. R. Ebbeler, 7030 Ellen Ave., Cincinnati 39, Ohio.

April 19-21, 1961

SWIRECO, South West IRE Conference & Electronics Show, Dallas Memorial Auditorium and Baker Hotel, Dallas, Tex.

Exhibits: Mr. B. Williams, Texas Instruments, Inc., 6000 Lemmon Ave., Dallas 9, Tex.

April 26-28, 1961

Seventh Region Technical Conference and Trade Show. Westward Ho Hotel, Phoenix, Ariz.

Exhibits: Mr. G. T. Royden, 912 W. Linger Lane, Phoenix, Ariz.

May 8-10, 1961

National Aerospace Electronics Conference (NAECON), Miami & Dayton-Biltmore Hotels, Dayton, Ohio.

Exhibits: Mr. Robert J. Stein, 136 W. Second St., Rm. 202, Dayton 2, Ohio.

May 9-11, 1961

Western Joint Computer Conference, Ambassador Hotel, Los Angeles, Calif.

Exhibits: John H. Whitlock Associates, 253 Waples Mills Road, Oakton, Va.

May 22-24, 1961

Fifth National Global Communications Symposium (GLOBECOM V), Sherman Hotel, Chicago, Ill.

Exhibits: Mr. Fred Hilton, Motorola, Inc., 1501 W. Augusta Blvd., Chicago, Ill.

May 22-24 1961

National Telemetering Conference, Sheraton Towers Hotel, Chicago, Ill.

Exhibits: Mr. Frank Finch, 795 Gladys Ave., Long Beach 4, Calif.

June 6-8, 1961

Armed Forces Communications & Electronics Show, Sheraton Park and Shoreham Hotels, Washington, D.C.

Exhibits: Mr. William C. Copp, 72 W. 45th St., New York 36, N.Y.

June 13-14, 1961

Fifth National Conference on Product Engineering & Production, Philadelphia, Pa.

Exhibits: Mr. Paul J. Riley, Radio Corp. of America, Building 10-6, Camden 2, N.J.

(Continued on page 10A)

SWEEP AUDIO FREQUENCIES and HIGH-Q FILTER CIRCUITS with the Ease and Precision of RF Sweep Techniques

NEW KAY *Sona-Sweep* MODEL M

FEATURES

- Built-In Audio Detector
- Sharp, Pulse-Type Markers
- Logarithmic and Linear Frequency Sweep
- Both Swept and Manual Frequency (and scope display) Control
- Variable Center Frequency
- Variable Sweep Width Built-In Attenuators
- Zero Reference Line
- All-Electronic

SPECIFICATIONS

Frequency Range: 20 cps to 200 kc, variable.

Sweep Width: 20 cps to 20 kc, variable.

Repetition Rate: 0.2 to 25 cps, variable.

Price: \$895.00 plus \$22.00 per Marker F.O.B., Factory (\$985.00 plus \$25.00 per Marker F.A.S., N. Y.)

KAY *Ligna-Sweep*® MODEL SKV

ALL ELECTRONIC—AUDIO, VIDEO, VHF SWEEPING OSCILLATOR COVERS WIDE RANGE 200 CPS TO 220 MC.

FEATURES

- From 10 mc Down to 1 kc in One Wide Video Sweep.
- Highly Stable, Narrow-Band Video Frequency Sweeps (20 kc on Variable Bands, 200 cps on Fixed).
- Logarithmic Sweep for Low-End Expansion. Linear Sweeps 0.2 cps to 30 cps; Linear Sweep Locked to Line Frequency.
- Audio Sweep—200 cps to 20,000 cps. 8 Fixed, Narrow-Band Video Frequency Sweeps for Repetitive Operations.
- Fundamental Frequency 10 mc to 220 mc. (Widths to 30 mc Plus.)
- Continuously Variable Center Freqs. Direct-Reading Dial 10 kc to 220 mc.
- High-Level RF Output—1.0-v rms Into 70 ohms. AGC'd to ±0.5 db Over Widest Sweep.
- Price: \$1295.00 F.O.B., Factory (\$1425.00, F.A.S., New York).

For high-frequency work, the Kay *Ligna-Sweep Model SKV* provides 9 sweep bands, operating at fundamental frequencies, for wide, stable sweeps from 10 to 220 mc. At the low end of the spectrum, an audio-frequency sweep from 200 to 20,000 cps is provided.

For checking high-Q circuits and low-frequency response characteristics, variable rep-rates down to 0.2 cps are available. This wide choice of sweep rates (continuous to 30 cycles, and fixed 60-cycle lock) makes it easy to select that highest *rep-rate* which gives both an *accurate response* display and easiest, brightest viewing on the scope screen. A nominally logarithmic 30-cycle sweep, most useful for studying audio and video low-pass circuits, provides an expanded view of the low-frequency end, while showing over-all frequency characteristic.

Write for Complete Catalog Information

KAY ELECTRIC COMPANY

DEPT. I-4, MAPLE AVENUE, PINE BROOK, N. J. CApital 6-4000

Meetings with Exhibits

(Continued from page 8A)

June 19-20, 1961

Second National Conference on Broadcast and Television Receivers, O'Hare's Inn, Des Plaines, Ill.

Exhibits: Mr. Ray Lee, Philco Corp., 6957 West North Ave., Oak Park, Ill.

June 26-28, 1961

Fifth National Convention on Military Electronics, Shoreham Hotel, Washington, D.C.

Exhibits: Mr. L. David Whitelock, 6514 Greentree Road, Bethesda 14, Md.

July 16-21, 1961

Fourth International Conference on Medical Electronics & Fourteenth Conference on Electrical Techniques in Medicine & Biology, Waldorf-Astoria Hotel, New York, N.Y.

Exhibits: Mr. Lewis Winner, 152 W. 42nd St., New York 36, N.Y.

August 22-25, 1961

Western Electronic Show and Convention (WESCON), Cow Palace and Fairmont Hotel, San Francisco, Calif.

Exhibits: Mr. Don Larson, WESCON, 701 Welch Road, Palo Alto, Calif.

September 6-8, 1961

National Symposium on Space Electronics & Telemetry, Albuquerque, N.M.

Exhibits: Mr. V. V. Myers, 2912 Texas N.E., Albuquerque, N.M.

October 2-4, 1961

Seventh National Communications Symposium, Hotel Utica & Utica Municipal Auditorium, Utica, N.Y.

Exhibits: Mr. R. E. Bischoff, 19 Westminister Road, Utica, N.Y.

October 2-4, 1961

IRE Canadian Convention, Automotive Building, Exhibition Park, Toronto, Canada.

Exhibits: Business Manager, IRE Canadian Convention, 1819 Yonge St., Toronto 7, Ontario, Canada.

October 9-11, 1961

National Electronics Conference, Hotel Sherman, Chicago, Ill.

Exhibits: Mr. Rudy Napolitan, National Electronics Conference, 228 N. LaSalle St., Chicago, Ill.

Δ

Note on Professional Group Meetings: Some of the Professional Groups conduct meetings at which there are exhibits. Working committeemen on these groups are asked to send advance data to this column for publicity information. You may address these notices to the Advertising Department and of course listings are free to IRE Professional Groups.

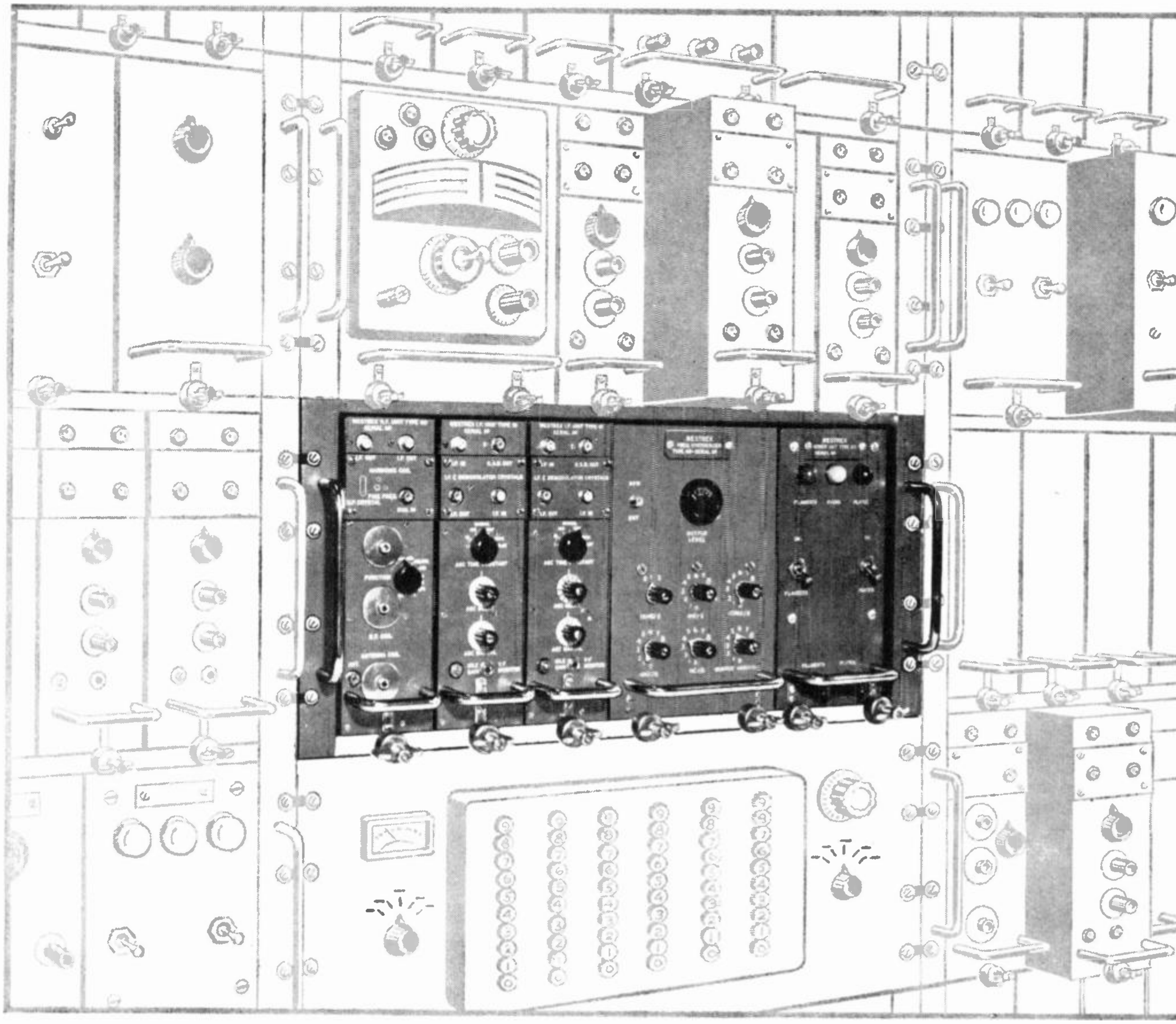

New HF SSB Receiver heart of a whole new "state of the art"

New flexibility. Building block modules make the Westrex 600 receiving system the most versatile communications receiver. The RF, IF, AFC, synthesizer, test and power supply modules can be arranged in any manner dictated by user requirements. As an example, a typical 4-voice channel SSB circuit can be established using one RF and four IF modules. As many RF channels as required can be accommodated using fixed frequency or continuously tunable RF modules. Operation can be either "local" or "remote."

New high performance. Significant features are:

- Extremely low third-order distortion (85-90 db) is made possible by a breakthrough in receiver front-end design.
- The sensitivity is very high. Image and IF spurious rejection is excellent. The AGC is extremely flat over a range of 130 db.
- The SSB filters have exceptionally high performance with very low pass-band phase distortion and very steep selectivity skirts.
- Cast aluminum housings are used for the RF, IF, and synthesizer modules, keeping radiation to a fraction of common receiver values.

Learn more about this significant receiver development. Write or phone today.

Westrex Corporation

A DIVISION OF LITTON INDUSTRIES

Communications Equipment Department, Section 163

540 W. 58th St., New York 19, N. Y. 1625 I St., N.W., Wash. 6, D. C.

SPECIAL PRODUCTS
SPECIAL SYSTEMS
SPECIAL SERVICES
FROM A SPECIAL SOURCE **LIONEL**

Special Announcement:

From its long history in the development of dependable products, the Lionel Corporation is emerging as a new force in U.S. industry. Together with the outstanding experience and proven products of its newly acquired subsidiaries, Lionel represents a strong new combination . . . an important single-source for the electronics industry, with dynamic management, engineering, production, and quality control. We believe it is to the interest of every electronic, electrical, and nucleonics engineer to investigate the products and services available from Lionel. A capsule listing of our products follows. For full facts, fill out coupon.

from LIONEL/TELERAD, Flemington, New Jersey

R-F Systems and Components: A full line of r-f coaxial and waveguide transmission components, plus complete transmission systems, are offered by our Telerad Division. These are precision products, with an established reputation for high performance. A few of the individual components are: ▪ power supplies ▪ signal generators ▪ feeds and horns ▪ antennas ▪ missile radar beacons ▪ mixers ▪ duplexers ▪ directional couplers ▪ rotary joints ▪ filters ▪ attenuators ▪ waveguides, fixed and flexible ▪ frequency meters ▪ and many other products manufactured to rigid industrial and MIL specifications. We welcome special orders for either components or r-f transmission systems, constructed to your exact requirements.

from LIONEL/ANTON, Brooklyn, New York

Connectors, Tubes, Nuclear Systems: The Anton Division of Lionel produces a wide line of *precision connectors* and *voltage regulator tubes.* It is also well known, of course, for its *nuclear radiation-sensing tubes, chambers,* and *nuclear systems,* which are truly standards for the industry. *Anton corona-discharge V-R tubes* run the full gamut of sizes and voltage ratings . . . from subminiature to miniature to standard dimensions, from 300 Volts to 30 KV. All operate in the microampere and very low milliampere range, with voltage tolerances of ±1% when required, ±2% standard. *Anton V-R tubes* are highly reliable units and are designed to meet MIL specs wherever applicable. *Anton precision connectors* are designed and tested to withstand severe environmental conditions such as shock, altitude, vibration, and moisture. Offered as standard are miniature rack and panel types, printed circuit types, and housed rack and panel types. Special designs are available on request. All standards are designed to meet MIL requirements.

from LIONEL, Hillside, New Jersey

Electromechanical Systems and Components: Our central plant has for years been a major producer of miniaturized electromechanical systems for both commercial and military use. Now for the first time, we are offering many of these components to industry at large. Some of the components now available include: *sequence relays, latching relays, time delay* and *power switches, bi-directional sequence relays, military low-energy transfer switches,* and a series of *miniaturized D.C.* and *universal motors.* In addition to our primarily commercial line, we also produce *miniature servo motors, servo-mechanisms, electrical* and *mechanical fuses, precision instruments, ordnance* and *communications equipment,* and other electronic products to customer specifications.

Our subsidiary, the LIONEL/INTERCONTINENTAL MANUFACTURING COMPANY, at Garland, Texas, is an important, experienced producer of *rocket motor casings, thrust nozzles, missile air frames,* and other parts and components for many weapons, including NIKE HERCULES, HONEST JOHN and LITTLE JOHN. We have demonstrated our competence on numerous prime and subcontracts to the government and industry, and have established an enviable reputation for fine product design and delivery on schedule.

For more information on any of the Lionel Corporation's products, systems, or services, check your area of interest on the coupon below, or contact us by phone or letter.

THE LIONEL CORPORATION

Hoffman Place, Hillside, New Jersey

I am interested in receiving information on the following:

- ☐ Frequency meters
- ☐ Coaxial lines
- ☐ Mixers
- ☐ Duplexers
- ☐ Feeds and horns
- ☐ Power supplies
- ☐ Signal generators
- ☐ Missile beacon
- ☐ The complete line of Anton connectors
- ☐ Flexible waveguide
- ☐ Directional couplers
- ☐ Rotary joints
- ☐ Antennas
- ☐ Filters
- ☐ Straight waveguide sections
- ☐ Voltage regulator tubes
- ☐ Precision potentiometers
- ☐ Relays
- ☐ Switches
- ☐ Motors
- ☐ Nuclear radiation sensing tubes and chambers
- ☐ Nuclear systems
- ☐ R-F transmission systems
- ☐ Lionel facilities and capabilities

NAME____________________ TITLE________________

DEPT.____________ COMPANY____________________

ADDRESS____________________________________

IRE News and Radio Notes

Current IRE Statistics

(As of February 28, 1961)
Membership—88,353
Sections*—110
Subsections*—29
Professional Groups*—28
Professional Group Chapters—281
Student Branches†—200

* See March, 1961 issue for a list.
† See October, 1960 issue for a list.

Calendar of Coming Events and Authors' Deadlines*

1961

Symp. on Information and Decision Processes, Purdue Univ., Lafayette, Ind., Apr. 12–13.

15th Ann. Spring Tech. Conf., Hotel Alms, Cincinnati, Ohio, Apr. 12–13.

SWIRECO, Dallas, Tex., April 19–21.

7th Region Tech. Conf. & Trade Show, Westward Ho Hotel, Phoenix, Ariz., April 26–28.

URSI-IRE Spring Mtg., Georgetown Univ., Washington, D. C., May 1–4.

Electronic Components Conf., Jack Tar Hotel, San Francisco, Calif., May 2–4.

2nd Nat'l. Symp. on Human Factors in Electronics, Marriott Twin-Bridges Motor Hotel, Arlington, Va., May 4–5.

Workshop in Graph Theory, University of Illinois, Urbana, May 6.

5th Midwest Symp. on Circuit Theory, Allerton Park & Urbana Campus, Univ. of Ill., Urbana, May 8–9.

NAECON, Miami & Biltmore Hotels, Dayton O., May 8–10.

Western Joint Computer Conf., Ambassador Hotel, Los Angeles, Calif., May 9–11.

Microwave Theory and Tech. Nat'l. Symp., Sheraton Park Hotel, Washington, D. C., May 15–17.

GLOBECOM V, Sherman Hotel, Chicago, Ill., May 22–24.

Nat'l. Telemetering Conf., Chicago, Ill., May 22–24.

Electro-Optical Devices Symp., Los Angeles, Calif., May.

3rd Nat'l. Symp. on Radio Frequency Interference, Sheraton-Park Hotel, Washington, D. C., June 12–13.

5th Nat'l. Symp. on Product Engrg. and Production, Hotel Sheraton, Philadelphia, Pa., June 14–15.

2nd Nat'l. Conf. on Broadcast and Television Receivers, O'Hare Inn, Des Plaines, Ill., June 19–20.

MIL-E-CON 1961, Shoreham Hotel, Washington, D. C., June 26–28.

JACC, Univ. of Colorado, Boulder, June 28–30.

Int'l. Conf. on Elec. Engrg. Education, Syracuse, N. Y., June.

* DL = Deadline for submitting abstracts.

(*Continued on page 15A*)

SWIRECO Announces Program Moderators

Moderators for twelve technical sessions have been announced for the 13th Annual Southwestern IRE Conference and Electronics Show (SWIRECO) in Dallas, Tex., on April 19–21, 1961, at the Dallas Memorial Auditorium and the Baker Hotel.

According to technical program chairman, Orville Becklund of Texas Instruments, Inc., the moderators and their panels are:

Dr. H. Huskey, University of California, Berkeley, "Computer Design" and "Computers"; Dr. G. E. Moore, Fairchild Semiconductor Corp., Palo Alto, Calif., "Semiconductor Devices"; F. Hefer, Dresser Electronics, Houston, Tex., "Microminiature Devices and Digital Design"; Maj. J. E. Steele, M.D., Wright Air Development Div., Wright-Patterson AFB, Ohio, "Bionics and Medical Electronics."

Also, Prof. W. L. Hughes, Oklahoma State University, Stillwater, "Magnetic Devices"; G. T. Bennett, Curtis Mathes Manufacturing Co., Dallas, "Equipment Design"; Dr. W. H. Hartwig, The University of Texas, Austin, "Circuit Theory"; J. C. McElroy, Collins Radio Co., Cedar Rapids, Iowa, "Communications and Telemetry"; Dr. J. F. Reagan, Chance Vought Corp., Dallas, Tex., "Systems"; Dr. H. T. Born, Geophysical Research Corp., Tulsa, Okla., "Geophysics"; and F. C. Smith, Jr., Dannemiller-Smith, Inc., Houston, Tex., "Industrial Electronics."

Dr. W. W. Hagerty, Dean of the College of Engineering, The University of Texas, Austin, will moderate a panel on engineering education.

Dr. Lloyd V. Berkner, President of the IRE, will be a special guest speaker at the Conference. His topic is "Graduate Education in the Southwest and the Graduate Research Center." Dr. Berkner will address the entire Conference at a special session on Thursday afternoon, April 20, in the Dallas Memorial Auditorium.

It was also announced that F. J. Ocnaschek has replaced F. J. Fogarty, Chance Vought Corp., Dallas, as registration chairman for the Conference. Preregistration and hotel reservation forms are available from Mr. Ocnaschek at Collins Radio Co., 1200 N. Alma Rd., Richardson, Tex.

Professional Group News

At its meeting on February 14, 1961, the IRE Executive Committee approved the following new chapters: Joint PG on **Antennas and Propagation and Microwave Theory and Techniques**—Seattle Chapter; PG on **Automatic Control**—Pittsburgh Chapter; PG on **Engineering Writing and Speech**—Twin Cities Chapter; PG on **Military Electronics**—Omaha-Lincoln Chapter; PG on **Military Electronics**—Ottawa Chapter; and PG on **Radio Frequency Interference**—Philadelphia Chapter.

IRE Canadian Conference Announces New Meeting Dates

The IRE Canadian Electronics Conference announces that the dates for its 1961 meeting have been changed from October 4–6 to October 2–4. In addition, the name of the Conference has been changed officially to "IRE Canadian Electronics Conference." The deadline for submitting abstracts of papers to be presented at this Conference has been set at May 15, 1961.

Reliability Training Course To Be Held in Syracuse

The arrangements for a Northeast Reliability Training Course, sponsored jointly by the IRE and the Electronic Division of the American Society for Quality Control, have been completed. The course will be held at the Sheraton Inn in Syracuse, N. Y., on May 22–27, 1961.

During the past decade, the field of reliability engineering has grown rapidly. Reliability specifications are becoming common form in military contracts, and understanding of their significance from a cost standpoint as well as from a technical standpoint is becoming vital.

Companies sending representatives to this Reliability Training Course will benefit directly. Completion of this course will equip the individual with the basic tools and knowledge required to pursue a systematic approach to reliability problems and to upgrade the reliability jobs in his company.

Persons spending a majority of their time on reliability work such as analysis testing, design review, statistical quality control, component application, malfunction reporting, etc., will benefit most from this course which is designed to furnish techniques for, and practice in, solving day to day problems in component and system reliability. The course will be especially helpful for the military, aircraft and missile industry, and for the military electronic component and systems manufacturer, but it is not limited to problems in these fields.

The course will be directed by foremost consultants in the field of reliability and quality control. Classes will total 50 hours, from 9 A.M. Monday, May 22, until 4 P.M. Saturday, May 27. In the evenings noted guest speakers will talk and lead discussions on various aspects of reliability. Registration is limited to 35 persons in order to preserve an atmosphere of individual tutorship.

Registration is open to all applicants and is complete only upon the receipt of the full registration fee, which includes the cost of course materials, lunches, and one dinner.

The registration fee of $225, as well as the name, address, and company affiliation of the registrant, should be sent to the Registrar: Mrs. N. J. McAfee, 2106 Tucker Lane, Apt. A-8, Baltimore 7, Md. For further information, contact: F. A. Gall, Chairman, Reliability Training Course, General Electric Co., French Road, Utica, N. Y.

Program Highlights of MIL-E-CON 1961 Announced

Five state-of-the-art reports by specialists will highlight the technical program of the Fifth National Convention on Military Electronics (MIL-E-CON 1961), according to Harry Davis, Chairman of the Technical Program Committee.

MIL-E-CON 1961 will meet at the Shoreham Hotel, Washington, D. C., on June 26–28, 1961. This annual meeting is sponsored by the Professional Group on Military Electronics of the IRE. Major General F. L. Ankenbrandt, USAF (Ret.), member of the Technical Staff of Defense Electronic Products, RCA, Camden, N. J., is Convention President for MIL-E-CON 1961.

The topics and sponsors of the five state-of-the-art sessions are: Low-Noise Amplifiers, Dr. M. N. Lebenbaum, Airborne Instruments Laboratory; Computer Technology, Dr. S. N. Alexander, National Bureau of Standards; Space Physics, Dr. R. Jastrow, National Aeronautics and Space Administration (NASA); Plasma Physics, Prof. W. K. Kahn, Polytechnic Institute of Brooklyn; and Radio and Radar Astronomy, Dr. J. P. Hagen, NASA.

The United States Air Force Research and Development Command (ARDC) will sponsor five classified sessions at MIL-E-CON 1961. Tentative arrangements have been made for the following topics to be discussed: Anti-Submarine Warfare, Office of Naval Research; Aerospace Physics, Aerospace Corporation; Command and Control, Mitre Corporation and Command and Control Development Division, ARDC; Satellite Communications, U. S. Army Research and Development Laboratories and Defense Communications Agency; Project DEFENDER, Advanced Research Projects Agency.

The 1961 *Conference Proceedings* will be distributed free to all registrants at the Convention and will contain the unclassified papers, except those presented in the state-of-the-art sessions.

In addition to hearing technical papers at a total of 25 sessions, registrants will see displays of components, instrumentation, equipment and systems of particular interest and significance in military electronics. According to L. D. Whitelock, Exhibits Chairman, more than half of the 214 exhibit booths had already been reserved by the middle of February. The exhibits will also be open to the scientific public.

More than 5000 engineers, scient sts, and executives from industry, government agencies and laboratories, and universities attended MIL-E-CON 1960, and an even larger attendance is indicated this year.

"HERO" Congress To Be Held in May

The Congress on *H*azards of *E*lectromagnetic *R*adiation to *O*rdnance, sponsored by the U. S. Naval Weapons Laboratory, Dahlgren, Va., will be held at the Franklin Institute, Philadelphia, Pa., on May 24–26, 1961.

The purpose of this Congress is to review the present state of knowledge of the hazards to ordnance from environmental radio frequency fields. The program is to include progress of current investigations, surveys and discussions of new ideas, techniques, components, and materials, and anticipation of future needs. It is believed that the Congress will provide for exchange of information and ideas, stimulate efforts toward early solutions to present problems, help to identify new problem areas, serve as a means of reviewing over-all program objectives, and provide, in the *Proceedings*, a state-of-the-art report.

Plans call for the presentation of formal papers and informal discussion periods. *Proceedings* will be distributed to attendees at a later date. The following subjects are tentatively scheduled:

1) Determination of Extent of Hazard of Current Weapons—Testing and Analysis, Instrumentation and Measuring Techniques, and Theory and Prediction.

2) Fixes for Existing Weapons—Components and Materials, Systems, and Evaluations.

3) Optimum Design Features and Specifications.

Secret security clearance and, in case of non-government organizations, certification of need-to-know by the cognizant military agency will be required for attendance.

Further details, security forms, and hotel reservations information will be mailed directly by the Franklin Institute at a later date.

Call for Papers

1961 Western Electronic Show and Convention (WESCON)

August 22–25, 1961

Cow Palace, San Francisco, Calif.

The 1961 Western Electronic Show and Convention now issues a call for papers for its 1961 meeting, which is to be held August 22–25, at the Cow Palace in San Francisco, Calif.

Prospective authors are required to submit 100- to 200-word abstracts and 500- to 1000-word detailed summaries of their papers by May 1, 1961, in order to be considered for inclusion in the program. They will be notified by June 1, 1961, of acceptance or rejection of their papers.

Submissions should be sent to: E. W. Herold, c/o WESCON's Northern California Office, 701 Welch Road, Palo Alto, Calif.

Calendar of Coming Events and Authors' Deadlines*

(Continued from page 14A)

4th Int'l. Conf. On Medical Electronics & 14th Conf. on Elec. Techniques in Medicine & Biology, Waldorf-Astoria Hotel, N. Y., N. Y., July 16–21. (DL*: April 1, 1961, H. P. Schwan, Moore School of E.E., Philadelphia 4, Pa.)

WESCON, San Francisco, Calif., Aug. 22–25. (DL*: May 1, E. W. Herold, WESCON North Calif. Office, 701 Welch Rd., Palo Alto, Calif.)

3rd Int'l. Conf. on Analog Computation, Belgrade, Sept. 4–9.

1961 Nat'l. Symp. on Space Electronics and Telemetry, Albuquerque, N. M., Sept. 6–8.

Joint Nuclear Instrumentation Symp., North Carolina State College, Raleigh, N. C., Sept. 6–8.

Engrg. Writing and Speech Symp., Bellevue Stratford Hotel, Philadelphia, Pa., Sept. 14–15.

9th Ann. Engrg. Management Conf., New York, N. Y., Sept. 14–16.

10th Ann. Industrial Electronics Symp., Boston, Mass., Sept. 20–21.

7th Nat'l. Communications Symp., Utica, N. Y., Oct. 2–4. (DL*: June 1, R. K. Walker, 34 Bolton Rd., New Hartford, N. Y.)

IRE Canadian Electronics Conf., Automotive Bldg., Toronto, Canada, Oct. 2–4.

IRE Canadian Conv., Exhibition Park, Toronto, Can., Oct. 4–6.

Nat'l. Electronics Conf., Chicago, Ill., Oct. 9–11.

5th Nat'l. Symp. on Engrg. Writing and Speech, Kellogg Ctr. for Continuing Education, Michigan State Univ., East Lansing, Oct. 16–17. (DL*: July 15, J. Chapline, Philco Corp., Computer Div., 3900 Welsh Rd., Willow Grove, Pa.)

East Coast Conf. on Aerospace & Navigational Electronics, Lord Baltimore Hotel, Baltimore, Md., Oct. 23–25.

URSI-IRE Fall Mtg., Univ. of Texas, Austin, Oct. 23–25.

PGNS 8th Ann. Mtg., Hotel Riviere, Las Vegas, Nev., Oct. 23–26.

Elec. Tech. in Medicine & Biology Conf., Univ. of Nebraska, Lincoln, Oct. 26–27.

Symp. on Instrumentation Facilities for Biomedical Res., Sheraton Fontenelle Hotel, Omaha, Neb., Oct. 26–27.

1961 Electron Devices Mtg., Sheraton-Park Hotel, Washington, D. C., Oct. 26–28.

Radio Fall Mtg., Hotel Syracuse, Syracuse, N. Y., Oct. 30–31.

NEREM, Boston, Mass., Nov. 14–16.

MAECON, Kansas City, Mo., Nov. 14–16.

PGVC Conf., Hotel Leamington, Minneapolis, Minn., Nov. 30–Dec. 1.

Eastern Joint Computer Conf., Sheraton-Park Hotel, Washington, D. C., Dec. 3–7.

1962

8th Nat'l. Symp. on Reliability and Quality Control, Statler Hilton Hotel, Washington, D. C., Jan. 9–11. (DL*: May 15, 1961, E. F. Jahr, IBM Corp., Owego, N. Y.)

* DL = Deadline for submitting abstracts.

TIMS To Meet In Brussels

The 8th Annual International Meeting of The Institute of Management Sciences will be held in the Palais des Congrès at Brussels, Belgium, on August 23–26, 1961. The following topics will be included in the program: 1) Programming under Uncertainty, 2) Simulation and Gaming, 3) Rational Investment Decisions, 4) Organization Theory and Analysis, 5) Subjective and Objective Probability, 6) Reality and Theory in Management Science, 7) Adaptive Systems, and 8) Behavioural Sciences. Arrangements will be made for meetings of the colleges, and special sessions are also being planned, including one which will be devoted to reports on research from the newly founded International Center for Management Science at Rotterdam, The Netherlands.

The registration fee is $12 for TIMS members and $15 for others. Registration for North Americans is handled by H. H. Cauvet, Executive Director of TIMS, 250 North St., White Plains, N. Y. All other registrations are handled by Max Duval, Office Belge pour l'Acroissement de la Productivité, 60, rue de la Concorde, Brussels, Belgium. The registration will be closed on April 1, 1961. Prospective participants who fail to apply before that date are advised to write to Dr. Jacques Drèze, Chairman of the Local Arrangements Committee, Department of Economics, University of Louvain, Louvain, Belgium; no guarantee can be given that registration will then be possible in view of space limitations. Participants who want to contribute a paper are required to submit either the paper or an adequate abstract to the Program Chairman, Professor W. W. Cooper, Graduate School of Industrial Administration, Carnegie Institute of Technology, Pittsburgh 13, Pa.

Changes Indicated for 1961 WESCON Program

Early planning of the technical program for the 1961 WESCON has developed several points of immediate interest to authors expecting to participate in the convention August 22–25, 1961, in San Francisco.

E. W. Herold, Chairman of the Technical Program Committee, recently reported for A. J. Morris, WESCON Board Chairman, and Dr. J. V. N. Granger, Convention Director, the decision of the WESCON Board to reproduce individual preprints of the papers. They will be made available at a nominal charge in advance of the presentations.

Authors scheduled for the technical program will be asked to submit papers to WESCON Headquarters in reproducible form by July 1, 1961.

There will be no restriction on authors for post-convention publication of their material in journals and magazines of choice. Authors will be encouraged to seek publication, and are assured of assistance from WESCON.

The Technical Program Committee has decided to develop further the "new look" approach initiated at the 1959 WESCON.

In this approach, technical sessions will include invited discussion of all formal papers by internationally known experts, as well as floor discussion, thereby enhancing interest considerably over presentation of the papers alone. In addition to submitted papers, the committee promises to exploit new media for exceptional invited papers and expects the program's content to be the best in history.

Although all the detailed session topics are not yet available, it is expected that most professional groups of the IRE will be represented.

It was further announced that a special radio astronomy session will be held jointly with the International Astronomical Union, whose worldwide members will be meeting simultaneously at Berkeley, Calif.

Among the program departures, special attention will be given to the generation, detection and application of coherent infrared and optical electromagnetic radiation, using the latest quantum-electronic techniques.

Still other sessions are planned for other new advances in the electronic art, for which the committee has requested particular suggestions.

Prospective authors are asked to send 100–200-word abstracts and 500–1000-word summaries for committee use by May 1, 1961. Submissions are to be directed to the attention of E. W. Herold at WESCON's Northern California Office, 701 Welch Road, Palo Alto, Calif. Notifications of acceptance or rejection will be made by June 1, 1961.

PGPEP Announces June Conference

The Fifth Annual Conference of the Professional Group on Product Engineering and Production (PGPEP) of the IRE will be held at the Sheraton Hotel in Philadelphia, Pa., on June 14–15, 1961. The program, entitled "Mechanical Engineering in Space Age Electronics," will consist of four main sessions: 1) Research—"Better Products through Advances in Design Technology," Dr. A. N. Goldsmith, RCA consultant, moderator; 2) Digital Technology—"Computers and Data Processing," I. Auerbach, President, Auerbach Electronics, moderator; 3) Packaging—"Packaging Applications for Missile and Space Vehicles," J. B. Duryea, GE Staff Engineer, moderator; 4) Systems Technology—"Systems Engineering and Related Research-Development," Dr. H. Krutter, Chief Scientist, USNADC, Johnsville, Pa., moderator.

Approximately 30 firms will exhibit products pertinent to the technical program of the Conference.

In addition to the regular program, T. A. Smith, of RCA, and another prominent speaker will deliver talks on subjects which will be announced at a later date.

The Conference committee consists of the following: Chairman, P. Riley, RCA; Vice Chairman, F. Dougherty, Turbo Machine Company; Program Chairman, J. Knoll, RCA; Registration, W. Welsh, RCA; Arrangements, W. Hennessy, Burroughs; Exhibits, A. Ansley, Arthur Ansley Company, and L. Schwartz, Remington Rand Univac; Publicity, R. Renner, Turbo Machine Company, and H. Olson, RCA.

Denver Research Institute Announces Symposium

The Denver Research Institute of the University of Denver will hold its 8th Annual Symposium on Computers and Data Processing at the Elkhorn Lodge in Estes Park, Colo., on June 22–23, 1961. The continuing theme of this series of meetings has been the advanced treatment of basic problems in computer technology. Papers will be presented in the fields of Components and Devices, Logic Design, Philosophy of Computer Design, and Computers and Education.

Although it is anticipated that the program will be comprised largely of invited papers, a limited number will be selected from papers submitted without invitation.

For further information, contact: W. H. Eichelberger, Denver Research Institute, University of Denver, Denver 10, Colo.

P. K. McElroy (*left*), Chairman of the PGRQC, presented the "1960 IRE Professional Group on Reliability and Quality Control Award" to the joint recipients, R. L. Easton and M. T. Votaw (*center* and *right*), of the Naval Research Laboratories, at the Seventh National Symposium on Reliability and Quality Control, which was held at the Bellevue-Stratford Hotel, Philadelphia, Pa., on January 9–11, 1961.

In Quantity Production

SUPER POWER KLYSTRONS

Varian Associates has developed quantity production techniques for the super-power VA-842 amplifier klystron.

These mighty tubes are the largest production-model klystrons in the world. VA-842 tubes operate at 400-450 Mc., providing 75 kW average power and 1.25 megawatts peak power. 40 db gain, efficiency to 40%. Pulse duration: 2000 microseconds.

Varian's broad experience in the design and manufacture of super-power tubes made possible the VA-842's record transition time from drawing board to delivery and acceptance—just nine months!

FEATURES ▪ Tunable 400 to 450 Mc. ▪ 75 Kilowatts Average ▪ 40 db Gain ▪ 1.25 Megawatts Peak ▪ Efficiency over 40% ▪ Pulse duration 2000 microseconds

Varian's production capacity in super-power tubes may be of use to you. For full information and technical data, write Tube Division.

VARIAN associates

PALO ALTO 2, CALIFORNIA

BOMAC LABORATORIES, INC.
VARIAN ASSOCIATES OF CANADA, LTD.
S-F-D LABORATORIES, INC.
SEMICON ASSOCIATES, INC.
SEMICON OF CALIFORNIA, INC.
VARIAN A. G. (SWITZERLAND)

IRE Begins Work in Nuclear Instrumentation

At its 25th Annual Meeting in New Delhi, India, last November 1–12, the International Electrotechnical Commission (IEC) began standardization activities in the field of nuclear instrumentation. The IEC, with the ultimate objective of enhancing international trade, functions mainly through specialized technical committees which formulate recommendations in various electrical technologies. These recommendations are reviewed and ratified by 33 member countries. The IEC emphasizes the engineering aspects of international electrotechnology, as compared to other international scientific bodies that stress definitions of fundamental quantities, terminology, etc.

Organized at the suggestion of West Germany, TC-45 on Electrical Measuring Instruments Used in Connection with Ionizing Radiation met to define its scope, its method of operation, and to initiate activities in the area of nuclear instrumentation. As a first task, the committee reviewed in detail a draft recommendation on safety prepared by the secretariat. The following countries were represented at its deliberations: Belgium, (Communist) China, Czechoslovakia, France, India, Sweden, U.K., U.S.A., and West Germany.

The chairman of TC-45 is W. H. Hamilton of Westinghouse—Bettis, while the secretariat is in West Germany (Dr. J. Troger, Siemens and Halske). U. S. delegate was Dr. A. B. Van Rennes of United Research Inc. (Hamilton is also Chairman, and Van Rennes a member of American Standards Association's Sectional Committee N-3 on Nuclear Instrumentation. This committee is sponsored by the IRE.)

Four working groups were constituted in TC-45, each of which plans to formulate one recommendation during the coming year. Members of each working group in various countries cooperate in arriving at suitable details of a recommendation, after which it is submitted to each IEC member country for formal ratification. The recommendations are expected to be based on standards already compiled, or in process of development, in one of the member countries. The four working groups are:

a) Terminology. Chairman: France—J. Auzouy, Inspecteur General au Commissariat a l'Energie Atomique, 127 Rue de l'Universitat, Paris 7.
b) Safety Requirements. Chairman: U.K.—S. J. Dagg, c/o Central Electricity Generating Board, Friars House, 157/168 Blackfriars Road, London.
c) Interchangeability. Chairman: Germany—Prof. Dr. K. Franz, Telefunken Forschungsinstitut, Ulm (Donau), Soflingerstr 100.
d) Reactor Instrumentation. Chairman: U.S.A.—Dr. A. B. Van Rennes, United Research Inc., 138 Alewife Brook Parkway, Cambridge 40, Mass.

The 26th Annual Meeting of IEC will convene in Switzerland during the summer of 1961. TC-45, however, expects to meet separately during the fall, possibly in Austria.

Hosts for the New Delhi IEC meeting were the Indian Standards Institution and the Indian Government, which, in addition to providing excellent conference facilities for the 350 delegates, afforded many off-hour opportunities to learn about Indian culture, customs, and industrial progress through local tours, visits to research laboratories, and through cultural programs. Notable among these opportunities were trips to the historical city of Agra (site of the Taj Mahal) and to the large Bakra-Nangal power dam in the state of Punjab.

NEREM 1961 Issues Call for Papers

Technical papers describing significant original advancements—focused on research and development—are invited for presentation at the 1961 Northeast Electronics Research and Engineering Meeting (NEREM), which will be held on November 14–16, 1961, in the Commonwealth Armory and the Somerset Hotel, Boston, Mass.

This year's meeting will feature a marked departure in technical program format, scope and size, as well as type and number of exhibits. The program will include many invited state-of-the-art tutorial sessions, discussion panels, as well as contributed topical papers on new developments.

All IRE member registrants will receive at the Conference, free of additional charge, a copy of the NEREM Record, a printed 200-page conference report with 600–1000-word digests (supported by drawings and photographs) of every paper presented at the meeting.

A suggested, but not inclusive list of subject areas for NEREM 1961 is as follows:

Computers—Logic, Design, Applications and Components.
Microwaves—Components, Interaction Phenomena, and Diagnostics.
Systems—Surveillance, Communications, Radar, Guidance, Data-Handling.
Plasma—Theory and Applications as Energy Convertors, Millimeter-Wave Generators.
Solid-State Devices—Semiconducting, Paramagnetic, Ferrimagnetic, Ferromagnetic, and Ferroelectric.
Engineering Management—Marketing, Production Techniques, Reliability.
Communication and Control—Theory and Applications.
Also, Antennas and Wave Propagation, Medical Electronics, Microelectronics and Electron Devices.

To permit the development of well-integrated technical sessions, speakers are requested to furnish either complete papers or 400–500-word abstracts, in triplicate, plus 50-word summaries for advance program mailings.

All material should be mailed on or before June 15, 1961, to the NEREM 1961 Program Chairman: F. K. Willenbrock, Pierce Hall, Harvard University, Cambridge 38, Mass.

Authors will be notified of paper acceptance or rejection by August 1, 1961. For further information, contact: L. Winner, 152 W. 42 St., N. Y. 36, N. Y., or telephone BRyant 9-3125.

Air Force MARS Announces Schedule

The schedule of broadcasts of the Air Force MARS Eastern Technical Net, operating Sundays from 2 to 4 P.M. EDT on 3295, 7540, and 15,715 kc, has been announced as follows:

April 16—"Modern Techniques in Speech Communications," Captain J. D. Griffiths, USAF, Rome Air Development Center.

April 23—"Basic Electronics for the Radio Amateur," P. E. Hatfield, General Electric Company.

April 30—"Custom Building Via Home Construction," E. A. Neal, General Electric Company.

May 7—"Telemetry: Modern Concepts and Applications," W. Bonney, Tele-Dynamics Division, American Bosch-Arma Corporation.

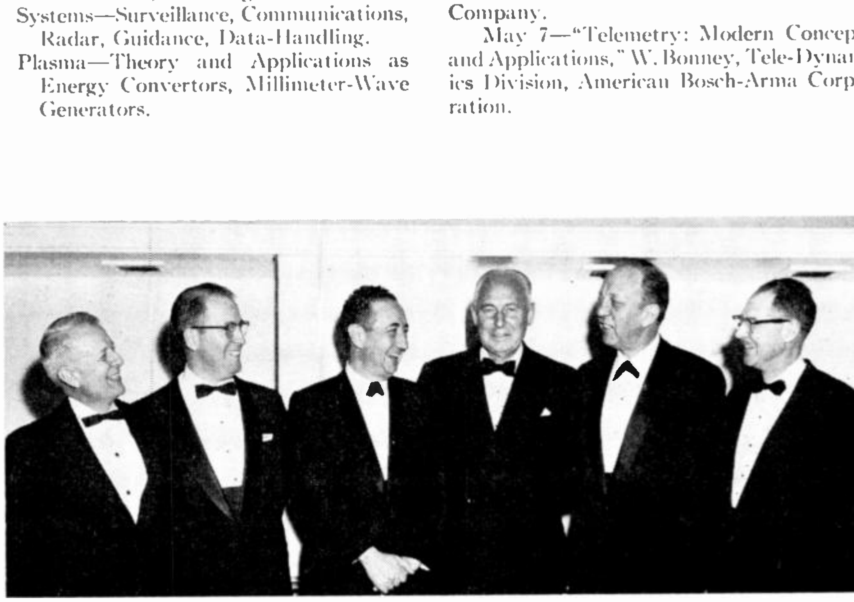

Dr. Lloyd V. Berkner, President of the IRE, was the main speaker at the Washington Section Annual Banquet, which was held on Saturday, February 11, 1961, at the Statler Hilton Hotel in Washington, D.C. The Honorable R. E. Lee, of the Federal Communications Commission, acting as guest chairman, presented Fellow, Student, and Patron Awards. Shown in the above photograph are (*left* to *right*): B. S. Melton, Vice Chairman of the Washington Section; C. R. Busch, Secretary; R. E. Lee, FCC Commissioner; Dr. Berkner; C. L. Engleman, Treasurer; and D. C. Ports, Chairman.

Radio Propagation Course Announced by NBS

The National Bureau of Standards will present a three-week course in Radio Propagation this summer, according to a recent announcement by Dr. F. W. Brown, Director of the NBS Laboratories in Boulder, Colo.

The course is designed to give scientists and engineers from universities, industry and government agencies access to the latest advances in radio propagation research, and to show how this knowledge can best be applied to the design of systems for radio communication and navigation. It will consider the entire range of useable radio frequencies, and will extend into the types of propagation which are being explored for the future.

The problems of sending a radio wave through the lower and upper atmosphere will be considered in two separate sections which may be taken individually or in succession. The first, a one-week course in Tropospheric Propagation, will be offered July 31–August 4; the second, a two-week course in Ionospheric Propagation, will be offered August 7–18. The problem of "static" or radio noise—of atmospheric, man-made, or cosmic sources—will be considered in the section on Ionospheric Propagation. In both sections, the continuing emphasis will be on those elements of propagation which affect system design and frequency allocation.

Prerequisites for the course are the bachelor's degree in electrical engineering, physics, or other suitable academic or practical experience. The tuition will be \$100 for Tropospheric Propagation, \$200 for Ionospheric Propagation, or \$300 for the entire course.

Registration will be limited and early application should be made to ensure consideration. Further details of the course and registration forms will be available March 1, 1961, from: E. H. Brown, Educational Director, Boulder Labs., National Bureau of Standards, Boulder, Colo.

Auerbach Receives Philadelphia Section Award

Isaac L. Auerbach (S'46–M'49–SM'52–F'58), President and Technical Director of Philadelphia's Auerbach Electronics Corporation has been cited by the Philadelphia Section of the IRE in a special award for "his personal contributions, stimulation, and leadership in the international exchange of information in the electronic computer field."

The award, first of its kind ever given by the organization, was presented at a Fellows' Night banquet, February 11, 1961, at the Philadelphia Cricket Club by W. T. Sumerlin (S'34–A'40–M'44–SM'50), Chairman of the IRE's Philadelphia Section.

The plaque was presented to Mr. Auerbach in recognition of "his many services in the advancement of the information processing sciences both here and abroad."

Mr. Auerbach is President of the International Federation of Information Processing Societies, with a Secretariat in Zurich, Switzerland. IFIPS is a society of societies, with representation from the technical societies of seventeen nations, dedicated to the advancement of the information processing sciences for the benefit of mankind.

Mr. Auerbach was one of the leading figures in the organization and development of this international organization to foster a greater interchange of information about the computer and information processing field. He is also the United States Representative to IFIPS via the National Joint Computer Committee (IRE, AIEE, ACM). He has been active in fostering exchanges of information about the burgeoning computer field for many years, first bringing together local IRE-AIEE groups for this joint purpose in 1950, and serving as Scientific Advisor to UNESCO on Automation and Information Processing from 1957 to 1960.

He helped to organize the UNESCO-sponsored First International Conference on Information Processing, June, 1959, in Paris. On this occasion, the City of Paris awarded him its Grand Medal for the key role he played in the success of the first such technical conclave.

Mr. Auerbach is a graduate of the Drexel Institute of Technology, Philadelphia, Pa., and earned the Master's degree in applied physics at Harvard University, Cambridge, Mass.

Also hailed at the IRE dinner was Dr. Britton Chance (M'46–SM'46–F'54), of the University of Pennsylvania, Philadelphia, who won the 1961 Prize Award of the Philadelphia Section's Professional Group on Bio-Medical Electronics. The following four newly-elected Fellows of the IRE were introduced: J. F. Fisher (SM'48–F'60), of the Philco Corporation; Y. H. Ku (SM'53–F'60), of the Moore School of Electrical Engineering, University of Pennsylvania; V. L. Ronci (SM'51–F'60), of Bell Telephone Laboratories, Allentown, Pa.; and T. A. Smith (J'25–A'26–SM'45–F'60) RCA, Camden, N. J.

Principal speaker at the dinner was Dr. Ferdinand Hamburger, Jr. (A'32–M'39–SM'43–F'53), Editor of the Proceedings, Professor, and Chairman of the Electrical Engineering Department of Johns Hopkins University, Baltimore, Md., and Director of their Radiation Laboratory.

A plaque for "leadership in the international exchange of information in the electronic computer field" was presented to I. L. Auerbach (*right*), President of the Auerbach Electronics Corporation, Philadelphia, Pa., and President of the International Federation of Information Processing Societies, with headquarters in Zurich, Switzerland.

W. T. Sumerlin (*left*), Chairman of the Philadelphia Section of the IRE, made the presentation at a Fellows' Night banquet, which was held on February 11, 1961, at the Philadelphia Cricket Club.

Components Conference to Meet in May

H. C. Ross, newly-appointed Chairman of the 1961 Electronic Components Conference, which will be held May 2–4, 1961, at the Jack Tarr Hotel, San Francisco, Calif., has announced that the themes of the Conference will include: "New Components and Their Impact on Engineering Progress," "New Products and New Requirements to Meet the Demands of Our New Engineering Age," and "New Techniques Which Make New Components Possible." The Conference will be sponsored by the IRE, AIEE, EIA, and WEMA. The subjects to be covered over the three-day period of the Conference will include papers on components using magnetic principles; semiconductors; microwaves; high voltage components; switching relays; control devices; pulse components; new components for power generation; space components and requirements; reliability of components; capacitors; resistors and potentiometers; super-cooled components; cryogenics; hardware plugs; terminals, printed circuits; wire, etc.; filters; microminiature components; optical, magneto-optical, and light sources; instruments and standard measuring devices; vacuum components and equipment; and tubes other than microwave and data processing components.

The topics to be covered are not only of great interest and importance in the electronics industry, but also in other industries where components problems are encountered.

For further information, contact: H. C. Ross, Jennings Radio Mfg. Corp., P. O. Box 1278, San Jose 8, Calif.

OBITUARIES

Dr. Hans Erich Hollmann (A'48–F'53) died on November 19, 1960. He was born on November 4, 1899, in Solingen, Germany.

H. E. Hollmann

He majored in physics at the Technical University of Darmstadt, Germany, and received the Doctor's degree in 1928. In 1930 he accepted a position with the "Heinrich-Hertz Institut für Schwingungsforschung" in Berlin. From 1934 to 1936 he wrote the first encyclopedia on microwaves and VHF, which contains a chapter on the field later to be known as radar. Much of his later work involved extensive studies and research in microwaves, VHF diathermy, and electrocardiography.

Over a hundred papers resulted from research in his "Laboratorium für Hochfrequenztechnik und Elektromedizin." The most outstanding were published in the U. S. and England. During this time he was also consulting scientist for the "Telefunken," "Siemens," and other companies. He was credited with nearly 300 inventions in the fields of microwaves, magnetrons, klystrons,

(*Continued on p. 22A*)

■ *A production reality based on 20 years of crystal engineering experience...*

Miniature Wide Band-Pass Crystal Filters Delivered In Quantity...To Specification

Filters just recently considered as "state of the art" are now a *production* reality. In addition to its many stock narrow band filters, Midland offers prototype and production quantities of practical Miniature Wide Band Filters in the .5 to 30 mc range. These filters are of exceptional quality.

They are essentially free from unwanted spurious modes which have previously limited the realization of many types of wide band filters. Small quantities for engineering evaluation are available *immediately* from stock. Consultation is available at any time to potential filter users.

Shown below are specifications for ten of our stock wide band filters, as well as actual characteristic response curves. These filters are actually being delivered to major weapons system manufacturers in quantities — to specification.

THESE ARE NOT LABORATORY CURIOSITIES OR IN PROTOTYPE DEVELOPMENT STAGE

Type	Center Freq.	3db Bandwidth Minimum	40db Bandwidth Max.	60db Bandwidth Max.	75db Bandwidth Max.	Ultimate Discrim. Minimum	Insertion Loss Max.	Impedance ohms	Inband Ripple Max.	Package Type
NJ-1	7.2MC	160KC	300KC			60db	6db	13K	1db	A
NJ-1B	7.2MC	160KC	300KC			60db	6db	13K	.5db	B
NJ-2	7.4MC	160KC	300KC			60db	6db	13K	1db	A
NJ-2B	7.4MC	160KC	300KC			60db	6db	13K	.5db	B
NG-1	5.09MC	160KC	350KC			60db	6db	20K	1db	A
NG-1B	5.09MC	160KC	350KC			60db	6db	20K	1db	B
NB-1	10.7MC	200KC		450KC		75db	12db	50	1db	A
NB-1B	10.7MC	200KC		450KC		85db	8db	50	.5db	B
RL-1	11.5MC	80KC		160KC	200KC	85db	6db	50	.5db	C
RL-1B	11.5MC	80KC		160KC	200KC	90db	5db	50	.5db	B

Operating Temp.: —55°C to +90°C Shock: 100g Vibration: 15g to 2KC Units hermetically sealed

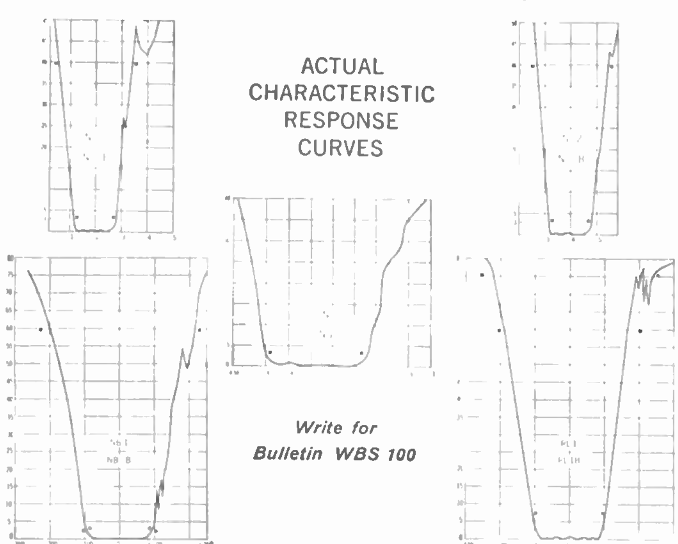

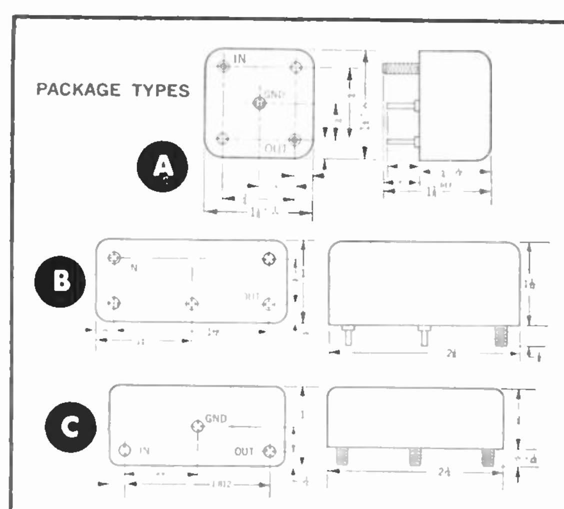

A limited number of opportunities for filter and communications engineers and technicians are available. Write Mr. Robert A. Crawford, Chief Engineer, Filter Division.

Midland MANUFACTURING COMPANY • 3155 Fiberglas Road, Kansas City 15, Kansas

WORLD'S LARGEST PRODUCERS OF QUARTZ CRYSTALS

DIVISION OF PACIFIC INDUSTRIES, INC.

MID 1-61

beam-riding, electrocardiography, and others. In addition he was the director of the "Forschungsgesellschaft für Funk und Tonfilmtechnik."

After the war, Dr. Hollmann became Professor in charge of the applied physics department at the Friedrich Schiller University in Jena, Germany. Subsequently he was a research scientist at the U. S. Naval Air Missile Test Center, Point Mugu, Calif., from 1947–1954. He was Director of Research at Hydro-Aire, Burbank, Calif. (1954–1955); consultant at National Aircraft Corp., also in Burbank (1955–1956); and consultant at H. R. Wagner Co., Van Nuys, Calif. (1956–1957). From 1957–1959, he was Vice President in charge of basic research at Dresser Dynamics, Inc., a division of Dresser Industries, Northridge, Calif.

During this period, Dr. Hollmann was in charge of basic research, to which he contributed many fundamental concepts on varying projects such as polaristors, sensitive magnetron magnetometers, a plasma amplifier to be used for converting thermal energy to electric energy, and a novel flowmeter for measuring the flow of a liquid. He also did various work in the fields of integrating accelerometers, double integrating accelerometers, position indicators, and the combination of these for inertial navigation. Applications for patents on many of these projects were filed. Indicative of his wide range of interests is the fact that patent applications relating to the automatic balancing of rotating members and a self-powered radio receiver were filed during this period of time.

After the dissolution of Dresser Dynamics in 1959, and until his death in 1960, Dr. Hollmann was retained as a consultant for Dresser Industries, Inc., where he worked on many problems relating to the varied fields in which the company is interested. He was also a consultant to Dresser Electronics, SIE Division. During this time, he was active in the field of well-drilling through an entirely new tool and was also active in work on devices for minimizing the effects of friction. His consultation work at Dresser Electronics, SIE Division, during this period included the fields of sonar, accelerometers, magnetometers, transistors, free-power devices, shock tubes, and flow meters.

Samuel A. Ferguson (SM'55), Vice President and General Manager—Mountain View Operations of Sylvania Electronic Systems, died Sunday, February 5, 1961, at Palo Alto—Stanford Hospital. He was 44.


S. A. FERGUSON

A leader in the West Coast electronics industry, he previously served as Chairman of the San Francisco Council of the Western Electronics Manufacturers Association. He played a significant role in the rapid growth of Sylvania's research, development and manufacturing complex in Mountain View.

He joined the company's Electronic Defense Laboratories in Mountain View in 1953 as manager of technical liaison, and was appointed Director of the Laboratories two years later. He was named Manager of the Mountain View Operations in 1957, and Vice President and General Manager in 1959.

A native of Columbia, S. C., he received the Bachelor's Degree in electrical engineering from Clemson College, Clemson, S. C., and the Master's Degree from Tulane University, New Orleans, La. He served in the U. S. Army Signal Corps during World War II, holding the terminal rank of Lieutenant Colonel.

He was an associate professor of electrical engineering at the University of South Carolina, Columbia, from 1947 to 1950, when he was recalled by the Army to serve for two years as Commanding Officer of the Signal Corps Engineering Laboratories' Field Station at White Sands, N. M.

Immediately prior to joining Sylvania, he was Assistant Technical Director of the DuMont Laboratories in Los Angeles, Calif.

Past Vice Chairman of the IRE Professional Group on Engineering Management, Mr. Ferguson also was a member of the American Institute of Electrical Engineers, Armed Forces Communications and Electronics Association, and the Association of the United States Army. In Mountain View, he was a Director of the Chamber of Commerce and the Rotary International.

Robert V. Werner (SM'58), Chairman of the IRE Professional Group on Space Electronics and Telemetry, died February 10, 1961, as the result of an accident while sailing his yacht outside San Diego Bay.

He was one of the three founders of the Cubic Corporation, and had served as part-time consultant on phase-comparison techniques from the founding of the company until 1955. Since 1955, he had served as Vice President, General Manager, and, most recently, as Executive Vice President of the Corporation. He was responsible for the day-to-day operation of the company, including engineering, administration, and production. He developed new concepts in trajectory-measuring, miss-distance indicating, and electronic surveying instrumentation.

His career began with Convair, in San Diego, as a project engineer. He was a junior engineer in 1940, and progressed rapidly to key engineering positions. He proposed and later directed command system for controlling the MX-774, and also developed the CW-phase-comparison baseline-type trajectory measuring systems for ballistic missile guidance. After a year (1948–1949) with the Raytheon Company, Point Mugu, Calif., as project engineer, during which time he was in charge of "Project Hurricane" at the U. S. Naval Air Missile Test Center, he returned to Convair. From 1949 to 1955, he directed the AZUSA tracking equipment program, the ATLAS guidance program, and other electronic system developments.

Mr. Werner was active in IRE affairs. He had served as a member of the publicity committee and was a speaker at the IRE National Symposium on Telemetry in 1958. He was a member of the Professional Group on Space Electronics and Telemetry, had been on its administrative committee and was its Chairman for 1960–1961. He was also a member of the Research Institute of America.

He had made numerous contributions to the field of trajectory instrumentation and held patents in telemetry and phase measurement. He had a number of pending patents which cover applications of phase measurement and feedback techniques to missile trajectory-measurement systems.

Mr. Werner was educated at the Universities of Arizona and California.

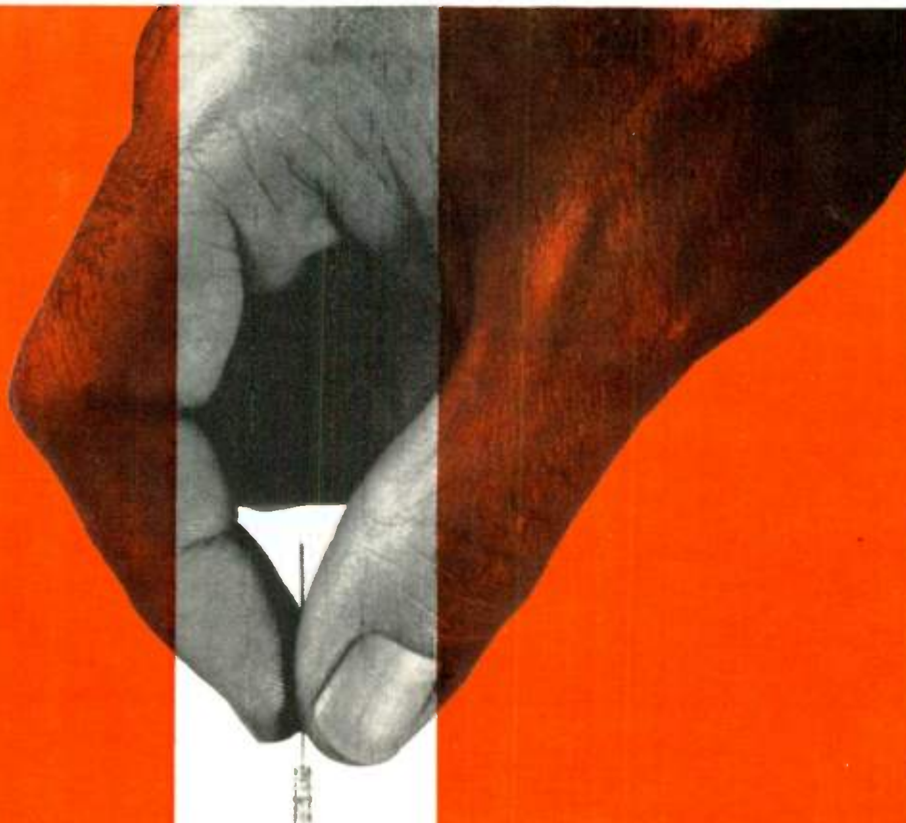

ALL-GLASS SUB MINIATURE RF DIODES

FM discriminator circuits
VHF/UHF general purpose
Low-noise balanced mixers through X-band
RF Harmonic Generation
AM clipping in IF amplifiers
RF Power Monitoring (pulsed & CW)
RF Sweep Circuits
RF Cavity Tuning (preselectors)
RF Leveling, Limiting & Switching
VHF/UHF Parametric Circuits
Microwave Computer Subharmonic Oscillators

A series of tiny, more adaptable, military-rugged diodes with axial wire leads designed for maximum convenience in all miniature strip-transmission-line or coaxial circuits.

All-glass sealing assures reliable hermetic seal, particularly when diodes are soldered into a circuit. All-glass packaging reduces shunt-capacitance for improved RF bandwidth at microwave frequencies.

A complete line of microwave diodes

Fixed-Base Cartridges | Reversible Polarity Cartridges | Special Purpose Diodes | Coaxial Diodes | "Pill" Varactors

Engineering Standards Data Sheets on all new Microwave Associates subminiature VARACTORS, MIXER DIODES, VIDEO DETECTORS, RF DISCRIMINATOR DIODES, and AM CLIPPER DIODES sent on request.

MICROWAVE ASSOCIATES, INC.
SEMICONDUCTOR DIVISION
Burlington, Massachusetts
BRowning 2-3000 · TWX Burlington, Mass. 942

1961 IRE INTERNATIONAL CONVENTION RECORD

The IRE INTERNATIONAL CONVENTION RECORD, containing all available Convention papers will be published in ten parts in July, 1961.

Professional Group members are entitled to purchase the Part sponsored by the Professional Group to which they belong at the special PG rate indicated below. Other parts may be purchased at the IRE member rate.

IRE members may purchase any part at the IRE member rate. However, if a member applies for membership in the appropriate Professional Group at the same time that he places his order, he will be entitled to the PG rate.

Nonmembers and libraries may place orders at the nonmember and library rates, respectively. Individuals who apply for IRE membership at the time they place their orders are entitled to the IRE member rate.

Subscription agencies are entitled to the library rate.

Clip out the order form and return it, with remittance, to the Institute of Radio Engineers, Inc., 1 East 79 St., New York 21, N. Y. In ordering, be sure to refer to the proper columns for subjects and prices.

Part	Sessions	Subject and Sponsoring IRE Professional Group	Prices for Members of Sponsoring Professional Group (PG), IRE Members (M), Libraries and Sub. Agencies (L), and Nonmembers (NM)			
			PG	M	L	NM
1	38, 46, 53	Antennas & Propagation	$0.70	$1.05	$2.80	$3.50
2	12, 20, 33, 40, 48	Audio Electronic Computers	1.00	1.50	4.00	5.00
3	8, 16, 23, 24, 32, 39	Electron Devices Microwave Theory & Techniques	1.00	1.50	4.00	5.00
4	1, 9, 17, 25, 34, 41, 49	Automatic Control Circuit Theory Information Theory	1.20	1.80	4.80	6.00
5	7, 15, 28, 36, 43, 45, 51	Aerospace & Navigational Electronics Human Factors in Electronics Military Electronics Space Electronics & Telemetry	1.20	1.80	4.80	6.00
6	6, 18, 22, 27, 31, 35, 42, 50	Component Parts Industrial Electronics Product Engineering & Production Reliability & Quality Control Ultrasonics Engineering	1.40	2.10	5.60	7.00
7	11, 19, 26	Broadcasting Broadcast & Television Receivers	0.70	1.05	2.80	3.50
8	4, 30, 37, 44, 52	Communications Systems Radio Frequency Interference Vehicular Communications	1.00	1.50	4.00	5.00
9	2, 10, 14, 21, 47, 54	Bio-Medical Electronics Nuclear Science Instrumentation	1.00	1.50	4.00	5.00
10	3, 5, 13, 29	Engineering Writing & Speech Engineering Management Education	0.80	1.20	3.20	4.00
		Complete Set (10 parts)	$10.00	$15.00	$40.00	$50.00

ORDER FORM

1961 IRE INTERNATIONAL CONVENTION RECORD

Part	1	2	3	4	5	6	7	8	9	10	Complete Set	
Number of Copies												Total Remittance
Amount Paid												

Name (Please Print): ____________________

Shipping Address: ____________________

new SOLA transistorized d-c supply...

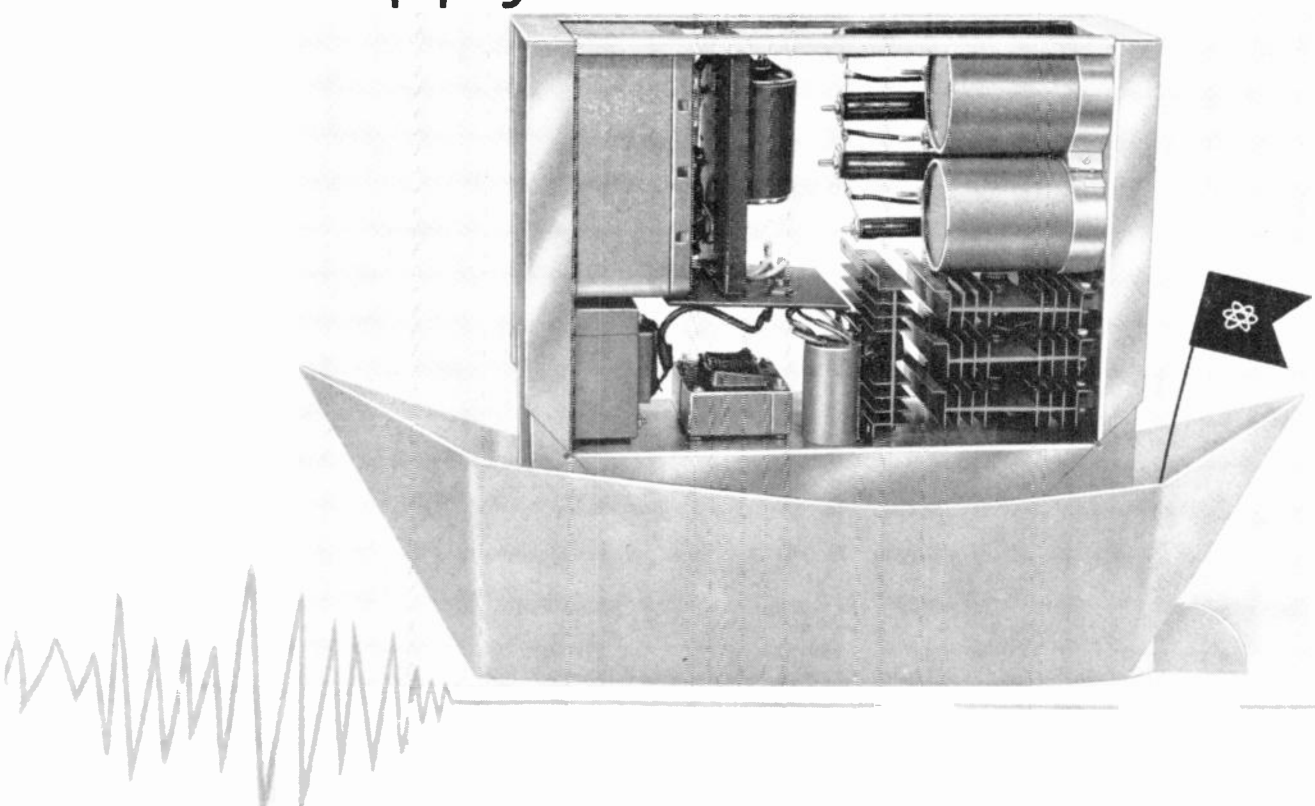

reliably regulates d-c voltage— right down to the last "**ripple**"!

New highly sensitive SOLA "CVQ" provides transistor-regulated d-c output ideal for computers and other *voltage-sensitive equipment.* Response to voltage change is so rapid the CVQ even attenuates 120-cycle ripple! Yet, with it all, this new d-c supply introduces a revolutionary circuit simplicity — providing significant savings in sizes . . . more watts per dollar!

CVQ combines exclusive transistorized shunt regulation with SOLA's inherently self-protecting, static-magnetic transformer . . . easily meets the most taxing demands of dynamic loading. Voltage holds in spite of widely fluctuating loads. The result is longer equipment life, more trouble-free operation. Contact our area representative for complete specifications and prices. Or write today for literature on CVQ.

- Standard models available at 5, 6, 10 and 12 volts d-c (100-130/181-235/200-260 volt input).
- Output regulated within ±0.04% for line voltage variations ±15%; 0.2% static-load regulation, 0 to full load.
- Excellent transient response.
- Inherent protection against output over-voltage safeguards both supply components and external circuitry.
- Short-circuit proof design.
- Compact mechanical layout — only 12¼ x 5¼ x 19″

SOLA

Division of Basic Products Corp.

BPC

SOLA ELECTRIC CO.
Busse Road at Lunt,
Elk Grove Village, Ill.
HEmpstead 9-2800.
IN CANADA, Sola-Basic Products Ltd., 377 Evans Ave., Toronto 18, Ontario

1961 Seventh Region IRE Technical Conference and Electronic Exhibits

HOTEL WESTWARD HO, PHOENIX, ARIZ., APRIL 26–28, 1961

The Seventh Region, comprising eleven western states, will hold its annual Technical Conference at the Westward Ho Hotel, Phoenix, Ariz., on April 26–28, 1961. Exhibits by electronic manufacturers will also be shown. The social program includes luncheons, a western barbeque dinner and a reception. Planned for the ladies are a style show and luncheon at the famous Mountain Shadows resort, a visit to nearby beautiful homes and luncheon, and a guided tour of Frank Lloyd Wright's Taliesin West and luncheon. Field trips to several industrial plants also will be offered. One session will be devoted to the Student Prize Paper Contest. The IRE Board of Directors, the Executive Committee, and the WESCON Board of Directors will meet concurrently.

The registration fee for the conference will be $1.00. No registration fee will be charged for students and ladies.

The technical program of the conference follows:

Wednesday Morning, April 26

Session I—New Problems for Electronic Engineers

Introduction: *W. C. Carnahan, Varian Associates, Palo Alto, Calif.*

"Problems Associated with Crowding of Frequency Spectrum," *Dr. D. E. Noble, Motorola, Inc., Scottsdale, Ariz.*

"Problems Associated with Electronic Control in Industrial Operations," *C. C. Lasher, General Electric Co., Phoenix, Ariz.*

Wednesday Afternoon

Session II-A—Panel Discussion—Spectrum Management

Moderator: *M. Davie, Jr., RAND Corporation.*

"Land Management Problems of the U. S. Forest Service on Mountain-Top Sites For Electronic Installations," *W. B. Morton, Albuquerque, N. M.*

"Status of the Defense Mutual Interference Problem," *Col. E. R. Reynolds, U. S. Army, and H. Randall, Office of the Director of Defense Research and Engineering, Washington 25, D. C.*

"Frequency Management in Army Electromagnetic Compatibility Program," *C. Gregory, USARFE Office, OCSigO, Washington 25, D. C.*

"Data Display Requirements for Interference Prediction and Control," *D. R. J. White, Frederick Research Corporation, Wheaton, Md.*

Session II-B—Control Theory and Practice

"A. C. Instrument Servo with Error Controlled Damping Coefficient," *P. B. Krishnaswamy, R. Schmoock, and D. L. Ham, Fischer & Porter Company, Hatboro, Pa.*

"A Special Purpose Cross-Correlator with Application to Servo Analysis," *R. C. Howard, Giannini Controls Corporation, Santa Ana, Calif.*

"Signal Filtering in Digital Contro Computer Systems," *W. M. Gaines, General Electric Company, Phoenix, Ariz.*

"Adaptive Sampling Frequency for Sampled Data Control Systems," *R. C. Dorf, M. C. Farren, and C. A. Phillips, U. S. Postgraduate School, Monterey, Calif.*

"Synthesis of Double-Terminated Active Networks Using Negative Impedance Converter," *King-sun Fu, Purdue University, Lafayette, Ind.*

Wednesday Evening

Session III—Student Prize Paper Contest

Organized by *Dr. C. L. Hogan, Vice President and General Manager, Motorola Semiconductor Products Division.*

Thursday Morning, April 27

Session IV-A—New Problems in Frequency Interference

"Survey of Electromagnetic Effects Associated with the Thermonuclear Devices TEAK and ORANGE," *R. Sanders, Hughes Communications Division, Los Angeles, Calif.*

Control of Interference Between Satellite Communication Terminals and Surface Services," *Dr. W. L. Firestone, Motorola, Inc., Chicago, Ill.*

"Control of Surface-Service Interference with Communication Satellites," *S. G. Lutz, Hughes Research Labs., Malibu, Calif.*

"Adaptive Communication Techniques as They Apply to Radio Control Systems," *J. Cohn, Motorola, Inc., Chicago, Ill.*

Session IV-B—Magnetic Logic in Computer Circuits

"Principles of Multiaperture Magnetic Logic," *L. Norde, Motorola, Inc., Scottsdale, Ariz.*

"The Use of Multiaperture Magnetic Logic in Digital Computers," *Dr. E. K. Van de Riet, Stanford Research Institute, Menlo Park, Calif.*

"Implementation of BOOLEAN Algebra with Integrated Magnetic Logic," *L. R. Smith, Motorola, Inc., Scottsdale, Ariz.*

Field Computer Using Pulsed Magnetics," *J. W. Heermons, IBM Corporation, Kingston, N. Y.*

Thursday Afternoon

Session V-A—Panel Discussion—The User Looks At Computer Control

Moderator: *Dr. T. L. Martin, Dean of Engineering, University of Arizona.*

Representatives of petroleum, steel, cement, and utilities industries will discuss applications of computers to their control problems. Dr. Martin will discuss engineering education oriented toward large electronic control systems.

Session V-B—Microwave Tubes and Antennas

"Generating High Power Gaussian Pulses in a Klystron Amplifier for TACAN Service," *H. R. Jones, Eitel-McCullough, Inc., San Bruno, Calif.*

"PPM Focusing of Low-Noise and Serrodyne TWT's," *W. J. Fleig, Microwave Electronics Corporation, Palo Alto, Calif.*

"Some New Crossed-Field Tubes for High Resolution Radars," *J. A. Saloom, S.F.D. Laboratories, Inc., Union, N. J.*

"Waveguide-Fed Biconical Horn," *A. Maestri, Jr., Melpar, Inc., Falls Church, Va.*

"Performance Characteristics of a Horn-Reflector Antenna," *L. E. Hunt, D. C. Hogg and A. B. Crawford, Bell Telephone Laboratories, Red Bank, N. J.*

Friday Morning, April 28

Session VI-A—Analysis Techniques for Radio Interference Problems

"Close-Channel Operation of SSB Receivers and Transmitters," *C. E. Blakeley, Georgia Institute of Technology, Atlanta, Ga.*

"A Model for Prediction of Radar Interference," *R. A. Rollin, Jr., G. Minty, W. DeHart, J. Dute, R. Legault, Y. Morita, J. Riordan, and N. Smith, University of Michigan, Ann Arbor, Mich.*

"Radio Frequency Interference Predictions for Quick Fix Decisions," *J. E. McShulskis, J. H. Mills, and D. R. J. White, Frederick Research Corporation, Wheaton, Md.*

Session VI-B—Process Control Instrumentation

"Automatic Electronic Quadrature Rejection in Electromagnetic Flowmeter Systems," *R. Schmoock and D. Ham, Fischer & Porter Company, Hatboro, Pa.*

"Transformers, Transformer-Type Transducers and Their Application in Process and Industrial Control Systems," *R. E. Claflin, Jr., Claflin Associates, Newtonville, Mass.*

"A Novel Electropneumatic Temperature Controller," *L. R. Axelrod, Powers Regulator Company, Skokie, Ill.*

"Some New Techniques For Recording and Processing Vibration Test Data," *R. M. Tidwell, Sandia Corporation, Livermore, Calif.*

Friday Afternoon

Session VII—Bandwidth Conservation and Interference Elimination

"Communications Central, AN/MRC-66," *A. J. Toberman, Motorola Research Laboratory, Phoenix, Ariz.*

"Hydroacoustic Simulation of Antenna Radiation Characteristics," *A. Maestri, Jr., Melpar, Inc., Falls Church, Va.*

"Practical Design Guides for Interference Reduction in Electronic Equipment," *R. F. Ficcki, RCA Service Company, Riverton, N. J.*

"Design and Development of a Bandwidth Compression System," *H. L. Morgan, Phoenix, Arizona.*

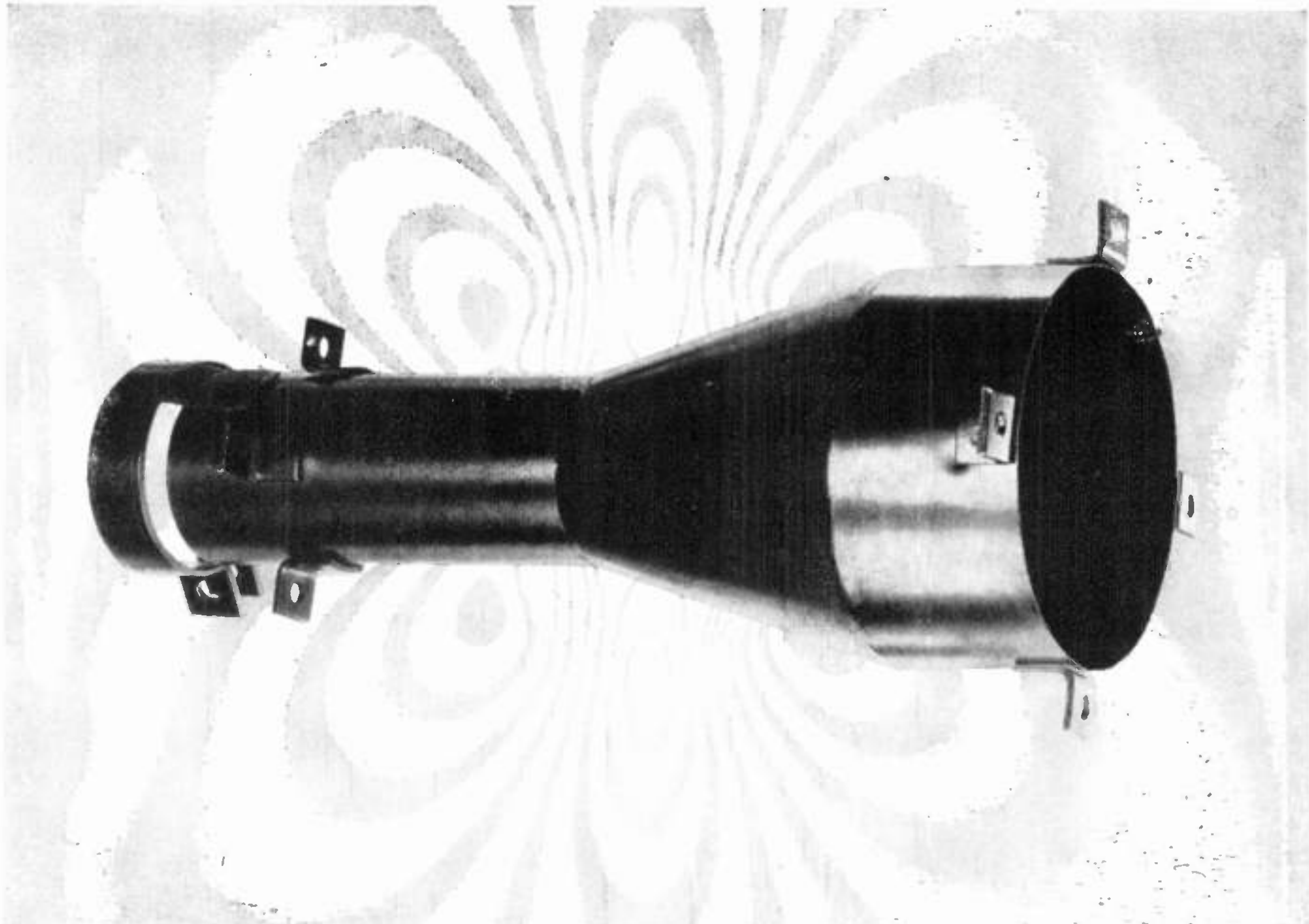

keep your signals clean with engineered magnetic shielding

Keep stray magnetic fields out of your high gain input transformers and cathode ray tubes. Keep your signals free of noise, hum, cross-talk and distortion. You can do it only with *engineered* magnetic shielding.

These high-permeability shields are made from existing tools in a broad variety of single and multiple structures—cylinders, spheres, truncated cones—for applications ranging from dc into the audio range and higher. They can be used with almost all conventional transformer core and coil assemblies to provide any degree of magnetic, electrostatic or RF shielding against undesired signals of all classes. Reduction of field strengths to 100 db and beyond is common.

With Magnetic Metals shielding, both the electrical and mechanical engineering is already done for you. Simply let us know your requirements . . . We'll engineer the exact type of shielding you need. In selection of raw material, design, fabrication, annealing, testing and gaging, Magnetic Metals has amassed a great backlog of shielding experience. For a better understanding of shielding and help in specifying it, write for our informative booklet, "Magnetic Shielding of Transformers and Tubes."

MAGNETIC METALS

MAGNETIC METALS COMPANY
Hayes Avenue at 21st Street, Camden 1, N.J.
853 Production Place, Newport Beach, California
transformer laminations • motor laminations • tape-wound cores
powdered molybdenum permalloy cores • electromagnetic shields

Fifth Midwest Symposium on Circuit Theory

University of Illinois, Urbana, May 6, 8–9, 1961

The final program for the Fifth Midwest Symposium on Circuit Theory has been announced. The Symposium is cosponsored by the IRE and will be held at Allerton Park and the Urbana Campus of the University of Illinois, Urbana, on May 6, 8–9, 1961. "Topology in Circuit Theory" is the subject of this year's Symposium.

Papers presented at the Symposium will be published in the March, 1961, issue of the Transactions on Circuit Theory.

Information concerning housing at Allerton Park and registration may be obtained by writing to: Professor M. E. Van Valkenburg, Dept. of Elec. Engrg., University of Illinois.

Saturday, May 6

Workshop in Graph Theory—*Lectures by S. L. Hakami, University of Illinois, Urbana; M. B. Reed, Michigan State University, East Lansing; S. Seshu, Syracuse University, Syracuse, N. Y.; and L. Weinberg, Hughes Research Labs.*

Monday Morning, May 8

Chairman: *R. M. Wainwright, Good-All Electric Mfg. Co., Ogallala, Neb.*

Address of Welcome: *E. C. Jordan, University of Illinois, Urbana.*

"Network Applications of Graph Theory," *S. Seshu, University of Syracuse, Syracuse, N. Y.* Commentator: *P. R. Bryant, General Electric Co., Wembley, England.*

"Linear Graphs: A Few Reflections on its Future in the Curriculum and in Research," *L. Weinberg, Hughes Research Labs., Malibu, Calif.* Commentator: *H. E. Koenig, Michigan State University, East Lansing.*

"Flowgraphs for Nonlinear Systems," *T. A. Bickart, Johns Hopkins University, Baltimore, Md.* Commentator: *C. L. Coates, General Electric Co., Schenectady.*

Monday Afternoon

Chairman: *B. R. Myers, University of Waterloo, Waterloo, Canada.*

"The Seg: A New Class of Subgraphs," *M. B. Reed, Michigan State University, East Lansing.* Commentator: *E. W. Hobbs,* McDonnell Aircraft Co., St. Louis, Mo.

"A Method of Tree Expansion in Network Theory," *H. Watanabe, Nippon Electric Co., Kawasaki City, Japan.* Commentator: *W. H. Kim, Columbia University, New York, N. Y.*

"On Realizability of a Set of Trees," *S. L. Hakami, University of Illinois, Urbana.* Commentator: *K. A. Pullen, Aberdeen Proving Ground, Md.*

Monday Evening

Panel Discussion—The Historical Development of Circuit Theory

H. W. Bode, Bell Telephone Labs., Whippany, N. J.; S. Darlington, Bell Telephone Labs., Murray Hill, N. J.; E. A. Guillemin, Mass. Inst. Tech., Cambridge.

Tuesday Morning, May 9

Chairman: *A. B. Macnee, University of Michigan, Ann Arbor.*

"On the Synthesis of Resistive N-Port Networks," *G. Biorci and P. P. Civalleri, Instituto Elettrotecnico Nazionale, Torino, Italy.* Commentator: *S. Okada, Stromberg-Carlson, Rochester, N. Y.*

"Paramount Matrices and Synthesis of Resistive N-Ports," *I. Cederbaum, Columbia University, New York, N. Y.* Commentator: *F. M. Reza, Syracuse University, Syracuse, N. Y.*

"On the Synthesis of R-Networks," *D. P. Brown and Y. Tokad, Michigan State University, East Lansing.* Commentator: *H. C. So, University of Rochester, Rochester, N. Y.*

Tuesday Afternoon

Chairman: *W. B. Boast, Iowa State University, Ames.*

"Analysis and Synthesis Techniques of Oriented Communication Nets," *D. T. Tang and R. T. Chien, IBM Res. Labs., Yorktown Heights, N. Y.* Commentator: *S. S. Yau, University of Illinois, Urbana.*

"Optimal Synthesis of a Communication Net," *O. Wing, Columbia University, New York, N. Y., and R. T. Chien, IBM Res. Labs., Yorktown Heights, N. Y.* Commentator: *W. Mayeda, University of Illinois, Urbana.*

"The Structures of Switching Nets," *L. Lofgren, University of Illinois, Urbana.* Commentator: *P. M. Lewis, General Electric Co., Schenectady, N. Y.*

1961 PGMTT National Symposium

Sheraton Park Hotel, Washington, D. C., May 15–17, 1961

Monday Morning, May 15

Registration

Opening Address: R. O. Stone, *Symposium Chairman, National Bureau of Standards, Washington, D. C.*

Keynote Address: *A. G. Clavier, (Ret.) ITT Labs., Nutley, N. J.*

Session I—Millimeter Waves

Chairman: *R. O. Stone, National Bureau of Standards, Washington, D. C.*

"Quasi-Optical, Surface-Waveguide, and Other Components for the 100 to 300 KMC Region," *F. Sobel and J. C. Wiltse, Electronic Communications, Inc., Timonium, Md.*

"A Millimeter Wave Fabry-Perot Maser," *W. Culshaw and R. C. Mockler, National Bureau of Standards, Boulder, Colo.*

"Broadband Isolators and Variable Attenuators for Millimeter Frequencies," *C. E. Barnes, Bell Telephone Labs., Murray Hill, N. J.*

Monday Afternoon

Session II—Parametric Devices

Chairman: *W. W. Mumford, Bell Telephone Labs., Whippany, N. J.*

"Transmission Phase Relations of Four-Frequency Parametric Devices," *D. B. Anderson and J. C. Aukland, North American Aviation, Anaheim, Calif.*

"A Traveling-Wave Parametric Amplifier," *T. H. Lee, Lockheed Aircraft Corporation, Sunnyvale, Calif.*

"An Electronically Tuneable Traveling-Wave Parametric Amplifier," *R. C. Honey, Stanford Research Institute, Menlo Park, Calif.*

"Practical Design and Performance of Nearly Optimum, Wideband, Degenerate Parametric Amplifiers," *M. Gilden and G. L. Matthaei, Stanford Research Institute, Menlo Park, Calif.*

"Design Theory of Up-Converters for Use as Electronically Tuneable Filters," *G. L. Matthaei, Stanford Research Institute, Menlo Park, Calif.*

"Passive Phase-Distortionless Parametric Limiters," *I. T. Ho and A. E. Siegman, Stanford University, Calif.*

Monday Evening

"The Business of Inventing," *J. Rabinow, Rabinow Engineering Co., Washington, D. C.*

Tuesday Morning, May 16

Session III—Ferrites

Chairman: *F. Reggia, Diamond Ordnance Fuze Labs., Washington, D. C.*

"Field Displacement Devices," *G. J. Wheeler, Sylvania Electric Products, Mountain View, Calif.*

"A Field Displacement Isolator at 57 KMC," *C. E. Fay and E. F. Kankowski, Bell Telephone Labs., Murray Hill, N. J.*

"Solid State X-band Power Limiter," *W. F. Krupke, T. S. Hartwick, and M. R.*

MISSILES AND AIR-BORNE EQUIPMENT

call for resistors that never fail catastrophically. A 30,000 hour load life test* of 150 Corning tin oxide resistors has proved 1% drift capability, and not one failed catastrophically.

Tin oxide and glass are among the most stable materials known, both electrically and environmentally. Fuse the two together and you have the basis for an outstanding resistor.

This holds true whether you buy ten or ten million, because we have developed the manufacture of this type of resistor to a science. Assembly is completely automatic and exact. And, if you think you have to pay a lot extra for this reliability, our price sheets hold some pleasant surprises for you.

The proof of what we say is spoken eloquently by typical specs like these:

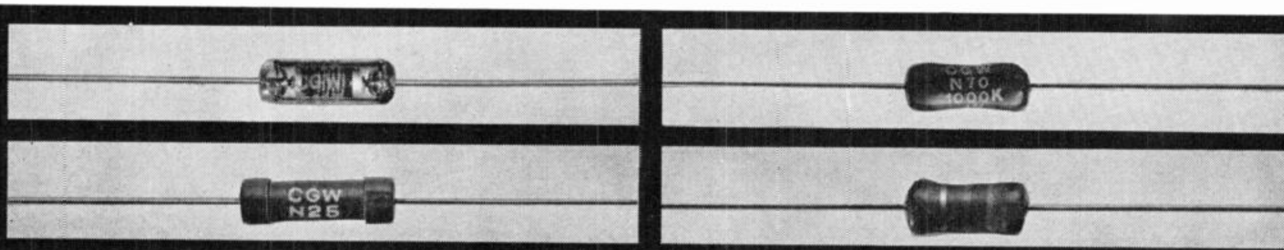

TYPE	DESCRIPTION	CORNING MODEL	WATTAGE	RESISTANCE (ohms)	TC	LOAD LIFE	OVERLOAD	MOISTURE RESISTANCE
NF	Glass ENCAPSULATED MIL-R-10509C, Char. B	NF60 NF65	1/8 1/4	100 100K 100 348K	150ppm/°C. −55 +150°C.	0.3%	0.03%	0.2% (Char. B)
N EPOXY	MIL-R-10509C, Char. B	N60 N65 N70	1/8 1/4 1/2	10 133K 10 499K 10 1Meg	150ppm/°C. −55 +105°C.	0.5%	0.03%	0.5% (Char. B.)
N	MIL-R-10509B, Char. X	N12 N20 N25 N30	1/4 1/2 1 2	100 133K 10 500K 10 1.5Meg 30 4.12Meg	150ppm/°C. −55 +105°C.	0.35%	0.1%	0.15% (Char. X)
C	Lowest cost film resistor; silicone insulation MIL-R-11C	C20 C32 C42	1/2 1 2	51 150K 51 470K 10 1.4Meg	150ppm/°C. −55 +125°C.	1.5%	0.2%	0.3%

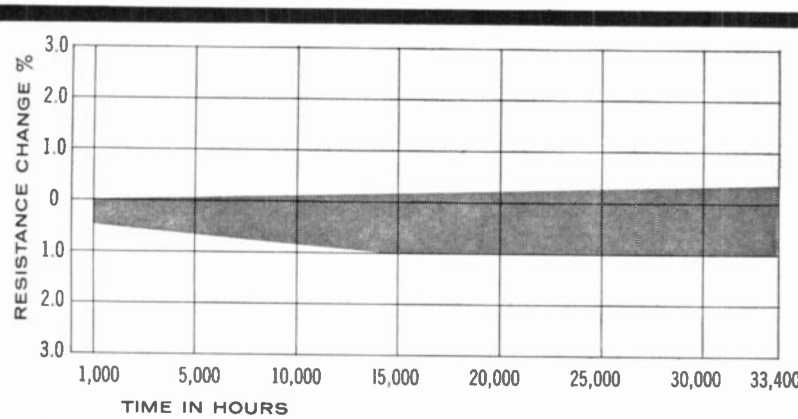

Results of 30,000 hour load life test on Corning Resistors representing 5,000,000 resistor hours. Resistors were run at 140% of rated load. There were no catastrophic failures.

For data sheets on Corning Type NF, N, N-Epoxy or C resistors, and the names of the distributors nearest you, write Corning Glass Works, 542 High Street, Bradford, Pa. If you also would like a booklet giving 30,000 hour test results, write on company letterhead.

*Test conducted by Remington Rand Univac

CORNING ELECTRONIC COMPONENTS

CORNING GLASS WORKS, BRADFORD, PA.

Weiss, Hughes Aircraft Co., Culver City, Calif.

"Frequency Doubling with Planar Ferrites and Isotropic Ferrites with Large Saturation Magnetizations," *I. Bady, USASC Research and Development Lab., Fort Monmouth, N. J.*

"Octave Bandwidth UHF/L-Band Circulator," *F. Arams, B. Kaplan and B. Peyton, Airborne Instrument Lab., Melville, L. I., N. Y.*

"A New Balanced Type Ferrite Switch," *T. Kuroda and A. Cho, Nippon Electric, Tokyo, Japan.*

Tuesday Afternoon

Session IV—High Power Microwave Techniques Panel

Chairman: *C. Jones, Mass. Inst. Tech., Cambridge.*

"Spurious Outputs from High Power Microwave Tubes and Their Control," *K. Tomiyasu, General Electric Co., Schenectady, N. Y.*

"Windows," *D. B. Churchill, Sperry Gyroscope Co., Great Neck, N. Y.*

"High Power Duplexers," *E. Muehe, Mass. Inst. Tech., Cambridge.*

Panel Members: *C. R. Beitz, Cornell Aeronautical Lab., Buffalo, N. Y.; J. B. Griemsman, Polytechnic Institute of Brooklyn, Brooklyn, N. Y.; L. Gould, Microwave Associates, Burlington, Mass.*

Session V—Low-Noise Microwave Amplifiers

Chairman: G. Wade, Raytheon Co., Burlington, Mass.

"Traveling Wave Tubes," *D. A. Watkins, Stanford University, Stanford, Calif.*

"Parametric Amplifiers," *R. D. Weglein, Hughes Aircraft Co., Malibu, Calif.*

"Masers," *H. E. D. Scovil, Bell Telephone Labs., Murray Hill, N. J.*

Panel Members: *K. K. N. Chang, RCA Labs., Princeton, N. J.; J. W. Meyer, Mass. Inst. Tech., Cambridge; J. Weber, University of Maryland, College Park.*

Session VI—Plasma

Chairman: *N. Marcuvitz, Polytechnic Institute of Brooklyn, Brooklyn, N. Y.*

"Microwave Instrumentation for Plasma Research," *E. G. Schwartz and H. H. Grimm, General Electric Co., Syracuse, N. Y.*

"Precision Measurements of Plasma Afterglows," *E. H. Holt, K. C. Stotz, and S. Pike, Rensselaer Polytechnic Institute, Troy, N. Y.*

"Electromagnetic Properties of Weakly Ionized Argon," *F. L. Terelow and H. D. Curchack, Diamond Ordnance Fuze Lab., Washington, D. C.*

"The Radiation Field and Q of a Resonant Cylindrical Plasma Column," *W. D. Hershberger, UCLA.*

"A Plasma Guide Microwave Selective Coupler," *W. H. Steier and I. Kaufman, Space Technology Labs., Canoga Park, Calif.*

Wednesday Afternoon

Session VII—System and Receiver Noise Performance Clinic

Chairman: *H. Haus, Mass. Inst. Tech., Cambridge.*

"Measurement of System and Receiver Performance," *R. S. Engelbrecht, Bell Telephone Labs., Whippany, N. J.*

"Some Typical Examples," *R. Adler, Zenith Radio Corporation, Chicago, Ill.*

"Commentary on Methods of Measurements," *M. T. Lebenbaum, Airborne Instruments Labs., Melville, L. I., N. Y.*

Fifth National Symposium on Global Communications (GLOBECOM V)

HOTEL SHERMAN, CHICAGO, ILL., MAY 22–24, 1961

Under the sponsorship of the AIEE and the IRE Professional Group on Communication Systems, the Fifth National Symposium on Global Communications will be held at the Hotel Sherman in Chicago, Ill., on May 22–24, 1961.

The three-day program will feature some ninety papers covering all phases of the communications engineering field. These will be presented in three simultaneous sessions during each morning and afternoon of the conference. Exhibits by more than two dozen manufacturers and engineering organizations in the communications industry will be displayed on all three days. A social hour will complete the activities of Monday, and a luncheon meeting will be held on Tuesday, May 23.

The program and advance registration forms will be sent to the symposium mailing list by April 1. Names will be added to the list upon request to C. F. Wittkop, Motorola, Inc., 1450 N. Cicero Ave., Chicago 51, Ill.

The tentative program of papers to be presented is as follows:

Monday Morning, May 22

Session 1.1—Space Communication I

"Passive Communication Satellites With Diffuse Scattering Characteristics," *H. P. Raabe, General Mills, Inc., Minneapolis, Minn.*

"Advanced Communications Technology and Future Aircom System Design," *L. A. De Rosa and E. W. Keller, ITT Communication Systems, Inc., Paramus, N. J.*

"ULTRACOM, Ultraviolet Communications System," *J. W. Ogland, Westinghouse Electric Corp., Baltimore, Md.*

"Exotic Methods in Space Communications," *L. Bittman, The Martin Co., Baltimore, Md.*

"Space Communications with Gamma Radiation," *J. W. Eerkens, Nuclear Associates, San Francisco, Calif.*

Session 1.2—Data Transmission

"Global Digital Communications," *C. A. Deutschle, ITT Communications Systems, Inc., Paramus, N. J.*

"Reliable Data Transmission on Common Carrier Facilities," *J. L. Wheeler, Stromberg-Carlson Co., Rochester, N. Y.*

"Coded Feedback for Error Correction in Binary Data Transmission," *J. R. Wyer, Armour Research Foundation, Chicago, Ill.*

"Magnetic Tape to Printer Communications System," *T. P. Donaher, Stromberg-Carlson Co., Rochester, N. Y.*

"SYSEC: System Synthesizer and Evaluation Center," *T. R. Sheridan, RCA Labs., Rocky Point, N. Y.*

Session 1.3—Communications Systems

"Radio Wave Propagation Through the Earth's Deep Rock Strata—A New Medium of Communication," *G. J. Harmon, Raytheon Co., Waltham, Mass.*

"Global Communications for Project Mercury Using Facilities of Common Carriers," *R. E. Mollbert, Western Electric Co., New York, N. Y.*

"Discussion Of Slow Scan TV System," *N. Hoag, ITT Labs., Fort Wayne, Ind.*

"Microwave Wire (G-Line) As A Broadband Information Highway Using Established Pole Routes," *T. Hafner, Surface Conduction, Inc., New York, N. Y.*

"Electronic Transmission of Mail," *L. Feit, ITT Labs., Nutley, N. J.*

Monday Afternoon

Session 2.1—A Large Scale Four-Wire Switched Communications Network for Military Communications

"Philosophy and General Features of the System," *J. W. Gorgas, Bell Telephone Labs., New York, N. Y.*

"The Transmission Plan," *H. H. Felder and D. T. Osgood, Bell Telephone Labs., New York, N. Y.*

RCA Announces The "TO-1" Rectifier

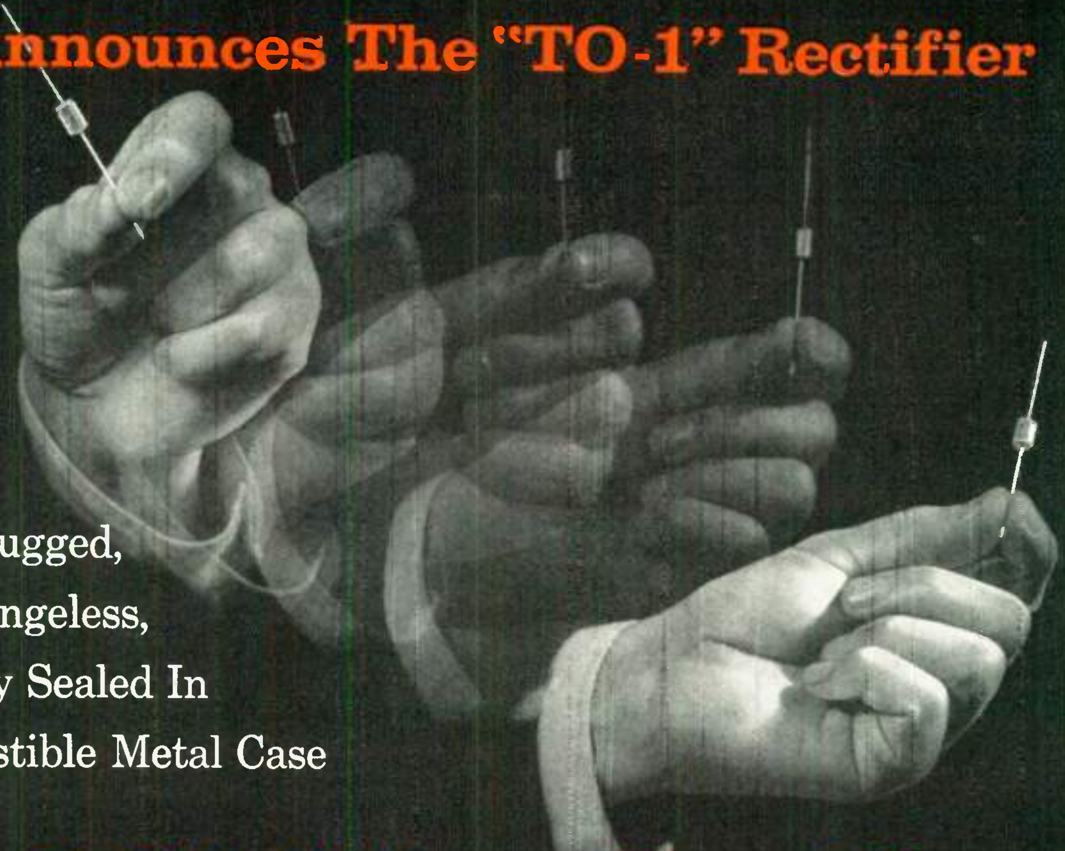

New Tiny, Rugged,
Tubular, Flangeless,
Hermetically Sealed In
Non-Combustible Metal Case

4 New RCA Silicon Rectifiers

for Industrial Applications

¾ Amp. from 200 to 600v–½ Amp. at 800v.

Here's RCA's brand-new idea in rectifier case design—four new silicon rectifiers in hermetically sealed flangeless metal packages. These four new types now make silicon rectifiers as easy to handle and mount as other standard tubular components. They are designed to outperform plastic-packaged rectifiers and meet the stringent heat and humidity requirements of today's industrial and commercial applications.

Using a unique combination of a silicon diffused-junction and a new case, these units can be operated at temperatures up to 75°C without derating. They are designed and priced to bring you economy and performance plus easy handling and assembly.

Sample these new RCA SILICON RECTIFIERS yourself and put them to work in your product. Call your RCA representative today at the Field Office near you. For additional technical information, write RCA Semiconductor and Materials Division, Commercial Engineering, Section D-35-NN, Somerville, N. J.

Available Through Your RCA Distributor

The Most Trusted Name in Electronics
RADIO CORPORATION OF AMERICA

RCA "TO-1" SILICON RECTIFIERS

Type	Max Ratings PIV	Max Ratings Forward Current* @ 75°C	Max Ratings Recurrent Peak Current @ 75°C	Max Instantaneous Forward Voltage Drop @ 0.5 DC amp @ 25°C	Max. Reverse Current @ 25°C and rated PIV
1N3193	200 v	750 ma	6 amp.	1.2 v	10 μa
1N3194	400 v	750 ma	6 amp.	1.2 v	10 μa
1N3195	600 v	750 ma	6 amp.	1.2 v	10 μa
1N3196	800 v	500 ma	5 amp.	1.2 v	10 μa

*Resistive or inductive load

RCA SEMICONDUCTOR & MATERIALS DIVISION FIELD OFFICES... **EAST:** 744 Broad Street, Newark, N. J., HUmboldt 5-3900 • 731 James Street, Room 402, Syracuse 3, New York, GRanite 4-5591 • **NORTHEAST:** 64 "A" Street, Needham Heights 94, Mass., HIllcrest 4-7200 • **EAST CENTRAL:** 714 New Center Bldg., Detroit 2, Mich., TRinity 5-5600 • **CENTRAL:** Suite 1154, Merchandise Mart Plaza, Chicago, Ill., WHitehall 4-2900 • P. O. Box 8406, St. Louis Park Branch, Minneapolis, Minn., FEderal 9-1249 • **WEST:** 6355 E. Washington Blvd., Los Angeles, Calif., RAymond 3-8361 • 1838 El Camino Real, Burlingame, Calif., OXford 7-1620 • **SOUTH:** Calmar Building, 1520 Edgewater Drive, Suite 1, Orlando, Florida, GArden 4-4768 • **SOUTHWEST:** 7905 Empire Freeway, Dallas 7, Texas, FLeetwood 7-8167 • **GOV'T.:** 224 N. Wilkinson St., Dayton, O., BAldwin 6-2366 • 1725 "K" St., N.W., Washington, D.C., FEderal 7-8500

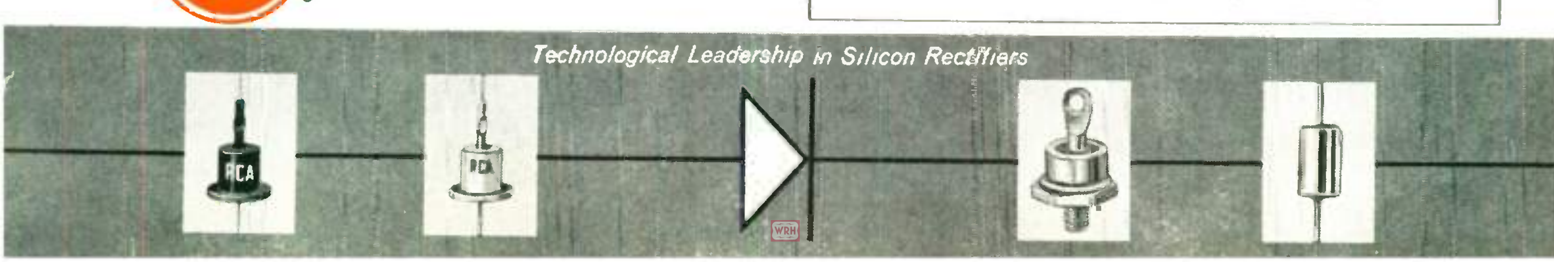

"Switching Features," *J. W. Brubaker, Bell Telephone Labs., New York, N. Y.*

"Employment of the Signal Corps Automatic Network," *Lt. Col. McNeil, U. S. Army Communications Agency, Washington, D. C.*

"Systems Engineering Aspects of the Signal Corps Automatic Network," *L. L. Gaddis, A.T.&T. Long Lines Dept., New York, N. Y.*

Session 2.2—System Performance

"Noise and Transmission Level Terms in American and International Practice," *H. H. Smith, ITT Communications Systems, Inc., Paramus, N. J.*

"Nomograms For The Statistical Summation of Noise in Multihop Communication Systems," *B. Sheffield, ITT Communication Systems, Inc., Paramus, N. J.*

"Multiplex Stability and Interface Requirements For Aircom Circuits," *G. Goltsos and P. H. Bourne, ITT Communication Systems, Inc., Paramus, N. J.*

"Synthesis of a Global Communications System Using Wideband Radio Relay Systems," *J. B. Potts, Radio Corporation of America, Camden, N. J.*

"Performance Rating of Communications Systems," *J. C. G. Carter, Westinghouse Electric Corp., Baltimore, Md.*

Session 2.3—HF Communications

"Optimum HF Prediction," *H. Greenberg, S. Krevsky, and G. Bumiller, RCA, New York, N. Y.*

"The AVCO Natural Communication System," *S. C. Coroniti, G. E. Hill, N. J. Macdonald, and R. Penndorf, AVCO Corp., Wilmington, Mass.*

"Frequency Sounding Techniques for HF Communications Over Auroral Zone Paths," *G. W. Jull, G. W. Irvine, and J. P. Murray, Defence Research Telecommunications Establishment, Ottawa, Ont., Canada.*

"Modern Ionospheric Measuring Equipment," *D. H. Covill, E.M.I., Cossor Electronics Ltd., Dartmouth, N. S., Canada.*

"Radiotelephone Communications on the Great Lakes and the Seaway," *H. H. Herrick, Lorain Coun y Radio Corp., Lorain, Ohio.*

Tuesday Morning, May 23

Session 3.1—Space Communication II

"Unfurlable Antennas for Space Communication," *P. D. Kennedy, Lockheed Aircraft Corp., Sunnyvale, Calif.*

"A Broadband HF Antenna System for Use In a Satellite Ionospheric Sounder," *J. R. Richardson and A. R. Molozzi, Defence Research Telecommunications Establishment, Ottawa, Ont., Canada.*

"Communications Satellites Using Active Van Atta Arrays," *R. C. Hansen, Aerospace Corp., Los Angeles, Calif.*

"Phase-Locked Loops for Electronically Scanned Antenna Arrays," *R. C. Colbert and W. L. Rubin, Sperry Gyroscope Co., Great Neck, L. I., N. Y.*

"Advanced Scann ng Feed for the AT-36 60′ Diameter Automatic Tracking Antenna," *E. Villaseca, Dynatronics, Inc., R. E. Moseley, Scientific Atlanta, Inc.*

Session 3.2—Modulation Techniques

"An Experimental Delta Modulator," *M. Kozuch and A. Lender, ITT Labs., Nutley, N. J.*

"The Use of Log Differential PCM for Speech Transmission in UNICOM," *R. L. Miller, Bell Telephone Labs., Inc., Whippany, N. J.*

"A High Speed, Serial, Four-Phase Data Modem for Regular Telephone Circuits," *G. L. Evans, E. Enriquez, and Q. C. Wilson, Hughes Communications Div., Los Angeles, Calif.*

"A New Digital Communication System-Modified Diphase," *G. Aaronson, D. A. Douglas, and G. J. Meslener, RCA, New York, N. Y.*

"Wideband Frequency Modulator," *L. D. Westenburg and H. D. Hern, Collins Radio Co., Dallas, Tex.*

Session 3.3—Pacific Scatter Communication System

"Pacific Scatter Communication System," *J. Rose, Defense Communications Agency; A. A. Childers, U. S. Army, Office of the Chief Signal Officer; H. H. Jones, Jr., U. S. Army Signal Engineering Agency; R. Bateman, Page Communication Engineers, Inc.; D. F. Brittle, Jr., Page Communication Engineers, Inc.*

"Improved Ionoscatter Receiving Techniques Used on the Pacific Scatter Communication System," *J. Rose, Defense Communications Agency; A. A. Childers, U. S. Army, Office of the Chief Signal Officer; H. H. Jones, Jr., U. S. Army Signal Engineering Agency; G. E. Boggs, Page Communication Engineers, Inc.*

"Performance Monitoring of the Pacific Scatter Communications System," *J. Rose, Defense Communications Agency; A. A. Childers, U. S. Army, Office of the Chief Signal Officer; H. H. Jones, Jr., U. S. Army Signal Engineering Agency; J. S. McLeod, Page Communication Engineers, Inc.*

"The Piggy-Back Dual Corner Reflector Antenna," *J. Rose, Defense Communications Agency; A. A. Childers, U. S. Army, Office of the Chief Signal Officer; H. H. Jones, Jr., U. S. Army Signal Engineering Agency; J. S. Stotsky, Page Communication Engineers, Inc.; J. McMahon, Page Communication Engineers, Inc.*

Tuesday Afternoon

Session 4.1—Switching Systems I

"Network Compatibility in Global Telephone Switching Systems," *C. A. Parry and P. O. Dahlman, Page Communications Engineers, Inc., Washington, D. C.*

"Parametron Applications in Military Switchboards," *S. Kaplan and L. Stambler, RCA, New York, N. Y.*

"Alternate Routing Computer," *A. Kritz and H. Roberts, RCA, New York, N. Y.*

"Message Storage in Automatic Switching," *W. F. Spanke, U. S. Army Communications Systems Div., Washington, D. C.*

"Traffic Management Techniques," *A. G. Steinmayer, O. O. Jones, and H. B. Collins, Jr., General Electric Co., Philadelphia, Pa.*

Session 4.2—Microwave Radio Relay

"A Modern Approach to Microwave Communications Systems," *G. I. Carlson, Motorola, Inc., Chicago, Ill.*

"A Transistorized Multi-Channel SSB Carrier Telephone System," *F. Correia, Motorola, Inc., Chicago, Ill.*

"Transistor Alarm and Control System for Unattended Microwave Repeater Stations," *L. Moore, Moore Associates, Inc., Redwood City, Calif.*

"Possibility of Noise Figure Reduction of a Microwave Receiver Using a Reflex Klystron Amplifier," *K. Ishii, Marquette University, Milwaukee, Wis.*

"Design of a TD-2 Microwave Repeater with Transmitters and Receivers on the Same Frequency," *P. B. Engh, Pacific Telephone & Telegraph Co., San Diego, Calif.*

Session 4.3—Reliability and Survivability

"The Planning of Space Communication System Reliability," *E. D. Karmiol, A. Sternberg, and J. S. Youthcheff, General Electric Co., Philadelphia, Pa.*

"Communication Error Rate Instrumentation System," *V. Chewey, J. Wittman, J. Rabinowitz and A. Tepfer, RCA, New York, N. Y.*

"A Technique for the Physical Survivability Analysis of a Communications Network," *D. F. Pascucci and N. P. Albrecht, ITT Labs., Nutley, N. J.*

"Circuits, Networks, and Survival," *J. W. Halina, ITT Communication Systems, Paramus, N. J.*

"Availability—New Approach to the Measurement of System Reliability," *M. Barow, S. R. Calabro, and V. Selman, International Electric Corp., Paramus, N. J.*

Wednesday Morning, May 24

Session 5.1—Space Communication III

"A Global Party Line Concept of Satellite Communication," *J. L. Walker, ITT Communications, Inc., Paramus, N. J.; D. R. Campbell and W. L. Glomb, ITT Labs., Nutley, N. J.*

"Optimization of System Parameters for Deep Space Communication Systems," *M. E. Breese and P. J. Sferrazza, Sperry Gyroscope Co., Great Neck, L. I., N. Y.*

"The Delay/Coverage Problem in Telecommunications Via Satellites," *A. J. Vadasz, General Electric Co., Lynchburg, Va.*

"Theoretical Considerations in Design of Delayed Time Satellite Repeater Systems," *J. Dressner, U. S. Army Signal Research and Development Lab., Fort Monmouth, N. J.*

"Some Studies of Special Orbital Configurations for Global Communications," *S. C. Hight and J. G. Kreer, Bell Telephone Labs., Whippany, N. J.*

Session 5.2—Data Handling

"Micro Programmed Digital Data Handling System," *J. C. Augustine, Space Technology Labs., Inc., Los Angeles, Calif.*

"A Binary Information Exchange," *R. C. P. Hinton, ITT Communication Systems, Inc., Paramus, N. J.; C. E. Haller, ITT Labs., Nutley, N. J.*

Automatic Keyboard-Operated Morse Code System Without Tape," *R. W. Johnson Co., Anaheim, Calif.*

"DIGIKEY—A Keyboard Technique for Digitalizing Human Information," *S. G. Lutz, Hughes Research Labs., Malibu, Calif.*

"A Technique for Converting Analog Voltages to Digital Codes at Sampling Rates Above Five Million Samples Per Second With Accuracies of Seven Bits," *C. F. Crocker, Raytheon Co., Waltham, Mass.*

Session 5.3—Forward Scatter

"Latest and Future Trends in Tropospheric Scatter Communications," *C. P.*

A-B QUALITY

Dependability PROVED!

...in tests at 5 Times mil specs for shock, vibration and acceleration

Potentiometers Type J and Type K	Potentiometers Type G and Type L	Adjustable Fixed Resistors Type R	Hermetically Sealed Ceramic Encased Resistors Type TS Type CS Type ES

About the test

At the United States Testing Co., Inc.* the above Allen-Bradley resistors and potentiometers were subjected to a constant acceleration of 300g, impact shock of 150g and vibration of 50g from 55 to 2,000 cps. All tests were conducted in accordance with procedures outlined in the latest Mil Specs.

*Test Report #71801, Sept. 1960.

In these severe tests, Allen-Bradley resistors and potentiometers have demonstrated their complete dependability in environmental extremes.

The ruggedness of A-B fixed resistors is obtained through an *exclusive* process in which the resistance element and the insulating jacket are hot molded into an integral unit of unusual mechanical strength. This unit is then hermetically sealed in a ceramic tube. Also, please remember, A-B fixed resistors are *completely free from catastrophic failures.*

A-B potentiometers have the resistance elements molded into, and are an integral part of, the base; therefore, they are virtually indestructible. In addition, operation is quiet and smooth when the potentiometer is new, and these characteristics improve with use.

For maximum reliability under severe operating conditions, insist on Allen-Bradley *quality* electronic components.

Allen-Bradley Co., 222 W. Greenfield Ave., Milwaukee 4, Wis.
In Canada: Allen-Bradley Canada Ltd., Galt, Ont.

2-61-E

ALLEN-BRADLEY | ***QUALITY ELECTRONIC COMPONENTS***

H. F. Fluorescent Lights

Television

Missiles

Radio

Radar

Telephone Systems

Electric Organs

Automatic Machine Tools

Hi-Fi Stereo

Durnovo, Adler Electronics, Inc., New Rochelle, N. Y.

"Basic Considerations of Economy-Type Troposcatter Systems," *L. P. Yeh, Page Communication Engineers, Inc., Washington, D. C.*

"Propagation Phenomena and Diversity Combiner Problems Encountered on a 690 Mile Multichannel Tropo-Scatter System," *W. H. Gentry, Jr., General Electric Co., Lynchburg, Va.*

"Radio Propagation at UHF by Incoherent Scattering in the F-Region," *H. W. Briscoe and V. C. Pineo, MIT Lincoln Lab., Lexington.*

"Mutual Interference Between Point-to-Point and Space Communications Systems," *W. J. Hartman and M. T. Decker, National Bureau of Standards, Boulder, Colo.*

Wednesday Afternoon

Session 6.1—Switching Systems II

"The Problem of the Tributary Area in Planning a Military Switched Global Network," *P. M. King and G. C. Hartley, ITT Communication Systems, Inc., Paramus, N. J.*

"Terminal Area Distribution and Processing," *H. H. Pine, ITT Communication Systems, Inc., Paramus, N. J.*

"A Fully Electronic TDM Solid State Switching Center for Military Communications—Grouping, Signalling, Logic," *A. K. Bergmann, North Electric Co., Galion, Ohio.*

"A Fully Electronic TDM Solid State Switching Center for Military Communications—Transmission Characteristics and Their Measurements," *G. Svala, North Electric Co., Galion, Ohio.*

"An Automatic Electronic System for Handling International Telegrams," *E. D. Becken and R. K. Andres, RCA Communications, Inc., New York, N. Y.*

Session 6.2—System Planning

"Application for Transmission Media," *J. H. Vogelman, Capehart Corp., Richmond Hill, N. Y.*

"The Economies of Communications Satellites," *W. Meckling and S. Reiger, The RAND Corp., Santa Monica, Calif.*

"Optimization Methods in Economics Planning of Telecommunications Systems," *Z. Prihar, Page Communications Engineers, Inc., Washington, D. C.*

"Value Engineering Applied to a Large Scale Electronic Communications System," *B. Ellison, International Electric Corp., Paramus, N. J.*

"Communications Cost Control Analysis—Integration of Communication and Data Processing Systems," *J. K. Mulligran, T. R. McKee, and J. P. Macri, RCA, Camden, N. J.*

Session 6.3—Speech Compression and Spectrum Sharing

"The Speech Bandwidth Compression Problem," *F. H. Slaymaker and R. A. Houde, Stromberg-Carlson Co., Rochester, N. Y.*

"A 1000 Bit Per Second Speech Compression System," *J. S. Campanella, D. C. Coulter, and R. Irons, Melpar, Inc., Falls Church, Va.*

"Band Economy Multiplex Equipment Applied to Long Distance Trunk Groups," *G. Atkinson, ITT Communications Systems, Inc., Paramus, N. J.*

"Unscheduled Spectrum Sharing in Communication," *D. P. Harris, Lockheed Aircraft Corporation, Sunnyvale, Calif.*

Designing Interference-Free Space Communication Systems Using Computer Simulation Techniques," *D. R. J. White, Frederick Research Corp., Wheaton, Md.*

Western Joint Computer Conference

Ambassador Hotel, Los Angeles, Calif., May 9–11, 1961

The tentative program for the 1961 Western Joint Computer Conference has been announced. This year's Conference will include a Ladies' Program, which will be held Monday morning, May 9. Phyllis Huggins, of Bendix Computer Division, Los Angeles, Calif., is the Chairman of this portion of the program, which will include a coffee and an invited panel, consisting of J. W. Granholm, Editor, *Computing News*, Thousand Oaks, Calif.; Vincent van Praag, President, Electro-Logic Corp., Los Angeles, Calif.; and G. G. Vosatka, Western Regional Manager, Bendix Computer Corp., Los Angeles. Another highlight of the Conference will be the luncheon, which will be held on Wednesday, May 10. W. F. Bauer, Chairman of the 1961 WJCC, will be the Master of Ceremonies, and Simon Ramo, Executive Vice President of Thompson Ramo Wooldridge, Inc., will speak on "Future Applications of Electronic Intelligence."

Tuesday Morning, May 9

Session IA—Opening Session

Chairman: *K. W. Uncapher, The RAND Corp., Santa Monica, Calif.; Vice Chairman, 1961 WJCC.*

Welcoming Address: *W. F. Bauer, Thompson Ramo Wooldridge, Inc., Canoga Park, Calif.; Chairman, 1961 WJCC.*

Keynote Address: *T. J. Watson, Jr., IBM Corp., New York, N. Y.*

General Remarks: *M. Rubinoff, University of Pennsylvania, Philadelphia; Chairman, National Joint Computer Committee.*

Tuesday Afternoon

Session IIA—Digital Simulation

Chairman: *H. H. Harman, System Development Corp., Santa Monica, Calif.*

"Simulation: A Survey," *H. H. Harman, System Development Corp., Santa Monica, Calif.*

"Computers and Management Games," *J. M. Kibbee, Remington Rand Univac, New York, N. Y.*

"Simulation of Airborne Anti-Submarine Systems," *T. Guinn, Douglas Aircraft Co., El Segundo, Calif.*

"An On-line Management System Using English Language," *A. Vazsonyi, Ramo-Wooldridge, Canoga Park, Calif.*

"Application of Digital Simulation Techniques to Highway Design Problems," *A. Glickstein and S. L. Levy, Midwest Research Institute, Kansas City, Mo.*

"The Use of Manned Simulation in the Design of an Operational Control System," *M. A. Geisler and W. A. Steger, The RAND Corp., Santa Monica, Calif.*

Session IIB—Microsystem Electronics

Chairman: *R. A. Kudlich, A. C. Spark Plug, El Segundo, Calif.*

"The Present Status of Microsystem Electronics," *P. B. Meyers, Motorola, Inc., Phoenix, Ariz.*

"Testing of Micrologic Elements," *R. Anderson, Fairchild Semiconductor Corp., Mountain View, Calif.*

"Interconnection Techniques for Semiconductor Networks," *J. S. Kilby, Texas Instruments, Inc., Dallas, Tex.*

"Microcircuit Interconnection Problems," *G. Anderson, C. Walant, and G. Selvin, Sylvania Electronic Systems, Waltham, Mass.*

"Microsystem Computer Techniques," *E. Luedicke and A. Medwin, RCA, Camden, N. J.*

Wednesday Morning, May 10

Session IIIA—Modeling Human Mental Processes

Chairman: *H. A. Simon, The RAND Corp., Santa Monica, Calif., and Carnegie Institute of Technology, Pittsburgh, Pa.*

"Introduction: Modeling Human Mental Processes," *H. A. Simon, Carnegie Institute of Technology, Pittsburgh, Pa.*

"The Simulation of Verbal Learning Behavior," *E. Feigenbaum, University of California, Berkeley.*

"The Simulation of Behavior in the Binary Choice Experiment," *J. Feldman, University of California, Berkeley.*

"Programming a Model of Human Concept Formulation," *C. I. Hovland and E. B. Hunt, Yale University, New Haven, Conn.*

Session IIIB—Recent Advances in Computer Circuits

Chairman: *C. T. Leondes, University of California, Los Angeles.*

"Parallelism in Computer Organization Random Number Generation in the Fixed Plus Variable Computer System," *M. Aoki* *and G. Estrin, University of California, Los Angeles; T. Tang, National Cash Register Co., Hawthorne, Calif.*

"The CELLSCAN System—a Leucocyte Pattern Analyzer," *K. Preston, Jr., Perkin-Elmer Corp., Norwalk, Conn.*

"Application of Computers to Circuit Design for UNIVAC LARC," *G. Kaskey, N. S. Prywes, and H. Lukoff, Remington-Rand Univac, Philadelphia, Pa.*

"Wide Temperature Range Coincident Current Core Memories," *R. S. Weisz, and N. Rosenberg, Ampex Computer Products Co., Culver City, Calif.*

"Tunnel Diode Storage Using Current Sensing," *E. R. Beck, D. A. Savitt, and A. E. Whiteside, Bendix Corp., Detroit, Mich.*

"Tunnel Diode Balanced Pair Circuit as a Building Block for High-Speed Computers," *W. E. Barnette, G. A. Brown, S. Fiarman, H. S. Miller, and R. A. Powlus, RCA Labs., Princeton, N. J.*

Session IVA—Problem Solving and Learning Machines

Chairman: *M. Minsky, M. I. T., Cambridge.*

"Problem Solving and Learning Machines: A Survey," *M. Minsky, M. I. T., Cambridge.*

"Baseball: An Automatic Question-Answerer," *B. F. Green, Jr., A. K. Wolf, C. Chomsky, and K. Laughery, M. I. T., Lexington.*

"A Basis for a Mathematical Theory of Computation," *J. McCar hy, M. I. T., Cambridge.*

Wednesday Afternoon

Session VA—Information Retrieval

Chairman: *D. R. Swanson, Ramo-Wooldridge, Canoga Park, Calif.*

"Information Retrieval: State of the Art," *D. R. Swanson, Ramo-Wooldridge, Canoga Park, Calif.*

"A Systems Approach to Scientific Communication," *M. M. Kessler, M. I. T., Lexington.*

"A Screening Method for Large Information Retrieval Systems," *R. T. Moore, Princeton University and the National Bureau of Standards, Washington, D. C.*

Session VB—Automata Theory and Neural Models

Chairman: *P. M. Kelley, Aeronutronic, Newport Beach, Calif.; Session arranged by H. von Foerster, University of Illinois, Urbana.*

"What is an Intelligent Machine?" *W. R. Ashby, University of Illinois, Urbana.*

"Automata Theory and Neural Models: A Survey," *P. M. Kelley, Aeronutronic, Newport Beach, Calif.*

"Physiology of Automata," *M. L. Babcock, University of Illinois, Urbana.*

"Analysis of Perceptrons," *H. D. Block, Cornell University, Ithaca, N. Y.*

Session VC—New Hybrid Analog-Digital Techniques

Chairman: *G. A. Korn, University of Arizona, Tuscon,*

"Hybrid Analog-Digital Computers," *H. Schmid, General Precision, Inc., Binghamton, N. Y.*

"Optimization of Linear System Dynamic Characteristics," *C. H. Single and E. M. Billinghurst, Beckman Instruments, Inc., Richmond, Calif.*

"Design and Development of a Sampled-Data Simulator," *J. E. Reich and J. J. Perez, Space Technology Labs., Inc., Los Angeles, Calif.*

"Digital Control Systems for a Repetitive Electronic Analog Computer," *T. Brubaker and H. Eckes, University of Arizona, Tuscon.*

Session VIA—Large Computer Systems

Chairman: *C. W. Adams, Charles W. Adams Associates, Bedford, Mass.*

"Trends in Design of Large Computer Systems," *C. W. Adams, Charles W. Adams Associates, Bedford, Mass.*

Thursday Morning, May 11

Session VIIA—Automatic Programming

Chairman: *A. Opler, Computer Usage Co., New York, N. Y.*

"Current Problems in Automatic Programming," *A. Opler, Computer Usage Co., New York, N. Y.*

"A First Version of UNCOL," *T. B. Steel, Jr., System Development Corp., Santa Monica, Calif.*

"Method of Combining Algol and Cobol," *J. E. Semmet, Sylvania Electric Products, Needham, Mass.*

"ALGY—An Algebraic Manipulation Program," *M. D. Bernick, E. D. Callender, and J. R. Sanford, Philco Corp., Palo Alto, Calif.*

"A New Approach to the Functional Design of a Digital Computer," *R. S. Barton, Computer Consultant, Altadena, Calif.*

"The JOVIAL Checker," *M. Blauer, System Development Corp., Paramus, N. J.*

Session VIIB—Memory Devices and Components

Chairman: *P. V. Levonian, Space Technology Labs., Inc., Los Angeles, Calif.*

"Factors Affecting Choice of Memory Elements," *C. F. King, Claude King Associates, Los Angeles, Calif.*

"A Nondestructive Readout Film Memory," *R. J. Petschauer and R. D. Turnquist, Remington Rand Univac, St. Paul, Minn.*

"A Technique for High Speed Information Transfer in Magnetic Films," *J. I. Raffel, A. H. Anderson, and T. S. Crowther, M. I. T., Lexington.*

"The Development of a New Nondestructive Memory Element," *A. W. Vinal, IBM Corp., Owego, N. Y.*

"A High Speed Metastable Memory Element and Pulse Delay Line," *L. C. Clapp, Sylvania Electronic Systems, Needham, Mass.*

Session VIIC—Applied Analog Techniques

Chairman: *R. R. Favreau, Electronic Associates, Inc., Long Branch, N. J.*

"The Optimization of Radar Designs Using GEESE Techniques," *E. L. Berger, General Electric Co., Syracuse, N. Y.*

"The Spectral Evaluation of Iterative Analyzer Integration Techniques," *M. Gilliland, Beckman Instruments, Richmond, Calif.*

"An Iteration Procedure for Model Building and Boundary Value Problems," *W. Brunner, Princeton Computation Center, Princeton, N. J.*

"Analog Simulation of Underground Water Flow in the Los Angeles Coastal Plain," *D. A. Darms, Electronic Associates Los Angeles Computation Center, Los Angeles, Calif.*

Thursday Afternoon

Session VIIIA—Pattern Recognition

Chairman: *O. Selfridge, M. I. T., Cambridge.*

"Pattern Recognition," *F. C. Frick, M. I. T., Cambridge.*

"A Self-Organizing Recognition System," *P. M. Kelley and R. J. Singer, Aeronutronic, Newport Beach, Calif.*

"A Learning Program for Pattern Recognition," *L. Uhr, University of Michigan, Ann Arbor; C. Vossler, System Development Corp., Santa Monica, Calif.*

"An Experimental Program for the Selection of Disjunctive Hypotheses," *M. Kochen, IBM Corp., Yorktown, N. Y.*

"Time-Analysis of Logical Processes in Man," *U. Neisser, Brandeis University, Waltham, Mass.*

Session VIIIB—Computers in Control

Chairman: *A. J. Rowe, Hughes Aircraft Co., Culver City, Calif.*

"Computer-Based Management Control," *A. J. Rowe, Hughes Aircraft Co., Culver City, Calif.*

"Some Comments on Military Control Applications of Computers," *W. S. Melahn and R. E. Olsen, System Development Corp., Santa Monica, Calif.*

"American Airlines 'SABRE' Electronic Reservations Systems," *M. N. Perry and W. R. Plugge, American Airlines, New York, N. Y.*

"Real-Time Management Control at Hughes Aircraft," *D. R. Pardee, Hughes Aircraft Co., Culver City, Calif.*

"Project Mercury—Command—Control Program System," *B. G. Oldfield, IBM Corp., Rockville, Md. and A. M. Pietrasanta, IBM Corp., Washington, D. C.*

"The 4651 (SACCS) Computer Application," *P. D. Hildebrandt, System Development Corp., Lexington, Mass.*

Session VIIIC—The "Human" Side of Analog Systems

Chairman: *L. A. Ohlinger, Norair, Hawthorne, Calif.*

"The Computer Simulation of Colonial, Socio-economic Society," *W. D. Howard, General Motors Corp., Warren, Mich.*

"X-15 Analog Flight Simulation—Systems Development and Pilot Training," *N. Cooper, North American Aviation, Inc., Los Angeles, Calif.*

"Analog-Digital Hybrid Computers in Simulation with Humans and Hardware," *O. F. Thomas, U. S. Naval Ordnance Test Station, Pasadena, Calif.*

"The Automatic Determination of Human and Other System Parameters," *T. F. Potts, G. N. Ornstein, and A. B. Clymer, North American Aviation Inc., Columbus, Ohio.*

General Instrument Semiconductor... Leader in Reliability!

GI ANNOUNCES INDUSTRY'S MOST RELIABLE SILICON MESA TRANSISTORS!

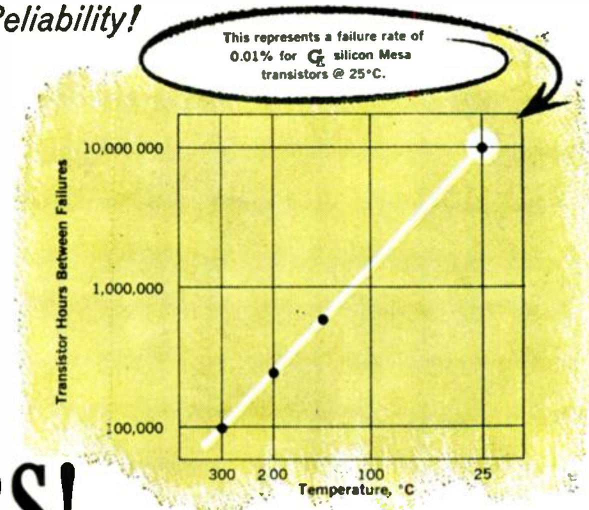

PROOF! Extended life tests at each of temperatures shown above, demonstrate GI superior mesa performance with 0.01%/per 1000-hrs. failure rate at 25°C.

General Instrument Semiconductor has achieved a major breakthrough in transistor manufacture! Through detailed research, careful product development and advanced production techniques we offer *the most reliable silicon mesa transistors available today!*

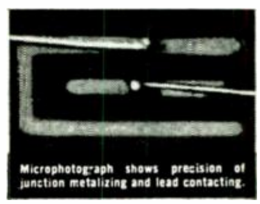
Microphotograph shows precision of junction metalizing and lead contacting.

Exclusive combination of reliability benefits offered by GI through long-term R & D:

- Advanced techniques of junction metalizing;
- Superior junction contacting;
- Permanent surface passivation;
- 100% lot stabilization with 96-hour bake at 300°C; and
- Critical analysis with automatic equipment for exhaustive parameter testing.

COMPLETE LINE OF GI SILICON MESAS...FROM STOCK

What are *your* needs? General Instrument offers a full line of double diffused NPN silicon mesas for your most exacting applications. Abbreviated ratings and characteristics below indicate a wide range of usefulness: Very high speed saturated switching; VHF tuned amplifiers; and units with high beta linearity for magnetic memory drivers and video amplifiers.

Available in accordance with MIL-S-19500/99A (GI 2N696, 2N697) and MIL-S-19500/120 (GI 2N706). Contact General Instrument today for more information on these realistically-priced units, and the name of your local authorized stocking distributor.

GENERAL INSTRUMENT NPN SILICON MESA TRANSISTORS

Type	Case	RATINGS			CHARACTERISTICS					
		BV_{CBO}	BV_{EBO}	Maximum Dissipation ($T_{CASE}=25°C$)	I_{CBO}	h_{FE} $V_{CE}=10$ v $I_C=150$ ma pulsed	h_{fe} $V_{CE}=10$ v $I_C=50$ ma f = 20 Mc	V_{BE} $I_B=15$ ma $I_C=150$ ma	V_{CE} (SAT.) $I_B=15$ ma $I_C=150$ ma	C_{ob} @ $I_E=0$ $V_{CB}=10$ v
2N696	TO-5	60 v	5 v	2 watts	@ $V_{CB}=30$ v T = 25°C Ambient: 1 μ a max T = 150°C Ambient: 100 μ a max	20 min 60 max	2 min	1.3 v max	1.5 v max	35 pf max
2N697	TO-5	60 v	5 v	2 watts	@ $V_{CB}=30$ v T = 25°C Ambient: 1 μ a max T = 150°C Ambient: 100 μ a max	40 min 120 max	2.5 min	1.3 v max	1.5 v max	35 pf max
2N699	TO-5	120 v	5 v	2 watts	@ $V_{CB}=60$ v T = 25°C Ambient: 2 μ a max T = 150°C Ambient: 200 μ a max	40 min 120 max	2.5 min	1.3 v max	5.0 v max	20 pf max
2N706	TO-18	25 v	3 v	1 watt	@ $V_{CB}=15$ v T = 25°C Ambient: 0.5 μ a max T = 150°C Ambient: 30 μ a max	$V_{CE}=1$ v $I_C=10$ ma 15 min	$V_{CE}=15$ v $I_C=10$ ma f = 100 Mc 2 min	$I_B=1$ ma $I_C=10$ ma 0.9 v max	$I_B=1$ ma $I_C=10$ ma 0.6 v max	6 pf max
2N1252	TO-5	30 v	5 v	2 watts	@ $V_{CB}=20$ v T = 25°C Ambient: 10 μ a max T = 150°C Ambient: 600 μ a max	15 min 45 max	2 min	1.3 v max	1.5 v max	45 pf max
2N1253	TO-5	30 v	5 v	2 watts	@ $V_{CB}=20$ v T = 25°C Ambient: 10 μ a max T = 150°C Ambient: 600 μ a max	30 min 90 max	2.5 min	1.3 v max	1.5 v max	45 pf max
2N1420	TO-5	60 v	5 v	2 watts	@ $V_{CB}=30$ v T = 25°C Ambient: 1.0 μ a max T = 150 C Ambient: 100 μ a max	100 min 300 max	2.5 min	1.3 v max	1.5 v max	35 pf max

GENERAL INSTRUMENT
GENERAL TRANSISTOR

SEMICONDUCTOR
DIVISION OF GENERAL INSTRUMENT CORPORATION
65 Gouverneur Street, Newark 4, New Jersey

IN CANADA: General Instrument Ltd., Semiconductor Division, P.O. Box 9, 151 Weber Street South, Waterloo, Ont., Canada.

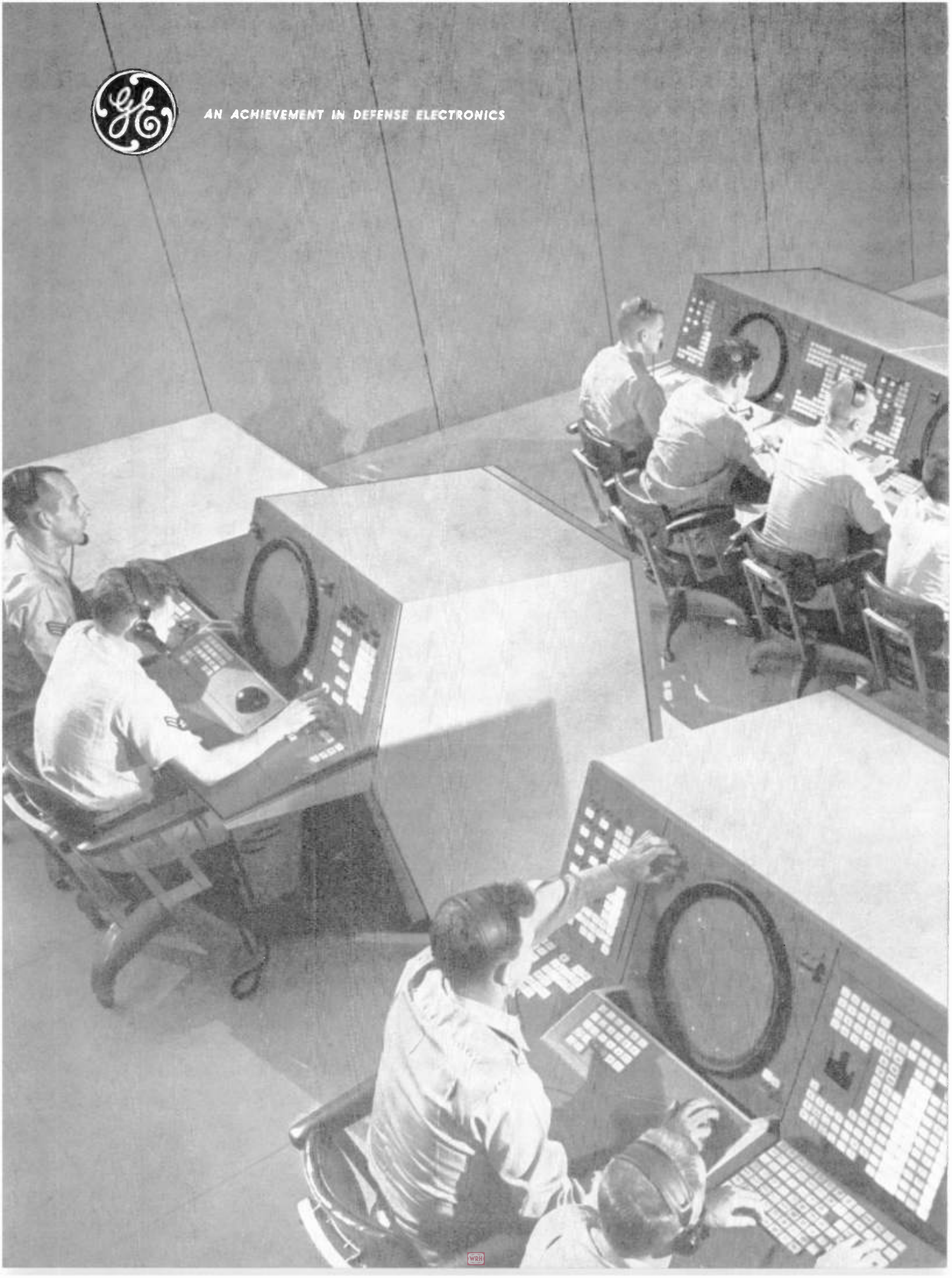
AN ACHIEVEMENT IN DEFENSE ELECTRONICS

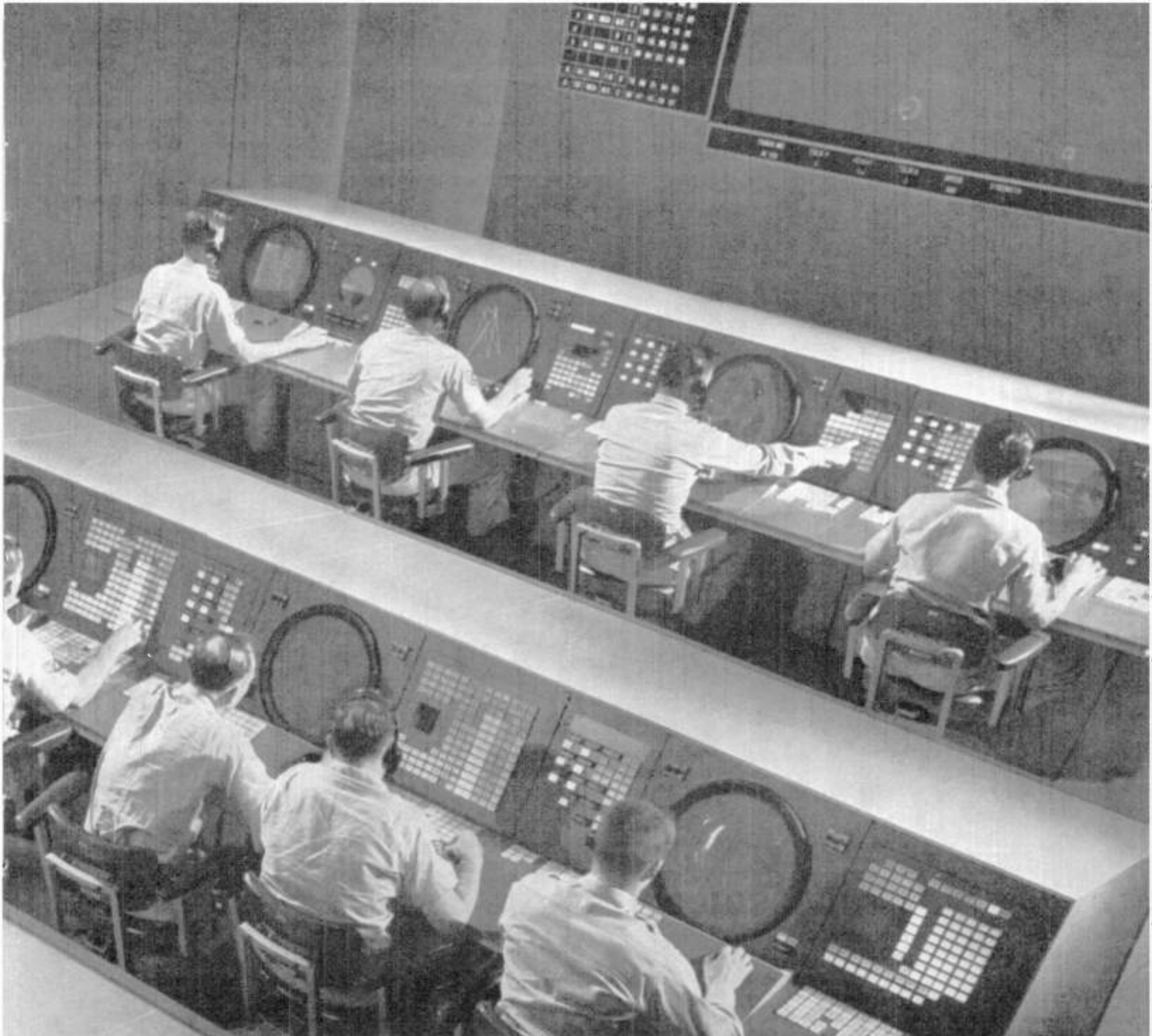

Industrial Engineering Notes*

Association Activities

Publication of an Educational Television Guidebook, representing the most complete work available on TV as an instruction tool was announced by Ben Edelman (Western Electric Co.), Chairman of the EIA Educational Coordinating Committee. The book presents nearly 100 illustrations in a sequence designed to develop a basic understanding of the components and workable combinations of television facilities to meet varying educational applications. It deals also with such innovations in electronic instruction as translators, video tape, the Midwest Program on Airborne Instructional Television, the Galveston experiments with Phonoscope, low-power educational television provisions, and closed-circuit library reference system. Preparation of the guidebook was financed by EIA and was under the direction of a task force headed by P. A. Jacobson (Motorola, Inc.). Members of the task force included leading educators in the field of television instruction and experts from EIA member and non-member companies. The book was written by Dr. P. Lewis, Director of the Bureau of Instructional Materials of the Chicago Board of Education. The McGraw-Hill Book Co., Inc., publisher of the guidebook, is selling the book to the public for \$4.95 a copy. Price to representatives of EIA member-companies, however, is \$3.30, reflecting a one-third discount granted by the publisher. To take advantage of the discounted price, EIA member-companies should address purchase orders, made out to McGraw-Hill, to P. H. Cousins, Staff Director, EIA Educational Coordinating Committee, EIA Headquarters. Orders will be forwarded to the publisher. . . . **A special EIA committee has begun the preparation of "A Technical Guide for the Purchase and Use of Language Laboratory Facilities and Equipment" at the request of the U. S. Office of Education.** EIA was invited by the Office of Education to prepare a simple technical guide on the use and facilities of language laboratories through a government contract authorized by Title VII of the National Defense Education Act. The booklet will be designed to acquaint language teachers and school administrators with the many facets of the rapidly increasing techniques of teaching foreign languages by electronic devices. The booklet will be prepared in a three- to four-month period under a "crash" program. Supervision and direction of the manuscript will be provided by the Language Laboratory Guide Book Project Task Force of the EIA Educational Coordinating Committee. The Task Force is chaired by R. G. Frick (General Electric Co.) and is composed of manufacturers of electronic language teaching devices, both members and non-members. Actual writing of the booklet will be performed by the Howard W. Sams Co., Inc., under Subcontract with EIA. The Association will perform its functions under the contract on a cost basis only. The pedagogical aspects of the manuscript will be supervised by an Office of Education committee of experts under Dr. Seth Spaulding, Chief, Educational Materials and Services Section.

* The data on which these Notes are based were selected by permission from *Weekly Reports*, issues of January 25 and 30, February 6, 13, and 20, 1961, published by the Electronic Industries Association, whose helpfulness is gratefully acknowledged.

Engineering

A new "OTS Selective Bibliography" listing government research reports, translations, and other technical documents on semiconductors has been published by the Office of Technical Services, U. S. Department of Commerce. The bibliography shows literature on properties of sulfide semiconductors, semiconducting properties of boron, reurtron dosimetry research, surfaces in semiconductors, and a number of other subjects. A list of government-owned patents available for license is also included. The document is available from OTS, U. S. Department of Commerce, Washington 25, D. C., at 10 cents a copy. Order SB-435. . . . **The Navy has issued an instruction to eliminate the "indiscriminate and incorrect" use of the word "module" and establish a standard terminology to be used for unitized electronic equipment.** According to Technical Logistics Divisions Instruction 9670.3, "module" has become "so loosely and improperly" used in industry and government that considerable confusion exists as to its actual meaning. It is incorrectly used, the Navy says, to mean a plug-in or any removable portion of an electronic equipment, and some manufacturers have extended its use to ancillary items of equipment such as microphones, antennas, headphones, and battery packs. The Navy pointed out that Military Specification MIL-E-16400D supplements the dictionary definition of "module" as a standard or unit or measurement by adding "a fixed dimension." When the word is used in conjunction with equipment assemblies having outline dimensions which are multiples of a module or fixed dimension, it becomes "modular assembly." Moreover, the instruction continues, for electronic equipment built up of a group of easily replaceable units, there are two expressions which apply—"unitized construction" and "modular construction." "For the former, the replaceable units can be of any size or form factor (which is the case with most of the current equipment). In the case of 'modular construction,' however, the units must

(Continued on page 44A)

Interchangeable SLOTTED SECTIONS

convenient and positive

- conveniently interchangeable waveguide sections
- no slope adjustment required
- vernier position scale readable to 0.1 mm.
- dial gauge holder and movable stop
- tapered slots to minimize residual VSWR

INTERCHANGEABLE WAVEGUIDE SECTIONS

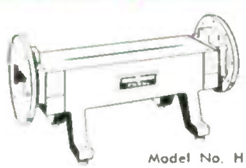

Model No. H115A

Model No. C115A

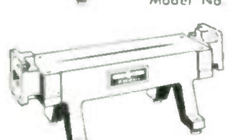

Model No. W115A

Model No. X115A

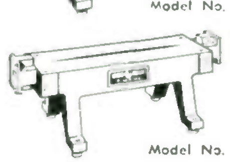

Model No. Y115A

UNIVERSAL CARRIAGE

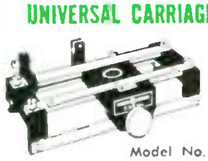

Model No. Z116A

Like the finest camera with a precisely fitted set of lenses, the FXR Universal Carriage and family of five Interchangeable Slotted Sections are matched to perfection. "Togetherness" with this unrivalled modular waveguide system gains new meaning . . . more rapid interchange of each section without tools or need for alignment, and more dependable performance over the entire frequency range from 3.95 kmc to 18.00 kmc. Another fine FXR "package" with quality and reliability built into it—from the first mark on the drawing board.

SERIES 115 PRECISION SLOTTED SECTIONS

MODEL NO.	FREQUENCY RANGE (KMC)	WAVEGUIDE DIMENSIONS (Inches)	INSERTION LENGTH	WAVEGUIDE TYPE	FLANGE TYPE
H115A	3.95- 5.85	2 x 1	$10\frac{3}{8}$ in.	RG-49/U	UG-149A/U
C115A	5.85- 8.20	$1\frac{1}{2} \times \frac{3}{4}$	$10\frac{3}{8}$ in.	RG-50/U	UG-344/U
W115A	7.05-10.00	$1\frac{1}{4} \times \frac{5}{8}$	$10\frac{3}{8}$ in.	RG-51/U	UG-51/U
X115A	8.20-12.40	$1 \times \frac{1}{2}$	$10\frac{3}{8}$ in.	RG-52/U	UG-39/U
Y115A	12.40-18.00	0.622 x 0.311 ID	$10\frac{3}{8}$ in.	RG-91/U	UG-419/U

ACCESSORY: FXR Model No. B200A Tunable Probe.
All units when mounted in Z116A Carriage:
Slope—1.01 max. Irregularity—1.005 max.

Write for Bulletin No. SS115 or contact your local FXR representative.

FXR, Inc.

Design • Development • Manufacture

25-26 50th STREET
WOODSIDE 77, N. Y.

RA. 1-9000
TWX: NY 43745

PRECISION MICROWAVE EQUIPMENT • HIGH-POWER PULSE MODULATORS • HIGH-VOLTAGE POWER SUPPLIES • ELECTRONIC TEST EQUIPMENT *another Sarkes Tarzian production breakthrough!*

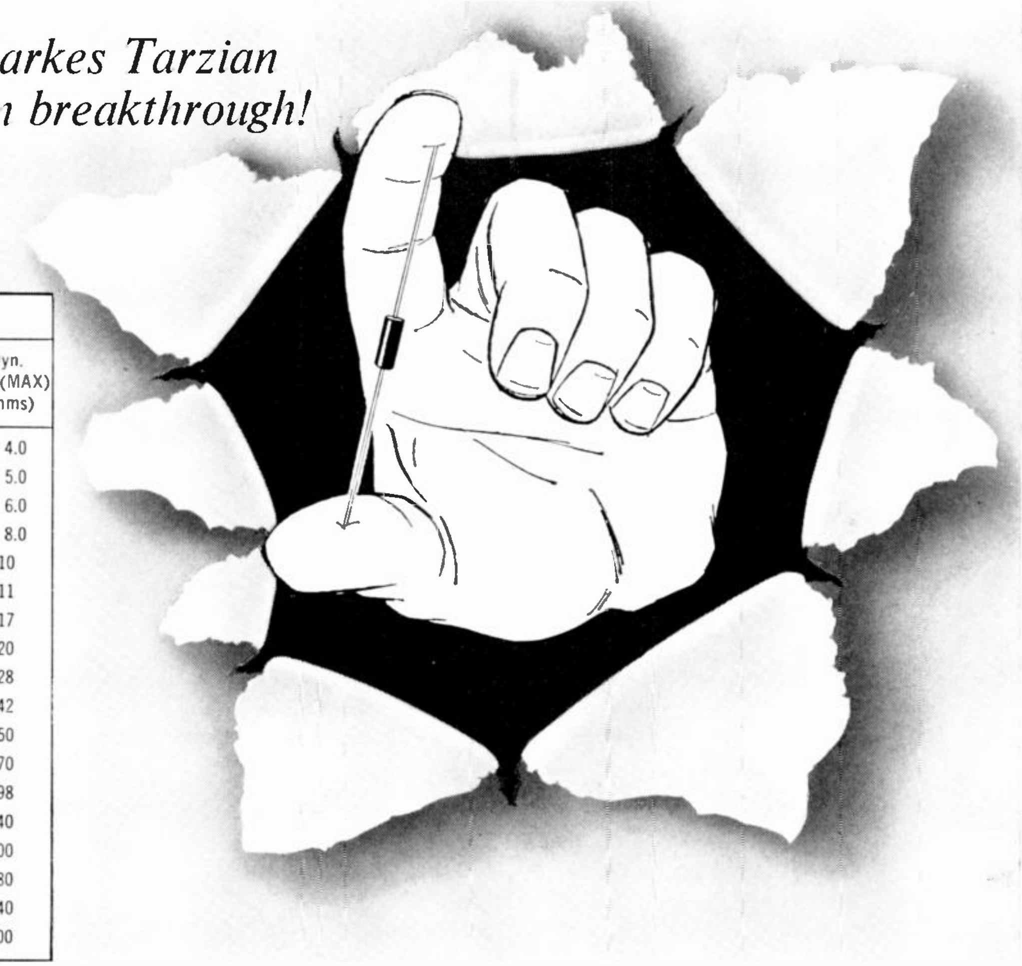

Specifications at 25° C			
Tarzian Type	Zener Voltage (V)	Test Current (MA)	Dyn. Imp.(MAX) (Ohms)
VR6	6	25	4.0
VR7	7	25	5.0
VR8.5	8.5	25	6.0
VR10	10	12	8.0
VR12	12	12	10
VR14	14	12	11
VR18	18	12	17
VR20	20	4	20
VR24	24	4	28
VR28	28	4	42
VR33	33	4	50
VR39	39	4	70
VR47	47	4	98
VR56	56	4	140
VR67	67	2	200
VR80	80	2	280
VR90	90	1	340
VR105	105	1	400

Tarzian Silicon Voltage Regulators now at workday prices

1-watt

Epoxy enclosed

6 to 105 volts, in 20% increments

Standard tolerance is 20%
(all common tolerances available on request)

Immediate availability

Sarkes Tarzian did it in 1957 for silicon rectifiers and has done it again in 1961 for silicon voltage regulators...devised production methods that make it possible to offer quality silicon semiconductor devices at a price level that permits their use not only in Sunday circuits but also in workday circuits.

At the new low prices, more circuits can be better protected or improved in performance by the use of these small and inherently rugged devices as clippers, limiters, and regulators.

Send for price and ordering information.

Where highest quality is in volume production

SARKES TARZIAN, INC.

World's Leading Manufacturers of TV and FM Tuners • Closed Circuit TV Systems • Broadcast Equipment • Air Trimmers • FM Radios • Magnetic Recording Tape • Semiconductor Devices

SEMICONDUCTOR DIVISION • BLOOMINGTON, INDIANA

In Canada: 700 Weston Rd., Toronto 9 • Export: Ad Auriema, Inc., New York

first in the industry

TPS

a complete new miniature UG series coaxial cable connector

DAGE

ACTUAL SIZE

1/3 smaller and lighter than standard BNC series

DAGE manufactured prototypes of a new series miniature connector for the U. S. Army Signal Corps. This series replaces standard BNC connectors used with RG 58 C/U cable.

The TPS series features and exclusive three-pin lock which minimizes rocking of the mated pair and eliminates electrical discontinuity due to shock and vibration. The TPS series is now available in the quantity you need.

Make your connections with DAGE

Write or call for catalog and facilities brochure

DAGE ELECTRIC COMPANY, INC.
Beech Grove, Indiana
STate 7-5305

Industrial Engineering Notes

(Continued from page 40A)

have fixed dimensions or multiples of these fixed dimensions. This method of construction is clearly explained and illustrated in MIL-E-16400D." The Navy, therefore, has adopted the term "electronic assembly" to satisfy the need for an expression to cover all types of easily replaceable portions of electronic equipment regardless of size, shape, or type of construction. The term is defined in MIL-E-16400D as: "A commonly-mounted group of two or more parts combined to perform a specific electronic function, and capable of being easily removed and replaced as an integral item." The instruction points out that there is one main difference between the terms "subassembly," "assembly," and "electronic assembly," as defined in MIL-E-16400D. The first two terms apply to units which are not necessarily easily replaceable, while the latter term includes this feature in its definition. In general, the term "electronic assembly" best applies where "module" was formerly used, according to the instruction. The instruction was issued by the Assistant Chief of The Navy Bureau of Ships for Technical Logistics. It cancels and supersedes Electronics Division Instruction 9670.12 Ser 674 672-43 of January 15, 1960.

Governmental and Legislative

The American Telephone and Telegraph Company last week was authorized to operate experimental radio stations for research on earth-satellite communications. The Federal Communications Commission granted AT&T's application to use a station in Holmdel, N. J., for communications with as many as six satellites to be launched by the National Aeronautics and Space Administration. The operation will be an extension of space research activities jointly conducted by AT&T and NASA under the Echo project. It was the second FCC approval in as many weeks of plans by commercial firms for space communications research. International Telephone and Telegraph Laboratories last week received an FCC go-ahead for a year of tests of bouncing signals off passive satellites and the moon. The AT&T tests were authorized to run until January 1, 1962. During that period, the firm proposes to launch up to six satellites at an estimated cost of $250,000 apiece. Cost of the Holmdel station is estimated at $106,000. The Commission authorized the earth station to operate in the 6325–6425 Mc region and the satellite stations in the 4100–4200 region. At the same time, it denied an AT&T request to use the 6425–6925 Mc band for satellite relay. The FCC order said opening up the band to international fixed public radio services would be premature, a position supported by the EIA Microwave Section. The experimental stations will share frequencies

(Continued on page 47A)

Industrial Engineering Notes

(Continued from page 44A)

with common carriers now operating within the assigned frequencies. The FCC stipulated that AT&T will make special tests to determine the feasibility of frequency sharing by space communications and common carrier operations in the 4000–6000 Mc region. AT&T plans test of communications via the satellites with earth stations operated for space research by the United Kingdom, France, and Germany. In another space communications development, Lockheed Aircraft Corporation recommended that major communications concerns pool funds to form a joint common carrier firm to handle commercial space telecommunications. In a proposal submitted to the FCC, the National Aeronautics and Space Administration, and other agencies involved in communications, Lockheed recommended establishment of an initial jointly owned satellite system estimated to cost about $260 million. Other common carriers would contract for use of the system for world-wide communications. Lockheed said that a thorough study of anti-trust regulations uncovered no rules which might restrict space communications operations by a jointly financed concern. . . . **The Final Eisenhower Budget: What Does It Hold For the Electronics Industry during Fiscal 1962?** DOD—Small but steady increase; NASA—Under $100 million for electronics; FAA—More for EDP, less for radars; FCC—$1 million for UHF TV testing; FTC—Quicker trials of deceptive practices.

Industry Marketing Data

Shipments of electronic components declined about five per cent during the third quarter of 1960, the Electronics Division of the Business and Defense Services Administration has reported. Most of this decline—at a time of year when components output usually reaches the annual peak—was in components shipped for military end-use, BDSA said. Non-military electronic components output, however, failed to show the normal upward movement during the latter half of the year, due to the contra-seasonal leveling-off of consumer electronics equipment output. Only the output of television picture tubes, quartz crystals, and transformers exceeded second quarter levels. Shipments of other components either decreased or remained at second quarter rates during the third quarter. For the second successive quarter, output of semiconductor devices (transistors, diodes and rectifiers, and related devices) declined in value, the agency reported. This decline was entirely due to lower prices, since unit output continued to rise. . . . **Radio sales at retail hit a monthly record of 2,378,853 during December and moved the total for the entire year to 10,705,128—the high for sales during any year since 1948, according to final 1960 statistics**

(Continued on page 194A)

The Highest Sensitivity
and the lowest noise.....

Advanced electronic research by Hitachi technicians has now resulted in the development of a superb frame grid type twin triode (6R-HH8) with excellent high gain and low noise characteristics. As a component of the tuner, the 6R-HH8 ensures an excellent picture with a remarkable degree of definition.

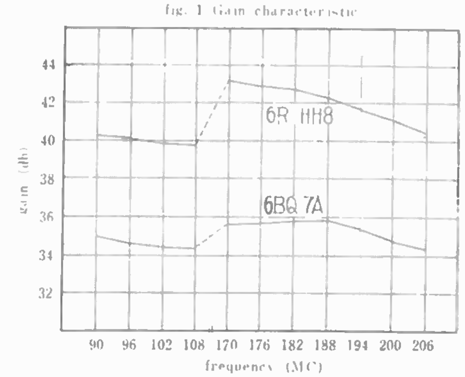

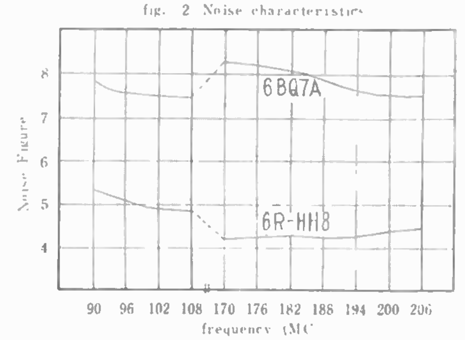

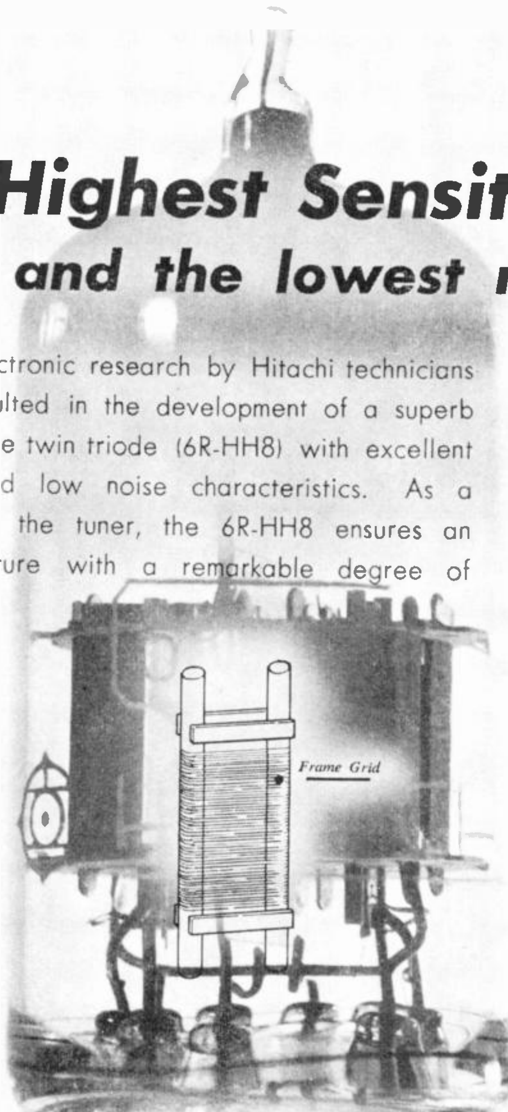

Frame Grid (6R-HH8)

Hitachi also produces other receiving tubes and components for television which, when used together with the new 6R-HH8, cannot fail to earn any maker a market reputation even better than he currently enjoys.

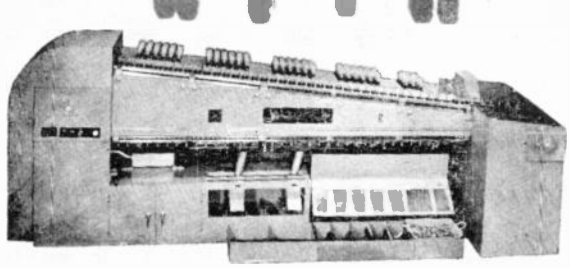

Automatic tube testing equipment

Hitachi, Ltd.

Tokyo Japan

Cable Address: "HITACHY" TOKYO

Industrial Engineering Notes

(Continued from page 47A)

released by the Marketing Data Department. Retail sales for television also reached the highest monthly mark during December, a total of 768,140. For the year, a total of 5,945,045 TV sets were sold to consumers, 196,369 more than during 1959 and the best total since 1957. . . . Factory sales of transistors scored another healthy advance during 1960, following the yearly growth pattern which has characterized the industry since production began, according to year-end totals released by the EIA Marketing Data Department. A total of 127,928,586 transistors valued at $301,132,285 were sold at the factory during the past year. The year before, 82,294,120 units were sold and revenue accrued totaled $222,009,722.

Military and Space

A report describing scientific and engineering problems facing the Navy has been published with the hope that industrial firms and institutions will help solve them. The report, "Navy Research and Development Problems," contains concise descriptions of the problems, their background, and the need for solutions. Included are sections on data processing, electronic sciences, and energy conversion. The publication is available without charge from the Chief of Naval Materiel, Department of the Navy, Washington 25, D. C., Attn: Code M42. . . . Navy scientists have reported successful transmission of radio signals over unusually long distances by guiding the waves through "ducts" in the air formed between dry and wet air layers. Scientists from the U. S. Naval Research Laboratory at Washington, D. C., and the U. S. Navy Electronics Laboratory at San Diego, Calif., transmitted signals from California which were received in Hawaii 2,600 statute miles away. The same signals, if not directed by the air ducts, would have travelled only about 575 miles. Exploring a new phase of radio communication between July 5 and August 25, the Navy scientists used three WV-2 (Constellation) aircraft flying between California and the Hawaiian Islands to investigate elevated duct radio propagation and its correlation with such meteorological phenomena as temperature and humidity. Unusually long range radio transmissions were accomplished using the duct, which follows the boundary between the dry air aloft and the wet air next to the ocean. This boundary climbs from about 1,000 feet over San Diego to 7,000 feet above Hawaii. Basic equipment used in the project, called Trade Winds III, consisted of dual frequency receiver equipment aboard one of the four engined NRL aircraft, very-high frequency transmitter equipment in a second NRL aircraft, NEL transmitters in San Diego and Oahu Island, and the ultra-high-frequency moonbounce transmitter at Oahu. The third WV-2 aircraft, a Navy Pacific Barrier picket plane, gathered additional weather data to assist the experiment.

Both Portable and Stationary

FREQUENCY and TIME STANDARDS

DECADE FREQUENCY SYSTEMS

Generate and Measure Frequencies from Zero to Kilomegacycles with Crystal Accuracy

FEATURES

- Frequency range from d.c. to 12.6 kilomegacycles.
- Accuracy and stability better than 1 x 10^{-9}/day, according to crystal oscillator used.
- Smallest crystal locked step 10 cps.
- Smallest frequency increment 5 millicycles.
- Crystal control steps rigidly locked to frequency standard.
- Continuous variable output voltage from less than 100μv to more than 1 volt.
- Simplicity of operation by small number of front panel controls.

The decade frequency measuring system is based on the principle of the frequency synthesizer, which generates a continuously variable frequency with the accuracy of the driving standard oscillator. Unknown frequencies are measured by heterodyning with this variable reference frequency, and the difference frequency is measured on a precision meter with magnifier. Facilities for recording also are available.

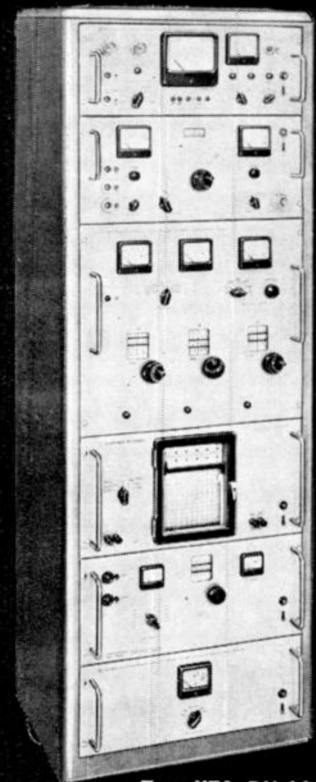

Type XZA BN 444044

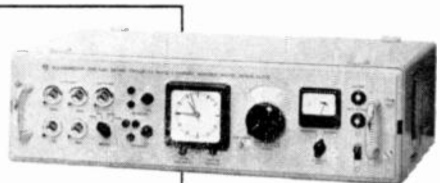

Type CAQ BN 7850

PORTABLE, FULLY TRANSISTORIZED FREQUENCY AND TIME STANDARD

STANDARD TIME SYSTEMS

Permits Measurement of Drift in Frequency Standards by means of Comparison of Time Signals

FEATURES

- This system embodies more than 20 years' experience in the field of time and frequency standards.
- Simplicity of operation obtained by completely integrated system.
- Special time-comparison oscilloscope for photographic logging.
- Emergency power supply prevents loss of calibration due to line failure.
- Special accessories, such as sidereal time converters, are available.

The standard time system generates a time signal, derived from the frequency standard, for comparison with time signals from WWV, etc., on a special time-comparison oscilloscope. Daily log without calculation may be kept by a photographic recording. The system provides frequency divider, motor-driven phase shifter, and all-wave receiver for time signals from 14 kc to 28 mc. Frequency standard has built-in servo system for remote control from VLF standard frequency by means of a phase comparator.

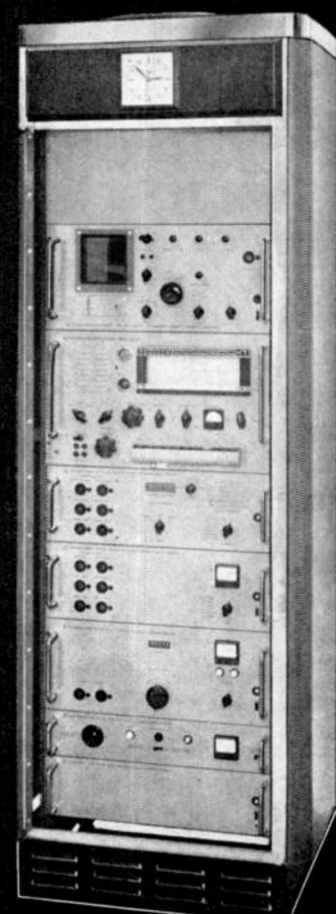

Type CAA BN 78012

ROHDE & SCHWARZ
111 Lexington Ave., Passaic, N. J. • PRescott 3-8010

Professional Group Meetings

Aerospace and Navigational Electronics

Boston—January 24

"Lightweight Inertial Navigation Systems," S. S. Kolodkin, RCA, Burlington.

Metropolitan New York—January 12

"The Changing Face of General Aviation," C. L. Cahill, Aircraft Radio Corp., Boonton, N. J.

Oklahoma City—October 24

"Cockpit Indicators for Instrument Navigation," L. C. Keene, American Airlines Jet Maintenance and Engineering Center, Tulsa, Okla.

"Differences in Engineering Requirements and Philosophy between Commercial and Military Aircraft," L. C. Keene.

Oklahoma City—June 21

"The FAA Glide Slope," J. Park, Federal Aviation Agency.

"The FAA Localizer," W. Dunn, Federal Aviation Agency.

Antennas and Propagation

Boston—January 25

"Radar Exploration of the Solar Atmosphere," J. H. Chisholm, Lincoln Laboratory.

"Design of Cassegrain and Gregorian Antennas," D. H. Archer, Raytheon, Bedford.

Los Angeles—January 12

"Data Processing Antennas," A. A. Ksienski, Hughes Aircraft Co., Culver City, Calif.

"Information Theory and Antenna Design," G. O. Young, Hughes Aircraft Co., Culver City, Calif.

San Francisco—January 11

"Some Recent Antenna Inovations," J. W. Carr, Lockheed Missile & Space Division, Sunnyvale, Calif.

Washington, D. C.—January 17

"Effect of a Re-Entry Plasma Sheath on the Performance of a Slotted Sphere Antenna," J. W. Marini, University of Maryland.

Tour of the Antenna Laboratory and Physical Sciences Laboratory of Melpar, Inc.

Antennas and Propagation Microwave Theory and Techniques

Columbus—November 15

"Log Periodic Antennas and Circuits," R. H. DuHammel, Collins Radio Co., Cedar Rapids, Iowa.

(Continued on page 52A)

Professional Group Meetings

(Continued from page 51A)

Philadelphia—January 11

"Performance of 2 Monopulse Antennas," E. S. Lewis, RCA, Moorestown.

"Antennas Boresighting in Fresnal Zone or by Auto Collimation," A. J. Bogush, RCA, Moorestown.

San Diego—January 16

"Satellite Signals Received at Trans-horizon Distances," L. J. Anderson, Smythe Research Associates, San Diego, Calif.

Audio

Philadelphia—January 25

"Power Amplifiers for High Fidelity," B. de Palma, formerly of Dynakit.

Automatic Control

Dallas-Fort Worth—January 23

"RH-2 Digital Flight Control Computer," R. D. Watson, Bell Helicopter Co., Hurst, Texas.

Los Angeles—January 10

"Atlas Control System and Mercury Abort and Pilot Safety System," R. Goad, D. R. White, Space Technology Labs., Arbor Vitae St., Los Angeles, Calif.

Milwaukee—February 7

"Automatic Control Applied to Industrial Processes," W. E. Korsan, Allis-Chalmers Co., West Allis, Wis.

Bio-Medical Electronics

Boston—January 17

"Modern Theories of Hearing," Dr. N. Y-S. Kiang, MIT and Massachusetts Eye and Ear Infirmary.

Columbus—January 10

"Physiological Instrumentation of Man in Space," Capt. G. Poter, U. S. Air Force, Wright-Patterson AFB, Ohio.

Memphis—January 6

Business Meeting—Officers voted on and accepted; bylaws voted on and accepted.

Philadelphia—November 17

"Highly Sensitive Spectrophotometer for Cellular and Sub-Cellular Instrumentation," Dr. R. Perry, Institute for Cancer Research & the Johnson Foundation; J. Cowles, The Johnson Foundation.

Broadcasting

Florida West Coast—January 25

"Transistors Related to Vacuum Tubes," A. C. Brunner, Electronic Communications, Inc., Saint Petersburg, Fla.

(Continued on page 56A)

AVAILABLE NOW...

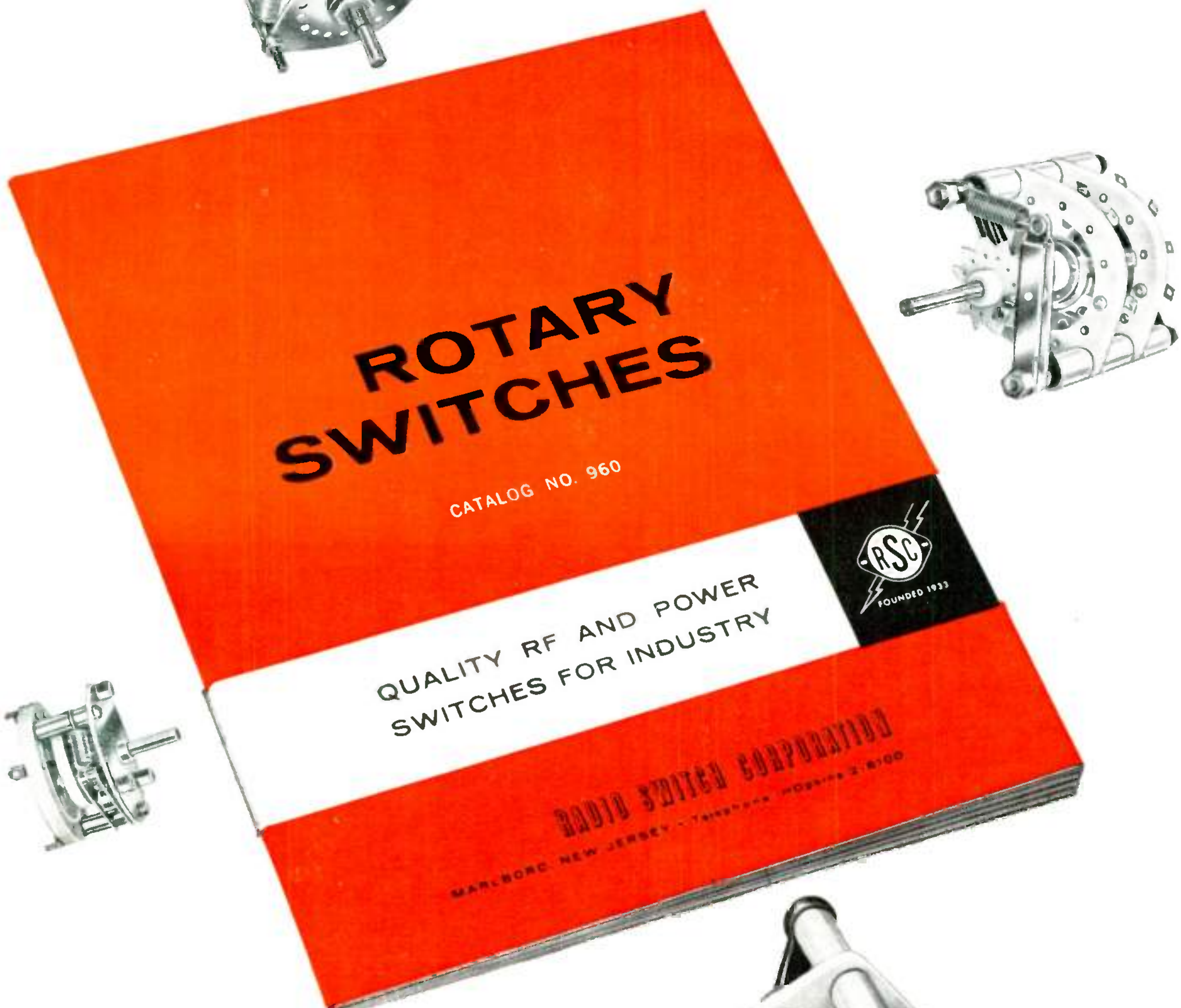

Request your copy today!

The new 1961 RSC Catalog No. 960 will be of interest to every designer and engineer concerned with radio frequency and power switching. It contains complete specifications on each switch in the RSC Line. Write for your copy today.

RCA AIRBORNE SINGLE SIDEBAND

Performance proven in Operation "Deep Freeze"

RCA's single sideband modification of the 618S-1 high frequency communication equipment has demonstrated proven capability under actual flight operations during Operation "DEEP FREEZE," now being conducted jointly by the U. S. Navy and U. S. Air Force, with the support of MATS.

The RCA concept of modifying proven, existing equipments, such as the AN/ARC-65, has resulted in the most economical approach to the utilization of single sideband performance capabilities. The 618S-1/MC and AN/ARC-38A SSB modifications are the latest additions to the family of RCA Communications Equipments now providing extra capability to meet present and future military and civil operational communications requirements.

Several thousand RCA Airborne Single Sideband Equipments are now in flight operation.

For further information on the 618S-1/MC, AN/ARC-38A, and other airborne communication equipments write: Marketing Dept., Airborne Systems Division, Defense Electronic Products, Radio Corporation of America, Camden 2, New Jersey.

The Most Trusted Name in Electronics
RADIO CORPORATION OF AMERICA

THE IMPROVED
MINCOM
SERIES CM-100
1.2 mc

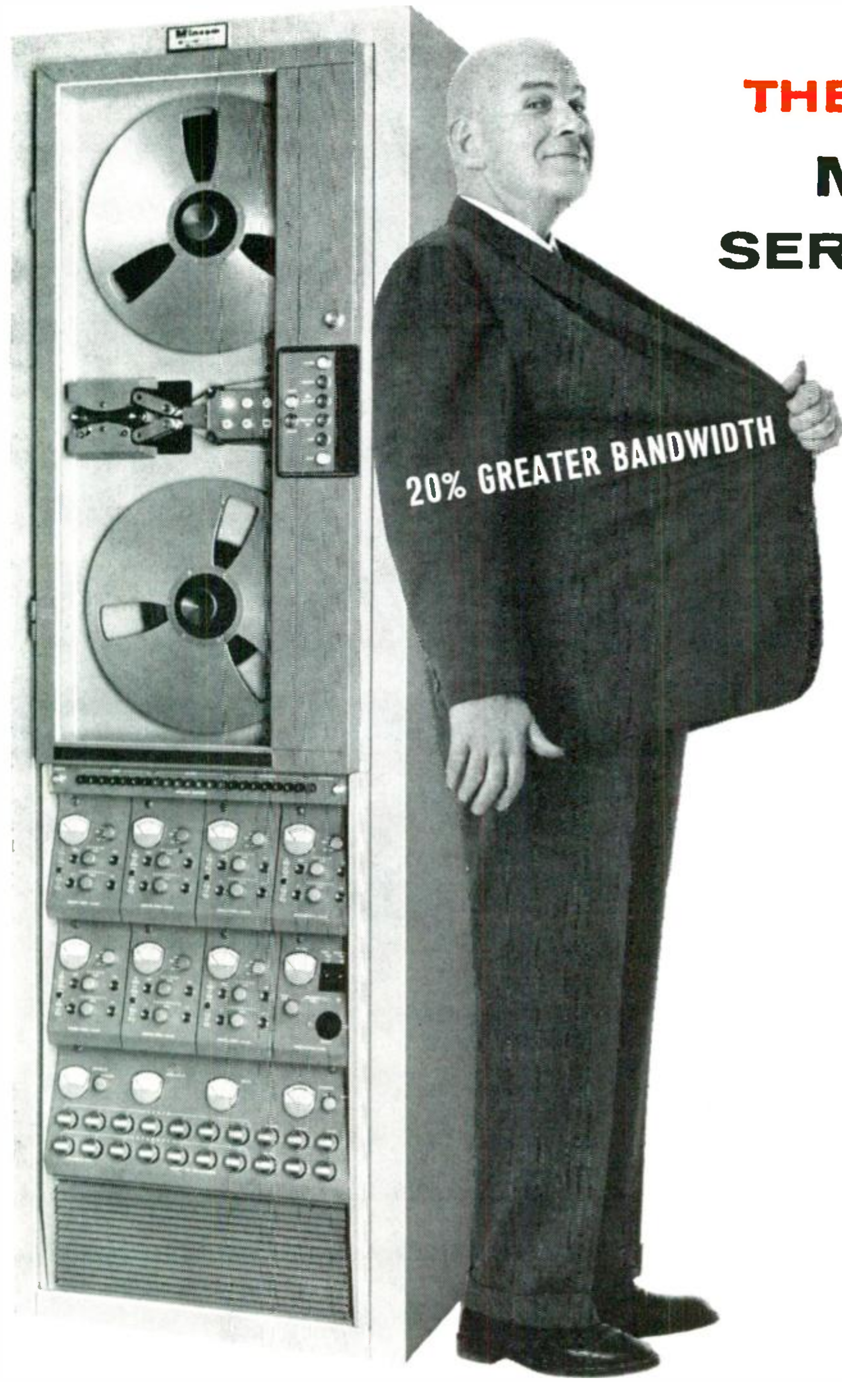

At 120 ips the Mincom Series CM-100 now delivers 1.2 mc with the same reliability that has been typical of Mincom's 1-megacycle performance for years. 20% extended bandwidths also are obtained at CM-100's other five speeds (see table at right). Tape previously recorded at 1 mc can be played back on the CM-100 with improved reproduction. Consistently good pulse response, due to constant phase equalization at all speeds, enables this system to perform predetection recording/reproducing on an operational basis—in FM, FM/FM modulation, PCM and PCM/FM. Plug-in rack easily converts CM-100 from 7 to 14 tracks. Write for brochure and specifications.

New Series CM-100 Frequency Response

7½ ips— 75 kc	30 ips—300 kc
12 ips—120 kc	60 ips—600 kc
15 ips—150 kc	120 ips—1.2 mc

3M COMPANY . . . WHERE RESEARCH IS THE KEY TO TOMORROW

MINCOM DIVISION **MINNESOTA MINING AND MANUFACTURING COMPANY**

2049 SO. BARRINGTON AVE., LOS ANGELES 25, CALIFORNIA • 529 PENN BLDG., 425 13th STREET N.W., WASHINGTON 4, D.C.

Professional Group Meetings

(Continued from page 52A)

Philadelphia—January 12

"Development of TK Image-Orthicon Camera," J. Rhoe, RCA, Camden.

San Francisco-Sacramento—January 10

"Bauer AM Transmitters (1 KW & 5 KW)," P. Gregg, Bauer Electronics Corp., San Carlos, Calif.

Broadcasting Vehicular Communications

Florida West Coast—January 25

"Transistors Related to Vacuum Tubes," A. C. Brunner, Electronic Communications, Inc., St. Petersburg, Fla.

Circuit Theory

Syracuse—January 10

"Adaptive Waveform Recognition," Dr. C. V. Jakowatz, General Electric Co., Schenectady, N. Y.

Communications Systems

San Francisco—November 23

"Step Frequency Sounders for High Frequency Communications," L. Seader, Granger Associates, Palo Alto, Calif.

Toronto—November 3

"The Use of Microwave to Support a High Altitude Platform," Dr. R. L. McFarlan, IRE.

Toronto—September 22

"Manning and Operation of Microwave Systems in Arctic and Sub-Arctic Areas," Col. B. A. Rorholt, Norwegian Joint Signals Administration.

Communications Systems Military Electronics

Rome-Utica—November 15

"Lasers," Dr. R. C. Mack, Hughes Aircraft Co., Culver City, Calif.

Component Parts

Washington—November 9

"Infra-Red," C. Ravistky, Diamond Ordnance Fuze Labs., Washington, D. C.

(Continued on page 60A)

The 1961 IRE DIRECTORY
Bigger and better than ever! Use it!

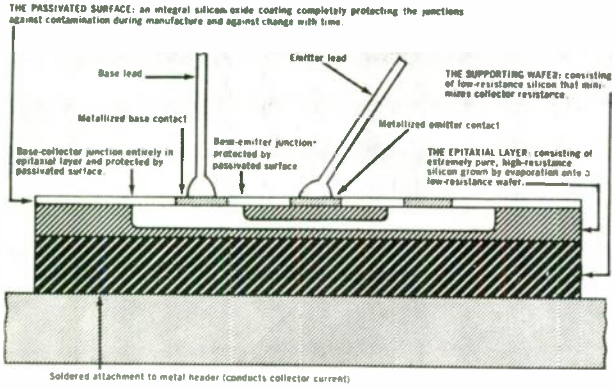

Silicon PLANAR epitaxial cross section

PLANAR

- GREATEST RELIABILITY, STABILITY AND UNIFORMITY
- LOWEST GUARANTEED I_{CBO}

EPITAXIAL

- LOWEST GUARANTEED V_{CE} (sat)
- HIGHER MAXIMUM I_C
- NO SACRIFICE IN VOLTAGE BREAKDOWN

COMBINED IN ONE TRANSISTOR
FAIRCHILD SILICON 2N914

This combination means extremely fast propagation time in digital circuits, excellent high-frequency response in amplifiers, high-speed performance in current drivers. Typical f_T is 300 mc.

To the EPITAXIAL advantages, PLANAR adds extreme stability, reliability, low leakage and low noise figure. PLANAR and EPITAXIAL TOGETHER achieve usable current gain over a broader current range than either alone.

ELECTRICAL CHARACTERISTICS AT 25°C—2N914

	Min.	Max.	Conditions
h_{FE}	20	80	I_C 10mA, V_{CE} = 1.0V
BV_{CBO}	40V	—	I_C = 10μA, I_E = 0
BV_{EBO}	5 0V	—	I_E = 10μA, I_C = 0
V_{CE} (Sat)	—	0.18V	I_C = 10mA, I_E 1mA
V_{CE} (Sat)		0.7V	I_C 200mA, I_B 20mA
h_{fe}	3		I_C 10mA, f 100mc
C_{ob}		6pf	V_{CB} 10V, I_E = 0

Write for full specifications.

FAIRCHILD
SEMICONDUCTOR CORPORATION

545 WHISMAN ROAD, MOUNTAIN VIEW, CALIF.·YORKSHIRE 8-8161·TWX: MN VW CAL 853
A wholly owned subsidiary of Fairchild Camera and Instrument Corporation

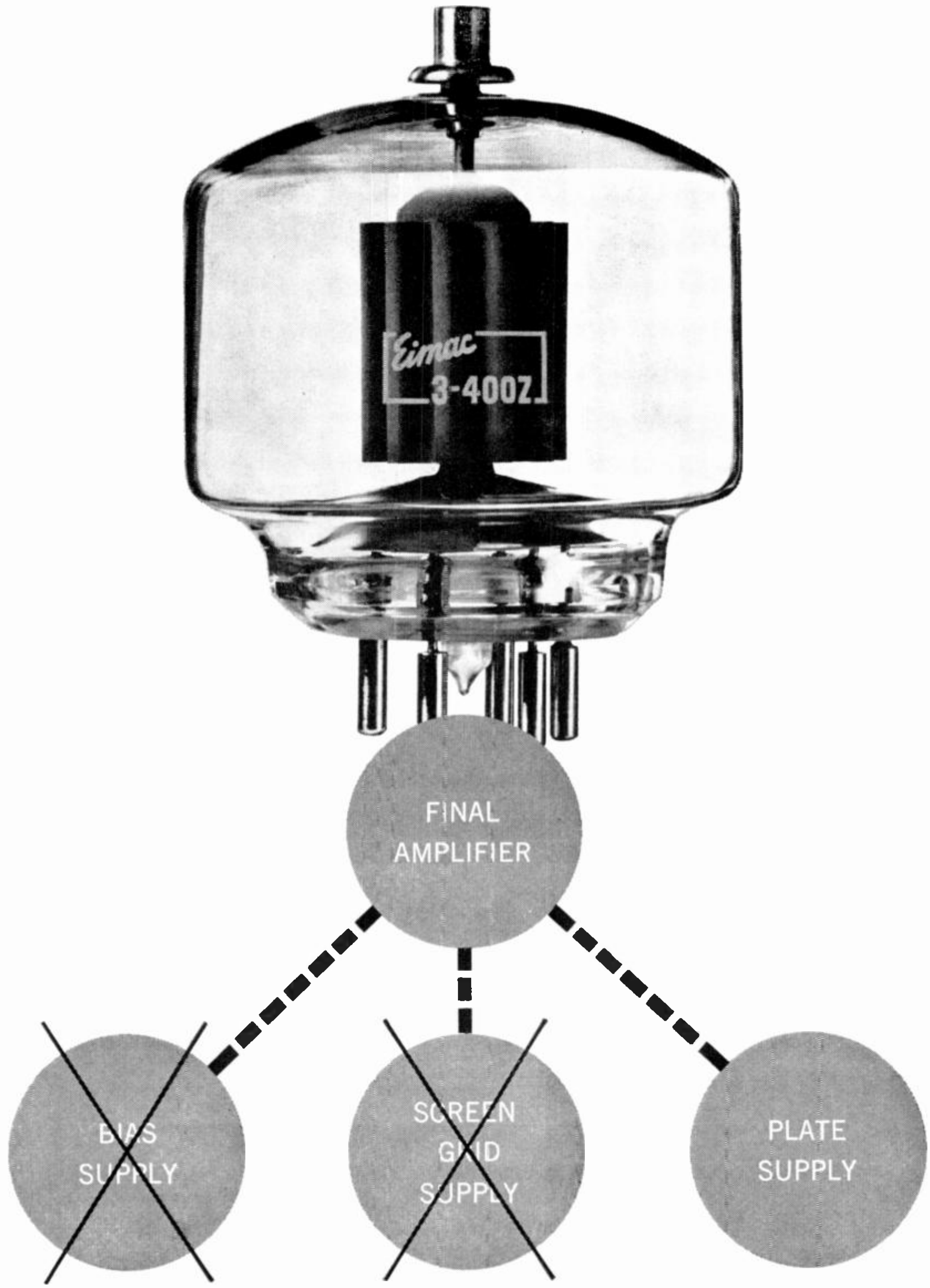

Cross off two power supplies with one of Eimac's new zero-bias triodes!

Another major advance from Eimac: the first high power zero-bias triodes anywhere. Just one of these new tubes will eliminate *both* screen grid and bias power supplies to simplify your circuit designs. Take your pick of the 3-400Z, shown above actual size, (plate dissipation: 400 watts) ... the 3-1000Z (1000 watt plate dissipation) ... the ceramic-metal 3CX10,000A7 (10,000 watt plate dissipation). Each offers a power gain of over *twenty times* in grounded grid service. And their small size accommodates today's lower, more compact equipment. You'll find these zero-bias triodes ideal for class B RF and audio amplifiers. And you'll find them *only* at Eimac...world leader in transmitting tubes. For ratings, specifications, other details, write: Power Tube Marketing, Eitel-McCullough, Inc., San Carlos, California.

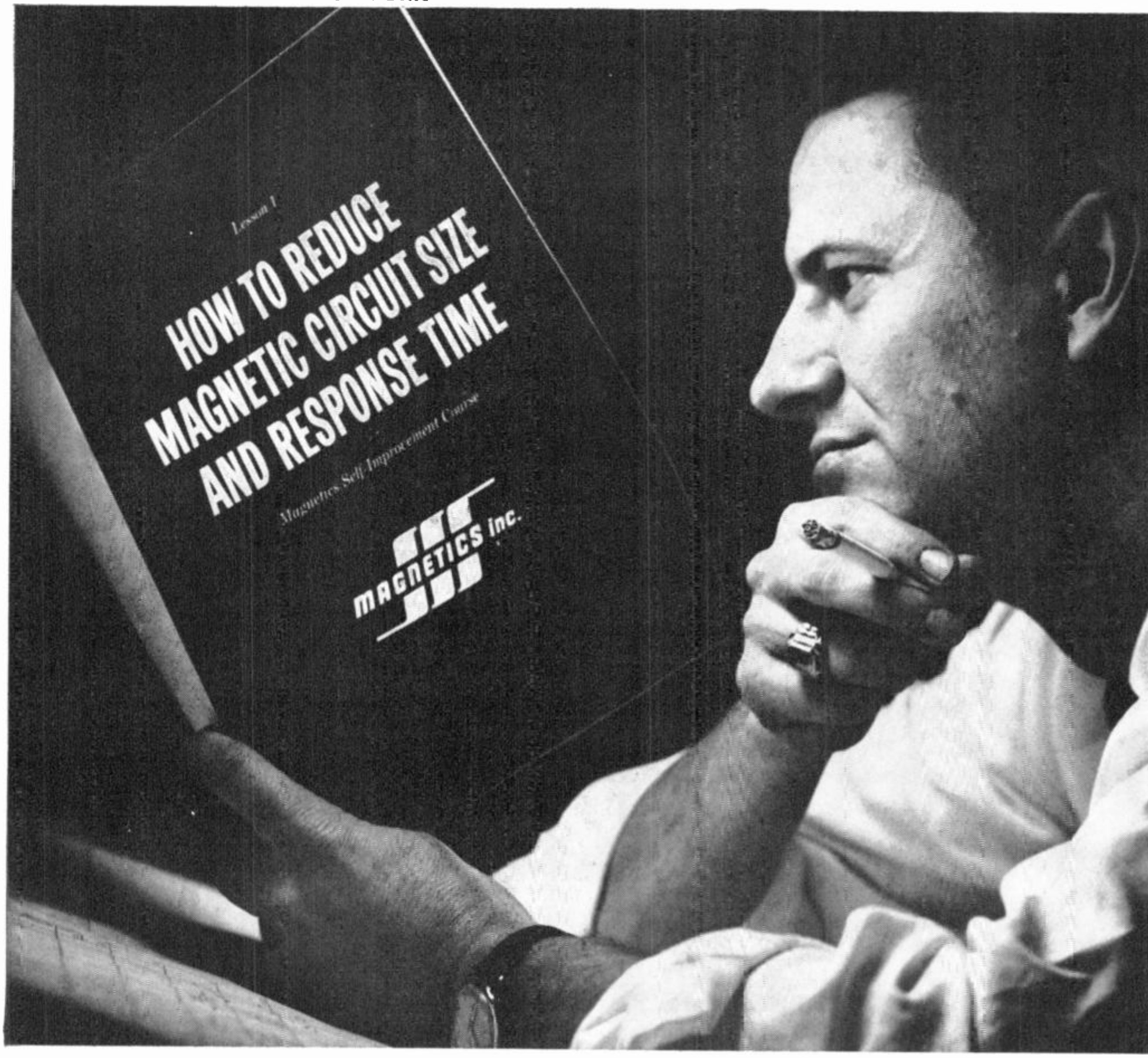

Sign up for the Magnetics self-improvement course:

Here's free help to enable you to improve yourself—and your position as a magnetic circuit designer. You need it if:

You don't know how to work with $E = n\frac{d\phi}{dt}$ to reduce the size of magnetic amplifier circuits. Most men who design amplifiers for cramped operation in missiles have found it invaluable.

What's more, you may only vaguely remember $H = .4\pi\frac{NI}{\ell_m}$, so how can you use it to cut circuit size by two to ten times, and shorten response time proportionately?

It's quite possible that you, like many engineers, may have bypassed or been bypassed by magnetic circuit theory *as a working tool* while you were in school. Yet this science has opened frontiers of static control which makes an understanding imperative if you are to do your job—and further your career. For your sake (and for ours, too, because we manufacture and sell high permeability tape wound cores and bobbin cores which are used in amplifier circuits), we have started this course. Lesson 1, "How to Reduce Magnetic Circuit Size and Response Time," will be on its way to you immediately if you use the coupon below.

MAGNETICS inc. ®

MAGNETICS INC., DEPT. P-86, BUTLER, PA.

Please enroll me in your free self-improvement course, and send me "How To Reduce Magnetic Circuit Size and Response Time."

name____________________

title____________________

company____________________

address____________________

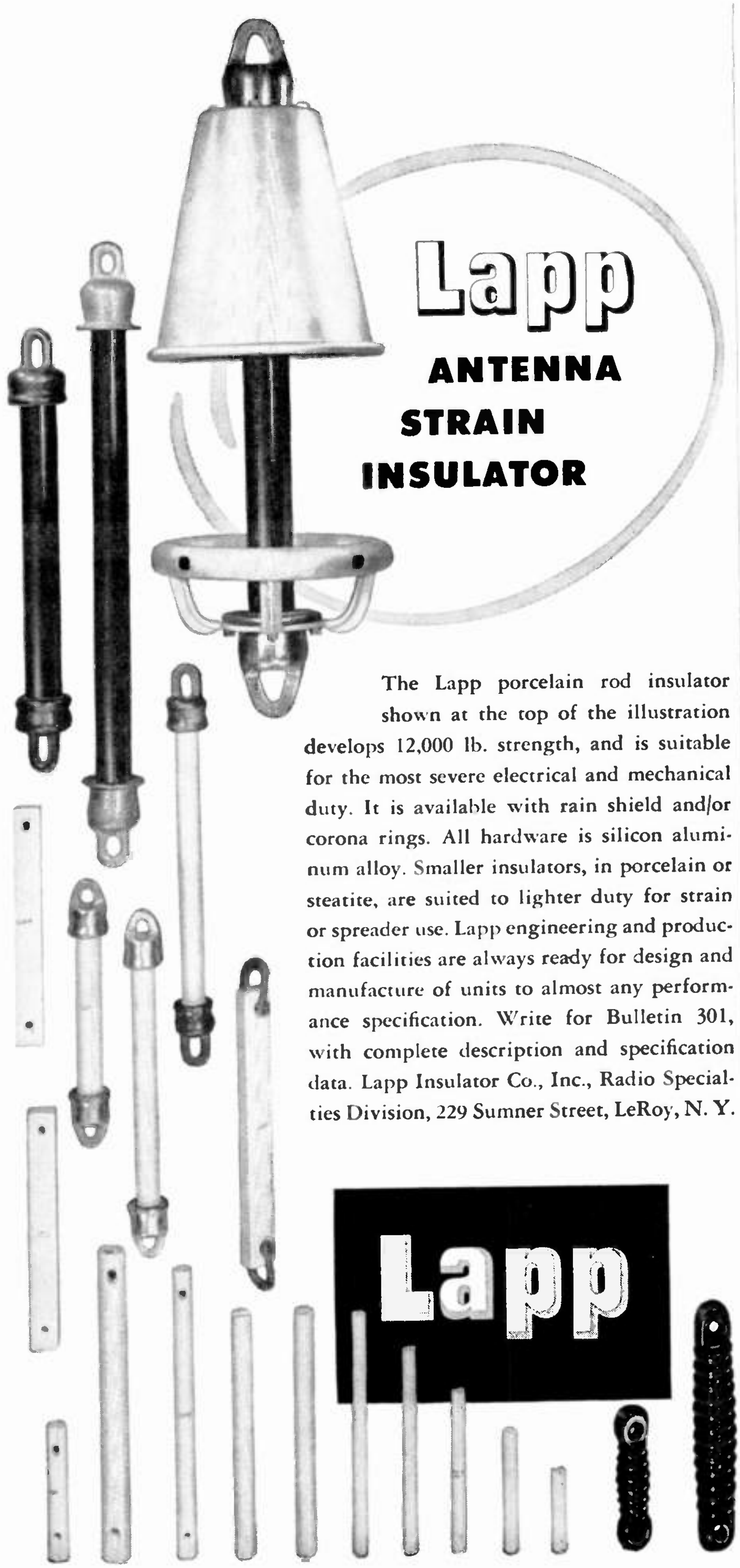

The Lapp porcelain rod insulator shown at the top of the illustration develops 12,000 lb. strength, and is suitable for the most severe electrical and mechanical duty. It is available with rain shield and/or corona rings. All hardware is silicon aluminum alloy. Smaller insulators, in porcelain or steatite, are suited to lighter duty for strain or spreader use. Lapp engineering and production facilities are always ready for design and manufacture of units to almost any performance specification. Write for Bulletin 301, with complete description and specification data. Lapp Insulator Co., Inc., Radio Specialties Division, 229 Sumner Street, LeRoy, N. Y.

Professional Group Meetings

(Continued from page 56A)

Component Parts Product Engineering and Production

Los Angeles—January 9

"Microcircuitry with Tantalum Thin Films," Dr. L. J. Vernerin, Jr., Bell Telephone Labs., Murray Hill, N. J.

"Thin Film Circuit Techniques," B. Solow, International Resistance Co., Philadelphia, Pa.

Electron Devices

Los Angeles—January 10

"The Ruby Optical Maser," Dr. G. Birnbaum, Hughes Res. Labs., Malibu, Calif.

Metropolitan New York—December 1

"Epitaxial Diffused Transistors," Dr. H. H. Loar, Bell Telephone Labs.

Metropolitan New York—October 20

"Pinch Plasma Engine," C. Cavalconte, Republic Aviation Corp., Farmingdale, N. Y.

San Francisco—January 25

"The Application of Mass Spectrometry, and Emission Spectroscopy, to the Manufacture of Vacuum Tubes," R. D. Culbertson, Eitel-McCullough, Inc., San Bruno, Calif.

Washington, D. C.—January 23

"The Superconducting Tunneling Diode," K. Mergerle, General Electric Res. Lab., Schenectady, N. Y.

Electron Devices Microwave Theory and Techniques

Boston—January 12

"Closing the Spectrum-Areas for Research and Development in the Millimeter Wavelength Region," G. S. Heller, MIT.

Electronic Computers

Los Angeles—January 19

"Survey of Guidance Computers," C. King, Space Technology Labs.

Los Angeles—December 15

"Sub Microsecond Magnetic Memories," Dr. A. L. Houde, Aeronutronics, Newport Beach, Calif.

Los Angeles—November 17

"UNIVAC Real Time 1106," D. Cota, Remington Rand Corp.

(Continued on page 62A)

HOW TO GET 380 mw at 250 mc

250 MC PUSH-PULL POWER AMPLIFIER

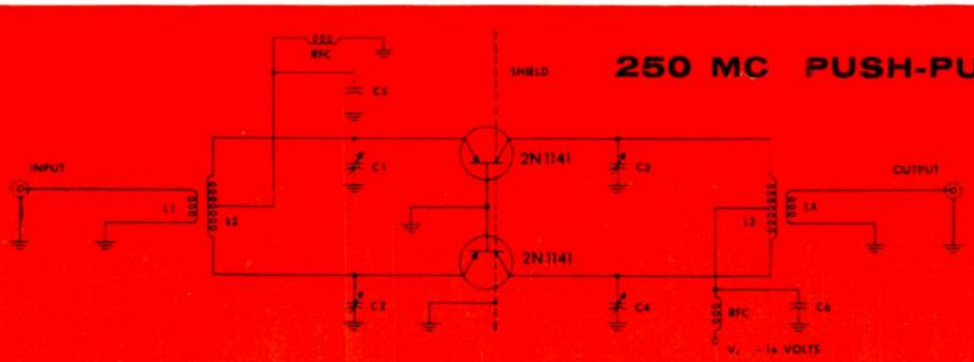

C1, C2, C3, C4 = 3—12pf CTC Trimmer Cap.
C5, C6 = 1000 pf Sprague T. V. Bypass Cap.
L1 = 4 turns No. 18 tinned copper wire; $\frac{9}{16}$" diam.; $\frac{1}{2}$" length
L2 = 6 turns No. 18 tinned copper wire; $\frac{3}{8}$" diam.; $\frac{7}{16}$" length
L3 = 6 turns No. 18 tinned copper wire; $\frac{3}{8}$" diam.; $\frac{7}{16}$" length
L4 = 2 turns No. 18 tinned copper wire; $\frac{9}{16}$" diam.; $\frac{1}{4}$" length

Power in = 30 mw
Power out = 380 mw
V_{CB} = −25 v
I_c = −42 ma

Use TI 2N1142 transistors if only 330 mw output is required.

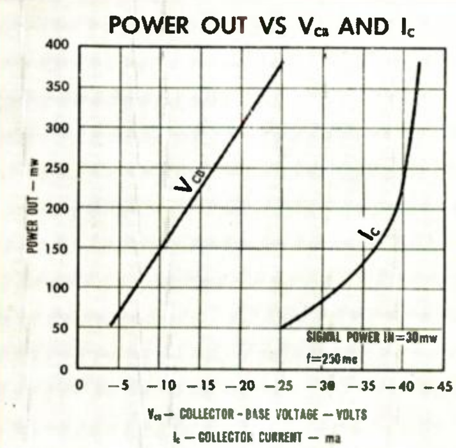

Specify TI 2N1141 P-N-P Germanium Mesa Transistor Series

Design-in Texas Instruments 2N1141 series transistors to obtain 380 mw output at 250 mc from your power amplifiers in telemetering applications in missiles and military communication systems.

TI 2N1141, 2N1142, 2N1143 germanium mesa transistors providing maximum dissipation of 750 mw at 25°C case temperature, 35 volts at 100 μa I_C, and f_{max} to 750 mc are ideal for your VHF power amplifier and oscillator circuits.

Order these TI "Tailored-to-the-Task" 2N1141 series devices *today* from your nearby authorized Texas Instruments distributor. Call him or your local TI sales engineer for price and delivery information including a detailed report on 2N1141 applications.

TYPICAL CHARACTERISTICS AT 25°C	2N1141	2N1142	2N1143
TYPICAL COMMON-EMITTER SHORT CIRCUIT FORWARD CURRENT TRANSFER RATIO AT 100 mc h_{fe}	13.5 db	11.5 db	9.5 db
TYPICAL MAXIMUM FREQUENCY OF OSCILLATION f_{max}	750 mc	600 mc	500 mc
TYPICAL COLLECTOR-BASE TIME CONSTANT $r_b' C_c$	30 ohm-$\mu\mu$f	40 ohm-$\mu\mu$f	50 ohm-$\mu\mu$f

Specify TI Germanium Transistors For Your: Computer / Power Supply / Communication / Industrial Control / Entertainment • Applications

IN TI DISTRIBUTOR STOCKS
3D
DEPTH - DELIVERY - DEPENDABILITY

SEMICONDUCTOR-COMPONENTS DIVISION

TEXAS INSTRUMENTS
LIMITED
DALLAS ROAD • BEDFORD, ENGLAND

TEXAS INSTRUMENTS
INCORPORATED
P. O. BOX 5012 • DALLAS 22, TEXAS

Professional Group Meetings

(Continued from page 60A)

New York and Northern New Jersey—January 5

"The Future of Computers—Fact or Fiction," (Panel Discussion) Prof. J. McCarthy, MIT; Prof. I. Azimov, Boston University; Dr. H. Gresch, Consultant.

New York and Northern N. J.—November 22

"An All-Digital Servo System," M. J. Dunne, Consolidated Controls, Bethel, Conn.

Philadelphia—January 10

"The Newest Development in Electronic Switching in the Bell System," B. I. Yokelson, Bell Telephone Labs.

Pittsburgh—October 25

"University of Pittsburgh plans for IBM 7070," W. B. Kehl, University of Pittsburgh, Pittsburgh, Pa.

"Rolls-Royce plans for IBM 7070," A. H. Helman, Rolls-Royce, Ltd., Derby, England.

Twin Cities—January 10

"Applications of Tunnel Diodes to High Speed Digital Computers," Dr. M. Lewin, RCA Sarnoff Res. Lab., Princeton, N. J.

"Instrumentation for Tunnel Diode Development," B. Lechner, RCA Sarnoff Research Lab., Princeton, N. J.

Engineering Management

Boston—January 19

"Management Problems in Small Electronics Companies," Dr. H. Krentzman, Northeastern University, Boston, Mass.

Boston—December 15

"Decision Making in Business Management and the Role of the Digital Computer," Prof. J. W. Forrester, M.I.T., Cambridge, Mass.

Los Angeles—January 5

"Investing in Small Electronics Firms," R. T. Silberman, Electronic Capital Corp., San Diego, Calif.

Los Angeles—November 18

"Computer Implementation of Project Management as Applied to the Polaris Missile Program," J. G. Sliney, Admiral, USN (ret.), Hughes Aircraft Co., Culver City.

Engineering Writing and Speech

Northern New Jersey—January 18

"Editing Your Own Writing," E. H. Ehrlich, Columbia University, New York, N. Y.

(Continued on page 64A)

Kodak reports on:

a definition of "very good"... a little literature before the 11 o'clock news... kits for oscillographers

High-fi photography for highbrows

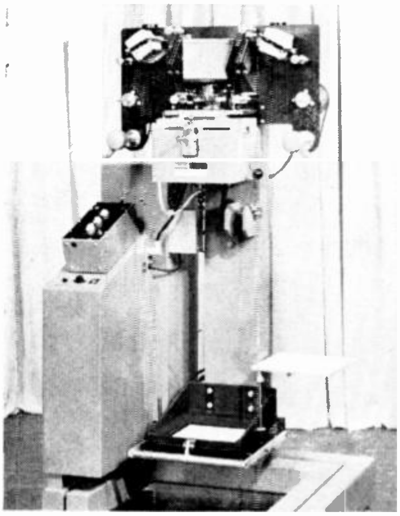

This enlarger was custom-built. The client's affairs are of such a nature that to supply him with anything short of the best-performing merchandise that money can buy could have disastrous consequences for all men of good will. The enlarger is a link in an astonishing chain on which much depends.

It is indeed a very good enlarger. We are tempted to resort to the cant of the times and call it a breakthrough in enlargers. We shall resist the temptation because we hate to lie. Nothing as climactic as a "breakthrough" has occurred in enlargers.

The reason it's a very good enlarger (the best in the world, we hope) is that some years ago it became apparent that descriptions like "very good" don't help much in dealing with such problems and that more precise-sounding terms like resolving power don't tell a full and honest story either. Progress came when we adopted the *weltanschauung* of the sound engineer, of all people!

Can you imagine the audacity of treating a photographic lens or a photographic emulsion or a combination of the two as though it were a loudspeaker or a telephone line and developing equations for its sine-wave frequency response? Yet this is what we were forced to do and it worked. The enlarger above can prove that it worked. The photographic-emulsion men and the lens men are given a common language, which they had lacked. The frequency response of a combination as in the above enlarger can be cascaded with the frequency response of other elements in the total picture-handling system, including the electronic, if any.

We have good reason to want to convince you that this nonsense is not as foolish as it sounds. We think that in the long run we shall be better off if we let you in on the principles by which we design a photographic *system* even though, under certain circumstances, we wish you would let us (George's successors) do it for you.

Education had best begin by studying a review paper, "Methods of Appraising Photographic Systems," by one of our men who has been up to his ears in this subject for a couple of decades. Get your free copy from Eastman Kodak Company, Apparatus and Optical Division, Rochester 4, N. Y. Freshman calculus and doggedness required.

A primer for metallography

You would think we had nothing better to do than write letters and be friendly, helpful, and cheerful.

Though this policy hasn't sunk us yet, we do go through motions to put the dispensing of technical photographic wisdom on a slightly self-sustaining basis. For those who have not yet delved deep enough to frame specific questions, we publish what we call *Kodak Data Books* and print on the cover a small cash price, like 50¢.

Recently issued is a new one, "Photomicrography of Metals." It contains 13 pages on the metallographic microscope (unbiased toward any particular make of instrument, since we are not in that business), 3 pages on illumination, 5 on filters, 3 on photographic materials (which we do make), 5 on exposure determination, and 8 on processing and printing—just enough for thoughtful perusal between the evening paper and the 11 o'clock news. The pages are meaty; the illustrations are there to explain, not just fill space; the author (anonymous) is a photomicrographer, not an ad-writing hack.

Theoretically the purchase of these data books from your Kodak dealer draws him and you closer together. Those willing to forego the personal touch can obtain them from Special Sensitized Products Division, Eastman Kodak Company, Rochester 4, N. Y., which is also the place to address specific questions.

1000 feet, no smell

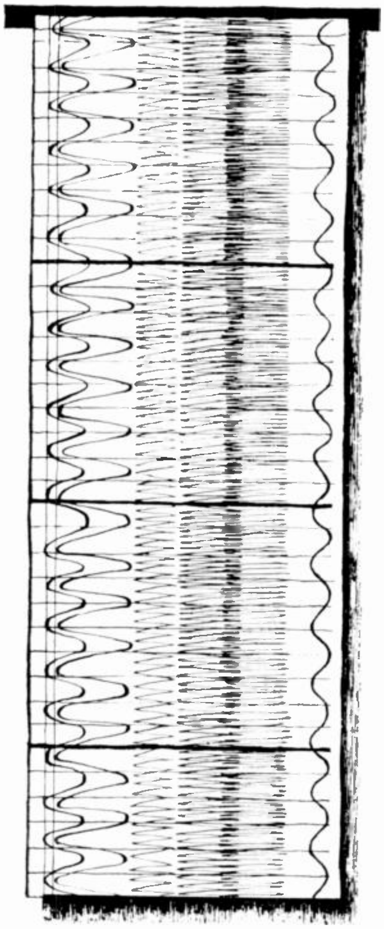

Doing paper oscillograms in a stabilization processor?

We have advice for you.

Get a supply of Kodak Linagraph 1000 Processing Kits. They're new, based on a new chemical idea.

Each one supplies a chemical loading to do two 475-foot rolls of 12-inch paper

WITHOUT POOPING OUT, WITHOUT REDUCING SPEED.

Records look magnificent

AND THERE IS NO PROCESSING SMELL.

Get some "1000" kits from your usual source of Kodak Linagraph photorecording supplies. See and smell for yourself.

This is another advertisement where Eastman Kodak Company probes at random for mutual interests and occasionally a little revenue from those whose work has something to do with science

Kodak
TRADE MARK

Professional Group Meetings

(Continued from page 62A)

Northern New Jersey—November 16

"Taking the Pain Out of Report Writing," C. W. Sall, RCA, Camden, N. J.

Northern New Jersey—October 19

"How to Write Effectively for Engineering Magazines," J. Lippke, Electronic Design, New York, N. Y.

San Francisco—January 17

"The Preparation and Writing of Successful Proposals," Panel Members—C. A. Smith, Sylvania EDL; R. R. Faerber, IBM; W. G. Notz, Philco WDL; M. Grushkin, Lenkurt; N. James, LMSD; J. E. Bert, U. S. Army Signal Electronic Research Unit; P. M. Reinhardt, Sylvania RSL.

Human Factors in Electronics

Los Angeles—January 10

"Panel Discussion on System and Equipment Maintainability," Lt. Col. B. McKown, BMC, Inglewood, Calif.; Dr. D. Meister, Convair Astronautics, San Diego; T. B. Slattery, TEMPO, GE, Santa Barbara; A. Kurth, BMC, Inglewood, Calif.

Information Theory

Boston—December 5

"Communication Theory and Optics," E. L. O'Neill, Boston University, Boston, Mass.

Instrumentation

San Francisco—January 12

"The Relative Merits of Nanosecond Sampling Techniques vs Direct Readout," Rod Carlson, Hewlett Packard, Palo Alto, Calif., and Cliff Moulton, Tektronix, Portland, Ore. (The two speakers discussed complementary parts of a vital subject and so are listed together.)

HP Model 185A Oscilloscope and the Tektronix Type 519 Oscilloscope were demonstrated.

Microwave Theory and Techniques

Albuquerque-Los Alamos—January 31

"Unbalanced Line Directional Couplers," L. J. Allen, Sandia Corp., Albuquerque, N. M.

Boston—January 12

"Closing the Spectrum—Areas for Research and Development in the Millimeter Wavelength Region," G. S. Heller, Lincoln Lab., Lexington, Mass.

Los Angeles—December 8

"The Challenge of a Young Industry," R. Krause, Rantec Corp., Calabasas.

Northern New Jersey—February 15, 1961

"Electron Density Measurements in the Field of Hot Plasma Research," W. P. Ernst, Forrestal Research Center, Princeton, N. J.

"Applications of Microwave to Plasma Research," Dr. R. W. Motley, Forrestal Research Center, Princeton, N. J.

Northern New Jersey—January 19

"Courier Satellite Communications System," E. Imboldi, ITT Labs., Nutley, N. J.

Northern New Jersey—November 16

"Quadrapole Amplifiers," Dr. E. Gordon, Bell Telephone Labs., Murray Hill, N. J.

Northern New Jersey—October 19

"LASERS," H. Cummins, Columbia Radiation Labs., New York, N. Y.

Omaha-Lincoln—January 20

"The Engineer's Responsibility," T. Saad, Sage Co., Natick, Mass.

Tokyo—July 26

"Review of Recent Developments of Microwave Theory and Techniques," Prof. K. Morita, Tokyo Institute of Technology.

Washington, D. C.—February 7

"TEM Diode Switching," R. V. Garver, Diamond Ordnance Fuze Labs.

Washington—January 10

"World's Largest "S" Band Radar Transmitter," T. Anderson, FXR, Woodside, N. Y.

(Continued on page 66A)

Professional Group Meetings

(Continued from page 64A)

Microwave Theory and Techniques/Electronic Computers

Baltimore—January 24

"Application of Microwave Techniques to Computers," R. L. Wigington, Dept. of Defense.

Military Electronics

Detroit—January 26

"MASER and LASER Programs at University of Michigan," L. Cross, University of Michigan, Ann Arbor, Mich.

Long Island—January 17

"New Techniques for Improvement of Reliability," J. J. Naresky, Rome Air Development Center.

North Carolina—December 6

"Effects of Nuclear Weapons," P. H. Hunter, Western Electric Co.

Rochester—December 22

"Electronic Switching in Military Communications," R. Dobbin, Stromberg-Carlson.

A Tour showing Stromberg-Carlson Transistorized Telephone System Equipment built for the U. S. Army Signal Corps followed the discussion.

San Francisco—December 7

"The Polaris Missile and the Fleet Ballistic Missile Weapon System," Commander N. Brango, BUWEPS Rep., Sunnyvale, Calif.

Nuclear Science

Albuquerque-Los Alamos—January 10

"Pulse Code Modulation," J. P. Knight, Radiation, Inc., Melbourne, Fla.

Albuquerque-Los Alamos—October 26

"Reduction of Noise in Data Transmission Systems," C. Taylor, Beckman Instruments, Inc., Anaheim, Calif.

Conducted discussion of above paper—R. Kramer, Beckman Instruments.

Heard a request from R. Krohn and F. Schonfeld of the local Boy Scout organization for backing of a Science Explorer post by the professional societies of Los Alamos.

Atlanta—January 12

"IBM 7090," A. Pfaff, IBM.
Tour of Building.

Los Angeles—January 17

"Detecting Beryllium with Berylometer," G. Ryan, Isotopes Specialties, Burbank, Calif.

(Continued on page 68A)

New Improved CBS PNP Power Transistors

2N538(A) • 2N539(A) • 2N540(A)

FEATURE MORE POWER, LESS WEIGHT, LESS SPACE

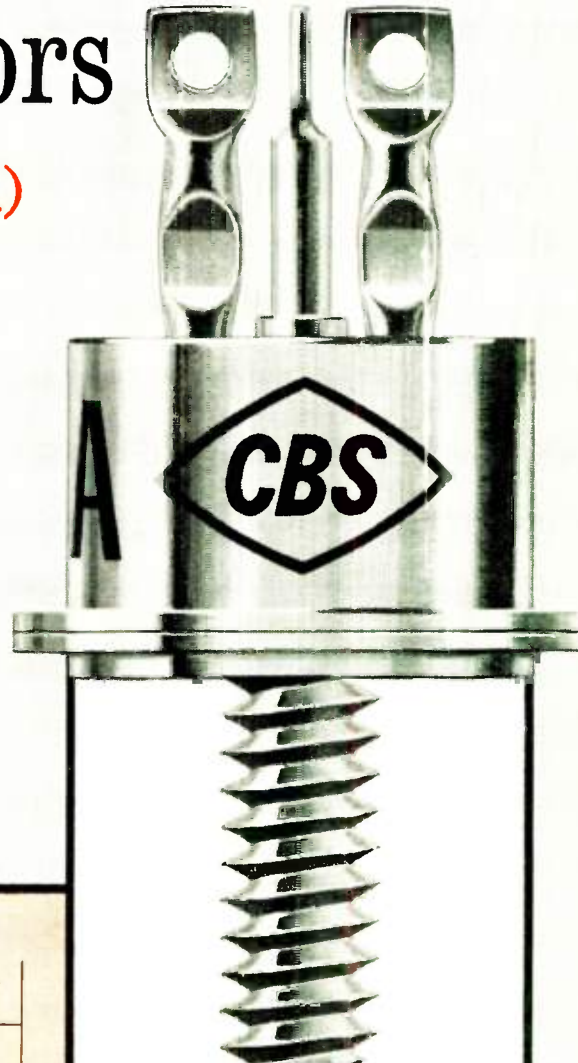

The CBS 2N538(A), 2N539(A) and 2N540(A) have a maximum dissipation of 30 watts at a base mounting temperature of 25 deg. Centigrade. Yet, each transistor weighs less than 5 grams and requires only 1/3 square inch of chassis space.

Compact and rugged, these hermetically-sealed CBS PNP Germanium Power Transistors are ideal for military and industrial power applications demanding high reliability. They are especially suited for servo motor controls, power amplifiers, converters, power supply regulators and low-speed power switches.

Note the major characteristics and advantages. Call or write today for complete technical data and delivery information from your local sales office or Manufacturer's Warehousing Distributor.

ELECTRICAL CHARACTERISTICS

Type	Max. VCBO	Min. V_{CE} ($\alpha=1$)	hFE ($I_C=2A$, $V_{CE}=-2V$) Min.	Max.	V_{BE} ($I_C=2A$, $V_{CE}=-2V$) Min.	Max.	Gp (mhos) ($I_C=2A$, $V_{CE}=-2V$) Min.	Max.
2N538	—80	—55	20	50	1.33	3.33		
2N538A	—80	—55	20	50	1.33	3.33	17.5	52
2N539	—80	—55	30	75	1.00	2.50		
2N539A	—80	—55	30	75	1.00	2.50	35	105
2N540	—80	—55	45	113	0.75	1.88		
2N540A	—80	—55	45	113	0.75	1.88	71	213

All types have: Max, collector current, 3.5 amps; junction temperature, −65 to +95°C; max, saturation voltage 0.6 volts ($I_C=2A$, $I_B=200$ mA). Minimum alpha cutoff frequency is 200 KC ($I_C=100$ MA, $V_{CE}=-4$ volts); max, thermal resistance, 2.2°C/W.

CBS PNP Power Transistors with an improved industrial male package offer:

- Single, sturdy 8-32 mounting stud
- Matched glass-to-metal seal for greater mechanical strength and resistance to thermal shock
- Rugged welded construction through the selection of matched materials having excellent welding properties
- Typical leakage three to five times lower than specification limits.
- High dissipation with minimum size
- High collector-to-base voltage
- High collector-emitter breakdown voltage
- Wide range of operating and storage temperatures

CBS semiconductors®

More Reliable Products through Advanced Engineering

CBS ELECTRONICS, Semiconductor Operations, Lowell, Massachusetts
A Division of Columbia Broadcasting System, Inc. • Semiconductors • tubes • audio components • microelectronics

Sales Offices: Lowell, Mass., 900 Chelmsford St., GLenview 2-8961 • Newark, N. J., 231 Johnson Ave., TAlbert 4-2450
Melrose Park, Ill., 1990 N. Mannheim Rd., EStebrook 9-2100 • Los Angeles, Calif., 2120 S. Garfield Ave., RAymond 3-9081
Toronto, Ont., Canadian General Electric Co., Ltd., LEnnox 4-6311.

Professional Group Meetings

(Continued from page 66A)

Radio Frequency Interference

Fort Worth—January 10

"Interference Problems of Mobile Two-Way Radio," D. W. Land, Motorola, Dallas.

Reliability and Quality Control

Philadelphia—November 22

Discussion of the "Darnell Report," P. Darnell, Bell Telephone Labs.

Space Electronics and Telemetry

Washington, D. C.—January 17

"Design Characteristics of SOLAR RADIATION I," M. J. Votaw, Naval Research Lab.

Vehicular Communications

Detroit—January 25

"A New Concept in Personal Communications," D. Petersen, Motorola Co., Chicago, Ill.

Metropolitan New York—January 24

"Bell System's Radio 'Bell Boy,'" R. R. Barnes, AT&T, New York, N. Y.

Paper illustrated with slides—demonstration of service being given. Appointment of N. Monk and S. C. Bartlett as Nominations Committee. Appointment of E. R. Saul and J. J. Algeo as Committee on Arrangements for the annual Dinner Meeting of PGVC.

Twin Cities—January 3

"Activities in Launching and Tracking High Altitude Balloons," A. Zmeskal and H. Jenson, General Mills, Inc., Minneapolis, Minn.

The Convention Record

gives the complete text of all technical papers presented at the IRE Convention.

The Convention Record will be issued in ten Parts according to subject, and will be available in July. Members of IRE Professional Groups may purchase corresponding parts at special reduced rates.

Orders for the Convention Record should be sent to the Institute of Radio Engineers, 1 East 79th St., New York 21, N.Y. Please include payment with order.

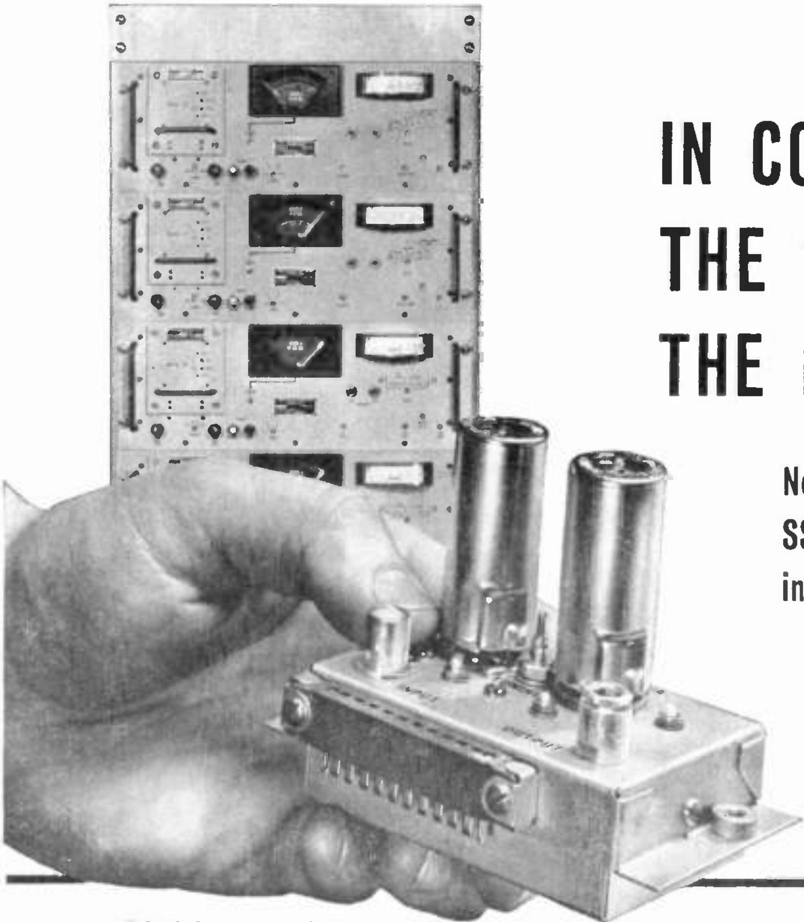

IN COMMUNICATIONS... THE SIMPLER THE BETTER

New Hallicrafters all-modular SSB strip receiver cuts costs, increases reliability.

- **50% less maintenance**
- **Far greater stability and reliability**
- **Down time almost entirely eliminated**
- **Lower initial cost**

Hallicrafters' new SX-116 SSB Receiver is the essence of simplicity—key to reliability in the Hallicrafters Series 116 communication system.

The SX-116 is entirely modular in construction, *virtually eliminating "down time" and cutting maintenance cost by over 50%.* The unit is quickly and easily adaptable to existing systems, entirely compatible with future requirements.

It is extremely stable—1 part in 10^6 per month (standard) or 1 part in 10^8 per month (special) . . . it permits, for the first time, continuous, unattended operation with *maximum reliability.*

The SX-116 weighs in at just 36 lbs.—equally practical for fixed, mobile, air or seaborne installations. *And its initial cost is very substantially lower.*

Finding a better and simpler solution to complex communications problems has been a Hallicrafters habit for over a quarter-century.

hallicrafters

Military Electronics Division, Chicago 24, Illinois

100% modular construction—only seven basic components

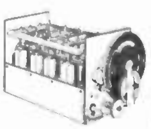

RF Module. Image and IF rejection maintained at better than 70 db. Single tuned circuit between antenna and RF grid. Four-channel, continuous tuning—2.0 mc. to 30 mc. range.

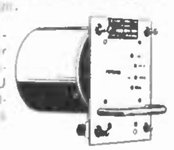

HF Crystal Oscillator Module. Stability, 1 in 10^8 per month. Capacity is four crystals; designed for HC-6/U metal or glass crystal holders. Oven temp. varies less than ± 0.01°C.

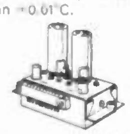

Injection Amplifier Module. AGC-controlled wide-band video amplifier provides constant injection level.

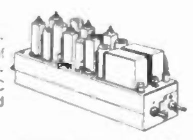

IF Module. Allows simultaneous reception of upper and lower sideband, independent AGC control of upper and lower sideband.

BFO Module. Operates at 1650.000 kc. Oscillator frequency stabilized in separate oven. Plate and filament voltages regulated.

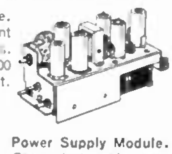

Audio Amplifier Module. Features dual, independent 100-milliwatt line amplifiers. Hum level is 80 db. below 100 milliwatts. Harmonic dist. less than 0.5%.

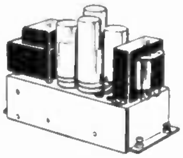

Power Supply Module. Separate transformers provided for regulated and non-regulated voltages. Local oscillator and BFO filament supply are regulated for $\pm 10\%$ line voltage variations!

Write for complete specifications on the SX-116.

HALLICRAFTERS REGIONAL SALES ENGINEERS

William E. Peugh—Joseph A. Small
4401 W. 5th Avenue, Chicago 24, Ill.
VAn buren 6-6300

Thomas H. Pretorius
7558 S.E. 15th St.,
Oklahoma City, Okla.
PErshing 7-2456

Earl L. Giffin
Box 568, Far Hills Br.,
Dayton 9, O.
AXminster 8-5239

Merle J. Long
513 E. Manchester Blvd.,
Suite 201,
Inglewood 1, Calif.
ORchard 2-6861

H. Kenneth Hudson
626 Lakeview Dr., Falls Church, Va.
CLearbrook 6-4978

James R. Spencer
Box 435, Lincroft, N.J.
SHadyside 7-2369
(Red Bank, N.J.)

LOOKING FOR A CHALLENGING OPPORTUNITY? We have openings for communications systems and equipment design engineers at all levels. Please write to William F. Frankart, Director of Engineering.

IRE People

Charles Askanas (S'54–M'60) has been named Project Manager in charge of automatic instruments at Lumatron Electronics, Inc., New Hyde Park, L. I., N. Y. He will head a new group which will emphasize the automatic aspects of millimicrosecond instruments and switching devices test sets in the nanosecond range.

He was previously employed by the General Instrument Company. He is a graduate of the New York University College of Engineering, New York, N. Y.

Mr. Askanas is a member of the IRE Professional Group on Electron Devices and the author of a number of papers on transistor circuits and the applications of solid state devices.

❖

Dr. Bristow Guy Ballard (SM'47–F'55), Vice President (Scientific) of the National Research Council, has been elected President of the Engineering Institute of Canada for the year 1961–1962. Dr. Ballard, who was awarded the Order of the British Empire for distinguished scientific contributions during the Second World War, will assume office during the 75th Annual Meeting of the Institute in Vancouver May 31–June 2, 1961. He will succeed Dr. G. McK. Dick of Sherbrooke, Que.

A native of Fort Stewart, Ont., he received the Bachelor of Science degree from Queen's University, Kingston, Ont., in 1924. After completing a Westinghouse graduate course in electrical engineering, he joined the staff of the Westinghouse Electric and Manufacturing Company, East Pittsburgh, Pa., in 1925.

He was appointed to the National Research Council of Canada in 1930 and spent the following 10 years building the electrical engineering section of the Division of Physics. The O.B.E. was awarded to Dr. Ballard for his wartime contributions which included the development of mine sweepers and other means of protecting ships against enemy magnetic mines.

In 1946 he was appointed Assistant Director of the Division of Physics and Electrical Engineering of the NRC, and two years later, when a full Division of Radio and Electrical Engineering was established, he was named its Director. He was appointed Vice President (Scientific) in 1954.

He has been associated with the Institute since 1931. For his paper entitled "Recent Canadian Radar," he received the Institute's Ross Medal in 1948. He served as Chairman of the Ottawa Branch in 1951, as Branch Councillor from 1952 until 1954, and as Vice President of the Institute representing Ontario from 1954 until 1956. He was elected an Honorary Member of the Institute in 1960. He is now serving as Chairman of the Institute's Committee on Technical Operations.

He is a Fellow of the American Institute of Electrical Engineers, and a member of the Association of Professional Engineers of Ontario, and of the Professional Institute of the Public Service of Canada.

The Doctor of Science degree was bestowed upon Dr. Ballard by Queen's University in 1956.

❖

Dr. Robert M. Bowie (A'34–M'37–SM'43–F'48), Vice President of General Telephone & Electronics Laboratories, Inc., and General Manager of that organization's Bayside, N. Y., Laboratories, has been assigned to the New York headquarters staff of GT&E Laboratories, it was recently announced.

R. M. Bowie

Born in Table Rock, Neb., he was graduated from Iowa State College, Ames, where he received the B.S. degree in chemistry, and M.S. and Ph.D. degrees in physics. He is a veteran in the field of electronics. In 1933 he joined the engineering staff of Hygrade Sylvania Corp., a predecessor company of Sylvania Electric Products Inc., which is a subsidiary of General Telephone & Electronics Corporation. He helped establish a research laboratory at Sylvania, and did pioneering work on television tube research. He was also responsible for the formation of the Physics Laboratory at Sylvania's Bayside Laboratories, now a part of General Telephone & Electronics Laboratories, Inc. Since then, he has held a number of positions at Bayside, including that of Manager, Director of Engineering, Director of Research, and Vice President.

He has made significant contributions to vacuum tube and television research. He was chairman of Panel 19 of the National Television Systems Committee and is chairman of Panel 5 on Analysis and Theory of the Television Allocations Study Organization. Last year, he was appointed by the Governor of the State of New York to serve on the Advisory Council for the Advancement of Scientific Research and Development in New York. He is also on the Advisory Committee of the Long Island Graduate Studies and Research Center of the Polytechnic Institute of Brooklyn, Brooklyn, N. Y.

Dr. Bowie is a member of Pi Mu Epsilon, Phi Lambda Upsilon, Phi Kappa Phi, Sigma Xi, and Alpha Chi Sigma. He is a Fellow of the American Physical Society, and in 1960 was Chairman of its Division of Electron Physics. He has been granted

(Continued on page 72A)

IRE People

(Continued from page 70A)

22 U. S. patents, chiefly in the fields of television, thermionics, and microwaves, and is the author of some 40 technical and managerial articles.

❖

Daniel B. Campbell (A'46–M'55) has been named manager of field service for the Military Products Division of General Dynamics/Electronics, according to a recent announcement.


D. B. Campbell

In this capacity, he will have complete responsibility for all field service operations of the Military Products Division. This will encompass recruitment, training and supervision of personnel engaged in the servicing and maintenance of military electronic installations around the globe under defense contracts held by General Dynamics/Electronics.

Prior to joining General Dynamics he had been with the Philco Corporation for 14 years in various sales, engineering and management positions. His last position with Philco was as marketing representative of the Communications Systems Division.

A native of Dillon, S. C., he attended Clemson A. & M. College, Clemson, S. C., majoring in electrical engineering. On the outbreak of World War II, he left during his junior year to join the U. S. Air Force, and served until 1946 at several installations in the United States.

Mr. Campbell is a member of the Electronic Industries Association and the Petroleum Electric Supply Association.

❖

Dr. Malcolm R. Currie, 33 (S'52–A'55–SM'58), Hughes Aircraft Company scientist, has been named one of five "outstanding young men" of 1960 by the California Junior Chamber of Commerce for his contributions in space propulsion and microwave electronics.


M. R. Currie

He presently heads a team of Hughes scientists working under a National Aeronautics and Space Administration (NASA) contract on ion engine propulsion for space travel. Ion propulsion uses an electronic flow of ions to propel a space vehicle.

He is manager of the physics laboratory at Hughes Research Laboratories at

(Continued on page 76A)

℞ how to cure traveling wave tube headaches

If you have TWT headaches—finding a microwave amplifier *now*—which produces high gain and wide bandwidth *with* high average and peak powers—Hughes may have just the prescription for you. Hughes TWT's provide all these desirable features with built-in long life, ruggedness and dependability. They fully exploit the advantages of permanent magnet periodic focusing in both glass and metal-ceramic structures, and many are available in either gridded or ungridded versions.

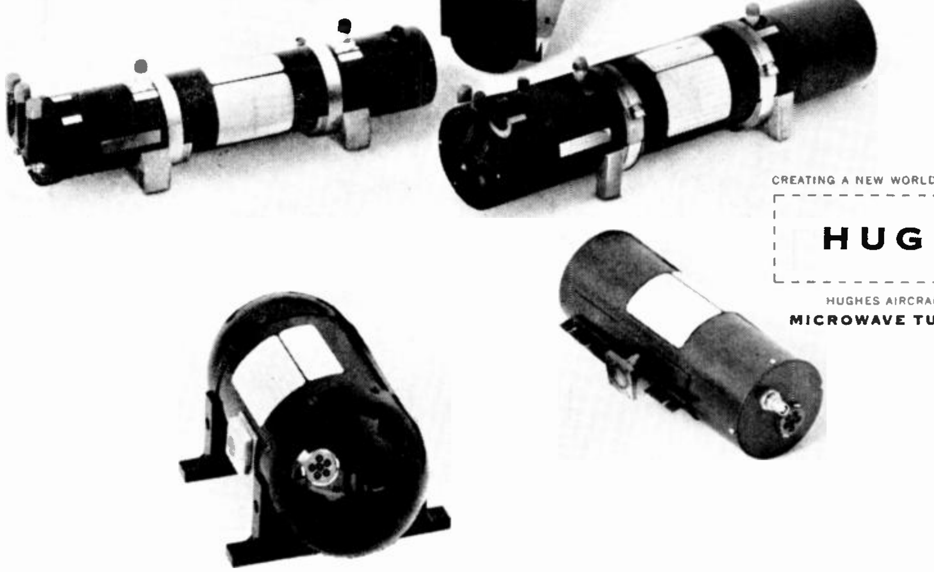

CREATING A NEW WORLD WITH ELECTRONICS

HUGHES

HUGHES AIRCRAFT COMPANY

MICROWAVE TUBE DIVISION

typical twt's available now:

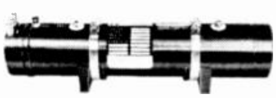

311H 2.0-4.0 KMC Gridded 1 KW minimum peak power output, 1% duty, 36db small signal gain @ 50 mw input. Weight 13 lbs. Length 17-7/16".

312H 2.0-4.0 KMC Gridded 1 KW minimum peak power output, 1/2% duty, 36db small signal gain @ 50 mw input. Weight: 11 lbs. Length: 15-3/8".

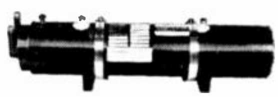

304H 2.0-4.0 KMC Ungridded, 1 KW minimum peak power output, 1% duty, 37db small signal gain @ 1 mw input. Weight: 12-1/2 lbs. Length: 17-31/32".

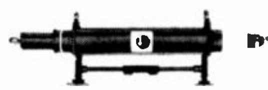

307H 8.5-9.5 KMC 50 KW minimum peak power output (500 watt average), metal-ceramic construction, 54db saturation gain, 1% maximum duty cycle, beam voltage = 38 kv. Wt. 21 lbs. Length: 24".

Hughes also has a complete line of K_u-band backward-wave oscillators for commercial and military applications.
Write or telephone today for full information or a catalogue concerning the broad line of Hughes TWT's available in L, S, C & X bands.
Hughes Microwave Tube Division, P. O. Box 90427, Los Angeles 45, California.

Model 860-1500P—handles low level DC data signals in the presence of high common mode

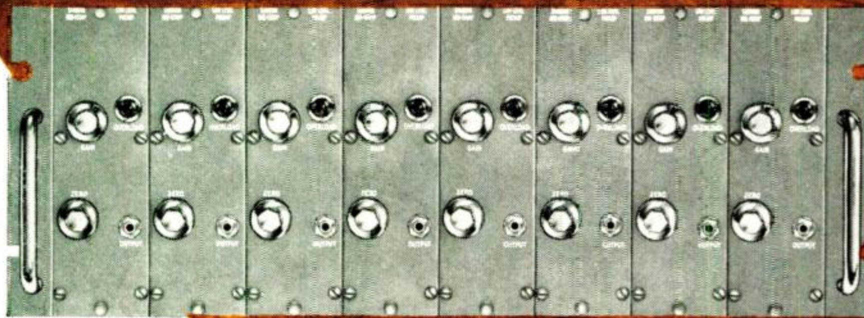

Model 658-3400 — drives high frequency optical galvanometers to 5 KC

COMPACT 7″ HIGH 8-CHANNEL UNITS ARE COMPLETELY TRANSISTORIZED, HAVE FLOATING INPUT ISOLATED FROM OUTPUT

Sanborn precision amplifiers

Data Preamplifier — Model 860-1500P

Designed for precise, economical amplification of signals with source impedance of zero to 10,000 ohms, such as thermocouples, strain gage bridges, etc. in presence of severe ground loop noise, and for driving digital voltmeters, scopes, tape recorders and similar devices. Each plug-in unit is only 2″ x 7″ x 14½″ deep; 64 channels with blower require only 60″ of rack-panel space. Separate 868-500 Power Supply required for every 8 preamplifiers. Power consumption 2.5 watts per channel.

Noise	3 uv peak-to-peak
Gain	100 (10 mv in gives 1 v out) (Model 860-1500PA with gain of 1000 also available)
Output	± 1 v across 300 ohms, DC-70 cps; ± 1.5 v to 40 cps. Output impedance 100 ohms. (10 v across 10K available on special order.)
Linearity	± 0.1% of full scale output (2 v)
Common Mode Performance	120 db rejection at 60 cps, 160 db at DC, with 5000 ohms unbalance in source. Inphase tolerance 220VAC.
Input Impedance	Greater than 200,000 ohms
Gain Stability	± 0.1% for 24 hours
Drift	± 2 uv referred to input
Rise Time	to 99.9% less than 25 ms

Optical Galvanometer Amplifier — Model 658-3400

Eight channels of amplification and common power supply. Each channel provides for sensitivity, compensation, damping and current limiting. Inputs floating and guarded, impedance 100,000 ohms on all ranges. All amplifier elements except output transistors are plug-in assemblies.

Sensitivity	± 10 mv input gives ± 400 ma output into 20 ohm load (max.). Eleven attenuator steps to X2000 in 1-2-5 ratio, smooth gain control.
Common Mode Performance	± 500 volts, max; rejection 140 db min at DC.
Gain Stability	Better than 1% to 50°C and for line voltage variation from 103-127 volts.
Frequency Response	0 to 5 KC within 3 db; can accomodate wide range of galvanometers.
Output	Output networks available for wide range of galvanometers.
Power Consumption	125 watts for 8 channels.

Your Sanborn Sales-Engineering Representative (offices throughout the U. S., Canada and overseas) will provide detailed information and application assistance. Call him or write plant in Waltham, Mass.

SANBORN COMPANY
INDUSTRIAL DIVISION
175 Wyman Street, Waltham 54, Massachusetts

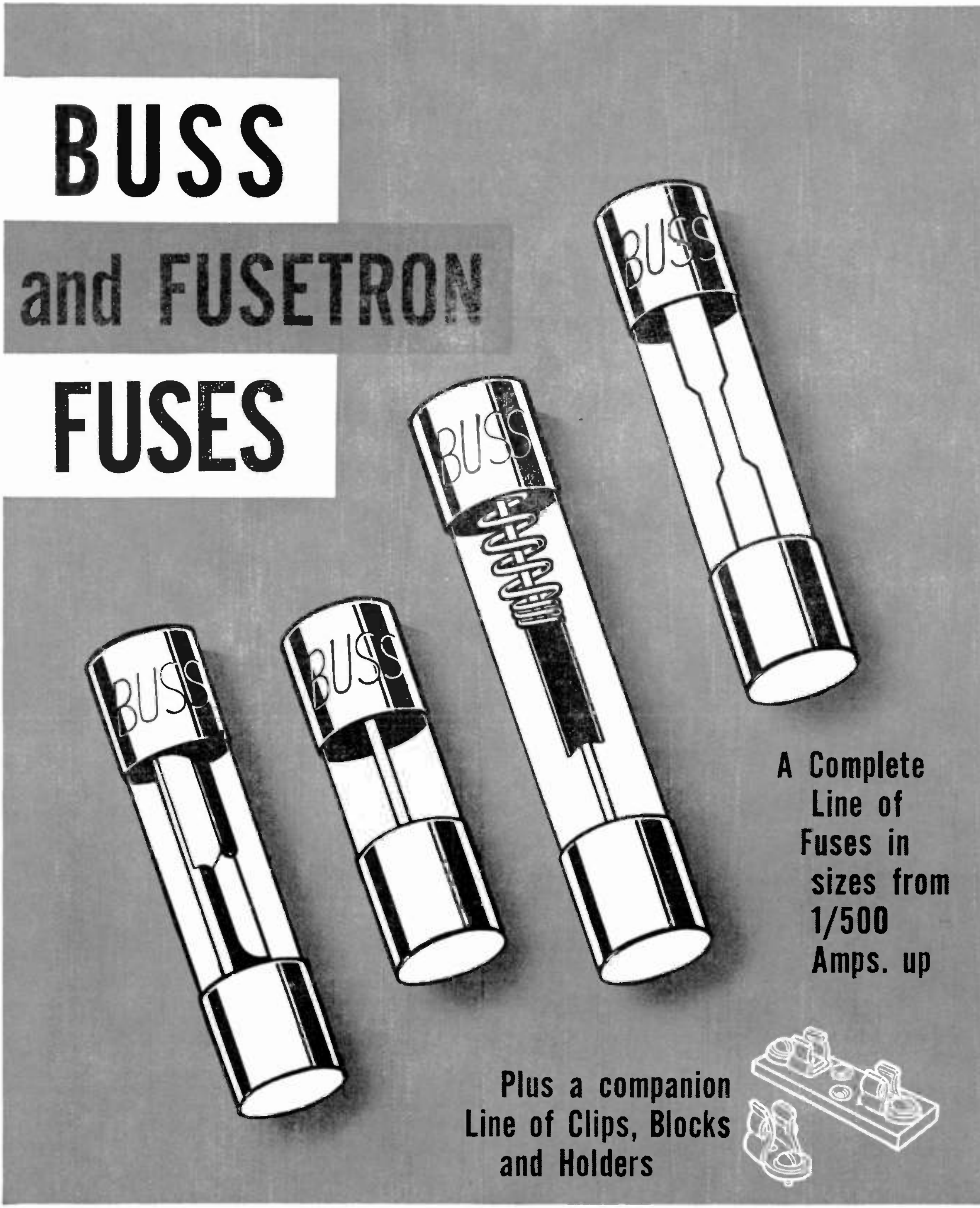

When you specify BUSS and FUSETRON fuses you can be sure of safe, dependable, trouble-free protection for your equipment under all service conditions.

Every BUSS and FUSETRON fuse is tested in a sensitive electronic device that automatically rejects any fuse not correctly calibrated, properly constructed and right in all physical dimensions.

Chances are you will find in the complete BUSS line the fuse and fuse mounting to fit your requirements — but if your protection problem is unusual, let our engineers work with you and save you engineering time.

To get full data for your files, write for BUSS bulletin on small dimension fuses and fuseholders. Form SFB.

461

BUSSMANN MFG. DIVISION, *McGraw-Edison Co.,* **UNIVERSITY AT JEFFERSON, ST. LOUIS 7, MO.**

Partial listing from

TABLE OF CONTENTS

. . . 19 Sections . . . over 100 fact-filled pages

Now...the industry's most comprehensive reference guide to semiconductor rectifiers

Here is another must for your reference library from General Electric. In the tradition of the famous G-E Transistor and Controlled Rectifier manuals, the new SEMICONDUCTOR RECTIFIER COMPONENTS GUIDE is an encyclopedia of semiconductor rectifier data and information.

Comprehensive, reliable, up-to-date information is at your fingertips for constant, convenient reference. Take advantage of this introductory offer — *You* fill in the coupon and mail it to us: *we* send you a SEMICONDUCTOR RECTIFIER COMPONENTS GUIDE without charge.

Progress Is Our Most Important Product

GENERAL ELECTRIC

Rectifier Components Department, Section 54D11
General Electric Company
Auburn, New York

Please send me my FREE copy of the new General Electric SEMICONDUCTOR RECTIFIER COMPONENTS GUIDE.

Name__________ **Title**__________

Company__________

Address__________

City__________ **Zone**____ **State**____

IRE People

(Continued from page 90A)

He was appointed to the chief staff position of WESCON, the largest trade show and technical convention in the West, in the fall of 1956.

Mr. Larson makes his headquarters at WESCON'S Business Office, 1435 South La Cienega Blvd., Los Angeles, Calif., and spends considerable time in the Northern California Office at 701 Welch Road, Palo Alto.

❖

The promotion of **Burtis E. Lawton** (S'41–A'46–M'48), to the post of eastern regional sales manager for the Electronic Tube Division, Allen B. DuMont Laboratories, Clifton, N. J., Division of Fairchild Camera and Instrument Corporation, has been announced.

B. E. Lawton

In his new post he will supervise and coordinate the activities of the division's sales engineering personnel and sales representative firms in the eastern third of the nation.

He has been associated with DuMont since 1956. Before his new appointment he was regional manager for the southeast. Prior affiliations were with the H. S. Martin Company, Evanston, Ill., as sales and service manager and with the Westinghouse Electric Company, Bloomfield, N. J., as an applications engineer.

Mr. Lawton is a member of the American Institute of Electrical Engineers.

❖

Microwave Associates, Inc., Burlington, Mass., have announced the appointment of **Dr. Kenneth E. Mortenson** (S'47–A'50–M'55–SM'57) to head a research group working on active solid-state microwave devices. In this newly created position, he will direct research and development activities on new microwave solid-state semiconductor tunnel-diode oscillators, and other solid-state amplifiers.

K. E. Mortenson

Prior to joining Microwave Associates, he was a research physicist with the General Electric Company's Research Laboratory, Schenectady, N. Y. He was also associate professor of electrical engineering at the Rensselaer Polytechnic Institute, Troy, N. Y., and a consultant to the RPI Radio Astronomy Observatory.

He received the B.S. and B.E.E. de-

(Continued on page 96A)

For greater versatility... longer life... increased reliability...

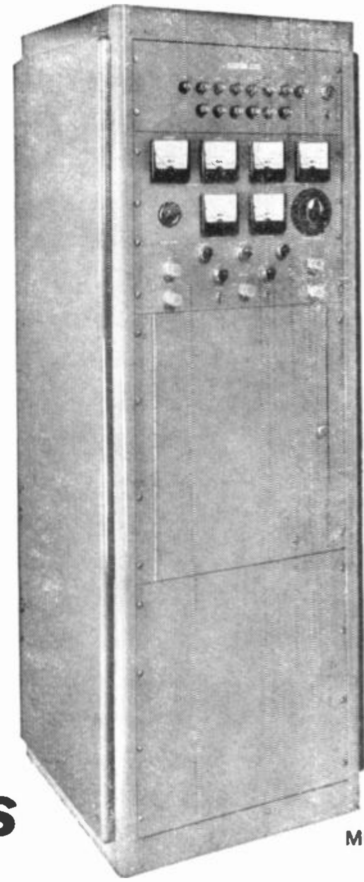

MODEL 10002
35 KV

Specify NARDA Microwave Modulators

Here's a line of new Microwave Modulators, designed to operate a maximum number of existing magnetrons, without any alterations to the modulator. In addition, provision has also been made for quickly converting the unit to handle any new or uncommon pulse microwave tubes.

Models 10001 and 10002 are designed to handle high-power magnetrons with provision for internal mounting of the tube. Model 10003 is designed for pulsing low-power magnetrons of the type now used in beacon transmitters and for low-power commercial pulse applications.

Since all units utilize silicon rectifiers and diodes, you can expect increased life and more reliable operation. At the same time, over-all size has been considerably reduced. Every Narda Microwave Modulator is complete with built-in safety provisions, built-in meters and viewing connectors for all principal parameters, a continuously variable repetition rate, and a standard pulse width of 1 microsecond (other widths available on special order) on Models 10001 and 10002; continuously variable on Model 10003.

The specifications below indicate those characteristics of the three new models which vary from each other. The listing of features indicates those features common to all models. For additional information, and a copy of our free catalog, write to us at Dept. P-60-9

SPECIFICATIONS

Narda Model ‡	Maximum Peak Pulse Power	Pulse Width (Microseconds)	Maximum Duty Cycle ‡ at Maximum Power	Size H x W x D
10001	18KV @ 20A	1*	0.001	38x22x18
10002	35KV @ 40A	1*	0.001	67x24x24
10003	4.5KV @ 2A	0.5-2.2†	0.002	8½x18x12

* Other values of pulse width can be readily substituted.
† Pulse width is continuously adjustable over given range.
‡ Internal continuously variable trigger generator for adjusting repetition rate and duty cycle.

FEATURES

Built-in Meters:
- High voltage power supply voltage
- High voltage power supply current
- Magnetron filament supply voltage
- Magnetron filament supply current
- Clipper average supply current*

*Models 10001 and 10002

Viewing Connectors (BNC):
- Magnetron pulse voltage
- Magnetron pulse current
- Primary pulse voltage*
- Thyratron pulse current*
- PFN charging voltage*

*Models 10001 and 10002

Output sync pulses (BNC Connectors):
- Positive + 50 v min. at 2 sec.
- Negative − 25 v min. at 2 sec.

Input sync (BNC Connectors):
- Sine wave: 20 v RMS min.
- Pulse: 20 v at .25 sec min.

the narda microwave corporation
HIGH POWER ELECTRONICS DIVISION
118-160 HERRICKS ROAD, MINEOLA, L. I., N. Y. • PIONEER 6-4650

IRE People

(Continued from page 94A)

grees in 1947 and 1948, respectively; the Masters degree in electrical engineering and the Ph.D. degree in applied physics in 1950 and 1954, respectively, all from the Rensselaer Polytechnic Institute.

He has published numerous professional papers on the following subjects: semiconductor diode and transistor development and related circuitry particularly as applied to solid-state microwave amplifying devices.

Dr. Mortenson is a member of Eta Kappa Nu and Sigma Xi.

❖

Conductron Corporation, New York, N. Y., has announced the appointment of **Alan D. Nichols** (A'53–M'58), as Research Engineer. He received the B.S. degree from Iowa State College, Ames, in 1949 and the M.S. degree from the University of Michigan, Ann Arbor, in 1956, both in electrical engineering. Since 1952 he has been with the Willow Run Laboratories of the University of Michigan, where he held the rank of Associate Research Engineer. His experience is in radar systems, microwave circuit design, and low-noise receiver design.

A. D. Nichols

Mr. Nichols is a member of Eta Kappa Nu, Tau Beta Pi, and Sigma Xi.

❖

Atherton Noyes, Jr. (SM'47), formerly vice president of research and development at Aircraft Radio Corporation, Boonton, N. J., has joined the General Radio Company, West Concord, Mass., as an engineering consultant. He will specialize in the development of precision, crystal-controlled digital-frequency sources.

A. Noyes, Jr.

Dr. Noyes served as an assistant to G. W. Pierce at Cruft Laboratory, from 1931–1937. In 1934, he received the Sc.D. degree from Harvard University, Cambridge, Mass.

❖

Erwin Tomash (S'46–A'48–SM'54), has been elected vice president of Ampex Corporation, and manager of Ampex Computer Products Company, Culver City, Calif., it was recently announced.

He received a degree in electrical engineering from the University of Minnesota, Minneapolis. Following his military service, he joined Engineering Research Associates, St. Paul, Minn., as an electronics engineer on digital system design for their facility in Washington, D. C., and later returned to St. Paul to become assistant director of computer development. In 1953, he joined Remington Rand as West Coast Director, and later moved to New York to assist in the establishment of their UNIVAC Division. In 1955, he joined Telemeter Magnetics, Inc., as director of marketing, and in 1956 was elected president.

Mr. Tomash is a member of the Association for Computing Machinery.

❖

Robert M. Peterson (S'47–A'49–M'55), has been appointed Chief of Design Requirements at Ryan Transdata, Inc., it was recently announced by W. G. Alexander, President of the company's San Diego subsidiary. He has an extensive background in engineering management for electronic printing, display and specialized computer equipment, IFF, radar and microwave systems. He was a key contributor to the concept and early design of high speed electronic label printing.

R. M. Peterson

Mr. Peterson received the B. S. and M.S. degrees in electrical engineering from the University of Wisconsin, Madison. He was Assistant Chief Engineer at Stromberg-Carlson, a Supervisory Engineer at Hazeltine Electronics Corporation, Little Neck, N. Y., and electrical engineering instructor at the University of Wisconsin, before joining Ryan Transdata, Inc. He served as a communications officer with the U. S. Army Air Force during World War II.

❖

Edwin Shuttleworth III (A'55) assistant vice president of Driver-Harris Company, Harrison, N. J., has been appointed assistant sales manager, it was recently announced.

He joined Driver-Harris Company in 1950 and became the technical assistant to the president three years later. In 1957, he was made director of this company's Italian manufacturing facility. He was named assistant to the vice president in 1958 and became the director of the Driver-Harris Company, Ltd., in England in 1959.

E. Shuttleworth

Mr. Shuttleworth received the B.S. degree in industrial engineering from Lehigh University, Bethlehem, Pa., in 1950.

❖

(Continued on page 100A)

AN EXTRAORDINARY PUBLISHING ACHIEVEMENT OF OUR TIME!

Here Are the Many Fields Covered:

ACOUSTICS
AERONAUTICAL AIRFRAMES
AGRICULTURE & SOILS
ANIMAL ANATOMY
PLANT ANATOMY
ANIMAL SYSTEMATICS
ASTRONOMY
ATOMIC, MOLECULAR AND NUCLEAR PHYSICS
BIOCHEMISTRY
BIOPHYSICS
CHEMICAL ENGINEERING
ANALYTICAL CHEMISTRY
INORGANIC CHEMISTRY
ORGANIC CHEMISTRY
PHYSICAL CHEMISTRY
CIVIL ENGINEERING
COMMUNICATIONS
CONSERVATION
CONTROL SYSTEMS
CYTOLOGY
ANIMAL ECOLOGY
PLANT ECOLOGY
ELECTRICAL ENGINEERING
ELECTRICITY
ELECTRONICS
FLIGHT SCIENCE
FOOD ENGINEERING
FORESTRY
GENETICS & EVOLUTION
GEOCHEMISTRY
PHYSICAL GEOGRAPHY
SURFICIAL AND HISTORICAL GEOLOGY
GEOPHYSICS
GRAPHIC ARTS
GROWTH AND MORPHOGENESIS
HEAT
INDUSTRIAL AND PRODUCTION ENGG.
LOW TEMPERATURE PHYSICS
MACHINE DESIGN
MATHEMATICS
MECHANICAL POWER
CLASSICAL MECHANICS
METALLURGICAL ENGINEERING
METEOROLOGY AND CLIMATOLOGY
MICROBIOLOGY
MEDICAL MICROBIOLOGY
MINERALOGY AND PETROLOGY
MINING ENGINEERING
NAVAL ARCHITECTURE AND MARINE ENGG.
NUCLEAR ENGINEERING
OCEANOGRAPHY
OPTICS
PALEONTOLOGY
ANIMAL PATHOLOGY
PLANT PATHOLOGY
PETROLEUM CHEMISTRY
PETROLEUM ENGINEERING
GENERAL PHYSIOLOGY
PLANT PHYSIOLOGY
SOLID STATE PHYSICS
THEORETICAL PHYSICS
PLANT TAXONOMY
PROPULSION
PHYSIOLOGICAL AND EXPERIMENTAL PSYCHOLOGY
INVERTEBRATE ZOOLOGY

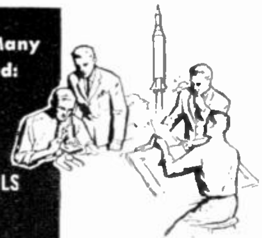

The Entire Span of Today's Scientific, Engineering and Technical Knowledge Encompassed in a Monumental Reference Work Containing 8,500 pages of Text, 800 Index Pages, 7,200 Articles and 9,700 Illustrations

includes developments so recent they are still major news!

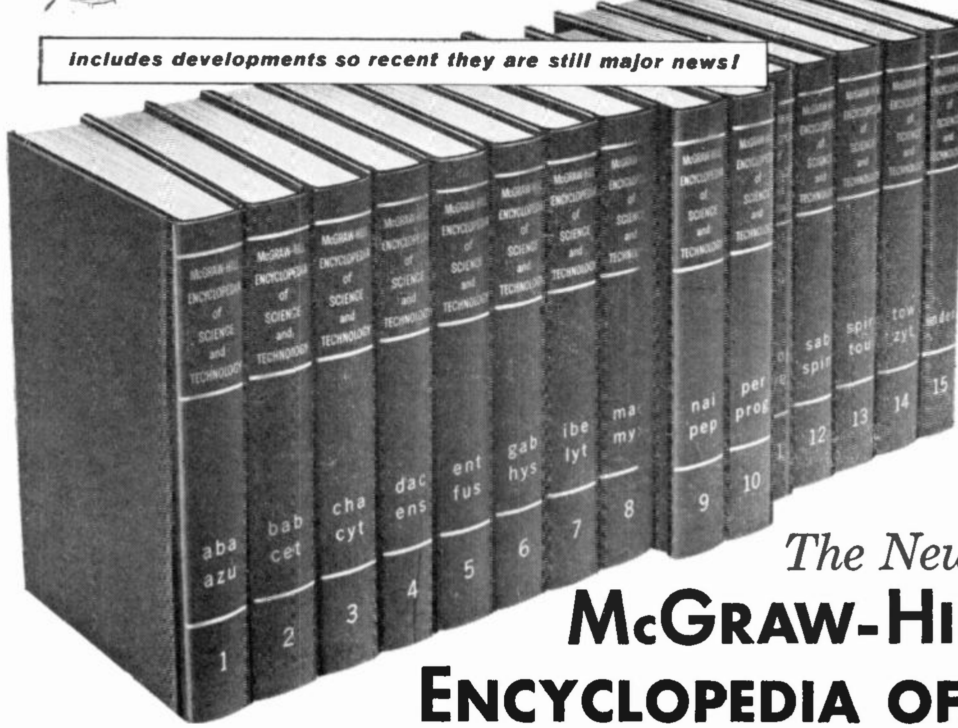

The New McGRAW-HILL ENCYCLOPEDIA OF SCIENCE and TECHNOLOGY

2,015 Contributors, including Nobel Prize Winners, Respected Leaders of Research and Industry . . . Over 6,000,000 Words — from Concise Articles to Amazingly Comprehensive Treatments . . . 100,000-Entry Index . . . a Wealth of Maps, Charts, Diagrams, Drawings, Photographs . . . many more than in any comparable work of reference.

AN epoch-marking publishing venture — providing up-to-date, authoritative information on all the sciences of our day — is now completed. The new McGRAW-HILL ENCYCLOPEDIA OF SCIENCE AND TECHNOLOGY makes readily accessible within its 15 volumes a vast fund of knowledge covering hundreds upon hundreds of subjects dealing with the whole spectrum of the physical sciences, life sciences, earth sciences, and engineering.

This major work fulfills a prime need of the scientist, the engineer, the technician — whether concerned with pure research or practical applications — whether his work is of a design or operating nature — whether he wants to review or keep abreast of the vastly enlarged knowledge of his own field or must bridge the gap between his specialty and unfamiliar areas into which his work leads him.

Unequalled in Timeliness, Clarity, Depth

This unique library makes it possible for you to have as near as your office, laboratory, plant, or home an all-knowing corps of specialists to which you can turn for precise, authoritative information. You can get answers to specific questions raised through daily professional activities or simply explore in a random way the universe of today's scientific, engineering, and technical knowledge — distilled into 7,224 comprehensive articles. Whatever your own field, whatever field your work is related to, you will find it here.

A Work of Unsurpassed Authority

The names of the contributors read like a "Who's Who" of the world's scientific community. All are recognized specialists — in many instances, articles were written by the very person credited with new discoveries and developments in a given field. Among them are Nobel Prize Winners and others who have distinguished themselves for their original and significant work.

Nothing comparable in breadth of conception, in authority, in usefulness, has ever before been offered in a reference work of this kind. As an all-embracing general reference or a practical working tool, this Encyclopedia belongs in the home and professional library of everyone with an interest in science and engineering. *An annual Supplement Volume keeps it always up to date.*

You are cordially invited to examine all fifteen volumes. There is, of course, no obligation on your part. Mail the coupon below for full details.

MAIL THIS COUPON

McGraw-Hill Book Company Dept. IRE-4
327 West 41 Street, New York 36, N.Y.

Please send me without obligation your pre-view brochure on the new McGRAW-HILL ENCYCLOPEDIA OF SCIENCE AND TECHNOLOGY in 15 volumes; also detailed information about the convenient time-payment plan I may use to purchase this set.

Name. . . . .

Address. . . . .

City & Zone. . . . .

State. . . . .

IRE-4

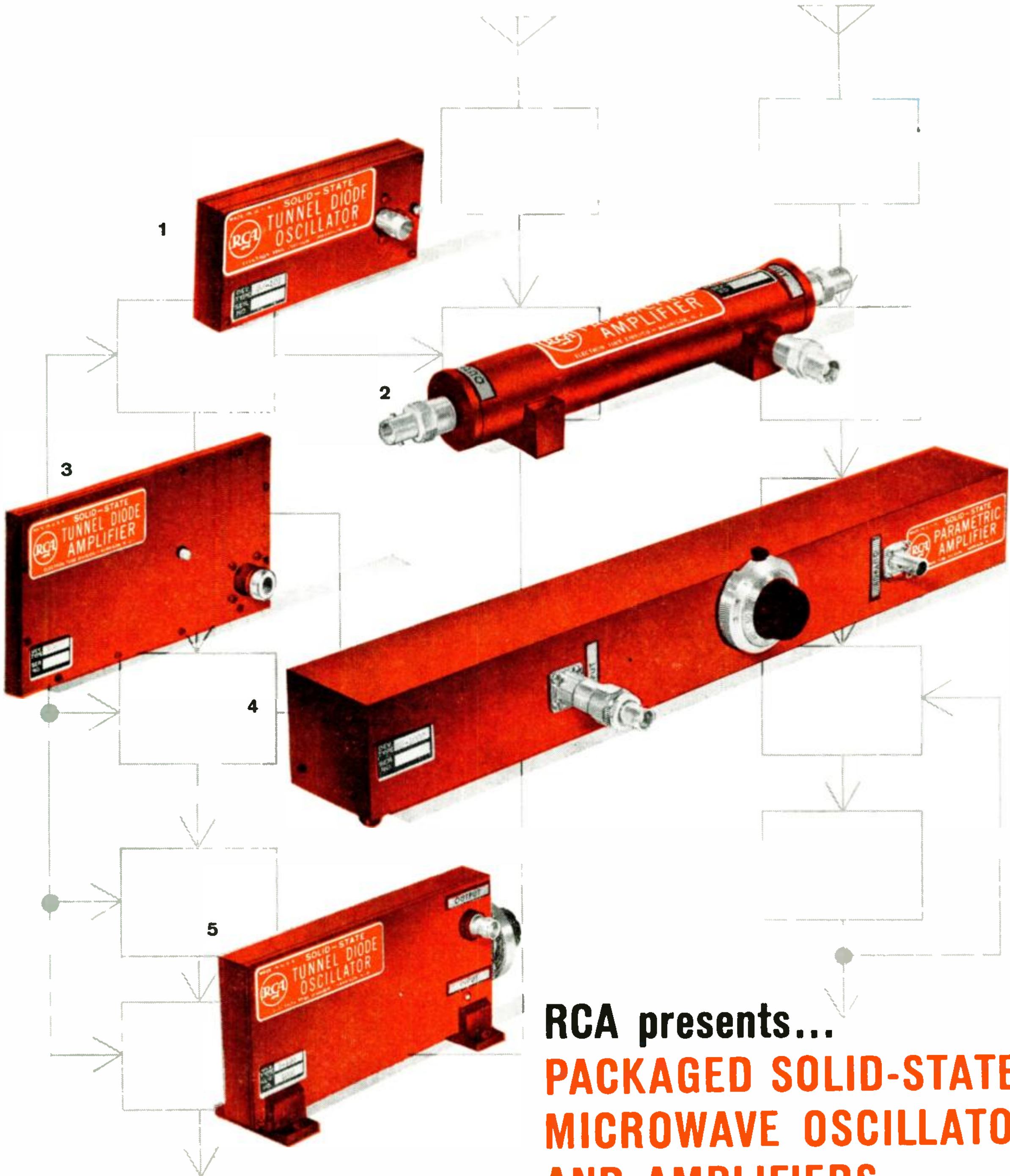

RCA presents...

PACKAGED SOLID-STATE MICROWAVE OSCILLATORS AND AMPLIFIERS

Now, RCA takes a major step ahead in microwave technology—to integrate packaged microwave circuits with RCA developed solid-state diodes and provide an important, new line of components for the needs of microwave designers. Low power requirements, and compact packaging using RCA Semiconductor and Materials Division's latest tunnel and varactor diodes open new possibilities for miniaturization, improved systems reliability, and systems cost reduction. Here are the first members of a growing family of packaged microwave circuits.

In addition to the performance characteristics of the packaged circuits shown here, RCA Solid-State Microwave Oscillators and Amplifiers can be designed to meet your special requirements for gain, power, frequency, and noise characteristics. For delivery quotations and technical data on circuits to meet your needs, contact the RCA Field Office nearest you. Or write: Microwave Marketing, RCA Electron Tube Div., Harrison, N. J.

1. **Fixed-Tuned Tunnel-Diode Oscillator** (Dev. No. SS-107) Delivers a minimum power output of 1 milliwatt at your specified frequency between 500-2000 Mc. DC input; 160 ma at 0.40 volt.
2. **Helix Parametric Amplifier** (Dev. No. SS-1000) Stable minimum gain of 15 db from 2200-2300 Mc with a 5-7.5 db noise factor. Typical saturated power output of 1 milliwatt; with 300 milliwatts pump power at 3000 Mc.
3. **Tunnel-Diode Amplifier** (Dev. No. SS-500) Stable minimum gain of 15 db from 1275-1325 Mc with 6 db max. noise factor, including typical circulator loss. Saturated power output of 30 microwatts. DC input; 10 ma at 0.1 volt.
4. **Tunable Low-Noise Parametric Amplifier** (Dev. No. SS-1002) Tunable with 5 Mc bandwidth from 1250-1350 Mc, with stable minimum gain of 15 db. Max. noise factor, 3 db. Saturated power output of 0.5 milliwatt, with 60 milliwatts pump power at 10,800 Mc.
5. **Tunable Tunnel-Diode Oscillator** (Dev. No. SS-100) Delivers a minimum power output of 0.3 milliwatt from 1050-1400 Mc. Coax. output. DC input; 30 ma at 0.2 volt.

RCA Electron Tube Division Field Offices

INDUSTRIAL PRODUCTS SALES

Detroit 2, Michigan, 714 New Center Building, TR 5-5600 • Newark 2, N. J., 744 Broad St., HU 5-3900 • Chicago 54, Illinois, Suite 1154, Merchandise Mart Plaza, WH 4-2900 • Los Angeles, California, 6801 East Washington Boulevard, RA 3-8361 • Burlingame, California, 1838 El Camino Real, Ox 7-1620.

GOVERNMENT SALES

Harrison, N. J., 415 South 5th St., HU 5-3900 • Dayton 2, Ohio, 224 North Wilkinson St., BA 6-2366 • Washington 7, D. C., 1725 "K" St., N.W., FE 7-8500.

The Most Trusted Name in Electronics

RADIO CORPORATION OF AMERICA

John V. L. Hogan

1890–1960

The Board of Directors of The Institute of Radio Engineers, joining with his many friends and colleagues, expresses its sense of profound regret and deep loss at the passing of their distinguished companion,

JOHN VINCENT LAWLESS HOGAN

The membership of The Institute, and indeed the entire fraternity of communications and electronic workers, owe John Hogan their gratitude for his pioneering energy and farsightedness in acting as a Founder of The Institute, and in devoting unremitting energy and skillful planning, over many years, to its organization and growth.

His participation in major deliberative bodies like the Joint Technical Advisory Committee was also noteworthy for its great value.

His contributions to the technology and procedures of the communications field were both numerous and outstanding. They ranged over many and diverse basic fields and they were both generic and specific.

Mr. Hogan exhibited as well exceptional executive ability and organizing skill in his professional, society, and industrial activities.

As a single typical example of his major organizing and planning contributions, exemplary mention is made of his widely acclaimed development of high-fidelity during the early years of radio broadcasting, with the related establishment of programming of notable cultural content combined with strong audience appeal.

In the midst of a busy life, he found the time and strength to contribute repeatedly and worthily to the National Defense of his country through the development and construction of many types of equipment, notably in the facsimile field and serving as an executive in the Office of Scientific Research and Development during World War II.

To those who were so fortunate as to know John Hogan personally, his passing will be a particular cause for sorrow. He was a rare combination of manly strength, great tenacity of purpose, unfailing dependability, and dignified and friendly courtesy. He will long be remembered with respect and affection.

The Board of Directors of The Institute of Radio Engineers conveys its sympathy to Mrs. Edith Hogan, and the family, in this time of their loss, which they too share.

The foregoing is the text of a resolution adopted by the IRE Board of Directors at its meeting of January 4, 1961.

Franz Ollendorff

Vice President, 1961

Professor Franz Ollendorff (SM'52–F'60), Overseas Vice President of the IRE for 1961, holds the Gerard Swope Chair in Electrical Engineering at the Technion, Israel Institute of Technology, Haifa. He was born in 1900, studied at the technical universities of Berlin and Danzig, and later became a member of the faculty at Berlin. He left this position in 1933, and until he joined the staff of the Technion, was Director of a school for children of the Youth Aliyah.

In 1928 he attracted international attention with the publication of a paper which pointed the way to the development, many years later, of radar. The paper dealt with the defraction of electromagnetic waves on mountains, hills, houses, and other objects. It showed that the reflection coefficient could be calculated in advance, and that, from the strength of the reflected waves, it is possible to judge the nature of the object causing the reflection. This is one of the principles on which radar is based.

Professor Ollendorff also made an important contribution to electronics. The formula for an electronic lens, which he published in 1932, has become a textbook classic, and the same is true of his well-known formula concerning the amplification factor of a triode.

More recently, the Technion scientist's ideas in connection with the development of electronic aid devices for the blind and deaf have attracted universal interest. One of his papers, "Contributions to the Geometry of Color Space," deals with electroencephalographic methods of aiding sight.

In 1955 he was appointed Research Professor at the Technion, the first staff member to be granted this rank. The title is conferred only upon scientists of high international repute, whose standing qualifies them for membership in institutions such as the Royal Society, the National Academy of Science, or the Academie des Sciences, and who have achieved distinction at a relatively early age.

He has won several prizes, including the Weizmann Prize for Exact Science for his work on electrophysiology, the Israel Prize for Exact Science in 1954 for his book, "Calculations of Magnetic Fields," and the David Lebeson Prize of the Hebrew University for his "Introduction to Electron Optics," also in 1954.

He is the author of a number of books and scientific papers and presently is editing a comprehensive work on electronics, two volumes of which already have been published, the third to appear shortly, and the fourth now being edited.

In 1959 Professor Ollendorff was elected a member of the Israel Academy of Science and, in the same year, was awarded the honorary degree of Doctor by the University of Berlin.

April, 1961
Vol. 49 No. 4

Proceedings of the IRE

Poles and Zeros

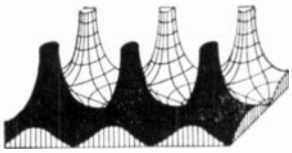

Satellite Communications. Poles and Zeros is pleased to present the following paragraphs prepared especially for it by Lieutenant General James D. O'Connell.

Satellite relays for common carrier communications appear to provide excellent long range communication channels and they are undergoing careful evaluation by private industry. Evidence of this interest was clearly demonstrated by the testimony of various firms presented to the FCC at recent hearings.

Engineering studies show that relay equipment can be placed into orbit with currently available rockets and currently available relay package designs. A telephone relay of several hundred voice channels is feasible. A television relay is feasible. The use of microwave frequencies eliminates the effects caused by ionospheric storms; fading as experienced by high-frequency signals is virtually nonexistent; and relatively simple ground installations are required.

The impact on world-wide communications will be great. Broadband communications to remote locations can be established almost as easily as between two highly developed countries. The number of available channels will surpass current capability by an order of magnitude. Cost studies indicate economic as well as technical feasibility. Current rate structures can be maintained, perhaps even lowered, and can adequately support an active satellite relay for common carrier purposes. Almost overnight a new communication medium will be available for the use of the world population.

A few questions remain unanswered, one of the most prominent being: Where will we obtain the spectrum space? Spectrum allocations for satellite relays will be discussed at the 1963 International Telecommunications Union Conference in New Delhi; however, the need for technical answers is immediate. It now appears that satellite relays must be accommodated within existing allocations. This implies mutual sharing of frequency allocations between satellite and existing ground services. The Federal Communications Commission is currently faced with these questions, and much theoretical and experimental work remains to be done before reliable answers can be given. If sharing of the same spectrum space can be accomplished in the design of satellite communications systems, this will have very great possibilities for over-all relief of spectrum congestion. But it appears too early to say with assurance that this noninterfering sharing can be accomplished. The Joint Technical Advisory Committee of the Electronic Industries Association and The Institute of Radio Engineers has formed an Ad Hoc Subcommittee chaired by Lieutenant General James D. O'Connell, USA Ret., now with General Telephone and Electronics Laboratories Inc., to study the technical problems imposed by satellite relays. Multiple use of frequency allocations will be one of the areas investigated by the committee. The Boulder Laboratories of the National Bureau of Standards and the Communication and Propagation Laboratory of Stanford Research Institute have been placed under contract to assist the committee in technical studies. A report containing preliminary JTAC findings was published early in March.

Members of the Committee, the National Bureau of Standards, and Stanford Research Institute invite the comments and views of industry concerning technical problems of satellite communication systems. Members of the Committee are:

Dr. Richard Emberson, Associated Universities, Inc., New York, N. Y.
Mr. Richard P. Gifford, General Electric Co., Lynchburg, Va.
Dr. John P. Hagen, National Aeronautics & Space Administration, Washington, D. C.
Dr. J. W. Herbstreit, National Bureau of Standards, Boulder Colo.
Dr. Donald MacQuivey, Office of Chief of Telecommunications, Department of State, Washington, D. C.
Mr. Ross Peavey, Space Science Board, National Academy of Sciences, Washington, D. C.
Dr. Allen M. Peterson, Stanford Research Institute, Stanford, Calif.
Mr. C. A. Petry, Aeronautical Radio Inc., Washington, D. C.
Mr. Thomas F. Rogers, Lincoln Laboratory, M.I.T., Lexington, Mass.
Dr. L. C. Tillotson, Bell Telephone Laboratories, Red Bank, N. J.
Lt. Gen. James D. O'Connell, USA Ret., Vice President, General Telephone & Electronics Labs., Inc., Menlo Park, Calif.

WWV and WWVH: With this issue of letters to the editor we note an improvement in reporting the standard frequencies broadcast by WWV. The corrections to these frequencies as broadcast now provide accuracy to ± 3 parts in 10^{11} with respect to the United States Frequency Standard, instead of the 1 part in 10^{10} of previous corrections. This is 30 parts in one million million and it is interesting to note that the standard frequency services, including those on LF and VLF, are required to give such high accuracy in meeting the needs of science and technology. It is even more interesting to realize that such requirements exist.

On the general subject of Standard Frequencies and Time Signals we received a copy of the National Bureau of Standards Miscellaneous Publication 236, "Standard Frequencies and Time Signals from NBS Stations WWV and WWVH," which can be purchased from the U. S. Government Printing Office for 10 cents. This publication contains complete, current information on standards of frequency, time interval, and musical pitch and on time signals and radio propagation forecast notices. Since issuance of Miscellaneous Publication 236, a Timing Code was added to WWV; it is described in PROC. IRE, p. 379, January, 1961.—F. H. Jr.

Scanning the Issue

Transistor Internal Parameters for Small-Signal Representation (Pritchard, *et al.*, p. 725)—The physicist or device designer looks at the transistor from the standpoint of its internal physical structure and operating mechanisms. The user, on the other hand, is concerned chiefly with its external characteristics. Numerous attempts have been made over the past decade to tie together these differing viewpoints by means of equivalent circuit representations, with varying degrees of success. In order to carry forward standardization work in this area, a Task Group on Transistor Internal Parameters (28.4.7) was formed a few years ago by the IRE-AIEE Committee on Semiconductor Devices. This joint Committee, which operates within the IRE as a subcommittee of the IRE Technical Committee on Solid-State Devices, will be remembered as the group that organized the June, 1958 Transistor Issue of the PROCEEDINGS. It soon became evident to the Task Group that before any standardization could be effected a tutorial paper on the subject would be required. Their report develops a complete equivalent-circuit representation of the transistor from its basic physical mechanisms and relates it to certain simplified representations that are useful in specific practical design situations. In so doing, the Task Group has taken an important step toward providing a common language for transistor designers and users.

A Noise Investigation of Tunnel-Diode Microwave Amplifiers (Yariv and Cook, p. 739)—Although the tunnel diode will probably never compete with the maser or parametric amplifier as a low-noise device, its high-frequency capabilities and simple structure make it a device of great promise and widespread interest. Consequently, there is a good deal of interest in the noise behavior of tunnel diodes, which is determined in large measure by the shot noise accompanying the tunneling process. This paper provides an analysis and derivation of the noise figure in a simple manner which emphasizes the physical interpretation of the results. These results will be of both practical and theoretical interest.

Tunnel-Diode Microwave Oscillators (Sterzer and Nelson, p. 744)—Tunnel-diode oscillators are compact and rugged, are relatively insensitive to nuclear radiation, have very modest power-supply requirements, and can be easily tuned by either mechanical or electrical means. Thus, they have significant advantages over low-power vacuum-tube oscillators and have great potential at UHF and microwave frequencies. During the past year or so, several workers have reported using tunnel diodes as oscillators with microwatt power outputs. The tunnel-diode oscillators described in this paper have power outputs an order of magnitude greater than any previously reported, ranging from 10 milliwatts at 610 Mc to 0.7 milliwatts at 2800 Mc to 0.01 milliwatt at 7130 Mc—a noteworthy advance in the state of the solid-state microwave generator art.

Three-Layer Negative-Resistance and Inductive Semiconductor Diodes (Gärtner and Schuller, p. 754)—Many different negative-resistance semiconductor devices have been discussed in recent years, including point-contact transistors, *p-n-p-n* structures, avalanche transistors, parametric and tunnel diodes. This revival of interest in negative resistance is understandable when one considers the wide variety of uses which such devices can have, such as bi-state devices for pulse circuitry, oscillators, oscillator-mixers, and novel amplifier circuits. This paper shows that under appropriate conditions negative resistance can be observed in a transistor-like three-layer structure with the base either open-circuited or shorted to the emitter region and that at higher frequencies an inductance is often evident, too. The conceivable circuit applications of this type of structure are numerous and impressive: oscillators, amplifiers, frequency converters, switching elements, multipliers, solid-state inductances to replace coils in miniature circuitry, distributed negative-resistance structures for microwave amplification, and parametric amplifiers of the variable-inductance as well as the variable-capacitance type.

A Low-Noise *X*-Band Radiometer Using Maser (Cook, *et al.*, p. 768)—The maser is unequalled as a nearly noiseless amplifying device. This attribute has made the maser an extremely valuable tool in the field of radio astronomy. This paper describes the characteristics and performance of the 4-level ruby maser system installed last year in the University of Michigan's 85-foot-diameter radiotelescope. It provides an excellent sequel to the June, 1959 PROCEEDINGS paper which described the first application of an *X*-band maser in a radiotelescope by the Naval Research Laboratory, and indicates the considerable advance which has been made since then in radio astronomy technology. The paper gives valuable information to those involved in space communications, as well as to radio astronomers, concerning the practical merits of the use of masers in the continuing quest for improved tools. In addition, the discussion of the practical problems encountered should stimulate further work on the part of research workers in the maser and large antenna fields.

An Analysis of the Magnetic Second-Subharmonic Oscillator (Lavi and Finzi, p. 779)—A second-subharmonic oscillator can operate in either of two phases, 180 degrees apart, thus providing in effect a device that can be switched back and forth between two states. Such a device can, therefore, be utilized to perform digital and logic operations in binary data-handling systems and indeed has been so used, for example, in the Parametron. This paper considers a second-subharmonic parametric oscillator with two ferromagnetic cores and presents a novel analysis of its steady-state performance and transient build-up which is in good agreement with experimental observations over a wide range of frequencies. The analysis will be of interest not only to computer engineers but to circuit theorists as well.

Properties of Tropospheric Scattered Fields (Ortwein, *et al.*, p. 788)—The general manner in which microwave transmissions are scattered by the troposphere is understood well enough to permit the design of tropospheric scatter communication systems. Nevertheless, there is still considerable disagreement as to the exact cause of the scattering phenomenon and only an incomplete understanding of a number of its properties. Further light is shed on these properties by this paper, which reports the results of a three-year series of over-water tropospheric scatter tests performed by the U. S. Navy Electronics Laboratory. It represents a great amount of careful work, yielding significant new experimental data that will be of lasting reference value to workers in this field.

IRE Awards, 1961 (p. 841)—Only one per cent of IRE's nearly 90,000 members have achieved the distinction of being named to its highest grade of membership. An even fewer number, 139, have had the high honor of receiving an award from the IRE. Last month, the 76 members who have been elevated to Fellow grade and the 8 who received an IRE award in 1961 were honored at the IRE annual banquet during the International Convention. The names, pictures, and award citations of these leaders of our profession are included in this issue as a tribute to them and to their work.

Annual Index to Transactions (follows p. 876)—Last year, the IRE Professional Groups published over 1000 papers and letters, accounting for more than 50 per cent of the total publication output of the IRE during 1960. As in past years, this April issue contains a consolidated author and a subject index to the 99 issues of IRE Transactions that appeared in 1960.

Scanning the Transactions appears on p. 855.

Transistor Internal Parameters for Small-Signal Representation*

R. L. PRITCHARD†, FELLOW, IRE, J. B. ANGELL‡, SENIOR MEMBER, IRE, R. B. ADLER||, FELLOW, IRE, J. M. EARLY§, FELLOW, IRE, AND W. M. WEBSTER¶, FELLOW, IRE

Summary—**The joint IRE-AIEE Task Group 28.4.7, on Transistor Internal Parameters, was organized with the following objectives:**

1) To formulate a small-signal equivalent-circuit representation of a transistor, the parameters of which emphasize separately the principal physical mechanisms of the device.

2) To recommend symbols for these parameters consistent with accepted usage and other standards.

3) To exhibit the relationship between the equivalent-circuit representation described in item 1 above and those simplified representations commonly employed in circuit analysis or design.

4) To propose and discuss methods of determining these parameters from electrical measurements at the terminals.

This report summarizes the work of the group on the first three of these objectives.

I. Introduction

IN characterizing a transistor for small-signal operation, one can adopt different philosophies depending on his immediate interest. From the standpoint of the user, it is sufficient to give the input, output, and transfer impedances as functions of the operating point, frequency, and ambient temperature. To the physicist or device designer, the transistor is characterized by the distribution of fixed charge within its volume, *i.e.*, by its dimensions, the conductivities of the active regions, etc. There is an appreciable gap between these two philosophies, requiring some tie-in between the physical structure and the four-pole parameters. Numerous equivalent-circuit representations have been proposed which attempt to make the connection and do so with varying degrees of success.[1] A need remained, however, to supply in a systematic manner a relatively complete single representation that could serve as a basis for a common language between the transistor designer and the user. This was the principal problem that motivated the present work; the fact that the complete circuit representation is usually too complicated for practical circuit calculations made it necessary also to detail its relationship with various well-known simplified forms.

In this report, the complete equivalent-circuit representation is developed from the basic physical mechanisms of the transistor in two steps. First, in Sections II and III, an idealized junction transistor is introduced (Fig. 1), and its structure is related to the elements of an equivalent-circuit representation (Fig. 2) through the physics of the minority-carrier and majority-carrier flows. Second, Section IV points out how a number of idealized transistors may be combined in a distributed fashion to simulate a real transistor. This section also indicates some simplifications that may be made of the resulting circuit representation in certain practical cases. Finally, in Section V are presented several of the common lumped equivalent-circuit representations that are useful for special classes of transistors or under special conditions of operation.

The idealized transistor is considered here in terms of the movement of minority charge carriers through the base region, including the finite time required for them to do so. Historically, this viewpoint has been used most widely in discussing transistor equivalent-circuit representations. The admittance representation em-

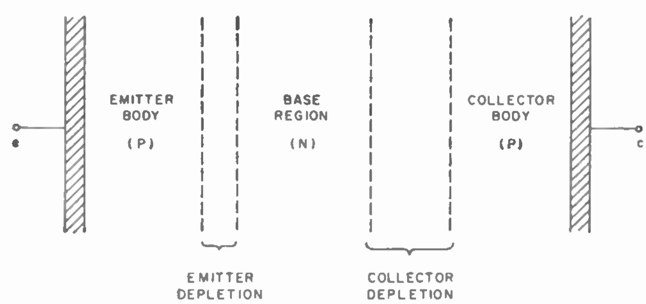

Fig. 1—Regions of idealized transistor.

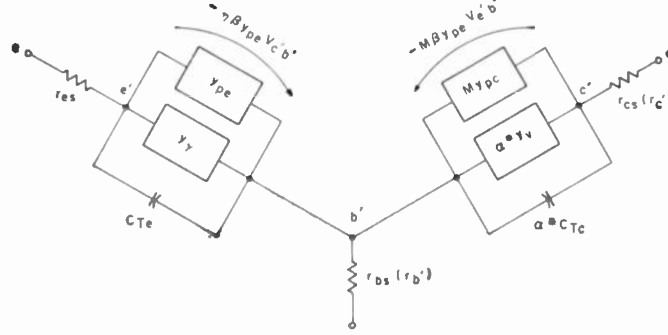

Fig. 2—Basic equivalent-circuit representation of idealized transistor.

* Received by the IRE, August 17, 1960; revised manuscript received December 19, 1960.

† Texas Instruments Inc., Dallas, Tex.
‡ Stanford University, Stanford, Calif.; formerly Philco Corp., Philadelphia, Pa.
|| Mass. Inst. Tech., Cambridge, Mass.
§ Bell Telephone Labs., Murray Hill, N. J.
¶ RCA Labs., Princeton, N. J.

[1] For a survey of this subject, see Pritchard [1].

ployed here is, of course, not the only possible choice. Other interesting viewpoints have been developed in considerable detail (see, for example, Zawels [2]), in which the compromise between physical representation of the device and convenience of the representation for equivalent-circuit purposes is made at a different place.

An alternative approach [3] also may be used, however, in which the time variation of stored charge, rather than the movement of charge, in the base region is considered to be fundamental. This stored-charge approach circumvents certain difficulties, such as defining the transit time of a diffuse flow; however, this formulation is less exact than the representation employed here. For example, the explicit dependence of all currents upon the barrier voltages usually disappears in a stored-charge analysis. In the use of a stored-charge analysis, portions of the stored charge must be related to the various physical phenomena discussed in this report.

For convenience, the entire report is phrased in terms of a *p-n-p* transistor.

II. The Idealized Transistor

Flow of minority carriers is basic to the operation of a junction transistor. However, majority-carrier flow is also important, giving rise to effects which will be considered in Section III. In the *p-n-p* transistor under discussion here, holes are injected into the base region by application of a forward bias to the emitter-base junction. The relation between the concentration of injected holes $[p_B(e') - p_{0B}]$ at the emitter edge of the base region and the applied forward voltage, $v_{E'B'}$ across the emitter junction[2] is exponential, according to the well-known [4] Boltzmann relation

$$p_B(e') - p_{0B} = p_{0B}[\exp(qv_{E'B'}/kT) - 1], \tag{1}$$

where p_{0B} is the equilibrium hole density in the base and kT/q is thermal voltage (about 25 millivolts at room temperature).

Inasmuch as the hole current is proportional to this injected hole concentration, current naturally appears as an exponential function of junction voltage. Consequently, the current-voltage relationship is most simply expressed with voltage taken as the independent variable, and this fact in turn makes it convenient to employ admittance parameters. A second reason for the choice of an admittance representation is that several individually analyzable currents may be associated with each junction voltage.

For an example of the second reason, note that the relation between incremental emitter hole current and emitter-base junction voltage gives rise to the admittance y_{pe} in Fig. 2. The same emitter-base junction voltage, $v_{E'B'}$, also causes injection of electrons into the emitter from the base region. Inasmuch as the total emitter current comprises both contributions, the small-signal effect corresponding to the electron current is represented by the admittance y_γ in parallel with the admittance y_{pe}. The electron flow into the emitter decreases the amplification of the device, and the transistor generally is designed to keep this current small relative to the hole current, *i.e.*, $|y_\gamma| \ll |y_{pe}|$.

The holes injected into the base region flow toward the collector. However, some of the holes recombine en route with the electrons in the base, so that only a fraction $|\beta|$ of the injected current reaches the collector depletion layer. There is also dispersion and delay associated with the flow of holes through the base region. These effects are included in the complex quantity β.

On reaching the edge of the collector depletion layer, holes move into the region of strong electric field. Even though they drift at a high velocity because of the field in this region, the holes may have a significant transit time through the depletion layer. In addition, some of the holes may have sufficient energy to produce hole-electron pairs by impact ionization. This "avalanche" phenomenon results in a multiplication within the collector depletion layer of the hole current which enters it. Finally, the flow of holes out of the collector depletion layer sets up an electric field in the collector body, which in turn causes a flow of electrons from the collector body into the base. This effect is called "collector-body multiplication," and makes the collector current larger than the hole current entering the collector depletion layer, as does avalanche multiplication. These three effects—depletion-layer transit time, avalanche, and body multiplication—vary in relative importance with individual transistor designs but they are all incorporated in the factor M which appears in Fig. 2. Collector body multiplication also produces additional effects requiring the factor α^* to appear separately in Fig. 2.

Thus far, consideration has been given only to the control of the flow of carriers by variation of emitter-to-base voltage, with the implicit understanding that collector-to-base voltage has remained fixed. Variations in collector-to-base voltage, however, cause changes in base-layer thickness through changes in the width of the collector depletion layer. These variations in base-layer thickness produce increments both in the hole current entering the collector barrier and in that leaving the emitter barrier. The dependence of the hole current entering the collector barrier on collector-to-base voltage is represented by the admittance y_{pc} in Fig. 2, and the corresponding change in hole current leaving the emitter is represented by the current generator between e' and b'.

The phenomenon of carrier multiplication due to impact ionization in the collector depletion layer is voltage-dependent. Therefore, the collector current may vary with collector-to-base voltage, even though the hole current arriving at the base edge of the collector

[2] The voltages $v_{E'B'}$ and $v_{C'B'}$, and their ac or dc counterparts, are the emitter-to-base junction voltage and collector-to-base junction voltage, respectively, and not the terminal voltages v_{EB} and v_{CB}, which may include significant voltage drops through one or more lead impedances.

depletion layer is constant. This variation of collector current with collector-to-base voltage, caused by changes in impact ionization, is represented by the avalanche admittance, y_v, in Fig. 2.

In order for us to proceed with the detailed definitions of the various parameters discussed above, it will be convenient to refer to various currents and voltages within the idealized transistor, of which some are shown in Fig. 3.[3] Upper-case symbols with lower-case subscripts are used to represent the rms magnitude and phase of single-frequency small-signal ac quantities; it should be understood that, in accordance with IRE Standards on Letter Symbols for Semiconductor Devices (56 IRE 28.S1), the corresponding static (or dc) quantities will be indicated by change from lower-case to upper-case subscripts. Lower-case symbols with upper-case subscripts denote instantaneous total values.

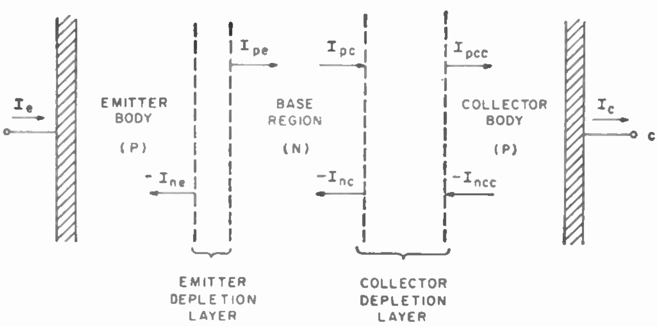

Fig. 3—Currents in idealized transistor.

A. Minority-Carrier Injection

1) *Injection into the Base* (y_{pe}): The admittance y_{pe}, associated with hole injection from the emitter into the base region, is defined as the ratio of the emitted hole current I_{pe} to the junction voltage $V_{e'b'}$ at constant collector voltage ($V_{c'b'}=0$):

$$y_{pe} = \frac{I_{pe}}{V_{e'b'}}\bigg|_{V_{c'b'}=0}. \tag{2}$$

At low frequencies, for transistors in which I_{pe} represents a major fraction of the emitter current, y_{pe} is approximately equal to the conductance of the emitter-base diode [5]:

$$y_{pe} \approx \frac{di_E}{dv_{E'B'}} \equiv \frac{1}{r_{e'}} \approx \frac{qI_E}{kT}. \tag{3}$$

[3] The directions of the various currents shown in Fig. 3 follow the flow pattern in a *p-n-p* transistor, in order to simplify the definition of transfer functions such as β. The collector current I_c flows out of the transistor, in contrast to usual network theory practice, where positive directions for currents are chosen into a circuit element. The internal hole currents, I_{pe}, I_{pc}, and I_{pcc}, flow from emitter to collector, as shown by the corresponding arrows. The arrows on the electron currents, however, point in the direction in which the electrons move; the minus signs on I_{ne}, I_{nc}, and I_{ncc} show that these currents actually are in the same direction as the hole currents.

On the other hand, the ac emitter junction voltage also gives rise to a time variation of the charge stored in the base by the direct current I_{PE}. This effect can be represented as a (diffusion) capacitance in parallel with the low-frequency conductance. However, at higher frequencies, the admittance y_{pe} must be considered as a more elaborate complex, frequency-dependent, admittance.

In the case of a transistor in which minority carriers flow only by diffusion [6]–[8], y_{pe} is given approximately by

$$y_{pe} \approx \frac{1}{r_{e'}} \zeta \coth \zeta \tag{4}$$

where ζ is defined as

$$\zeta \equiv \frac{W}{L_B}\sqrt{1 + j\omega\tau_B} = \sqrt{\left(\frac{W}{L_B}\right)^2 + j\omega\frac{W^2}{D_B}}, \tag{5}$$

with W as the base width, τ_B, L_B and D_B, respectively, the minority-carrier lifetime, diffusion length, and diffusion constant in the base region.

2) *Injection into the Emitter* (y_γ): The admittance y_γ is associated with the flow of electrons from the base into the emitter region, where the electrons are minority carriers. This admittance is the ratio of the electron current I_{ne} to the emitter junction voltage $V_{e'b'}$, with the collector voltage constant.

$$y_\gamma = \frac{I_{ne}}{V_{e'b'}}\bigg|_{V_{c'b'}=0}. \tag{6}$$

For the conventional transistor defined in Section II-A, 1), it is given approximately by

$$y_\gamma \approx \frac{q}{kT} I_{NE}\sqrt{1 + j\omega\tau_E}, \tag{7}$$

where τ_E is the effective electron lifetime in the emitter.

3) *Injection Efficiency* (γ): The injection efficiency, γ, is introduced at this point for convenience and defined as that fraction of the total emitter conduction current (as distinct from displacement current through the emitter transition capacitance) which is composed of holes [4]. Specifically,

$$\gamma = \frac{I_{pe}}{I_{pe} + I_{ne}}\bigg|_{V_{c'b'}=0} = \frac{y_{pe}}{y_{pe} + y_\gamma}. \tag{8}$$

Since only the hole current gives rise to amplification, transistors usually are designed to have values of γ close to one. This, of course, means that y_γ is much smaller in magnitude than y_{pe}. For a given forward emitter-junction voltage, the ratio of hole current to electron current crossing the junction is determined in the first order by the ratio of hole density in the emitter to electron density in the base. To make I_{pe} large compared to I_{ne}, the transistor is designed to have a much higher concentration of holes in the emitter region than electrons in the base region. For example, in the conventional transistor discussed previously [6]–[8],

$$\left.\frac{I_{ne}}{I_{pe}}\right|_{V_{c'b'}=0} \approx \frac{I_{NE}\sqrt{1+j\omega\tau_E}}{I_{PE}\zeta\coth\zeta} = \frac{n_{0E}D_E W}{p_{0B}D_B L_E} \times \frac{\sqrt{1+j\omega\tau_E}}{\zeta\coth\zeta}, \tag{9}$$

in which n_{0E} and p_{0B} are the equilibrium minority-carrier densities, D_E and D_B are the minority-carrier diffusion constants in the emitter and base regions respectively, and L_E is the minority-carrier diffusion length in the emitter. It should be noted that if the thickness of the emitter region is small relative to the diffusion length in the emitter material, the factors L_E and τ_E are determined by the emitter thickness and by the nature of the contact to the emitter region.

B. Carrier Flow Through the Base Region (β)

The collector current generator of Fig. 2 represents the flow through the collector depletion layer of carriers controlled by the emitter-base voltage. It is composed of M, which includes effects occurring in transit through the depletion layer [as will be discussed in Section II-D,1) below]; β, which indicates the efficiency of hole transport through the base region; and $y_{pe}V_{e'b'}=I_{pe}$, that portion of the emitter current which results in useful amplification. The present section concerns β, the base transport factor, which is defined as the ratio of the hole current (I_{pc}) leaving the base region at the collector depletion layer to the hole current (I_{pe}) entering the base region at the emitter, with the collector voltage held constant [5].

$$\beta = \left.\frac{I_{pc}}{I_{pe}}\right|_{V_{c'b'}=0}. \tag{10}$$

This ratio always is less than one in magnitude and in general is complex, owing to time delays in the diffusion and drift processes. At low frequencies, I_{pc} is less than I_{pe} because of recombination of holes in the base.[4] The smaller the base width W, the less β departs from one. Also, I_{pc} lags behind I_{pe} in such a way that β has a negative phase angle which increases with increasing frequency. In general, the smaller the base width, the less the time delay and, hence, the smaller the phase lag at a given frequency. Furthermore, diffusion during transport through the base region results in a spread of carrier transit time, *i.e.*, dispersion. This dispersion causes the magnitude of I_{pc} to decrease, relative to that of I_{pe} with increasing frequency; therefore, $|\beta|$ decreases with increasing frequency. In some high-frequency transistors, a built-in electric field in the base region reduces the transit time for a fixed base width, and reduces the dispersion even more.

For a transistor in which minority carriers flow only by diffusion [5], the transport factor β is given by

$$\beta = \operatorname{sech}\zeta \tag{11}$$

where ζ is defined in (5). In the more general case, particularly when electric fields in the base region affect transit time, a useful approximation for β is [9]–[11]

$$\beta \approx \frac{\beta_0 e^{-j\nu(\omega/\omega_\beta)}}{1 + j(\omega/\omega_\beta)}, \tag{12}$$

where β_0 is the low-frequency value of β, ω_β is the frequency at which $|\beta|$ has decreased to $1/\sqrt{2}$ times its low-frequency value β_0, and ν is a constant that represents the "excess phase" or additional phase shift of β over and above the particular RC-type phase shift associated with the simplified attenuation $[1+(\omega/\omega_\beta)^2]^{-1/2}$ assumed for β in (12). Eq. (12) does not imply that the frequency dependence of β is necessarily of a nonminimum phase type; in fact, it can be shown that precisely minimum-phase behavior is to be expected in common cases [11], although the phase shift obviously is not of the simple RC variety.

For transistors in which minority carriers flow only by diffusion [see (11)],

$$\beta_0 = \operatorname{sech}(W/L_B) \approx 1 - \tfrac{1}{2}(W/L_B)^2, \quad (W/L_B)^2 \ll 1,$$
$$\omega_\beta \approx 2.4 D_B/W^2, \qquad \nu \approx 0.2. \tag{13}$$

Note that $\frac{1}{2}(W/L_B)^2 \approx T_B/\tau_B$, which is the ratio of transit time through the base region, $T_B \approx W^2/2D_B$, to hole lifetime in the base region, τ_B. The ratio T_B/τ_B is simply the proportion of carriers which recombine in transit through the base region.

C. Base-Width Modulation [12]

1) *Reverse Transfer Admittance* ($-\eta\beta y_{pe}$): The emitter-base current generator (short-circuit reverse transfer admittance of the part of Fig. 2 between terminals e', b' and c') represents the change in emitter current caused by a change of collector junction voltage, with emitter junction voltage held constant. For convenience, this reverse transfer admittance has been written as the product of three factors, two of which have already been discussed (β and y_{pe}). The third one, η, must be the main concern of this section.

Called the voltage feedback factor, η is defined as $1/\beta$ times the ratio of emitter-junction voltage $V_{e'b'}$ to collector junction voltage $V_{c'b'}$, with the emitted hole current entering the base region held constant ($I_{pe}=0$):

$$\eta = \left.\frac{V_{e'b'}}{V_{c'b'}}\right|_{I_{pe}=0} \times \frac{1}{\beta} \tag{14}$$

[4] In a practical transistor, recombination of carriers at the surface must be considered. See Section IV-A).

Defined in this way, η is frequency-independent for idealized one-dimensional transistors of either the homogeneous-base or the Kroemer drift type.

Physically, the emitter-junction voltage variation involved in η arises from a variation in base width with collector-junction voltage, as discussed in Sections II and III-A. For a transistor in which minority-carrier flow through the base region is by diffusion only, an approximate expression for the factor η may be deduced by referring to Fig. 4, which illustrates the hole distribution through the base for two different values of collector voltage. For simplicity, a constant hole-concentration gradient is shown. This implies that the dc hole current is constant through the base and hence that $\beta_0 = 1$. Moreover, the gradient is the same for both values of collector voltage, which implies that the dc hole current at the emitter is being maintained constant, as required in the definition of η.

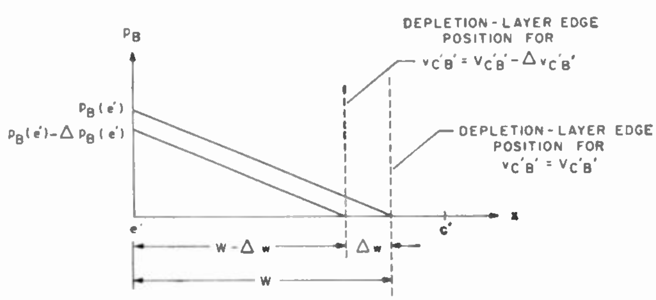

Fig. 4—Hole concentrations in the base layer, illustrating the reverse-transfer effect of base-width modulation at low frequencies when i_{PE} = Constant.

From the geometry of Fig. 4,[5]

$$\frac{\Delta p_B(e')}{p_B(e')} = \frac{\Delta w}{W}. \tag{15}$$

The relation between the excess hole concentration at the emitter edge of the base, $p_B(e')$, and the emitter junction voltage $v_{e'b'}$ has been given in (1), differentiation of which yields

$$\Delta p_B(e') = p_B(e')(q/kT)\Delta v_{E'B'}. \tag{16}$$

Noting that

$$\Delta w = \Delta v_{C'B'}(dw/dv_{C'B'}), \tag{17}$$

combining the above results, and recalling that $\beta_0 = 1$, we find that

$$\eta = \frac{1}{\beta_0}\frac{V_{e'b'}}{V_{c'b'}}\bigg|_{I_{p_e}=0} = \frac{\Delta v_{E'B'}}{\Delta v_{C'B'}} \approx \frac{kT}{q}\frac{1}{W}\left(\frac{dw}{dv_{C'B'}}\right). \tag{18}$$

The value of the space-charge layer widening factor $(dw/dv_{C'B'})$ depends on the nature of the collector-base junction. In most transistors, the feedback ratio η is of the order of 10^{-3} to 10^{-5}. In circuit applications, the feedback associated with η is usually negligible. However, this feedback affects the choice of the equivalent-circuit representation of the transistor, as described further in Section V-B.

2) *Collector Admittance* (y_{pc}): The factor y_{pc} in the admittance My_{pc} of Fig. 2 represents the collector-base admittance produced by depletion-layer widening effects alone. It is defined as the (negative of the) ratio[3] of the hole current I_{pc}, entering the collector depletion layer from the base, to the junction voltage $V_{c'b'}$, with emitter-base junction voltage held constant ($V_{e'b'} = 0$):

$$y_{pc} = \frac{-I_{pc}}{V_{c'b'}}\bigg|_{V_{e'b'}=0}. \tag{19}$$

In order to incorporate this admittance into the equivalent-circuit representation of Fig. 2, we must multiply y_{pc} by the collector-current multiplication ratio M relating I_{pc} to I_c [Section II-D, 1)]. It might be noted that M is defined in terms of $V_{c'b'} = 0$, whereas a short-circuit output admittance requires $V_{e'b'} = 0$. This difference in boundary conditions does not affect My_{pc} *per se* but rather gives rise to the presence of the admittances $\alpha^* y_e$ and $j\omega\alpha^* C_{Te}$ in Fig. 2, representing the collector current that flows for unit $V_{c'b'}$ when $V_{e'b'} = 0$.

For the simple case of the transistor in which minority-carrier flow through the base is by diffusion only, an expression for y_{pc} at low frequency can be derived, in a manner similar to that used in deriving (18), by referring to the sketch shown in Fig. 5. This sketch differs from that of Fig. 4, however, in that the hole concentration at the emitter is the same for both values of collector voltage, which reflects the condition that the emitter junction voltage $v_{E'B'}$, rather than the emitter hole current, is held constant. Inasmuch as the hole current is proportional to the gradient of the hole concentration, $p_B(e')/w$, a change in base width due to a change in collector voltage gives rise to a change in hole current such that

$$\Delta i_{PC} = -(I_{PC}/W)\Delta w. \tag{20}$$

By referring to (17), and to the definition (19) for y_{pc}, we see that

$$y_{pc} \approx \frac{-\Delta i_{PC}}{\Delta v_{C'B'}} = I_{PC}\frac{1}{W}\left(\frac{dw}{dv_{C'B'}}\right). \tag{21}$$

In addition to the low-frequency conductance effect in (21), the decrease of base width also involves susceptance [13]. At low frequencies, the minority-carrier charge q_B stored in the base by the dc bias current must be changed by an amount, as indicated by the shaded portion of Fig. 5,

$$\Delta q_B = qA\Delta w p_B(e')/2, \tag{22}$$

where A is the cross-section area of the junction. When this charge Δq_B is removed through the collector terminals by an incremental collector voltage $\Delta v_{C'B'}$, the effec-

[5] Lower-case w is used to designate the instantaneous value of base width, whereas upper-case W indicates the base width with quiescent collector voltage ($V_{c'b'} = 0$).

tive shunt capacitance is $C_{eq} = \Delta q_B / \Delta v_{C'B'}$. A more useful form for this capacitance can be obtained by introducing the proportionality constant between dc hole current and hole concentration:

$$I_{PC} = qAD_B p_B(e')/W \tag{22}$$

and by employing (17); thus

$$C_{eq} = \frac{\Delta q_B}{\Delta v_{C'B'}} = I_{PC}\left(\frac{W}{2D_B}\right)\left(\frac{dw}{dv_{C'B'}}\right). \tag{23}$$

In general, at higher frequencies, y_{pc} must be considered as a more elaborate complex admittance, with frequency-dependent conductive and susceptive parts.

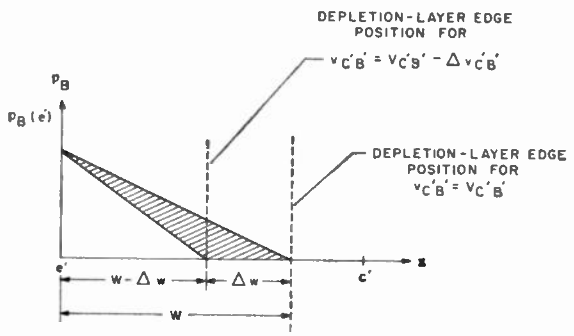

Fig. 5—Hole concentrations in the base layer, illustrating one output admittance effect of base-width modulation at low frequencies, when $v_{E'B'}$ = Constant.

D. Collector Action

"Collector action" as defined here comprises only those injection-induced conduction processes occurring *within* either the collector depletion layer or the collector body region (Fig. 3).[6] These processes relate portions of the incremental collector terminal current I_c to: 1) incremental hole current I_{pc} incident from the immediately adjacent part of the base region; and 2) incremental collector junction voltage $V_{c'b'}$. Effects similar to item 2), but associated with collector depletion-layer widening, are discussed in Sections II-C, 2) and III-A.

The portion of collector action relating I_c to I_{pc}, at fixed collector junction voltage ($V_{c'b'} = 0$), is contained in the over-all collector current-multiplication factor M (Fig. 2). It is treated in Sections II-D, 1)–II-D, 4).

The remaining portion of collector action contains the effect of the voltage $V_{c'b'}$ upon that portion of I_c produced by the avalanche process within the collector depletion layer, at fixed incident hole current ($I_{pc} = 0$). The corresponding small-signal admittance is y_v (Fig. 2). It is discussed in Section II-D, 5).

1) *Collector Current-Multiplication Factor* (M): At fixed collector junction voltage, the ratio of incremental collector terminal current, I_c, to the incremental hole current βI_{pe} incident from the emitter upon the base boundary of the collector depletion layer is the complex current-multiplication factor M:

$$M = \left.\frac{I_c}{\beta I_{pe}}\right|_{V_{c'b'}=0} = \left.\frac{I_c}{I_{pc}}\right|_{V_{c'b'}=0}. \tag{24}$$

The factor M defined above may always be represented as the product of two others

$$M = \left.\frac{I_{pcc}}{I_{pc}}\right|_{V_{c'b'}=0} \times \left.\frac{I_c}{I_{pcc}}\right|_{V_{c'b'}=0} \equiv M'\alpha^*, \tag{25}$$

where

$$\alpha^* \equiv \left.\frac{I}{I_{pcc}}\right|_{V_{c'b'}=0} \tag{26}$$

is the collector-body multiplication factor and

$$M' \equiv \left.\frac{I_{pcc}}{I_{pc}}\right|_{V_{c'b'}=0} = \left.\frac{I_{pcc}}{\beta I_{pe}}\right|_{V_{c'b'}=0} \tag{27}$$

is the collector depletion-layer multiplication factor.

In spite of the general factorability of M exhibited in (25), calculation of the values of M' and α^* from the physics of the device requires, in principle, the solution of a boundary-value problem involving both the collector depletion layer and the collector body region at the same time. Thus, in principle, M' and α^* cannot be evaluated independently when both are simultaneously greater than one.[7] Moreover, under such conditions, the appropriate boundary-value problem referred to above has never been investigated carefully. Nevertheless, in contemporary practice, it is unusual to find important conditions under which M' and α^* are simultaneously much larger than one; and when either factor is close to one, a first-order calculation of the other can be made by neglecting the interaction between them.

More detailed discussions of α^* and M' are given below, with examples of their analytical expressions under appropriate simplifying conditions.

The depletion-layer multiplication factor M' in (27) relates to those processes occurring within the collector depletion layer which are responsible for a difference in either phase or magnitude between the hole current I_{pcc} in Fig. 3 and the portion βI_{pe} of the injected hole current entering the depletion layer from the base. Both the transit time of carriers through the depletion layer and their avalanche multiplication processes are involved in M', generally in a more or less complicated way.

Most of the important practical situations at present are cases in which either barrier transit time is important without significant avalanche multiplication (low collector bias voltage and high frequency), or avalanche multiplication is important without significant transit time (high collector bias voltage and low frequency).

[6] In this connection, any avalanche process considered must not be so great that it destroys the validity of separating these regions conceptually.

[7] An extreme case of this situation is the one rejected in footnote 6.

The relevant special values of M' under these circumstances are important enough to be given identifying symbols:

B = barrier transit time factor (complex)
m = avalanche multiplication factor (real).

Further discussion of these parameters will be given in Sections II-D, 2) and II-D, 3), respectively.

2) *Barrier Transit-Time Factor* (B): In the absence of any avalanche multiplication, a single hole (hole-current impulse) entering the collector depletion layer from the base produces a pulse of collector terminal current. This pulse lasts for the time, T, that it takes the hole to traverse the depletion zone, and is essentially rectangular because the hole velocity is approximately constant in transit. Hence, the sinusoidal response for the barrier transit-time factor, B [14], is the Fourier transform of this rectangular pulse of duration T:

$$B = \frac{1 - e^{-j\omega T}}{j\omega T}. \tag{28}$$

When collector-body multiplication is either absent or at least very small ($\alpha^* \approx 1$), the collector body current is almost entirely composed of holes, and

$$B = \frac{1 - e^{-j\omega T}}{j\omega T} \approx \left.\frac{I_{pcc}}{\beta I_{pe}}\right|_{\substack{V_{c'b'}=0 \\ \text{No avalanche}}} = \left. M' \right|_{\text{No avalanche}}. \tag{29}$$

3) *Avalanche Multiplication Factor* (m): At low frequencies, when depletion-layer transit time is negligible, the only effect upon hole current through the depletion layer is the avalanche multiplication process. Then,

$$m = \left.\frac{I_{pcc}}{\beta I_{pe}}\right|_{\substack{V_{c'b'}=0 \\ \text{Low Frequency}}} = \left. M' \right|_{\text{Low Frequency}} \tag{30}$$

is the avalanche multiplication factor.

Values of m in germanium and silicon have been measured only on a dc (or very low-frequency) basis, and in the absence of collector-body multiplication. That is, they have been measured under conditions in which

$$m = \left.\frac{I_C - I_{CO}}{\beta_0 I_{PE}}\right|_{\substack{r_{C'B'}=\text{const} \\ \alpha^*=1}} \tag{31}$$

where I_{CO} is the collector reverse-bias current with $i_E = 0$. It has been found experimentally for these materials that [15], [16]

$$\left. m \right|_{\substack{\alpha^*=1 \\ \text{Low Frequency}}} \approx \frac{1}{1 - \left(\frac{V_{C'B'}}{V_B}\right)^n} \tag{32}$$

where V_B and n are empirical constants depending upon both the semiconductor material and the incident carrier (holes or electrons).

4) *Collector-Body Multiplication Factor* (α^*): In the collector body region (Fig. 3), there is considerable hole current flowing as a result of transistor action, notwithstanding the reverse bias on the collector junction. At a distance greater than a diffusion length from the junction, this hole current is accompanied by an electric field. Associated with this field there is an electron current, I_{ncc}, flowing toward the collector junction. Hence, the total incremental collector current I_c exceeds the incident hole current I_{pcc} by an amount I_{ncc} which is proportional to I_{pcc}. Therefore, (26) for the collector-body multiplication factor α^* may be written as [6], [17]

$$\alpha^* = \left.\frac{I_c}{I_{pcc}}\right|_{V_{c'b'}=0} = 1 + \left.\frac{I_{ncc}}{I_{pcc}}\right|_{V_{c'b'}=0}. \tag{33}$$

Normally, the incremental electron current I_{ncc} is small relative to I_{pcc}, inasmuch as the former is proportional to electron concentration in the collector body, whereas the latter is proportional to hole concentration. However, when the collector body material approximates an intrinsic semiconductor, *e.g.*, with increasing temperature, the ratio I_{ncc}/I_{pcc} may become appreciable.

In general, α^* is a function of the collector bias current I_C and the frequency ω, as well as of the physical parameters of the collector body region [6], [17]. For a one-dimensional transistor, under conditions of large collector bias current, low frequency, and no avalanche, α^* can be expressed in terms of collector-body conductivities as:

$$\alpha^* \approx \left(1 + \frac{\sigma_{nc}}{\sigma_c}\right) \tag{34}$$

where σ_{nc} is the equilibrium collector-body conductivity due to minority carriers only, and σ_c is the equilibrium collector conductivity. For small collector currents, the ratio $(\alpha^* - 1)$ must be reduced by a factor of 2. In either case, at high frequencies the ratio $(\alpha^* - 1)$ varies as $(j\omega)^{-1/2}$. Normally, $\sigma_{nc} \ll \sigma_c$, and α^* is not significantly different from 1.

At those frequencies for which barrier transit time is negligible, (25) suggests that

$$M = m\alpha^*. \tag{35}$$

This is correct; but use of (32) and (34) for m and α^* respectively in (35) can never be justified unless both m and α^* are nearly equal to one (in addition to the other restrictions placed on these equations).

5) *Avalanche Admittance* (y_r): The collector-current multiplication factor M has been related to the current-transfer action of the collector depletion-layer region and the collector body region, when the collector junction voltage does not vary ($V_{c'b'} = 0$). We must now consider the effect of collector junction voltage upon the action of these regions, when the incident hole current does not vary. Fixing the incident hole current means setting $I_{pe} = 0$ in Fig. 3, even though the col-

lector-junction voltage is allowed to change. Under different constraints, I_{pc} ordinarily varies as a result of the collector depletion-layer widening, which accompanies changes of the junction voltage [Section II-C, 2)]. Therefore, the condition $I_{pc}=0$, with $V_{c'b'}\neq 0$, implies a variation of emitter voltage, and consequent emitter injection, just sufficient to counteract the effect of collector space-charge layer widening upon I_{pc}. In terms of the equivalent circuit of Fig. 2, the current generator between b' and c' is being actuated to counteract exactly the current through the admittance My_{pc} produced by $V_{c'b'}$.

Under the foregoing conditions, which make $I_{pc}=0$, $V_{c'b'}$ produces a terminal current I_c that must meet several demands. First, it supplies a charging current required to change the depletion-layer width. This current is associated with the depletion-layer capacitance C_{Tc} (Section III-A). Secondly, it must include any current associated with changes in the avalanche process accompanying the changes in voltage. Third, the changes in barrier transit time accompanying the changes in depletion-layer width require additional "charging current" components in I_c. The last two items come under the heading of voltage dependence of the conditions encountered by carriers traversing the depletion layer; the corresponding current is associated with the avalanche admittance y_v.

In general, it is difficult to separate clearly (in terms of the currents in Fig. 3) those processes (y_v) having to do with carriers traversing the depletion layer from those relating directly to the changing of the dimensions of that layer (C_{Tc}). Thus, it is best to define simply

$$y_v + j\omega C_{Tc} = \left.\frac{-I_c}{V_{c'b'}}\right|_{\substack{I_{pc}=0\\ \alpha^*=1}} = \left.\frac{-I_{pcc}}{V_{c'b'}}\right|_{I_{pc}=0}. \tag{36}$$

Nevertheless, the depletion-layer widening responsible for C_{Tc} takes place so quickly with applied voltage, compared to the carrier transit time across the barrier, that there is no conceptual difficulty in isolating the effects whenever they have any meaning. Essentially this requires that the avalanche multiplication be small enough to permit thinking of a depletion layer in the first place.[6] Treatment of situations in which this is not possible falls beyond our present scope of discussion.

If conditions are such that (31) and (32) apply, y_v can be identified as follows [18]

$$y_v = \left.\frac{\partial i_C}{\partial v_{C'B'}}\right|_{I_{PE}=\text{const}} = \beta_0 I_{PE}\left(\frac{dm}{dv_{C'B'}}\right)$$

$$\approx n(m-1)\left(\frac{-I_C}{V_{C'B'}}\right). \tag{37}$$

6) *Other Effects of Collector-Body Multiplication:* As a result of the current multiplication processes in the collector body and collector depletion layer, the various collector admittances y_{pc}, y_v, and $j\omega C_{Tc}$ must be multiplied by appropriate factors M or α^*. The validity of this procedure can be established by treating the region between the base edge of the collector depletion layer and the collector terminal as a pair of cascaded transducers, voltage-current equations for which can be written down from (26), (27) and (36):

$$I_c = \alpha^* I_{pcc}$$

$$I_{pcc} = M' I_{pc} - (j\omega C_{Tc} + y_v)V_{c'b'}. \tag{38}$$

The equation relating hole current to the emitter-base and collector-base junction voltages follows from (10), (2), and (19):

$$I_{pc} = \beta y_{pe} V_{e'b'} - y_{pc} V_{c'b'}. \tag{39}$$

Combining the above equations and introducing (25) leads to

$$I_c = M\beta y_{pe} V_{e'b'} - [My_{pc} + \alpha^*(y_v + j\omega C_{Tc})]V_{c'b'} \tag{40}$$

which describes the voltage-current relations between terminals c' and b' of Fig. 2.

III. The Idealized Transistor – Majority-Carrier Flow

This section treats phenomena associated with majority-carrier flow. These phenomena are not basic to the amplifying properties of a transistor, but may limit its performance. They are of two kinds: 1) the depletion-layer capacitances across the junctions, and 2) resistances within the device due to the resistivities of the semiconducting regions.

A. Depletion-Layer Transition Capacitances (C_{Te} and C_{Tc})

A contact potential exists between p- and n-type semiconductors. At a p-n junction, a depletion layer is formed in which this potential difference is absorbed. The depletion layer extends on both sides of the junction, and in it the electric field is relatively high. This field is in such a direction as to push majority carriers away from the junction on their own sides and to accelerate minority carriers which diffuse into the depletion layer across to the opposite side of the junction. Applied reverse or forward voltages add to or subtract from, respectively, the contact potential. As the reverse potential across the junction increases, the layer widens, pushing majority carriers back through the bulk semiconductor on both sides. The depletion layer thus behaves as a capacitor, requiring charging current to flow in the external circuit. This capacitance is exactly that of a parallel-plate capacitor filled with material having the dielectric constant ϵ of the semiconductor, the junction area, A, and the plate spacing equal to the depletion-layer width, x_m, which is a function of junction voltage:

$$C = A\epsilon/x_m. \tag{41}$$

The junction has a depletion layer even when forward-biased, because of the internal contact potential between the n- and p-type semiconductors which, in effect, acts as a built-in reverse bias. A net reverse junction potential therefore exists even with very large forward currents. However, the depletion layer of a forward-biased emitter is much thinner than at the reverse-biased collector, so that the emitter depletion-layer capacitance is usually much larger than that at the collector.

The depletion layer capacitances are indicated by elements C_{Te} and C_{Tc} in the equivalent-circuit representation of Fig. 2. The collector depletion-layer capacitance in the representation is multiplied by α^*, as described in Section II-D, 5), because the current through this capacitance contributes to the majority-carrier current, I_{pcc}, in the collector body.

The variation of the depletion-layer capacitance with applied voltage depends upon the impurity distribution in the neighborhood of the junction. In the case of an abrupt transition between homogeneous n-type and homogeneous p-type materials, where the resistivity of one type is very much lower than the other (as in an alloy transistor or surface-barrier transistor) the depletion-layer capacitance varies inversely with the square root of the junction voltage [4]

$$C_T = A[qN\epsilon/2(V + V_0)]^{1/2}, \tag{42}$$

where N is the impurity concentration in the higher resistivity material (base region in an alloy transistor), V_0 is the magnitude of the internal contact potential (*e.g.*, for germanium, $V_0 \approx 0.3$–0.5 volt), and V is the applied reverse voltage. On the other hand, if the impurity concentration varies in a linear fashion from n- to p-type, as in most grown-junction transistors and in some diffused-base transistors, then [4]

$$C_T = (A\epsilon)[qa/12\epsilon(V + V_0)]^{1/3} \tag{43}$$

where a is the impurity-concentration gradient.

In some types of high-frequency transistors, the capacitance may vary with voltage in one of the ways described above for voltages up to a critical value, beyond which the capacitance effectively saturates, *i.e.*, further increases in voltage cause no further decrease in capacitance.

For the reverse-biased collector-base junction, the applied voltage $V = |V_{C'B'}|$ generally is much greater than the internal contact potential V_0. Hence, an equation for C_{Tc} can be obtained from (42) above by replacing $(V_0 + V)$ by $|V_{C'B'}|$. In an alloy transistor, for example,

$$C_{Tc} \approx A_c[qN\epsilon/2\ |V_{C'B'}|\ ]^{1/2}. \tag{44}$$

On the other hand, for the forward-biased emitter junction, the applied voltage $V = -V_{E'B'}$ is small but of opposite sign from V_0. Hence, the net junction voltage for the emitter junction is considerably smaller than for the collector junction. Moreover, in many high-frequency transistors, the impurity distribution in the vicinity of the emitter-base junction is such that the impurity concentration and/or gradient are much greater than at the collector-base junction. As a result of these factors, the emitter transition capacitance generally is many times greater than that of the collector.

B. Extrinsic Lead Resistances (r_{es}, r_{bs}, r_{cs})

In any practical transistor structure, the majority-carrier current must flow through the three semiconductor regions to the emitter and collector junctions. The resistances of these regions are accounted for in the equivalent-circuit representation of Fig. 2 by series resistors in each of the three leads. At low current densities the magnitudes of these resistances (for the ideal structure considered here) can be calculated approximately in a relatively straightforward manner from the geometry and resistivity of the material. That is, $r_s = \rho l/A$, where ρ is the resistivity of the region, l and A respectively are the path effective length and effective cross-section area for current flow through the region. At high current densities, conductivity modulation of the regions must be taken into account, *i.e.*, ρ will decrease with increasing current density.

The relative importances of these elements varies with the type of transistor construction, and in many cases some of these resistances are negligible insofar as their influence on performance is concerned. Generally, the most important is the one in the base lead (r_{bs}), since this resistance is inversely proportional to the width of the base region (cross-section area for current flow transversely through the base region is directly proportional to base width.)

IV. Practical Transistors

In the foregoing sections, the physical mechanisms involved in the idealized transistor have been discussed in detail. No real transistor is exactly like the ideal one. To the first approximation, however, any real transistor can be considered as a three-dimensional array of ideal, but not necessarily identical, transistors, whose emitter, base, and collector terminals are interconnected by means of the incremental lead resistances similar to r_{es}, r_{bs}, and r_{cs}, respectively [19].

In general, such an array is extremely difficult to analyze. An alternative procedure, which is reasonably satisfactory in many cases, is to represent the practical transistor structure by an equivalent circuit of the form shown in Fig. 2 but with the series resistances replaced by impedances, as illustrated in Fig. 6 [20]. These impedances are assumed to be complex in general, in order to account for three-dimensional interactions. They also may be functions of the dc bias in order to take account of changes in the dc flow pattern with dc bias. Note that even those elements of the equivalent-circuit representation of Fig. 6 which appear to be identical with those of the ideal transistor of Fig. 2 (elements between c', b', and c') actually are determined by the entire structure, rather than by any one portion of it. The situation regarding the depletion-layer capacitances is described more fully in Section IV-B.

A. Surface Recombination

The parameter β of Fig. 6 must include the influence of minority-carrier recombination at the free surfaces adjacent to the emitter and collector junctions. This effect was not discussed above because, strictly speaking, surface recombination cannot exist in the ideal model. However, the effect of carriers recombining at the surface of a practical three-dimensional transistor must be included in β just as are those recombining in the bulk. To a first approximation, this effect can be represented by a surface-recombination velocity.

Surface-recombination velocity is a phenomenological parameter characteristic of a surface. It represents the average rate at which minority carriers flow to the surface and recombine. Physically, it is a function of the density of recombination centers on the surface, surface potential, and capture cross section of the recombination centers. The minority-carrier lifetime produced by recombination on the surface alone can be calculated for a given geometery and surface recombination velocity [21]–[24]. This lifetime is combined with that corresponding to bulk recombination alone by adding reciprocals, thus forming a new "effective lifetime" which includes both surface and volume effects. If this value is used in making the calculations for β from the otherwise idealized model, according to equations like (11) and (13), a good approximation to β for the actual transistor can be achieved for incorporation into Fig. 6. In most practical transistors, surface recombination is the dominant mechanism and cannot be ignored.

B. Effects of Collector Geometry

The equivalent-circuit representations shown in Fig. 6 apply particularly to most grown-junction types of transistors [20]. If the elements z_{es} and z_{cs} are omitted, and if the element z_b' is replaced by a pure resistance r_b', an equivalent-circuit representation is obtained which is widely used, but which is most applicable to transistors having the junction geometry of alloy units.

On the other hand, additional modifications which are useful for representing other types of transistors in common use are shown as Figs. 7–9. The first two of the representations are useful lumped approximations for structures in which the collector area is substantially larger than the emitter area, so that the effects of current flow and voltage drops in the transverse directions are significant. The circuit of Fig. 7 applies to nonsymmetrical alloy and surface-barrier transistors [6]. In this case, the base impedance z_b' is purely resistive and may be split into two portions, r_{b1}' and r_{b2}'. The resistance of r_{b1}' is associated only with the base current from the ideal portion of the equivalent-circuit representation (terminal b'), whereas reactive current flowing through the collector transition capacitance flows only through the portion r_{b2}' of the total base re-

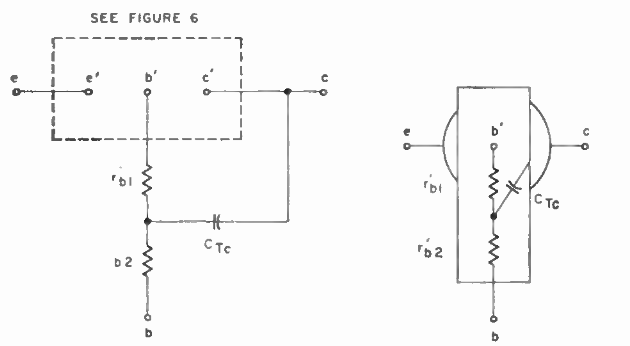

Fig. 7—Alloy or SBT approximation.

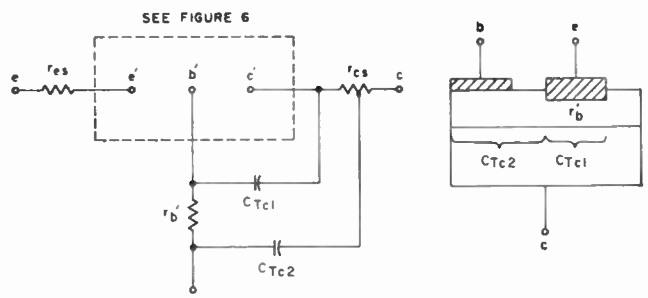

Fig. 8—Diffused-base approximation.

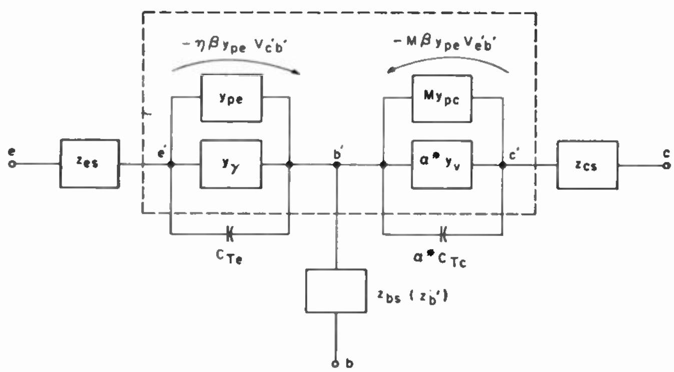

Fig. 6—General equivalent-circuit representation.

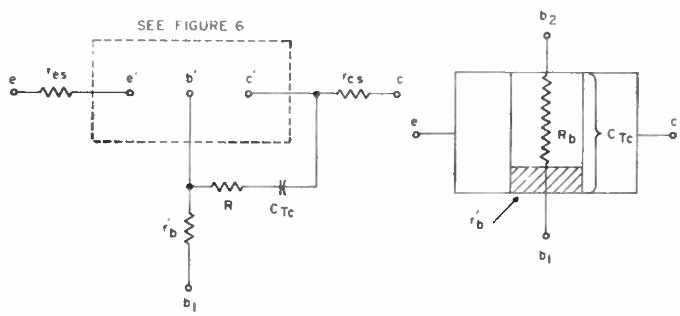

Fig. 9—Tetrode approximation.

sistance. This separation of the base resistance into two parts mirrors the physical fact that the collector region on the average is closer to the base contact than is the emitter region.

A somewhat similar equivalent-circuit representation which is useful for certain diffused-base transistors is shown in Fig. 8. In such transistors, a substantial portion of the charging current of the collector transition capacitance does not flow through any appreciable series resistance in the base terminals between b and c. Hence, the total capacitance can be split into two parts, as shown in Fig. 8 [25], [26].

A third type of modified equivalent-circuit representation which is applicable for tetrode junction transistors is shown in Fig. 9 [27]. In this case, the resistance R in series with C_{Tc} reflects the fact that the charging current for the collector transition capacitance flows throughout the entire region, even though the active portion of the transistor has been crowded toward base contact b_1. Hence, base current from the ideal portion of the equivalent-circuit representation (terminal b') flows through a much smaller resistance $r_b' \ll R$. The value of R is a fraction of the total base-to-base resistance R_b that depends on the termination of b_2 relative to b_1, *i.e.*, whether b_2 is open circuited for ac or shorted to b_1.

V. Equivalent-Circuit Representations

The basic equivalent-circuit representation shown in Fig. 6 includes the various physical phenomena thought to be significant for transistor action, without any particular consideration of the ease with which this representation can be applied directly by the circuit engineer. In this section, the intrinsic parts of the basic representation (the "intrinsic transistor" comprising just the elements within e', b', and c') are transformed into alternative forms. When combined with extrinsic lead impedances of the form discussed in the preceding section, these alternative representations lead to readily applied configurations for practical transistors.

A. Transformations of the Basic Equivalent-Circuit Representation

One of the most useful small-signal equivalent-circuit representations is based on a π-equivalent representation of the intrinsic transistor in a common-emitter connection [28]–[30]. This π-equivalent circuit representation is shown in Fig. 10, together with equations relating its parameters to those of the intrinsic part of the basic representation of Fig. 6. The interrelationships are determined simply by equating appropriate terminal parameters of the representations.

A second small-signal equivalent-circuit representation for the intrinsic transistor, shown in Fig. 11, is suggested by the hybrid parameters of the common-base connection. This representation uses a voltage-generator representation for the space-charge feedback effect from collector to emitter [12].

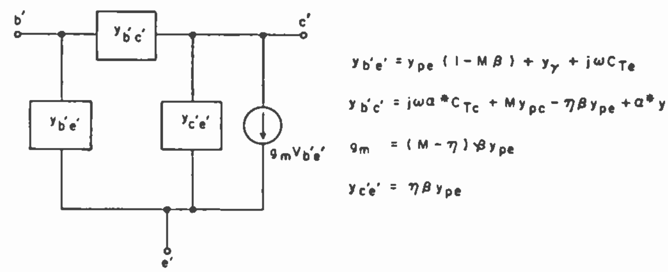

Fig. 10—Common-emitter pi-equivalent-circuit representation.

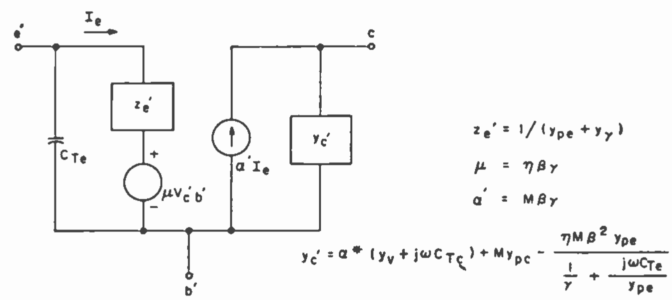

Fig. 11—Hybrid equivalent-circuit representation.

B. Commonly Used Equivalent-Circuit Representations

Virtually all of the equivalent-circuit representations that have been used in circuit design are based upon the simple model shown in Fig. 6, in which only a single impedance has been inserted in series with each element of the intrinsic transistor and in which only a single capacitance is associated with the emitter and collector transition regions, *i.e.*, no direct account has been taken of distributed effects as illustrated by the models of Figs. 7–9. Hence, only equivalent-circuit representations based on this simple model will be discussed below. Note, however, that the representations presented below could be modified easily for one of the other models, if desired. Moreover, in some cases such modifications might be desirable for circuit design: *e.g.*, in the case of Fig. 8, only the capacitance C_{Tc1} contributes to internal feedback for common-base operation, whereas the capacitance C_{Tc2} may be tuned out without appreciable loss of gain.

When series lead resistances are added to the common-emitter equivalent-circuit representation of Fig. 10, the "hybrid-π" equivalent-circuit representation proposed by Giacoletto [28]–[30] is obtained, as shown in Fig. 12. In actual use, it is frequently possible to omit one or more of the elements of a representation, because such elements may be relatively insignificant in particular cases. A simplified version of Fig. 12, frequently used for high-frequency amplifier applications, is shown in Fig. 13. An even greater simplification, useful when the load conductance is much greater that the transistor output conductance (as for video-amplifier applications), is shown in Fig. 14 [31].

When extrinsic lead impedances are added to the equivalent-circuit representation of Fig. 11, the "Early"

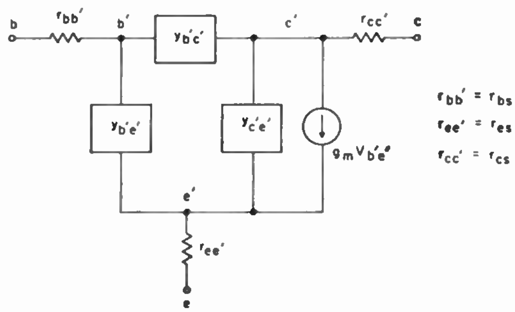

Fig. 12—Hybrid-pi (Giacoletto) equivalent-circuit representation.

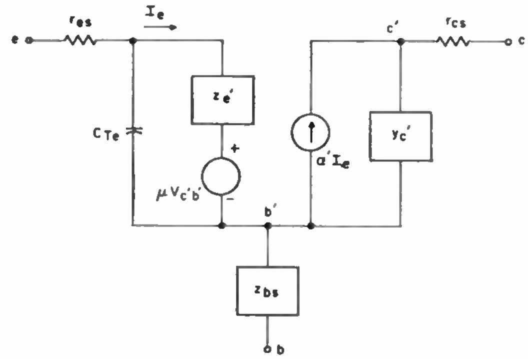

Fig. 15—"Early" equivalent-circuit representation.

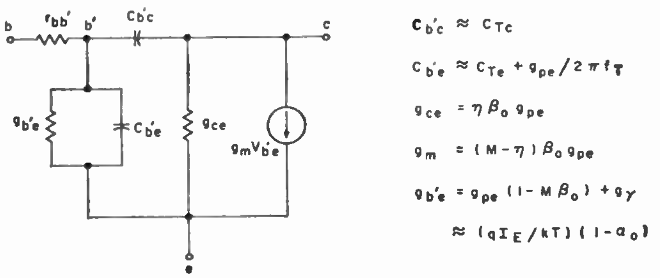

Fig. 13—Hybrid-pi equivalent-circuit approximation for high-frequency amplifiers.

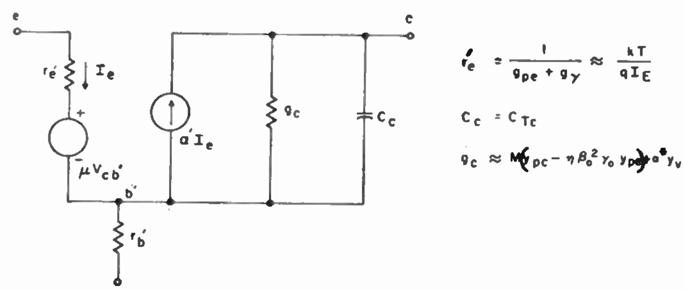

Fig. 16—"Early" equivalent-circuit low-to-intermediate-frequency approximation.

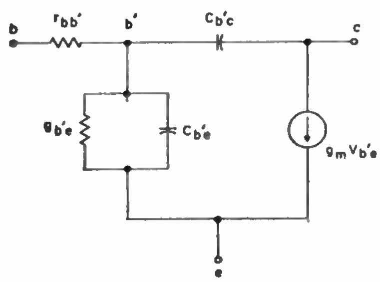

Fig. 14—Hybrid-pi equivalent-circuit approximation for video amplifier.

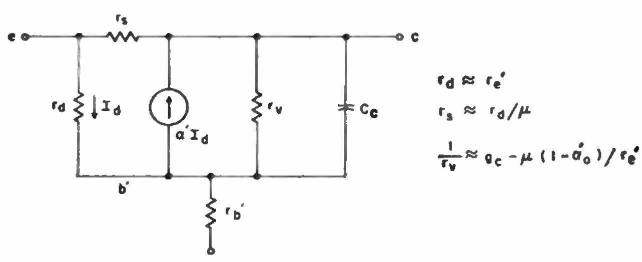

Fig. 17—"Keiper" equivalent-circuit approximation for "wafer" transistors.

equivalent-circuit representation shown in Fig. 15 results [12]. This representation or its simplifications are particularly convenient for grounded-base circuit analysis. An approximation of the "Early" equivalent-circuit representation suitable for most intermediate-frequency amplifier applications is shown in Fig. 16. A modification of this representation, using a resistive voltage divider to represent the feedback due to space-charge widening, is shown in the "Keiper" equivalent-circuit representation of Fig. 17 [32], [33]. This circuit has found its widest use in the analysis of intermediate-frequency amplifiers employing "wafer" transistors having substantial base spreading resistance. A further simplification of the "Early" equivalent-circuit representation is shown in Fig. 18 [14]; this simplification has been found adequate for many applications requiring control of the high-frequency capabilities of the transistor in use, where performance is limited more by transit time, base spreading resistance, and transition capacitances than by space-charge layer widening.

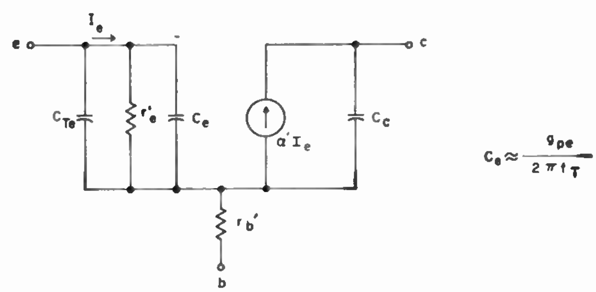

Fig. 18—"Early" equivalent-circuit high-frequency approximation.

The classical T-equivalent circuit representation, employing the parameters r_e, r_b, and r_c, a complex internal current generator aI_e (and occasionally a collector capacitance, C_c, across r_c) has been omitted deliberately from this section on equivalent-circuit representations. This representation was originally suggested for the point-contact transistor [34], [35], and has on occasion been applied to the junction transistor in small-signal low-frequency applications. However, if the passive elements (the resistances and capacitance) of this representation are assumed to be frequency-independent real numbers, then this equivalent-circuit representation will not predict junction-transistor behavior (gain or impedance level) satisfactorily as a function of frequency over a significant, practical band. By contrast, such representations as are shown in Figs. 13 or 16 frequently provide adequately accurate information for circuit calculations over a very significant frequency range, without requiring variable passive elements in the representation. Furthermore, even the low-frequency values of the T-equivalent circuit representation do not relate in a direct and simple manner to physically explainable quantities and, unlike the elements of Figs. 13 and 16, they cannot be computed to a good approximation directly from the physical structure. As an example of this point, the base resistance r_b must include the reverse transfer impedance caused by space-charge layer widening ($r_b = r_b' + \mu r_c$). For these reasons, the T-equivalent circuit representation is not recommended for junction-transistor computations, and is consequently excluded from this report. For similar reasons, the equivalent-circuit representation based on common-base impedance parameters is not shown or recommended.

List of Symbols

(Numbers in brackets refer to the equation, section, or figure where the symbol is defined.)

B = barrier transit-time factor [Section II-D, 2)]
C_{eq} = low-frequency capacitive component of y_{pc} [Section II-C, 2)]
C_{Tc}, C_{Te} = collector and emitter depletion-layer capacitances, respectively [Section III-A)]
D_B = minority-carrier diffusion constant in the base [Section II-A, 1)]
D_E = minority-carrier diffusion constant in the emitter [Section II-A, 3)]
f_T = the characteristic frequency $f_{MEAS} \times |h_{fe}|$, where $|h_{fe}|$ is determined at f_{MEAS}, and f_{MEAS} is chosen so that $2 < |h_{fe}| < 10$. To a good approximation, f_T is the frequency at which $|h_{fe}| = 1$ [Fig. 3]
I_c = collector terminal current [Fig. 3]
I_e = emitter terminal current [Fig. 3]
I_{nc} = current due to flow of electrons from the collector depletion layer into the base [Fig. 3]
I_{ncc} = current due to electron flow from the collector body into the collector depletion layer [Fig. 3]
I_{ne} = current due to electron flow from the base into the emitter [Fig. 3]
I_{pc} = current due to flow of holes from the base into the collector depletion layer [Fig. 3]
I_{pcc} = current due to the flow of holes from the collector depletion layer into the collector body [Fig. 3]
I_{pe} = current due to flow of holes from the emitter into the base [Fig. 3]
kT/q = thermal voltage (about 25 mv at room temperature) [Section II]
L_B = minority carrier diffusion length in the base region $= \sqrt{D_B \tau_B}$ [Section II-A, 1)]
L_E = minority-carrier diffusion length in the emitter [Section II-A, 3)]
m = avalanche multiplication factor [Section II-D, 3)]
M = over-all collector multiplication factor $= M'\alpha^*$ [(24)]
M' = collector depletion-layer multiplication factor [(27)]
n_{OE} = equilibrium electron concentration in the emitter [Section II-A, 3)]
N = ionized impurity concentration in the higher resistivity region [Section III-A]
$p_B(e')$ = hole concentration in the base at the emitter junction [Section II]
p_{OB} = equilibrium hole concentration in the base [Section II]
q = negative electronic charge
r_e' = low-frequency emitter-base resistance [Section II-A, 1)]
r_{es}, r_{cs}, r_{bs} = extrinsic lead resistances [Section III-B]
T_B = minority-carrier transit time through base region [Section II-B]
V_0 = internal contact potential [Section III-A]
W = base width [Fig. 4]
y_{pc} = collector admittance associated with depletion-layer widening effects [(19)]
y_{pe} = admittance associated with hole injection from the emitter into the base region [(2)]
y_v = avalanche admittance [Section II-D, 5)]
y_γ = admittance associated with the flow of electrons from the base into the emitter [(6)]
α^* = collector-body multiplication factor [([illegible]

List of Symbols (*Cont'd*)

β = base transport factor [(10)]
β_0 = low-frequency value of the base transport factor [Section II-B]
γ = emitter minority-carrier injection efficiency [(8)]
ϵ = dielectric permittivity
ζ = (dimensionless parameter)—normalized base width [(5)]
η = voltage feedback factor [(14)]
ν = proportionality constant for the "excess phase" in β [Section II-B]
σ_c = equilibrium collector-body conductivity [Section II-D, 4)]
σ_{nc} = equilibrium collector-body conductivity due to minority carriers only [Section II-D, 4)]
τ_E = minority-carrier lifetime in the emitter [Section II-A, 2)]
τ_B = minority-carrier lifetime in the base [Section II-A, 1)]
ω_β = frequency at which β has decreased to $\beta_0/\sqrt{2}$. [Section II-B]

Acknowledgment

The authors wish to thank a number of their colleagues, in particular Prof. J. G. Linvill of Stanford University, for contributing many helpful comments about the Task Force Report at its various stages of development. In addition, we are especially grateful to J. G. Hilibrand of the RCA Laboratories for many helpful suggestions, for his skill in effecting a compromise between the authors' different points of view on various occasions, and for compiling the Glossary of Symbols. Last but not least, special thanks are due Mrs. D. Wilson for untiring secretarial assistance at a number of our Task Force meetings and for compiling numerous drafts of this report.

Bibliography

[1] R. L. Pritchard, "Electric-network representation of transistors—a survey," IRE Trans. on Circuit Theory, vol. CT-3, pp. 5–21; March, 1956.
[2] J. Zawels, "Physical theory of new circuit representation for junction transistors," *J. Appl. Phys.*, vol. 25, pp. 976–981; August, 1954.
[3] R. Beaufoy and J. J. Sparkes, "The junction transistor as a charge-controlled device," J. ATE, vol. 13, pp. 310–317; April, 1957. Also in, Proc. IRE, vol. 45, pp. 1740–1742; December, 1957.
[4] W. Shockley, "The theory of *p-n* junctions in semiconductors and *p-n* junction transistors," *Bell Sys. Tech. J.*, vol. 28, pp. 435–489; July, 1949.
[5] W. Shockley, M. Sparks, and G. K. Teal, "*P-N* junction transistors," *Phys. Rev.*, vol. 83, pp. 151–162; July, 1951.
[6] J. M. Early, "Design theory of junction transistors," *Bell Sys. Tech. J.*, vol. 32, pp. 1271–1312; November, 1953.
[7] R. L. Pritchard, "Frequency variations of junction-transistor parameters," Proc. IRE, vol. 42, pp. 786–799; May, 1954.
[8] H. Krömer, "Zur Theorie des diffusions und des drifttransistors," *Arch. elekt. Übertragung*, vol. 8, pp. 223–228, May, 1954; pp. 363–369, August, 1954; pp. 499–504, November, 1954.
[9] R. L. Pritchard, "Frequency variations of current-amplification factor for junction transistors," Proc. IRE, vol. 40, pp. 1476–1481; November, 1952.
[10] W. F. Chow and J. J. Suran, "Transient analysis of junction transistor amplifiers," Proc. IRE, vol. 41, pp. 1125–1129; September, 1953.
[11] D. E. Thomas and J. L. Moll, "Junction transistor short-circuit current gain and phase determination," Proc. IRE, vol. 46, pp. 1177–1184; June, 1958.
[12] J. M. Early, "Effects of space-charge layer widening in junction transistors," Proc. IRE, vol. 40, pp. 1401–1406; November, 1952.
[13] R. L. Pritchard, "Collector-base impedance of a junction transistor," Proc. IRE, vol. 41, p. 1060; August, 1953.
[14] J. M. Early, "*P-N-I-P* and *N-P-I-N* junction transistor triodes," *Bell Sys. Tech. J.*, vol. 33, pp. 517–533; May, 1954.
[15] S. L. Miller, "Avalanche breakdown in germanium," *Phys. Rev.*, vol. 99, pp. 1234–1241; August, 1955.
[16] S. L. Miller and J. J. Ebers, "Alloyed junction avalanche transistors," *Bell Sys. Tech. J.*, vol. 34, pp. 883–902; September, 1955.
[17] L. P. Hunter, "Transistor action," in "Handbook of Semiconductor Electronics," McGraw-Hill Book Co., Inc., New York, N. Y., sec. 4, pp. 4–6 to 4–7; 1956.
[18] A. W. Matz, "Thermal turnover in germanium *p-n* junctions," *Proc. IEE*, pt. B, vol. 104, pp. 555–564; November, 1957.
[19] G. Brouwer, "Three-dimensional electric-circuit model of the high-frequency phenomena in a junction transistor," *Philips Res. Repts.*, vol. 14, pp. 132–142; April, 1959.
[20] R. L. Pritchard, "Two-dimensional current flow in junction transistors at high frequencies," Proc. IRE, vol. 46, pp. 1152–1160; June, 1958.
[21] J. Laplume, "Evaluation du gain en courant dans le transistor à jonction obtenu par fusion," *Compt. Rend. Acad. Sci.*, vol. 238, pp. 1300–1301; March, 1954. Also, "Sur l'influence de la recombinaison en surface sur le gain en courant du transistor à jonction," *Compt. Rend. Acad. Sci.*, vol. 239, pp. 1274–1276; November, 1954.
[22] W. M. Webster, "On the variation of junction-transistor current-amplification factor with emitter current," Proc. IRE, vol. 42, pp. 914–920; June, 1954.
[23] A. R. Moore and J. I. Pankove, "The effect of junction shape and surface recombination on transistor current gain," Proc. IRE, vol. 42, pp. 907–913; June, 1954.
[24] K. F. Stripp and A. R. Moore, "The effects of junction shape and surface recombination on transistor current gain—Part II," Proc. IRE, vol. 43, pp. 856–866; July, 1955.
[25] J. T. Nelson, J. E. Iwersen, and F. Keywell, "A five-watt ten-megacycle transistor," Proc. IRE, vol. 46, pp. 1209–1215; June, 1958.
[26] R. L. Pritchard, "Transistor equivalent circuits," *Proc. IEE*, pt. B, suppl. no. 17, vol. 106, pp. 1012–1017; May, 1959.
[27] R. L. Pritchard, "High-frequency parameters of tetrode junction transistors," GE Res. Lab. Rept. 58-RL-1850; April, 1958.
[28] L. J. Giacoletto and H. Johnson, "Considerations of Admittance Representation of Junction Transistors," presented at Transistor Standardization Forum, AIEE Summer Meeting, Atlantic City, N. J.; June 17, 1953.
[29] C. W. Mueller and J. I. Pankove, "A *p-n-p* triode alloy-junction transistor for radio-frequency amplification," *RCA Rev.*, vol. 14, pp. 586–599; December, 1953. Also in, Proc. IRE, vol. 42, pp. 386–391; February, 1954.
[30] L. J. Giacoletto, "The study and design of alloyed-junction transistors," 1954 IRE Convention Record, pt. 3, pp. 99–103.
[31] L. J. Giacoletto, "Comparative high-frequency operation of junction transistors made of different semiconductor materials," *RCA Rev.*, vol. 16, pp. 34–42; March, 1955.
[32] J. B. Angell, "Circuit Implications of Surface-Barrier Transistors," presented at IRE-AIEE Conf. on Transistor Circuits, Philadelphia, Pa., February 18, 1954.
[33] R. J. Turner, "Surface-barrier transistor measurements and applications," *Tele-Tech*, vol. 13, p. 78; August, 1954.
[34] L. C. Peterson, "Equivalent circuits of linear active four-terminal networks," *Bell Sys. Tech. J.*, vol. 27, pp. 593–622; October, 1948.
[35] R. M. Ryder and R. J. Kircher, "Some circuit aspects of the transistor," *Bell Sys. Tech. J.*, vol. 28, pp. 367–401; July, 1949.

A Noise Investigation of Tunnel-Diode Microwave Amplifiers*

A. YARIV†, MEMBER, IRE, AND J. S. COOK†, MEMBER, IRE

Summary—An analysis and derivation of the noise figure of a tunnel-diode microwave amplifier are presented. The agreement between the measured noise figure and the theoretical results is an indirect check on the existence of full shot noise in germanium tunnel diodes at microwave frequencies. The limiting noise temperature of the amplifier is $eI_0R/2k$, and can be approached by using diodes with small (RC) products in which the extreme overcoupling (load mismatch) and high gain can be achieved simultaneously.

Introduction

Amplifiers utilizing tunnel diodes were first reported by Chang[1] at frequencies up to 80 Mc. He also suggested that the noise contribution of the diode was due to the shot noise accompanying the tunneling process. This suggestion was confirmed by Lee and Montgomery,[2] who showed by measurements at 5 Mc that full shot noise was indeed generated by the tunnel diode. Tiemann[3] has reported results similar to those of Lee and Montgomery, obtained from noise measurements at 500 kc on germanium diodes.

Approximate noise analyses of tunnel-diode amplifiers were given by Sommers, *et al.*,[4] Tiemann,[3] and Hines and Anderson.[5] The simplified equivalent circuits used were sufficient to derive the limiting noise behavior for very high gain and extreme overcoupling. Yariv, *et al.*,[6] reported the operation of a tunnel-diode amplifier at microwave frequencies and measured its noise figure.

In this paper, the details are given of the noise analysis which led to the noise temperature formula stated by Yariv, *et al.*[6] This analysis is based on an "exact" equivalent circuit, and its results are useful in the intermediate range of small or medium gain as well as in the limiting case described above. The theoretical results are compared with the noise measurements.

I. The Physical Sources of Noise

In addition to the omnipresent noise generated by the ohmic losses in the spreading and contact resistance of the diode and the surrounding microwave structure, we must consider the shot noise accompanying the tunneling process.[7] There are two separate and independent tunneling currents, one consisting of electrons tunneling from the N to the P side of the junction, which we denote by i_1, and a second current, i_2, made up of electrons crossing the junction in the opposite direction. The net measurable dc current is $I_0 = |i_1| - |i_2|$. Since the currents i_1 and i_2 are uncorrelated, the total shot noise[8] is represented by a current generator of mean-square amplitude,

$$\overline{i^2} = 2e(|i_1| + |i_2|)B, \tag{1}$$

where e is the electronic charge and B is the bandwidth in cycles per second in which the noise is considered. When the diode is biased so as to operate in the negative resistance region (see Fig. 1), the current i_2 is negligibly small and the approximation

$$I_0 \approx |i_1| + |i_2|$$

may be used.

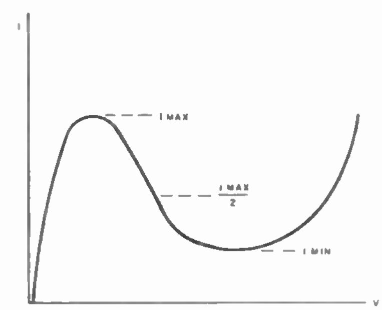

Fig. 1—A typical voltage-current characteristic curve of an Esaki diode.

II. The Equivalent Circuit

The amplifier constructed for the noise experiment consists of a germanium diode mounted in a single port cavity which is coupled to the load and the source by a low-loss circulator as shown in Fig. 2, the coupling being continuously variable. The equivalent circuit of this amplifier is shown in Fig. 3. The diode is represented by a negative resistance $-R$, shunted by a capacitance C,

* Received by the IRE, October 3, 1960.
† Bell Telephone Labs., Inc., Murray Hill, N. J.

[1] K. K. N. Chang, "Low-noise tunnel-diode amplifier," Proc. IRE (Correspondence), vol. 47, pp. 1268–1269; July, 1959.

[2] C. A. Lee and H. C. Montgomery, "Determination of forward and reverse tunneling currents in Esaki diodes by shot noise measurements," *Bull. Am. Phys. Soc.*, vol. 3, p. 160; March 21, 1960.

[3] J. J. Tieman, "Shot noise in tunnel diode amplifiers," Proc. IRE, vol. 48, pp. 1418–1423; August, 1960.

[4] H. S. Sommers, Jr., *et al.*, "Tunnel diodes for low noise amplification," 1959 IRE WESCON Convention Record, pt. 3, pp. 3–8.

[5] M. E. Hines and W. W. Anderson, "Noise performance theory of Esaki (tunnel) diode amplifiers," Proc. IRE (Correspondence), vol. 48, p. 789; April, 1960.

[6] A. Yariv, *et al.*, "Operation of an Esaki diode microwave amplifier," Proc. IRE (Correspondence), vol. 48, p. 1155; June, 1960.

[7] L. Esaki, "New phenomenon in narrow germanian *p-n* junctions," *Phys. Rev.*, vol. 109, pp. 602–603; June, 1958.

[8] See, for instance, J. R. Pierce, "Physical sources of noise," Proc. IRE, vol. 44, pp. 601–608; May, 1956.

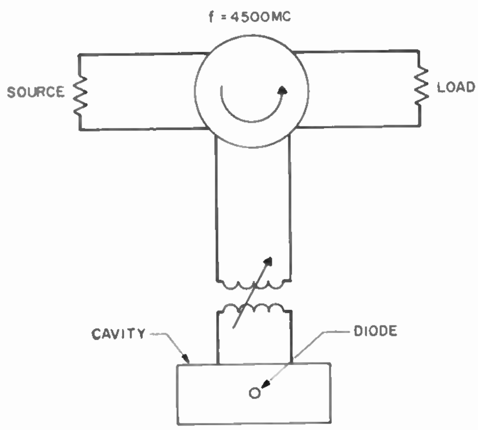

Fig. 2—A schematic view of the Esaki diode amplifier.

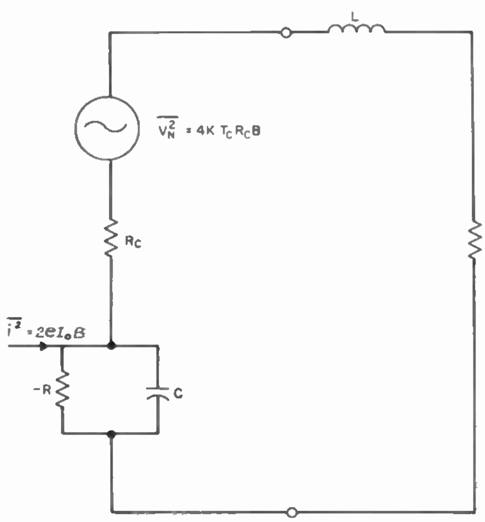

Fig. 3—The equivalent circuit of the Esaki diode amplifier.

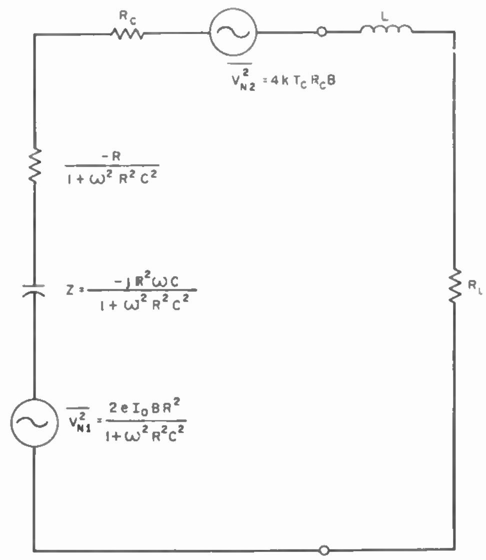

Fig. 4—The series equivalent circuit of the Esaki diode amplifier.

which accounts for the barrier capacitance. The spreading and contact resistance of the diode are lumped together with the ohmic losses of the cavity in R_c. The noise generated by the three sources of loss listed above is provided by a Johnson noise generator of mean-square voltage amplitude,

$$\overline{v^2} = 4kT_cR_cB,$$

where k is the Boltzmann constant and T_c is the ambient temperature of the cavity. L stands for the total inductance (parasitic and intentional). The shot noise generator

$$\overline{i_2} = 2eI_0B$$

was discussed above. The load resistance is R_L.

For the purpose of analysis, it is more convenient to transform the circuit to one in which all the elements are either in series or in parallel. The series equivalent circuit and the new expressions for the equivalent series circuit elements are shown in Fig. 4.

Series resonance occurs at

$$\omega_{res} = \omega_0 \sqrt{1 - \frac{1}{\omega_0^2R^2C^2}}, \tag{2}$$

where $\omega_0^2 = 1/LC$. For resonance to occur at real frequencies, we must fulfill the condition

$$\omega_0RC > 1 \tag{3}$$

for $\omega_0^2R^2C^2 \gg 1$, $\omega_{res} \approx \omega_0$.

A necessary and sufficient condition for positive gain is that the real part of the total series resistance, seen looking back into the amplifier terminals, be negative; or from Fig. 4,

$$\frac{R}{1+\omega^2R^2C^2} > R_c. \tag{4}$$

The highest frequency at which this can take place is called the cutoff frequency, f_{co}:

$$f_{co} = \frac{\sqrt{R/R_c - 1}}{2\pi RC}, \tag{5}$$

and represents the highest useful frequency for a given diode and circuit.

Since our main interest is in an amplifier operating at resonance, we evaluate the elements of the equivalent circuit of Fig. 4 for the condition $\omega = \omega_{res}$. The result is shown in Fig. 5. The effective negative resistance is now represented by the series resistance

$$R' = \frac{-R}{\omega_0^2R^2C^2}, \tag{6}$$

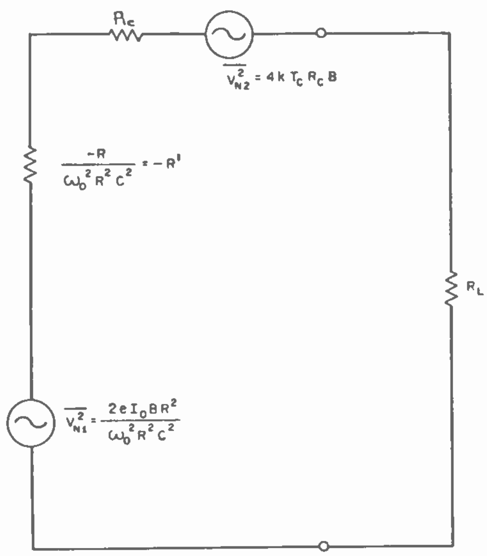

Fig. 5—The series equivalent circuit of the Esaki diode amplifier at resonance.

while the shot noise is now provided by a voltage generator of mean-square amplitude

$$\overline{V_{N1}^2} = \frac{2eI_0BR^2}{\omega_0^2R^2C^2}.$$

The physical importance attached to the elements of the equivalent circuit of Fig. 5 is of paramount importance and contains a number of pitfalls, so that a few pertinent remarks are in order. Since the resistances are all in series, they are proportional to power, with the result that one may wrongly infer, for instance, that the power generated by the diode is proportional to R and, therefore, that for large gain or large power output, diodes with large R are superior. In actuality, the generated power is proportional to $1/R$, which for a given diode material is proportional to the junction area. Physical significance can *only* be attached to ratios of any pair of resistances in Fig. 5. The quantity R'/R_L is equal to the ratio of power generated by the diode to that delivered to the load, while R_L/R_c, for instance, gives the ratio of the power consumed by the load to that expended in the cavity. R_L/R_c is often referred to as the coupling ratio of the cavity. (Ratio of cavity "Q" to external "Q".)

III. The Gain-Bandwidth Product

The power gain G of the amplifier is defined as the ratio of the power delivered to the load (the reflected power in our case) to the power available from the source (incident) and is thus equal to the squared magnitude of the reflection coefficient measured at the amplifier terminals. Using Fig. 5, we have

$$G = \left[\frac{R_L - (R_c - R')}{R_L + (R_c - R')}\right]^2. \tag{7}$$

The bandwidth Δf is the distance, in cps, between the half-power frequencies. It is derived by replacing $R_c - R'$ in (7) by the total series impedance away from resonance as given by Fig. 4. The result is

$$\Delta f = \frac{R_L + R_c - R'}{2\pi L\left(1 - \dfrac{1}{\omega_0^2R^2C^2}\right)},$$

yielding for the voltage gain-bandwidth product

$$(\sqrt{G})_{\text{res}}\Delta f = \sqrt{G}\Delta f = \frac{R_L + R' - R_c}{2\pi L\left(1 - \dfrac{1}{\omega_0^2R^2C^2}\right)}. \tag{8}$$

Eq. (8) takes a meaningful form upon substitution of the high gain condition[9]

$$R' \approx R_c + R_L \tag{9}$$

and the definition of R' as given by (6). The result is

$$(\sqrt{G}\Delta f)_{\text{high gain}} = \frac{1 - R_c/R'}{\pi RC\left(1 - \dfrac{1}{\omega_0^2R^2C^2}\right)}, \tag{10}$$

in which form it is amenable to experimental verification.

To increase the gain-bandwidth product, we have to use a diode with a small (RC). This happens, not only through the dependence of $\sqrt{G}\Delta f$ on (RC) as given by (10), but also through a less obvious decrease of R_c/R'. If we assume that the total inductance has been made as small as possible, operation at one frequency means using the same C. If one now goes to a diode material with an intrinsically smaller (RC) product, it becomes possible to operate at the same frequency with a diode having a smaller R,[10] *i.e.*, a diode generating more power, which corresponds to a smaller R_c/R' ratio.

IV. The Noise Temperature of the Amplifier

The noise temperature T_e of the amplifier,[11] which is sometimes called the effective input noise temperature, can be defined as the increase in the source temperature which is required to keep the noise power output a constant if the amplifier, hypothetically, were rendered noiseless. It is found by equating that part of the total noise output originating within the amplifier, N_A, to kT_eGB, *i.e.*,

$$N_A = kT_eGB,$$

[9] This condition, when taken with an equality sign, makes the gain infinite [see (7)] and becomes the "start-oscillation" condition.
[10] The new diode will have the same area as the old one, but will possess a larger current density and, consequently, a larger current.
[11] T_e is related to the noise figure F by

$$F = 1 + \frac{T_e}{290}.$$

or using the equivalent circuit of Fig. 5 and the gain definition of (7),

$$kT_eB\frac{(R_L - R_c + R')^2}{(R_L + R_c - R')^2} = 4kT_cB\frac{R_cR_L}{(R_L + R_c - R')^2} + \frac{2eI_0BRR'R_L}{(R_L + R_c - R')^2},$$

where T_c is the temperature of the cavity and diode. Solving for T_e yields

$$T_e = \frac{4T_cR_cR_L}{(R_L - R_c + R')^2} + \frac{2eI_0RR'R_L}{k(R_L - R_c + R')^2},$$

which can be transformed to

$$T_e = \frac{(\sqrt{G}+1)^2}{G}\left[T_c\left(\frac{R_c}{R_L}\right) + \frac{eI_0R}{2k}\left(\frac{R'}{R_L}\right)\right], \qquad (11)$$

in which form only ratios of resistance appear. This form is particularly useful, since in it the dependence of the noise temperature on the gain is separated from its dependence on the coupling ratios. This bracketing is justified operationally, since the same value of gain can be obtained with different combinations of coupling ratios.

V. Experimental Results

The pertinent characteristics of the phosphorus-doped germanium diode were:

$$I_{\text{peak}} = 1 \text{ ma},$$
$$I_0R = 8.6 \times 10^{-2} \text{ at the biasing point},$$
$$RC \cong 3.5 \times 10^{-10} \pm 10 \text{ per cent},$$
$$R = 175 \text{ ohms}.$$

The diode was mounted between the ridge and top wall of a short-terminated waveguide, the distance between the diode and the short being adjustable for tuning purposes. The ridge waveguide tapered gradually into a 2-inch×1-inch input waveguide which was coupled to the input and output via a low-loss circulator. The diode coupling was controlled by two screws placed, respectively, $\frac{1}{8}$ and $\frac{3}{8}$ guide wavelengths in front of the diode. Fig. 6 shows a photograph of the ridge waveguide cross section at the diode position, while Fig. 7 shows, with considerable magnification, the immediate area surrounding the diode.

The measured gain-bandwidth product at 4500 Mc was 3.6×10^8, and was checked at a number of gain settings between 17 db and 25 db, where it was found to be a constant, in agreement with (10). The gain-bandwidth product deteriorated for lower gain settings.

The measured noise temperature was 1740°K and was taken with the amplifier set for a gain of 25 db. To compare this result with that predictable from (8), it is necessary to know the power ratios R_c/R_L and R'/R_L. This was accomplished by using the measured values of

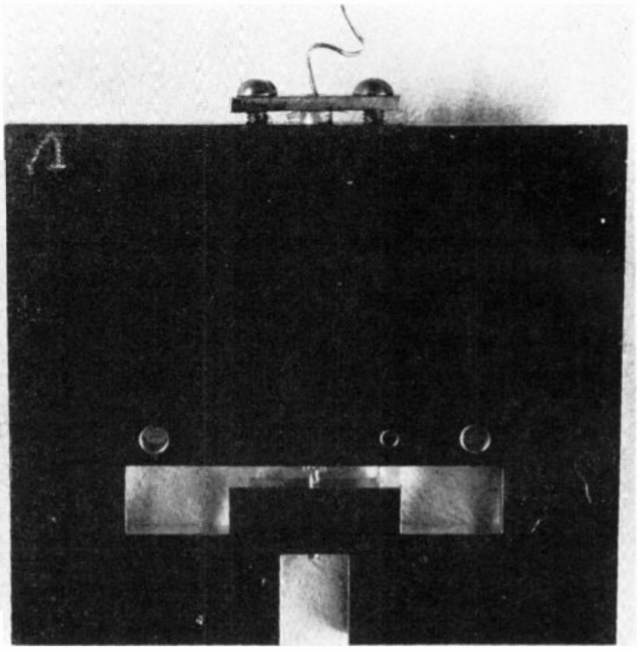

Fig. 6—Cross section of the ridge waveguide at the diode position.

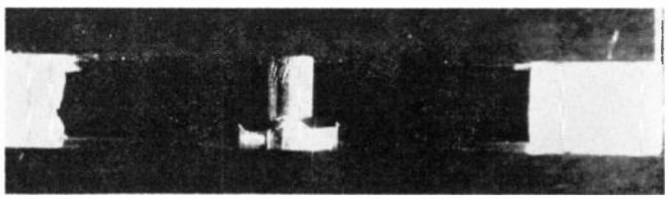

Fig. 7—An enlarged view of the diode and its surroundings. The diode is mounted between the two pins at the center of the photograph.

$\sqrt{G}\Delta f$ and (RC) to solve for R_c/R' in (10), and then by using the high gain condition (9) to solve for the required ratios. With the numerical data given above, the ratios are:

$$\frac{R_c}{R'} = 0.6, \qquad \frac{R'}{R_L} = 2.5, \qquad \frac{R_c}{R_L} = 1.5.$$

Substitution in (11) yields

$$(T_e)_{\text{calculated}} = 1890°\text{K} \pm 10 \text{ per cent},$$

which is to be compared with the experimental value of 1740°K. The main source of error is the uncertainty in (RC). The satisfactory agreement between the experimental and theoretical results serves as an indirect check on the existence of full shot noise at microwave frequencies in tunnel diodes. A more recent version of the same amplifier yielded a noise temperature of 1200°K.

VI. Concluding Remarks

A number of factors which are evident from (11) affect the noise temperature. We shall treat them separately.

The dependence of T_e on the gain G is contained in the factor $(\sqrt{G}+1)^2/G$, which decreases asymptotically toward unity with increasing gain so that high gain operation is imperative.

The shot noise contribution enters through the term I_0R. It can be minimized by optimum biasing of the diode in such a manner that the product I_0R is a minimum. In practice, it was found impractical to operate the diode for any considerable distance beyond the mid-range of the negative resistance, because the increasing value of R, due to the curvature of the V-I curve, more than offset the decrease in i_0. The problem of the exact shape of the V-I curve is intimately related to that of the excess current[12,13] and has not been settled yet.

The (I_0R) product is inherently smaller for semiconductors with small energy gaps (InSb—0.17 v, InAs—0.33 v, Ge—0.72 v) which should therefore be preferred for low noise applications. This advantage is offset to some extent by the fact that, assuming the same (RC) product, the high-energy-gap diodes generate more power and thus make it easier to overcouple the cavity and still achieve high gain.

The shot noise contribution to the noise temperature is proportional to R'/R_L, which, according to (9), is always larger than unity. In the limit when the cavity losses are very small compared to the generated power and the load power, *i.e.*, when $R_c/R' \approx R_cR_L \ll 1$, the ratio R'/R_L approaches unity. As pointed out at the conclusion of Section III, this situation is approached, for a diode operating at a fixed frequency, by using diodes with small values of (RC). The shot noise contribution to the amplifier's noise temperature is thus always larger, but hopefully not much larger, than $eI_0R/2k$. In our amplifier this was $\sim$500°K.

The same conditions that minimize the shot noise contribution also cause the ratio R_c/R_L to be a minimum, thus minimizing the contribution of the cavity losses at T_e [see (11)].

[12] R. A. Logan and A. G. Chynoweth, "Effect of radiation damage on excess current in Esaki diodes," *Bull. Am. Phys. Soc.*, vol. 5, series II, p. 375; June 15, 1960.

[13] T. Yajima and L. Esaki, "Excess noise in narrow germanium *p-n* junctions," *J. Phys. Soc. Japan*, vol. 13, pp. 1281–1287; November, 1958.

The reduction of (RC) has a beneficial effect on both the gain-bandwidth product and the noise temperature of the amplifier; it also creates a number of problems. The first is one of stability. For stable operation we must satisfy the condition[14]

$$L(\omega) < R_s(\omega)RC$$

at all frequencies. Where $L(\omega)$ and $R_s(\omega)$ are, respectively, the total inductance and resistance in series with the diode, they are shown as functions of frequency since stable operation has to obtain for all frequencies. The difficulty of satisfying the stability condition increases with smaller (RC) product.

A small value of RC makes R smaller, at a given frequency, and entails using a microwave structure with low characteristic impedances. In the diode used in our experiment, $R\sim175$ ohms and $RC\sim3.5\times10^{-10}$. Had we used instead a unit with $RC\sim10^{-11}$, which is available, the negative resistance R would have been $\sim$5 ohms, which is a very low impedance level in microwave circuitry and creates a gamut of problems, such as matching to standard components with much higher impedances and the high attenuation of low-impedance waveguides.

It is not likely that tunnel diode will ever threaten the maser and parametric amplifiers as a low-noise amplifier. It may still find application in cases where its extreme simplicity and economy may be traded for increased noise, especially when tunnel-diode amplifiers with noise figures substantially lower than the one reported above will be made. This improvement is mainly contingent on the utilization and taming of diodes with small (RC) products and on the use of low-energy-gap diodes—with small (I_0R) products.

Acknowledgment

The authors wish to express their indebtedness to P. E. Butzien for his able participation in the experimental work, and to E. Dickten for fabricating and mounting the diodes used in the experiment.

[14] R. L. Wallace, unpublished report.

Tunnel-Diode Microwave Oscillators*

F. STERZER†, MEMBER, IRE, AND D. E. NELSON†, MEMBER, IRE

Summary—**Several experimental tunnel-diode RF oscillators which operate at frequencies from 610 to 8350 Mc are described. Power outputs an order of magnitude greater than those previously reported in the literature were obtained: 10 mw at 610 Mc, 2 mw at 1600 Mc, 0.7 mw at 2800 Mc, 0.2 mw at 5500 Mc, and 0.01 mw at 7130 Mc. Problems relating to oscillation frequency, power output, and wave shape are treated analytically.**

Introduction

Tunnel diodes are heavily doped *p-n* junctions that exhibit an incremental negative resistance at a small forward dc bias.[1–4] These diodes hold great promise for high-frequency applications because they are not limited by transit-time effects even at microwave frequencies.

Previous authors have described tunnel diode oscillators with microwatt power outputs and have derived the conditions for self-starting oscillations in simple oscillator circuits.[4–8] This paper discusses the use of tunnel diodes in UHF and microwave oscillators with milliwatt power outputs. The diode parameters which determine the performance of the diode in oscillator circuits are described in detail. Several oscillator circuits are analyzed with special attention to the steady state. A number of practical oscillator circuits are described, and experimental results are presented.

Tunnel-Diode Parameters

An approximate equivalent circuit for an encapsulated tunnel diode consists of three elements connected in series: an inductance L_d, a resistance r_d, and a voltage-dependent resistance $[R_d(v)]_0$ shunted by a voltage-dependent capacitance $C_d(v)$, as shown in Fig. 1. L_d results mainly from the inductance of the housing; r_d is the resistance of the ohmic contact, the base, and the internal leads of the package, and is a function of frequency due to skin effect. $C_d(v)$ is the junction capacitance, and $[R_d(v)]_0$ is the total resistance of the junction, where v is the voltage across R_d and C_d.

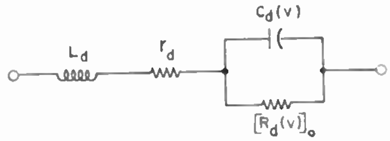

Fig. 1—Equivalent circuit of a tunnel diode.

Fig. 2, a photomicrograph furnished by Mueller of RCA Laboratories, shows the cross section of a typical high-performance microwave germanium tunnel diode. This particular unit had a peak current I_p of 27 ma, corresponding to a peak-current density of about 1.7×10^4 a/cm².

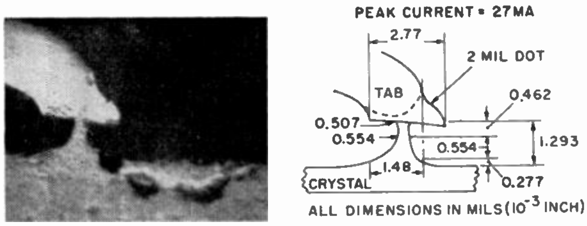

Fig. 2—Photomicrograph of cross section of germanium tunnel diode.

The dc bias voltage V_d across a tunnel diode is given by

$$V_d = I_d r_d + I_d[R_d(v)]_0, \tag{1}$$

where I_d is the direct current through the diode. At a reverse current, an order of magnitude greater than I_p, $[R_d]_0$ is usually very small compared to r_d, so that r_d can be measured directly. When r_d is known, $[R_d]_0$ can be determined from the current-voltage characteristics of the diode.

Fig. 3 shows the current-voltage characteristics of typical germanium and gallium-arsenide tunnel diodes. In each of these diodes, $I_d r_d$ is much less than V_v (valley voltage) for $0 < I_d < I_p$ (peak current), and, therefore, V_d is approximately equal to $I_d[R_d(v)]_0$ over the current range shown in Fig. 3. For diodes of this type, in which the voltage drop across r_d can be neglected, the shape of the curve of I_d/I_p as a function of V_d usually depends very little on I_p and r_d. For diodes in which the voltage drop across r_d is appreciable, the current-voltage curve generally shifts to the right, *i.e.*, voltages corresponding to peak and valley currents are higher than shown in Fig. 3.

* Received by the IRE, October 24, 1960; revised manuscript received, February 3, 1961.

† Electron Tube Div., RCA, Princeton, N. J.

[1] L. Esaki, "New phenomenon in narrow Ge *p-n* junctions," *Phys. Rev.*, vol. 109, pp. 603–604; January, 1958.

[2] H. S. Sommers, Jr., "Tunnel diodes as high frequency devices," Proc. IRE, vol. 47, pp. 1201–1206; July, 1959.

[3] L. Esaki and Y. Miyahara, "A new device using the tunneling process in narrow *p-n* junctions," *Solid State Electronics*, vol. 1, pp. 13–21; March, 1960.

[4] M. E. Hines, "High-frequency negative-resistance circuit principles for Esaki diode applications," *Bell Sys. Tech. J.*, pp. 477–514; May, 1960.

[5] R. F. Rutz, "A 3000-Mc lumped-parameter oscillator using an Esaki negative-resistance diode," *IBM J.*, vol. 3, pp. 372–374; October, 1959.

[6] J. K. Pulfer, "Voltage tuning in tunnel diode oscillators," Proc. IRE (Correspondence), vol. 48, p. 1155; June, 1960.

[7] R. Trambarulo and C. A. Burrus, "Esaki diode oscillators from 3 to 40 kMc," Proc. IRE, vol. 48, pp. 1776–1777; October, 1960.

[8] C. A. Burrus, "Millimeter wave Esaki diode oscillators," Proc. IRE (Correspondence), vol. 48, p. 2024; December, 1960.

Presently available tunnel diodes have values of I_p varying from about one-tenth to a few hundred milliamperes. The ratio of I_p to I_v (I_v is the value of current corresponding to V_v) usually exceeds 5:1; in some cases ratios of better than 20:1 have been obtained.[9,10]

In ac applications, the quantity of most interest is not the total value of the junction resistance $[R_d(v)]_0$, but rather its incremental value $R_d(v) = dv/dI_d$. Fig. 4 shows R_d as a function of voltage for the two diodes of Fig. 3. The graph indicates that R_d is negative over a voltage range from 0.05 to 0.27 volt for the germanium diode and 0.09 to 0.42 volt for the gallium-arsenide diode.

The series inductance L_d and the junction capacitance $C_d(v)$ of a tunnel diode can be determined from ac impedance measurements.[11] Theoretically, the variation of C_d with voltage when V_d is less than V_v may be approximated by

$$C_d(v) \approx K(\phi - v)^{-1/2}, \tag{2}$$

where K and ϕ are constants. Fair agreement between experimental values of C_d and the values predicted from (2) may be obtained by setting the value of ϕ equal to 0.6 volt for germanium and 1.1 volts for gallium arsenide.[9]

In commercially available tunnel diodes, L_d varies from about 4×10^{-10} to 20×10^{-9} henry. Experimental units using a housing similar to one described by Hilibrand, *et al.*,[12] have a value of L_d of about 3×10^{-10} henry. C_d in commercially available diodes (C_d is usually measured at V_v) varies from 4×10^{-12} farad to 300×10^{-12} farad. Experimental diodes may have capacitances from about 0.4×10^{-12} to 500×10^{-12} farad.

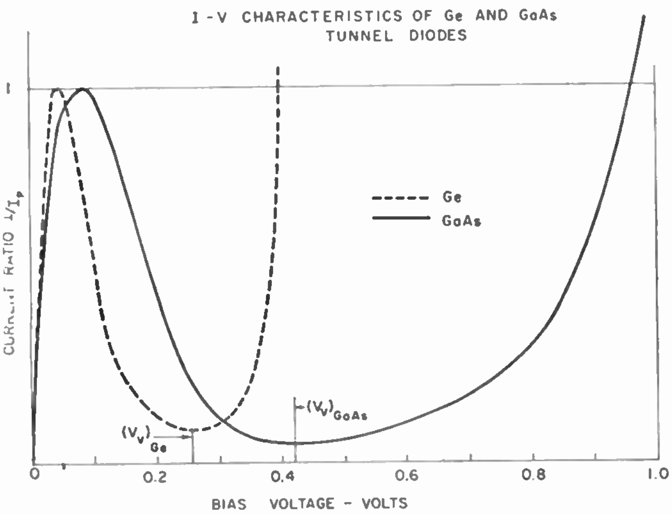

Fig. 3—Current-voltage characteristics of typical germanium and gallium-arsenide tunnel diodes.

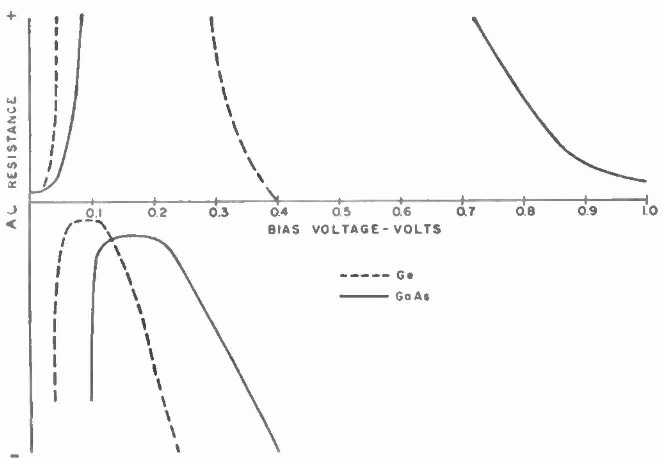

Fig. 4—Incremental resistance of the two diodes of Fig. 3.

Impedance of Tunnel Diodes

In terms of the incremental resistance R_d, the small-signal ac impedance Z_d across the terminals of a tunnel diode may be written as follows:

$$Z_d = \left(r_d - \frac{|R_d|}{R_d^2C_d^2\omega^2 + 1}\right) + j\left(\omega L_d - \frac{R_d^2C_d\omega}{R_d^2C_d^2\omega^2 + 1}\right), \tag{3}$$

where it is assumed that the diode is biased in a region where R_d is negative.[13] In order that the diode exhibit negative resistance, $|R_d|$ must be greater than r_d. The real part of the impedance, Re (Z_d), is equal to $(r_d - |R_d|)$ at zero frequency and increases monotonically with frequency. The frequency at which Re (Z_d) becomes zero is called the cutoff frequency f_c, and is given by

$$f_c = \frac{\sqrt{|R_d|/r_d - 1}}{2\pi|R_d|C_d}. \tag{4}$$

At frequencies above f_c, Re (Z_d) is positive.

The imaginary part of Z_d, Im(Z_d), becomes zero at frequency f_r, where

$$f_r = \frac{\sqrt{R_d^2C_d/L_d - 1}}{2\pi|R_d|C_d} = \frac{1}{2\pi}\sqrt{\frac{1}{L_dC_d} - \frac{1}{R_d^2C_d^2}}. \tag{5}$$

Usually f_r is referred to as the self-resonant frequency of the diode. Below self-resonance, the reactance of the diode is capacitive; above self-resonance, it is inductive.

[9] J. Hilibrand, H. S. Sommers, and C. W. Mueller, RCA Labs., Princeton, N. J.; private communication.

[10] D. J. Donahue, RCA Semiconductor Div., Somerville, N. J.; private communication.

[11] U. S. Davidsohn, Y. C. Hwang, and G. B. Ober, "Designing with tunnel diodes, Part II," *Electronic Design*, vol. 8, pp. 66–71; February 17, 1960.

[12] J. Hilibrand, C. W. Mueller, C. F. Stocker, and R. D. Gold, "Semiconductor parametric diodes in microwave computers," IRE Trans. on Electronic Computers, vol. EC-8, pp. 287–297; September, 1959.

[13] Unless otherwise noted, it will be assumed throughout this paper that R_d is negative.

Both f_c and f_r are functions of dc bias. If $|R_d| > 2r_d$, $[f_c]_{max}$ occurs at the bias voltage corresponding to $|R_d|_{min}$ (neglecting the small effect of the variation of C_d with bias). For $|R_d| < 2r_d$, $[f_c]_{max}$ is at a lower bias voltage. $[f_r]_{max}$ always occurs at the bias voltage, V_p.

The maximum values of f_c, $1/|R_d|C_d$ and f_r for commercially available tunnel diodes are about 5 kMc, 1.5×10^{10} per second and 2 kMc respectively. For experimental units, the maximum values obtained at RCA Laboratories are about 40 kMc, 2×10^{11} per second and 8 kMc.

The design of distributed tunnel-diode oscillator circuits usually requires a plot of diode impedance (or admittance) as a function of frequency. In Fig. 5, Re $(Z_d)/|R_d|$ is plotted as a function of $\omega C_d|R_d|$, with $r_d/|R_d|$ as a parameter. Fig. 6 shows Im $(Z_d)/|R_d|$ as a function of $\omega C_d|R_d|$, with $L_d/C_dR_d^2$ as a parameter.

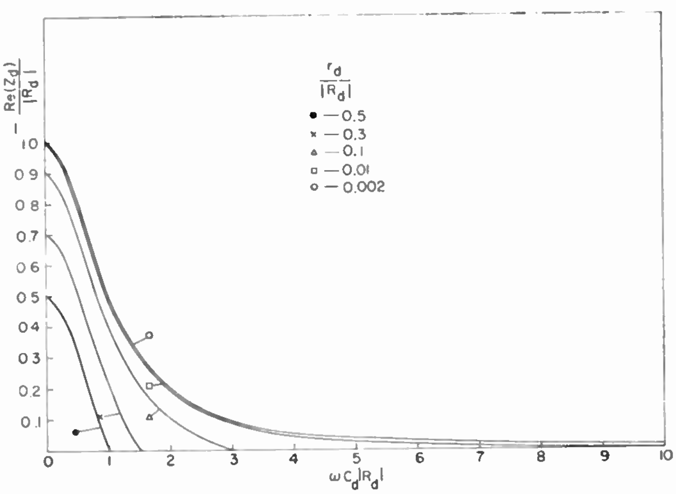

Fig. 5—Graph of the real part of $(Z_d)/|R_d|$ as a function of $\omega C_d|R_d|$ with $r_d/|R_d|$ as a parameter.

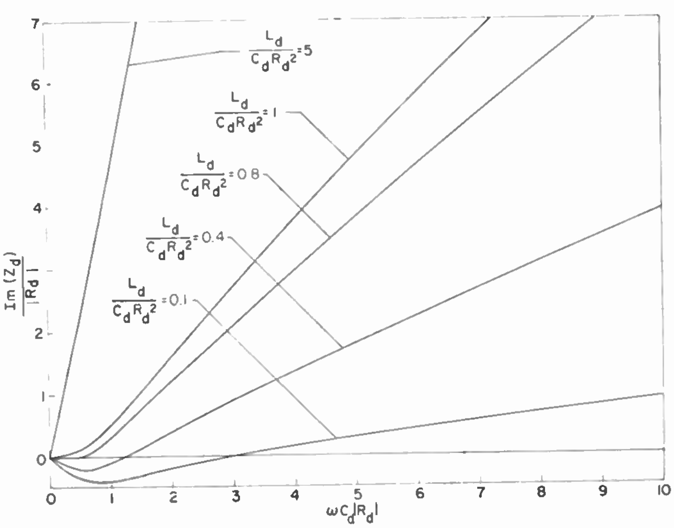

Fig. 6—Graph of the imaginary part of $(Z_d)/|R_d|$ as a function of $\omega C_d|R_d|$ with $L_d/C_dR_d^2$ as a parameter.

OSCILLATORS USING LUMPED-CIRCUIT PARAMETERS

Circuits for Operation Below the Maximum Self-Resonant Frequency of the Diode

From an analytical standpoint, the simplest possible tunnel-diode oscillator circuit consists of a diode shunted by the series combination of an inductance L_c, a series resistance r_c, and a dc voltage source V_b, as shown in Fig. 7(a). This circuit, which is useful in many practical applications, is analyzed in some detail below.[14]

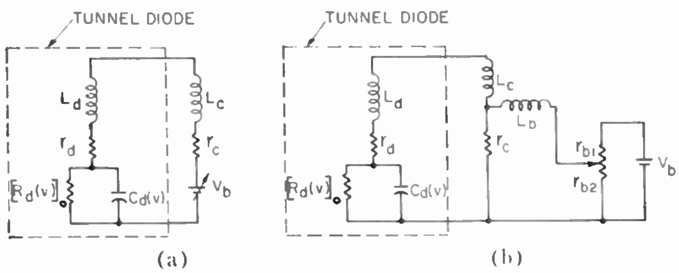

Fig. 7—Tunnel-diode oscillator circuits for operation below the maximum self-resonance frequency of the diode.

In many tunnel-diode oscillators, the inductance of the leads from the dc power supply to the oscillator is much greater than the desired value of L_c. The problem of lead inductance can be obviated through use of the circuit shown in Fig. 7(b). Here the resistor r_c can be placed close to the diode, and the inductance of the bias leads L_b does not affect the performance of the circuit provided both r_{b1} and r_{b2} are much larger than r_c.

If it is assumed that the value of $C_d(v)$ is given by (2), the application of Kirchhoff's laws to the circuit of Fig. 7(a) leads to the following simultaneous equations:

$$f(v) + \frac{Kdv}{dt}(\phi - v)^{-1/2}[1 + v/2(\phi - v)] + I$$

$$= 0 \approx f(v) + \frac{Kdv}{dt}(\phi - v)^{-1/2} - I, \quad (6)$$

$$Ir + L\frac{dI}{dt} + v = V_B, \quad (7)$$

where v = voltage across R_d and C_d,

$$f(v) = \frac{v}{[R_d(v)]_0},$$

$$r = r_d + r_c,$$

$$L = L_d + L_c,$$

$$I = \text{current through } L \text{ and } r.$$

Eqs. (6) and (7) are nonlinear differential equations which cannot be solved in closed form. Therefore, some

[14] A small signal analysis of this circuit is carried out by H. J. Reich in "Theory and Application of Electron Tubes," McGraw-Hill Book Co., Inc., New York, N. Y.; 1944. Reich's analysis does not include variation of C with voltage.

of the general properties of the solutions to these equations are first obtained by a small signal analysis.

The initial response of the network to a small signal excitation can be determined by taking the Laplace transform of (6) and (7). Initial conditions for (6) and (7) are chosen to make R_d negative at time t equal to zero. The resultant characteristic equation is given by

$$s^2LC_{di} + s(rC_{di} - L/|R_{di}|) + (1 - r/|R_{di}|) = 0, \quad (8)$$

where R_{di} and C_{di} are the initial values of R_d and C_d, respectively. Eq. (8) can be solved for s, the familiar generalized frequency, as follows:

$$s_{1,2} = \sigma_i \pm j\omega_i$$

$$s_{1,2} = -\frac{1}{2}\left(\frac{r}{L} - \frac{1}{C_{di}|R_{di}|}\right) \pm\left[\frac{1}{4}\left(\frac{r}{L} - \frac{1}{C_{di}|R_{di}|}\right)^2 - \frac{1 - r/|R_{di}|}{LC_{di}}\right]^{1/2}. \quad (9)$$

A growing solution is obtained if $\sigma_i > 0$. This condition for σ_i is satisfied if either one or both of the following inequalities hold:

$$L > r|R_{di}|C_{di} \quad (10)$$

$$r > |R_{di}|. \quad (11)$$

The initial growth can be either purely exponential ($\omega_i = 0$) or sinusoidal ($\omega_i \neq 0$). The conditions for sinusoidal growth are inequality (10) and

$$\frac{1}{LC_{di}} > \frac{1}{4}\left(\frac{r}{L} + \frac{1}{C_{di}|R_{di}|}\right)^2. \quad (12)$$

The initial frequency of oscillation ω_i is given by the second term of (9). The steady-state frequency ω_s differs, however, from ω_i because of the nonlinearities of the diode. Also, although the oscillations grow initially at the rate $e^{\sigma_i t}$, there can be, of course, no net growth in the steady state. This difference between initial and steady-state behavior of the oscillator can be accounted for by the assumption that both ω and σ are functions of time:[15]

$$\omega(0) = \omega_i \qquad \lim_{t\to\infty} \omega(t) = \omega_s \quad (13)$$

$$\sigma(0) = \sigma_i, \qquad \lim_{t\to\infty} \sigma(t) = 0. \quad (14)$$

For the steady state, (9), (13) and (14) yield

$$L = r|R_{de}|C_{de} \quad (15)$$

$$\omega_s = \left(\frac{1 - r/|R_{de}|}{LC_{de}}\right)^{1/2}, \quad (16)$$

[15] If inequality (11) holds, there exists the possibility of a non-oscillating steady state [$\lim t \to \infty\ \sigma(t) < 0$].

where R_{de} and C_{de} are the effective steady-state values[16] of R_d and C_d, respectively.

For steady-state oscillations, the sum of the impedances or admittances at any point in the circuit (using the effective values R_{de} and C_{de}) must be zero. Eqs. (15) and (16) can also be easily derived by using this principle.

Accurate values of R_{de} and C_{de} can be obtained only by use of lengthy numerical or graphical methods. However, if only moderate variations in R_d and C_d are encountered, then, to a first approximation, R_{de} and C_{de} can be replaced by their average values $\overline{R}_d$ and $\overline{C}_d$, and (15) and (16) become

$$L \approx r|\overline{R}_d|\overline{C}_d \quad (17)$$

$$\omega_s \approx \left(\frac{1 - r/|\overline{R}_d|}{L\overline{C}_d}\right)^{1/2}. \quad (18)$$

Substitution of $r = L/\overline{C}_d|\overline{R}_d|$ and $L = L_d + L_e$ in (18) results in

$$\omega_s \approx \left[\frac{1}{(L_d + L_e)\overline{C}_d} - \frac{1}{\overline{R}_d^2\overline{C}_d^2}\right]^{1/2} = \left[\frac{1}{(L_d + L_e)\overline{C}_d} - \frac{r^2}{(L_d + L_e)^2}\right]^{1/2}. \quad (19)$$

Comparison of (19) with (5), the equation for the self-resonance frequency f_r, shows that ω_s is less than or equal to $|\omega_r|_{\max}$, *i.e.*, the circuits of Fig. 7 cannot produce oscillations above the maximum self-resonance frequency of the diode.

The RF power, P, delivered by a linear negative resistance is

$$P = V_r I_r, \quad (20)$$

where V_r and I_r are the rms values of voltage across and current through the negative resistance, respectively. To a first approximation, one can consider the tunnel diode to be a linear negative resistance in the voltage range from V_p to V_v, and the power delivered by the diode (assuming $r_d = 0$) for an RF voltage swing in this range is

$$p \approx \tfrac{1}{8}(V_v - V_p)(I_p - I_v). \quad (21)$$

A better approximation to the I-V characteristics of the diode can be obtained, in analogy with the classical theory of vacuum tube oscillators,[17] by writing the current as a third degree polynomial of the voltage.[18] This cubic approximation changes the constant in (21) from 1/8 to 3/16.

Complete solutions, including power output, har-

[16] A similar effective resistance is discussed by C. Brunetti, "The clarification of average negative resistance with extensions of its use," Proc. IRE, vol. 25, pp. 1595–1617; December, 1937.

[17] B. Van Der Pol, "Non-linear theory of electric oscillations," Proc. IRE, vol. 22, pp. 1051–1086; September, 1934.

[18] K. K. N. Chang, RCA Labs., Princeton, N. J.; private communications.

TABLE I*

Case	V_b (volts)	L (henrys)	$\frac{r\lvert R_{di}\rvert C_{di}}{L}$	f_1 (Mc)	f_2 (Mc)	Calculated values of: (v) min (volts)	(v) max (volts)	f_s (Mc)	RF power to load r† (milliwatts) Harmonic 1	2	3
1	0.13	8×10^{-11}	0.6	10,540	11,300	0.040	0.187	11,370	0.296	9.8×10^{-4}	1.4×10^{-3}
2	0.13	2×10^{-10}	0.2	6,670	7,580	0.005	0.233	7,140	0.185	7.9×10^{-4}	4.9×10^{-5}
3	0.13	8×10^{-10}	0.06	3,330	3,620	−0.012	0.312	3,030	0.124	3.7×10^{-2}	1.2×10^{-4}
4	0.156	8×10^{-10}	0.1	3,613	3,820	−0.01	0.349	3,252	0.139	1.9×10^{-3}	2.9×10^{-6}
5	0.11	8×10^{-10}	0.07	3,480	3,920	−0.009	0.256	2,604	0.116	3.5×10^{-3}	1.1×10^{-4}
6	0.085	8×10^{-10}	0.08	3,640	3,980	−0.003	0.189	1,865	0.063	5.0×10^{-3}	4.5×10^{-4}

* Results of solutions of equations (6) (approximate form) and (7) obtained on the digital computer. The current-voltage characteristics of a germanium tunnel diode having a peak current of 10 ma were used in the calculations. Other parameters were: $K=1.4\times10^{-12}$ volts $^{1/2}$ farad, $\phi=0.58$ volt, $r=2.5$ ohms.

$$f_1 = \frac{1}{2\pi}\left[\frac{1 - r/\lvert R_{di}\rvert}{LC_{di}}\right]^{1/2}$$

$$f_2 = \frac{1}{2\pi}\left[\frac{1}{LC_{di}} - \left(\frac{r}{L}\right)^2\right]^{1/2}.$$

† The approximation $P=\frac{1}{8}(V_v - V_p)(I_p - I_v)$ yields a value of 0.25 mw for the power delivered to r.

monic content and frequency, of (6) and (7) can be obtained to any desired degree of accuracy by use of numerical calculus.[19] The required calculations using the approximate form of (6) were programmed for an automatic digital computer. The program used a subroutine (written by Dr. F. Edelman of the RCA Laboratories) for the solution of systems of first-order ordinary differential equations. The subroutine is based on methods originated by Milne[20] and Runge-Kutta-Gill.[21] The tunnel-diode current I_d was approximated by the following expression[22] in which $A_1, A_2 \cdots A_6$ are constants:

$$I_d = A_1V_d + A_2V_d^2 + A_3V_de^{-2/3}\left(\frac{V_d}{A_4}\right)^{3/2} + A_5(e^{A_6V_d} - 1). \tag{22}$$

An excellent fit of each of the tunnel-diode characteristics shown in Fig. 3 was obtained by proper choice of the six constants.

Table I summarizes some of the results obtained on the computer. Fig. 8 shows the computed steady-state wave shapes.

The following qualitative conclusions can be drawn from this table:

1) The voltage swing across the diode junction (*i.e.*, across R_d and C_d) increases as L is increased if all other diode and circuit parameters are held constant (see cases 1, 2 and 3). This fact can be explained as follows: in the steady state $r\lvert R_{de}\rvert C_{de}/L=1$ (15). As L is increased, $\lvert R_{de}\rvert C_{de}$ must increase proportionally, *i.e.*, the voltage swing across the diode must increase.
2) Although the voltage swing across the diode junction increases as L increases (cases 1, 2, 3), the RF power delivered to the load decreases, primarily because the voltage drop across L increases.
3) Cases 1, 2 and 3 show that, for a diode biased in the center of the negative-resistance region, the harmonic power output increases as the voltage swing across the diode increases. This result is to be expected because the V-I characteristic of the diode is more nonlinear for large voltage swings.
4) The maximum power output of a tunnel-diode oscillator usually occurs at a bias somewhere between the maximum negative-resistance point and

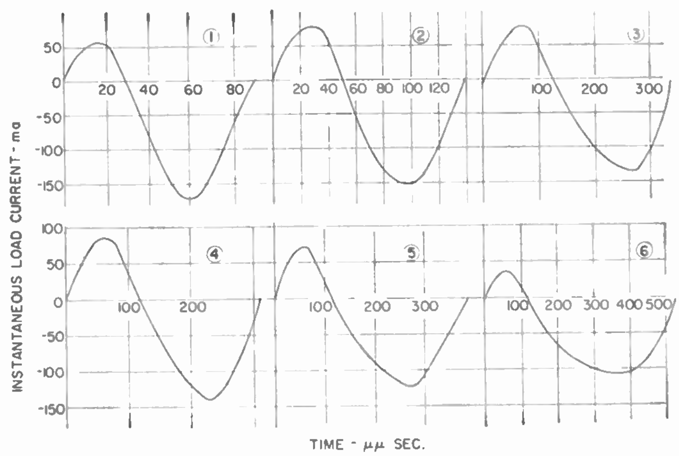

Fig. 8—Calculated steady-state wave shapes of tunnel-diode oscillators.

[19] An alternative method is to use a combination of graphical and analytical procedures. See for example L. Strauss, "Wave Generation and Shaping," McGraw-Hill Book Co., Inc., New York, N. Y., ch. 15; 1960.

[20] W. E. Milne, "Numerical Calculus," Princeton University Press, Princeton, N. J.; p. 134; 1949.

[21] S. Gill, "A process for the step-by-step integration of differential equations in an automatic digital computing machine," *Proc. Cambridge Phil. Soc.*, vol. 47, p. 96; 1951.

[22] This approximation was developed by Dr. R. Klopfenstein and A. H. Simon of the RCA Laboratories.

V_v. Cases 3 to 6 illustrate the increase in power with increasing bias voltage at voltages below the bias voltage corresponding to maximum-power-output. These cases also show that the frequency decreases with bias voltage in this voltage range.

5) Finally, the table also indicates that (19) with $\overline{R}_d$ equal to R_{di} and $\overline{C}_d$ equal to C_{di} represents at least a fair approximation of the steady-state solution for the frequency in (6) and (7), as long as the diode is biased near the center of the negative resistance region.

Fig. 9(a)-(h) shows oscilloscope tracings of the output of a germanium tunnel-diode oscillator of the type shown in Fig. 7(b) as a function of bias across the diode. As predicted by the analytical solutions of (6) and (7), the oscillations are nearly sinusoidal if the diode is biased in the middle of the negative-resistance region. The experimental wave shapes and the variation in frequency with bias agree well with those calculated. It is interesting to note that this oscillator can produce almost undistorted sine waves even though the ratio $r|R_{di}|C_{di}/L$ is about 0.006 and inequality (12) is not satisfied. Thus the initial growth must be purely exponential, *i.e.*, nonperiodic.

Circuits for Operation Above the Maximum Self-Resonant Frequency of the Diode

Above self-resonance, the reactance of the diode is inductive. Therefore, to obtain oscillations at frequencies above the maximum self-resonance frequency it is necessary to use a circuit which presents a capacitive reactance at the oscillation frequency. A simple circuit suitable for operation above the self-resonance frequency of the diode is shown schematically in Fig. 10(a). However, the circuit shown in Fig. 10(b) must be used if the inductance of the power-supply leads L_b is appreciable. The results obtained for the circuit shown in Fig. 10(a) are also applicable to the circuit shown in Fig. 10(b), provided that r_{b1} and r_{b2} are much greater than r_c.

Proceeding in the same fashion as in the preceding section, it can be shown that for small amplitude oscillation, the following relationships exist:

$$(|\overline{R}_d| - r_d - r_c)r_cC_c$$
$$\approx (r_dr_cC_c/L_d - r_cC_c/|\overline{R}_d|\overline{C}_d + 1)(r_c|\overline{R}_d|\overline{C}_d + |\overline{R}_d|r_cC_c + r_d|\overline{R}_d|\overline{C}_d - L_d - r_dr_cC_c), \quad (23)$$

and

$$\omega_r \approx \left[\frac{|\overline{R}_d| - r_d - r_c}{L_d|\overline{R}_d|\overline{C}_d + r_cC_c(|\overline{R}_d|\overline{C}_dr_d - L_d)}\right]^{1/2}. \quad (24)$$

A proper choice of parameters of the circuit of Fig. 10(a) can lead to an oscillation frequency higher than the maximum self-resonance frequency of the diode. Of course, the cutoff frequency of the diode must be higher than the self-resonance frequency.

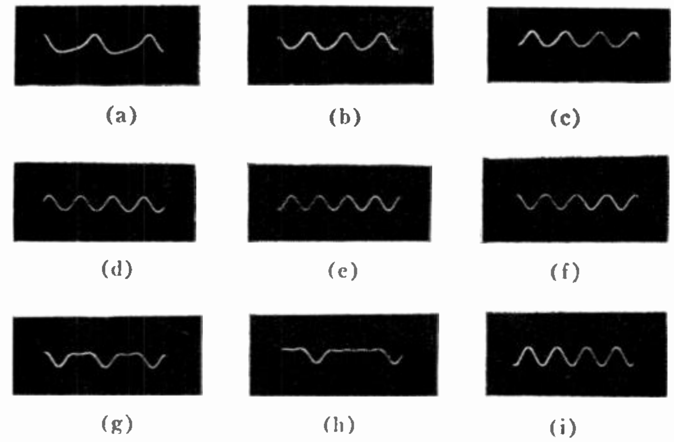

Fig. 9—(a)-(h). Oscilloscope tracings of the output of a germanium tunnel-diode oscillator of the type shown in Fig. 7(b) as a function of bias across the diode. (i). A calibrating 17.9-Mc sine wave with 0.025-volt rms amplitude. The parameters of the oscillator were as follows: $|R_d| = 4.3$ ohms, C_d (measured at 0.35 volt) $= 75 \times 10^{-12}$ f_d, $r_d = 0.3$ ohm, $L_d = 2. \times 10^{10}$ henry, $L_c = 1.8 \times 10^{-7}$ henry, $r_c = 3.33$ ohms. The bias voltage across the diode was varied as follows: (a) 0.093 volt; (b) 0.13 volt; (c) 0.15 volt; (d) 0.175 volt; (e) 0.25 volt; (f) 0.28 volt; (g) 0.295 volt; (h) 0.305 volt.

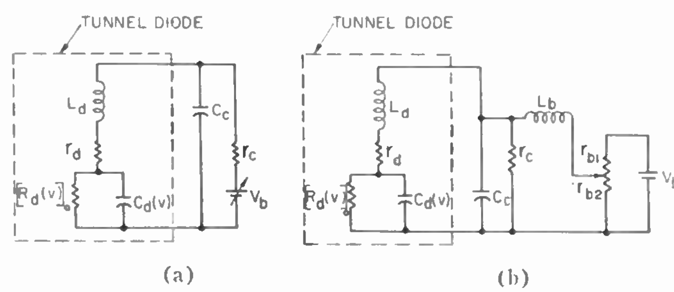

Fig. 10—Tunnel-diode oscillator circuits for operation above the maximum self-resonance frequency of the diode.

Experimental oscillators of the type shown in Fig. 10(b), operated at a frequency of a few megacycles, have produced almost perfect sinusoidal oscillations well above the self-resonant frequency of the diode.

Oscillators Using Distributed Circuits

In tunnel-diode oscillators operating above a few hundred megacycles, it is convenient to use transmission-line resonators. Suitable resonators can be built from coaxial lines, strip transmission lines, waveguides, and the like. The mathematical description of an oscillator using this type of resonator generally involves nonlinear partial differential equations, for which complete solutions are very difficult to obtain. The solutions of these equations are simplified when it is valid to assume that the oscillator circuit consists of lumped elements connected by uniform transmission lines. This assumption is valid for many practical microwave oscillators. Tunnel diodes can be packaged in housings that are sufficiently small to be considered lumped-circuit elements up to frequencies well above 10 kMc. It is also possible to build stabilizing resistors that can be treated as lumped-circuit elements up to these frequencies.

The characteristic equations of circuits consisting of lumped elements connected by transmission lines can be found in the conventional manner by using the generalized frequency, $s=\sigma+j\omega$ in the expression for either the impedance or admittance of the circuit. In general the characteristic equation will be transcendental and will have an infinite number of eigenfrequencies, $s_n=\sigma_n+j\omega_n$. If σ_n is greater than zero, then oscillations can occur at frequency ω_n. However, if there exists no σ_n greater than zero, the circuit will be stable. Unlike the two cases of lumped circuits treated previously, in the distributed case it is very difficult to express the condition for start oscillation in closed form. It is possible, however, to determine the stability of a particular circuit by solving its characteristic equation by either numerical or graphical means.

For steady-state oscillations, the sum of the impedances or admittances at any point in the circuit must be zero. For small amplitude oscillations, the effective values of R_d and C_d are nearly equal to their initial values, and an approximation of the steady-state frequency of oscillation can be calculated. In Fig. 11 the conductance and susceptance of a tunnel diode are plotted as a function of frequency. The stabilizing resistors in a number of oscillator circuits using this diode were adjusted to a value at which oscillations were just maintained. The conductance and susceptance of the circuits were calculated and their negative values plotted in Fig. 11 for comparison with the diode curve. It can be seen that the sum of the initial admittance of the diode and the admittance of the circuit is indeed nearly zero.

For oscillations with appreciable amplitude, the effective average value of R_d is several times as large as the minimum value. Therefore, in the design of circuits for oscillators with appreciable power output, it is helpful to plot the impedance or admittance of the tunnel diode vs frequency for a value of R_d several times the minimum value. This curve differs, in general, by only a relatively small amount from that for a minimum R_d except in the neighborhood of self-resonance, where the difference may be very large. Thus at frequencies removed from f_r, the exact choice of $\overline{R}_d$ is not critical. Figs. (5) and (6) are usually very helpful in constructing the graphs of impedance vs admittance described above.

Figs. 12 and 13 show tunnel-diode oscillator circuits which use straight and re-entrant strip transmission-line resonators, respectively. These circuits have also proven to be useful in amplifier applications. If it is assumed that the RF energy propagates in a pure TEM mode and there are no losses in the line, the admittance

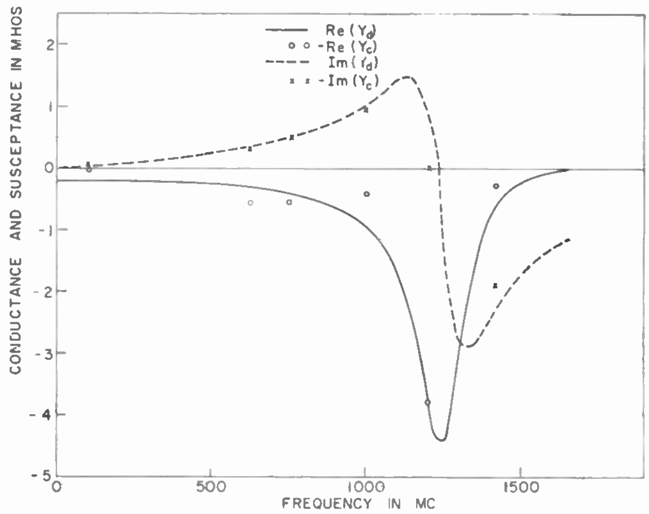

Fig. 11—Plot of conductance and susceptance as a function of frequency for a tunnel diode and its oscillator circuits.

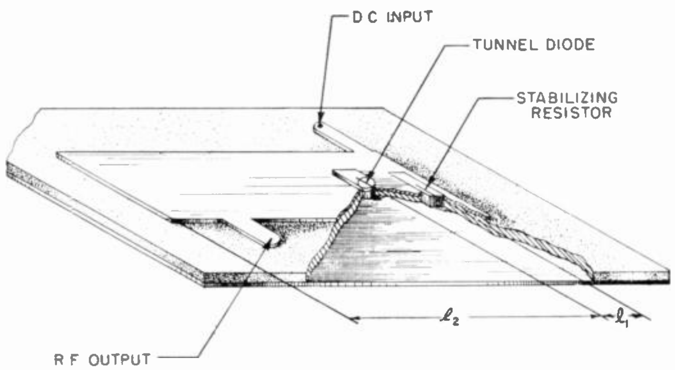

Fig. 12—Tunnel-diode oscillator using a straight strip transmission-line cavity.

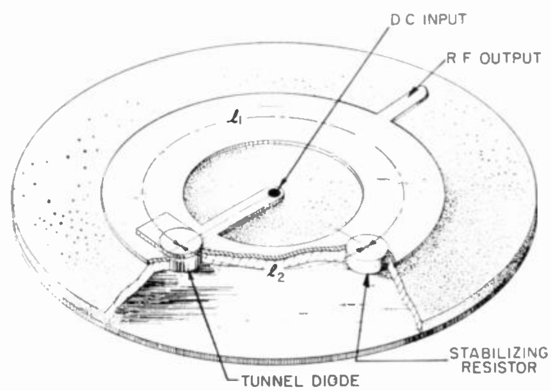

Fig. 13—Tunnel-diode oscillator using a re-entrant strip transmission-line cavity.

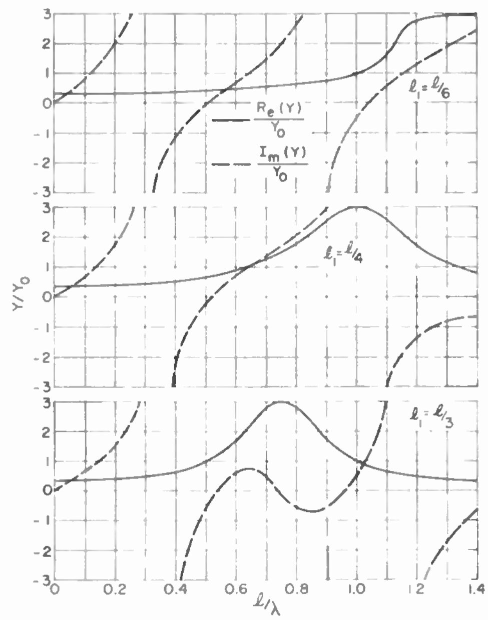

Fig. 14—Plot of the real and imaginary parts of Y/Y_0 for the circuit of Fig. 12 as a function of l/λ for three values of $l_1(Z_0/Z_R=3)$.

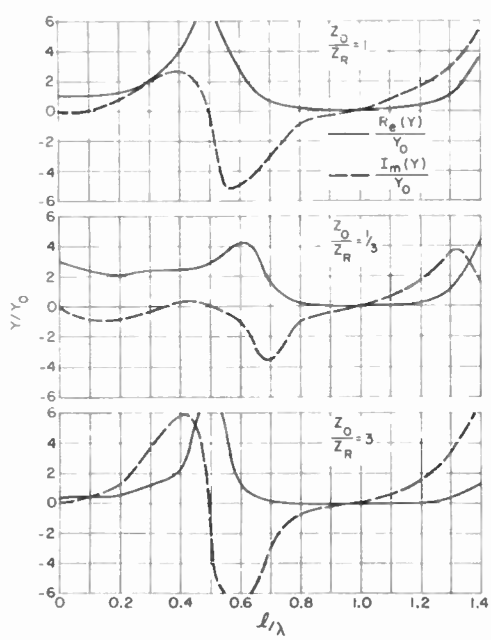

Fig. 15—Plot of the real and imaginary parts of Y/Y_0 for the circuit of Fig. 13 as a function of l/λ for three values of $Z_0/Z_R(l_1/l=1/4)$.

of the circuit, Y_c, at the location of the diode can be written for the straight cavity as follows:

$$\frac{Y_c}{Y_0} = \frac{Z_0/Z_R}{(Z_0/Z_R)^2 \sin^2 \beta l_1 + \cos^2 \beta l_1} + j\left[\tan \beta l_2 + \frac{1-(Z_0/Z_R)^2 \sin \beta l_1 \cos \beta l_1}{(Z_0/Z_R)^2 \sin^2 \beta l_1 + \cos^2 \beta l_1}\right], \quad (25)$$

and for the re-entrant cavity as follows:

$$Y_c/Y_0 = \frac{B^2}{Z_0/Z_R - jA} - jA = \frac{B^2}{A^2+(Z_0/Z_R)^2}\,\frac{Z_0}{Z_R} + jA\left[\frac{B^2}{A^2+(Z_0/Z_R)^2} - 1\right], \quad (26)$$

where

Y_0 = characteristic admittance of the strip transmission line,
Z_0 = characteristic impedance of strip transmission line,
Z_R = impedance of the stabilizing resistor,
β = propagation constant in the strip transmission line,
$A = \cot \beta l_1 + \cot \beta l_2$,
$B = \csc \beta l_1 + \csc \beta l_2$,
l_1 and l_2 are defined in Figs. 12 and 13.

Eqs. (25) and (26) neglect the effect of RF output loading.

The frequency of oscillation of the circuits of Figs. 12 and 13 can be electrically varied by insertion of a variable capacitor in regions of high electric field. The circuit of Fig. 12 can also be mechanically tuned by varying l_2.[23]

Fig. 14 shows curves of the real and imaginary parts of (25) as a function of l/λ (l is equal to l_1+l_2) for three values of $l_1(Z_0/Z_R=\frac{1}{3})$. Fig. 15 shows the real and imaginary parts of (26) as a function of l/λ for three values of $Z_0/Z_R(l_1/l=\frac{1}{4})$. These figures show that it is possible to vary the conductances and susceptances of the circuits of Figs. 12 and 13 over wide ranges by adjusting l_1, l_2, and Z_R. Thus, it is possible to design oscillator circuits for diodes having widely different parameters.

A Rieke diagram showing the variation of oscillator frequency and power as the load impedance is varied is shown in Fig. 16. This Rieke is for a re-entrant strip transmission-line oscillator for which Z_0/Z_R was 2; l_1/l was $\frac{1}{4}$; and l/λ was 1.2.

It is possible to lock the frequency of any tunnel-diode oscillator to the frequency of an external signal. The locking signal can be introduced by means of a simple power divider, but in this case, part of the locking signal is not effective and part of the oscillator output

[23] R. Steinhoff of the RCA Electron Tube Division has designed a 1000-to-1500-Mc mechanically tunable oscillator, of the type shown in Fig. 12, suitable for commercial production.

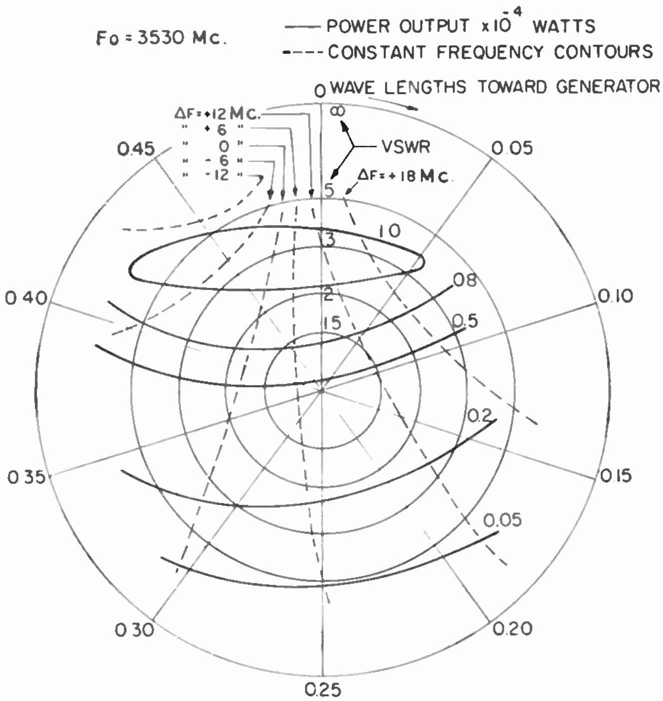

Fig. 16—Rieke diagram of tunnel-diode oscillator.

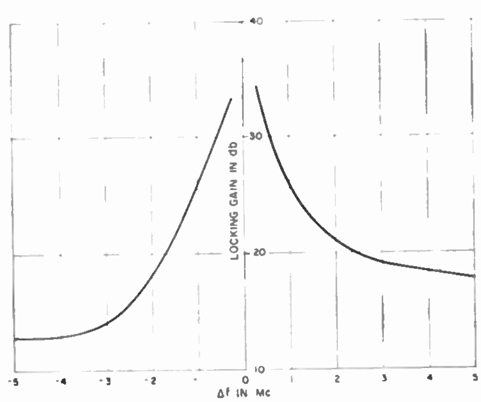

Fig. 17—Plot of locking gain vs difference frequency for two 860-Mc tunnel-diode oscillators having a total power output of 2.3 mw. The two oscillators were locked by means of a hybrid circuit.

must be absorbed in the locking generator. Both these difficulties can be overcome by using either a ferrite circulator or a hybrid ring connecting two similar oscillators (a suitable hybrid ring circuit is shown in Fig. 9 of Sterzer[24]). A hybrid arrangement using two 860-Mc tunnel-diode oscillators having a total power output of 2.3 mw was locked by means of a klystron generator. Fig. 17 is a plot of locking gain (the ratio of power output from the hybrid to the minimum required locking power) vs frequency difference (the difference between the natural frequency of the two oscillators and the frequency of the locking signal). The figure shows that the locking signal can be orders of magnitude smaller than the power output, provided the locking frequency is close to the natural frequency of the oscillators. The locking signal can, if desired, be derived from the harmonics of a crystal-controlled lower-frequency oscillator.

Three tunnel-diode oscillators may be paralleled using a single hybrid ring. The hybrid arrangement described above is used with the locking generator replaced by the third tunnel-diode oscillator. Multiple hybrid circuits may be used to parallel larger numbers of diodes. A single hybrid-ring circuit has been tested. Three oscillators with maximum power outputs of 1.7, 2.0 and 2.5 mw were paralleled producing a total 850-Mc power output of 5.6 mw or 90 per cent of the total available power.

Fig. 18 is a photograph of some straight and re-entrant strip transmission-line and waveguide oscillators. The experimental results obtained with these oscillators are listed in Table II. The power outputs obtained are an order of magnitude greater than those previously reported in the literature.[5,6] At the lower frequencies, the power output from these oscillators approaches, and in one case even exceeds, $\frac{1}{8}(I_p - I_v)(V_v - V_p)$. At the higher frequencies where the effects of series resistance, series inductance and circuit losses are appreciable, the power output is considerably lower.

The oscillators shown in Fig. 18 used experimental tunnel diodes. For example, the results listed in the second line of Table II (using the strip transmission circuit in the extreme right of Fig. 18) were obtained with a gallium-arsenide diode with the following parameters: $I_p = 53$ ma, $|R_d|_{min} \approx 3.8$ ohms, $C_d = 15$ $\mu\mu$f (measured at V_v), $r_d = 1.2$ ohms, $L_d \approx 500$ $\mu\mu$h.

There is little doubt that power outputs an order of magnitude higher than those listed in Table II can be obtained in the near future. Methods that can be used to increase the power output include: paralleling a large number of individual oscillators, use of a number of diodes in a single oscillator circuit, and the use of high-

[24] F. Sterzer, "Microwave parametric subharmonic oscillators for digital computing," Proc. IRE, vol. 47, pp. 1317–1324; August, 1959.

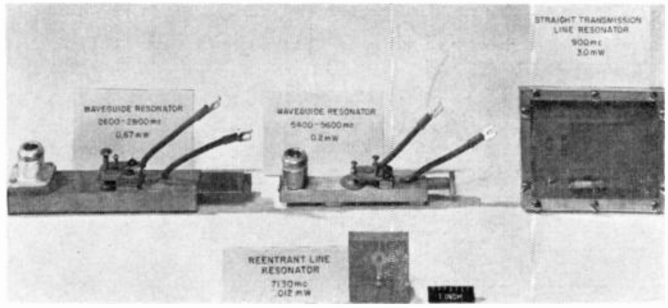

Fig. 18—Photograph of tunnel-diode oscillators.

TABLE II

CHARACTERISTICS OF EXPERIMENTAL TUNNEL-DIODE OSCILLATORS

Type of Circuit	Diode Peak Current (ma)	Diode Material	Number of Diodes	Frequency of Oscillation (Mc)	Power Output (mw)	Tuning Range (Mc)	$\frac{1}{8}(I_p - I_v)(V_v - V_p)$ (mw)
Straight strip cavity	210	Ga-As	1	610	10		8.6
Straight strip cavity	53	Ga-As	1	900	1.7		2.4
Straight strip cavity	50	Ga-As	2	950	3		4.8
Re-entrant strip cavity	210	Ga-As	1	1,600	2		8.6
Ridge-waveguide cavity	37	Ge	1	2,800	0.7	2,700–2,900	1.3
Ridge-waveguide cavity	37	Ge	1	5,500	0.2	5,400–5,600	1.3
Strip-line re-entrant cavity	13.7	Ge	1	7,130	0.012		0.5
Strip waveguide	13.7	Ge	1	8,350			0.5

current tunnel diodes with distributed junctions. Also research on semiconductor materials may permit the development of higher voltage tunnel diodes.

CONCLUSION

Experimental oscillators described in this paper have produced power outputs of 10 mw at 610 Mc, 2.0 mw at 1600 Mc, 0.67 mw at 2800 Mc, 0.2 mw at 5500 Mc, and 0.01 mw at 7100 Mc. It is anticipated that considerably higher power outputs will be obtained in the near future. Tunnel-diode oscillators are compact and rugged, are relatively insensitive to nuclear radiation, have very modest power-supply requirements, and can be easily tuned by either mechanical or electrical means; thus, they have significant advantages over low-power vacuum-tube oscillators.

ACKNOWLEDGMENT

The authors extend their thanks to Dr. D. J. Donahue, Dr. C. W. Mueller, Dr. H. S. Sommers, and H. Nelson for supplying the tunnel diodes; and to Dr. J. Hilibrand, H. C. Johnson, A. Presser, Dr. H. S. Sommers, F. E. Vaccaro, and L. M. Zappulla for their discussions and assistance.

Three-Layer Negative-Resistance and Inductive Semiconductor Diodes*

W. W. GÄRTNER†, SENIOR MEMBER, IRE, AND M. SCHULLER†, MEMBER, IRE

Summary—**This paper shows that in transistor-like three-layer structures with the base either open-circuited or directly shorted to the emitter region, negative resistances are observed when any two of several effects listed occur simultaneously. At higher frequencies, an inductance is often associated with the negative resistance. A few typical devices are analyzed illustrating an approach to the design theory and showing that the component values achieved ($-R$ and L) lie in the region of major circuit interest. Some of the structures offer hope of providing negative resistances and variable inductances in the microwave region; others appear promising as fast switching elements or as replacements for wound coils in microcircuitry.**

Introduction

INTEREST in negative-resistance diodes has increased in the last few years[1] since they promise to provide simple monostable and bistable devices for pulse circuitry; simple two-terminal oscillators as they are needed, *e.g.*, in all-solid-state parametric amplifiers; oscillator-mixer combinations that would utilize their nonlinearities; and novel amplifier circuits. The advent of microelectronics has also spurred some interest in semiconductor inductances to replace bulky coils. In this paper, we concentrate on three-layer transistor-like structures in which the base region is either open-circuited or shorted to the emitter contact, and which exhibit a negative resistance and inductance across their two terminals due to several possible combinations of effects. We shall discuss these effects in some detail below. It is of particular interest to investigate the frequency dependence of these devices since it no longer seems to be limited by the base-spreading impedance of the corresponding transistor structure, but only by the carrier transit time. Therefore, it no longer appears necessary to compromise between transit time and base-spreading resistance, but merely to optimize the device for short transit times only. The hope is therefore justified that, with a given state of technology, it will be possible to build three-layer negative-resistance diodes with a higher cutoff frequency than the corresponding transistor structure. An exception is the case where the base region is shorted to the emitter contact, but here, too, the manufacturing problem is greatly simplified since it is no longer necessary to attach a base contact insulated from, but very close to, the emitter contact.

Many different negative-resistance structures in semiconductors and their associated circuitry have been described and discussed in the literature. We may mention only point-contact transistors, p-n-p-n structures, avalanche transistors, parametric and tunnel diodes. The following discussion is concerned with listing the various obvious effects whose combinations could give a negative resistance in three-layer diodes, and analyzing quantitatively the dc and small-signal ac characteristics of several typical examples.

List of Symbols Not Defined in Text

A—conducting cross section (of device or junction)
a_0—low-frequency common-base short-circuit current-amplification factor
C_c—collector-junction capacitance
C_e—emitter-junction capacitance
c_1—capacitance describing emitter efficiency in high-frequency equivalent circuit of Fig. 13
D_{nB}—diffusion constant of electrons in base region
D_{nC}—diffusion constant of electrons in collector region
D_{nE}—diffusion constant of electrons in emitter region
D_{pB}—diffusion constant of holes in base region
D_{pC}—diffusion constant of holes in collector region
D_{pE}—diffusion constant of holes in emitter region
ds—line element in (1)
$\boldsymbol{E}$—electric field vector
g_1—conductance describing emitter efficiency in high-frequency equivalent circuit of Fig. 13
I_B—dc base current
I_C—dc collector current
I_{C0}—dc collector current for $i_E=0$
I_C'—dc collector current with avalanche multiplication
I_E—emitter current
I_{nE}—dc electron current through emitter junction
I_{pE}—dc hole current through emitter junction
I_{nC}—dc electron current through collector junction
I_{pC}—dc hole current through collector junction
J_C—dc current density through collector junction
J_{nC}—dc electron-current density through collector junction
J_{nE}—dc electron-current density through emitter junction

* Received by the IRE, July 20, 1960; revised manuscript received, December 13, 1960.
† CBS Labs., Stamford, Connecticut; formerly with the U. S. Army Signal Res. and Dev. Lab., Fort Monmouth, N. J.

[1] See, *e.g.*, W. Shockley, "Negative resistance arising from transit time in semiconductor diodes," *Bell Sys. Tech. J.*, vol. 33, pp. 799–826, July, 1954; "Transistor-diodes," *Proc. IEE*, vol. 106, pp. 264–278, May, 1959; "Whither Transistor Electronics?" presented at Transistor and Solid State Circuits Conf., Philadelphia, Pa., February 20, 1958; "The four-layer transistor diode: An example of a solid state circuit or molecular engineering," *Wave Guide*, vol. 10, pp. 15–30, March, 1959.

J_{pC}—dc hole-current density through collector junction
J_{pE}—dc hole-current density through emitter junction
$j=\sqrt{-1}$
k—Boltzmann constant
L_B—diffusion length in base region
L_C—diffusion length in collector region
L_E—diffusion length in emitter region
L_{pC}—diffusion length of holes in collector region
M—avalanche-multiplication factor
m—empirical exponent in expression for avalanche multiplication factor M
n_{0B}—equilibrium density of electrons in base region
n_{0C}—equilibrium density of electrons in collector region
n_{0E}—equilibrium density of electrons in emitter region
n_{1B}—electron density in base region at emitter junction
n_{10B}—dc electron density in base region at emitter junction
n_{20B}—dc electron density in base region at collector junction
p_{0B}—equilibrium density of holes in base region
p_{0C}—equilibrium density of holes in collector region
p_{0E}—equilibrium density of holes in emitter region
p_{1E}—hole density in emitter region at emitter junction
p_{10E}—dc hole density in emitter region at emitter junction
p_{20C}—dc hole density in collector region at collector junction
q—electronic charge
r_B'—base-spreading resistance
r_{B0}'—base-spreading resistance with no applied collector voltage
T—absolute temperature
V_{BD}—breakdown voltage (due to avalanche multiplication)
V_C—dc collector-junction voltage
V_{CE}—dc voltage between collector and emitter
V_E—dc emitter-junction voltage
V_{PT}—punch-through voltage
v—total voltage across diode
v_C—total collector-junction voltage
v_E—total emitter-junction voltage
v_e—ac emitter-junction voltage
W—dc base width
W_0—dc base width with no applied collector voltage
w—total base width
y_{ikb}'—common-base four-pole admittances describing diffusion, junction capacitances and collector multiplication
$\bar{y}_{ik,\mathrm{diff}}$—diffusion admittances in the case of current-dependent emitter efficiency
z_B'—base-spreading impedance
ϵ_0—permittivity of free space
κ—dielectric constant (=12 for silicon, =16 for germanium)
μ_{pB}—hole mobility in base region
μ_{pC}—hole mobility in collector region
ρ_B—resistivity in base region
ρ_C—resistivity in collector region
ρ_E—resistivity in emitter region
ω—frequency
ω_a—cutoff frequency of common-base short-circuit current-amplification factor
τ_{nE}—electron lifetime in emitter region
τ_{pE}—hole lifetime in emitter region.

Three-Layer Negative-Resistance Diodes in General

A semiconductor diode in the general sense is a piece of semiconductor material between two contacts, as shown in Fig. 1(a). For it to have a negative resistance, it is necessary that for some voltage v and current i the following relationship holds

$$0 > \frac{dv}{di} = -\frac{d}{di}\int_A^B E(x, y, z)ds. \tag{1}$$

This means that along a certain line element between A and B,

$$\frac{dE}{di} < 0. \tag{2}$$

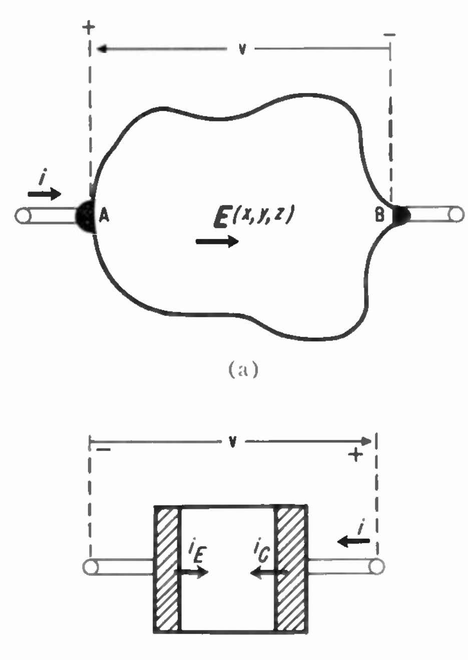

Fig. 1—On the analysis of negative resistance diodes in general.

To invent negative-resistance diodes, it is then necessary to find mechanisms which satisfy this inequality.

Although extremely general, this approach does not prove very helpful in the discussion of the two-junction three-layer diodes which we propose to analyze. Rather, it appears more suitable to base the discussion on the general transistor structure of Fig. 1(b), and on general transistor relationships. The emitter and collector currents, i_E and i_C, which are equal, of course, in the diode, are different functions of the emitter and collector junction voltages, v_E and v_C, and provide the following two relationships:

$$i_E = f_1(v_E, v_C) = -i \tag{3}$$

and

$$i_C = f_2(v_E, v_C) = i. \tag{4}$$

By eliminating v_E, these relationships may be combined in principle into the following not entirely logical, but later very useful, form

$$i = f(i, v_C) + g(v_C). \tag{5}$$

where f incorporates all the terms which contain i explicitly, and g contains those which do not. In a more familiar form, we may write

$$i_C = -a(i_E, v_C)i_E + g(v_C), \tag{6}$$

where $a(i_E, v_C)$ corresponds approximately to the current-amplification factor, and $g(v_C)$ corresponds approximately to the collector-cutoff current for $i_E=0$. Since in the diode

$$i_C = -i_E = i, \tag{7}$$

one obtains

$$i = g/(1-a). \tag{8}$$

This equation indicates that appreciable current will flow through the diode either if the collector-cutoff current is very high, or if the current-amplification factor is very close to unity, or both.

We may now ask ourselves under what conditions does the device exhibit a negative resistance, *i.e.*,

$$di/dv < 0. \tag{9}$$

Considering the usual situation in a transistor structure, we may assume that

$$dv_C/dv \simeq 1, \tag{10}$$

and then find from (8) that

$$\frac{di}{dv} = \frac{(1-a)\dfrac{dg}{dv_C} - g\dfrac{\partial a}{\partial v_C}}{(1-a)^2 - g\dfrac{\partial a}{\partial i}}. \tag{11}$$

Considering that all the derivatives in this equation are usually positive (with special effects, however, the opposite may be true), we may immediately distinguish three obvious cases which will yield a negative resistance:

A.

$$(1-a)^2 < g(\partial a/\partial i) \tag{12}$$

and

$$dg/dv_C = 0 \tag{13}$$

and

$$g(\partial a/\partial v_C) > 0. \tag{14}$$

B.

$$(1-a)^2 < g(\partial a/\partial i) \tag{15}$$

and

$$(1-a)(dg/dv_C) > 0 \tag{16}$$

and

$$\partial a/\partial v_C = 0. \tag{17}$$

C.

$$(1-a)^2 < g(\partial a/\partial i) \tag{18}$$

and

$$(1-a)(dg/dv_C) > 0 \tag{19}$$

and

$$g(\partial a/\partial v_C) > 0. \tag{20}$$

We shall obviously have a small-signal negative-resistance diode if, for some operating point determined by the dc current I through the device, and by the dc voltage V across its terminals, any of these three sets of conditions is satisfied. The exact magnitude of the low-frequency negative resistance may, of course, be obtained from a plot of the dc V-vs-I characteristic.

The ac small-signal analysis of these three-layer structures is conveniently approached via the small-signal four-pole parameters of the corresponding transistor. When the base is open, we may use, *e.g.*, h_{22e} (the common-emitter open-circuit output admittance), and when the base region is shorted to the emitter contact, we may use y_{22e} (the common-emitter short-circuit output admittance), which is equal to y_{22b} (the common-base short-circuit output admittance).

We therefore take the following approach to the analysis of these diodes: We first calculate the dc V-vs-I characteristic over as wide a range of values as is reasonable to expect of a finished device. Then we calculate the complex small-signal four-pole parameters over the same range of operating points and as a function of frequency. (If this procedure is reversed by constructing first the small-signal four-pole parameters to achieve the negative resistance, one must assure afterwards that the necessary dc operating point may actually be reached.)

Before we consider certain structures in detail, we want to list those current and voltage dependences of the current-amplification factor and the collector-cutoff current whose combination may lead to a negative resistance. They are shown in a schematic way in Fig. 2.

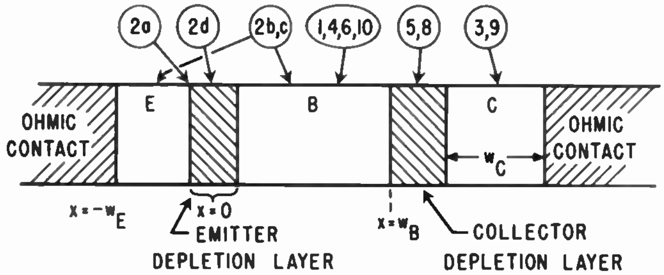

Fig. 2—Three-layer diode structure and location of different effects which may contribute to negative resistance.

List of Effects Whose Combinations May Lead to Negative Resistances

1) Increase in current-amplification factor a with current due to field-enhanced diffusion in base region. (Aiding field for minority carriers increases with injection level,[2,3] and therefore increases the "transport factor.")

2) Increase or decrease in current-amplification factor a with current due to the current dependence of the emitter efficiency. Several entirely independent possibilities exist here:

a) The geometry of the emitter junction is such that the percentage of minority carriers injected into the base increases.[4]

b) The base region is shorted to the emitter contact around its periphery. With increasing total current, the percentage through the emitter junction increases, and the percentage through the ohmic base contact decreases, leading to an effective increase in emitter efficiency (see calculations below).

c) The emitter efficiency decreases with emitter-current density when the emitter resistivity is lower than the base resistivity; the emitter efficiency increases with emitter current when the base resistivity is lower than the emitter resistivity. This latter case is, of course, usually avoided in transistors because the emitter efficiency is low at all current levels, but it may be called for in negative-resistance diodes.

d) The emitter efficiency increases with current due to recombination and generation inside the emitter-junction depletion layer, which effect decreases in importance as the emitter current increases.

3) Increase in current-amplification factor a with collector current due to field-enhanced diffusion in the collector region ("collector multiplication"), which increases the minority carrier current from the collector region into the base with increasing total collector-current density.[5]

4) Increase or decrease in current-amplification factor a with current due to injection-level dependent recombination mechanism in the base region.

5) Increase in current-amplification factor a with collector voltage due to avalanche multiplication in the collector junction.

6) Increase in current-amplification factor a with collector voltage due to narrowing of the effective base region and, thus, increase in the transport factor. In a variation of this effect, the recombination mechanism in the base region (density and level of recombination centers) may be a function of distance and may produce a certain voltage dependence of the transport factor. If most of the recombination takes place very close to the collector junction, whereas the rest of the base region has a very long life-time, the increase of the transport factor with reverse collector voltage may be much more pronounced than with uniform lifetime throughout the base region.

7) Surface recombination velocity could be used for a current-dependent mechanism if the recombination velocity were a function of injection density near the surface, or it could be used for a voltage-dependent mechanism if variation in base width due to collector voltage changes the surface area over which recombination takes place.

8) Increase in collector-cutoff current with collector voltage due to avalanche multiplication in collector junction.

9) Increase in collector cutoff current with collector voltage due to the proximity of the ohmic collector contact. As the depletion layer of the collector junction expands towards the ohmic collector contact (somewhat analogous to punch-through), the collector cutoff current increases because of the steeper gradient of minority carriers towards the collector junction.

10) Increase in current through the device with collector voltage due to approaching punch-through in the base region. Even with no external forward bias on the emitter junction, the gradient of minority carriers in the base region becomes high enough to pull current out of the emitter region.

[2] W. M. Webster, "On the variation of junction-transistor current-amplification factor with emitter current," Proc. IRE, vol. 42, pp. 914–920; June, 1954.
[3] E. S. Rittner, "Extension of the theory of the junction transistor," *Phys. Rev.*, vol. 94, pp. 1161–1171; June, 1954.
[4] S. L. Miller and J. J. Ebers, "Alloy junction avalanche transistors," *Bell Sys. Tech. J.*, vol. 34, pp. 883–902; September, 1955.
J. R. A. Beale, W. L. Stephenson and E. Wolfendale, "A study of high-speed avalanche transistors," *Proc. IEE*, vol. 104, pp. 394–402; July, 1957.
R. Emeis and A. Herlet, "The blocking capability of alloyed silicon power transistors," Proc. IRE, vol. 46, pp. 1216–1229; June, 1958.

[5] J. M. Early, "Design theory of junction transistors," *Bell Sys. Tech. J.*, vol. 32, pp. 1271–1312; November, 1953.
R. L. Pritchard, "Frequency variations of junction transistor parameters," Proc. IRE, vol. 42, pp. 786–799; May, 1954.
W. W. Gärtner, "Transistors: Principles, Design and Applications," D. Van Nostrand Co., Inc., Princeton, N. J., ch. 5; 1960.

Avalanche Transistor with Base Shorted to Emitter ("Miller-Ebers" Diode)

This negative-resistance diode consists of an ordinary avalanche transistor whose base region is directly shorted to the emitter contact, as shown in the cross section of Fig. 3. Due to the avalanche multiplication, the device has a current gain and collector reverse current which increase with increasing collector voltage, and the transverse voltage drop through the base-spreading resistance causes the effective emitter efficiency (and thus the "alpha") to increase with current. Thus, the prerequisites for a dc negative resistance are met. Although the base-spreading resistance is here part of the ac circuit, the construction of the device is considerably simpler than that of the corresponding transistor structure because there is no need to attach a base contact which is insulated from the emitter contact. There is hope, therefore, that such a diode can be built with a higher frequency cutoff than an optimized transistor structure based on the same state of technology.

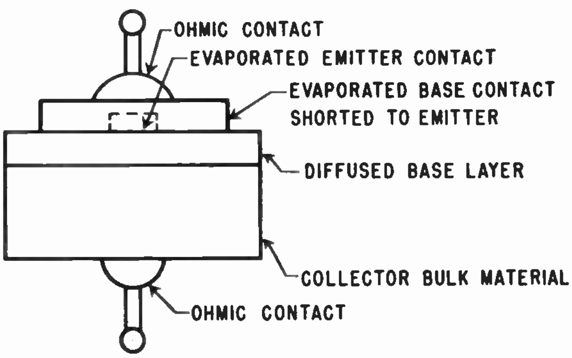

Fig. 3—Cross section of negative-resistance diode consisting of avalanche transistor with base shorted to emitter (typical realization).

DC Characteristics

The negative resistance of avalanche transistors has been studied intensively.[4] Our analysis, based on Fig. 4, will therefore be restricted to aspects not yet discussed in these references. To analyze the high-frequency small-signal behavior we must first establish a dc operating point by means of the following simultaneous equations:

$$I = I_C' = -I_E - I_B \tag{21}$$

$$V = V_{CE} = V_C - V_E \tag{22}$$

$$I_C' = I_C M \tag{23}$$

$$M = 1/[1 - (V_C/V_{BD})^m] \tag{24}$$

$$I_B = V_E/r_B' \tag{25}$$

$$r_B' \equiv 1/g_B' = r_{BO}' W_O/W \tag{26}$$

$$W = W_O[1 - (V_C/V_{PT})^{1/2}], \tag{27}$$

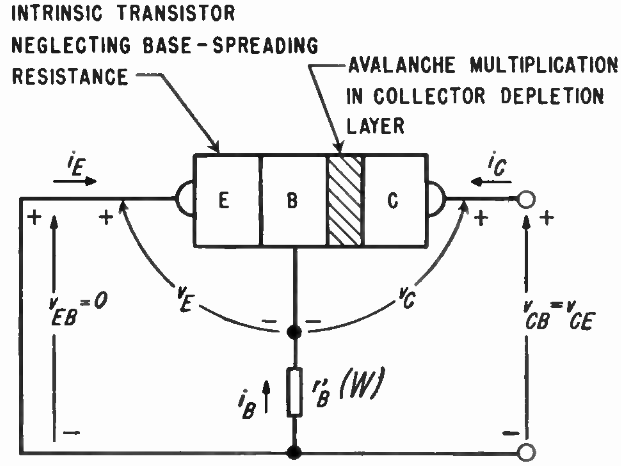

Fig. 4—On the analysis of an avalanche transistor with base shorted to emitter.

where (for the *n-p-n* diode discussed below) the dc diffusion currents, I_E and I_C, are given by (79), (82)–(84), (87) and (88), and the other notation is explained in the List of Symbols.

Fig. 5 shows the dc V/I characteristics of several such typical structures, the design parameters for which are given in the legend. The characteristic quantities of the dc curves are: the peak voltage, V_P; the value, V_∞, to which the voltage drops for $i \to \infty$; and the current value at which the negative resistance region starts. An inspection of the underlying equations together with Fig. 5 and approximate calculations shows that:

1) The peak voltage V_P is close to the breakdown voltage V_{BD} or the punch-through voltage V_{PT}, depending on which value is lower;

2) V_∞ is approximately given by

$$V_\infty \simeq V_{BD}(1 - \alpha_\infty)^{1/m}, \tag{28}$$

where m is the exponent in (24) and α_∞ is the applicable high-current value of $\alpha = |I_C/I_E|$;

3) The drop in voltage with increasing current begins approximately where

$$I_B \simeq I_E. \tag{29}$$

I_B must be substituted from (25) and I_E from (79). One may then solve this approximate equation for V_E and I_C. Curves 1, 2, and 3 in Fig. 5 have the same value of breakdown voltage, $V_{BD} = 100$ volts, leading to approximately the same values for V_∞. They differ only by the thickness of the base layer W_O, and therefore of the punch-through voltage, V_{PT}, which is 200, 100 and 70 volts, respectively, leading to a lower value for V_p in Curve 3. One also observes that lower punch-through voltage produces a higher value of r_B' at the peak voltage V_P [see (26) and (27)] which shifts the onset of the negative-resistance region towards lower currents. Curves 4 and 5 are also closely related, and represent structures with a relatively high-frequency response.

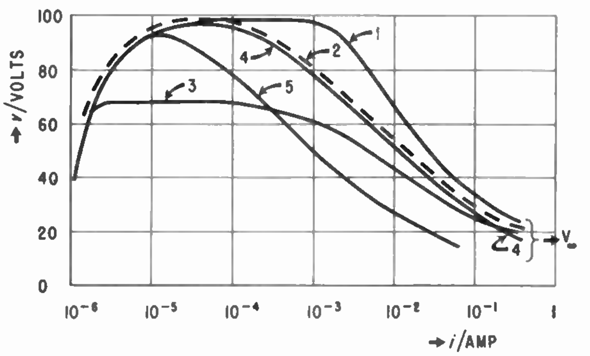

Fixed constants:

Symbol	Units	Value
q	Cb	1.6×10^{-19}
$q/(kT)$	v^{-1}	38.7
m		2.3
ϵ_O	$f\cdot cm^{-1}$	8.854×10^{-14}
κ		12
n_{OE}	cm^{-3}	4.31×10^{18}
p_{OE}	cm^{-3}	5.23×10^{2}
D_{pE}	cm^2s^{-1}	1.59
L_{pE}	cm	9.4×10^{-4}
V_{BD}	v	100
I_{CO}	amp	10^{-6}

Varying parameters:

Symbol	Units	Values in curve no.				
		1	2	3	4	5
W_O	cm	8.06×10^{-4}	5.695×10^{-4}	4.76×10^{-4}	7.55×10^{-5}	same
A	cm^2	10^{-3}	same	same	10^{-5}	same
n_{OB}	cm^{-3}	5.54×10^{4}	same	same	6.25×10^{4}	same
p_{OB}	cm^{-3}	4.06×10^{15}	same	same	3.6×10^{15}	same
p_{OC}	cm^{-3}	5.23×10^{2}	same	same	3.38×10^{5}	same
n_{OC}	cm^{-3}	4.31×10^{18}	same	same	6.67×10^{15}	same
D_{nB}	cm^2s^{-1}	34	same	same	10	same
L_{nB}	cm	2.49×10^{-3}	1.763×10^{-3}	1.475×10^{-3}	3.77×10^{-4}	same
V_{PT}	v	200	100	70	100	same
α_O	—	0.95	same	same	0.98	same
r_{BO}'	ohm	100	same	same	100	1000

Fig. 5—DC characteristics of three-layer avalanche diode with base shorted to emitter (silicon, n-p-n)

The difference between the two curves lies in the value of the base-spreading resistance, r_{BO}', a high value of which leads to a negative-resistance, region at lower currents. A comparison of Curves 2 and 4 shows that the dc characteristics are largely independent of the conducting cross section and of the base thickness, W_O, provided V_{BD} and the voltage-dependence of r_B' (punch-through voltage) are the same.

AC Characteristics

With the base shorted to the emitter, the small-signal high-frequency admittance between emitter and collector contact is described by y_{22e} (common-emitter short-circuit output admittance), which we must calculate taking into account the base-spreading resistance and avalanche multiplication.[6] We find

$$y_{22e} = y_{22b}$$

$$= \frac{My_{22,\text{diff}}' + I_C(\partial M/\partial v_C) + j\omega C_c + r_B'\Delta_M{}^{y'}}{1 + r_B'\sum y_M'}, \qquad (30)$$

[6] Gärtner, *Ibid.*, p. 207.

where

$$\Delta_M{}^{y'} = (y_{11,\text{diff}}' + j\omega C_e)[My_{22,\text{diff}}' + I_C(\partial M/\partial v_C) + j\omega C_c] - My_{12,\text{diff}}'y_{21,\text{diff}}' \qquad (31)$$

and

$$\sum y_M' = y_{11,\text{diff}}' + j\omega C_e + y_{12,\text{diff}}' + My_{21,\text{diff}}' + My_{22,\text{diff}}' + I_C(\partial M/\partial v_C) + j\omega C_c. \qquad (32)$$

Rather than use the complicated expressions for the diffusion admittances,[5] we shall base the high-frequency analysis on the customary equivalent circuit of Fig. 13 where we must make only the changes indicated in Fig. 6(a).

We find

$$y_{22e} = g_{22e} + jb_{22e}, \qquad (33)$$

where

$$g_{22e} = (AC + BD)/(A^2 + B^2) \qquad (34)$$

and

$$b_{22e} = (AD - BC)/(A^2 + B^2) \qquad (35)$$

with

$$A = g_e'(1 - a_O M) + g_B' + Mg_c + I_C(\partial M/\partial v_C) - (\omega^2/\omega_a)(C_e + C_e' + C_c) \qquad (36)$$

$$B = \omega\{(1/\omega_a)[g_e' + g_B' + Mg_c + I_C(\partial M/\partial v_C)] + C_e'(1 - a_O M) + C_e + C_c\} \qquad (37)$$

$$C = [Mg_c + I_C(\partial M/\partial v_C)][g_e' + g_B' - (\omega^2/\omega_a)(C_e + C_e')] - \omega^2 C_c[(g_e' + g_B')/\omega_a + C_e' + C_e] \qquad (38)$$

$$D = \omega\{[Mg_c + I_C(\partial M/\partial v_C)][(g_e' + g_B')/\omega_a + C_e' + C_e] + C_c[g_e' + g_B' - (\omega^2/\omega_a)(C_e' + C_e)]\}. \qquad (39)$$

The various symbols are defined in the Appendix and in (21)–(27). $\partial M/\partial v_C$ and $\partial w/\partial v_C$ are calculated from (24) and (27) [replacing W and V_C in (27) by w and v_C]. The multiplication factor M and its derivatives have been considered frequency-independent, which may not be a valid assumption at very high frequencies.

Fig. 6(b) shows the equivalent circuit of the negative-resistance diode (base shorted to emitter) which is a direct consequence of the transistor-equivalent circuit in Fig. 6(a).

Figs. 7(a) and 7(b) (next page) give the real and imaginary parts of the diode impedance $1/y_{22e}$ for a typical high-frequency structure (Curve 4 in Fig. 5) plotted vs operating point $I_C = I$, with the frequency as the curve parameter.

One observes that the negative resistance prevails up to relatively high frequencies and with additional modifications in the structure may reach the microwave range. The diode inductance persists even beyond the range where the diode exhibits a negative resistance; however, it is then no longer constant but is approxi-

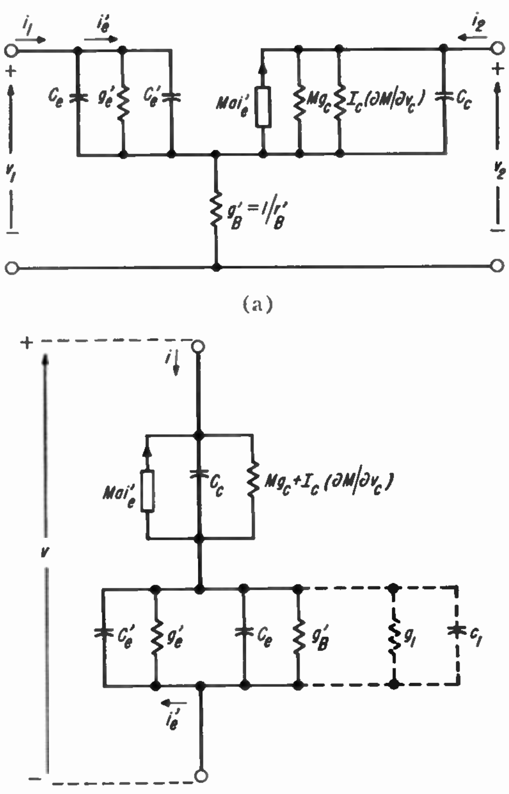

Fig. 6—(a) Common-base high-frequency equivalent circuit for avalanche transistor. (b) High-frequency equivalent circuit of negative-resistance diode consisting of avalanche transistor with base shorted to emitter.

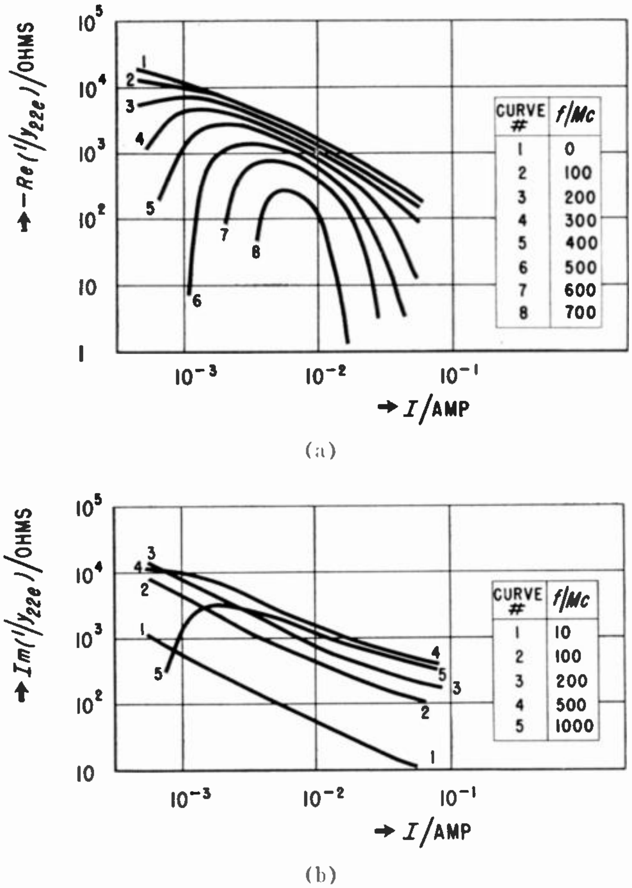

Fig. 7—Real and imaginery parts of small-signal diode impedance, $1/y_{22e}$, at various frequencies as a function of dc bias current, I. The design parameters are those of Curve 4 in Fig. 5.

mately proportional to $1/f$. Because of the complicated nature of the underlying equations, there are no simple design rules to achieve high-frequency response. Typically, one finds that the quantity A in (33)–(36) is always negative, B is always positive, C is positive at low frequencies and becomes negative at high frequencies (which removes the negative resistance), and D is positive as long as $\omega < \omega_a$. By a comparison of the magnitude of the individual terms in typical numerical calculations, it becomes apparent that for high-frequency operation ω_a should be very large (small W), g_e' should be large (negative resistance at high currents, therefore small r_B'), and C_e, C_c should be very small.

Avalanche Transistor with Base Open and Emitter Efficiency Increasing with Current

Miller and Ebers[4] have already pointed out that a negative-resistance diode may be obtained from an avalanche transistor whose base is open-circuited, and whose emitter efficiency increases with emitter current. Various mechanisms are conceivable which will yield this increase in emitter efficiency. We shall concentrate in the following analysis on a structure in which the base region has a higher doping than the emitter region (opposite to the usual situation in transistors), so that the emitter efficiency will increase with increasing injection level.

To simplify the analysis, we shall base it on the diffusion equation only, rather than also take into account the electric fields which arise at high injection levels.[7] We shall find its solution under the boundary conditions for large injection into emitter and base regions. The following are for an n-p-n transistor:[8]

$$p_{1E} = \frac{p_{0E}e^{-qV_E/(kT)} - p_{0E}\left(\frac{n_{0B}}{p_{0B}}\right)e^{-2qV_E/(kT)}}{1 - \frac{p_{0E}n_{0B}}{n_{0E}p_{0B}}e^{-2qV_E/(kT)}}, \tag{40}$$

and

$$n_{1B} = \frac{n_{0B}e^{-qV_E/(kT)} - n_{0B}\left(\frac{p_{0E}}{n_{0E}}\right)e^{-2qV_E/(kT)}}{1 - \frac{p_{0E}n_{0B}}{n_{0E}p_{0B}}e^{-2qV_E/(kT)}}, \tag{41}$$

[7] W. M. Webster, "On the variation of junction-transistor current amplification factor with emitter current," Proc. IRE, vol. 42, pp. 914–920; June, 1954.
E. S. Rittner, "Extension of the theory of the junction transistor," *Phys. Rev.*, vol. 94, pp. 1161–1171; June, 1954.
T. Misawa, "Emitter efficiency of junction transistor," *J. Phys. Soc. Japan*, vol. 10, pp. 362–367; May, 1955.
[8] W. W. Gärtner, *op. cit.*, see Eqs. (4.25a) and (4.26a), on p. 81.

where p_{1E} is the hole density in the emitter at the emitter junction and n_{1B} is the electron density in the base at the emitter junction.

DC Characteristics.

We thus obtain the following expressions for the direct currents at the emitter and collector junctions:

$$I_E = -I = -qA\big[(D_{nB}/L_{nB})(n_{10B} - n_{0B})\coth(W/L_{nB}) - (D_{nB}/L_{nB})(n_{20B} - n_{0B})\operatorname{csch}(W/L_{nB}) - (D_{pE}/L_{pE})(p_{10E} - p_{0E})\big] \quad (42)$$

$$I_C = I = MqA\big[(D_{nB}/L_{nB})(n_{10B} - n_{0B})\operatorname{csch}(W/L_{nB}) - (D_{nB}/L_{nB})(n_{20B} - n_{0B})\coth(W/L_{nB}) - (D_{pC}/L_{pC})(p_{20C} - p_{0C})\big], \quad (43)$$

where n_{10B} is the dc electron density in the base region at the emitter junction, obtained from (41) by setting $v_E = V_E$; p_{10E} is the dc hole density in the emitter at the emitter junction, obtained from (40) by setting $v_E = V_E$; n_{20B} and p_{20C} are the respective minority carrier densities at the collector junction, which may be set equal to zero under reverse-bias conditions.

Eqs. (40)–(43) together with (24), (27) and

$$V = V_C - V_E, \quad (44)$$

determine the dc V-vs-I characteristic of the diode for which typical examples have been plotted in Fig. 8. When the punch-through voltage is high, the peak voltage V_P is given approximately by

$$V_P \simeq V_{BD}(1 - \alpha_0)^{1/m}, \quad (45)$$

where α_0 denotes the dc current amplification at low current levels, as given approximately by

$$\alpha_0 = \big[\cosh(W/L_{nB}) - (D_{pE}/D_{nB})(L_{nB}/L_{pE})\sinh(W/L_{nB})(p_{0E}/n_{0B})\big]^{-1}. \quad (46)$$

Thus, the peak voltage increases for decreasing α_0. Curve 1 in Fig. 8 has the lowest V_P, because W_0/L_{pE} is small and n_{0B} is large. Curves 2–4 illustrate how V_P can be raised by increasing W_0/L_{pE} and/or decreasing n_{0B}.

The voltage V_∞ for high currents is again given by (28), where, however, the high-current α_∞ has a different algebraic form than in the previous case, and is approximately given by

$$\alpha_\infty = \big[\cosh(W/L_{nB}) + (D_{pE}/D_{nB})(L_{nB}/L_{pE})\sinh(W/L_{nB})\big]^{-1}. \quad (47)$$

One observes that V_∞ is independent of doping level in emitter and base regions, so that Curves 2 and 3 in Fig. 8 have the same V_∞. In Curve 1, V_∞ is smaller because

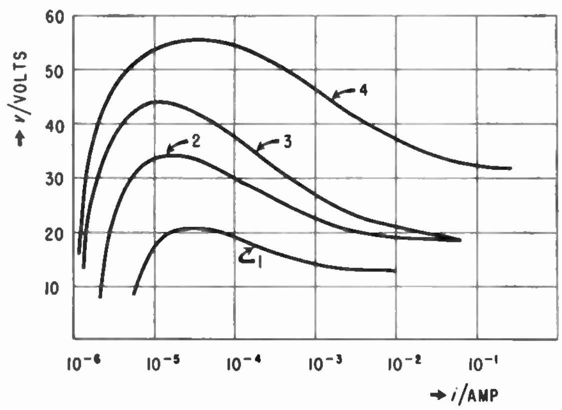

Fixed constants:

Symbol	Units	Value
q	Cb	1.6×10^{-19}
$q/(kT)$	v^{-1}	38.7
m	—	2.3
ϵ_0	$f\cdot cm^{-1}$	8.854×10^{-14}
κ	—	12
n_{0E}	cm^{-3}	1.25×10^{15}
p_{0E}	cm^{-3}	1.8×10^{6}
D_{pE}	cm^2s^{-1}	11.2
V_{BD}	v	60.86
I_{C0}	amp	10^{-6}
A	cm^2	10^{-5}
p_{0C}	cm^{-3}	5×10^{5}
n_{0C}	cm^{-3}	4.46×10^{15}
D_{pC}	cm^2s^{-1}	11
D_{nB}	cm^2s^{-1}	16.4

Varying Parameters:

Symbol	Units	Values in curve No. 1	2	3	4
W_0	cm	3×10^{-4}	same	same	10^{-4}
p_{0B}	cm^{-3}	1.56×10^{16}	same	5×10^{16}	same
n_{0B}	cm^{-3}	1.44×10^{5}	same	4.5×10^{4}	same
L_{nB}	cm	1.8×10^{-3}	same	same	1.8×10^{-4}
L_{pE}	cm	7.5×10^{-3}	2.4×10^{-3}	same	2.4×10^{-4}

Fig. 8—DC characteristics of three-layer avalanche diode with base open and higher-doped than emitter region (silicon, n-p-n).

W_0/L_{pE} is smaller than in Curves 2 and 3; in Curve 4, V_∞ is bigger because this ratio is larger.

The current I_P at which the peak voltage V_P is observed is subject to various conflicting influences: Large α_0, *i.e.*, large n_{0B} and small W/L_{pE}, shift I_P to the right; small n_{0B}/W and high L_{pE} shift it to the left. This explains the relative position of the maxima in Fig. 8. The latter condition (small n_{0B}/W, high L_{pE} for low I_p) is derived by considering the current at which the emitter efficiency begins to increase, causing a negative resistance. This will occur approximately where the minority-carrier density injected into the emitter region becomes comparable to the majority-carrier density there. Thus, from (42), with $p_{10E} \simeq n_{0E}$, we have

$$I \simeq qAn_{0E}\big[2(n_{0B}/p_{0E})(D_{nB}/L_{nB})\coth(W/L_{nB}) - D_{pE}/L_{pE}\big]. \quad (48)$$

AC Characteristics

The small-signal high-frequency admittance of the diode is given by the h_{22e} of the corresponding transistor structure, as follows:

$$h_{22e} = \{(\bar{y}_{11,\mathrm{diff}} + j\omega C_e)[M\bar{y}_{22,\mathrm{diff}} + I_C(\partial M/\partial v_C) + j\omega C_c] - M\bar{y}_{12,\mathrm{diff}}\bar{y}_{21,\mathrm{diff}}\}\{\bar{y}_{11,\mathrm{diff}} + j\omega C_e + \bar{y}_{12,\mathrm{diff}} + M\bar{y}_{21,\mathrm{diff}} + M\bar{y}_{22,\mathrm{diff}} + I_C(\partial M/\partial v_C) + j\omega C_c\}^{-1} \quad (49)$$

where the $\bar{y}_{ik,\mathrm{diff}}$ describe the diffusion effects. The expressions for the diffusion admittances of the ordinary transistor, however, cannot be used here because they are derived under small-injection boundary conditions. Rather, we must solve the time-dependent diffusion equation under linearized large-injection boundary conditions. For small ac voltages, v_e, v_c, superimposed on the dc voltages, V_E, V_C,

$$v_E = V_E + v_e \quad (50)$$

and

$$v_C = V_C + v_c. \quad (51)$$

The large-injection boundary conditions (40) and (41) may be linearized by the customary series expansion to give

$$p_{1E} \simeq p_{1OE} + p_1'v_e \quad (52)$$

where

$$p_1' \equiv (\partial p_{1E}/\partial v_E)_{v_E=V_E}$$
$$= -\frac{q}{kT}\, p_{OE}e^{-qV_E/(kT)}\{1 + (2n_{OB}/p_{OB})e^{-qV_E/(kT)} + [p_{OE}n_{OB}/(n_{OE}p_{OB})]e^{-2qV_E/(kT)}\} \cdot\{1 - [p_{OE}n_{OB}/(n_{OE}p_{OB})]e^{-2qV_E/(kT)}\}^{-2} \quad (53)$$

and

$$n_{1B} \simeq n_{1OB} + n_1'v_e, \quad (54)$$

where

$$n_1' \equiv (\partial n_{1B}/\partial v_E)_{v_E=V_E}$$
$$= -\frac{q}{kT}\, n_{OB}e^{-qV_E/(kT)}\{1 + (2p_{OE}/n_{OE})e^{-qV_E/(kT)} + [p_{OE}n_{OB}/(n_{OE}p_{OB})]e^{-2qV_E/(kT)}\} \cdot\{1 - [p_{OE}n_{OB}/(n_{OE}p_{OB})]e^{-2qV_E/(kT)}\}^{-2}. \quad (55)$$

Solving the time-dependent diffusion equations under these boundary conditions finally yields the following expressions for the diffusion admittances, including the effect of the bias-current dependent emitter efficiency:

$$\bar{y}_{11,\mathrm{diff}} = -Aqn_1'(D_{nB}/L_{nB})(1 + j\omega\tau_{nB})^{1/2} \cdot\coth[(W/L_{nB})(1 + j\omega\tau_{nB})^{1/2}] - Aqp_1'(1 + j\omega\tau_{pE})^{1/2}(D_{pE}/L_{pE}) \quad (56)$$

$$\bar{y}_{12,\mathrm{diff}} = Aq(D_{nB}/L_{nB}^2)[(n_{1OB} - n_{OB})\,\mathrm{csch}\,(W/L_{nB}) + n_{OB}\coth(W/L_{nB})] \times(\partial w/\partial v_C)(1 + j\omega\tau_{nB})^{1/2} \cdot\mathrm{csch}\,[(W/L_{nB})(1 + j\omega\tau_{nB})^{1/2}] \quad (57)$$

$$\bar{y}_{21,\mathrm{diff}} = Aqn_1'(D_{nB}/L_{nB})(1 + j\omega\tau_{nB})^{1/2} \cdot\mathrm{csch}\,[(W/L_{nB})(1 + j\omega\tau_{nB})^{1/2}] \quad (58)$$

$$\bar{y}_{22,\mathrm{diff}} = -Aq(D_{nB}/L_{nB}^2)[(n_{1OB} - n_{OB})\,\mathrm{csch}\,(W/L_{nB}) + n_{OB}\coth(W/L_{nB})] \times(\partial w/\partial v_C)(1 + j\omega\tau_{nB})^{1/2} \cdot\coth[(W/L_{nB})(1 + j\omega\tau_{nB})^{1/2}]. \quad (59)$$

Fig. 9 shows a plot of the real and imaginary parts of h_{22e} as a function of operating point I, as calculated from (49) and (56)–(59). The design parameters are the same as for Curve 4 in Fig. 8. Again one observes that the negative resistance is constant over a wide frequency range and then vanishes rapidly as the cutoff frequency is approached. The imaginary part is again

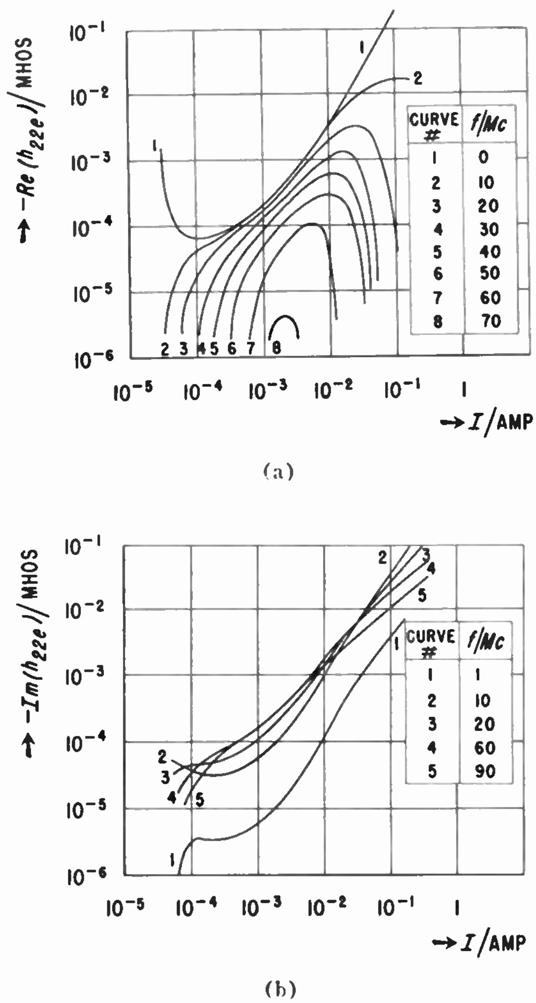

Fig. 9—Real and imaginary parts of small-signal diode admittance, h_{22e}, at various frequencies as a function of dc bias current. The design parameters are those of Curve 4 in Fig. 8.

inductive, and the inductance becomes frequency dependent in the neighborhood of the cutoff frequency.

An analysis shows that the appearance of a small-signal negative resistance depends on a value of

$$|h_{21b}| > 1, \tag{60}$$

which at low frequencies is achieved by avalanche multiplication. At high frequencies (and M constant for a given operating point), the emitter efficiency drops because of the increase in the term

$$-Aqp_1'\sqrt{D_{pE}}(1/\tau_{pE} + j\omega)^{1/2}, \tag{61}$$

in $\bar{y}_{11,\text{diff}}$ (56), reducing h_{21b} below unity. To achieve high-frequency response, it is therefore necessary to make the lifetime in the emitter region as small as possible. To preserve the general shape of the dc characteristics, one must also reduce the base width W. The ultimate frequency limit of these devices thus depends on the technological control of small dimensions (in one direction).

Ordinary Transistor with Field-Enhanced Diffusion in Collector Region

It is well known that transistors with high-resistivity collector bodies exhibit a negative resistance between emitter and collector. This effect has been explained by Early[5] as a modulation by the collector current of the minority-carrier current from collector to base. The modulation mechanism is the enhancement of minority-carrier diffusion in the collector towards the collector junction, by the electric field produced by the total collector current. The effect may be observed experimentally in grown-junction, diffused-base and *p-n-i-p* units with high collector resistivity, often only at elevated temperatures.

Let us assume that a dc operating point has been established in such a transistor (see Fig. 10), and that through suitable blocking no ac is allowed to pass through the base lead, so that as far as ac is concerned, we are dealing with a *diode* only.

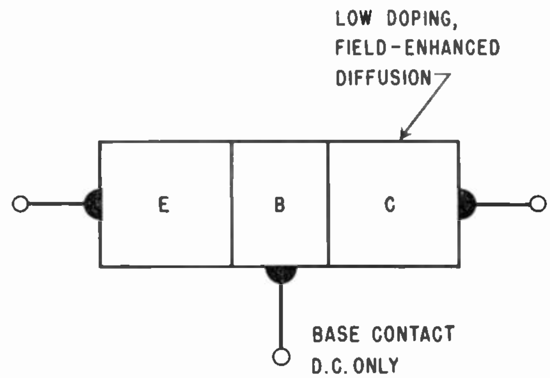

Fig. 10—Ordinary transistor with field-enhanced diffusion in collector region ("collector multiplication"). AC-wise the device is operated as a diode between emitter and collector.

With the base-contact open-circuited for ac, the small-signal admittance between emitter and collector leads is given by h_{22e} (open-circuit output admittance in common-emitter configuration). Expressing h_{22e} in terms of the common-base four-pole parameters, one may show rigorously that this admittance is given by

$$h_{22e} = \frac{y_{11b}'y_{22b}' - y_{12b}'y_{21b}'}{y_{11b}' + y_{12b}' + y_{21b}' + y_{22b}'}, \tag{62}$$

where the y_{ikb}' are the common-base intrinsic "diffusion" admittances $y_{ik,\text{diff}}'$ including the junction capacitances.[5] One notices that h_{22e} is not affected by the magnitude of the base-spreading impedance z_B', which is intuitively plausible. The frequency-dependence of the admittance, in which we are interested here, will therefore be independent of the base-spreading resistance, and the geometry of the device may be optimized for short transit times.

Early[5] has derived the influence of field-enhanced diffusion in the collector region on the small-signal four-pole parameters of a transistor. $y_{11b}' = y_{11,\text{diff}}' - j\omega C_e$ (C_e being the emitter junction capacitance), and $y_{12b}' = y_{12,\text{diff}}'$, are unaffected, whereas the new y_{21b}' and y_{22b}' are given by

$$y_{21b}' = y_{21,\text{diff}}\alpha_C \tag{63}$$

and

$$y_{22b}' = (y_{22,\text{diff}}' + j\omega C_c)\alpha_C, \tag{64}$$

where α_C has been called the "collector-multiplication" factor and is equal to

$$\alpha_C = 1/(1 - \beta_C), \tag{65}$$

where for an *n-p-n* transistor,

$$\beta_C = \frac{p_{0C}qD_{pC}\mu_{pC}\rho_C}{j\omega}[B + (B^2 + L_{pC}^{-2})^{1/2}] \cdot [(B^2 + L_{pC}^{-2} + j\omega/D_{pC})^{1/2} - (B^2 - L_{pC}^{-2})^{1/2}] \tag{66a}$$

and

$$B = \mu_{pC}\rho_C J_C(2D_{pC}). \tag{66b}$$

Fig. 11 shows the real and imaginary parts of α_C as a function of collector current, assuming typical design parameters. The curve parameters are diffusion length in the collector region and frequency. This diffusion length, which affects the frequency response, also enters the expression for the collector reverse current I_{pC}, which is given in (88). If a certain value of L_{pC} is chosen in a design, one must verify through (88) that the reverse current is not prohibitively high (causing heating and possible destruction of the device).

Instead of basing the computations of the frequency dependence of h_{22e} on the complete and complicated expressions for the diffusion admittances, one may obtain a much simpler estimate by using the equivalent circuit for transistors, as shown in Fig. 13. Its four-pole pa-

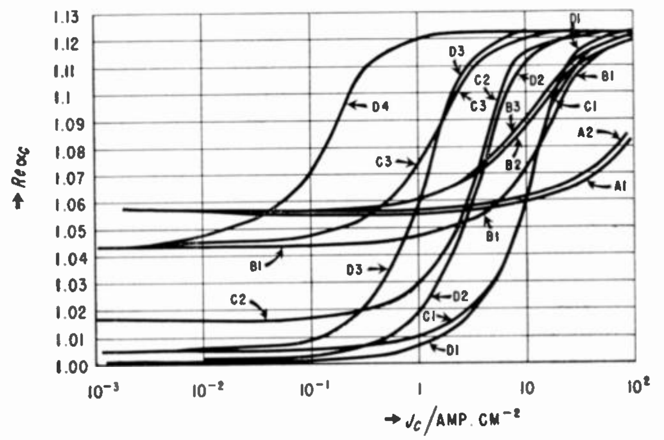

(a)

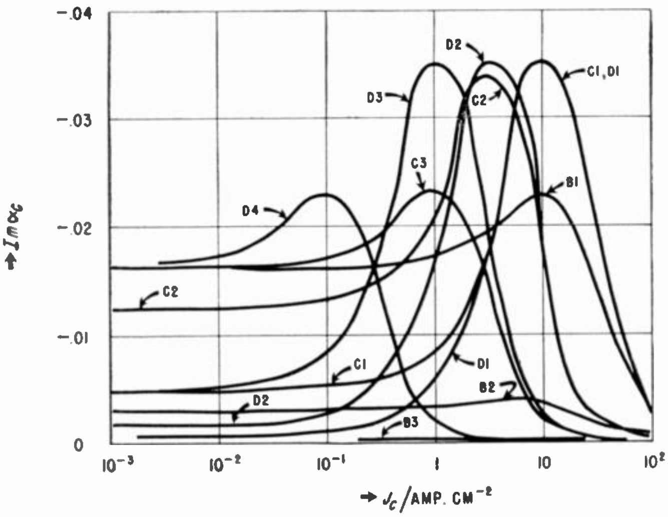

(b)

Curve No.	L_{pc}^{-1}/cm^{-1}	ω/sec^{-1}
A1	10^5	10^{10}
A2	10^5	10^9
B1	10^4	10^{10}
B2	10^4	10^9
B3	10^4	10^8
C1	10^3	10^{10}
C2	10^3	10^9
C3	10^3	10^8
D1	10^2	10^{10}
D2	10^2	10^9
D3	10^2	10^8
D4	10^2	10^6

Fig. 11—(a) Real and (b) imaginary parts of "collector multiplication factor" α_c in typical n-p-n germanium transistor with field-enhanced diffusion in the collector region. Parameters: $\rho_C = 29.7$ ohm.cm, $p_{0c} = 1.2 \times 10^{13}$ cm^{-3}, $\mu_{pc} = 1900$ cm$^2 \cdot v^{-1} \cdot$sec^{-1}, $D_{pC} = 49.4$ cm$^2 \cdot$sec^{-1}. (The imaginary parts of Curves A1 and A2 lie below that of B3)

rameters for negligible "collector multiplication" are given by (91)–(94). To take the field-enhanced diffusion into account, we need only to multiply y_{21}'' and y_{22}'' by α_c and we finally obtain

$$h_{22} = \frac{\alpha_c(g_c + j\omega C_c)(g_c' + j\omega C_c' + j\omega C_e)}{(1 - \alpha_c a)(g_c' + j\omega C_c') + j\omega C_e + \alpha_c(g_c + j\omega C_c)}. \quad (67)$$

Under the assumptions that

$$|\alpha_C - 1| \ll 1, \quad (68)$$

$$C_e \ll C_c', C_c \quad (69)$$

and

$$|(g_c + j\omega C_c)/(g_c' + j\omega C_c')| \ll |1 - \alpha_c a|, \quad (70)$$

one finds the approximate expression

$$h_{22e} \simeq (g_c + j\omega C_c)/(1 - \alpha_c a). \quad (71)$$

When the series resistance r_c' of the collector body cannot be neglected, as may the be case for a thick high-resistivity collector region, the following expression for the modified open-circuit output-admittance, $\bar{h}_{22e}$, must be used:

$$\bar{h}_{22e} = h_{22e}/(1 + r_c' h_{22e}), \quad (72)$$

where h_{22e} is given by (71) or (62).

For the purpose of discussing the high-frequency operation of the Early diode, we assume that the quantity a in (71) is real, *i.e.*, that the base width is very thin, and thus the alpha-cutoff frequency is very high. Then, from (71), one finds the real part of h_{22e} to be equal to

$$\text{Re } h_{22e} = \frac{g_c(1 - a \text{ Re } \alpha_c) - \omega C_c a \text{ Im } \alpha_c}{(1 - a \text{ Re } \alpha_c)^2 + (a \text{ Im } \alpha_c)^2}. \quad (73)$$

From (73) it is obvious that for Re h_{22e} to be negative at high frequencies, $g_c (>0)$ should be large, $0 < a < 1$ should be high, C_c should be small, Re α_c (>0) should be large, and Im $\alpha_c (<0)$ should be small. The novel feature in the frequency dependence of the Early diode, as compared to that of the ordinary transistor, thus lies in the frequency dependence of α_c as shown in Figs. 11(a) and 11(b). Since

$$\text{Re } \alpha_c \simeq 1 + \text{Re } \beta_c \quad (74)$$

and

$$\text{Im } \alpha_c \simeq -\text{Im } \beta_c, \quad (75)$$

these curves are best understood by considering the frequency and current dependence of β_C.

Eq. (66) indicates that β_c is an increasing function of current density. The high-current limit $\beta_c°$ of β_c is independent of frequency and diffusion length L_{pc} in the collector region. For low current density, Re β_c also reaches a limit which, however, does depend on ω and L_{pC} except in the case of $\omega \to 0$, when it becomes independent of L_{pC} and equal to $\beta_C°/2$. For $\omega>0$, the low-current limit of Re β_C is always smaller than $\beta_C°/2$. The change from low-current β_C to high-current β_C occurs where the following conditions are satisfied:

$$B^2 = \left(\frac{\mu_{pC}\rho_C J_C}{2D_{pC}}\right)^2 \geq \frac{\omega}{D_{pC}} \tag{76}$$

and

$$B \geq 1/L_{pC}. \tag{77}$$

These relations are shown schematically in Fig. 12(a). Small values of L_{pC} and high frequencies require high values of collector current to bring about an increase in Re β_C and Re α_C. On the other hand, the low-current limit of Re α_C at high frequencies is highest for small L_{pC}.

Since β_C always approaches a real value $\beta_C°$ at high current densities, the imaginary part of α_C vanishes at high currents. At low current densities, Im α_C reaches a limit which depends on L_{pC} and ω, and which may be estimated from the following expression:

$$\lim_{J_C\to 0} \beta_C = \frac{\beta_C°}{j\omega}\frac{1}{L_{pC}}\left[\left(\frac{1}{L_{pC}^2} - \frac{j\omega}{D_{pC}}\right)^{1/2} - \frac{1}{L_{pC}}\right] \tag{78}$$

For $\omega\to 0$, one obtains $\beta_C=\beta_C°/2$ and for $\omega\to\infty$, one finds $\beta_C=0$, *i.e.*, the low-current value of Im α_C is equal to zero in both cases, and reaches a maximum at some finite frequency, as indicated in Fig. 12(b). Depending on whether one operates on the left or right of the maximum in Fig. 12(b), the low-current limit of Im α_C will increase or decrease with frequency. Examples for both cases are shown in Fig. 11(b).

One observes from Figs. 11 and 12 that the large values of Re α_C and small values of Im α_C necessary for high-frequency operation are obtained by high current densities and short diffusion lengths in the collector region.

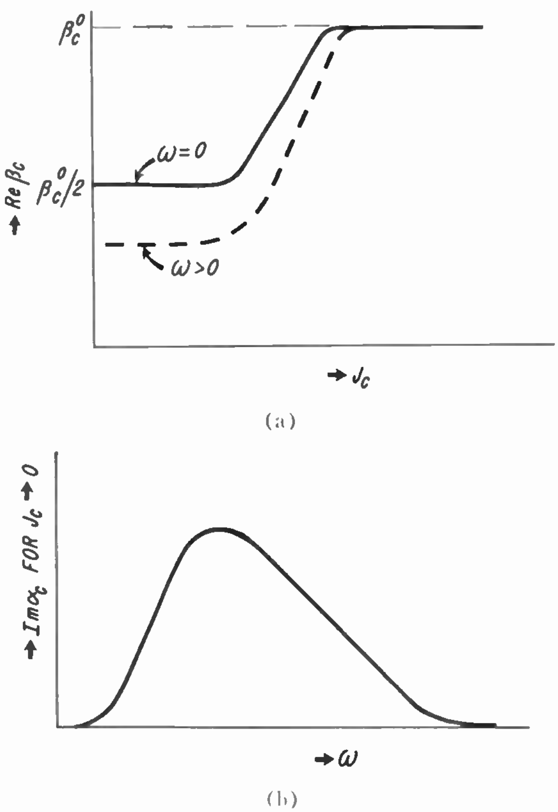

Fig. 12—(a) Schematic on the current and frequency dependence of Re β_C. (b) Schematic on the frequency dependence of the low-current value of Im α_C.

Other Three-Layer Negative-Resistance Diodes

In addition to the structures discussed in detail above, there are several others which also involve an increase in current gain a, with current due to field-enhanced diffusion in the collector region ("collector multiplication"). These shall be the subject of future quantitative investigations; we mention here only the underlying mechanisms:

1) A combination of field-enhanced diffusion in the collector region, relatively high I_{CO}, and an increase of the transport factor across the base with increasing applied voltage. The latter effect usually comes about as the collector depletion layer spreads into the base region.

2) A combination of field-enhanced diffusion in the collector region, constant transport factor, and I_{CO} increasing with collector voltage (due to the proximity of the ohmic collector contact and depletion-layer widening into the collector region and/or by approaching punch-through in the base region).

3) A combination of field-enhanced diffusion in the collector region and avalanche multiplication.

The approach to the analysis of these structures is analogous to that used earlier in this paper.

Circuit Applications

The conceivable circuit applications of the devices discussed in this paper are numerous and will be the subject of separate investigations and publications when such negative-resistance and inductance diodes have been built and are being used in exploratory circuitry; here we will give a list of the more important applications:

1) Oscillators, amplifiers, frequency converters, monostable and bistable switching elements analogous to those extensively discussed in recent months in connection with tunnel diodes.

2) Variable Q-multipliers realizing electronically tunable bandwidth of tank circuits.[9]

[9] M. Schuller and W. W. Gärtner, "Inductive elements for solid-state circuits," *Electronics*, vol. 33, pp. 60–61; April, 1960.

3) Solid-state inductances replacing coils in miniature circuitry.[9] These will usually be electronically tunable.

4) Parametric microwave amplifiers using the nonlinear inductance of the diode. The variable inductance may be self-oscillating or externally pumped.

5) Parametric microwave amplifiers using the nonlinear variable junction capacitance of an oscillating negative-resistance diode.

6) Distributed negative-resistance structures for microwave amplification.

Conclusions

The paper has shown that combinations of effects in three-layer semiconductor diodes may lead to a large number of different negative-resistance and inductive devices with a large range of interesting circuit applications. The analysis given for a few typical cases has illustrated a general approach to the design problem, and has shown that operating frequency, component values ($-R$ and L) and voltage and current swings lie in the range of major circuit interest.

On the other hand, many additional questions remain to be answered even on the structures analyzed in this paper. What are the highest frequencies at which negative resistances and high-Q inductances may be realized? What are the optimized geometries in this respect, given a minimum dimension realizable by state-of-the-art technology? What dc to ac efficiency can be realized with such structures, particularly in comparison with transistors and tunnel diodes? To answer the last question for switching applications, it may be necessary to develop a large-signal high-frequency circuit theory for these devices, as has recently been done for tunnel diodes.[10]

In addition, one might develop a considerably more accurate large-signal high-frequency device design theory based on the direct electronic-computer solution of the nonlinear differential equations underlying carrier motion in semiconductors.

Some of the effects described in this paper may occur in ordinary transistors and may explain observations incompatible with simple transistor design theory. Among these are oscillations and amplification at very high frequencies, possibly beyond the cutoff frequency of the transistor involved. Amplification in particular could be accomplished by the variable emitter or collector capacitance of a transistor oscillating as a three-layer negative-resistance diode, or by the transistor operating as a negative-resistance amplifier.

[10] M. Schuller and W. W. Gärtner, "Large-signal high-frequency circuit theory for negative-resistance diodes, in particular tunnel diodes," presented at AIEE Winter Meeting, New York, N. Y., January 30, 1961.

Appendix

Reference Material

This Appendix consists of generally-known formulas and diagrams, and a list of symbols on which the derivations in this paper are based.

DC Current-Voltage Relationships

$$I_E = I_{nE} + I_{pE}. \tag{79}$$

For p-n-p transistor (small-injection diffusion currents only):

$$I_{nE} = AqD_{nE}n_{0E}(e^{qV_E/(kT)} - 1)/L_E \tag{80}$$

$$I_{pE} = -Aq\frac{D_{pB}p_{0B}}{L_B}\left[\frac{e^{qV_C/(kT)} - 1 - (e^{qV_E/(kT)} - 1)\cosh(W/L_B)}{\sinh(W/L_B)}\right] \tag{81}$$

For n-p-n transistor (small-injection diffusion currents only):

$$I_{nE} = +Aq\frac{D_{nB}n_{0B}}{L_B}\cdot\left[\frac{e^{-qV_C/(kT)} - 1 - (e^{-qV_E/(kT)} - 1)\cosh(W/L_B)}{\sinh(W/L_B)}\right] \tag{82}$$

$$I_{pE} = -AqD_{pE}p_{0E}(e^{-qV_E/(kT)} - 1)/L_E \tag{83}$$

$$I_C = I_{nC} + I_{pC}(+I_{CO}). \tag{84}$$

I_{CO} is approximately equal to the *measured* collector current for open-circuited emitter and is added as an empirical quantity, since the calculated theoretical value is frequently unrealistically small. The value for I_{CO} assumed in the numerical calculations is given in the legends of Figs. 5 and 8.

For p-n-p transistor (small-injection diffusion currents only):

$$I_{nC} = AqD_{nC}n_{0C}(e^{qV_C/(kT)} - 1)/L_C. \tag{85}$$

$$I_{pC} = Aq\frac{D_{pB}p_{0B}}{L_B}\cdot\left[\frac{(e^{qV_C/(kT)} - 1)\cosh(W/L_B) - (e^{qV_E/(kT)} - 1)}{\sinh(W/L_B)}\right]. \tag{86}$$

For n-p-n transistor (small-injection diffusion currents only):

$$I_{nC} = -Aq\frac{D_{nB}n_{0B}}{L_B}\cdot\left[\frac{(e^{-qV_C/(kT)} - 1)\cosh(W/L_B) - (e^{-qV_E/(kT)} - 1)}{\sinh(W/L_B)}\right]. \tag{87}$$

$$I_{pC} = -AqD_{pC}p_{0C}(e^{-qV_C/(kT)} - 1)/L_C. \tag{88}$$

Junction breakdown voltage V_{BD}:

The junction breakdown voltage as a function of impurity density and thus of resistivity may be determined from empirical graphs such as the ones given in McKay and McAfee, and others.[11]

Punch-through voltage V_{PT} (collector step junction):

$$p\text{-}n\text{-}p: \quad V_{PT} = \frac{q}{2\kappa\epsilon_0} W_0^2 \frac{n_{0B}(p_{0C} + n_{0B})}{p_{0C}} \tag{89}$$

$$n\text{-}p\text{-}n: \quad V_{PT} = \frac{q}{2\kappa\epsilon_0} W_0^2 \frac{p_{0B}(n_{0C} + p_{0B})}{n_{0C}}. \tag{90}$$

Four-Pole Admittance for the Equivalent Circuit in Fig. 13.

Four-pole admittances for $z_B' = 0$ (approximations to

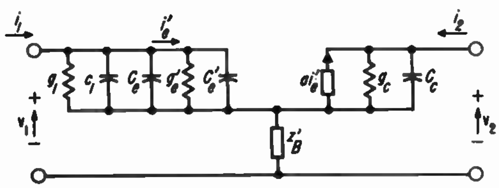

Fig. 13—Common-base high-frequency equivalent circuit for junction transistor with no avalanche multiplication.

diffusion admittances plus junction capacitances):

$$y_{11}'' = g_e' + j\omega C_e' + j\omega C_e + g_1 + j\omega c_1 \tag{91}$$

$$y_{12}'' = 0 \tag{92}$$

$$y_{21}'' = -a(g_e' + j\omega C_e') \tag{93}$$

$$y_{22}'' = g_c + j\omega C_c \tag{94}$$

$$\Delta^{y''} = y_{11}'' y_{22}'' \tag{95}$$

$$g_e' = q|I_E|/(kT) \tag{96}$$

[11] K. G. McKay and K. B. McAfee, "Electron multiplication in silicon and germanium," *Phys. Rev.*, vol. 91, pp. 1079–1084; September, 1953.
K. G. McKay, "Avalanche breakdown in silicon," *Phys. Rev.*, vol. 94, pp. 877–884; May, 1954.
S. L. Miller, "Avalanche breakdown in germanium," *Phys. Rev.*, vol. 99, pp. 1234–1241; August, 1955.
W. W. Gärtner, *op. cit.*, chs. 3.H and 4.D, pp. 65–89.

$$C_e' = 0.81 g_e'/\omega_a \tag{97}$$

$$g_c = a_0 |I_E| (W/L_B^2) |\partial w/\partial v_C| \tag{98}$$

$$a = a_0 e^{-j(0.2)\omega/\omega_a}/(1 + j\omega/\omega_a)$$

$$\simeq a_0/(1 + j\omega/\omega_a). \tag{99}$$

g_1, c_1:

$$p\text{-}n\text{-}p: \quad g_1 = Aqn_{10E}D_{nE}/L_{nE} \tag{100}$$

$$c_1 = g_1 \tau_{nE}/2 \tag{101}$$

$$n\text{-}p\text{-}n: \quad g_1 = Aqp_{10E}D_{pE}/L_{pE} \tag{102}$$

$$c_1 = g_1 \tau_{pE}/2. \tag{103}$$

g_1 and c_1 describe the emitter efficiency of the transistor, and may be neglected in the analysis unless indicated otherwise.

ω_a:

$$p\text{-}n\text{-}p: \quad \omega_a = 2.43 D_{pB}/W^2 \tag{104}$$

$$n\text{-}p\text{-}n: \quad \omega_a = 2.43 D_{nB}/W^2 \tag{105}$$

$$C_e = A\left[\frac{\kappa\epsilon_0 q}{2} \frac{p_{0B} n_{0E}}{p_{0B} + n_{0E}}\right]^{1/2} \frac{1}{\sqrt{|V_{EQ} - V_E|}}$$

$$V_{EQ} = \frac{kT}{q} \ln \frac{p_{0B}}{p_{0E}} \tag{107}$$

$$C_c = A\left[\frac{\kappa\epsilon_0 q}{2} \frac{p_{0B} n_{0C}}{p_{0B} + n_{0C}}\right]^{1/2} \frac{1}{\sqrt{V_C}}. \tag{108}$$

Four-pole impedances for $z_B' \neq 0$:

$$z_{11}'' = y_{22}'/\Delta^{y''} + z_B' \tag{109}$$

$$z_{12}'' = z_B' \tag{110}$$

$$z_{21}'' = -y_{21}''/\Delta^{y''} + z_B' \tag{111}$$

$$z_{22}'' = y_{11}''/\Delta^{y''} + z_B'. \tag{112}$$

ACKNOWLEDGMENT

The authors would like to thank Dr. W. Shockley for the interesting discussion in which he first brought their attention to the theoretical aspects of the subject, and J. Armstrong of the United States Army Signal Research and Development Laboratory, Fort Monmouth, N. J., for having carried out all numerical computations.

A Low-Noise *X*-Band Radiometer Using Maser*

J. J. COOK†, L. G. CROSS†, M. E. BAIR†, MEMBER, IRE, AND R. W. TERHUNE†

Summary—**A low-noise *X*-band radiometer, using a ruby maser preamplifier in radio astronomy measurements, is discussed. The radiometer uses a reflection-cavity maser with voltage-gain bandwidth products as high as 300 Mc at 4.2°K. Less than 1 per cent short-term gain instability and dependable performance are obtained. A system noise factor (excluding antenna spillover) of 0.6 db (43°K) has been obtained. The system bandwidth is limited to 8 Mc by the intermediate frequency bandwidth, with maser bandwidths of 20–30 Mc available. RMS noise fluctuations of approximately 0.01°K with a 12-second integration time and 0.007°K with a 42-second integration time are obtained. Gain instability of 0.6 per cent up to 10 minutes and 2 per cent up to 30 minutes has been measured. Electrical and mechanical features as well as measurement and operational techniques are described. Performance data and radio astronomy observations are discussed.**

I. Introduction

THE first successful operation of a ruby maser amplifier at Willow Run Laboratories of the University of Michigan on December 20, 1957[1] stimulated interest in many fields. Since this initial operation, the number of research and development programs in masers and maser systems has greatly increased. Among these programs is the development of reliable, low-noise systems for both active and passive astronomical applications. The system to be described is a modified Dicke system,[2] *X*-band radiometer specifically designed for use in a long-term radio astronomy research program. It is presently operating on The University of Michigan's 85-foot-diameter radiotelescope (Fig. 1).

The radiometer utilizes a four-level ruby maser preamplifier[3] operating at 8.72 Gc.[4] The maser gain is typically 20–23 db with a voltage-gain bandwidth product of 200 Mc at 4.2°K. Maser bandwidths to 30 Mc and voltage-gain bandwidths to 550 Mc at 4.2°K have been obtained. An equivalent system input temperature of approximately 75°K, including about 30°K caused by antenna spillover and backlobes, has been observed. The remaining 45±5°K results from input-guide noise and a superheterodyne receiver with a noise figure of 9.5 db (including all noise resulting from components following the maser preamplifier). The input-guide

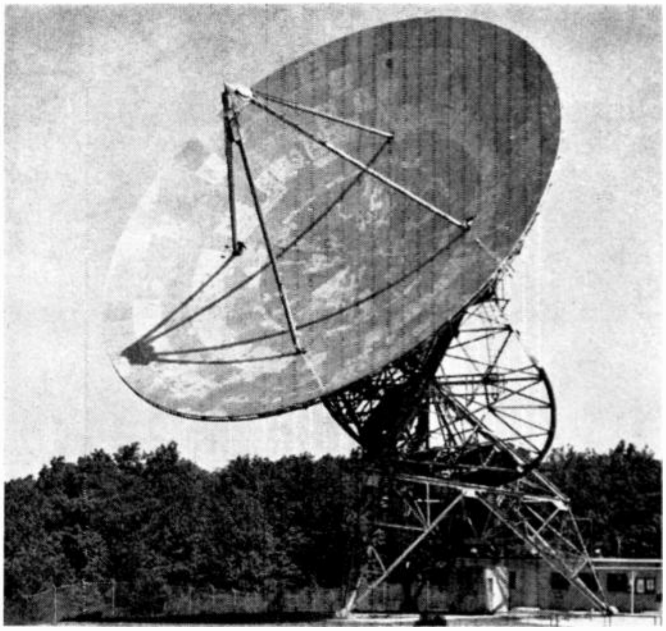

(a)

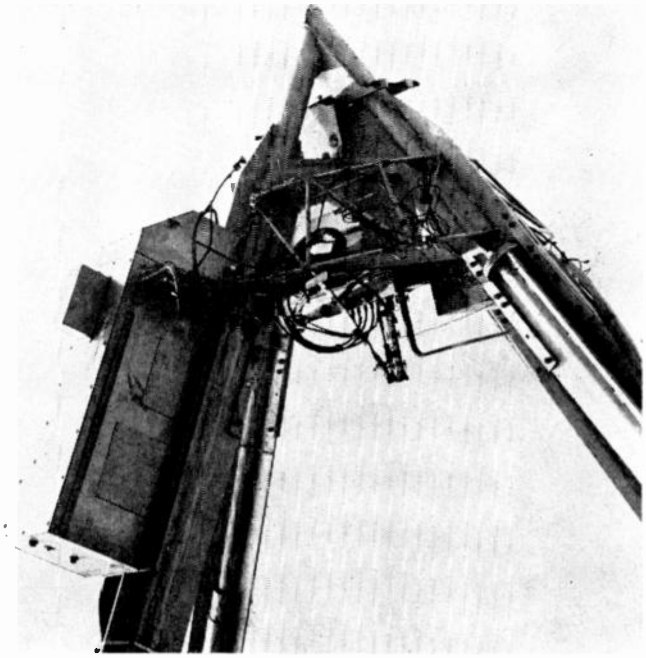

(b)

Fig. 1—(a) The University of Michigan's 85-foot diameter radio telescope. (b) Detail showing mounting arrangement of packaged maser system, as well as other 2- and 3-cm receivers.

* Received by the IRE, August 31, 1960; revised manuscript received, December 12, 1960. This work was conducted by Project MICHIGAN under Dept. of the Army Contract (DA-36-039-7801) administered by the U. S. Army Signal Corps.

† Willow Run Labs., University of Mich., Ann Arbor.

[1] G. Makhov, C. Kikuchi, J. Lambe, and R. W. Terhune, "Maser action in ruby," *Phys. Rev.*, vol. 109, p. 1399; February, 1958.

[2] R. H. Dicke, "Measurement of thermal radiation at microwave frequencies," *Rev. Sci. Inst.*, vol. 17, p. 268; July, 1946.

[3] C. Kikuchi, J. Lambe, G. Makhov, and R. W. Terhune, "Ruby as a maser material," *J. Appl. Phys.*, vol. 30, p. 1061; July, 1959.

[4] Throughout this paper Gc is used in conformance to the National Bureau of Standard's newly adopted prefixes as recommended by the International Committee on Weights and Measures, accordingly, Gc replaces the former kMc designation.

noise is intended to include all loss noise as well as cavity-wall radiation and spontaneous emission. The system contribution of 45°K was obtained with a maser gain of 23 db and bath temperature of 4.2°K.

The development program was initiated in the fall of 1958 and, following a six-month testing and reliability study on a six-foot van-mounted antenna, was concluded in January, 1960. The system was installed on January 29, 1960 and successfully received the first extraterrestrial radiation on the same day.

II. System Components and Characteristics

A. Physical Description

The radiometer system is shown in simplified block form in Fig. 2. All components to the left of the dashed line are mounted at the apex of the 85-foot antenna and, with the exception of the input guide, are housed in a single weatherproof package, approximately one foot square and four feet long (Fig. 3). The package weighs approximately 250 lbs. The necessary electrical connection into the equipment house is through a system of 20 individually shielded weatherproof cables which are 285 feet long. All electrical power to the antenna-mounted components is dc, a precautionary measure to prevent possible pick-up into signal lines.

The mounting arrangement, along the outside of one of the feed supports, is shown in Fig. 1(b). This position allows the mounting of several other receivers inside the "cone." The dewar orientation is such that the entire antenna positioning range is permissible with a maximum angle, dewar axis to the vertical, of 67°. Refrigerant transfer is accomplished at the apex mount, and no disassembly is required. Maser performance is such that it is unnecessary to reduce the bath temperature, and all performance data are taken at 4.2°K.

B. The Microwave System

The microwave system consists of two major subdivisions: K-band pump (18–26 Gc) and X-band signal (8.2–12.4 Gc).

The K-band pump power is provided by either of two klystrons: the Varian VA 96B or the Raytheon 2K33. The primary requirement of the pump tube is that it provide sufficient power to saturate the ruby crystal. The klystron is housed in its own case to allow forced-air cooling. A ferrite isolator and variable attenuator follow the klystron. The variable attenuator is used to check the degree of saturation. If a 1- or 2-db loss in the pump line causes no maser-gain change, the saturation is sufficient. A 20-db coupler and crystal mount allow monitoring of the pump signal. The remaining system consists of standard bends and straight sections.

The X-band system includes a signal-input line and a comparison-signal line. The Dicke system switching, between the two inputs, is accomplished with a switchable, four-port ferrite circulator. Direct current measurements, in an unmatched system, indicate insertion losses of 0.20 ± 0.05 db and isolations of greater than 25 db. A second (nonswitchable) circulator provides the necessary isolation for a reflection-cavity maser. The input path of this device has a measured insertion loss of 0.12 ± 0.05 db. An additional 0.10-db loss arises from the silver-plated input guide. The total line loss is about 0.45 db.

The amplified maser signal feeds into a balanced mixer using 1N23EMR crystals. Local-oscillator power is provided by a stabilized microwave generator with a 10-mw output. Long-term frequency drift is 1 part in 10^6. An electronically controlled variable attenuator and ferrite isolator complete the local-oscillator line.

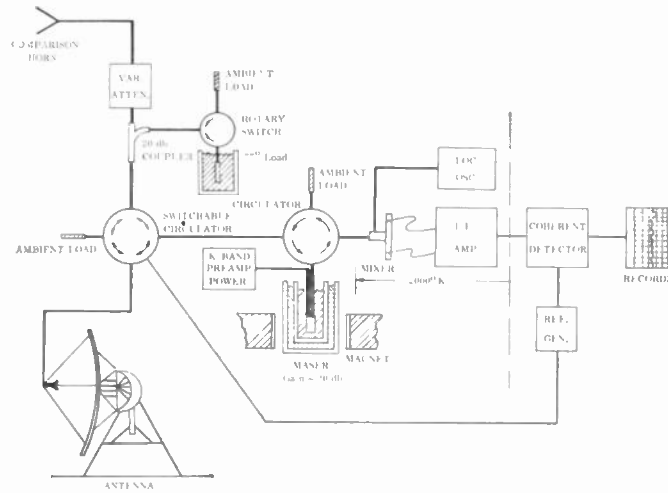

Fig. 2—Basic block diagram of maser radiometer. All equipment to left of dashed line (except input waveguide) is mounted in a single weather-proof package.

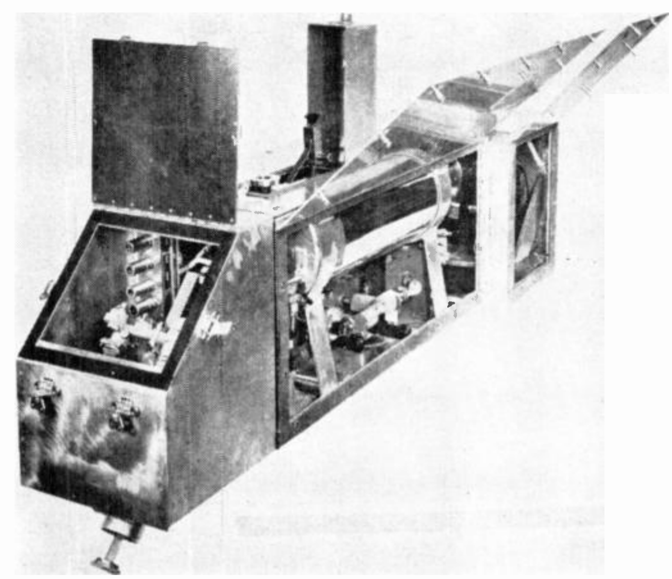

Fig. 3—Packaged maser radiometer showing service openings. The complete unit is approximately one foot square and four feet long. It weighs about 250 pounds.

Three methods of obtaining the necessary comparison signal have been used. First, a wide-beam horn pointed away from the antenna at "cold sky" receives an average sky-signal temperature of about 10–20°K. Its disadvantages are its obvious dependence upon antenna position and its insensitivity to atmospheric conditions. As the antenna is moved, varying amounts of ground radiation affect the switching temperature. Its wide-beam averaging effect makes the comparison horn somewhat insensitive to atmospheric changes, while the narrow antenna beam is not. This also has a variable effect upon the switching temperature.

A second method utilizes a cooled microwave termination of sufficient loss to provide approximate black-body radiation. In liquid helium, this can theoretically produce a comparison signal of 4–5°K. Commercial waveguide terminations are not suitable as the absorption characteristics are drastically reduced at liquid-helium temperature. One method, presently under investigation, is the use of a broad-band, matched, dielectrically loaded cavity.

A third method of obtaining a comparison signal is the so-called "double-horn technique." In this scheme, two identical horns are pointed at the antenna surface. By placing these horns a few inches apart, rather large beam separation is possible. In this manner, one can compare two signals originating at discrete points in the sky. Preliminary tests of this technique indicate there is essentially no balancing problem. The two horns see essentially the same spillover and backlobe radiation; therefore, their temperature balance becomes almost independent of antenna motion. Although the narrow beams are quite susceptible to atmospheric changes, such as clouds, etc., their relatively close proximity results in similar effects in each arm.[5]

Regardless of the source of the comparison signal, some device to "balance-out" the two inputs is necessary. This is accomplished with a remotely controlled 0 to 0.3-db attenuator in each line. Physically, a tiny strip of resistance card is inserted into either input as needed. These give a total equivalent-noise-input tuning range of approximately 16°K in each arm.

Calibration of the system is accomplished with two matched waveguide loads, one at ambient temperature and the other in liquid nitrogen. These loads are attached to the two input ports of a rotary, three-port, waveguide switch. The output port feeds, through a 20-db coupler, into the comparison arm. The system is balanced with the switch to ambient; a change to liquid nitrogen produces a signal equivalent to an antenna temperature increase of

$$T_{\text{test}} = 0.01[T_{\text{ambient}} - T_{77,\text{eff}}] \tag{1}$$

where $T_{77,\text{eff}}$ is the temperature equivalent of the liquid nitrogen load, at the switch input.

The cavity assembly (discussed more fully in connection with the maser preamp.) uses a silver-plated ruby cavity.[6] This design yields dependable, stable performance with voltage-gain bandwidth products of over 200 Mc. It has shown experimentally the possibility of products up to 550 Mc.

Closely associated with the waveguide system is the magnet-dewar assembly. The magnet is a permanent alnico magnet having a $1\frac{1}{2}$-inch gap and a field strength of 3850 gauss. Coils are provided to vary the field ± 150 gauss. The dewar tip is narrowed to fit into the gap of the externally mounted magnet. Refrigerant capacities are 3.4 and 8.1 liters for liquid helium and liquid nitrogen, respectively. These amounts evaporate completely in about 36 hours in a vertical, stationary dewar; however, during operation a maximum of 17 hours has been obtained.

A liquid-helium level indicator has been provided to allow continuous monitoring of the refrigerant level. The device consists of five carbon resistors spaced at various points along the cavity-assembly waveguide.

C. Associated Electronics

The balanced mixer output is amplified by a 30-Mc amplifier before it leaves the antenna mount. The preamplifier has a bandwidth of 8 Mc, a gain of 30 db, and a noise figure of 1.9 db. The postamplifier has a bandwidth of 10 Mc and a gain of 60 db. The IF output is fed into a selective amplifier and a synchronous detector system. The synchronous detector output is displayed on a recorder. All dc supplies are regulated to at least 1 per cent and a few millivolts ripple. The switchable circulator is driven by a square wave input at 90 cps with a 60-microsecond rise time.

III. The Maser Preamplifier

A. Gain-Bandwidth Requirements

The performance requirements of the preamplifier are determined by the characteristics of the receiver system in which it is used. If we define

- $T_i \equiv$ the total input-noise temperature including contributions from sky, antenna, input guide, and preamplifier;
- $G \equiv$ power gain of the preamplifier; $\Delta\nu_M =$ bandwidth of the preamplifier;

[5] Concerning the authors' "double-horn technique," see also: M. E. Bair, J. J. Cook, L. G. Cross, and C. B. Arnold, "Recent developments and observations with a ruby maser radiometer," IRE Trans. on Antennas and Propagation, vol. AP-9, pp. 43–49; January, 1961.

This method of comparison has been used successfully in the recent detection of radio radiation from the planet Saturn: J. J. Cook, L. G. Cross, M. E. Bair, and C. B. Arnold, "Radio detection of the planet Saturn," *Nature* (Letters to the Editor), vol. 188, p. 393; October, 1960.

Also in the detection of the first radio radiation from a planetary Nebula: A. H. Barrett, W. E. Howard, F. T. Haddock, J. J. Cook, L. G. Cross, and M. E. Bair, "Measurement of Microwave Radiation at λ3.45 cm from the Planetary Nebula NGC6543," paper presented at the American Astronomical Soc. Meeting, New York, N. Y.; December 28–31, 1960. Further investigation into the use of the "double-horn technique" will be reported as soon as possible.

[6] L. G. Cross, "Silvered ruby maser cavity," *J. Appl. Phys.*, vol. 30, No. 9, p. 1459; 1959.

$T_R \equiv$ noise temperature of one sideband of the receiver; and

$\Delta\nu_R \equiv$ the bandwidth of one sideband of the receiver,

then the effective input temperature is just

$$(T_{IN})_{\text{eff}} = T_i + T_R\left[(G-1)\frac{\Delta\nu_M}{2\Delta\nu_R} + 1\right]^{-1}. \tag{2}$$

This applies only when $\Delta\nu_M \leqq \Delta\nu_R$. Since in our system $\Delta\nu_M$ was always greater than $\Delta\nu_R$ and $G \gg 1$, (2) can be replaced by the simplier expression:

$$(T_{IN})_{\text{eff}} = T_i + \frac{2T_R}{G}. \tag{3}$$

and the figure of merit for the whole system for any given integration time, τ, is

$$\text{Fig. of merit} = F = \frac{2}{\pi}\sqrt{\tau}\,\Delta T_{\text{RMS}} = \frac{T_i}{\sqrt{\Delta\nu_S}} + \frac{2T_{R,G}}{\sqrt{\Delta\nu_S}} \tag{4}$$

where $\Delta\nu_S$ is the net bandwidth of the system and ΔT_{RMS} is the rms value of the system noise output, °K. If $\Delta\nu_S$ was limited by $\Delta\nu_M$ only, where $\Delta\nu_R = \Delta\nu_M$, then minimizing F for any given gain-bandwidth relation would determine the optimum values of G and $\Delta\nu_M$.

For our preamplifier, the following relation applies

$$G^{1/4}\Delta\nu_M \cong C_0 \tag{5}$$

where C_0 is a constant of the maser material. This shall be discussed in Section III, B. Solving then for the optimum gain, with $\Delta\nu_S$ limited only by $\Delta\nu_M$:

$$\text{Optimum } G = 14\frac{T_R}{T_i}. \tag{6}$$

A typical value of C_0 is 70 Mc, corresponding to a voltage gain-bandwidth product, at 20-db gain, of ~ 220. Using $T_R \sim 1000$°K and $T \sim 50$°K, one would obtain the optimum values $G = 24.5$ db and $\Delta\nu_M = 17.1$ Mc.

However, this optimum point is not at all critical. Fig. 4 shows a plot of F vs preamplifier gain, and it is seen that a wide variation of G with little change in sensitivity is possible. For this reason, G is always chosen to be a little low (20–23 db) to reduce gain instability, and $\Delta\nu_M$ is always more than sufficient to cover the 8-Mc band-pass of the superheterodyne receiver.

B. Theory of Operation

The preamplifier is a reflection-type, resonant-coupled cavity maser using 0.1 per cent ruby at the double-pump operation point ($\theta \cong 54°$). The gain and bandwidth relations for a single-cavity amplifier using nonresonant coupling are just

$$G_0^{1/2} = \frac{\Delta\nu_C + \Delta\nu_m'}{\Delta\nu_C - |\Delta\nu_m'|} \tag{7}$$

$$\Delta\nu_S = \Delta\nu_C - |\Delta\nu_m'| \tag{8}$$

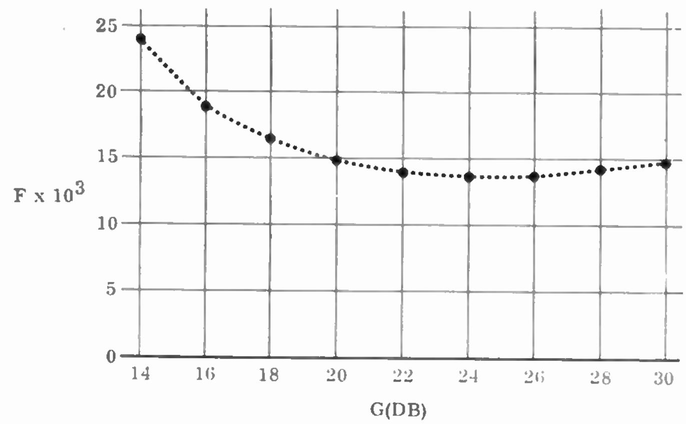

Fig. 4—Plot of radiometer figure of merit vs preamplifier gain for a 2000°K receiver and 50°K input temperature.

where G_0 is the center gain at the resonant frequency, ν_0, $\Delta\nu_S$ is the $\frac{1}{2}$ power bandwidth, $\Delta\nu_C$ is the coupling bandwidth, and $\Delta\nu_m'$ is the effective magnetic bandwidth. That is,[7]

$$\Delta\nu_C = \frac{\nu_0}{Q_C} \quad Q_C = \text{external or coupling } Q\text{, and} \tag{9}$$

$$\Delta\nu_m' = \Delta\nu_L + \Delta\nu_m \tag{10}$$

where

$$\Delta\nu_L = \frac{\nu_0}{Q_L} \quad Q_L = \text{unloaded or loss } Q \tag{11}$$

$$\Delta\nu_m = \frac{\nu_0}{Q_m} \quad Q_m = \text{magnetic } Q. \tag{12}$$

If one introduces a resonant cavity in front of the maser cavity, the center gain equation is essentially unchanged, functionally; but the bandwidth characteristics are greatly altered. The two resonances will tend to push each other in frequency and the typical double-humped response is obtained, as shown in Fig. 5. The separation of the humps $\Delta\nu_k$ is related to the coupling coefficient k between the two cavities as given by

$$\Delta\nu_k = \nu_0 k. \tag{13}$$

By analyzing a simple equivalent circuit one can obtain the above characteristics and show that the voltage gain bandwidth product is not a constant, but is proportional to $G^{1/4}$; *i.e.*, for high gains

$$(G^{1/2} - 1)\Delta\nu_S \cong 2\Delta\nu_m G^{1/4} \tag{14}$$

or

$$G^{1/4}\Delta\nu_S \cong 2\Delta\nu_m. \tag{15}$$

This dependence has been experimentally verified on this preamplifier over a range of 20–40 db, the voltage-

[7] Here the external and unloaded Q's have the conventional definition in terms of the electromagnetic field, and Q_m is defined in (21).

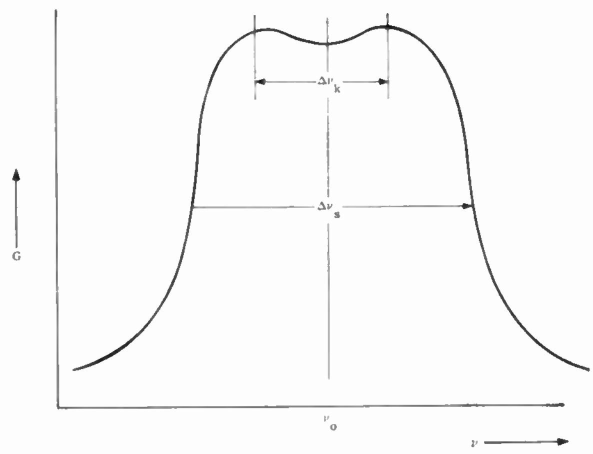

Fig. 5—Gain vs frequency response for the resonant coupled maser cavity.

gain bandwidth product ranging from 200 to 550 Mc.

As stated before, however, the gain instability at high gains has prevented the practical use of gains greater than ~30 db. The gain instability in the high-gain approximation is given by

$$\frac{\delta G}{G} = G^{1/2}\frac{\delta x}{x} \tag{16}$$

where x may be $\Delta\nu_m$, $\Delta\nu_c$ or VSWR. At a gain of 30 db, for instance, $G^{1/2} \cong 32$; hence any variation in the coupling magnetic Q or the VSWR in the waveguide will be amplified by a factor of 32.

The negative magnetic Q obtained is ~200, giving a negative magnetic bandwidth at 8.7 Gc of ~40 Mc under optimum conditions. However, in operation $|\Delta\nu_m'|$ is somewhat less because of the magnetic gain control which is discussed in Section III-C.

The theoretical negative magnetic Q may be obtained from the dynamics of the four-level spin system which determine the paramagnetic properties of ruby. The Zeeman splitting of the ground state of Cr^{+++} in Al_2O_3 shows a symmetry when the angle θ between the applied magnetic field and the crystalline axis is

$$\theta = \arc\cos\frac{1}{\sqrt{3}} \sim 54.7°. \tag{17}$$

The diagram of the energy level vs the magnetic field is shown in Fig. 6(a). Everywhere $\nu_{13}=\nu_{24}$ and $\nu_{12}=\nu_{34}$ and, at $H=3850$ gauss, $\nu_{23}\cong 8.7$ Gc and $\nu_{13}=\nu_{24}\cong 22.3$ Gc, which is a typical operating point for our preamplifier.

The population distribution of electrons among these levels is dependent on the ambient temperature T, the twelve relaxation probabilities ω_{ij} ($i, j=1$ through 4), and the presence of pump power at frequency $\nu_{13}=\nu_{24}$. In Fig. 6(b) and 6(c), the population of the levels is shown without and with pump saturation, respectively. Without saturation the population ratio of any two levels, i and j, is given by the Boltzmann factor

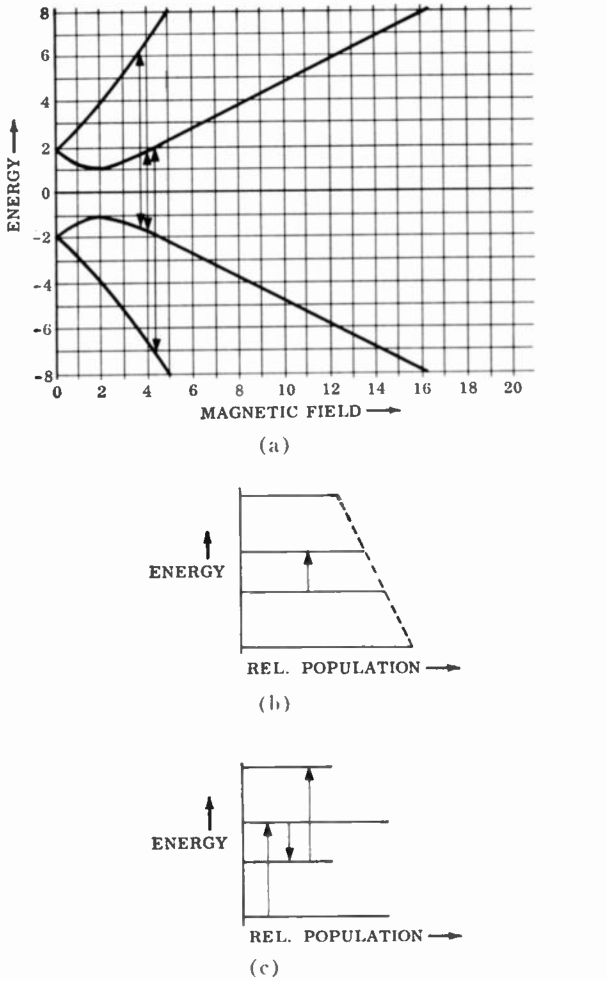

Fig. 6—Electron energy levels in ruby at $\theta=54.7°$ (a) vs magnetic field, (b) at fixed magnetic field without pump, (c) at fixed magnetic field with pump showing electron population changes.

$$\frac{n_i}{n_j} = e^{h\nu_{ij}/kT} \quad \text{where} \quad i > j, \tag{18}$$

but even at 4.2°K, $h\nu \ll kT$ for the frequencies involved, and thus the population difference, in particular for levels 2 and 3, is approximately

$$n_2 - n_3 \cong \frac{N}{4}\frac{h\nu_{23}}{kT}. \tag{19}$$

The power absorbed from the cavity at frequency ν_{23} is given by P_{23},

$$P_{23} = h\nu_{23}(n_2 - n_3)\overline{W}_{23}, \tag{20}$$

and the magnetic Q is given by

$$Q_m = \frac{2\pi\nu_{23}\overline{H_{r-f}^2}}{P_{23}}\frac{V_0}{8\pi} \tag{21}$$

where $\overline{W}_{23}$ is the average transition probability over the ruby, H_{r-f} is the microwave magnetic field, and V_0 is the volume of the cavity. Thus, the functional dependence of the magnetic bandwidth $\Delta\nu_m$ is seen to be

$$\Delta\nu_m = (n_2 - n_3)(h\nu_{23})(f) \tag{22}$$

where f is a rather complex function of the cavity mode configuration and the quantum mechanical transition probability. For our mode configuration and crystal orientation, f is close to its maximum value.

Now, for the case of pump saturation $n_1 = n_3$ and $n_2 = n_4$. The resulting population difference in levels 2 and 3 is:

$$(n_2 - n_3) = \frac{N}{4} \frac{h}{kT} \left[\frac{\nu_{23}\omega_{23} - \nu_{14}\omega_{14} - \nu_{12}\omega_{12} - \nu_{34}\omega_{34}}{\omega_{23} + \omega_{14} + \omega_{12} + \omega_{34}} \right] \quad (23)$$

having a maximum negative value, if $\omega_{14} \gg \omega_{23}, \omega_{12}, \omega_{34}$ of

$$(n_2 - n_3)_{\max} = -\frac{N}{4} \frac{h\nu_{14}}{kT}. \quad (24)$$

A convenient parameter to measure is the inversion factor I defined as the ratio of negative magnetic Q to positive magnetic Q.

$$I = \frac{|n_2 - n_3|_{\text{saturation}}}{|n_2 - n_3|_{\text{ambient}}}. \quad (25)$$

Eqs. (24) and (19) show the maximum value of I to be

$$I_{\max} = \frac{\nu_{14}}{\nu_{23}} \sim 4 \text{ at } \nu_0 = 8.7 \text{ Gc}. \quad (26)$$

I can be easily calculated from the values of the maser gain with pump on and off, G_1 and G_2, respectively.

$$I = \frac{(G_1^{1/2} - 1)(1 + G_2^{1/2})}{(G_1^{1/2} + 1)(1 - G_2^{1/2})}. \quad (27)$$

We have found that $I = 2.3$, which means that ω_{14} does not predominate, at least at $\nu_{23} = 8.7$ Gc.

C. Physical Description

The cavity and assembly are shown in Fig. 7. The active element is a rectangular parallelopiped of silvered ruby. The size of the silvered ruby for 8.7-Gc operation is $0.7'' \times 0.5'' \times 0.27''$, and the signal mode is the (1, 1, 1) mode. In reliability and stability of operation, the silvered-ruby cavity is a significant improvement over the conventional machined-cavity designs that we have investigated. The microwave coupling is provided through slots cut in the silver with a dust cutter which provides a thin stream of air carrying abrasive powder at high velocity. The coupling plate contains a resonant iris operating in a semicoaxial mode because of the insertion of a silver pin. The side of the coupling cavity facing the waveguide is completely open; therefore, it is very heavily coupled to the waveguide. A typical value of $\Delta\nu_C$ for the coupling cavity is 250 Mc.

The cavity and coupling plate are firmly clamped to the waveguide as shown in Fig. 7(a). In this manner, several cavities can be used in the same assembly with a minimum of alteration. The frequency of the coupling cavity is tunable to allow for the change in resonant frequency of the ruby cavity at 4.2°K. This tuning is ac-

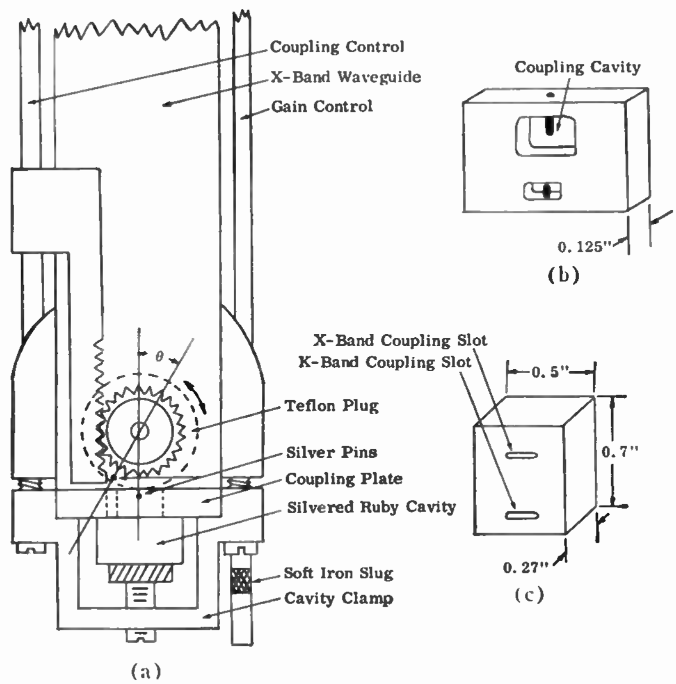

Fig. 7—The maser cavity assembly showing (a) complete assembly, (b) coupling plate containing the coupling cavity, (c) the silvered ruby cavity.

complished by a 5/8-inch diameter, 0.4-inch thick, teflon plug located in the waveguide near the coupling plate. It contains two small pieces of 0.040-inch diameter silver wire. As it is rotated, the silver wire perturbs the resonance field of the coupling cavity and produces a frequency change given by

$$\Delta\nu_0 = 1.2|\cos\theta| \text{ Gc} \quad (28)$$

where θ is as shown in Fig. 7(a). The teflon plug is rotated by means of a rack and pinion arrangement.

The gain of the preamplifier can be varied continuously from 10 to 30 db by the magnetic tuning rod. In this scheme, a small piece (0.125 inch diameter $\times$ 0.150 inch) of soft iron is soldered into a 1/8-inch stainless steel rod which can be moved up and down. As the iron is moved near the cavity, it produces an inhomogeneity in the magnetic field which lowers the magnetic bandwidth $\Delta\nu_m'$ by broadening the resonance line. The gain-control rod is driven by a 1-rpm motor which advances the rod 1/17 inch per minute. This method of gain control is superior to varying the gain by means of the coupling Q since it does not change the cavity or coupling configuration and thus removes a possible source of instability.

Pump energy is coupled in a manner similar to the signal coupling. There is an abundance of cavity modes at the pump frequency, and saturation can usually be obtained in any of them.

Both signal and pump waveguides are filled with Styrafoam to reduce gain instability caused by a fluctuating liquid-helium level.

D. Setup and Operation

In order to obtain double-pump operation, the magnet angle must be very close to 54.7° ($\pm\frac{1}{2}$°). This adjustment must be made when the cavity is changed or other alterations are made. This is accomplished by monitoring the pump transition as the angle is varied. Since the 1–3 transition is stronger than the 2–4 transition, they can be easily differentiated. If the angle is less than 54°, the 1–3 transition will occur at a lower field than the 2–4, and vice versa.

The maser gain is monitored by sweeping the local-oscillator klystron over a 60-Mc range, displaying the receiver output on the y axis and the klystron sweep on the x axis of an oscilloscope. The resulting presentation is the frequency variation of the preamplifier gain, to a resolution of 8 Mc. Fig. 8 shows a typical oscilloscope pattern obtained in this manner. The gain may be calculated if the receiver noise temperature and the input noise temperature are known. If $T_R \gg T_I$, G is given by

$$G = \frac{T_R}{T_I}\left(\frac{R_2}{R_1} - 1\right). \qquad (29)$$

Here R_2 and R_1 are in volts, and the detector is assumed to be operating in the square-law region.

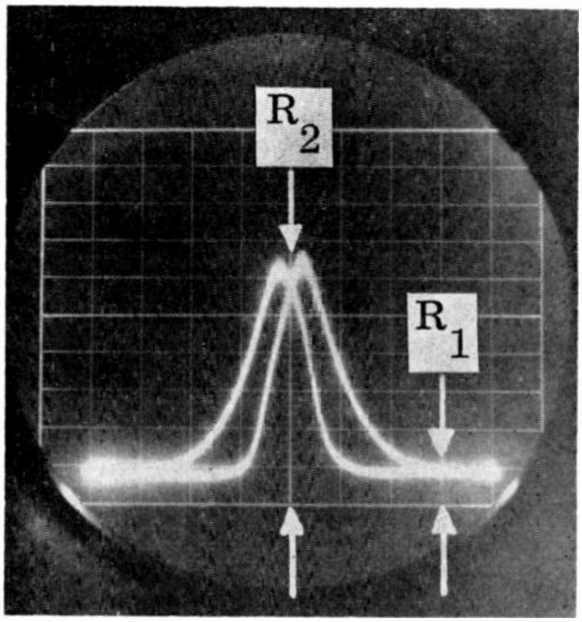

Fig. 8—Noise output of receiver vs local oscillator frequency showing the amplification of the input noise by the maser.

IV. System Performance

A. Threshold Sensitivity

The noise fluctuation, which establishes a lower limit for the sensitivity of a Dicke-system radiometer, arises from internally generated noise and gain instability. The noise contribution of each can be analyzed and their combined rms level taken as a measure of system sensitivity.

If we define a threshold sensitivity, due to internally generated noise, as that signal giving an output equal to the rms noise fluctuations, we get:

$$(\Delta T)_{\text{in}} = \frac{\pi}{2}\frac{(T_{\text{in}})_{\text{eff}}}{\sqrt{\Delta\nu_{ST}}} = \text{rms value of internally generated noise.} \qquad (30)$$

Analysis of the gain-variation effect upon the output signal is an extremely complicated problem. Fluctuations throughout the system can occur from vibration, changes in ambient temperature, line voltages, etc., as well as from spurious changes in the components themselves. Assuming that these gain variations are random, they will have a probability density centered about G_0, and a rapidly decreasing frequency spectrum.[8]

One can presumably modulate at such a frequency rate, (f_{mod}), as to make the contribution of these gain variations small. However, there will still be a gain-instability threshold, caused by a nonzero switching signal, given by:

$$(\Delta T)_{GI} = \alpha(\gamma - 1)(|T_{\text{ant}} - T_{\text{comp}}|)$$
$$= \text{rms value of gain-instability noise.} \qquad (31)$$

where γ = the gain-fluctuation factor $= 1 + (\delta G/G_0)$; $\delta G/G_0$ = percentage gain change. The term α depends upon the detection technique. In the case of synchronous detection, α is a rapidly decreasing function of frequency, centered about $\alpha = 1.0$, for gain variations at the modulation frequency, (f_{mod}).

In addition, very low-frequency gain "drift" will result in output changes which follow the drift. The input noise will be amplified by a varying amount; that is, in effect, the equivalent input temperature of (30) will change with maser gain. This type of drift can generally be removed in data reduction by merely adjusting the base line. The maser radiometer system has been affected only slightly by such low-frequency "drift."

Eq. (31) shows the desirability of keeping the temperature contributions of antenna and comparison source as closely balanced as possible. If there are large signals, or if the system cannot be balanced ($|T_{\text{ant}} - T_{\text{comp}}| > 1°$K), the gain-fluctuation threshold becomes quite large.

Summing the threshold rms noise levels as determined by internally generated noise and gain instability from (30) and (31), the resultant sensitivity threshold becomes

$$(\Delta T)_{\text{rms}} = \frac{\pi}{2}\frac{(T_{\text{in}})_{\text{eff}}}{\sqrt{\Delta\nu_{ST}}} + \alpha(\gamma - 1)(|T_{\text{ant}} - T_{\text{comp}}|). \qquad (32)$$

[8] P. Strum, "Considerations in high sensitivity microwave radiometry," Proc. IRE, vol. 46, pp. 43–53; January, 1958.

B. Noise-Measurement Techniques

The sensitivity threshold of a radiometer has been shown to depend heavily upon the equivalent input temperature. Consequently, it is necessary to develop methods for precise system measurements as well as methods for convenient, approximate measurements.

1) *Precision Noise Measurements:* The circuit for system-noise measurement is shown in Fig. 9. The switchable circulator is dc energized, with the reversing switch thrown to look alternately at T_1 and T_2. The output power level is monitored on a dc microammeter, and the precision 30-Mc attenuator is varied to give an identical output with either T_1 or T_2 as input. If $T_1 > T_2$, we will necessarily add an amount of 30-Mc attenuation (Δ db) when the input is T_1, where:

$$\Delta \text{db} = 10 \log \frac{T_S + T_1}{T_S + T_2} \cdot \tag{33}$$

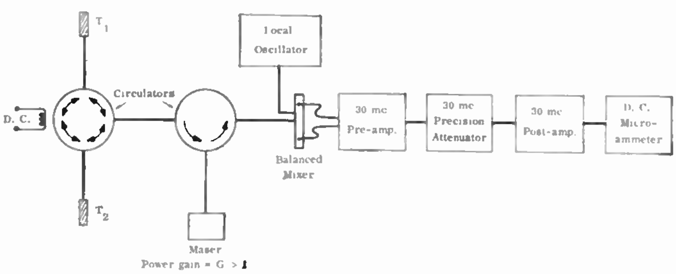

Fig. 9—Block diagram of noise measurement circuit.

In the case of the radiometer system *without maser*, we simply tune the magnetic field off resonance, leaving the system otherwise intact. Since input power of the same level enters the IF amplifiers from both signal and image bands, T_S is one half the excess noise temperature of the receiver and the total equivalent input temperature is $2T_S$.

For the system *with maser*, Δ db is measured as before and T_S obtained from (33). Now, however, input power in the signal band is multiplied by the maser gain (G), whereas the image power is not. T_S is therefore $G/(G+1)$ of the total excess noise temperature of the receiver and to the equivalent input is $T_S(G+1/G)$. Since G is the maser power gain and generally $G \gg 1$, we can quite accurately use a total equivalent input temperature T_S, as given by (33).

2) *Approximate Noise Measurements:* It is advantageous to devise quick checks on system performance which can be made before and during operation. In the case of system-noise temperature, two very convenient approximations have been used. These approximate measurements are adequate for routine checks, and precision methods are required only in special circumstances.

According to (33), the power output ratio between the two input arms is

$$\text{ratio} = \frac{T_S + T_1}{T_S + T_2} = R. \tag{34}$$

Thus, if we know T_1 and T_2, we can calculate T_S from the ratio taken from an oscilloscope display of the IF postamplifier square-wave output. If we carefully measure T_2 as the total antenna arm input temperature (T_A) in, say, the access position, we need only establish T_1. Experience has shown that a hand over the comparison horn serves as an approximate ambient load. Thus, it becomes quite simple to approximate T_S from:

$$T_S \cong \frac{T_{\text{ambient}} - R(T_A)}{(R-1)} \cdot \tag{35}$$

A second method, which does not require the antenna to be in the access position, allows a quick approximation of $(T_{\text{in}})_{\text{eff}}$, even during operation. This method, dependent only upon short-term gain stability (a very dependable maser property), utilizes a calibrated test signal. The temperature of the available test signal has been discussed in connection with (1).

The 2°K test signal (T_{test}) will produce a synchronous detector output to the recorder having an off-signal peak-to-peak noise fluctuation, $N = 4(\Delta T)$, and a dc level S due to the signal. We can now calculate $(T_{\text{in}})_{\text{eff}}$ from (30), where $T = \frac{1}{4}$ of the peak-to-peak noise (N).

$$\Delta T = \frac{T_{\text{test}}}{4}\left[\frac{N}{S}\right] \tag{36}$$

which, when substituted in (30), gives:

$$(T_{\text{in}})_{\text{eff}} = \frac{T_{\text{test}}}{2}\left[\frac{N}{S}\sqrt{\Delta \nu_S T}\right]. \tag{37}$$

It should be noted that this approximation includes the input temperature, and hence is *not* an *excess* noise measurement.

C. Performance Characteristics

The two most significant characteristics of the radiometer system are its equivalent input temperature and gain stability. The effect of these two parameters upon threshold sensitivity has been discussed [see (32)]. Extensive measurements of these and other operational characteristics have been made and compared with theoretical calculations.

The total system's excess noise temperature T_S may be predicted from the measured performance values:

Ambient temperature, input line loss = 0.45 db: $L_1 = 1.109$

Complete superheterodyne noise figure = 9.5 db; $T = 2000°$K

Cavity radiation and spontaneous emission $\cong 4°$K.

We may therefore calculate T_S, dependent only upon maser gain (G), as:

$$T_S = 2000\left(\frac{L_1}{G}\right) + 4(L_1) + 290(L_1 - 1)$$
$$= 2220\left(\frac{1}{G}\right) + 36°\text{K}. \quad (38)$$

This results in a predicted T_S of 58 and 47°K with maser gains of 20 and 23 db, respectively. Actual precision measurements have given values of 70, 57, and 43°K with maser gains of 17, 20, and 23 db, respectively.

The off-source antenna temperature is about 30°K largely because of spillover and backlobe radiation. Conventional horn designs which are 10 or even 20 db down at the dish edge are unsatisfactory for maser radiometer use. The illumination beyond the dish edge adds a variable input noise temperature, negligible even with a 1000°K system, but of great importance as the system temperature is reduced to the maser radiometer range ($T<100$°K). Preliminary studies indicate that it is possible to design a multi-element horn to illuminate the dish in an essentially flat pattern, dropping very rapidly at the dish edges. Such a design is expected to yield an antenna temperature of approximately 10°K, essentially independent of antenna position.

The gain-stability performance of the complete system, taken experimentally with a maser gain of 20 db is approximately

Short term: < 10 minutes: 0.6 per cent
< 30 minutes: 2.0 per cent
Long term: <100 minutes: 5.0 per cent.

The variable-attenuator balance controls are capable of an off-source input signal zeroing to within:

$$T_{\text{ant}} - T_{\text{comp}} \mid < 0.02°\text{K}. \quad (39)$$

This amount of unbalance, together with a system gain instability of 2 per cent, contributes an rms output fluctuation as given by (31) of:

$$\alpha(\gamma - 1)(\mid T_{\text{ant}} - T_{\text{comp}} \mid)$$
$$< 1.0(0.02)(0.02) = 0.0004°\text{K}. \quad (40)$$

Thus, for present system temperatures, the gain-fluctuation threshold is negligible.

The rms fluctuation due to internally generated noise becomes of primary concern. Theoretically, the threshold is predicted by (30):

$$(\Delta T)_{\text{rms}} = \frac{\pi}{2}\frac{(T_{\text{in}})_{\text{eff}}}{\sqrt{\Delta\nu_S\tau}}$$

where:

$(T_{\text{in}})_{\text{eff}} = T_S + T_{\text{antenna}} \cong 55+30 = 85$°K
$\Delta\nu_S$ = bandwidth = 8 Mc (IF limited)
τ = integration time = 2 seconds.

These values result in a threshold sensitivity of:

$$(\Delta T)_{\text{rms}} = \frac{\pi}{2}\frac{85}{\sqrt{16 + 10^6}} = 0.034°\text{K}. \quad (41)$$

Gain instability is such that long integration times are also usable. For example, $\tau = 42$ seconds gives, theoretically,

$$(\Delta T)_{\text{rms}} = \frac{\pi}{2}\frac{85}{\sqrt{336 \times 10^6}} = 0.0073°\text{K}. \quad (42)$$

Actual measurements, based upon a 2°K test signal are in very close agreement with these theoretical predictions. Measurements have given a no signal ($|T_{\text{ant}} - T_{\text{comp}}| < 0.02$°K) ΔT_{rms}, taken as $\frac{1}{4}$ the peak-to-peak fluctuation, of:

$$(\Delta T)_{\text{rms}} \cong 0.033°\text{K}; \qquad \tau = 2 \text{ seconds}$$
$$\cong 0.007°\text{K}; \qquad \tau = 42 \text{ seconds}. \quad (43)$$

The latter $(\Delta T)_{\text{rms}}$ output fluctuation was maintained for 16 time constants (11 minutes). Table I summarizes the actual operational sensitivities obtained with a 2°K test-signal input.

TABLE I
SENSITIVITY VS INTEGRATION TIME
UNIVERSITY OF MICHIGAN MASER RADIOMETER

Integration time (τ) (seconds)	$(\Delta T)_{\text{rms}}$; threshold sensitivity ($\frac{1}{4}$ peak-to-peak fluctuation)°K
2	~0.033
12	~0.012
42	~0.007

Maser gain = 20 db; Post-maser noise temperature = 2000°K
Equivalent input temperature = 85°K; system bandwidth = 8 Mc
$\gamma \leqq 1.02$; ($|T_{\text{ant}} - T_{\text{comp}}|$) $\leqq 0.02$°K

V. RADIO ASTRONOMY OBSERVATION

The final test of any radio astronomy receiver is in the astronomical observations. Several drift curves, representative of the system sensitivity and performance are presented. In this type of observation, wherein the earth's rotation moves the antenna beam past the source, the antenna is stationary relative to the earth, thus eliminating spillover variations. Sources resulting in antenna temperature increases of 35°K to 0.4°K have been observed, using integration times from $\frac{1}{2}$ second to 42 seconds. In all cases, the system is balanced prior to the drift to minimize gain-instability fluctuations. A test-signal calibration is used to measure the antenna-temperature increase caused by the source.

Fig. 10 is a drift curve of the radio source Cassiopeia A, obtained with an integration time of $\frac{1}{2}$ second. No rms fluctuation has been calculated because the operation was relatively insensitive. The peak source con-

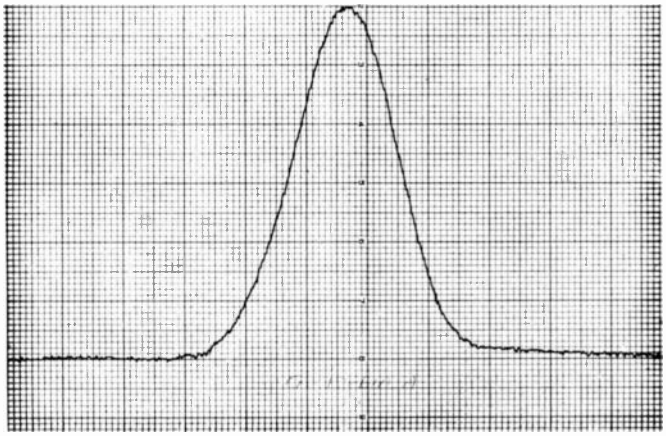

Fig. 10—Drift curve of radio source Cassiopeia A obtained with the maser radiometer (March 10, 1960). Peak antenna temperature increase is about 35°K. Integration time is ½ second.

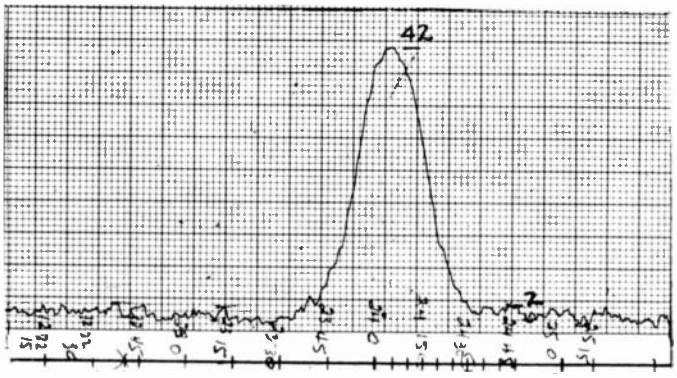

Fig. 11—Drift curve of radio source Virgo A obtained with the maser radiometer (February 25, 1960). Peak antenna temperature increase is 2.8°K. Integration time is 2 seconds.

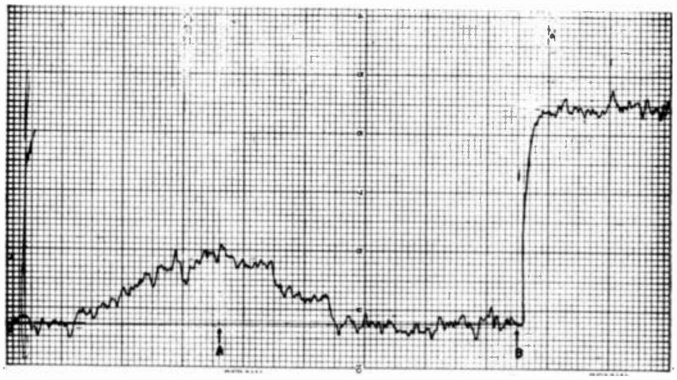

Fig. 12—Drift curve of Tycho Brahe's Super Nova 1572 obtained with the maser radiometer (March 14, 1960). Peak antenna temperature increase is 0.61°K. Test signal is 2.05°K. Integration time is 2 seconds.

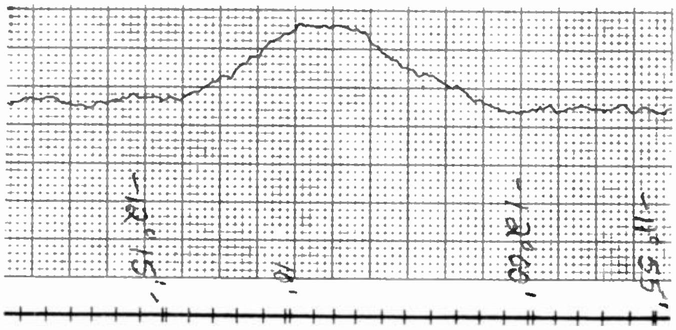

Fig. 13—Drift curve of Hydra A obtained with maser radiometer (March 2, 1960). Peak antenna temperature increase is 0.45°K. Integration time is 12 seconds.

tribution to antenna temperature is approximately 35°K.

Proceeding to more sensitive system performance, Fig. 11 shows a drift curve of Virgo A (M87, NGC 4486), obtained with a 2-second integration time. The resulting peak antenna-temperature increase was measured as 2.8°K, and the ratio of the signal to the peak-to-peak noise is about 21 to 1. Use of these values in (36) indicates an rms off-source noise fluctuation of 0.033°K; this is in very close agreement with the theoretical prediction of 0.034°K obtained from (41).

The response to Tycho Brahe's Super Nova 1572 is shown in Fig. 12. This figure also shows the calibration signal, in this case 2.05°K. The peak antenna-temperature increase is approximately 0.61°K; integration time is again 2 seconds. The rms value of the noise fluctuation, taken as ¼ of the peak-to-peak, is, in this case, approximately 0.055°K. The theoretical prediction is again about 0.034°K. Because the results are, in general, in excellent agreement with theory, this disagreement is attributed to the least understood variable of the system: the atmospheric effects upon antenna temperature.

Fig. 13 shows the signal from Hydra A, the antenna temperature increase is 0.45°K and the integration time 12 seconds. RMS noise fluctuation is approximately 0.016°K which compares favorably with a theoretical prediction of 0.013°K. Assuming an antenna efficiency of 0.50 (as determined by comparing the results from several strong sources with expected results on the basis of published flux values), the point-source flux from Hydra A at 8.72 Gc (3.45 cm) is $(4.8 \pm 1.4) \times 10^{-26}$ watts/m²/cps.

VI. Conclusion

The performance of this system has shown the maser radiometer to be a dependable, useful addition to radio astronomy equipment. The maser amplifier can be incorporated into a long-term program and engineered to assure reliable, high-sensitivity operation upon installation. With careful design and operation, the ratio of operational to down time has been proven to be as good as a conventional, high-sensitivity, nonmaser receiver.

RMS noise fluctuations of approximately 0.01°K with integration times as short as 12 seconds have been obtained for the first time. The faster response, because of the shorter integration time, has great operational significance since it makes it unnecessary to spend many minutes, or even hours, obtaining sensitive observations. Further, the first maser gain stabilities suf-

TABLE II
COMPARISON OF EXISTING AND FUTURE X-BAND RECEIVERS

X-Band System	$(T_{in})_{eff}$(°K)	$\Delta\nu_S$(Mc)	τ (sec) for $(\Delta T)_{rms}=0.02$°K	τ (sec) for $(\Delta T)_{rms}=0.003$°K
Presently existing, broad-band, nonmaser receivers	4000	1000	~100	~4400
Presently existing, narrow-band, maser receiver	75	8	~4.5	~200
Predicted, broad-band, maser receiver	40	100	~0.1	~4.4

ficient to allow long integration have been obtained. RMS noise fluctuations of approximately 0.007°K, with an integration time of 42 seconds, are possible. Improved techniques, such as the use of a cooled-load test signal rather than a noise tube and the "double-horn" comparison technique for sources of small extent (planets, point sources), offer simpler, more reliable operation.

Results obtained with the present system indicate that it is possible to design an even more advanced system, capable of an order-of-magnitude improvement in sensitivity. By increasing the system bandwidth, decreasing the equivalent input temperature, and further increasing maser gain stability, it now appears possible to construct a radiometer with a threshold rms fluctuation of a few thousandths of a degree. Specifically, the rms fluctuations, with an integration time of 12 seconds, are theoretically <0.003°K.

Since atmospheric limitations are, as yet, somewhat unknown, there is some feeling that pushing the radiometer sensitivity below a few thousandths of a degree offers little return. However, the benefit of shorter integration times still exists. Table II illustrates the potential of such a receiver to yield a given threshold sensitivity $(\Delta T)_{rms}=0.02$°K as calculated from (30):

$$(\Delta T)_{rms} = \frac{\pi}{2} \frac{(T_{in})_{eff}}{\sqrt{\Delta\nu_S \tau}}.$$

On the other hand, since the atmospherics may allow greater sensitivities, and considering the possible, future, radiometer applications outside the atmosphere, Table II also indicates the response possible with $(\Delta T)_{rms}=0.003$°K.

The fast response and high sensitivity of predicted maser receivers will be important to space communications and observations above the atmosphere.

All integration times are based upon the threshold due to internal noise only. Thus, due to gain variations during the extremely long integration times, this sensitivity is improbable with present nonmaser systems.

Future maser receivers will doubtlessly utilize mechanical refrigerators, eliminating much of the troublesome manpower and time requirement of maser operation. Continuous 4.2°K cooling will allow radio astronomy maser receivers to be operated by one man. Also, the constantly refrigerated maser assembly will require essentially no setup adjustment, and routine operation at the flip of a switch is conceivable. Although the present system has been successfully operated by semitrained (in maser operation) radio astronomy personnel, the initial setup has required personnel more experienced in maser work. The predicted continuous cooling and single setup would eliminate this requirement.

ACKNOWLEDGMENT

The authors wish to thank Prof. C. Kikuchi for his guidance and support throughout the program. They wish to express their gratitude to Profs. R. L. Hess and F. T. Haddock, who initiated the program and devoted much time and effort to its support. Special acknowledgment is due A. J. Cote and F. Alred for their technical contributions and assistance throughout the design, construction and installation; C. B. Arnold, G. Latimer and J. Talen for their assistance in the installation and operation; and Drs. A. H. Barrett and W. E. Howard for their supervision of the astronomical observations.

An Analysis of the Magnetic Second-Subharmonic Oscillator*

A. LAVI†, MEMBER, IRE, AND L. A. FINZI†, SENIOR MEMBER, IRE

***Summary*—An analysis is given for the second-subharmonic parametric oscillator with two ferromagnetic cores. "Square-loop" reasoning is employed with extreme idealization of the magnetic core properties; the effects of hysteresis losses and saturated inductance are subsequently considered. The steady-state operation, both with voltage and with current pump drives, is studied to determine the values of the circuit parameters for which the subharmonic oscillations occur. The transient build-up is evaluated by means of difference equations, and the influence of the magnitude of the excitation signal upon the transient is illustrated.**

The experimental waveforms agree with the analytical predictions for a wide range of drive frequencies, the upper limit investigated being 3 Mc.

INTRODUCTION

BY VIRTUE of their quantized phase, second-subharmonic oscillators are utilized to perform digital and logic operations in binary data-handling systems. Von Neumann[1] suggested this idea, while Goto[2] independently produced such an oscillator, which he called the "Parametron" and analyzed the operation treating the nonlinear magnetic component as a periodically varying reactance. Similar work has been performed by many[3-5] considering circuits with nonlinear capacitors. Applications of the second-subharmonic oscillator in digital systems have been described by still others.[6-9]

In this paper the steady-state performance and the transient build-up of the parametric oscillator with two ferromagnetic cores are analyzed with methods based on a piece-wise linearization of the flux current (ϕ, i) relationship of the magnetic cores. In order to reduce the transcendentality of the resulting equations, and to present clearly the mechanism of operation, square-waved pump drives are considered here. An extension of this analysis to sinusoidal drives can be found in Lavi.[10]

GENERAL STUDY OF CIRCUIT: SQUARE-WAVE PUMP VOLTAGE

The general equations governing the system of Fig. 1 on a unit-turn basis are:

$$e_p = \dot{\phi}_1 + \dot{\phi}_2 + R_p i_p, \tag{1}$$

$$0 = \dot{\phi}_1 - \dot{\phi}_2 + R_c i_c + v_c, \tag{2}$$

$$F_1 = i_p + i_c + I_b,$$

$$F_2 = i_p - i_c + I_b, \tag{3}$$

where

$$\dot{\phi} = \frac{d\phi}{dt}; \; v_c = \frac{1}{c}\left(q_0 + \int_0^t i_c d\tau\right).$$

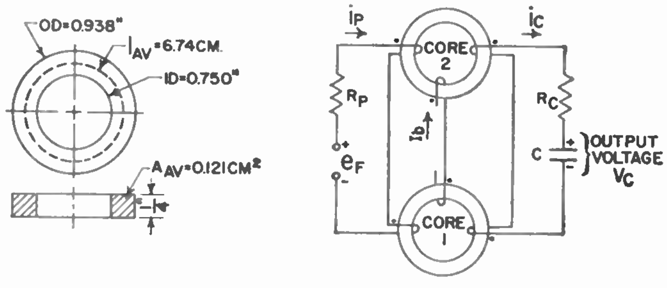

(a) (b)

Fig. 1—Circuit diagram and core description.

With the idealization of Fig. 2(a) three states are conceivable for either core:

1) Unsaturated $|\phi| < \phi_s$ (U state), $F = 0$;
2) Positively saturated $\phi = \phi_s$ (S^+ state), $F \geq 0$, $\dot{\phi} = 0$;
3) Negatively saturated $\phi = -\phi_s$ (S^- state), $F \leq 0$, $\dot{\phi} = 0$.

The "mode" of the system is defined at any time by specifying the magnetic states of the two cores; thus nine modes are possible.

* Received by the IRE, April 4, 1960; revised manuscript received, February 3, 1961. This is part of a dissertation submitted by A. Lavi in partial fulfillment of the requirements for the Ph.D. degree, Carnegie Inst. Tech., Pittsburgh, Pa. The work herein was performed under Office of Naval Res. Contract Nonr 760(09).

† Elec. Engrg. Dept., Carnegie Inst. Tech., Pittsburgh, Pa.

[1] J. von Neumann, "Nonlinear Capacitance or Inductance Switching, Amplifying and Memory Organs," U. S. Patent No. 2,815,488; December 3, 1957.

[2] E. Goto, "The parametron, a digital computing element which utilizes parametric oscillation," PROC. IRE, vol. 47, pp. 1304–1317; August, 1959.

[3] F. Kiyasu, *et al.*, "Parametric excitation using variable capacitance of ferroelectric materials," *J. Inst. Elec. Commun. (Japan)*, vol. 41, pp. 239–244; March, 1958.

[4] F. Kiyasu, *et al.*, "Parametric excitation using barrier capacitance of semi-conductor junction," *J. Inst. Elec. Commun. (Japan)*, vol. 40, pp. 162–169; February, 1957.

[5] F. Sterzer, "Microwave parametric subharmonic oscillators for digital computing," PROC. IRE, vol. 47, pp. 1317–1324; August, 1959.

[6] E. Goto, "On the application of parametrically excited nonlinear resonators," *Denki Tsushin Gakki-Shi (Japan)*, vol. 38, pp. 770–775; October, 1955.

[7] L. Onyshkevych, *et al.*, "Parametric Phase Locked Oscillators—Characteristic and Application to Digital Systems," presented at the Symp. on Microwave Techniques for Computers, Dept. of Interior, Washington, D. C.; March, 1959.

[8] S. Muroga, "Elementary principles of parametron and its applications to digital computors," *Datamation*, vol. 1, pp. 31–34; October, 1958.

[9] R. L. Wigington, "A new concept in computing," PROC. IRE, vol. 47, pp. 516–523; April, 1959.

[10] A. Lavi, "Large Signal Analysis of Parametric Subharmonic Oscillators," Ph.D. dissertation, Dept. of Elec. Engrg., Carnegie Inst. Tech., Pittsburgh, Pa.; September, 1959.

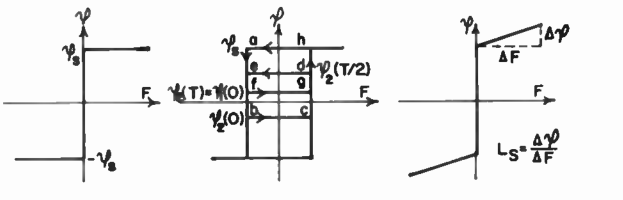

Fig. 2—Magnetic approximations. (a) Extreme idealization. (b) Approximated major and minor dynamic hysteresis loops. (c) Inclusion of saturated inductance.

In the four (S_1, S_2) modes, both cores are saturated $(\phi_{1,2} = \pm\phi_s)$ and the pump circuit is completely decoupled from the output circuit

$$i_p = e_p/R_p,$$

$$i_c = -\frac{v_{ss}}{R_c}\epsilon^{-(t-t_{ss})/\tau d},$$

$$v_c = v_{ss}\epsilon^{-t(-t_{ss})/\tau d};$$

where $\tau_d = R_c C$, and v_{ss} is the capacitor voltage at $t = t_{ss}$, the time both cores reach saturation.

In the (U_1, U_2) mode, both cores are unsaturated, $F_1 = 0$, $F_2 = 0$. Hence,

$$i_c = 0,$$

$$i_p = -I_b,$$

$$\dot\phi_1 = \frac{e_p + R_p I_b - v_c}{2},$$

$$\dot\phi_2 = \frac{e_p + R_p I_b + v_c}{2}. \qquad (4)$$

Throughout this mode v_c^2 remains constant.

In the modes $(S_1^\pm, U_2)$, $\dot\phi_1 = 0$, $F_2 = 0$. Defining v_{su} as the capacitor voltage when the (S_1, U_2) mode begins at $t = t_{su}$ with $\tau_c = (R_p + R_c)C$,

$$i_c = \frac{e_p + R_p I_b - v_{su}}{R_p + R_c}\epsilon^{-(t-t_{su})/\tau_c},$$

$$i_p = i_c - I_b,$$

$$v_c = (e_p + R_p I_b)(1 - \epsilon^{-(t-t_{su})/\tau_c}) + v_{su}\epsilon^{-(t-t_{su})/\tau_c},$$

$$\dot\phi_2 = (e_p + R_p I_b) - \frac{R_p}{R_p + R_c}(e_p + R_p I_b - v_{su})\epsilon^{-(t-t_{su})/\tau_c}. \qquad (5)$$

In the modes $(U_1, S_2^\pm)$, $\dot\phi_2 = 0$, $F_1 = 0$. Defining v_{us} as the capacitor voltage when the (U_1, S_2) mode begins at $t = t_{us}$,

$$i_c = \frac{e_p + R_p I_b + v_{us}}{R_p + R_c}\epsilon^{-(t-t_{us})/\tau_c},$$

$$i_p = -(i_c + I_b),$$

$$v_c = -(e_p + R_p I_b)(1 - \epsilon^{-(t-t_{us})/\tau_c}) + v_{us}\epsilon^{-(t-t_{us})/\tau_c},$$

$$\dot\phi_i = (e_p + R_p I_b) - \frac{R_p}{R_p + R_c}(e_p + R_p I_b + v_{us})\epsilon^{-(t-t_{us})/\tau_c}. \qquad (6)$$

A change from $+\phi_s$ to $-\phi_s$ or vice versa cannot take place in zero time; hence, a (U_1, S_2^+) mode cannot immediately follow a (U_1, S_2^-) mode, as there is a finite time during which core 2 is unsaturated. Since the pump waveform is square, v_c is bound between $\pm(E + R_p I_b)$. Therefore when $\dot\phi_1$ or $\dot\phi_2$ is positive, $e_p > 0$, and when $\dot\phi_1$ or $\dot\phi_2$ is negative, $e_p < 0$. In other words, positive saturation is not possible in negative half cycles. Also the (U_1, U_2) mode can initiate only at the beginning of a half cycle and must occur at least once during a pump cycle.

Summing up, in any operation:

1) The possible modes are (U_1, U_2), (S_1^+, S_2^+) and (S_1^+, U_2), or (U_1, S_2^+) if $e_p > 0$; and (U_1, U_2), (S_1^-, S_2^-) and (S_1^-, U_2), or (U_1, S_2^-) if $e_p < 0$.
2) The modes (S_1^+, S_2^-) and (S_1^-, S_2^+) are impossible at any time.
3) The appearance of a (U_1, S_2) mode rules out the possibility of an (S_1, U_2) mode in the same half cycle.
4) If the (S_1, S_2) is attained, it must persist till the end of the half cycle.

Therefore, the possible sequences over a half cycle of the pump are:

1) (U_1, U_2),
2) $(U_1, U_2) \to (S_1, U_2)$ or (U_1, S_2),
3) $(U_1, U_2) \to (S_1, U_2)$ or $(U_1, S_2) \to (S_1, S_2)$,
4) $(U_1, U_2) \to (S_1, S_2)$.

Subharmonic Oscillations in the Steady State: Square-Wave Pump Voltage

Second-subharmonic oscillations are obtained if a sequence of modes repeats itself every two cycles of the pump. The various possible sequences that satisfy this requirement are expressed in Table I(a) and I(b). Table I(a) presumes that the capacitor voltage at the beginning of a positive pump half cycle is zero, $v_c(0) = 0$, with both cores unsaturated following that instant. Possible modes that may follow from there are indicated by arrows. Table I(b) presumes $v_c(0) \neq 0$ (in particular, $v_c(0) < 0$). For a pair of identical cores, the output has half-cyclic symmetry, *i.e.*,

$$i_c(t) = -i_c(t + T) \text{ (no even harmonics of the subharmonic)}$$

$$i_p(t) = i_p(t + T) \text{ (no odd harmonics of the subharmonic)}$$

$$\dot\phi_1(t) = \dot\phi_2(t + T)$$

$$\phi_1(t) = \phi_2(t + T),$$

where τ is the period of the pump.

It is seen by inspection that certain sequences, marked with × in the table, do not satisfy the periodicity conditions. The remaining twenty-four sequences have been individually examined using (1)–(6), and

TABLE I

CONCEIVABLE SEQUENCES

(a) $V_1(0) = 0$.
(b) $V_c(0) < 0$.

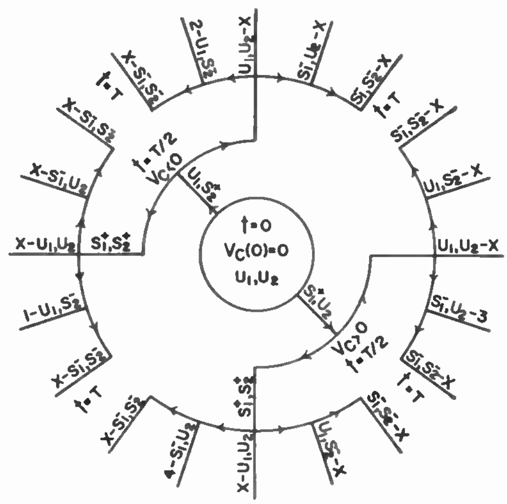

(a)

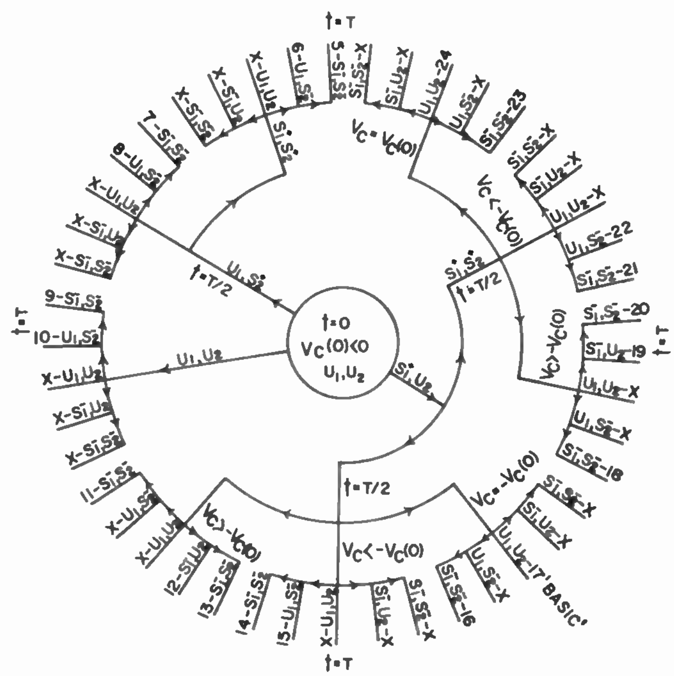

(b)

again a violation of the periodicity conditions resulted in some sequences. Ten sequences show no contradiction with the mode equations and with the periodicity conditions. Waveforms of $v_c(t)$ are given in Fig. 3. Sequence 17 is particularly simple and appealing, and is named henceforth the "basic sequence." Other sequences can be regarded as modifications thereof with some additional modes.

In the basic sequence, let $t=0$ be the beginning of an arbitrary positive half cycle which begins with the (U_1, U_2) mode, (4). The initial conditions at $t=0$ are $v_c = v_c(0) < 0$, $\phi_1 = \phi_1(0)$, $\phi_2 = \phi_2(0)$. At $t = t_1 (< T/2)$, $\phi_1 = \phi_s$ such that

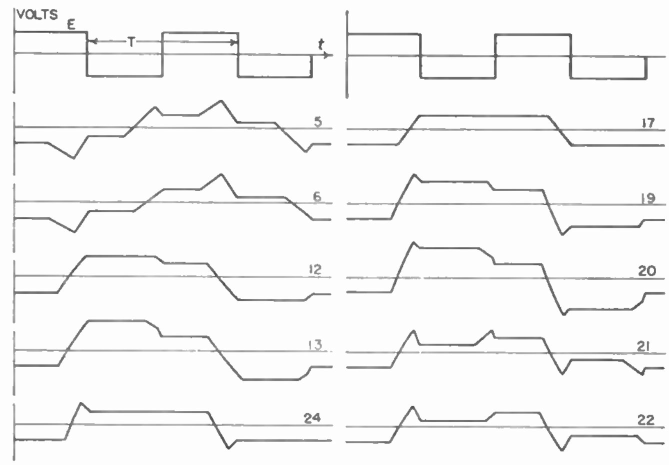

Fig. 3—Output waveforms of conceivable sequences.

$$\int_0^{t_1} \dot{\phi}_1 dt = \phi_s - \phi_1(0)$$

and

$$\int_0^{t_1} \dot{\phi}_2 dt = \phi_2(t_1) - \phi_2(0). \tag{7}$$

In the rest of the half cycle, $\dot{\phi}_2$ is given by (5). In this sequence ϕ_2 cannot reach ϕ_s before $t = T/2$, *viz.*,

$$\int_{t_1}^{T/2} \dot{\phi}_2 dt \leq \phi_s - \phi_2(t_1) \tag{8}$$

$$v_c(T/2) = (E + R_p I_b)(1 - \delta_1) + \delta_1 v_c(0) = -v_c(0); \tag{9}$$

hence

$$v_c(0) = -\frac{1 - \delta_1}{1 + \delta_1}(E + R_p I_b), \tag{9a}$$

where $\delta_1 = \epsilon^{-(T/2 - t_1)/\tau_c} < 1$. Thus given δ_1 or t_1, $v_c(0)$ can be calculated. It is seen that $v_c(0)$ is not linearly dependent on either E or I_b since δ_1 itself depends upon E and I_b.

The positive half cycle ends with $\phi_1 = \phi_s$, $\phi_2 \leq \phi_s$ and $v_c = -v_c(0)$. The negative half cycle begins immediately with the (U_1, U_2) mode which then persists throughout the half cycle without either core reaching $-\phi_s$ before $t = T$. For this the inequalities

$$-2\phi_s \leq \frac{-E + R_p I_b + v_c(0)}{2} \frac{T}{2}$$

$$-\phi_s - \phi_2\left(\frac{T}{2}\right) \leq \frac{-E + R_p I_b - v_c(0)}{2} \frac{T}{2} \tag{10}$$

must hold. Now if

$$\int_0^T \dot{\phi}_2 dt > 0$$

core 1 does not reach $-\phi_s$. Thus

$$\phi_2(T) - \phi_2(0) = E\left[\frac{T/2 - t_1 - 2R_pC(1-\delta_1)}{1+\delta_1}\right] + R_pI_b\left[\frac{T(2+\delta_1) - t_1 - 2R_pC(1-\delta_1)}{1+\delta_1}\right]. \quad (11)$$

If the coefficient of E is equal to or greater than zero,

$$t_1 \leq \frac{T}{2} - 2R_pC(1-\delta_1). \quad (12)$$

The latter is sufficient to conclude that $\phi_2(T) > \phi_2(0)$ if $\phi_1(T) > -\phi_s$. For $\phi_1(T)$ to be greater than $-\phi_s$, from (10)

$$2\phi_s \geq \frac{E - \delta_1 R_p I_b}{1+\delta_1}\frac{T}{2} \quad (13)$$

must hold.

Waveforms of v_c, $\dot{\phi}_1$, $\dot{\phi}_2$, i_c and i_p are calculated for typical values of parameters using the above equations (Fig. 4).

The unknown variables of the system are four: t_1, $v_c(0)$, $\phi_1(0)$ and $\phi_2(0)$. The known parameters are E, I_b, R_p, R_c, C, T and ϕ_s. These quantities are related by

$$\text{a)} \quad v_c(0) = -\frac{1-\delta_1}{1+\delta_1}(E + R_pI_b),$$

$$\text{b)} \quad \phi_s - \phi_1(0) = \frac{t_1}{1+\delta_1}(E + R_pI_b),$$

$$\text{c)} \quad \phi_s - \phi_2(0) = \frac{T/2}{1+\delta_1}(E - \delta_1 R_pI_b). \quad (14)$$

From the steady-state requirement $\phi_1(0) = \phi_2(T)$, (11) becomes

$$\text{d)} \quad \phi_1(0) - \phi_2(0) = \frac{T/2 - t_1 - 2R_pC(1-\delta_1)}{1+\delta_1}(E + R_pI_b) + \delta_1\frac{T}{2}R_pI_b.$$

Equating the difference between (14c) and (14b) with (14d), t_1 can be evaluated. The above equations hold if

$$\text{a)} \quad 2\phi_s \geq \frac{E - \delta_1R_pI_b}{1+\delta_1}\frac{T}{2}$$

$$\text{b)} \quad t_1 \leq \frac{T}{2} - 2R_pC(1-\delta_1)$$

$$\text{c)} \quad \phi_s \geq \phi_2(0) + |(E + R_pI_b)| \cdot \left[\frac{T}{2} - \frac{t_1}{1+\delta_1} - 2R_pC\frac{1-\delta_1}{1+\delta_1}\right]. \quad (15)$$

Condition (15c) is certainly satisfied if $t_1 \leq (T/2) - 2R_pC(1-\delta_1)$. Because of the transcendental character of (14), it is difficult to obtain a static characteristic expressing v_c as a function of E. A more convenient formulation res ılts by rea'izing that the pump current

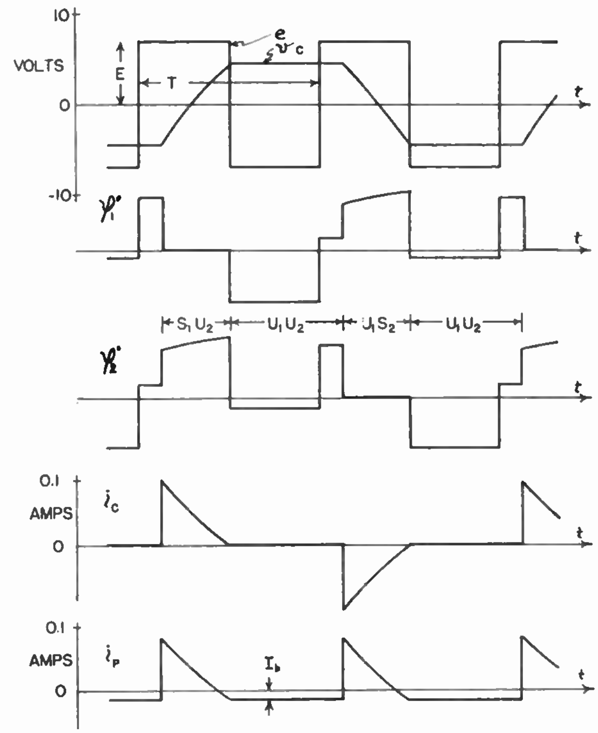

Fig. 4—Calculated waveforms for basic-steady-state sequence ($R_p = 12\ \Omega$, $R_c = 92\ \Omega$, $C = 6.2\ \mu f$, $T = 1/1200$ sec). $I_b = 10$ ma.

i_p' has no direct component, *i.e.*,

$$\int_0^{2T} i_p dt = 0.$$

Moreover, since

$$i_p(t) = i_p(t + T), \quad \int_0^T i_p dt = 0, \ i.e.,$$

$$-I_bT + (E + R_pI_b)(1-\delta_1)C + v_c(0)(1-\delta_1)C = 0. \quad (16)$$

From (14a) and (16),

$$\delta_1^2 - (1-K)\delta_1 + K = 0, \quad (17)$$

where

$$K = \frac{TI_b}{2C(E + R_pI_b)} > 0.$$

Hence, given E and I_b, $v_c(0)$ is obtained by evaluating δ_1 and substituting back in (14). The roots of (17) have physical significance only if they are real and less than unity; therefore K must be less than 0.171. In fact, two solutions for δ_1 exist for $0.171 > K > 0$; the static characteristic appears as double valued. However, the conditions of (15) must also be satisfied and this may rule out one of the roots. Fig. 5 gives calculated and measured static characteristics.

Experimentation has been performed with Orthonol cores at pump frequencies ranging between 250–1500 cps, with circuit parameters chosen to satisfy (15). The predicted waveforms of Fig. 4 show a good confirmation in the oscillograms of Fig. 6.

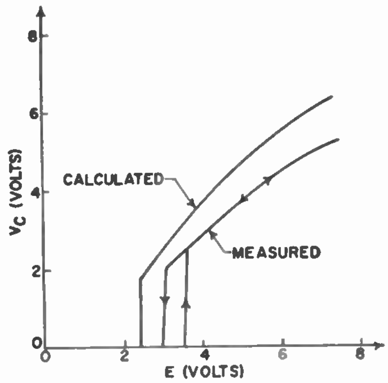

Fig. 5—Static characteristic parameters as given in Fig. 4. V_c is given in volts.

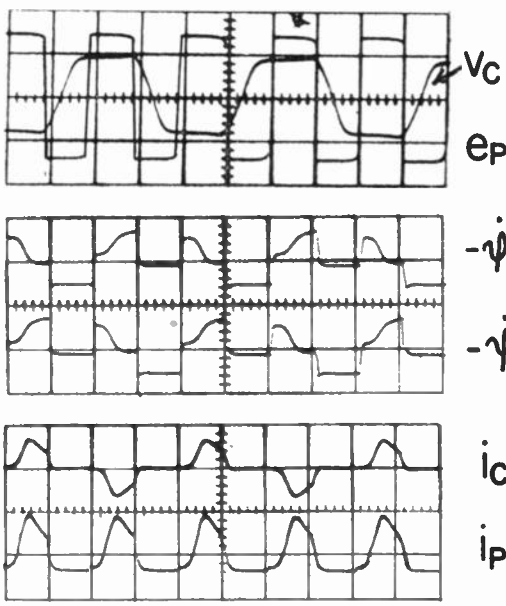

Fig. 6—Experimental waveforms of basic sequence parameters as given in Fig. 4. $V_c\dot{\phi}_1$ scales are 10 volts/div.

If the conditions of (15) are not met, second-subharmonic oscillators may still be obtained, but the basic sequence becomes impossible. Other sequences, 12, 19 and 24, analytically predicted, have been experimentally verified by Lavi.[10] Lavi also presents a comparison between analytical and experimental results for sinusoidal pump voltage at these frequencies with excellent agreement. Results obtained with sinusoidal pump voltage at 20-kc—3-Mc range, using small permalloy bobbin cores, also exhibit good qualitative agreement.

Modifications of the Extreme Magnetic Idealization

The extreme idealization of Fig. 2(a), used so far in the analysis, does not account for hysteresis and eddy current losses in the cores. An accurate representation of the core properties in dynamic processes of swinging fluxes is not manageable, but a reasonable approximation is to assume that the double-minor loop, described by a core in one subharmonic cycle, is inscribed within a rectangle of constant width as shown in Fig. 2(b). This approximation implies that when either core is unsaturated its total MMF, instead of being zero, is $\pm F_d$ depending on whether $\dot{\phi}$ is positive or negative. The MMF relation (3), applied to the various modes of the basic sequence, indicates that the quantity E appearing in the voltage equation (1), becomes $E-R_pF_d$ in positive half cycles, and $(-E+R_pF_d)$ in negative half cycles of the pump; *i.e.*, dynamic hysteresis losses can be accounted for by using a modified pump voltage $E'=E-R_pF_d$ in the previous analysis. With $F_d \simeq 30$ AT/m at 1200 cps, the calculated transfer characteristic of Fig. 5 shifts to the right by an amount $R_pF_d \simeq 0.25$ volts, thus improving upon the agreement with the experiment.

The idealization of Fig. 2(a) also implies that $d\phi/dF=0$ for $F>0$. That is, no further increase of ϕ is possible beyond the value ϕ_s, and $d\phi/dt$ is zero for the saturated core. If the circuit resistances are comparatively low, or if the frequency of operation is high, this assumption may be inaccurate. A linear relationship between ϕ and F for $\phi>\phi_s$ can be assumed then, resulting in the concept of a saturated differential inductance $L_s=(d\phi/dF)\big|_{\phi>\phi_s}$ as shown in Fig. 2(c). Thus the two coils of a saturated core exhibit a self-inductance L_s and also a mutual differential inductance M_s, with $L_s=M_s$ if leakage fluxes are neglected.

Eqs. (5) for the (S_1^+, U_2^-) mode modify to

$$E = \dot{\phi}_2 + R_pi_p + L_s\frac{di_p}{dt} + M_s\frac{di_c}{dt}$$

$$0 = -\dot{\phi}_2 + R_ci_c + v_c(t_1) + \int_{t_1}^{t}\frac{i_c}{C}\,d\tau + L_s\frac{di_c}{dt} + M_s\frac{di_p}{dt}. \quad (18)$$

Since core 1 is unsaturated, $i_p=i_c-I_b$, $di_p/dt=di_c/dt$. Adding (18) and eliminating i_p,

$$E_p - v_c(t_1) + R_pI_b = (R_p+R_c)i_c + 4L_s\frac{di_c}{dt} + \int_{t_1}^{t}\frac{i_c}{C}\,d\tau. \quad (19)$$

Eq. (19) is a second-order linear differential equation. If the solution is oscillatory, v_c is not bound any more between $\pm(E+R_pI_b)$; oscillatory overshoots are recognized in the waveforms of Fig. 7.

Altogether, the actual core properties can be represented by approximations which improve upon the extreme idealization of Fig. 2(a). This is feasible without substantial changes in the analysis.

Subharmonic Oscillations with Square-Wave Current Drive

The miniaturization of components and the use of a single pump to drive a number of oscillators in series may give the character of a current source to the pump supply.

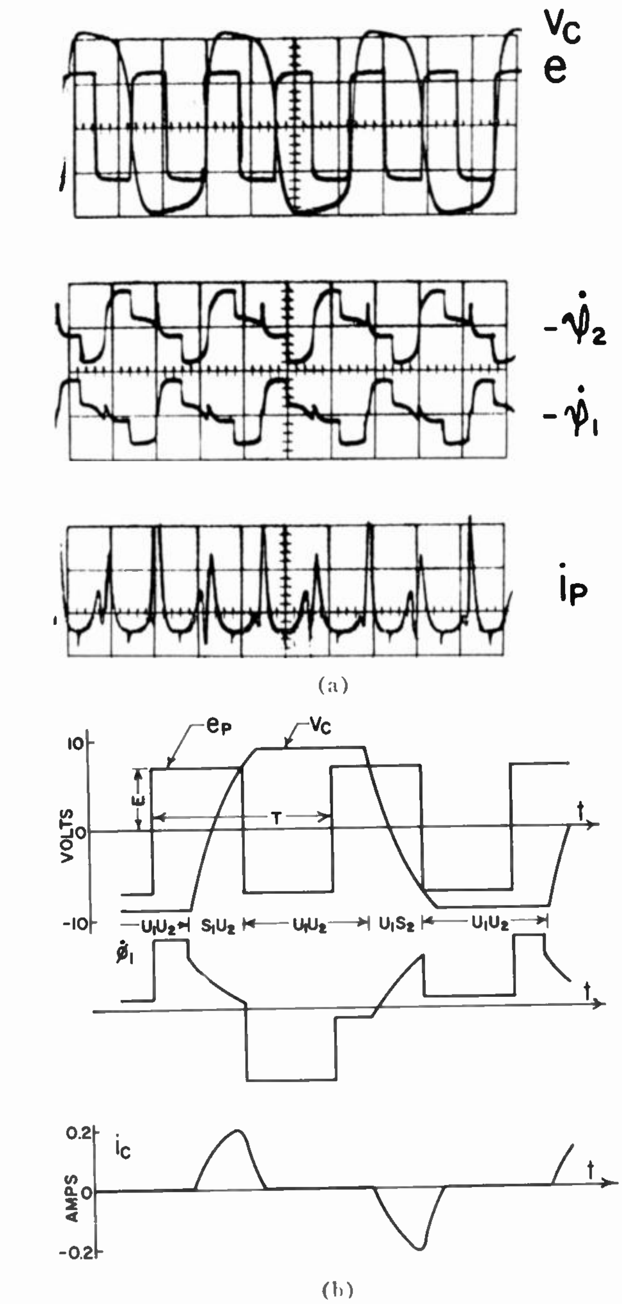

Fig. 7—Waveforms showing effect of saturated inductance. $|V_c| > E$, $\dot{\phi}_{1,2} > 0$ when $e_p > 0$. ($R_p = 12\ \Omega$, $R_c = 12$, $C = 1\ \mu f$, $T = 1/1200$ sec, $L_s = 6$ mh.) In (a) the experimental scale is 10 volts/div, in (b) it is calculated.

By prescribing $i_p(t)$, the pump-loop voltage equation loses its meaning, but nevertheless the remaining equations [(2) and (3)] are sufficient to describe the system. Assuming a square-wave pump current under the core idealization of Fig. 2(a), it appears that the (U_1, U_2) mode cannot appear at any time unless $i_p = I_b$. Eliminating negative saturation, the transition from one mode to the other has to be through an (S_1^+, S_2^+) mode. The only possible modes are (S_1^+, U_2), (U_1, S_2^+) and (S_1^+, S_2^+). Since immediate transition between the first two modes is excluded, the three modes form the sequences $(S_1^+, U_2) \rightarrow (S_1^+, S_2^+) \rightarrow (U_1, S_2^+) \rightarrow (S_1^+, S_2^+) \rightarrow$ etc. If the above sequence repeats itself every two pump cycles, second-subharmonic output is obtained.

In the mode (S_1^+, S_2^+), v_c decays exponentially as usual. If $v_{ss}/R_c \leq i_p + I_b$, the mode persists until i_p changes sign, otherwise a (U_1, S_2^+) or (S^+, U_2) mode initiates. In the mode (S_1^+, U_2),

$$F_2 = 0, \qquad \dot{\phi}_1 = 0,$$

$$F_1 = 2(i_p + I_b),$$

$$v_c(t) = v_{su} + (i_p + I_b) \frac{t - t_{su}}{C},$$

$$\dot{\phi}_2(t) = R_c(i_p + I_b) + v_c(t). \tag{20}$$

In the mode (U_1, S_2),

$$F_1 = 0, \qquad \dot{\phi}_2 = 0,$$

$$F_2 = 2(i_p + I_b),$$

$$v_c(t) = v_{us} - (i_p + I_b) \frac{t - t_{us}}{C},$$

$$\dot{\phi}_1(t) = -R_c(i_p + I_b) - v_c(t). \tag{21}$$

Consider an arbitrary positive half cycle such that at $t=0$, $\phi_1 = \phi_s$. The mode (S_1, U_2) prevails and both ϕ_2 and v_c are increasing. At $t = t_2$, the (S_1, S_2) mode is reached. From t_2 to $T/2$, v_c decays exponentially. In the negative half cycle, the mode (U_1, S_2) prevails such that $\phi_1(T) = \phi_2(0)$ and $v_c(T) = -v_c(0)$. Thus, the periodicity requirement is satisfied.

The calculations become very simple if $t_2 = T/2$, for then

$$v_c(T/2) = v_c(0) + (I_b + I_p) \frac{T}{2C};$$

$$v_c(T) = -v_c(0) = v_c(T/2) - (I_b - I_p) \frac{T}{2C}. \tag{22}$$

Therefore,

$$v_c(0) = -\frac{T}{2C} I_p; \qquad v_c(T/2) = \frac{T}{2C} I_b. \tag{22a}$$

The periodicity condition

$$\phi_s - \phi_2(0) = +\phi_s - \phi_1(T)$$

requires that

$$\frac{I_b}{I_p} = \frac{T}{4R_cC}. \tag{23}$$

Fig. 8 gives calculated waveforms for a typical set of values. Eq. (22) is very restrictive as it requires a critically adjusted ratio I_b/I_p. A wider range becomes permissible if $t_2 < (T/2)$. As before, ϕ_2 reaches ϕ_s at t_2,

$$v_c(t_2) = v_c(0) + (I_p + I_b) \frac{t_2}{C}. \tag{24}$$

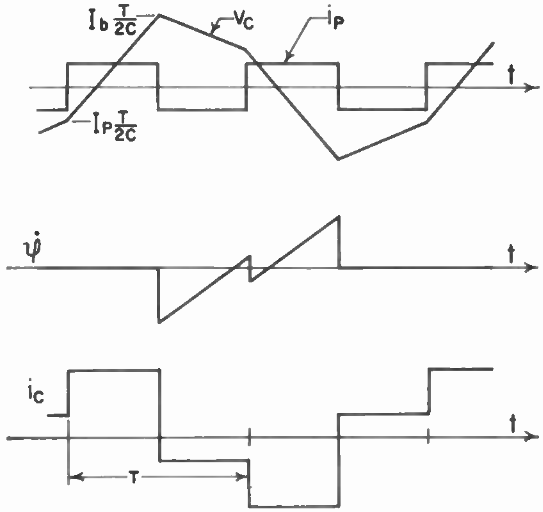

Fig. 8—Calculated waveforms for special case of current drive

$$\frac{I_b}{I_p} = \frac{T}{4R_cC} = 2; \frac{T}{2} = \frac{t}{2}.$$

The negative half cycle proceeds with the U_1, S_2^+ mode, implying

$$\frac{v_c(T/2)}{R_c} > I_b - I_p,$$

while $i_c < 0$. It can be shown that

$$v_c(0) = -\frac{\left(\delta_2 t_2 + \frac{T}{2}\right) I_p + \left(\delta_2 t_2 - \frac{T}{2}\right) I_b}{(1 + \delta_2)C}, \tag{25}$$

where $\delta_2 = \epsilon^{-(T/2 - t_2)/\tau_d}$. Thus a static characteristic v_c vs I_p can be calculated. The calculation is lengthy but feasible. Experimental waveforms of v_c and $\dot{\phi}$ are shown in Fig. 9.

The noticeable spikes appearing in $\dot{\phi}$ at the end of each pump half cycle are due to the existence of finite saturated inductances. Such inductances are practically helpful in reducing the discharge of the capacitor during the (S_1, S_2) mode.

The Transient Build-Up Voltage Drive

The system can be excited from rest either by applying the bias current while the pump supply is already energized or vice versa. Theoretically, if the system is symmetrical a build-up of oscillations can occur only if the capacitor is initially charged. Practically, a build-up is observed even without a charge, but the phase of the resulting steady-state oscillation is random. The control of the phase can be achieved by applying to the capacitor either a suitable initial charge or a small "signal" voltage with the desired phase; the signal can be removed while the transient build-up is in progress. In fact, a sufficiently large signal of a given phase may be adequate to switch the phase of oscillation without de-energizing the system.

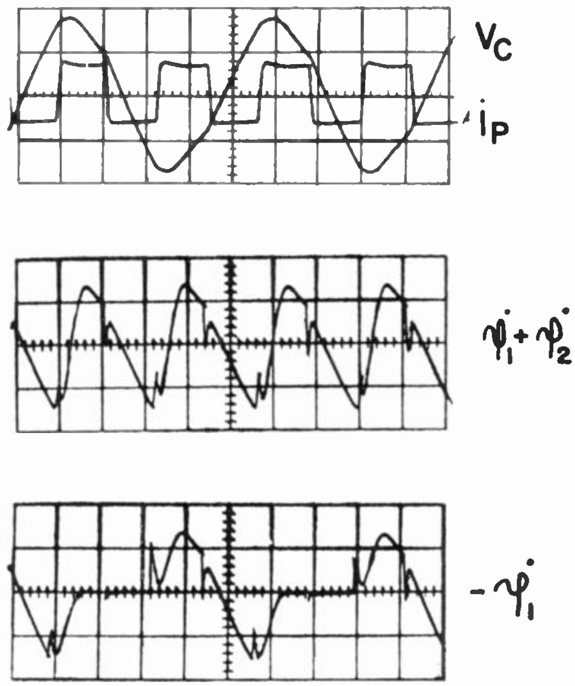

Fig. 9—Experimental waveforms for square-wave current drive. ($I_b = 20$ ma, $I_p = 15$ ma, $R_c = 40\ \Omega$, $C = 5\ \mu$f, $T = 1/1200$ sec.) Scale is $\frac{1}{2}$ volt/div.

The transient build-up is described by a set of difference equations. The symbol n is used to designate the nth half cycle of the pump: $\phi_{1,2}(n)$ can be defined as the core flux at the end of the nth half cycle, $t_1(n)$ as the time one core reaches ϕ_s in the nth half cycle, $t_2(n)$ as the time both cores reach ϕ_s in the nth half cycle, $v_c(n)$ as the capacitor voltage at the end of the nth half cycle.

Assume that the transient is initiated at the beginning of a negative half cycle with an initial capacitor charge $+Q_0$, while the bias is already energized. In negative half cycles (*i.e.*, n odd)

$$\phi_1(n) - \phi_1(n-1) = \frac{-E + R_pI_b - v_c(n-1)}{2} \cdot \frac{T}{2},$$

$$\phi_2(n) - \phi_2(n-1) = \frac{-E + R_pI_b + v_c(n-1)}{2} \cdot \frac{T}{2},$$

$$v_c(n) = -v_c(n-1). \tag{26}$$

In positive half cycles (n even), the (S_1^+, S_2^+) mode may appear; this is so if

$$\left|\frac{E + R_pI_b}{v_c(n-1)}\right| > \frac{1 + \delta_1(n)}{1 - \delta_1(n)}, \tag{27}$$

where

$$\delta_{1,2}(n) = \epsilon^{-(T/2 - t_{1,2}(n))/\tau_c},$$

$$t_1(n) = \frac{\phi_s - \phi_2(n-1)}{E + R_pI_b - v_c(n-1)}. \tag{28}$$

$t_2(n)$ is given by

$$\phi_s - \phi_1(n-1) = (E + R_pI_b)\left(t_2(n) - \frac{t_1(n)}{2} - R_pC\frac{\delta_1(n)}{\delta_2(n)}\right) - v_c(n-1)\left(\frac{t_1(n)}{2} + R_pC\frac{\delta_1(n)}{\delta_2(n)}\right), \quad (29)$$

$$v_c(n) = \left[-(E + R_pI_b)\left(1 - \frac{\delta_1(n)}{\delta_2(n)}\right) - v_c(n-1)\frac{\delta_1(n)}{\delta_2(n)}\right]\gamma(n),$$

$$\gamma(n) = \epsilon^{-(T/2 - t_2(n))/\tau_d}. \quad (30)$$

For a transient to build up the relation,

$$\left|\frac{E + R_pI_b}{v_c(n-1)}\right| > \frac{1 + \frac{\delta_1(n)}{\delta_2(n)}\gamma(n)}{\left(1 - \frac{\delta_1(n)}{\delta_2(n)}\gamma(n)\right)\gamma(n)} \quad (31)$$

must hold.

On the other hand, if

$$\left|\frac{E + R_pI_b}{v_c(n-1)}\right| < \frac{1 + \delta_1(n)}{1 + \delta_1(n)}. \quad (32)$$

the (S_1^+, S_2^+) vanishes.

$$\phi_1(n) - \phi_1(n-1) = (E + R_pI_b)\left(\frac{T - t_1(n)}{2} - R_pC\delta_1(n)\right) - v_c(n-1)\left(\frac{t_1(n)}{2} + R_pC\delta_1(n)\right)$$

$$v_c(n) = -(E + R_pI_b)(1 - \delta_1(n)) - v_c(n-1)\delta_1(n). \quad (33)$$

Eqs. (26)–(33) hold if $v_c(n-1)$ is positive for n odd; otherwise the subscripts 1 and 2 should be interchanged on ϕ and the sign of v_c reversed.

The difference equations derived above are nonlinear and transcendental; thus a closed-form solution is not readily obtainable. These equations, however, describe the physical processes involved and provide a concise algorithm for the computation of the transient half cycle by half cycle.

Evidently the larger the initial Q_0, the lower is $\phi_1(1)$ and the shorter is $t_1(2)$. Hence more time is available for the capacitor to charge in the first positive half cycle.

If the pump is applied at the beginning of a positive half cycle, the (S_1^+, S_2^+) mode persists throughout the half cycle while the capacitor loses some of its initial Q_0; hence, a larger number of cycles are required to attain the steady state.

Practically, the transient is started by applying a signal voltage to the capacitor through a high impedance. In this case, if the pump is energized at times other than $t = T/2$, a delay of up to one half cycle results. After $t = T/2$ the build-up proceeds and the signal can be removed.

A transient leading to the basic steady-state sequence is calculated in Fig. 10 for $v_c(T/2) = 0.1\ v_c(n = \infty)$ with the same circuit parameters used in Fig. 6. In Fig. 11, oscillograms are shown for various initial conditions.

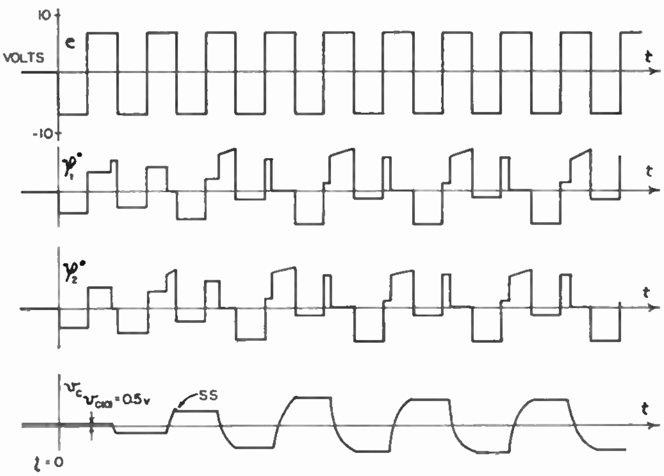

Fig. 10—Calculated transient build-up voltage drive. Parameters are given in Fig. 4.

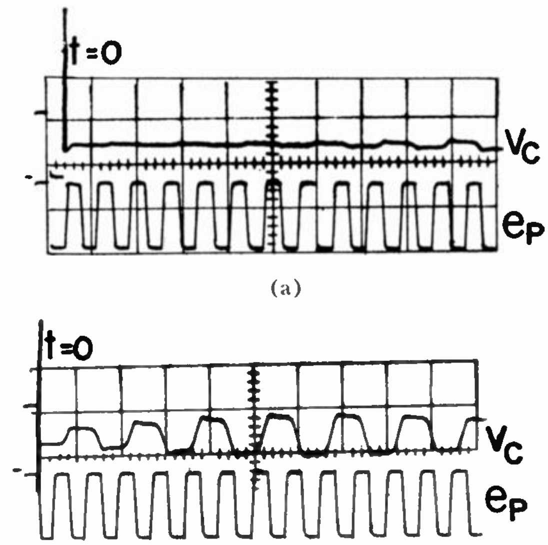

(a)

(b)

Fig. 11—Experimental transient build-up, voltage drive. (a) System energized early in a positive half cycle. (b) System energized early in a negative half cycle. $V_c(0) = 1$ volt. Parameters are given in Fig. 4.

Hysteresis effects can be accounted for in the transient with the same reasoning used in the steady state; namely, the amplitude of the pump voltage must be considered reduced to the value $E' = E - R_pF_d$.

The saturated inductance has a different influence upon the transient build-up depending whether the system is damped or oscillatory for the particular mode. In the damped case, while L_s slows the build-up in a U_1, S_2^+ or S_1^+, U_2 mode, it prevents the decay of the capacitor voltage in the S_1^+, S_2^+ mode which usually appears in the early stages of the build-up. In the oscillatory case, the presence of L_s causes overshoots in v_c and thus a quicker build-up in the U_1, S_2^+ or S_1^+, U_2 modes of the transient. Furthermore, it prevents the decay of the capacitor voltage in the S_1^+, S_2^+ mode as in the damped case.

The Transient Build-Up Current Drive

Assume again that the transient is initiated at the beginning of a negative half cycle with an initial capacitor charge Q_0 while the bias is already energized. For n odd:

$$i_c(n) = -(I_b - I_p),$$

$$\dot{\phi}_1(n) = (I_b - I_p)R_c - v_c(n-1) + (I_b - I_p)\frac{t}{C}\cdot$$

$$\phi_1(n) = \phi_s + \left[(I_b - I_p)R_c - v_c(n-1)\right]\frac{T}{2} + \frac{1}{2}\,\frac{I_b - I_p}{4}\,\frac{T^2}{C},$$

$$v_c(n) = v_c(n-1) - \frac{I_b - I_p}{C}\,\frac{T}{2}\cdot \qquad (34)$$

For n even:

$$i_c(n) = -(I_b + I_p),$$

$$\dot{\phi}_1(n) = (I_b + I_p)R_c - v_c(n-1) + (I_b + I_p)\frac{t}{C},$$

$$\phi_s - \phi_1(n-1) = \left[(I_b + I_p)R_c - v_c(n-1)\right]t_2(n) + \frac{I_b - I_p}{2}\,\frac{t_2^2(n)}{C},$$

$$v_c(t_2(n)) = v_c(n-1) - \frac{I_b + I_p}{C}\,t_2(n),$$

$$v_c(n) = v_c(t_2(n))\epsilon^{-(T/2 - t_2(n))/\tau_d}. \qquad (35)$$

For ordinary sets of values, the time constant τ_d is small compared to $T/2$, and it would be expected that the decay of capacitor voltage may be such to prevent the build-up. Actually, excitation is experimentally observed and suggests that the saturated inductance intervenes, hindering the decay of the capacitor voltage during the (S_1^+, S_2^+) intervals. This contention is substantiated by actual calculations in which measured values of L_s were introduced. Accounting for the existence of finite saturated inductance, (35) modifies into

$$v_c(n) = \frac{v_c(t_2(n))}{\alpha_1 - \alpha_2}\left[\alpha_1\epsilon^{\alpha_2((T/2)-t_2(n))} - \alpha_2\epsilon^{\alpha_1((T/2)-t_2(n))}\right], \qquad (36)$$

where $\alpha_{1,2}$ are the roots of the characteristic equation. The condition for transient build-up $|v_c(n)| > |v_c(n-2)|$ (n even) is easily met. Experimental transient build-ups are shown in Fig. 12.

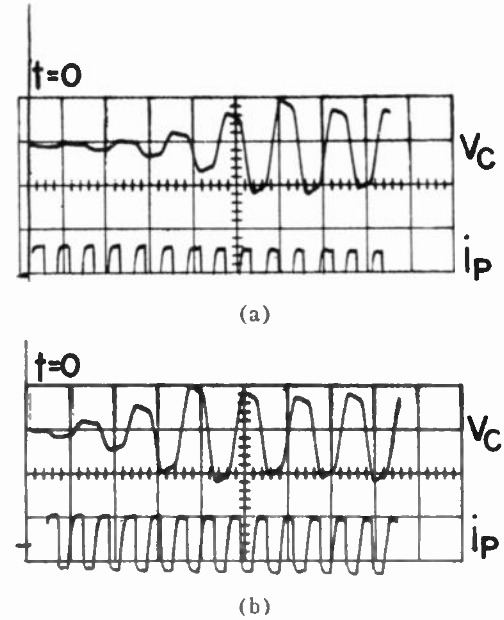

Fig. 12—Experimental transient build-ups, current drive. (a) System energized early in a positive half cycle. (b) System energized early in a negative half cycle. $v_c(0) = 0.1$ volt. Parameters are given in Fig. 9.

Conclusions

A method of analysis has been presented for the second-subharmonic parametric oscillator with nonlinear magnetic components. The system considered embodies two ferromagnetic cores to balance out the pump frequency and its harmonics at the output. The analysis is based on piece-wise linearizations of the magnetic core properties, avoiding the mathematics of nonlinear differential equations. In particular, the extreme idealization chosen dictates certain rules of logic that govern the sequence of events in the operation of the device.

The steady-state operation, with both voltage and current drives, was studied at first in order to determine the values of parameters of the circuit which give rise to the subharmonic oscillation.

For the intended use of the circuit as a binary computer element, the switching transients are of foremost importance. The method of analysis proves convenient in the evaluation of the switching transients in which oscillations are established from rest or are reversed in phase.

The results of the experimentation indicate that the general approach is well suited for this type of problem. At low frequencies, the agreement between predictions and experimental observations is astoundingly good, and at frequencies as high as 3 Mc no significant departures from the analytical predictions have been observed.

It is to be noted that the square-loop idealizations of the magnetic core, with or without hysteresis, exclude any storages of energy in magnetic form and, thus, any exchange of energy between the capacitor and the cores. The operation of the device has been explained without requiring concepts of tuned circuits and inductances of nonlinear elements.

Acknowledgment

The authors wish to thank A. W. Lo for his helpful comments and suggestions in the early stages of this paper.

Properties of Tropospheric Scattered Fields*

N. R. ORTWEIN†, R. U. F. HOPKINS†, MEMBER, IRE, AND J. E. POHL†

Summary—**Tropospheric scatter tests were performed in the Southern California region in conjunction with extensive meteorological measurements. The turbulent spectra were found to be, in the region of interest, proportional to $k^{-5/3}$. In general, the scattered signals were found to agree with the turbulent single scattering model predicted by such a dielectric spectrum.**

Horizontal beamswinging experiments gave a dependence on the scattering angle of $\theta^{-14/3}$. A stronger θ dependence was observed for vertical beamswinging and is explained by a height dependence of the turbulent fluctuation spectra rather than anisotropy. This explanation is further supported by agreement with Booker and deBettencourt aperture-to-medium coupling loss.

A $\lambda^{-1/3}$ wavelength dependence was observed under standard atmospheric conditions. In the presence of weak turbulent layers a $\lambda^{0.9}$ dependence in the lower frequency region was observed and is explained in terms of a frequency dependent layer reflection phenomena. The spectra of the envelope of the scattered signal are also given. They are generally Gaussian in shape with the width dependent upon the range, frequency and scattering angle. Other details of their fine structure are also discussed.

Introduction

Certain general characteristics of microwave fields scattered beyond the horizon by the troposphere are well known. The Rayleigh amplitude distributions, diversity distance and monthly means have been sufficiently well established to allow use of the phenomena in design of communications systems. However, in spite of extensive experimental and theoretical work, considerable disagreement is still present concerning the cause of the phenomena and the relations between such parameters as distance, scattering angle, wavelength, fading rate and the effect called aperture-to-medium coupling loss. Most of the disagreements are due to assumptions concerning the structure of the atmosphere. In addition, the signal envelope power spectrum has received little attention until recently.

During 1957–1959 NEL has conducted a new series of experiments designed to measure these properties of the tropospheric scattering process. Four overwater beyond-the-horizon propagation paths were established using from one to three frequencies in the microwave region. Meteorological measurements were also made simultaneously to relate the atmospheric structure to the observed microwave fields. An airborne refractometer and a captive balloon refractovariometer[1] were used to measure the index of refraction fluctuations, supplemented by special pibals, U. S. Weather Bureau maps, Raobs and Rawind sondes.

Theoretical Considerations

In 1950, Booker and Gordon[2] following the suggestion of Pekeris[3] proposed that the fields observed beyond the horizon in the microwave region could be explained by single scattering from fluctuations in the dielectric constant of the atmosphere. These "blobs" are usually assumed to be isotropic and are assumed to result from the turbulent motion of the atmosphere. Booker and Gordon used the spatial autocorrelation of dielectric constant as a measure of the fluctuations. Several others[4–10] have made the assumption that the Kolmogoroff velocity spectrum determines the spectral function, $E(k)$, which represents these spatial fluctuations. This spectrum is the Fourier transform of the autocorrelation function such as was used by Booker and Gordon.[11] Most of the disagreements in the single scattering theories have to do with the form of this dielectric turbulent spectrum.

Bauer[12] has suggested the signal may be due to reflection from the layers which are observed in most refractive-index height profiles. Friis, Crawford, and

* Received by the IRE, April 4, 1960; revised manuscript received, December 27, 1960.

† U. S. Navy Electronics Lab., San Diego, Calif.

[1] A. L. Crozier, "Captive balloon refractovariometer," *Rev. Sci. Instr.*, vol. 29, pp. 276–279; April, 1958.

[2] H. G. Booker and W. E. Gordon, "A theory of scattering in the troposphere," Proc. IRE, vol. 38, pp. 401–412; April, 1950.

[3] G. L. Pekeris, "Note on the scattering of radiation in an inhomogeneous medium," *Phys. Rev.*, vol. 71, pp. 268–269; February, 1947.

[4] A. D. Wheelon, "Spectra of turbulent fluctuations produced by convective mixing of gradients," *Phys. Rev.*, vol. 105, pp. 1706–1710; March 15, 1957.

[5] F. Villars and V. F. Weisskopf, "On the scattering of radio waves by turbulent fluctuations of the atmosphere," Proc. IRE, vol. 43, pp. 1232–1239; October, 1955.

[6] A. M. Obukhov, "Structure of the temperature field on turbulent flow," *Akad. Nauk. SSSR, Ser. Geograf. i Geofiz.*, vol. 13, pp. 58–69; 1949.

[7] G. K. Batchelor, "The Scattering of Radio Waves in the Atmosphere by Turbulent Fluctuations in Refractive Index," Cornell University School of Elect. Engr., Ithaca, N. Y., Res. Rept. No. EE-262; September 15, 1955.

[8] R. A. Silverman, "Turbulent mixing theory applied to radio scattering," *J. Appl. Phys.*, vol. 27, pp. 699–705; July, 1956.

[9] R. Bolgiano, Jr., "Turbulent Mixing and its Role in Radio Scattering," Cornell University School of Elect. Engr., Ithaca, N. Y., Res. Rept. No. EE 334; April, 1957.

[10] R. Bolgiano, Jr., "The role of turbulent mixing in scatter propagation," IRE Trans. on Antennas and Propagation, vol. AP-6, pp. 161–168; April, 1958.

[11] The dielectric-fluctuation spectrum and the index-of-refraction spectrum will both be referred to as the "turbulent spectrum" $E(k)$. The relation between fluctuations of the dielectric constant $\Delta\epsilon$ and refractive index Δn is $\Delta\epsilon = 2\Delta n$. "Envelope spectrum" here is the spectrum of the envelope of the scattered microwave field and the "RF spectrum" is the microwave carrier-frequency spectrum which is affected by the bandwidth of the medium.

[12] J. R. Bauer, "The Suggested Role of Stratified Elevated Layers in Transhorizon Short Wave Radio Propagation," M.I.T. Lincoln Lab., Lexington, Mass. Tech. Rept. No. 124; September 24, 1956.

Hogg[13] have proposed that reflection from a large number of small layers, or from several portions of a single wavy layer, may account for the fields. From rapid beamswinging experiments, Waterman has observed apparent high velocities of scatterers and has supported the wavy layer concept to explain them.

Several other explanations have been suggested but will not be discussed in detail in this paper. One of the best-known is the normal mode theory of Carroll and Ring.[14] Others include multiple scattering theories by Potter[15] and by Bugnolo.[16] An excellent summary of the theoretical work prior to 1959 is to be found in Staras and Wheelon.[17]

Single Scattering Theory

The single scattering theories characterize the medium by scattering eddies or blobs of dielectric constant ϵ;

$$\epsilon = \epsilon_0 + \Delta\epsilon \tag{1}$$

where ϵ_0 is the mean value and $\Delta\epsilon$ represents time and space variations of ϵ and is usually assumed constant over a blob of size l characterized by its wavenumber $k = 2\pi/l$. The ratio Q of the received power P_r to the free space power P_{FS} is obtained[18] by solving the wave equation in an inhomogeneous medium for the field at the receiver, expressing the solution as a function of the scattering coefficient σ per unit volume per unit solid angle per unit incident power and integrating the scattering coefficient over the common volume V formed by the intersection of the antenna beam patterns. The resulting expression is

$$Q = \frac{P_r}{P_{FS}} = 4D^2 \int_V \frac{\sigma d^3r}{R_t^2 R_r^2}, \tag{2}$$

where R_t and R_r are the distances between the incremental scattering volume d^3r and the transmitter and receiver respectively and D is the total path distance as shown in Fig. 1. The factor of 4 comes from assuming perfect reflection from the earth, as is the case for the completely over-water paths with small incidence angles used in the NEL experiments.

When the scattering blobs are isotropic for each wavenumber k, the scattering coefficient[7] may be written in terms of the spectrum of the dielectric fluctuations $E(k)$ as

$$\sigma = \frac{2\pi^4 \sin^2 x E(K)}{\lambda^4 K^2}. \tag{3}$$

where λ is the electromagnetic wavelength, x is the angle between the incident field and the direction of the line to the receiver and is approximately 90°. K is the value of the wavenumber k at which the spectrum must be evaluated.[19]

$$K = \frac{4\pi}{\lambda} \sin \frac{\theta}{2} \tag{4}$$

where θ is the scattering angle as shown in Fig. 1.

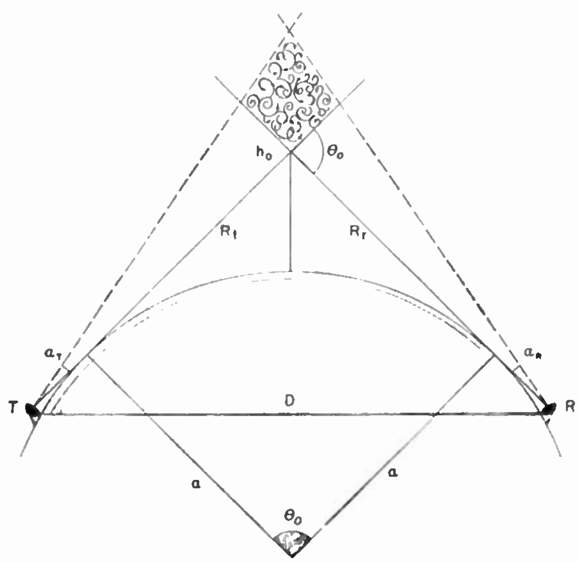

Fig. 1—Tropospheric scattering geometry.

The integral in (2) can be evaluated for two cases of special interest. For the case of narrow beam antennas, the scattering volume is determined by the intersection of the narrow antenna beams. For broad beam antennas, the effective scattering volume of the atmosphere is determined by the scattering process itself.

Narrow Beam Antennas: A narrow beam antenna for tropospheric scattering is usually defined somewhat arbitrarily[20] by the criterion

$$\alpha < \tfrac{2}{3}\,\theta_{\min} \tag{5}$$

[13] H. T. Friis, A. B. Crawford, and D. C. Hogg, "A reflection theory for propagation beyond the horizon," *Bell Sys. Tech. J.*, vol. 36, pp. 627–644; May, 1957.

[14] T. J. Carroll and R. M. Ring, "Propagation of short radio waves in a normally stratified troposphere," Proc. IRE, vol. 43, pp. 1384–1390; October, 1955.

[15] C. A. Potter, "Tropospheric scattering of microwaves," *Proc. Decennial Symp. of ONR*, Washington, D. C., March 19–20, 1957.

[16] D. S. Bugnolo, "A Transport Equation for the Spectral Density of a Multiply Scattered Electromagnetic Field," Columbia University Dept. of Elec. Engrg., New York, N. Y., Tech. Rept. No. T-3/D; November 17, 1959.

[17] H. Staras and A. D. Wheelon, "Theoretical research on tropospheric scatter propagation in the United States 1954–1957," IRE Trans. on Antennas and Propagation, vol. AP-7, pp. 80–87; January, 1959.

[18] W. E. Gordon, "Radio scattering in the troposphere," Proc. IRE, vol. 43, pp. 23–28; January, 1955.

[19] Note the difference between k and K. k is the characterization of the turbulent blobs. K, sometimes called the magnitude of the scattering difference vector, is the wavenumber of the particular blob size most effective in scattering the radio energy to the receiver and is determined by the path properties.

[20] H. G. Booker and J. T. deBettencourt, "Theory of radio transmission by tropospheric scattering using very narrow beams," Proc. IRE, vol. 43, pp. 281–290; March, 1955.

where α is the beamwidth between half-power points either of a transmitting or receiving antenna, and θ_{min} is the minimum scattering angle of the illuminated volume. For smooth earth, on-axis, tangent-ray transmission

$$\theta_{min} = \theta_0 = \frac{D}{a} \tag{6}$$

where a is the earth's radius. If the beams are narrow the effective scattering volume is determined by their pointing angles and free-space beamwidths. The scattering angle, the scattering coefficient and the distances may be assumed constant. Then for identical narrow beam transmitting and receiving antennas, (2) becomes

$$Q_N = \frac{64\sigma}{D^2}\int_V d^3r = \frac{64\sigma V}{D^2}, \tag{7}$$

where

$$R_t = R_r = \frac{D}{2}. \tag{8}$$

The total volume V may be approximated[20] by

$$V = \frac{D^3\alpha^3}{32\theta_0}, \tag{9}$$

and

$$Q_N = \frac{2D\alpha^3\sigma}{\theta_0}. \tag{10}$$

The α^3 factor in the numerator comes from the restriction of the common volume by the antenna patterns and is the cause of the phenomenon called aperture-medium coupling loss. Estimates of this loss may be made from comparison of (10) with (14) for the power received using broad beams.

Broad Beam Antennas: For broad beam antennas defined by

$$\alpha > \tfrac{2}{3}\theta_0, \tag{11}$$

the effective scattering volume is limited not by the antenna patterns but by the angular scattering cross section within the volume. Gordon[18] defines the width $H(\sigma)$ of the scattering volume by a scattering angle θ_1 corresponding to a scattering coefficient equal to half of that for the great circle path. This is analogous to the half-power beamwidth of an antenna. $H(\sigma)$ is given in terms of θ_1 by

$$H^2 = (\theta_1^2 - \theta_0^2)\frac{D^2}{4}. \tag{12}$$

The length Y of the scatter volume as a function of height h is determined by the distance between tangent rays and is given by

$$Y = \frac{4ha}{D}. \tag{13}$$

The incremental volume, d^3r, may then be written as the product of the length, width, and an incremental height dh; and for broad beams the volume integral becomes

$$Q_B = \frac{256a}{D^3}\int_{h_0}^{\infty}\sigma H(\sigma)h\,dh \tag{14}$$

where h_0 is the tangent intersection height and the assumption (8) is again made.

To obtain the received power for either (10) or (14), the spectrum of dielectric fluctuations $E(k)$ must be known to determine the scattering coefficient σ from (3).

The Dielectric-Fluctuation Spectrum $E(k)$: This spectrum is usually divided into the three ranges shown in Fig. 2. The input range characterized by small wavenumbers and large blob sizes corresponds to the region of insertion of fluctuation energy into the spectrum. The energy of the fluctuations is assumed to be conserved throughout the middle portion of the spectrum, called the inertial subrange. The form of the spectrum of the fluctuations in this range is the source of most of the theoretical disagreements. It is important because the wavenumber K at which the spectrum is evaluated as in (3) is located in this region. The fluctuations are finally lost by conversion to heat by the viscous forces in the dissipation range.

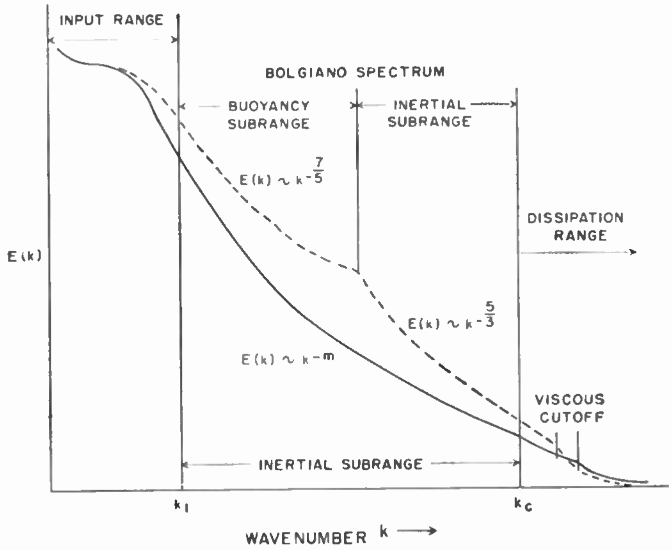

Fig. 2—Dielectric fluctuation spectrum.

The various distributions of the dielectric spectrum proposed for the inertial subrange result from assumptions concerning the generation of the dielectric fluctuations. The dielectric constant of the troposphere is determined mainly by the temperature and humidity, and it is the variations of these properties that is of interest in most cases.

Obukhov[6] and Batchelor[7] obtain the same spectral form for the squares of the temperature and refractive index fluctuations as for the square of the turbulent wind velocity predicted by the universal equilibrium theory.[21] The fluctuations are assumed to result from an impulse disturbance in the input range which decays so that there is no change in the square of the fluctuations throughout the inertial subrange of wavenumber space. Dimensional arguments then lead to a $k^{-5/3}$ dependence for the temperature spectrum $E(k)$. Similar results may be obtained for the humidity spectrum and thus the dielectric-fluctuation spectrum. Bolgiano[10] has treated the more realistic case of continuous input and arrived at the same wavenumber dependence.

Experimental results by Chisholm, Roche and Jones indicate that the way in which the received microwave power in a scattered field depends on electromagnetic wavelength is itself variable with meteorological conditions. Bolgiano[22] has extended his theoretical treatment to include the effects of buoyancy to explain the observed variability. He introduced a buoyancy subrange which separates the input range from the $k^{-5/3}$ inertial subrange. In the buoyancy subrange the spectrum appears to vary as $k^{-7/5}$. The occurrence and extent of the new range is determined by the stability of the atmosphere. The anomalies in the wavelength dependence may thus be attributed to variations of atmospheric stability with a very stable atmosphere yielding a predominant buoyancy subrange with little or no inertial subrange.

Inoue[23] assumes that the temperature fluctuations themselves rather than their squares are conserved and uses the same dimensional arguments to arrive at a $k^{-7/3}$ spectral dependence.

A mixing-in-gradient theory has been proposed[4,5] which treats turbulent convection in an atmosphere with an initial refractive index gradient. For this theory dimensional arguments lead to $E(k)$ proportional to $k^{-9/3}$.

Gordon has evaluated (14) by expressing the scattering coefficient in terms of the exponential correlation function of dielectric fluctuations and a height dependence of the mean-square fluctuations of the dielectric constant

$$\overline{\Delta\epsilon^2} = c_n h^{-n}. \tag{15}$$

for values of n from zero to three where c_n is a constant depending only on n. The same results may be obtained by using (3) for the scattering coefficient and a spectrum varying as $k^{-6/3}$ which is approximated by the transform of the exponential correlation function within the limits of the inertial subrange.

Received Power: Let the spectrum be assumed to be of the form

$$E(k) \sim k^{-m} h^{-n} \tag{16}$$

with the conditions

$$n \geq 0 \qquad m > 0. \tag{17}$$

Then substitution of (16) into (3) to get σ, and then σ into (10) and (14) gives

$$Q_N = \frac{N_{mn}\alpha^3 a^{m+n+3}\lambda^{m-2}}{D^{m+2n+2}} \tag{18}$$

for narrow beams, and

$$Q_B = \frac{B_{mn} a^{m+n}\lambda^{m-2}}{D^{m+2n-1}} \tag{19}$$

for broad beams, where N_{mn} and B_{mn} are constants for given values of m and n.

Even though $\overline{\Delta\epsilon^2}$ is assumed to be constant throughout the volume in the narrow beam case, a greater decrease of received power with antenna elevation angle than with azimuthal angle will be observed if $\overline{\Delta\epsilon^2}$ decreases with height because of the changed height of the scattering volume.

Aperture-Medium Coupling Loss: The ratio of (18) to (19) gives the aperture-to-medium coupling loss L which would be observed[20,24] by changing from broad to narrow beam antennas at both ends of the path.

$$L = \frac{N_{mn}}{B_{mn}}\left(\frac{\alpha a}{D}\right)^3 = \frac{N_{mn}}{B_{mn}}\left(\frac{\alpha}{\theta_0}\right)^3. \tag{20}$$

The aperture-to-medium coupling loss is then dependent on the atmospheric structure only through N_{mn} and B_{mn}. Also

$$\frac{N_{mn}}{B_{mn}} \approx 0.39(m + n). \tag{21}$$

The results of substituting the various forms of spectral dependence into (18) and (19) for the case where $n=0$ are shown in Table I. Parameters such as fading rate and beam broadening which may be predicted by one or more of the theories[25-27] will be discussed in detail with the results of the appropriate NEL experiments.

[21] G. K. Batchelor, "The Theory of Homogeneous Turbulence," The University Press, Cambridge, England; 1953.

[22] R. Bolgiano, Jr., "A Meteorological Interpretation of Wavelength Dependence in Transhorizon Propagation," Cornell University School of Elec. Engrg., Ithaca, N. Y., Res. Rept. No. EE 385; September 15, 1958.

[23] E. Inoue, "On the Temperature Fluctuations in a Heated Turbulent Fluid," Geophysical Notes, Tokyo University, Japan, vol. 3, no. 34, pp. 1–5; 1950.

[24] H. Staras, "Antenna-to-medium coupling loss," IRE Trans. on Antennas and Propagation, vol. AP-5, pp. 228–231; April, 1957.

[25] R. A. Silverman, "Fading of radio waves scattered by dielectric turbulence, *J. Appl. Phys.*, vol. 28, pp. 506–511; April, 1957.

[26] T. Laaspere, "An Analysis and Re-Evaluation of the Role of Horizontal Drift in Producing Fading in Troposphere Scattering Propagation," Cornell University School of Elec. Engrg., Ithaca, N. Y., Res. Rept. No. EE 380; August 31, 1958.

[27] F. Farner, "Signal Strength Distribution and Fading in Tropospheric Scatter Propagation," Syracuse University Res. Inst., Syracuse, N. Y., Tech. Phase Rept. No. 2, Contract AF 19(604)-1179; October, 1956.

TABLE I

	Booker and Gordon Gordon Booker and deBettencourt	Obukhov Batchelor Silverman Bolgiano	Inoui	Villars and Weisshopf Wheelon	Friis, Crawford and Hogg
Characterization of the medium.	Correlation $\rho \sim e^{-r/l}$ $\overline{\Delta\epsilon^2} = c_n h^{-n}$ $E(k) \sim k^{-6/3}$	Spectrum turbulent decay or continuous input $E(k) \sim k^{-5/3}$ Buoyancy subrange $E(k) \sim k^{-7/5}$	Spectrum (ΔT) conserved $E(k) \sim k^{-7/3}$	Spectrum mixing-in-gradient $E(k) \sim k^{-9/3}$	Layer reflection. Many intermediate size layers or a single large wavy layer.
Received power proportional to: (θ is eliminated when $\theta_{min} = \theta_0 = D/a$).	Narrow beams $\lambda^{\circ}(1+(2\theta_1/\theta_0)^2)^{-5/2}$ $\lambda^{\circ} D^{-4}\alpha^3 l^{-1}$ Broad beams $\lambda^{\circ} D^{-2n-1}$	Narrow beams $\lambda^{-1/3} D\theta_{min}{}^{-14/3}\alpha^3$ $\lambda^{-1/3} D^{-11/3}\alpha^3$ Broad beams $\lambda^{-1/3} D\theta_{min}{}^{-5/3}$ $\lambda^{-1/3} D^{-2/3}$ Buoyancy subrange λ^{-1} to λ^3	Narrow beams $\lambda^{1/3} D\theta^{-16/3}$ $\lambda D^{-13/3}$	Narrow beams $\lambda D\theta_{min}{}^{-6}$ λD^{-5} Broad beams $\lambda D\theta_{min}{}^{-3}$ λD^{-2}	Narrow beams $\lambda\theta^{-4}(\alpha/\theta)$ $\times(2+\alpha/\theta)^{-1} f(\alpha/\theta)$ $\sim \lambda D^{-4 \text{ to } -5}$ See (22) and (23).

The symbols are defined in the text with the exception of: T, Temperature; ρ, the space correlation function of the dielectric constant, and $l = 2\pi/k$, the blob size.

Layer Reflection

Friis, Crawford and Hogg[12] have computed the scattered field reflected from a large number of layers of limited dimensions which are located randomly in position and orientation. The received field Q relative to freespace is given by

$$Q = \frac{4M\lambda}{3\theta^4} \frac{(\alpha/\theta) f(\alpha/\theta)}{(2 + \alpha/\theta)} \tag{22}$$

where M is a function of the height, size and number of layers, and the change in atmospheric gradient at the tangent intersection which represents the effects of atmospheric structure and

$$f(\alpha/\theta) = 1 + \frac{1}{(1 + \alpha/\theta)^4} - \frac{1}{8}\left(\frac{2 + \alpha/\theta}{1 + \alpha/\theta}\right)^4. \tag{23}$$

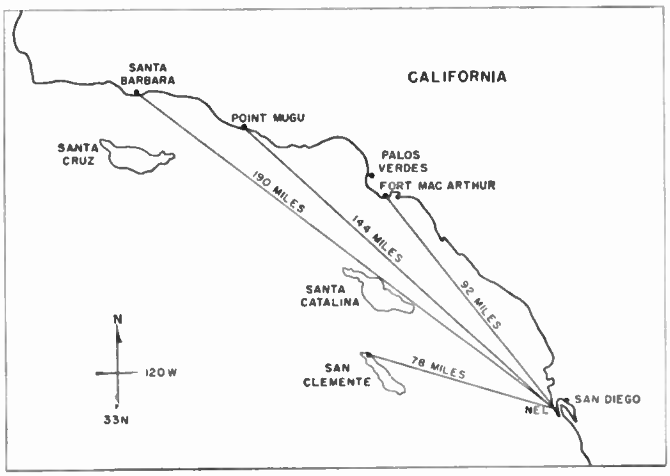

Fig. 3—NEL operations area for tropospheric scattering experiments.

INSTRUMENTATION

The station complex used for the NEL microwave beyond-the-horizon scattering experiments is shown in Fig. 3. All microwave receiving and recording instrumentation was located at the NEL Electromagnetic Propagation facility on Point Loma. The four transmitting stations were located at Santa Barbara, Point Mugu, Fort McArthur and San Clemente Island providing completely overwater transmission paths of 190, 144, 92 and 78 miles. The meteorological station at Palos Verdes controlled a captive balloon which lifted the NEL refractovariometer to the height of the scattering volume during the experiments. An airborne cavity refractometer was also flown along the transmission paths. All transmitting stations as well as the meteorological station were packaged in trailer vans.

Measurements were made using X, S and L bands with antenna diameters ranging from 1.5 to 28 feet. Table II summarizes the combinations of path, frequency and antenna size for each path.

Fig. 4 is a block diagram of the microwave system. Transmitters with peak powers between 75 and 200 kw were modulated with one microsecond pulses at the common rate of 500 cps. All receivers were time-gated by a system synchronizer to minimize interference from radars operating in Southern California. Width and relative delay of the gate for each path were individually adjustable. The type of receiver used was designed by NEL to provide an output voltage which is linearly related to the microwave field seen by the antenna. Linearity of better than 0.3 db was achieved over a 30-db range with corresponding sensitivity of 95–98 dbm for 6–8 Mc bandwidth. The IF strips were operated at constant gain and receiver gain was adjusted by precision calibrated attenuators in the waveguide prior to mixing.

TABLE II

CHARACTERISTICS OF NEL TROPOSPHERIC SCATTER LINKS

Location	Total distance from NEL (miles)	Effective path distance* (miles)	θ_0† degree	Frequency (Mc)	Antennas size (feet)	Antennas α (degree)	Freespace fields DBM	Year
Santa Barbara	190	165	1.79	*X*-Band 9365	10	0.78	− 0.6	1958
							+ 1.7	1959
					4	2.08	−12.7	1959
				S-Band 3406	10	2.1	− 1.8	1959
				L-Band 1365–58	10	5.2	− 7.9	1958
				1250–59	28	1.85	+ 5.4	1958
							+ 7.3	1959
Point Mugu	144	118	1.28	*X*-Band	10	0.78	− 8.1	1958
				L-Band	10	5.2	− 5.5	1958
Fort MacArthur	92	63	0.68	*X*-Band	10	0.78	+ 7.1	1959
					1.5	4.9	−21.4	1959
San Clemente	78	35	0.34	*X*-Band	6	1.26	+ 3.5	1958
					1.5	4.9	−20.4	1958
Palos Verdes	101	Location of refractovariometer						1958

* The effective distance is the total distance minus the horizon distances.
† θ_0 is calculated using effective distances and a 4/3 earth radius.

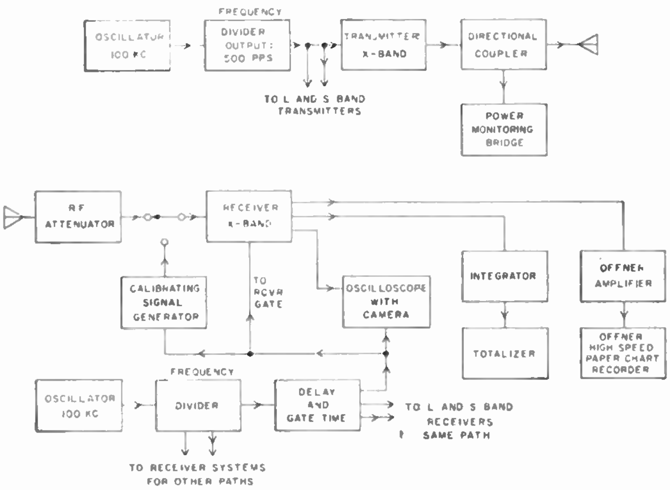

Fig. 4—Block diagram of experimental tropospheric scatter system.

The pulse train from detector output was passed through a peak reader with a time constant of several milliseconds and then recorded on Offner paperchart recorders to provide a continuous record of the envelope of the signal. These recorders have a flat frequency response from dc to approximately 30 cps for full-scale pen deflection.

Because scattered fields are characterized by rapid random fluctuations in amplitude which may be as much as 20 db relative to the mean signal amplitude, it is often difficult to obtain rapid and reliable estimates of the short term mean-signal amplitude. A special digital integrator designed by NEL providing an output display as a number on a mechanical counter was used to provide arithmetic means of field strength averaged over one-minute samples. The integration time over which the sample was averaged was simply the interval during which the integrator was turned on. The one-minute sample was chosen for convenience. This integrator received the output of the peak reader and provided an immediate estimate of the signal mean in convenient form.

The data recorded on the paper charts were converted to digitized form on punched cards by using a Telereader. The punched-card decks are in a form accepted by Datatron 205 and 220 computers for processing. The Datatron was programmed to determine the sample means (furnishing corroboration for the means given by the integrator), number of mean crossings per unit time (fading rate), cumulative distribution, and finite-sample estimates of the autocorrelation function and power spectrum. The techniques of data sampling and processing are described by Potter[28] based on smoothing functions discussed by Blackman and Tukey.[29]

Data were recorded in the months from January to July in 1958 and again in 1959 on the few days when tropospheric scattering was a significant mechanism for beyond-the-horizon propagation. Because a stable atmosphere with strong layers and elevated ducts

[28] C. A. Potter, "Information Recovery from Finite-Sample Fluctuation Data," U. S. Navy Electronics Lab., San Diego, Calif., NEL Rept. No. 831; February 25, 1958.

[29] R. B. Blackman and J. W. Tukey, "The measurement of power spectra from the point of view of communications engineering," *Bell Sys. Tech. J.*, vol. 37, pp. 185–282; January, 1958. (Also published by Dover Books, S507.)

normally exists over Southern California, suitable meteorological conditions occur only after the passage of frontal activity has wiped away these layers and persists for only hours or a few days at most. The experimental technique involved massive data collection during these relatively short and infrequent scattering periods and provided data on overwater scattered fields unobtainable in any other way. The behavior of the received signal as the front passes across the path and the transition from trapping by layers or ducts to scattering is discussed by Moler and Holden.[30]

The refractovariometer provided measurements of refractive-index fluctuations with time at a point in the scattering region. The fluctuations were recorded at the Palos Verdes station on Offner paperchart recorders and later processed similarly to the microwave envelope fluctuation data to provide autocorrelation functions and power spectra. Mean winds aloft, temperature, humidity, and refractovariometer altitude were recorded. The refractive index profiles obtained along the path by the airborne cavity refractometer were also recorded using Offner recorders. Refractive index spatial fluctuations measured by the cavity refractometer were processed to provide autocorrelation functions and power spectra for comparison with the single-point refractovariometer results.

Synchronized Beamswinging

Synchronous beamswinging of transmitting and receiving antennas such as suggested by Booker and deBettencourt[20] is an attractive method for studying the tropospheric scatter mechanism since it is easy to do and involves the measurement of only relative signal amplitudes. The main requirement of the experimental configuration is that the antenna beamwidth be small compared to the scattering angle θ. [See (5).]

The 1958–59 NEL experiments were designed to include such synchronized beamswinging experiments. Numerous synchronous azimuthal scans were performed during 1958 simultaneously on the 190, 144 and 78 mile paths using antenna dishes of 95 λ diameter. In 1959, simultaneous beam-swinging measurements were made on the 190 mile path and on the 92 mile path to Fort McArthur accompanied by considerably more extensive airborne refractometer measurements. The higher signal levels received on the short 92 mile path permitted wider angular deviations from the great circle antenna orientation.

Patterns of the average signal level were obtained for one-minute integration periods at 0.5° intervals by swinging from the maximum angle on one side of the great circle path in steps of 1° to the maximum on the other side and then repeating the scan at the intermediate 0.5° angles. Only the patterns whose average signal strength on the great circle bearing remained substantially constant for the 20-minute period required to obtain a pattern are reported.

Microwave refractometer measurements of the index-of-refraction fluctuation spectra as a function of height were made at the middle of the propagation path as well as the usual profiles. The results of the meteorological measurements have been reported by Gossard.[31] Those spectra required for interpretation of the propagation data are reproduced in Figs. 5 and 6.

Microwave refractometer index-of-refraction profiles are shown in Fig. 7. The data shown in Fig. 5 taken on February 12 were obtained during the period between the two index profiles measured at 1321 and 1430 hours. The slightly turbulent layer which is evident between two and three thousand feet had little effect on the field-strength measurements on the 92-mile path since the antenna product pattern was 6 db below the maximum at 2000 feet. The average field strength was observed constant within ± 1.5 db from 1100 until after 1600 that day. Thus even fairly strong elevated inversions had little effect on the fieldstrength during horizontal beamswinging. However vertical beamswingings were strongly effected by elevated inversions as observed on several of the profiles (February 9 and 10, March 23). Fig. 5 shows a series of index-of-refraction fluctuation power spectra at various altitudes also taken on February 12. Note that over at least a decade of wavenumbers, the data indicates that the atmosphere was characterized on this day by a spectral dependence of $k^{-5/3}$. The ranges of k computed from (4) for the 92-mile path at X-band and for X, L and S wavelengths on the 190-mile path are indicated along the abscissa. It has been pointed out by Gossard[31] that the spectra taken at various altitudes tend to coincide at high wavenumbers and to diverge at low wavenumbers.

Little is known experimentally about the behavior of the spectra for wavenumbers greater than about 2 per meter. However, it is reasonable to assume when the slope of the turbulent spectra and of the angular scattering crosssection $Q(\theta)$ are both smoothly varying and well-behaved that the spectra may be extrapolated to somewhat higher wavenumbers than could be measured. In Fig. 6, turbulent spectra for February 9 and 10 appear to reverse slope and increase with increasing wavenumber for k greater than 1 per meter. This effect appears in about half of the turbulence spectra but is not confirmed by the behavior of $E(k)$ inferred from the measurements of $Q(\theta)$.

The energy in the turbulent spectrum is eventually dissipated by viscosity, but the scale size at which this occurs is not evident from the measured spectra. Since the received power continues to vary nearly with $\theta^{-14/3}$

[30] W. F. Moler and D. B. Holden, "Tropospheric Scatter Propagation and Atmospheric Circulation," *NBS J. of Res.*, Section D, Radio Propagation, vol. 64D, pp. 81–93; January, February, 1960.

[31] E. E. Gossard, "Power spectra of temperature, humidity and refractive index from aircraft and tethered balloon measurements," IRE Trans. on Antennas and Propagation, vol. AP-8, pp. 71–90; March, 1960.

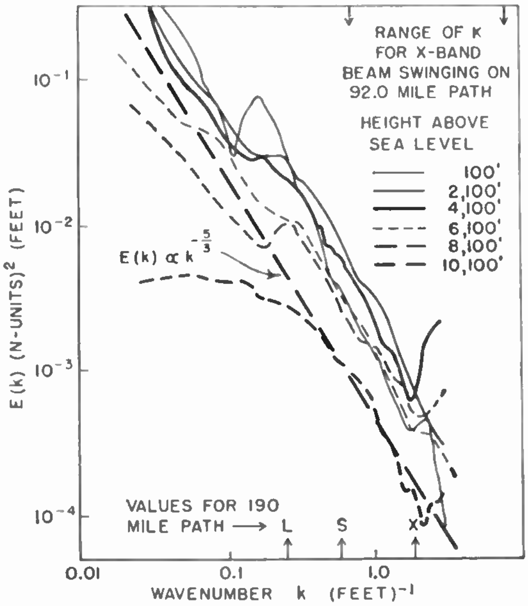

Fig. 5—Index of refraction fluctuation spectra taken from airborne refractometer data, February 12, 1959.

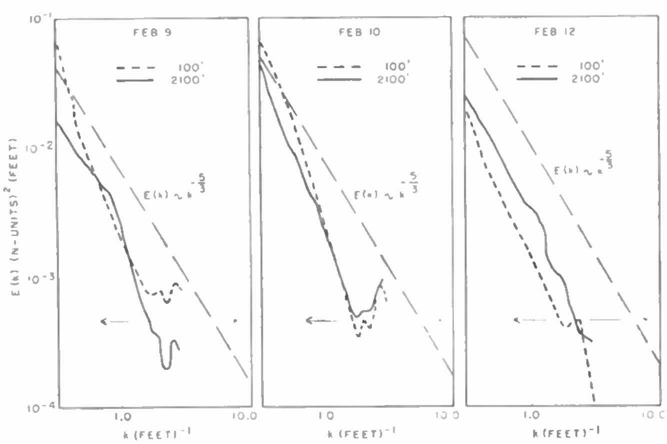

Fig. 6—Index of refraction fluctuation spectra taken with airborne refractometer at 100 and 2100 feet under different weather conditions. Partial layering on February 9 and 10 with no layering on February 12. The range of K for horizontal beamswinging on the 92-mile path are indicated by the double arrows.

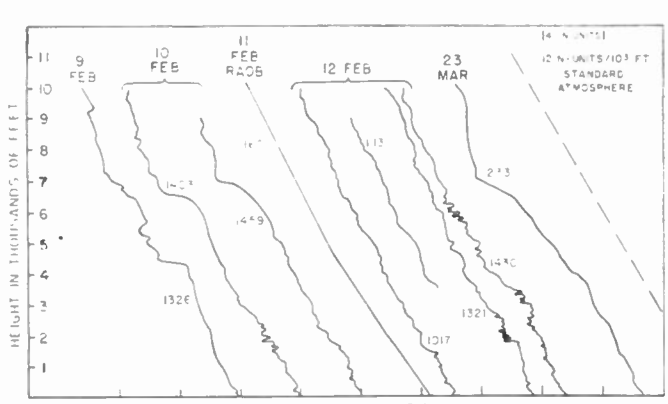

Fig. 7—Refractive index profiles. All profiles except the February 11 Raob were obtained using an airborne microwave refractometer.

for wavenumbers as large as 40 per meter, viscous cutoff is presumed to occur at some higher value of k, probably at a scale size of less than 0.4 feet.

An example of a typical beamswinging pattern is shown in Fig. 8. The sidelobes of the multiplied antenna pattern measured in free space were below the noise level. The predictions of Booker and deBettencourt are applicable in this particular example for off-axis angles greater than 2° but not near the great circle bearing since the antenna beamwidths used are not small compared to the minimum scattering angle.

Since scattering theories indicate a simple power law variation of received signal with scattering angle, a log-log presentation is used to obtain the exponent by slope matching. Fig. 9 shows two horizontal patterns at different elevation angles. This figure also shows a power-law curve for the exponent of the scattering angle which best matches the slope of the data. The experimental

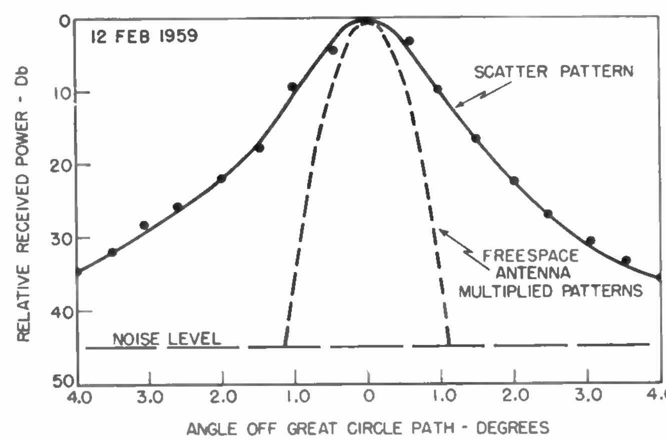

Fig. 8—X-band synchronized beamswinging pattern for the 92-mile path.

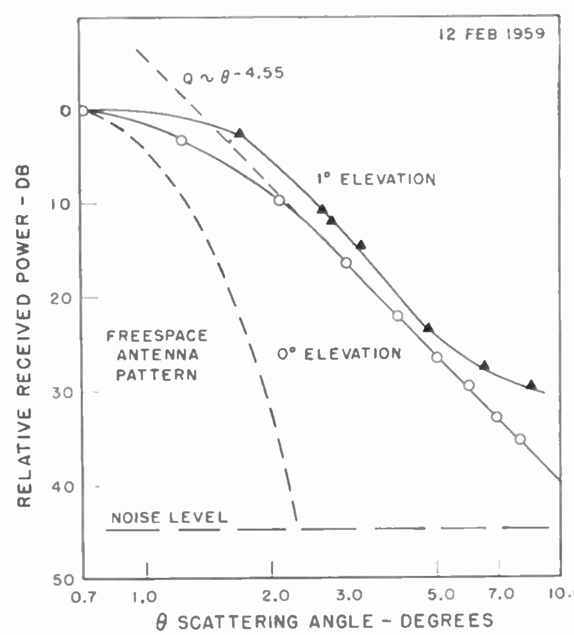

Fig. 9—X-band received power vs scattering angle with tangent ray and elevated antennas on 92-mile path.

curves in the figure have not been normalized and may be compared directly in magnitude. The slope of best fit ($Q \sim \theta^{-4.55}$) for the horizontal curves is very close to the exponent of -4.67 for θ corresponding to a turbulent spectrum proportional to $k^{-5/3}$, shown to exist at the time in Fig. 5. The break in slope near 6° on the tail of the horizontal scan at 1° elevation has not been resolved.

Day-to-day temporal changes have been observed in the angular scattering cross section $Q(\theta)$ which correspond to changes in the turbulent spectra. Fig. 10 shows horizontal beamswinging data which corresponds to the spectra in Fig. 6 taken at 100 and 2100 feet on the same three days. These measurements define the upper and lower boundaries of the common volume at midpath. Meteorological conditions at altitudes much above 2100 feet were not effective on the 92-mile path.

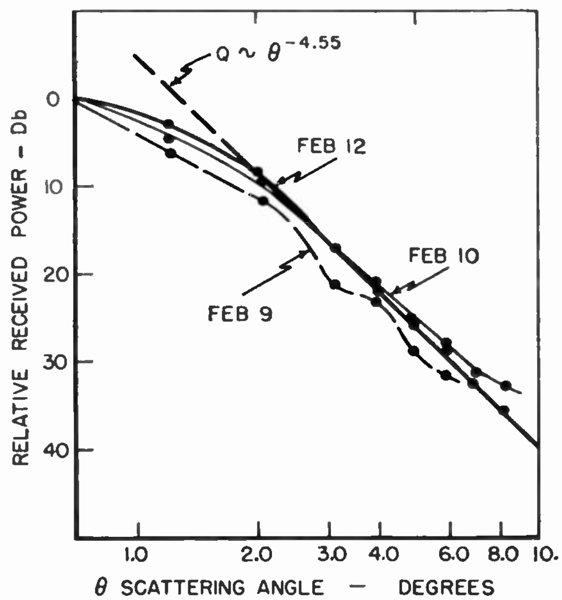

Fig. 10—X-band received power vs scattering angle on 92-mile path.

On February 9 and 10, there was a slight but definite tendency for the exponent of θ to decrease with increasing θ as would be expected from the behavior of the tails of the $E(k)$ curves for these days shown in Fig. 6. On February 12, the spectra closely followed $k^{-5/3}$ and the X-band angular cross section exhibited the expected $\theta^{-14/3}$ form.

The X-band beamswinging experiments on the 190, 144 and 78 mile paths showed a variability in the exponent of θ ranging from -3.0 to -4.5. Figs. 11–13 show curves corresponding to the maximum and minimum observed values of the exponent for each of the three paths. From these figures it may be seen that the range of the exponent is nearly the same for the two longest paths and that $-14/3$ represents a limiting value for all paths. Similar results using L band on the 190-mile path with different aperture sizes are also shown in Fig. 11.

On the 78-mile path the antenna beamwidth is several times larger than the minimum scattering angle so that for scattering angles less than the free-space beamwidth (about 3.5°), the slope is considerably different from that for an exponent of $-14/3$. However, when the narrow-beam criterion is satisfied the slope becomes constant and $Q(\theta)$ varies as $\theta^{-14/3}$, as predicted.

The results of vertical beamswinging experiments performed under various meteorological conditions are shown in Fig. 14 with a curve calculated by using the turbulent spectra for February 12. The computed curve of Fig. 14 has been normalized to the data at an elevation angle of 1.5° above which sea reflection effects are negligible. The dependence of received power on vertical scattering angle is greater than for horizontal scattering indicating that either the index-of-refraction fluctuations are diminishing with height or that the blobs are anisotropic.[32] A simple height dependence of the turbulent spectra such as observed in Fig. 5 is sufficient to explain the increased slope without recourse to anisotropic blobs.

On one other occasion (February 19) the results of vertical beamswinging were nearly the same as on February 12. No refractometer data was taken on the 19th, but radiosonde measurements indicated that no inversion layers existed at the time. The other three vertical patterns shown in Fig. 14 (February 9, 10, and March 23) were obtained on days when definite inversion layers were present as shown by the index profiles in Fig. 7. Enhancement of the microwave signal level greater than 15 db may occur when the antenna beams intersect at the height of the inversion, but is not present on days when the beams intersect at high angles in a well mixed atmosphere. The signal enhancement is believed to result from enhancement of the turbulent spectrum by mixing-in-gradient effects in the inversion rather than from specular reflection by the layer.

When scattering from atmospheric turbulence is the dominant mode of propagation, the results of the synchronized beamswinging experiments indicate that the dependence of the received fieldstrength on the scattering angle is predictable from the power density spectrum of the dielectric fluctuations. This conclusion is supported by the following observations:

1) On February 12, the dielectric fluctuation spectrum was measured to vary with $k^{-5/3}$, and the dependence of the received field strength on the horizontal scattering angle was $\theta^{-14/3}$.
2) On February 12, the dependence of the received fieldstrength on the vertical angle was greater than for the horizontal and agreed with that calculated from the measured height dependence of the dielectric fluctuation spectrum.

[32] S. O. Rice, "Statistical properties of a sine wave plus random noise," *Bell Sys. Tech. J.*, vol. 27, pp. 109–157; January, 1948.

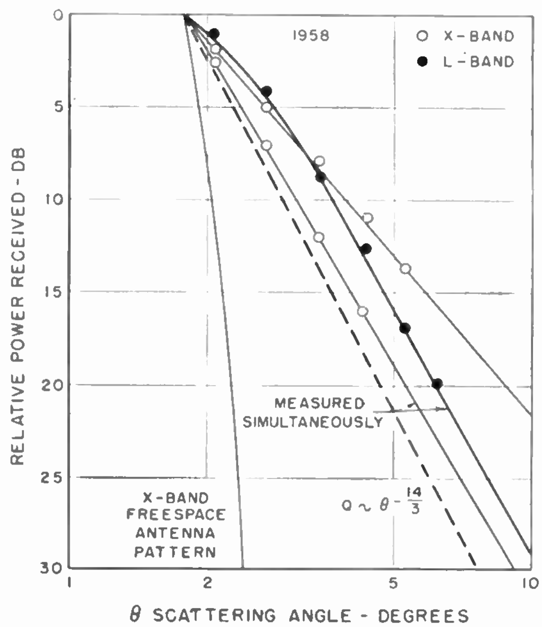

Fig. 11—Received power vs scattering angle over 190-mile path showing maximum and minimum observed slopes at X-band and one L-band beamswinging.

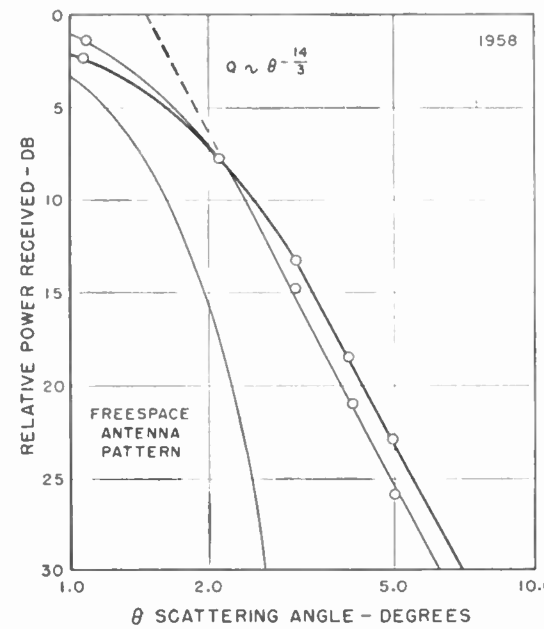

Fig. 13—X-band received power vs scattering angle on 78-mile path.

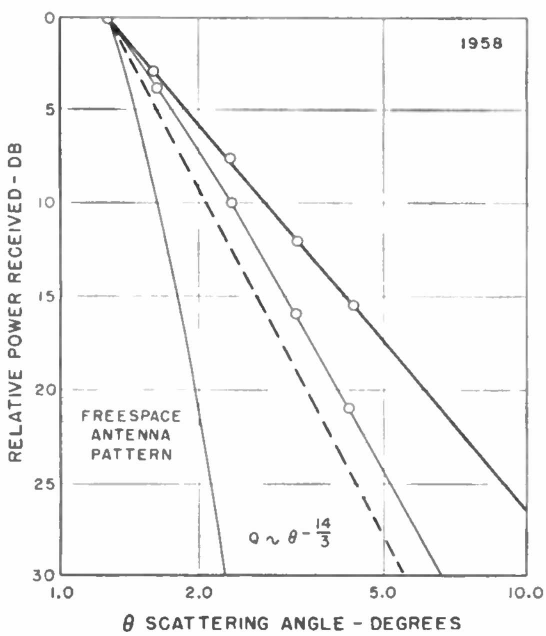

Fig. 12—X-band received power vs scattering angle over 144-mile path showing maximum and minimum slopes.

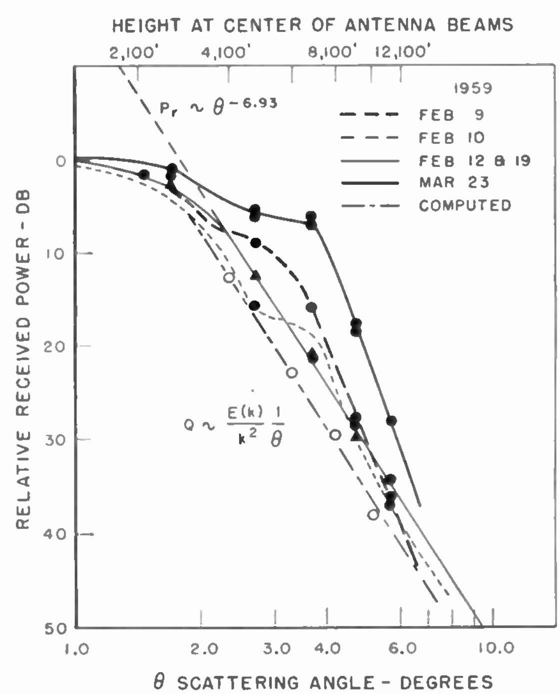

Fig. 14—X-band received power vs scattering angle for vertical beamswinging on 92-mile path under various meteorological conditions.

3) The greatest dependence of fieldstrength on scattering angle for many measurements on all paths was $\theta^{-14/3}$, and it always occurred on days with well mixed atmospheric conditions.
4) The same dependence of fieldstrength on scattering angle was observed for a simultaneous measurement on L-band and X-band yielding the value of $\theta^{-14/3}$. This implies consistance between overlapping regions of the dielectric fluctuation spectrum.

Multiple-Frequency Measurements with Equal Beamwidths

Theory predicts that the amplitude of the scattered field is a function of wavelength. Estimates of the wavelength factor range from $\lambda^{-1/3}$ to λ (Table I). Bolgiano's proposal of the buoyancy subrange was due to the distribution of wavelength dependence obtained by Chisholm at both 417 Mc and 2290 Mc, using antennas of equal beamwidth at both frequencies.

The NEL experiments on the 190-mile path extended measurements of the wavelength dependence to include the X-band region; 1250 Mc, 3406 Mc, and 9365 Mc were measured simultaneously on this path. Antennas with 2° beamwidth between 3-db points were used on all three frequencies to illuminate the same common volume. The difference in db of the signals received (in db below free space) at two frequencies was used to estimate the dependence on frequency between the two frequencies. The notation X-S, X-L, S-L refers to this "difference."

The one-minute averages of the received signals recorded on all three frequencies on February 11 and 12, 1959 are shown in Fig. 15 as a function of time of day. The cumulative distributions of the average differences $X-S$, $X-L$, and $S-L$ are given in Figs. 16 and 17 for February 11 and 12, in terms of the wavelength dependence n. Fig. 18 shows the medians, 0.10 and 0.90 limits of the cumulative distributions of the short-term averages for each day. The median values of a distribution reported by Chisholm are shown in Fig. 18 normalized to the median of the L-band data for comparison. The anomalies apparent in Fig. 18 are believed due to effects of the atmospheric structure.

Strong frontal activity with heavy rains on February 11 grounded the aircraft flying the microwave refractometer and prevented measurements of the turbulent spectra and profiles. However, the Raobs shown in Fig. 7 indicate that a standard atmosphere existed during that day. The refractive index profiles and turbulent spectra measured on February 12 are shown in Figs. 5 and 7.

The expected fieldstrength for February 12 calculated from the spectra of Fig. 5 using (19) is indicated by the open circles in Fig. 18. The calculated values are near the measured medians indicating wavelength dependence nearly proportional to $\lambda^{-1/3}$, as is expected for a turbulent spectrum with $k^{-5/3}$.

Comparison of predictions with the data for February 12 suggest either a dominant layer reflection phenomena or mixing-in-gradient (both give Q as directly

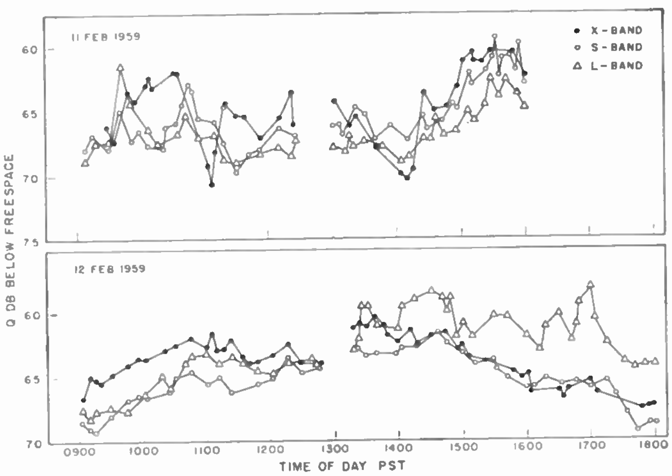

Fig. 15—Average received power vs time of day over 190-mile path using broad scaled beam antennas.

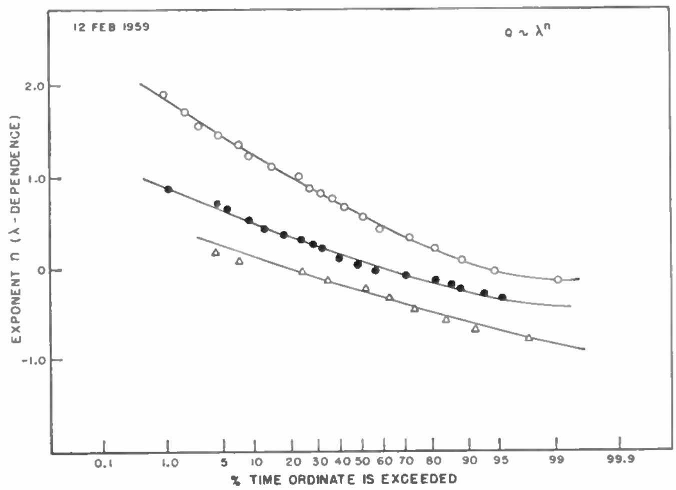

Fig. 17—Wavelength dependence vs per cent of time observed over the 190-mile path using broad scaled-beam antennas.

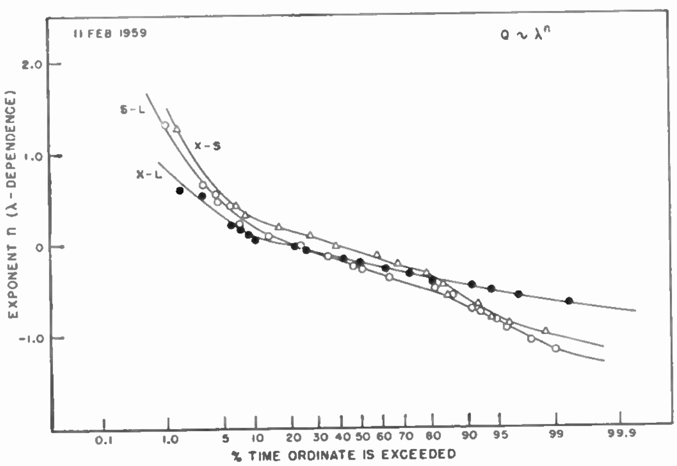

Fig. 16—Wavelength dependence vs percent of time observed over the 190-mile path using broad scaled-beam antennas.

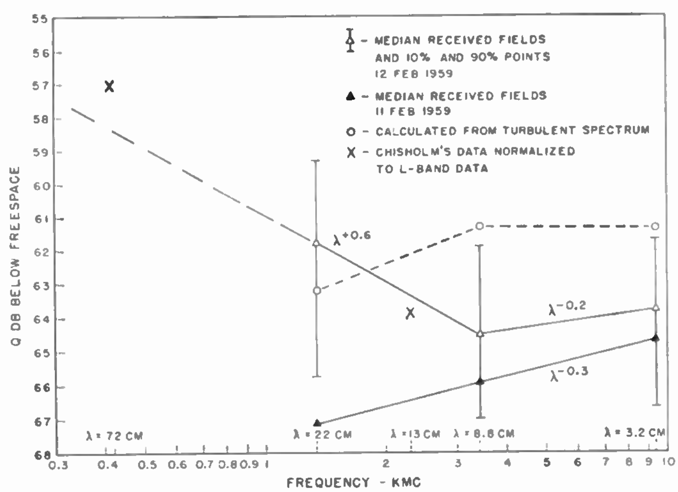

Fig. 18—Received power vs frequency.

proportional to λ) for the lower microwave frequencies and turbulent single scattering at higher frequencies. The $\lambda^{-0.3}$ dependence observed on the 11th followed the passage of a frontal zone which left an unstable standard atmosphere with no layering. Turbulent scattering was the dominant mode of propagation. The *L*-band field-strength increased in the afternoon of the 12th with the onset of a turbulent layer but the *S*-band and *X*-band signals remain unchanged. Data from the morning of February 12 indicated a $\lambda^{0.4}$ dependence when there were slight irregularities in the profile but a $\lambda^{0.9}$ dependence was observed in the afternoon when the turbulent layer had become more established. Little change was noted in the *S*-band and *X*-band signals on February 12.

The Microwave Envelope Spectrum

The random fluctuations in time of microwave fields scattered by the troposphere which have been observed are rapid compared to the slow fading resulting from layers or other multipaths but are extremely slow compared to the period of the microwave carrier frequency. They are observed as envelope fluctuations in the same general domain as refractive index fluctuations. Little is known of fluctuations at or near the carrier frequency at present.

The envelope signal contains information which may be related to the turbulence of the medium. Statistical functions of varying degrees of complexity can be used to characterize the random process of short-term envelope fluctuations. Estimates of these functions formed from sampling the received signal for a finite time can be formed.[28]

The first order probability function for envelope fluctuations is usually considered to follow a Rayleigh distribution. But for cases of mixed meteorological regimes when both scattering and reflection from layers (possibly broken) are present, the observed distribution may not be Rayleigh. In general, unless meteorological measurements indicate a standard well-mixed atmosphere free of layers at the time the microwave data is taken, the characteristics of pure scattered fields are difficult to estimate from the data. The occurrence of Rayleigh fading provides an additional indication of nearly pure scattering conditions.

More emphasis was placed on second-order functions such as finite-sample estimates of correlation functions and power spectra. These functions provide somewhat more insight into the process than the simple probability distribution. Spectra of the envelope fluctuations were obtained for combinations of range, frequency and scattering angle.

Examples of envelope spectra $U(f)$ are shown for data from March 7, March 28, 1958 and February 12, 1959. The antennas used in 1958 were 0.78° narrow-beam dishes on the 190- and 144-mile paths and 1.26° broad-beam dishes on the 78-mile path. In 1959, 2° broad-beam antennas were used on all three frequencies on the 190-mile path.

Some examples of *X*-band envelope correlation functions obtained on the afternoon of March 28, 1958 are shown in Fig. 19. The envelope spectra obtained from transforms of the correlation functions are shown in Fig. 20, which also includes *L*-band spectra which were obtained simultaneously. All spectra are normalized at zero frequency. The 0.90 confidence limits which are given in one case are approximately the same for all envelope spectra shown.

The spectra obtained on the February 12, 1959 equal-beamwidth multiple-frequency experiments are shown in Fig. 21. Figs. 22–24 show spectra for horizontal off-axis angles for the three paths in operation in 1958. Usually the spectra can be well-fitted by a Gaussian curve within the 0.90 confidence limits but occasionally an exponential gives a better fit.

Hogg and Lowry have shown that the spectrum approaches a Gaussian curve with a "standard deviation" proportional to the frequency, for the case of a large number of layers drifting across the path with the mean wind. A similar result is given by Rice[32] for the sum of a sine wave and random noise. An increase in the spread of the carrier spectra with distance was predicted by Laaspere.[26] An increasing spread with distance of the envelope spectra has been predicted quantitatively by Potter[15] and also by Bugnolo,[16] both using multiple scattering models.

An unexpected result appears in the log-log presentation of spectra shown in Fig. 25. In more than half of the cases, the tails of the spectra appear to follow a different power law at higher spectral frequencies rather than the initial Gaussian or exponential curve. Occasionally this frequency region is clearly divided into two subregions, each with a different exponent. The middle region is characterized by $U(f) \sim f^{-3}$ where the 3 is an average value of the exponent for all cases. The end of the tail (when distinct from the middle region) followed a power law form with a slope varying from -4 to -6 with an average value of -5.1.

In Fig. 25, f_b is the frequency at which the final tail starts. In Fig. 26, f_b is shown as a function of the maximum Doppler frequency f_d expected from the drift of the "scatterers" with the mean wind w across the volume defined by the antenna beamwidths.

$$f_d = \frac{2\alpha w}{\lambda}. \tag{24}$$

The mean wind velocities were obtained by averaging the normal components of the wind velocities in the lower 1000 meters of the scattering volume as reported by the U. S. Weather Bureau.

The correlation coefficient ρ_0 between f_d and f_b from Fig. 26 was 0.26. This weak correlation does imply some

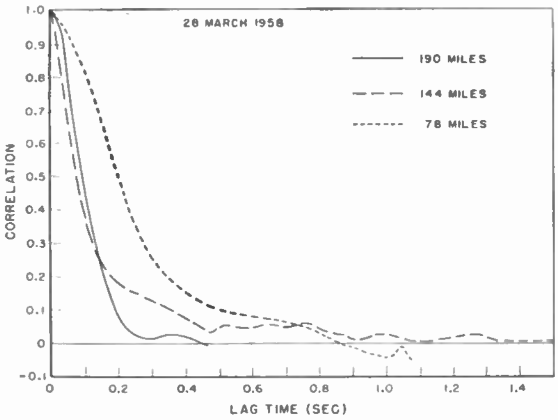

Fig. 19—X-band envelope correlation functions of scattered fields.

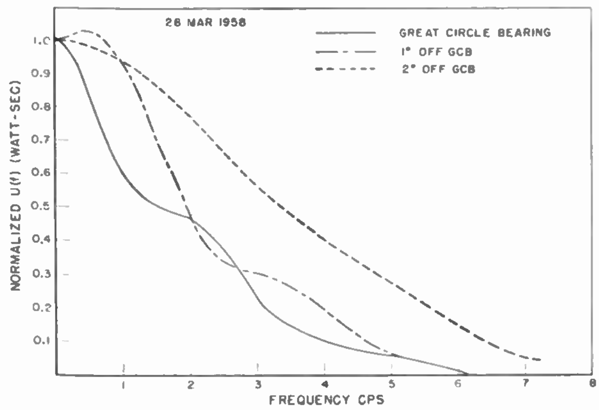

Fig. 22—X-band envelope spectra during beamswinging tests on 190-mile path.

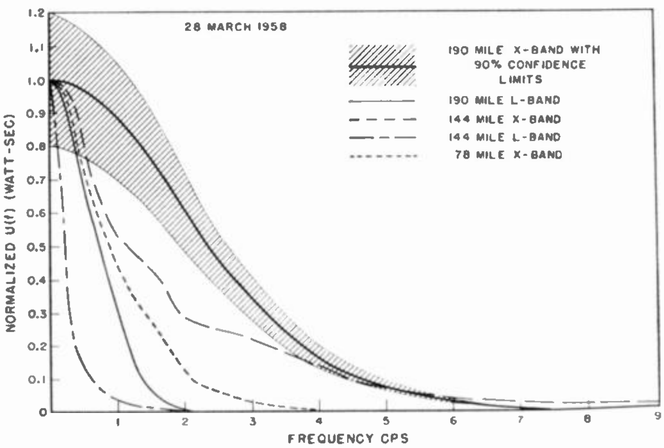

Fig. 20—Envelope spectra of scattered fields.

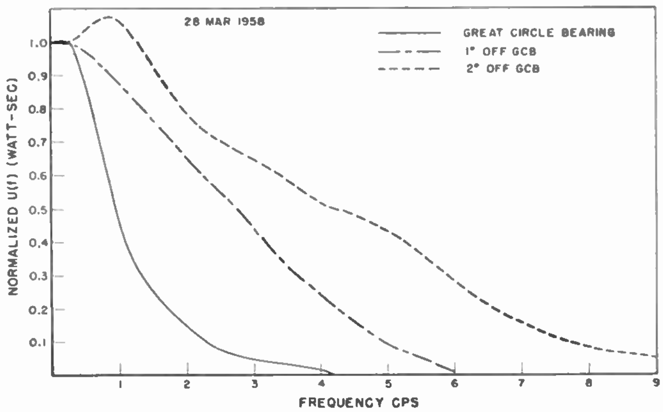

Fig. 23—X-band envelope spectra obtained during beamswinging tests on 144-mile path.

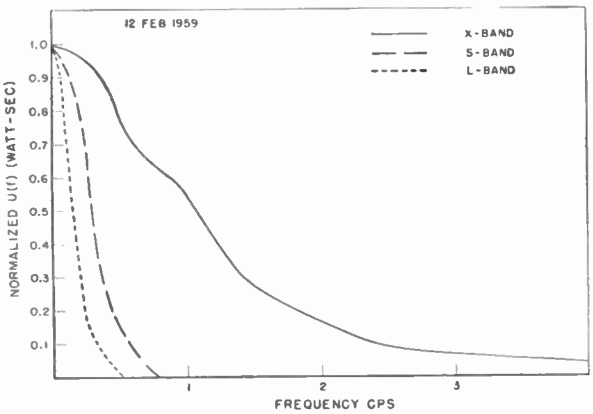

Fig. 21—Envelope spectra of scattered field with broad scaled-beam antennas on a 190-mile path.

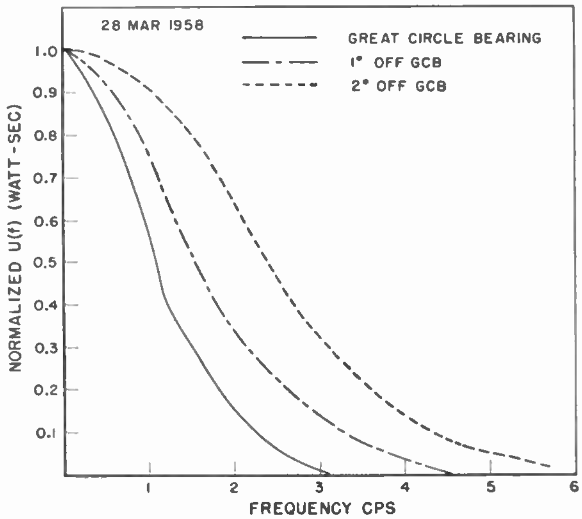

Fig. 24—X-band envelope spectra obtained during beamswinging tests on 78-mile path.

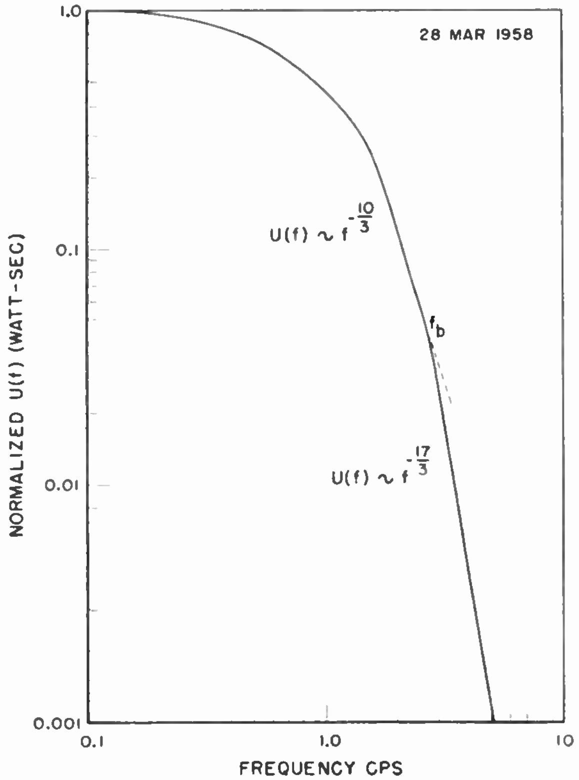

Fig. 25—X-band envelope spectrum of 78-mile path demonstrating the three regions observed. The middle region is often missing.

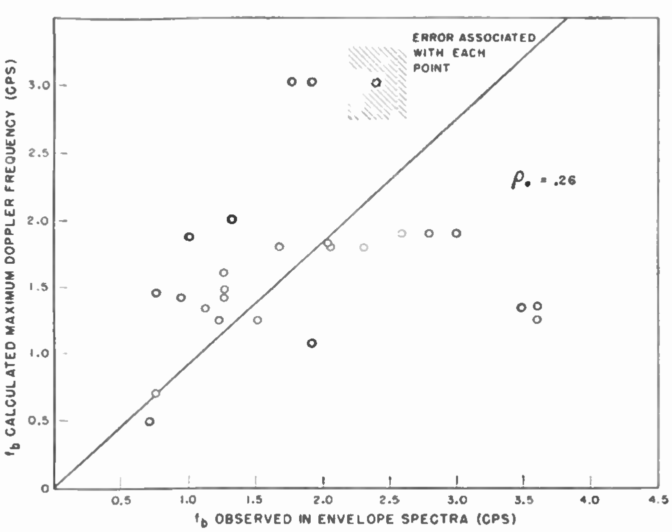

Fig. 26—Scatter plot of calculated maximum Doppler frequency vs beginning frequency of the upper region of the envelope spectra.

indication of Doppler shifts caused by a drift of the scatterers with the mean wind. This result was predicted in a different manner for Booker-Gordon single-scattering by Laaspere[26] from consideration of the shape of the carrier frequency spectrum alone. No definite relation has been discovered relating the occurrence of f_b to atmospheric conditions. However, the effect was less noticeable in the L-band spectra. If the small amount of energy in the portion of the spectra above f_b is due to turbulence, the spectrum of the signal being propagated by some other mechanism (L-band layer reflection) would not be expected to have such a tail.

Aperture-to-Medium Coupling Loss

Narrow-beam antennas restrict the size of the scatter volume preventing a system from realizing the total gain of the antennas. This loss of system gain is termed aperture-to-medium coupling loss. Broad-beam antennas do not restrict the scattering volume and exhibit no coupling loss. Thus a comparison of the signal received using a pair of narrow-beam antennas to that received with a pair of broad-beam antennas gives a measure of aperture-to-medium coupling loss.

Such comparisons were made on the 190- and 92-mile paths. Three to five one-minute integrator means were recorded using small broad-beam antennas. They were then changed to the large narrow-beam dishes, the mean similarly obtained and the procedure repeated. The results obtained in this manner over a three hour period on the afternoon of February 12, 1959, are given in Table III. Note they agree quite closely with the predictions of Booker and deBettencourt[20] and not that of Staras[24] which were obtained assuming anisotropy. This indicates a height dependence of the spectrum (Fig. 5) rather than anisotropy as the cause for the increased slope in the vertical beamswingings of Fig. 14.

Conclusions

1) The observed angular scattering dependence of the received field strength $Q(\theta)$ varies as $\theta^{-14/3}$, consistent with the turbulent spectra $E(k)$ varying as $k^{-5/3}$.
2) The multiple-frequency measurements indicate a layer reflection mechanism at low microwave frequencies and turbulent scattering at higher frequencies. This does not contradict the X-band beamswinging results where turbulent scattering was the dominant mechanism.

TABLE III

Path distance	Antenna pairs Size in feet		Plane wave gain ratio of large to small pairs db	Measured scatter response of pairs db	"Loss" of response db	Booker and deBettencourt "Loss" db	Staras "Loss" db
	small	large					
92	1.5	10	28.5	24.0±0.5	4.5±0.5	6.1	1.0
190	4.0	10	14.4	7.1±2.0	7.3±2.0	6.9	3.5

3) The turbulent spectra satisfactorily predicts the angular scattering and wavelength dependence of the received field.
4) The microwave envelope spectra can be fitted by Gaussian or exponential forms except near the tail.
5) These spectra in many cases have a tail which varies with spectral frequency raised to some power, occasionally characterized by two distinct frequency regions with different exponents. The maximum Doppler frequency is slightly correlated with the frequency at the beginning of the tail.
6) These spectra broaden with increasing range, scattering angle and frequency.
7) Aperture-medium coupling loss agrees with that predicted by Booker and deBettencourt.
8) In general, the results support the turbulent single-scattering concept with a dielectric spectrum proportional to $k^{-5/3}$. Layer reflection phenomena becomes important in the lower frequency range as the atmosphere begins to stabilize.

ACKNOWLEDGMENT

The cooperation shown by the University of California at Santa Barbara in connection with the operating site on their campus is gratefully acknowledged.

The authors would also like to express their appreciation to the members of the Electromagnetic Propagation Branch of the Navy Electronics Laboratory for the invaluable assistance in the collection and reduction of this data. Particular thanks go to E. E. Gossard and W. F. Moler for discussions and comments, and to F. A. Sabransky and J. B. Fedor for handling the many computer problems.

Correspondence

Behavior of Thermal Noise and Beam Noise in a Quadrupole Amplifier*

Because of a fundamental difference in the nature of thermal noise in resistors on one hand, and of cyclotron-wave noise in electron beams on the other, the terms corresponding to these noise sources in the single-channel noise figure of quadrupole amplifiers[1] exhibit significantly different frequency dependence. It is well known[2] that for any parametric amplifier, the contribution from the thermal noise in the idler channel is proportional to ω_1/ω_2, the ratio of signal frequency to idler frequency. In parametric amplifiers where thermal noise is dominant, an obvious way to improve the noise figure is to select a high idler frequency so that this ratio becomes small. The same is not necessarily true with respect to quadrupole amplifiers.

The purpose of this letter is to clarify the noise behavior of nondegenerate quadrupole amplifiers under the following mutually exclusive sets of conditions:

1) Beam noise, having been removed from the beam by appropriate fast-wave input couplers, is negligible at both signal and idler frequencies.
2) No fast-wave coupler is provided at the idler frequency; thus, the original beam noise is present at that frequency.

In both cases, we can assign to the beam an effective noise temperature at the idler frequency T_i. The minimum noise figure is then

$$F_{\min} = 1 + \frac{T_i}{T_0}\frac{\omega_1}{\omega_2}, \tag{1}$$

where T_0 is room temperature. How large is T_i in the two cases?

For case 1, we assume that an idler coupler succeeds in extracting all the beam noise at ω_2 and dissipating it in an external resistive load. The thermal noise generated in this external load, or in other resistive elements associated with the idler coupler, must be impressed upon the beam like an input signal at the idler frequency. Thus, T_i is the temperature of the external load or the resistive elements generating the noise. If this temperature is held at T_0, the minimum noise figure for case 1 becomes the familiar expression[2]

$$F_{\min(1)} = 1 + \frac{\omega_1}{\omega_2}. \tag{2}$$

The situation in case 2, where idler noise is not stripped from the beam, is quite different. We have shown in an earlier paper,[3] experimentally as well as theoretically, that the noise temperature of cyclotron waves is inversely proportional to ω_c, the cyclotron frequency. Specifically, the noise temperature T_ω observed at a frequency ω in a magnetic field having a cyclotron frequency ω_c is equal to

$$T_\omega = T_c\frac{\omega}{\omega_c}, \tag{3}$$

where T_c is the cathode temperature. Equating T_ω with T_i in (1) and ω with ω_2, we find that

$$F_{\min(2)} = 1 + \frac{T_c}{T_0}\frac{\omega_1}{\omega_c}. \tag{4}$$

Note that the idler frequency ω_2 no longer appears in the expression for the minimum noise figure. As the idler frequency is increased, the beam noise power available at ω_2 increases proportionately, thus cancelling the advantage one would normally expect. The cyclotron frequency now appears in the position previously occupied by the idler frequency; if idler noise is not removed, the magnetic field must be made high to reduce it.

In a practical nondegenerate quadrupole amplifier, one normally attempts to strip the beam noise at ω_2 in order to attain the superior performance corresponding to case 1. In practice, the match between beam and room temperature load at the idler frequency may not be perfect. The minimum noise figure will then be between the values given for the two cases.

R. ADLER
Zenith Radio Corp.
Chicago, Ill.
G. WADE
Raytheon Co.
Burlington, Mass.

* Received by the IRE, December 19, 1960.

[1] R. Adler, G. Hrbek, and G. Wade, "The quadrupole amplifier, a low-noise parametric device," PROC. IRE, vol. 47, pp. 1713–1723; October, 1959.

[2] H. Heffner and G. Wade, "Minimum noise figure of a parametric amplifier," *J. Appl. Phys.*, vol. 29, p. 1262; August, 1958.

[3] R. Adler and G. Wade, "Beam refrigeration by means of large magnetic fields," *J. Appl. Phys.*, vol. 31, pp. 1201–1203; July, 1960.

Tunnel Diode Large-Signal Simulation Study*

Crisson[1] has presented a method for producing a voltage-controlled negative resistance at the input terminals of an "ideal amplifier" with feedback. It can be shown that the network enclosed by the dashed line in Fig. 1 displays the same terminal characteristics as the "ideal amplifier."

Curve A in Fig. 2 is a broken-line approximation to the static V-I characteristics of a GE ZJ56 tunnel diode which was produced by an analog-computer mechanization of the aforementioned network. The $i(v)$ current generator in Fig. 1 delivers a current equal to $i_1(v)-i_j(v)$, which is a function of the junction voltage, v. $i_1(v)$ is defined by the linear equation relating v and i in region 1 of curve A, and the resistance r_1 is equal to the constant ratio of v to i in this same region. $i_j(v)$ is defined by the linear equations relating v and i in each of the j linear regions $(j=1, 2, 3, 4)$ of curve A, Fig. 2. Curve B in Fig. 2 is the broken-line output current from the $i(v)$ generator. Curve C is the plot of an analytic expression that was fitted to curve B, *i.e.*,

$$i(v) = k_1[1 - \exp(-k_2v^2)] \qquad (1)$$

where $k_1=0.008$ and $k_2=11.0$ for the GE ZJ56 tunnel diodes that were the basis for the simulation. The monotonic character of the $i(v)$ curves permitted good curve-following techniques during the analog simulation. The enclosed network in Fig. 1 is used to simulate the static voltage-current characteristics of the large-signal tunnel diode equivalent circuit shown in that figure. The L, C and R_s elements that complete the equivalent circuit have been treated in detail in the literature.[2] (An additional average

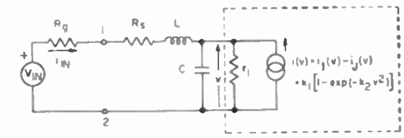

Fig. 1—Large-signal tunnel-diode equivalent circuit.

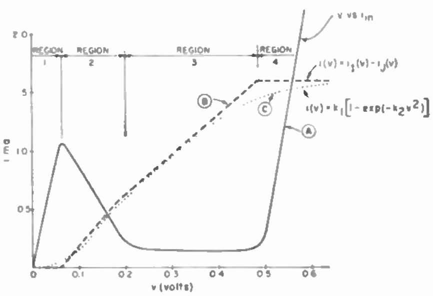

Fig. 2—Curve A: Approximation to GE ZJ56 tunnel diode static v-i characteristic obtained by analog computer simulation. Curve B: Broken-line approximation to current from $i(v)$ generator. Curve C: Analytic approximation to current from $i(v)$ generator.

diffusion capacitance can be switched in region 4 during analog simulation.)

The equivalent circuit was investigated for large-signal dynamic response using both analog simulation and graphical analysis techniques. An objective in this initial study was to determine the correlation between the analog and graphical techniques for arbitrary equivalent circuit parameters. Figs. 3 and 4 show some analog simulated results (dashed lines) with the analytic $i(v)$ current generator employed in the equivalent circuit. Fig. 3 displays the response of the equivalent circuit to a ramp driving function with the circuit operating in the switching mode, *i.e.*, $(R_g + R_s) > |-r|$, where $-r$ is the inverse slope in region 2. ($R_g+R_s=470$ ohms, $L=5.0$ nh and $C=2\mu\mu f$). Fig. 4 shows the sinusoidal response to a voltage step input that places the load line $(R_g+R_s)<|-r|$, in the negative resistance region (region 2) of the v-i characteristic. ($R_g+R_s=10$ ohms, $L=7.5$ nh and $C=2\mu\mu f$.)

A total, second-order, nonlinear differential equation employing the $i(v)$ function

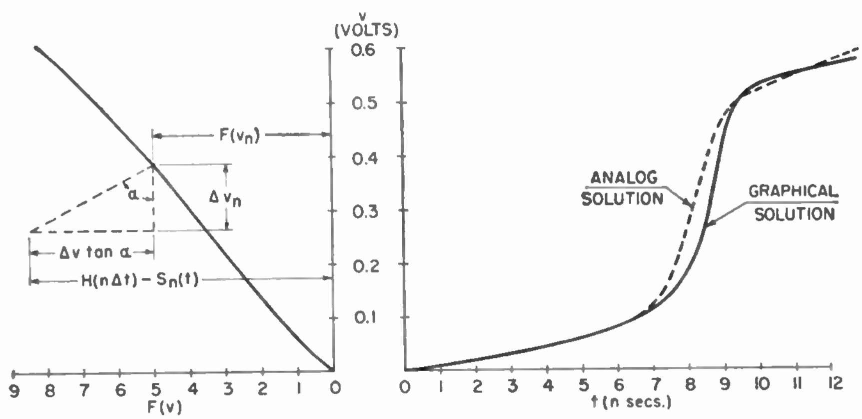

(a) (b)

Fig. 3—(a) Graphical construction in $F(v)$ vs v plane. (b) Analog computer and graphical solution for junction v vs time (switching mode).

* Received by the IRE, November 22, 1960; revised manuscript received, December 10, 1960.

[1] G. Crisson, "Negative impedances in the twin 21 type repeater," *Bell Sys. Tech. J.*, vol. 10, pp. 485–513; July, 1931.

[2] C. S. Davidsohn, Y. C. Hwang and G. B. Ober, "Designing with tunnel diodes," *Electronic Design*, vol. 8, pp. 50–55; February 3, 1960.

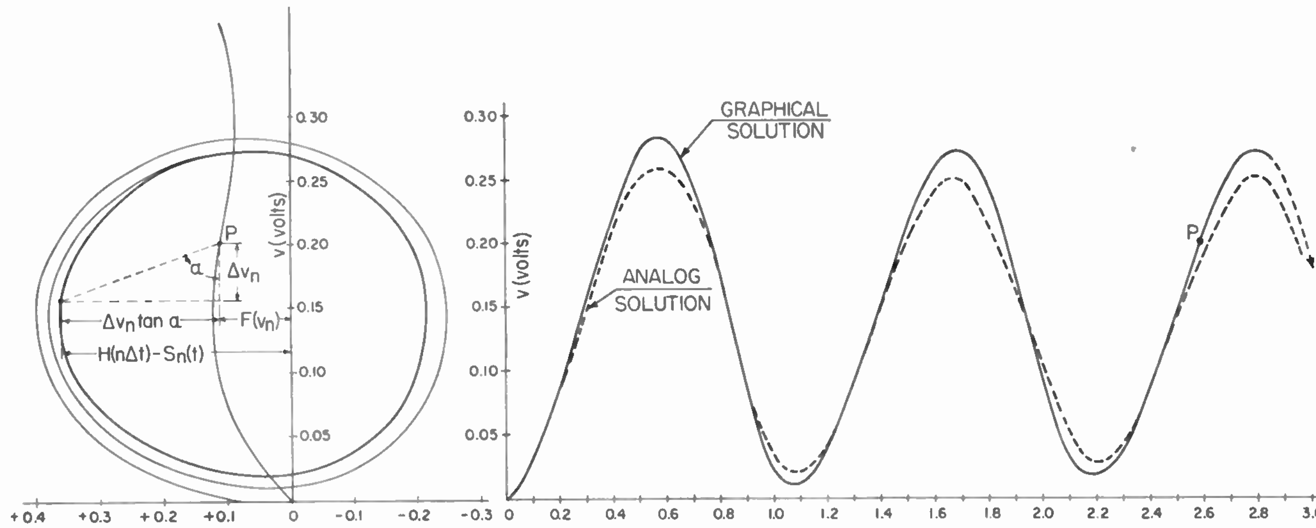

(a) (b)

Fig. 4—(a) Graphical construction in $F(v)$ vs v plane. (b) Analog computer and graphical solution for junction v vs time (oscillatory mode).

defined in (1) was written for the junction voltage v, *i.e.*,

$$\ddot{v} + \frac{1}{C}\left[\left(\frac{1}{r_1} + \frac{RC}{L}\right) - 2k_1k_2v\exp(-k_2v^2)\right]\dot{v} + W_0^2\left[\left(1 + \frac{R}{r_1}\right)v - Rk_1[1 - \exp(-k_2v^2)]\right] = E(t)W_0^2 \qquad (2)$$

where $R = R_g + R$, and $W_0^2 = 1/LC$. Although this equation does not lend itself to closed analytic solution, it was found to be solvable by Hsia's[3] graphical method when the construction technique is properly altered to accommodate the changes in the apparent driving conditions. This graphical method yields the solution of the equation

$$\Delta v_n \tan\alpha + F(v_n) = H(n\Delta t) - S_n(t) \qquad (3)$$

which is obtained from a term-by-term integration of (2).

Figs. 3 and 4 display the graphical solutions of (3) for the same circuit conditions used in the analog simulation process. The equivalent circuit in Fig. 1 also produced relaxation oscillations with the proper external circuit parameters.

S. B. Geller
P. A. Mantek
Data Processing Systems Div.
Natl. Bureau of Standards
Washington, D. C.

[3] P. S. Hsia, "A graphical analysis for nonlinear systems," *Proc. IEE*, vol. 99, pt. 2, pp. 125–134; 1952.

Radar Sensitivity with Degenerate Parametric Amplifier Front End*

The following analysis is presented to assess the role of the degenerate parametric amplifier as the front end of a radar receiver operated in the normal mode or as a coherent moving-target indicator (MTI). In both cases, it is assumed that the degenerate parametric amplifier, which can either be of the electron-beam[1] or junction-diode[2] type, is synchronously pumped[3]—that is, its pump voltage is derived from the second harmonic of a reference signal conerent with the transmitted RF.

It will be shown that when calculating the effect of the degenerate amplifier on normal mode sensitivity, a value between 1.6 and 3.2 db must be added to the broad-band noise figure of the amplifier. (The actual value depends on the characteristics of the radar set and is about 2.4 db for a typical search radar.) It will also be shown that the coherent MTI performance of the system will be severely degraded unless a filter can be used to eliminate one half of the IF amplifier's usual pass band, in which case 3 db must be added to the broad-band noise figure of the degenerate amplifier when calculating its effect on system MTI sensitivity.

The radar return from a target can either be considered to have the same frequency as the reference RF, but with a variable phase depending on the range of the target, or to have a frequency differing from the reference RF by the Doppler frequency corresponding to the target's radial velocity. Initially, consider the first viewpoint and denote the phase difference between the radar return and the reference RF for each pulse by θ. Then the complex output voltage of the degenerate amplifier V is given by

$$V = ABe^{j\theta}[1 + (1 - \delta)e^{-j2\theta}] \qquad (1)$$

where A is a gain factor, B is the amplitude of the received signal, and $(1-\delta)$ equals the idler voltage divided by the signal voltage ($\delta \ll 1$ for high gain).[2]

From (1), the magnitude and phase of V under high-gain conditions are given by

$$|V| \approx 2AB\cos\theta \qquad (2a)$$

$$\tan(\measuredangle V) \approx \frac{\delta\tan\theta}{2}. \qquad (2b)$$

Thus, the degenerate amplifier rejects those input signal (and noise) voltages in quadrature with the reference RF voltage. Furthermore, the output voltage of the degenerate amplifier contains the original phase information in the radar return θ principally in its magnitude and only slightly in its phase angle. The voltage V is then fed to either the normal or MTI receivers.

For the normal receiver, assume the use of a linear detector (square-law for weak signals) that delivers an output video voltage proportional to the envelope of the input voltage. Then, for comparison purposes, assume the receiver front end can either be a degenerate parametric amplifier, which rejects quadrature components, or of a conventional single-channel amplifier, which amplifies both in phase and quadrature components, and whose noise figure equals the broad-band noise figure of the degenerate amplifier. Then, if the noise contribution from the post receiver is negligible, the average signal-to-noise power ratio applied to the detector will be the same in both cases, but the video voltage probability density functions will be different, and are given by

$$P_d(v) = \frac{1}{\sigma\sqrt{2\pi}}\left\{\exp\left[-\frac{(v - a\cos\theta)^2}{2\sigma^2}\right] + \exp\left[-\frac{(v + a\cos\theta)^2}{2\sigma^2}\right]\right\} \qquad (3a)$$

$$P_c(v) = \frac{v}{\sigma^2}\exp\left\{-\left(\frac{v^2 + a^2}{2\sigma^2}\right)\right\}I_0\left(\frac{av}{\sigma^2}\right); \qquad (3b)$$

where $P_d(v)$ and $P_c(v)$ are the functions for the degenerate and conventional amplifiers, when $v \geq 0$; σ is the rms value of the Gaussian noise voltage applied to the detector, and a is the peak signal voltage applied to the detector.

For the degenerate amplifier, the mean and mean-square values of distribution (3a) are, respectively,

$$\overline{v_d} = \sigma\sqrt{\frac{2}{\pi}}\Big\}\exp\left(-\frac{a^2\cos^2\theta}{2\sigma^2}\right) + \frac{a\cos\theta}{\sigma}\int_0^{a\cos\theta}\exp\left(-\frac{t^2}{2}\right)dt \qquad (4)$$

$$\overline{v_d^2} = \sigma^2 + a^2\cos^2\theta. \qquad (5)$$

The mean-square fluctuation in the absence of the signal is then

$$\overline{v_d^2} - (\overline{v_d})^2 \approx \sigma^2\left(1 - \frac{2}{\pi}\right), \qquad (6)$$

and the video-signal component for weak signals is approximately

$$S_d \approx \sqrt{\frac{2}{\pi}}\left(\frac{a^2\cos^2\theta}{2\sigma}\right). \qquad (7)$$

For a large number of weak radar returns with arbitrary values of phase θ, the average signal component is

$$\overline{S_d} = \frac{1}{\sqrt{2\pi}}\left(\frac{a^2}{2\sigma}\right); \qquad (8)$$

thus, the average video signal-to-noise power ratio is

$$\frac{(\overline{S_d})^2}{\overline{v_d^2} - (\overline{v_d})^2} = \frac{a^4}{8\sigma^4}\left(\frac{1}{\pi - 2}\right). \qquad (9)$$

For strong signals, the video-signal component is

$$S_d' = a|\cos\theta|. \qquad (10)$$

For a large number of strong radar returns with arbitrary values of phase θ, the average signal component is

$$\overline{S_d'} = \frac{2a}{\pi}. \qquad (11)$$

and the average video signal-to-noise power ratio becomes

$$\frac{(\overline{S_d'})^2}{\overline{v_d^2} - (\overline{v_d})^2} = \frac{a^2}{\sigma^2\pi}\left(\frac{4}{\pi - 2}\right) \qquad (12)$$

Repeating the process for the conventional amplifier, we obtain the following video signal-to-noise power ratios for the weak and strong signal cases, respectively,

$$\frac{S_c^2}{\overline{v_c^2} - (\overline{v_d})^2} = \frac{a^4}{16\sigma^4}\left(\frac{\pi}{4 - \pi}\right) \qquad (13)$$

$$\frac{S_c'^2}{\overline{v_c^2} - (\overline{v_d})^2} = \frac{2a^2}{\sigma^2(4 - \pi)}. \qquad (14)$$

Comparing (9) with (13) and (12) with (14), we find that the loss incurred in average video signal-to-noise power ratio with the degenerate amplifier is $2(4-\pi)/\pi(\pi-2)$ or 3.2 db for both weak and strong signals. In the strong-signal case, this means a 3.2-db loss in sensitivity since the detector is linear. In the weak-signal case, this means a 1.6-db loss in sensitivity, since any detector characteristic is square-law for weak signals. The conclusion then is that 1.6 db must be added to the broad-band noise figure of the degenerate amplifier to determine normal mode sensitivity for a large number of weak

* Received by the IRE, July 8, 1960; revised manuscript received, October 26, 1960. The work reported here was performed under Contract AF 30(602)-1854 with the Rome Air Dev. Ctr., Griffiss Air Force Base, N. Y.

[1] R. Adler, G. Hrbek, and G. Wade, "The quadrupole amplifier, a low-noise parametric device," Proc. IRE, vol. 47, pp. 1713–1723; October, 1959.

[2] R. Gardner, *et al.*, "First Quarterly Progress Report on Application of Semiconductor Diodes to Microwave Low-Noise Amplifiers and Harmonic Generators," Airborne Instruments Lab., Rept. No. 5872-I-1, Section IVC; October 15, 1958.

[3] "High-frequency radar amplifier," New Products Section, Proc. IRE, vol. 48, pp. 174A–178A; June, 1960.

returns with random phases, while a value of 3.2 db must be added for the corresponding strong-signal case. The exact value to use in a given application depends on the circumstances. In a typical search radar case with 10 to 15 target returns per antenna scan, the minimum detectable signal is about equal to noise for each return and we are in the breakpoint region where the proper value is about 2.4 db.

Next, the coherent MTI receiver case is considered. Here, video detection is accomplished in a phase detector (operating from the reference RF) that is preceded by a limiting IF amplifier. The object is to sense moving targets by obtaining a phase-detector output-pulse amplitude that is a cosine function of the phase angle θ of the radar return. Then pulse-to-pulse subtraction in a subsequent canceller will generate outputs only for moving targets. When a degenerate amplifier front end is used, however, its output voltage contains the necessary phase information primarily in its magnitude. [See discussion following (2).] As a result, there is a severe degradation in MTI performance caused both by the generation of spurious target indications and by the failure to detect actual moving targets. Spurious target indications will be generated from the small perturbations in clutter returns that are caused by antenna scanning when the clutter return has the average phase necessary to produce a small output from the degenerate amplifier. On the other hand, if the clutter return has the phase necessary to produce a large output from the degenerate amplifier, the desired phase variation for a moving target in the presence of this clutter (which appears as an amplitude variation superimposed on clutter at the output terminals of the degenerate amplifier) will be masked by the limiting action of the IF amplifier. Furthermore, because of this same limiting action, a large moving target in the clear will be largely undetected except at near-optimum target speeds when an appreciable number of complete RF phase reversals from pulse-to-pulse occur in one scan of the antenna. Note that the use of a non-limiting IF amplifier should provide better moving-target detection, but it too would produce spurious target indications due to scanning clutter. These spurious indications can be detrimental in many applications.

The degradation in MTI operation that occurs with a degenerate amplifier can be avoided in theory by inserting a filter to eliminate one half of the IF amplifier's usual response. Aside from the practical difficulties of designing a filter of sufficiently sharp rejection, however, such a procedure would cause a degradation in optimum sensitivity. This can be seen most readily by considering the radar return from a moving target to be at either a frequency f_0+f_d (target approaching radar) or f_0-f_d (target moving away from radar), where f_0 is the transmitted frequency and f_d is the Doppler frequency corresponding to the target's radial velocity. Signals at either of these frequencies will then be amplified (either with or without frequency translation) and will appear at the output of the degenerate amplifier in the useful band (say in the vicinity of f_0+f_d, due to the subsequent IF filter). Input noise from the vicinity of both of these frequencies, however, will always be present in this useful output band, resulting in a 3-db degradation in optimum sensitivity (3 db must be added to the broad-band noise figure to determine system MTI sensitivity).

In conclusion, although synchronous pumping affords a convenient means for obtaining a pump source, it does not yield a significant improvement in search-radar performance over that obtainable by simply detuning the amplifier from the degenerate point, where a constant value of 3 db must be added to the broad-band noise figure of the amplifier to determine system sensitivity.

ACKNOWLEDGMENT

The authors are indebted to A. E. Ruvin and E. W. Sard of Airborne Instruments Laboratory for their helpful discussions, and to Dr. R. Adler of the Zenith Radio Corp. for his helpful and clarifying discussions of the noise properties of the degenerate amplifier.

J. C. GREENE
W. D. WHITE
Airborne Instruments Lab.
Melville, N. Y.

Comments from R. Adler[5]

Anyone who has seen a distant radar target suddenly light up with a certain setting of the pump-frequency control, only to find later that the setting was close to twice the signal frequency, will find it difficult to believe all of Greene and White's pessimistic conclusions.

Synchronous pumping of a degenerate parametric amplifier was suggested several years ago by Kenneth G. Eakin of Rome Air Development Center, for the purpose of increasing the sensitivity of coherent MTI radars. The idea was to take advantage of a property which the degenerate amplifier shares with the phase detector: both respond to one signal component (say cos θ) and reject the corresponding quadrature component (sin θ). Thus, with the pump synchronized and properly phased, the entire output from the degenerate amplifier, including signal and idler alike (see Greene and White's (2a), above) is accepted by the phase detector; the sin θ component rejected by the degenerate amplifier would have been suppressed by the phase detector in any event. For weak signals (below limiting level), one would therefore expect a sensitivity in accordance with the double-channel noise figure of the parametric amplifier, without any impairment whatever.

Such a system was tested in Rome, N. Y., early in 1960. An electron-beam parametric amplifier (EBPA) operating at about 1300 Mc was used in these experiments. The double-channel noise figure was 1.3 db (compared to 8.5 db without EBPA); more than 20-db gain was available and the results were exciting—the minimum detectable signal (MDS) in MTI mode improved by a full 10 db. Effective antenna temperature of substantially less than 290°K probably accounted for the nearly 3-db extra improvement beyond the 7.2-db difference in noise figures.

The expectation that the full-range increase corresponding to the double-channel noise figure would be realized in the MTI mode was clearly confirmed. This result, which had been Eakin's prime concern, does not seem to be the subject of controversy.

Unfortunately, an MTI setup is not usually concerned with weak targets at extreme range; its main purpose is to reject strong stationary targets, often at close range, while rendering moving targets visible. MTI circuits frequently employ a 30-db span between noise level and limiting level; stationary targets are often strong enough to cause limiting, and whenever this happens the degenerate amplifier impairs subclutter visibility, as explained by Greene and White. Not all the dire consequences predicted by them are observed—for instance, the range of blind speeds for large moving targets in the clear is narrowed, not widened—but the fact remains that MTI performance at close range is seriously degraded.

Greene and White mention the theoretical possibility of avoiding this degradation by means of a filter which eliminates half the IF response. Such a filter was considered after the difficulty was first discovered; it turned out, however, that a comb filter capable of separating the IF band into as many parts as there are lines in the pulse spectrum would be required. This is impractical.

Let us now return to the Rome experiments. The radar could be operated with conventional detection as well as with MTI. We had expected no particular advantage from synchronous pumping with conventional detection, and a switch was available to move the pump frequency a few megacycles away from the synchronous point. This had no measurable effect on gain or double-channel noise figure but it removed all signal power from the idler channel. To our surprise, we found immediately a substantial difference in MDS in favor of synchronous pumping; the difference appeared to be close to 3 db. It seemed that putting the idler into the receiver pass band restored the double-channel signal-to-noise ratio.

Today, after many more experiments and a little more thought, it appears that the signal-to-noise ratio using conventional detection and idler-in-pass band pumping (synchronism is not important in this case) is just 1.5 db poorer than would be expected from the double-channel noise figure. The magic number of 1.5 db results when one assumes square-law detection. It is interesting that it differs by only 0.1 db from Greene and White's figure (1.6 db) for this case. Let us show first how easily the result can be derived, then why square-law detection seems a proper and practical assumption, and finally give experimental data.

As stated before, the degenerate amplifier accepts cosine components and rejects sine components. It applies to the square-law detector a signal (and noise) of the form $a\cdot\cos\theta$. The detector output is thus $a^2\cos^2\theta$.

[5] Received by the IRE, November 9, 1960.

TABLE I

EXPERIMENTAL RESULTS (*L* BAND)

Equipment	Noise-Figure Improvement (Double-Channel Over Original)	MDS Improvement (Conventional Detection)	Source
FPS-8 Radar Rome, N. Y.	7.2	9	antenna
ARSR-1 Radar Wayland, Mass.	4.9	4.0	dummy load
MPS-11 Radar Glenview, Ill.	8.1	7.0	antenna
AASR-1 Radar North Bay, Ont.	5.5	4.5	dummy load
GRN-9B TACAN Patuxent River, Md.	6.3	4.3	dummy load
MPS-11 Radar Jacksonville, N. C.	8.3	7–10	antenna*

* Range increase of 45 to 70 per cent, PPI (controlled flight tests). Better figure corresponds to in-pass-band pumping.

This output includes the desired video signal as well as rectified noise having a certain fluctuation.

In principle, we could assume that the unused sine components might be utilized in a second degenerate amplifier and rectified by a second square-law detector, with a resulting output signal $a^2 \sin^2 \theta$. We could then add the two video voltages (each representing signal and noise power) to obtain simply a^2, the output from a conventional receiver followed by a square-law detector.

The two channels which we have thus combined contain, on the average, equal amounts of signal. Their noise fluctuations are not correlated. By combining the two channels we double the signal and the average dc level of the noise, but the noise fluctuation increases only by $\sqrt{2}$. Since output voltage represents input power, the improvement resulting from the combination is 1.5 db. Conversely, with the single degenerate amplifier operating alone, we lose 1.5 db compared to a conventional amplifier.

Greene and White point out that for large signals, video signal-to-noise ratio is impaired if linear detection occurs in place of square-law detection. But this is just as true in any other receiver; once a signal pulse sticks out of the noise by a detectable margin, flattening the detector characteristic from square-law to linear naturally reduces that margin. Since every detector becomes a square-law device at sufficiently low input level, proper receiver design provides enough video gain to permit operation of the detector in this region for signals close to the noise level. An operator who turns the IF gain up and the video gain down deprives himself of a certain degree of performance; but why assume operation of any radar receiver, conventional or otherwise, with misadjusted gain controls?

Before giving experimental results, let me correct another error: the 1.5-db impairment applies to the signal-to-noise ratio, not to the noise figure. The impairment in noise figure is 1.5 db only when the antenna-noise temperature is 290°K. Usually, this temperature is somewhat lower and the corresponding degradation of noise figure is then less than 1.5 db.

The experimental data are shown in Table I. Idler-in-pass-band pumping was used in all cases. In some locations where MTI was employed at close range, the range gate was used to shift the pump frequency so as to place the idler outside the pass band during MTI operation. Turning the pump off at close range, with the EBPA acting as a unity-gain isolator, has also been suggested.

One interesting puzzle remains: In a number of cases where the idler frequency could be shifted inside or outside the pass band, the MDS improvement resulting from in-pass-band pumping was measured directly. Theoretically, we would expect $3-1.5=1.5$ db; Greene and White would look for something from 1.4 db down to -0.2 db. But observers uninhibited by either theory keep finding 2.5 to 3 db.

To sum it all up, idler-in-pass-band pumping with conventional detection provides a significant improvement over offset-frequency pumping. The correction to be applied to the double-channel noise figure is 1.5 db or less.

It is a pleasure to thank J. C. Greene and W. D. White of Airborne Instruments Laboratory for the courtesy of making their manuscript available in advance of publication.

ROBERT ADLER
Research Dept.
Zenith Radio Corp.
Chicago, Ill.

Rebuttal from Greene and White[6]

Adler finds that distant targets appear brighter on the display of a radar set when a low-noise degenerate amplifier is used. This is not surprising, but we would expect that if the degenerate amplifier were replaced with a conventional amplifier having the same noise figure, distant targets would appear even brighter on the normal mode display while the MTI display would show far fewer spurious targets and more clearly reveal moving targets in chaff, in choppy seas, or near uneven terrain.

We have shown that, depending on relative signal level, the normal mode sensitivity of a radar set using a degenerate amplifier front end will be between 1.6 and 3.2 db worse than that obtained with an equivalent conventional amplifier. Adler suggests that by proper manipulation of receiver gain controls, one can operate the detector in the square-law region and thereby suffer only the minimum degradation of 1.6 db. Woodward[7] has shown why this cannot be done; he indicates that when a number of pulses are to be combined for detection purposes, the optimum detector characteristic is square law for weak signals but becomes asymptotically linear as the signal level increases. (The linear detector we assumed is a close approximation to the optimum detector and is used almost universally in receivers.) Thus, for the case of a conventional search radar where 10 to 15 pulse returns are received per antenna scan and each of these returns must be about equal to noise if the target is to be detected, even the optimum detector characteristic must depart significantly from square law. As a result, the minimum sensitivity degradation in this case becomes about 2.4 db as indicated in our letter.

We would like to point out that in modern radar sets with only a few target returns available per antenna scan, the increase in signal strength required for reliable target detection when using a degenerate amplifier rather than a similar conventional amplifier can be significantly larger than the 3.2 db limit we derived on the basis of a large number of returns. This occurs because the degenerate amplifier can entirely reject some of the few returns available. Detailed computations for the limiting case of detecting a single pulse with 90 per cent probability and a false alarm rate of 10^{-6} show a 14-db penalty for the degenerate amplifier. It is also of interest to note that if a degenerate amplifier is used in a radio astronomy application where the received signal is broadband noise, the system will be 1.6-db less sensitive than if a conventional amplifier having the same noise figure and total bandwidth is used.

The degradation in normal mode sensitivity caused by the degenerate amplifier is a result of the detection process, and we have indicated that for convenience this degradation may be added to the amplifier's broadband noise figure when calculating system sensitivity. We are, of course, aware that when the antenna temperature is other than 290°K, corresponding adjustments must be made in computing system sensitivity. However, noise figure is defined by the IRE Standards in terms of a source (antenna) at 290°K. To speak of the noise figure at some other reference temperature is to invite confusion. A more general way of expressing the degradation for an arbitrary value of antenna temperature, is to multiply the effective system noise temperature (antenna temperature plus receiver excess noise temperature) by the factor representing the actual sensitivity degradation.

[6] Received by the IRE, January 13, 1961.

[7] P. M. Woodward, "Probability and Information Theory with Applications to Radar," McGraw-Hill Book Co., Inc., New York, N. Y., p. 98, Eqs. 38 and 39; 1953.

Our objection to the degenerate amplifier for coherent MTI reception is based solely on the serious consequences of the loss of subclutter visibility and the generation of spurious targets, since there is no degradation in MTI sensitivity with synchronous pumping. Adler is correct in stating that the range of blind speeds for large moving targets in the clear is narrowed with the degenerate amplifier, but only to the extent that the degenerate amplifier noise figure is better than that of the amplifier it is compared with. For the case of equal noise figures, there should be little difference in the range of blind speeds.

The only published report available on the Rome experiments indicates that a Hewlett-Packard signal generator was used to simulate actual radar returns.[8] In such a case, an unlimited number of pulses is available for processing by the radar set, and we believe the puzzle reported by Adler can be explained on this basis. Thus, with degenerate operation, many of the incoming pulses will arrive with near optimum phase and produce an A-scope deflection consistent with no sensitivity degradation. Because of scope persistence, the observer should be able to detect this peak value, which should correspond to a signal level just about 3 db lower than that with the idler outside the amplifier pass band. In a practical radar case, where a limited number of pulses is available, one would *not* expect the same results.

In summary, we believe the conclusions stated in our original letter are correct, and that the experimental data presented by Adler would have been even better if the degenerate amplifier had been replaced with a conventional amplifier having the same noise figure.

J. C. Greene
W. D. White
Airborne Instruments Lab.
Melville, N. Y.

Rebuttal from R. Adler[9]

Apparently we are in substantial agreement with respect to the MTI mode: no sensitivity is lost there, but close-range performance is degraded. The disagreement centers on the normal mode (conventional detection): Greene and White expect that shifting the pump frequency from outside to inside the pass band should produce an improvement of only about 0.6 db; we expect the improvement to be 1.5 db, and field observers find even more, usually 2.5 to 3.0 db.

Greene and White's explanation of the puzzle (next-to-last paragraph of their rebuttal) has considerable merit. Let me add a detail: with degenerate operation, quadrature noise is rejected and therefore the dc level of the detected noise is one-half, its fluctuation amplitude $1/\sqrt{2}$ of what they would be with a conventional amplifier. Optimum phase signal pulses, on the other hand, produce the same scope deflection as with a conventional amplifier. If an observer were able to detect the peak value as Greene and White suggest, he could observe even weaker signals than with the conventional amplifier, because the noise is lower. There is no evidence for this; with signal generator and A-scope, the typical improvement observed with in-pass-band pumping is 3 db, no more. Greene and White's explanation may well account for this result.

But why are the results with search radars and PPI observation as good as reported? Let me briefly describe a controlled flight test: Typically, a test plane flies radially outward at fixed altitude. Each time the antenna sweeps across the selected azimuth, the radar paints a spot which is graded as follows: 1) persistent for the entire scan, 2) for only half the scan, 3) barely visible. Grade and distance are recorded; the results are quite reproducible. It is in tests of this kind that the 2.5- to 3.0-db improvement with in-pass-band pumping is observed.

These are conventional search radars with 10 to 15 hits per scan, so that considerable averaging takes place each time a spot is painted; the fluctuations resulting from the random phasing of individual hits are reduced by a factor of $\sqrt{10}$ to $\sqrt{15}$, or about 3 to 4 times. The residual fluctuation has not been observed. But the point raised by Greene and White regarding the probability of missing an individual pulse is very well taken: in those special radars which make use of single (or very few) pulses, instead of averaging over many, in-pass-band pumping should not be used.

No matter how good the averaging process, it does not explain why the PPI observations give better results than either theory. If we follow Greene and White in assuming that the detector is not square-law, the gap between theory and practice widens further. Could it be that there are other factors involved? Let me suggest one worth investigating.

The integration over the 10 to 15 hits occurs in the phosphor on the face of the cathode ray tube. The instantaneous light intensity of a spot is proportional to $V^{2.5}$ to $V^{3.5}$, where V is the drive voltage above black level.[10] Thus, even with a strictly linear detector, the light intensity varies much faster than the signal amplitude. Could this nonlinear reproduction process favor the degenerate amplifier by placing a premium on the large in-phase pulses?

Before closing, two minor points. First the matter of antenna temperature. We all agree, of course, that the noise figure must always be referred to a signal source of 290°K. In a conventional amplifier, the story ends right there. But a parametric amplifier has a noise leak in the form of its idler channel. The noise which enters through this leak does not come from the signal source but from the idler termination which, for instance, could be cooled even though the signal source remained at 290°K. The total excess noise of a parametric amplifier (used as a single-channel device) consists of the built-in noise on the signal channel, the built-in noise on the idler channel, and the external noise generated in the idler termination. To determine, for the signal channel, an equivalent single-channel noise figure, the idler termination temperature must be specified; it need by no means be 290°K. In practice it is often lower.

Second, with respect to the degenerate amplifier used in a radio astronomy (or radiometry) application: the suppression of all quadrature components (internal and external noise alike) is equivalent to cutting the information bandwidth (bits per unit time) in half; the two sidebands (above and below the half pump frequency) become symmetrical, therefore one is superfluous. This is probably another way of stating what Greene and White have said. The noise figure, in this case, is of course the double-channel noise figure.

To return to radar and summarize the points of diagreement: Greene and White's predictions with respect to the normal mode are unduly pessimistic. The degenerate amplifier performs surprisingly well with conventional search radars; so well, in fact, that its replacement by a conventional amplifier having the same noise figure would result in very little improvement.

Robert Adler
Research Dept.
Zenith Radio Corp.
Chicago, Ill.

[8] "Test and Evaluation of a Zenith Electron Beam Parametric Amplifier," RADC Rept.; February 26 1960.

[9] Received by the IRE, December 7, 1960.

[10] See, for instance: Donald G. Fink, "Television Engineering," McGraw-Hill Book Co., Inc., pp. 131–132; 1952.

Determination of Noise Temperature of a Gas-Discharge Noise Source for Four-Millimeter Waves*

A gas-discharge noise source has been calibrated against a hot-body standard for use in the measurement of the noise figure of crystal diode mixers at 70 Gc. The tube calibrated was a neon discharge tube (noise source GNW-V18 made by Roger White Electron Devices, Inc.) mounted in RG-98/U waveguide. The noise temperature of this tube at 70 Gc was determined to be 18.2±0.25 db relative to 290°K at an operating current of 35 ma.

The hot-body standard was made from a wedge of high-resistivity silicon (50 ohm-cm) inserted into a 5-inch section of RG-98/U waveguide, as shown in Fig. 1. The wedge was approximately 1 inch long, and a VSWR of 1.05 was achieved. The load was placed in an oven and heated to 780°C. To keep the temperature of the load uniform, and to achieve a high temperature gradient away from the load, the walls of the waveguide section adjacent to the silicon wedge were machined to a thickness of approximately 10 mils over a 2 1/16 inch length, as

* Received by the IRE, January 6, 1961. This work was supported in part by the U. S. Army Signal Corps under Contract No. DA-36-039-SC-78066.

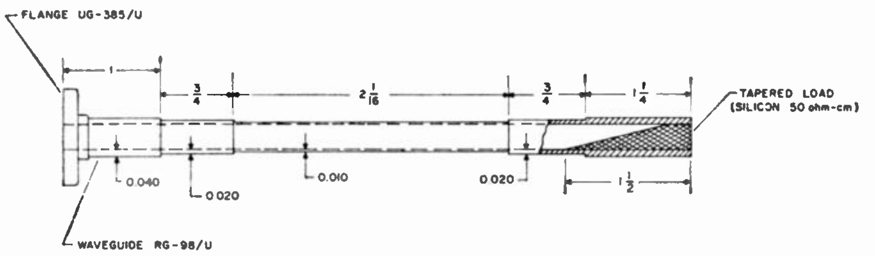

Fig. 1—"Hot-body" termination. (*Note:* drawing not to scale; dimensions in inches.)

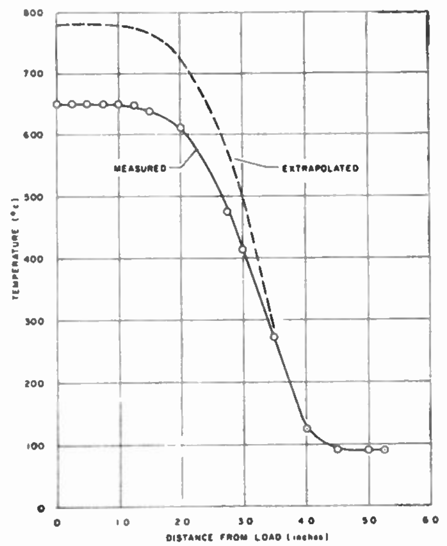

Fig. 2—Temperature gradient of "hot body."

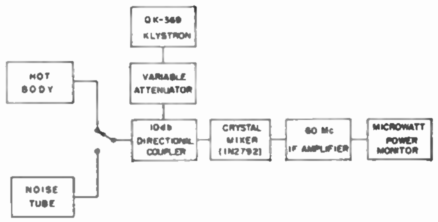

Fig. 3—Block diagram of 70-Gc receiver.

shown in Fig. 1. Just outside the oven, the waveguide was maintained at 100°C by water cooling. The waveguide temperature gradient, as shown in Fig. 2, was determined by moving a thermocouple inside the waveguide. (Measurements were made with a 650°C source and extrapolated to the 780°C hot-body temperature.) The waveguide insertion loss was also determined as a function of temperature. From these data the effective noise temperature was calculated, and found to be only 0.2 db less than the measured temperature of the silicon load. To prevent oxidation of the inner walls of the waveguide, the load was evacuated and filled with dry argon (this precaution proved to be unnecessary in subsequent measurements).

The hot-body standard was compared with the gas-discharge noise tube using a 70-Gc superheterodyne receiver employing a Philco 1N2792 mixer diode, as shown in Fig. 3. The receiver noise figure measurements were made with a standard deviation of 0.15 db. The uncertainty in the determination of the effective temperature of the hot load was less than 0.1 db.

It is of interest to note that a similar gas-discharge noise source was calibrated by Bridges[1] at approximately 37 Gc. He used a microwave radiometer for comparison with a load heated to 500°C and obtained the same noise temperature of 18.2 db for the gas-discharge noise source.

Nicoll and Warner[2] also measured the noise temperature of a neon gas discharge, at 30 mm Hg pressure, and found it to be about 13 db at 4-mm wavelength. The difference between their result and ours may be due to insufficient attenuation of the discharge they used, which would cause lowering of the effective temperature. In our case, the discharge attenuation was high enough so that a change in the termination behind the discharge tube did not affect the noise temperature within the experimental uncertainty.

W. Jasinski
G. Hiller
Special Products Operation
Philco Corp.
Lansdale, Pa.

[1] T. I. Bridges, "A gas-discharge noise source for eight-millimeter waves," Proc. IRE, vol. 42, pp. 818–819; May, 1954.
[2] G. R. Nicoll and F. L. Warner, T. R. E. Memorandum No. 544.

A Direct Graphical Solution for the Flux Distribution in a Magnetic Parallel Circuit*

A problem which is encountered in magnetic circuit analysis is that of the division of a flux ϕ_X between two different branches, Y and Z, of a parallel circuit (Fig. 1). By methods of successive approximations, a solution can be derived with a sufficient degree of accuracy. The present method provides a direct graphical solution. The principle of this method is one that is used in many nonlinear circuits problems.

* Received by the IRE, October 30, 1960.

Given, then, the following: 1) the flux ϕ_X; 2) the mean length of branch Y, l_Y, its cross-section area A_Y, and its average B-H curve; 3) the mean length l_Z, the cross-section area A_Z, and the B-H curve of branch Z, it is required to find ϕ_Y and ϕ_Z.

This case is the dual of a series circuit, consisting of two different branches connected in series, where it is required to find the division of the total magnetomotive force (mmf) between these branches.[1]

The equations pertaining to the solution of the present problem are

$$\phi_X = \phi_Y + \phi_Z, \tag{1}$$

$$U_Y = U_Z, \tag{2}$$

where U is the mmf.

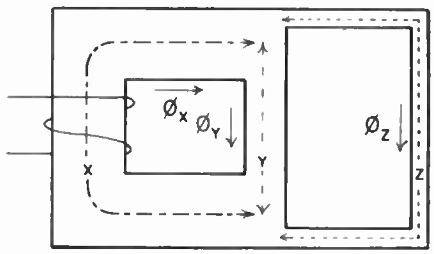

Fig. 1.

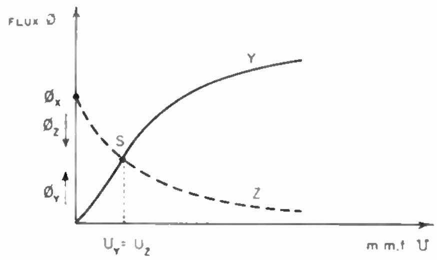

Fig. 2.

The relationship between the flux and the mmf for branch Y can be determined from the given data ($\phi_Y = B_Y A_Y$ and $U_Y = H_Y l_Y$) in a rationalized system of units. The curve of ϕ_Y as a function of U_Y is plotted in Fig. 2. Likewise, the relationship between ϕ_Z and U_Z can be determined. This curve is plotted in such a way that values on the ordinate axis increase from the top to the bottom, with the zero value starting at the point where ϕ_Y is equal to ϕ_X. That is to say, an *inverted magnetization curve* is plotted for branch Z. The intersection of the two curves at S satisfies (1) and (2), and therefore yields the required result.

Shlomo Karni
Elec. Engrg. Dept.
University of Illinois
Urbana, Ill.

[1] M.I.T. Staff, "Magnetic Circuits and Transformers," John Wiley and Sons, Inc., New York, N. Y.; 1949.

Comparative Figures of Merit for Available Varactor Diodes*

In a parametric amplifier using a varactor diode, optimum noise performance and, to a large extent, the maximum achievable gain-bandwidth product are both determined by the figure of merit M of the particular diode used.[1] However, M, defined as the product of the diode cutoff frequency and relative nonlinearity under pumped conditions, is not specified by the manufacturers of commercially available diodes. Thus, it may appear to the diode user that a silicon diode with a graded junction will not compare favorably with an abrupt-junction gallium arsenide diode having the same cutoff frequency, since the graded junction is reputedly "less nonlinear" than the abrupt junction. In determining the M values obtainable with the best commercially available abrupt- and graded-junction diodes, it has been found that the graded junction appears to have a larger effective nonlinearity. For the particular graded-junction diode considered, however, this advantage was offset by a lower cutoff frequency, resulting in similar M values of about 30 kMc for either type of diode. The good S-, C-, and X-band experimental data recently reported are consistent with such large M values.

For an analysis based on a parallel equivalent circuit, M has been defined as[1]

$$M = (f_c)(C_1/C_0) = (1/2\pi RC_0)(C_1/C_0), \quad (1)$$

where

f_c = diode cutoff frequency under pumped conditions,

R = diode series resistance,

$C(t) = C_0 + 2C_1 \sin wt + 2C_2 \sin 2wt + \cdots$ (the diode capacitance variation when pump frequency w is applied).

Barring complicated effects, maximum M values are ordinarily obtained when 1) the diode is biased slightly forward of the midway point between forward and reverse conduction, and 2) the pump amplitude is adjusted to drive the diode into the forward conduction region (the maximum allowable amplitude is determined by a compromise between rapidly increasing C_1/C_0 values and the additional loss and noisiness imposed by the onset of conductive current). This mode of operation is essentially optimum for the TI XD-503 gallium arsenide abrupt-junction diode. However, for silicon graded-junction diodes, such as the MA pill diode, there is an anomalous current effect due to a multiplication through collision ionization of the minority carriers injected during forward conduction.[2] As a result, the optimum bias point for such diodes is generally much closer to the forward conduction region.

For the silicon graded-junction diode, the necessity for driving into the forward region and the phenomenon of multiplication of stored carriers indicate that the capacitance due to minority carrier storage may be the dominant factor in obtaining large C_1/C_0 values. The theory of the graded junction does show an enhancement of storage capacitance effects when compared with the abrupt junction, indicating a larger ratio of susceptance to conductance for a given lifetime.[3,4] In any event, since the loss and noise due to RF conductive current actually determine the maximum obtainable M values, simple comparisons of M values based on assumed diode capacitance variations with the inverse square root or inverse cube root of applied voltage plus contact potential are meaningless.

To determine the M values obtainable with each type of diode, Fourier series for the capacitance-time characteristics were determined from curves of junction capacitance vs applied voltage derived from the manufacturer's published Smith chart data taken at microwave frequencies. Thus, although a sinusoidal junction voltage was assumed to facilitate analysis, no erroneous capacitance-voltage law was used in the all important forward conduction region (the assumed sinusoidal junction voltage actually gives a somewhat more pessimistic M value than that obtainable with a constant current pump source). The computed results are listed in Table I for several values of pump drive about fixed operating bias voltages. The assumed bias voltage of −1.0 volt for the MA diode is a nearly optimum value, as determined by experiment. The 2.0 volt value assumed for the TI diode is not quite optimum, but represents a good compromise between an optimum M value and reasonable pump requirements.

Table I shows that the diode nonlinearity factor C_1/C_0 increases rapidly, while the diode cutoff frequency f_c decreases rapidly (due to an increase in average diode capacitance) as the pump amplitude is increased. The figure of merit M which is the product of these quantities is seen to increase to a maximum of 25 kMc for the MA diode and then decrease as the drive level is further increased. M for the TI diode increases continuously with drive level to a value of 34 kMc for the assumed maximum drive level.

TABLE I

DIODE CHARACTERISTICS VS PUMP DRIVE

Diode Type	Peak Pumped Capacitance / 0 Bias Capacitance	Instantaneous dc Current Corresponding to Peak Pumped Capacitance in μa	$\frac{\text{Unpumped Capacitance}}{\text{Pumped Capacitance (Average)}} = \frac{\text{Pumped Cutoff Frequency}}{\text{Unpumped Cutoff Frequency}}$	$\frac{C_1}{C_0}$	$M = \left(\frac{C_1}{C_0}\right)(f_c)$ in kMc	$M_s = \frac{M}{1 - \left(\frac{C_1}{C_0}\right)^2}$
Microwave Associates MA-4298X Silicon Varactor	2.35	<1	0.70	0.37	23	27
Operating Bias = −1.0 v	4.0	1	0.55	0.50	25	33
Unpumped Cutoff Frequency at Operating Bias = 90 kMc	10	5	0.35	0.67	21	38
Texas Instruments XD-503 Gallium Arsenide Varactor	1.63	1	0.74	0.29	30	33
Operating Bias = −2.0 v Unpumped Cutoff Frequency at Operating Bias = 144 kMc	2.43	10	0.66	0.36	34	38

The peak of the drive level assumed for the MA diode corresponds to a point on the E-I curve where a forward current of 5 μa flows. Such a peak current does not cause a significant degradation in amplifier noise performance. The degradation in noise performance of the corresponding peak current value of 10 μa for the TI diode has not yet been determined.

Also shown in Table I are values for M_s, the diode figure of merit derived on the basis of a series equivalent circuit[5] (M is derived on the basis of a parallel equivalent circuit). M_s is larger than M by the factor $1-(C_1/C_0)^2$ and thus, for a given diode, the series analysis always predicts better amplifier noise performance than the parallel analysis. For the TI diode, the values of M and M_s are not significantly different, whereas for the MA diode, M_s becomes considerably larger than M at high drive levels. The actual diode circuit is neither a simple series nor parallel ar-

* Received by the IRE, January 6, 1961. The work reported here was performed with the Rome Air Dev. Ctr., Griffiss AFB, Rome, N. Y., under Contract AF 30(602)-1854.

[1] J. C. Greene and E. W. Sard, "Optimum noise and gain-bandwidth performance for a practical one-port parametric amplifier," PROC. IRE, vol. 48, pp. 1583–1590; September, 1960.

[2] K. Siegel, "Anomalous reverse current in varactor diodes," PROC. IRE, vol. 48, pp. 1159–1160; June, 1960.

[3] A. E. Bakanowski, "Crystal Rectifiers," Bell Telephone Labs., Ninth Interim Tech. Rept., Signal Corps Contract DA-36-039-sc-5589; October 15, 1956.

[4] W. Shockley, "The theory of p-n junctions in semiconductors and p-n junction transistors," *Bell. Sys. Tech. J.*, vol. 28, pp. 435–489; July, 1949.

[5] G. L. Matthaei, "A Study of the Optimum Design of Wideband Parametric Amplifiers and Up-Converters," presented at PGMTT meeting, San Diego, Calif.; May, 1960.

rangement if stray parasitic reactances are considered, but in most cases it is believed that the series circuit is the more representative.

It is also of interest to note that for diodes with unpumped cutoff frequencies different from those listed in Table I, the value of M can be readily computed, since the parameter M divided by unpumped cutoff frequency tends to be constant. The good experimental data recently reported at S, C, and X bands[6-8] require silicon diode M values between about 20 and 30 kMc, which, as shown in Table I, are not the best obtainable, but are consistent with the lower cutoff frequency values of the actual diodes used.

In summary, it appears that the MA linearly-graded silicon junction diode is considerably more nonlinear than the TI abrupt-junction gallium arsenide diode. However, due to a higher cutoff frequency, the TI diode has a comparable M value and therefore should give about the same noise performance in a parametric amplifier; but this has not yet been verified experimentally.

K. SIEGEL
Airborne Instruments Lab.
Division of Cutler-Hammer, Inc.
Melville, N. Y.

[6] I. Goldstein and J. Zorzy, "Some results on diode parametric amplifiers," PROC. IRE, (Correspondence), vol. 48, p. 1783; October, 1960.

[7] J. C. Greene, *et al.*, "Tenth Quarterly Progress Report On Application of Semiconductor Diodes to Low-Noise, Amplifiers, Harmonic Generators, and Fast-Acting TR Switches," Airborne Instruments Lab., Melville, N. Y., Rept. No. 4589-I-10; December, 1960.

[8] Microwave Associates advertisement, *Microwave J.*, vol. 3 p. 15; November, 1960.

Capacitance Coefficients for Varactor Diodes*

It has been shown[1] that the Fourier coefficients of a back-biased varactor, when driven by a constant voltage pump source, can be expressed in terms of hypergeometric functions. These coefficients are, of course, required in the preliminary design of single-tuned, as well as multiply-tuned, parametric amplifiers.[2] When the varactor is of the abrupt junction type, the hypergeometric function reduces to the complete elliptical integrals of the first and second kind and these are widely available in tabulated form.[3] The linearly graded junction, on the other hand, leads to nontabulated hypergeometric functions. Fortunately, these functions can be expressed in a power series, which rapidly converges for all values of the argument.[4] Calculations from this series expansion are presented in Figs. 1 and 2.

The form of the capacitance variation with instantaneous voltage was assumed as follows:

$$C = C_d(1 - \alpha \cos \theta)^{-1/3}, \qquad \theta = \omega t,$$

where

$$C_d = C_{0b}(1 - V_b/A)^{-1/3}$$
$$\alpha = V_0/(A - V_b),$$

with C_{0b} the zero-bias capacitance, V_b the negative bias voltage, A the built-in voltage,

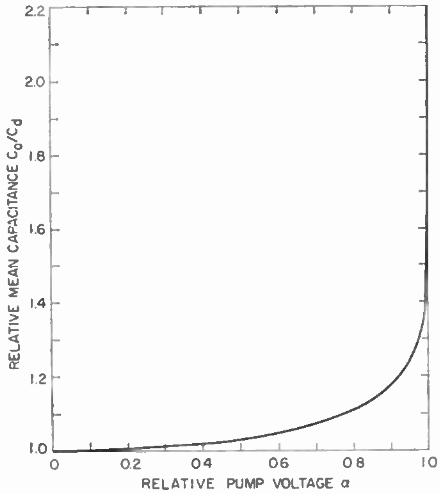

Fig. 1.

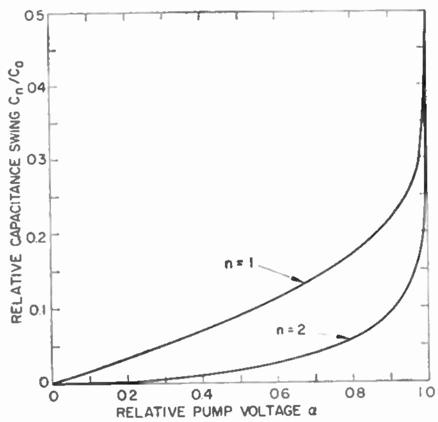

Fig. 2.

and V_0 the magnitude of the pump voltage at frequency ω. While, in particular, Fig. 2 shows the possibility of obtaining relatively large values of C_1/C_0 when the diode is driven severely, it should be remembered that under these conditions (that is, when the instantaneous voltage swings positive), there will be a contribution from the storage admittance. Although this admittance is capacitive in nature, its Q is frequency dependent and at microwave frequencies approaches unity, thus subtracting from the over-all Q of the varactor.[5] It follows that, if low noise is the objective, the permissible normalized capacitance swing suffers as the frequency is increased. In addition, as can be seen from Fig. 2, higher-order capacitance coefficients attain magnitudes comparable with C_1/C_0, under severe pumping conditions. These may lead to instabilities and spurious behavior in unsuspected places.

Finally, the authors wish to point out an error in their previous note.[1] The limits on the integral of (13) should be 0 and $\pi/2$.

R. D. WEGLEIN
Hughes Res. Labs.
Malibu, Calif.
S. SENSIPER
Space Electronics Corp.
Glendale, Calif.

* Received by the IRE, December 27, 1960.

[1] S. Sensiper and R. D. Weglein, "Capacitance and charge coefficients for parametric diode devices," PROC. IRE, (Correspondence), vol. 48, pp. 1482–1483; August, 1960.

[2] G. L. Matthaei, "A Study of the Optimum Design of Wideband Parametric Amplifiers and Up-Converters," PGMTT Natl. Symp., San Diego, Calif.; May 9–11, 1960.

[3] See, for example: E. Jahnke and F. Emde, "Tables of Functions," Dover Publications, Inc., New York, N. Y., 4th ed., pp. 78–80; 1945.

[4] W. Magnus and F. Oberhettinger, "Formulas and Theorems for the Special Functions of Mathematical Physics," Chelsea Publishing Co., New York, N. Y., pp. 9, 11; 1949.

[5] J. Hillibrand and C. F. Stocker, "The design of varactor diodes," *RCA Rev.*, vol. 21, pp. 457–474; September, 1960.

Note on a Balun: Solution by a Tapered Potential*

A recent paper[1] described a design of tapered balun (transducer between coaxial and two-wire transmission lines) with a reported excellent wideband performance. The design, however, was based on an intuitive approach, and it is the purpose of this note to draw attention to a powerful method which frequently leads to a simple solution of this type of problem. In this instance, a form of balun results which does not seem to have been known previously.

The method was devised for waveguide mode transducers[2] and may be explained briefly as follows. Suppose a two-dimensional field described by an eigenfunction, which in the waveguide case is a solution of the wave equation; then the walls of the guide must lie along boundaries set by the eigenfunction. Now suppose it is required to taper from one waveguide mode to another. Instead of considering directly how to choose a suitable boundary taper, the method is to construct an eigenfunction taper, changing gradually along the axis from the function appropriate to the first mode to the function appropriate to the second. Boundaries satisfying the function at each intermediate stage can often be assembled into the desired boundary taper.

For the balun, the first and second modes are transverse electromagnetic (TEM modes)[3] for which the fields are described by

* Received by the IRE, November 7, 1960.

[1] J. W. Duncan and V. P. Menerva, "100:1 Bandwidth balun transformer," PROC. IRE, vol. 48, pp. 156–164; February, 1960.

[2] L. Solymar and C. C. Eaglesfield, "Design of mode transducers," IRE TRANS. ON MICROWAVE THEORY AND TECHNIQUES, vol. MTT-8, pp. 61–65; January, 1960.

[3] S. A. Schelkunoff, "Electromagnetic Waves," D. Van Nostrand Co., Inc., Princeton, N. J.; p. 281; 1956.

a scalar potential satisfying the two-dimensional Laplace equation. The surfaces of the conductors follow equipotentials. The field of the concentric line is described by a potential proportional to

$$U_A = \log_{10} r,$$

the equipotentials being given by $r=\text{const.}$ The two-wire line is similarly described by

$$U_B = \log r_1 - \log r_2,$$

the equipotentials being circles surrounding (but not centered on) P and Q.

Now form

$$U = (1 - \epsilon)U_A + \epsilon U_B,$$

where ϵ is a slowly-varying function of the axial coordinate, changing from 0 to 1. Thus, U changes slowly from U_A to U_B. Being a sum of two solutions of the Laplace equation, U is also a solution and therefore describes a TEM wave.

Hence, U describes a wave changing gradually from the concentric to the two-wire configurations. The required balun is to be sought by finding conductor cross sections corresponding to each intermediate U and assembling them along the axis. Note that

$$U = \log r_1 - \epsilon \log r_2,$$

and consider Fig. 1, which shows an equipotential plot for the case of $\epsilon = 0.5$. It wil be seen that the equipotentials are closed loops surrounding either P or Q, or both. When U is small, the equipotential is a single loop around P, and when U is large, it is a pair of loops, one around Q and one around both P and Q. There is a transition value of U for which the two latter loops join. This general description applies for any value of ϵ.

Now if one boundary is taken along one value of U, U_2, and the other along U_1, then the impedance of the resulting transmission line is

$$138(U_2 - U_1) \text{ ohm}$$

if the dielectric is air.

As an example, a design of balun will be given on which the following restrictions have been imposed:

1) The impedance is constant, 150 ohms (*i.e.*, $U_2 - U_1 = 1.09$).
2) The outer loop and the small loop around Q are at the same potential U_2.
3) The small U_2 loop is arranged to have the same diameter as the U_1 loop.
4) The scale of the cross section is adjusted, for each value of ϵ, so that the diameter of the U_1 loop remains constant through the taper.

The third condition needs qualifying. The diameter referred to is along the PQ axis, although for most of the balun it turns out that the small loops are very nearly circular. But when ϵ is small, it is not possible to fulfill the condition and then the transition loop is taken.

Fig. 2 shows several 150-ohm sections assembled into the balun.

A simple physical explanation of the balun is that the outer conductor is gradually replaced by a second wire as the return path. This second wire starts as a rib on the outer conductor and at a certain stage separates, leaving the outer conductor to expand in the manner of a horn. The proportion of current carried by the second wire (measured by ϵ) gradually increases, but it is not possible to continue the taper until virtually all the current flows in the second wire.

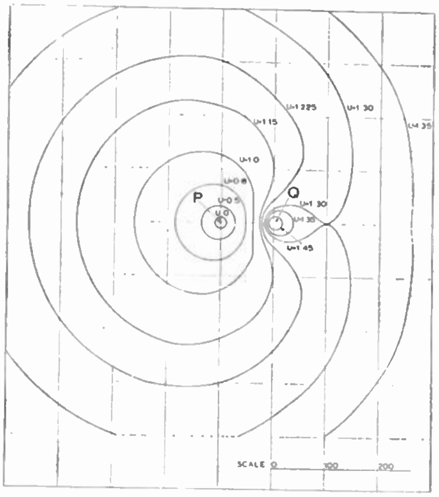

Fig. 1—Equipotentials for $\epsilon = 0.5$.

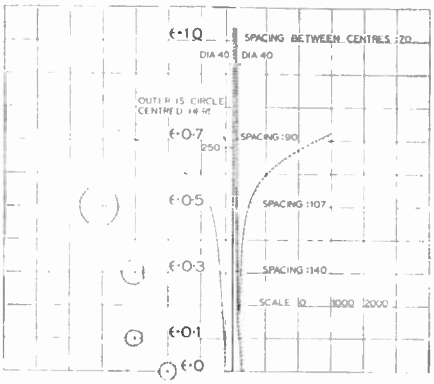

Fig. 2—Several sections assembled into the balun.

It can be shown that an approximate expression for the diameter D of the outer conductor is given in terms of the diameter d of a wire [for the conditions 1) to 4)] by

$$\log D/d = \frac{1.09}{1 - \epsilon^2}.$$

Practical limitations on D set a limit to ϵ of about 0.8.

At the section where the outer conductor is terminated, the spacing between the wires can be closed to the final spacing. This avoids reflection in the desired mode.

Due partly to the termination and partly to a finite angle of taper, other modes will be generated. Perhaps the most important is a TEM mode in which the second wire and the outer conductor are not at the same potential. This mode is reflected at the separation of the second wire from the outer conductor.

It may be desirable, in a practical device, to provide a mode suppressor which could take the form of a resistive card placed between the second wire and the outer conductor, in the PQ plane. In addition to suppressing the undesired TEM mode, this would probably be effective also on the higher modes. It would have little effect on the desired mode.

The fabrication of the balun does not seem to present great problems, although the shape of the outer conductor is a little inconvenient. It is possible that more convenient shapes could be substituted without appreciably changing the performance, for instance an outer conductor mainly circular and concentric with the first wire.

C. C. EAGLESFIELD
Standard Telecommun. Labs., Ltd.
Harlow, Essex, Eng.

Energy Fluxes from the Cyclotron Radiation Model of VLF Radio Emission*

In a recent note,[1] Santirocco makes a rough calculation of the energy radiated by gyrating protons in the magnetic field of the earth. Since he concludes that the energy is probably insufficient to explain the observed natural radiation known as "dawn chorus" as was proposed by MacArthur,[2] and accordingly favors the traveling wave amplifier hypothesis proposed by Gallet,[3] some comments on his note seem to be in order.

The geometry assumed by Santirocco, which for any one observer corresponds to an infinite plane sheet of radiators, is fairly realistic in one respect—that is, spectrographic observations in the auroral zone show that protons come in over large areas. It is not necessary to worry about geometry, however, since the radiation will be channeled down the magnetic field lines in the manner of whistlers, so that the result will be very nearly the same as the infinite plane source, whatever the actual shape of the emitting cloud.

Santirocco's note gives the impression that, in order to obtain the power he calculates, the protons must be oscillating in phase, but the power that he actually calculates is for oscillators in random phase. (His equation is $P = sn$, where P is the power, n the number of oscillators, and s the radiation flux per oscillator.) If the elementary oscillators are in phase, the power is proportional to the square of the number of oscillators, to within the approximation involved in assuming all oscillators to be at the same distance from the receiver.[4] The length of column assumed by Santirocco (700 km) is much too long to be considered

* Received by the IRE, November 18, 1960.

[1] R. A. Santirocco, "Energy fluxes from the cyclotron radiation model of VLF radio emission," PROC. IRE, vol. 48, p. 1650; September, 1960.

[2] J. W. MacArthur, "Theory of the very low frequency radio emissions from the earth's exosphere," *Phys. Rev. Lett.*, vol. 2, pp. 491–492; June, 1959.

[3] R. M. Gallet, "The very low frequency emissions generated in the earth's exosphere," PROC. IRE, vol. 47, pp. 211–231; February, 1959.

[4] L. Page and N. I. Adams, "Electrodynamics," D. Van Nostrand Co., Inc., Princeton, N. J., pp. 329–331; 1940.

in this way. To remove this difficulty, let us assume a cloud of particles of large horizontal extent, but of one kilometer thickness along the direction of the magnetic field. Such a structure is plausible in view of the auroral observations. Assuming a particle density of 10^3 protons cm^{-3} which corresponds to 10^{12} protons m^{-2} from the 1 km column, and using Santirocco's value of 2×10^{-33} for the flux from a single particle, the power becomes:

$$P = 2\times 10^{-33} n^2$$
$$= 2\times 10^{-33}\times 10^{24} = 2\times 10^{-11}\text{ watts } m^{-2}$$

for the phase coherent case. This is 100 times the power he calculates as minimum detectable. The density that he originally assumed (10^4 protons cm^{-3}) gives a signal of 2×10^{-7} watts m^{-2}, so it can be seen that there is no difficulty so far as the power is concerned, provided that the particles can be considered to gyrate as a group, or achieve phase coherence in some other manner.

Even supposing the elementary oscillators in random phase, the factor of 10^{-3} calculated by Santirocco is, as he says, not sufficient to be conclusive, in view of the roughness of the calculation. Actually, if the process is considered as taking place in the top of the ionosphere, which the writers consider the most favorable region, the factor is 10^{-2} rather than 10^{-3} because of the change in s due to the increase in magnetic field strength. Local concentrations of particles, some small degree of focusing action, or partial phase coherence could easily increase the signal strength by this much. Thus, it is impossible to discriminate against the gyrating proton mechanism on the basis of insufficient power.

There seems to be some impression that the traveling-wave amplification hypothesis has been shown to produce signals of sufficient power to be detectable. No calculation has been made which shows the traveling-wave mechanism capable of producing any signal at all, let alone a detectable one. In attempting to show that the power available from particle streams is sufficient to produce the observed signal, Helliwell[5] *assumed* an energy transfer of one per cent of the particle energy to the signal for the traveling-wave mechanism. The traveling-wave hypothesis consists solely of the suggestion that, since the velocity of electromagnetic radiation of the frequency range observed in chorus is comparable to that which might be expected of incoming charged particles, some interaction might lead to amplification of stray signals of these frequencies. Since no precise interaction is suggested, it is not possible to calculate what signal strength might be expected, nor is it possible to say whether the mechanism can work at all.

The writers are far from convinced that the proton gyration mechanism is the source of the phenomenon known as dawn chorus. It can be said, however, that protons approaching the earth will radiate in a manner which can be calculated, and that if this radiation is received on the ground it will have a frequency-time curve much like those observed in natural chorus. Whether the chorus actually observed is this radiation or not is still uncertain, and Dr. Santirocco's calculations are a valuable attempt to approach this problem from a new angle, even though the results are not conclusive.

This study was supported in part by the Electronics Research Directorate, U. S. Air Force Cambridge Research Center.

W. B. Murcray
J. H. Pope
Geophysical Inst.
University of Alaska
College, Alaska

[5] R. A. Helliwell, "Low Frequency Propagation Studies, Part 1: Whistlers and Related Phenomena," Radio Propagation Lab., Stanford University, Stanford, Calif., Final Rept., Contract AF 19(604)795, AFCR-TR-5(-189), ASTIA Document AD 110184; 1953–1956 (revised 1958).

Interpretation of the Transmission Line Parameters with a Negative-Conductance Load and Application to Negative-Conductance Amplifiers*

Introduction

In the study of negative-conductance amplifiers such as the maser, it is necessary to understand the effect of negative-conductance loads on transmission lines. Fig. 1 shows the normal configuration of a negative-conductance amplifier consisting of a circulator, transmission line, and a negative-conductance load. The signal enters the circulator, goes down the transmission line, encounters a negative conductance, returns up the transmission line amplified, and goes through the circulator to the receiver. The gain for such a configuration has been reported in the literature.[1]

Theory

Consider the transmission line and load of Fig. 1. Writing the standard equation[2] relating voltage and current at the load

$$I_1 + I_1' = I_L \tag{1}$$

$$V_1 + V_1' = V_L \tag{2}$$

and since $I_1 = V_1 Y_0$ and $I_1' = -V_1' Y_0$, we have

$$V_1 Y_0 - V_1' Y_0 = V_L Y_L. \tag{3}$$

Solving for the reflection coefficient,

$$\rho = \frac{V_1'}{V_1} = \frac{Y_0 - Y_L}{Y_0 + Y_L}. \tag{4}$$

If $Y_L = G$ and $Y_0 = G_0$

$$\rho = \frac{1 - \dfrac{G}{G_0}}{1 + \dfrac{G}{G_0}}. \tag{5}$$

Realizing that no restriction has been placed on the polarity of G, we can plot (5) in Fig. 2 for values of G/G_0 from -10 to $+10$. The reflected voltage V_1' is greater than V_1 for all values of $G/G_0<0$. In a negative-conductance amplifier $-1<G/G_0<0$ and the voltage gain is given by $|\rho|$.

If the load Y_L is complex and consists of a susceptance jB and two conductances G and G_1 and the transmission line, circulator, receiver, and source have the same conductance G_0, the power gain defined by the power delivered to the receiver divided by the power available from the source is given by

$$|\rho|^2 = \frac{\left(\dfrac{B}{G_0}\right)^2 + \left(1 - \dfrac{G}{G_0} - \dfrac{G_1}{G_0}\right)^2}{\left(\dfrac{B}{G_0}\right)^2 + \left(1 + \dfrac{G}{G_0} + \dfrac{G_1}{G_0}\right)^2}. \tag{6}$$

The standing-wave ratio is given by

$$S = \frac{V_{\max}}{V_{\min}} = \left|\frac{|V_1| + |V_1'|}{|V_1| - |V_1'|}\right|$$
$$= \left|\frac{1 + |\rho|}{1 - |\rho|}\right|. \tag{7}$$

Eq. (7) is plotted in Fig. 3 for values of G/G_0 from -10 to $+10$.

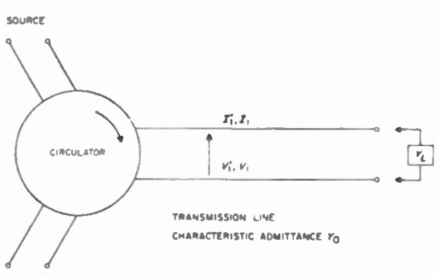

Fig. 1—Typical negative-admittance amplifier configuration.

Summary

The effect of connecting a negative-conductance load on a transmission line is to reflect a voltage which is larger than the forward traveling wave by the factor of the absolute value of the reflection coefficient. As shown in Fig 2, the gain goes to infinity as G/G_0 approaches -1 when the load reactance is tuned out. Since the reflected voltage is much greater than the forward traveling wave for high gain, there is little interference between the two waves. This results in a low standing wave ratio that approaches 1 as G/G_0 approaches -1 and the gain approaches infinity.

In the amplifying condition G/G_0 lies between 0 and -1. In an amplifier with a voltage gain of 10, $G/G_0=-0.82$, $\rho=10$ and $S=1.22$.

* Received by the IRE, August 5, 1960; revised manuscript received, November 7, 1960. This paper presents the results of one phase of research carried out at the Jet Propulsion Lab., California Inst. Tech., Pasadena, under Contract No. NASw-6, sponsored by the NASA.

[1] M. E. Hines and W. W. Anderson, "Noise performance theory of esaki (tunnel) diode amplifiers," Proc. IRE, vol. 48, p. 789; April, 1960.

[2] S. Ramo and J. Whinnery, "Fields and Waves in Modern Radio," 2nd ed., John Wiley and Sons, Inc., New York, N. Y.; 1953.

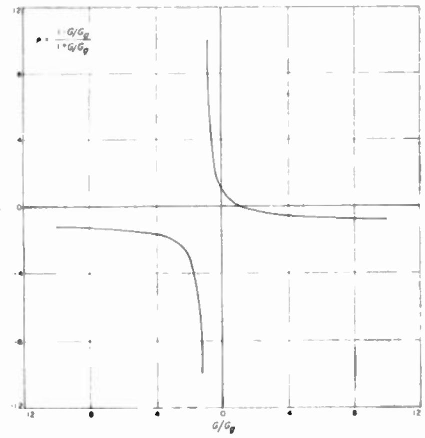

Fig. 2—Plot of transmission line reflection coefficient vs normalized load conductance.

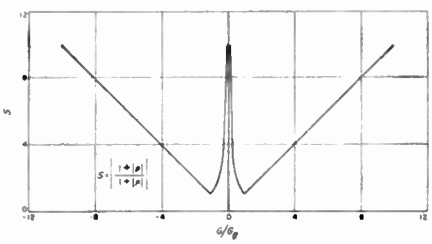

Fig. 3—Plot of transmission line standing-wave ratio vs normalized load conductance.

Ideally, the impedance of the transmission line, circulator, receiver, and source should be the same, so as to eliminate reflections and match the amplified signal to the receiver.

ACKNOWLEDGMENT

William Pilkington and Dr. Walter Higa contributed with helpful discussions.

GLOSSARY OF TERMS

B = Load susceptance.
G = Load conductance (not including losses).
G_0 = Real part of transmission line characteristic conductance.
G_1 = Circuit losses of load.
I_L = Current flowing into the load Z_L.
I_1 = Value of the current forward traveling wave at the load.
I_1' = Value of the current negative traveling wave at the load.
S = Standing wave ratio $= V_{max}/V_{min}$.
V_L = Voltage across the load Z_L.
V_{max} = The value of the maximum voltage along a transmission line.
V_{min} = The value of the minimum voltage along a transmission line.
V_1 = Value of the voltage forward traveling wave at the load.
V_1' = Value of the voltage negative traveling wave at the load.
Y_L = Transmission line load admittance.
Y_0 = Transmission line characteristic conductance.
ρ = Reflection coefficient $= V_1'/V_1$.

C. T. STELZRIED
Jet Propulsion Lab.
California Inst. Tech.
Pasadena, Calif.

WWV and WWVH Standard Frequency and Time Transmissions*

The frequencies of the National Bureau of Standards radio stations WWV and WWVH are kept in agreement with respect to each other and have been maintained as constant as possible with respect to an improved United States Frequency Standard (USFS) since December 1, 1957.

The nominal broadcast frequencies should, for the purpose of highly accurate scientific measurements, or of establishing high uniformity among frequencies, or for removing unavoidable variations in the broadcast frequencies, be corrected to the value of the USFS, as indicated in the table. The corrections reported have been improved by a factor of three over those previously reported, by means of improved measurement methods based on LF and VLF transmissions.

The characteristics of the USFS, and its relation to time scales such as ET and UT2, have been described previously,[1] to which the reader is referred for a complete discussion.

The WWV and WWVH time signals are also kept in agreement with each other. Also they are locked to the nominal frequency of the transmissions and consequently may depart continuously from UT2. Corrections are determined and published by the U. S. Naval Observatory. The broadcast signals are maintained in close agreement with UT2 by properly offsetting the broadcast frequency from the USFS at the beginning of each year when necessary. This new system was commenced on January 1, 1960. A retardation time adjustment of 20 msec was made on December 16, 1959; another retardation adjustment of 5 msec was made at 0000 UT on January 1, 1961.

WWV FREQUENCY WITH RESPECT TO U. S. FREQUENCY STANDARD

1961 January	Parts in 10^{10}†
1	−151.8
2	−151.4
3	−151.0
4	−150.8
5	−150.8
6	−150.9
7	−151.0
8	−151.1
9	−151.0
10	−151.1
11	−151.3
12	−151.5
13	−151.7
14	−151.9
15	−151.7
16	−151.1
17	−150.7
18	−150.5
19	−150.4
20	−150.1
21	−150.2
22	−150.4
23	−150.3
24	−150.2
25	−150.4
26	−150.7
27	−150.6
28	−150.6
29	−150.6
30	−150.5
31	−150.5

† A minus sign indicates that the broadcast frequency was low. The uncertainty associated with these values is $\pm 3 \times 10^{-11}$.

NATIONAL BUREAU OF STANDARDS
Boulder, Colo.

* Received by the IRE, February 23, 1961.
[1] "National Standards of Time and Frequency in the United States," PROC. IRE, vol. 48, pp. 105–106; January, 1960.

Minimum Power Set by Quantum Effects*

In gamma-ray spectroscopy, far more photons must be counted to determine the central frequency of a gamma-ray line spectrum than to merely measure its intensity. One might similarly expect that at radio frequencies the specific power level at which quantum limitations become important should depend on the information to be extracted from the signal. We shall demonstrate this possibility by estimating the minimum power set by quantum considerations in an idealized experiment intended to measure the frequency of a CW signal.

Let us suppose that it is desired to measure the frequency of a CW signal with as great precision as possible. It will be assumed that we have the advantage of knowing beforehand that the signal frequency lies between two limiting frequencies, f_1 and $f_2 (f_2 > f_1)$. We will also impose the restriction on integrating time that only one second of time is available for the measurement. Our problem is thus equivalent to that of measuring the frequency transmitted from a satellite within the frequency range set by the expected Doppler shift and within the time the frequency may be assumed to remain reasonably constant.

In order to make maximum use of all available signal power, it is proposed to determine the frequency by passing the signal through a lossless device which divides the signal into two portions appearing at separate output ports. The amounts of signal power P_1 and P_2 leaving the two output ports will be assumed to depend on frequency, as in a typical transmission line hybrid with two output ports separated from the input and each other by different fractions of a wavelength at different frequencies. In order to simplify calculations we will assume this power divider to have ideal linear characteristics, such that the ratio of the power P_1 leaving one output port to the total input power P equals the ratio of the amount by which the signal frequency f exceeds its lowest possible value f_1, to the frequency range $f_2 - f_1$ in which the signal frequency is known beforehand to lie.

The operation of the power divider may then be described by the two relationships,

$$P = P_1 + P_2 \text{ (no power loss)} \qquad (1)$$

$$\frac{P_1}{P_1 + P_2} = \frac{f - f_1}{f_2 - f_1} \qquad (2)$$

(power division proportional to position of f within frequency range).

Since the division of power between the output ports is frequency-dependent, the frequency may be found by measuring P_1 and P_2 separately. We will find that in order to accurately measure frequency this way a large number of photons are required.

We consider first the case $f - f_1 \geq f_2 - f$. Rewriting (2), we see that if P_1 and P_2 can be measured with perfect accuracy the dif-

* Received by the IRE, November 1, 1960; revised manuscript received, December 8, 1960. This work was supported by the Ballistic Res. Labs., Aberdeen Proving Ground, Md.

ference between the signal frequency f and f_1 is given by

$$f - f_1 = \left(\frac{P_1}{P_1 + P_2}\right)(f_2 - f_1). \quad (3)$$

If, on the other hand, it is possible to measure $P_1/(P_1+P_2)$ with only a relative accuracy r, we must regard the actual frequency as given by

$$f - f_1 = (f_2 - f_1)\frac{P_1}{P_1 + P_2}(1 \pm r), \quad (4)$$

when measured values are used for P_1 and P_2. Since

$$f = f_1 + (f_2 - f_1)P_1/(P_1 + P_2) \pm r(f_2 - f_1)P_1(P_1 + P_2),$$

the measured frequency can be considered to be determined only within

$$\Delta f = r(f_2 - f_1)P_1/(P_1 + P_2) \text{ cps}.$$

We now proceed to estimate the minimum relative accuracy r set by quantum considerations only. At optical or higher frequencies the powers P_1 and P_2 would be measured with photon counters. Gabor[1,2] has given a general theoretical proof that no more information can be obtained from a signal with radio equipment than that obtainable with photon counters. Accordingly, we will compute the minimum value of Δf as that which would result if P_1 and P_2 were measured with photon counters. Since photons are counted randomly in time, in successive equal intervals of time the number of counts fluctuates about its mean value n with the $\sqrt{n}$ standard deviation characteristic of the Poisson distribution governing events occurring randomly in time. Thus, if in a fixed time interval t one observes n_1 photons at output port 1, and n_2 photons at output port 2, then P_1 and P_2 must be considered to be determined only within relative uncertainties $\sqrt{n_1}/n_1$ and $\sqrt{n_2}/n_2$.

Applying these uncertainties to P_1 and P_2, one has for the ratio $P_1/(P_1+P_2)$ a relative uncertainty r of $\sqrt{P_1/P_2}/\sqrt{n_1+n_2}$ and, therefore, a measurement uncertainty

$$\Delta f = \sqrt{\frac{P_1}{P_2}}\,\frac{1}{\sqrt{n_1 + n_2}}\,\frac{(f_2 - f_1)P_1}{P_1 + P_2}. \quad (5)$$

If a one-second integrating time is assumed, $n_1 + n_2 = P/hf$, giving

$$\Delta f = \sqrt{\frac{P_1}{P_2}}\sqrt{\frac{hf}{P}}\,\frac{(f_2 - f_1)P_1}{P_1 + P_2}. \quad (6)$$

Solving for P gives the minimum power, permitting measurement with any given precision Δf as

$$P = \frac{P_1}{P_2}\left(\frac{f_2 - f_1}{\Delta f}\right)^2\left(\frac{P_1}{P_1 + P_2}\right)^2 hf. \quad (7)$$

If $f - f_1 < f_2 - f$, the ratio $P_2/(P_1+P_2)$ may be measured with greater accuracy than the ratio $P_1/(P_1+P_2)$, and (7) is replaced by

$$P = \frac{P_2}{P_1}\left(\frac{f_2 - f_1}{\Delta f}\right)^2\left(\frac{P_2}{P_1 + P_2}\right)^2 hf. \quad (8)$$

The greatest power is required when $P_1 = P_2$. Then the minimum power needed to measure, by this technique, to an accuracy Δf of one cps, the frequency f of a 100-Mc signal known beforehand to lie within a band $f_2 - f_1$ of 10 kc, is approximately 10^{-18} watts by either (7) or (8).

Another radio measurement in which quantum considerations might similarly prevent rapid measurement is radio direction finding. The determination of the direction of a distant transmitter with a rotatable receiving antenna is equivalent to using the distant source to measure the radiation pattern of the receiving antenna with sufficient precision to define the direction giving maximum intensity. In this case, the bearing giving maximum intensity can be found only by comparing intensity measurements on different bearings, each of which, like the powers P_1 and P_2 in the frequency measurement, requires a minimum number of photons for its precise measurement.

L. P. Bolgiano, Jr.
W. M. Gottschalk
Dept. of Elec. Engrg.
University of Delaware
Newark, Del.

[1] D. Gabor, "Communication theory and physics," *Phil. Mag.*, vol. 41, pp. 1161–1187; November, 1950.
[2] D. Gabor, "Der Nachrichtengehalt eines electromagnetischen Signals," *Arch. Elekt. Übertragung*, vol. 7, pp. 95–99; February, 1953.

Corrections and Coordination of Some Papers on Noise Temperature*

This note should clarify the applications of the noise temperature concept as given recently by various authors, and provide some corrections.

The literature mentions various noise temperatures which are related to each other in a receiving system. Radio astronomers seek the cosmic noise temperature, and communication engineers seek *CNR* of the received signal referred to some convenient point. Some important papers on the subject are incomplete in definition to the extent of not distinguishing the point of noise temperature reference, and of possibly obscuring the application to *CNR* calculations.

The following nomenclature is most common to the authors. The asterisk indicates reference to the input terminals of the receiver.

- C = *received rms power of desired signal, in watts
- $N = P$ = *summation of all noises that can be expressed by KTB, in watts
- K = Boltzmann's constant, 1.38×10^{-23} watts per cps per degree Kelvin
- B = bandwidth in cycles per second
- G = gain of receiver between input terminals and any later point
- L = loss ratio of input to output
- A = attenuation ratio of output to input, or $1/L$
- T = noise temperature in degrees Kelvin

Subscripts (all giving location of loss and/or temperature)

- a = antenna
- bl = back lobes of antenna
- x = mixer
- $h2o$ = atmospheric waver vapor
- g = galaxy
- if = intermediate frequency
- $o2$ = atmospheric oxygen
- s = *effective noise of entire antenna and receiver system
- e = *effective noise of receiver and prior hardware
- er = *effective noise of receiver alone
- L_0 = losses in hardware located between antenna aperture and input terminals in receiver
- $T_L = T_0$ = ambient temperature, which may be 290° Kelvin

To obtain *CNR*, $N = KT_sB$. Therefore, we will reduce the noise temperature expression given by each author to a value T_s. The clearest and simplest explanation of noise temperature and T_s may be that of Hogg and Mumford.[1] From their Fig. 1, and referencing the receiver output terminal,

$$N = \frac{GKB}{L}[T_a + (L - 1)T_L + LT_{er}]. \quad (1)$$

The last two terms in the brackets give the hardware noise and the receiver noise. Now referring the noise to the receiver input terminals by deleting G, and clearing the loss factor, we have

$$N = KB\left[\frac{T_a}{L} + \left(1 - \frac{1}{L}\right)T_L + T_{er}\right]. \quad (2)$$

Next, replacing the loss ratio with its reciprocal, the attenuation factor A_0, the terms in brackets become

$$T_s = A_0T_a + (1 - A_0)T_0 + T_{er}. \quad (3)$$

This seems completely clear and will be retained herein as a standard of comparison, with our reference retained as the receiver input terminals. Note that hardware noise temperature is proportional to its loss, and only a termination (absorbing all signal) has the same noise temperature as the ambient. [Our Eq. (7) is also convenient.]

Dimond[2] has given a particularly convenient delineation of noise temperature as related to *CNR*. Typographical errors include: 1) In the last equation, page 684, expression for P, change "182" to "172°", 2) in Fig. 3, the middle line, change "db" to "dbw," 3) in Fig. 4, change "db/cps bw" to "watts/cps bw expressed in dbw," 4) in Fig. 4, one may delete the left-hand arrow and also that at the lowest abscissae scale, and the "ANTENNA GAIN" arrow should refer to the number scale immediately above (100 db to −10 db).

The significant error is in Dimond's (6) and footnote 15, which presume that a noise source of 290° is connected. His (6) is most usefully changed to $P = KT_sB$ where T_s comes from Dimond's (7) or our (3). These

* Received by the IRE, November 14, 1960; revised manuscript received, December 15, 1960.

[1] D. C. Hogg and W. W. Mumford, "The effective noise temperature of the sky," *Proc. Natl. Conf. on Aeronautical Electronics* (*NAECON*), pp. 580–587; May, 1959.
[2] R. H. Dimond, "Interplanetary telemetering," Proc. IRE, vol. 48, pp. 679–685; April, 1960.

errors have been brought to the attention of Mr. Dimond, who is submitting corrections including his Fig. 3 and numerical work.

A report to the U. S. Government[3] states "the equivalent antenna input noise temperature is $T_e = T_a + T \ldots T_a$ (evaluates) a noise power, . . . generated by the thermal background radiation to which the radiation resistance is subjected. . . T is the ambient temperature surrounding the antenna ohmic losses. . . . " The assumption appears to be that the antenna, T, is inherently a 290° noise source; the value of T (our T_0) should be corrected as in (2) or (3).

Perlman, *et al.*,[4] in (7) express T_s, with antenna noise T_a taken twice for the case where there is no preselector, due to image noise.

$$T_s = T_x + T_{if} + 2T_a. \quad (4)$$

This is consistent with our (3) provided that the hardware losses $(1-A_0)T_L$ are added to (4).

Drake and Ewen[5] give

$$T_{e2} = \frac{T_{eq}}{(A_1 + A_2)} + T_b + T_t + T_{A_2} + T_l. \quad (5)$$

This is equivalent to our (3), with their nomenclature; the five terms on the right-hand side are, respectively, any noise generator connected to the system (with its coupling losses in the denominator), the galactic background radiation (equivalent black-body temperature of), tropospheric losses (oxygen and water vapor), hardware losses (theirs is expressed as a ferrite switch and the sidelobe losses), and man-made noises.

Madigan[6] gives similar information for the radar receiver:

$$T = T_a + (L-1)290 + L(F-1)290. \quad (6)$$

Replacing his $(F-1)290$ with our identical T_{er}, and his T with our T_s, we have

$$T_s = T_a + (L-1)290 + LT_{er}. \quad (7)$$

This expression assumes 290° Kelvin for the temperature of the lossy hardware, which could be true, or could be altered by sun heat, equipment-room heat, conducted RF current, or refrigeration. Eq. (7) is identical to our (3) except for the first $1/L$ factor in (1). Thus, Madigan's input terminal must be the input to the prereceiver hardware and not the receiver itself, although he states "the noise output of the ideal receiver will be KTB times the gain of the receiver. For this to be the same noise output as in the nonideal receiver, the effective operating temperature must be T. . . . " To arrange the Madigan equation in the Hogg and Mumford manner requires dividing Madigan's right-hand expression by L.

Ewen's[7] Fig. 1 illustrates temperatures and losses. For simplicity, his last equation assumes all temperatures equal. "T_1T_0" should read $T_1 = T_0$. With another simplification, $L_1L_{o2}L_{b2o}L = L_0$ (the combined losses from the receiver input terminals back out through the ionosphere), and otherwise using the above tabulated nomenclature, Ewen gives

$$T_s = (T_g + T_{b1}) + (L_0 - 1)T_0 + T_eL_0. \quad (8)$$

This apparently customary treatment by the radio astronomers increases the hardware losses and receiver temperature in order to reference all noises back to outer space,—the location of their target, and a convenient place to correct for nontarget noise sources. To use (8) for calculation of noise temperatures seen at the receiver input terminals (our T_s) requires dividing the whole expression by Ewen's L_0.

EDWIN DYKE
Melpar, Inc.
Falls Church, Va.

[3] McCallum, *et al.*, "Factors for Systems Considerations of Earth Satellites," Govt. Contract AF 33(616)-5471, June 30, 1960 (unclassified report).

[4] S. Perlman, *et al.*, "Concerning optimum frequencies for space vehicle communication," *Record of Natl. Symp. on Extended Range and Space Communications*, pp. 24–31; October, 1958.

[5] F. D. Drake and H. I. Ewen, "A broad-band microwave source comparison radiometer for advanced research in radio astronomy," PROC. IRE, vol. 46, pp. 53–60; January, 1958.

[6] T. W. Madigan, "Receiver sensitivity graph," *Electronics*, vol. 32, p. 62; April 3, 1959.

[7] H. I. Ewen, "Thermodynamic analysis of maser systems," *Microwave J.*, vol. 2, pp. 41–46; March, 1959.

Small-Signal Space-Charge Density in Drifting Ion-Neutralized Rectilinear-Flow Beams Immersed in an Axial Magnetic Field of Finite Magnitude*

In the small-signal field theory of electron beams,[1] the alternating part of the space-charge density ρ_1 is calculated under the assumption of an infinite confining axial magnetic field and is found to be proportional to the axial component of the high-frequency electric field E_z. When the constant axial magnetic field is relaxed so that transverse motions of electrons are permitted, a more general expression for the space-charge density ρ_1 is found. Analyses of waves in beams under such conditions, specifically of cyclotron waves,[2] for the frequencies where the phase velocity v_p is greater than the velocity of light c, may be useful in connection with the treatment of essentially transverse electric field tubes, such as the quadrupole amplifier at high frequencies (X band), which have recently attracted interest.

We shall now calculate the alternating space-charge density in a drifting rectilinear-flow ion-neutralized beam for a finite axial magnetic field. Since it has been shown by Hahn[3] and more recently by Suhl and Walker[4] that the electromagnetic waves in such media can no longer be resolved into purely TE and TM modes, the derivation should include also the effects of the high-frequency magnetic field. Consider that the ion-neutralized electron beam moves with a uniform velocity v_0 along the z-coordinate axis, immersed in a constant magnetic field of intensity B_0 in the direction of the z axis. It is assumed, as usual, that all alternating quantities (ρ_1, v_1, E, H) vary with time and the z coordinate as the function $\exp j(\omega t - \beta z)$; and, furthermore, all products of alternating quantities are neglected.

Definition of symbols:

ω = operating frequency
$\omega_p{}^2 = e\rho_0/m\epsilon_0 K$ plasma frequency (squared)
$\omega_c = (e/mK)B_0$ cyclotron frequency
β = propagation constant
ρ_0 = dc charge density in the beam
e/m = charge-to-mass ratio for electrons
e_z = unit vector in the direction of z axis
$K^2 = 1/[1-(v_0/c)^2]$ relativistic factor
$\omega_b = \omega - v_0\beta$ transformed operating frequency.

The force equation for charged particles is[5]

$$\frac{dv_1}{dt} = \frac{e}{mK}\Big[E + v_1 \times B_0 + \mu_0 v_0 \times H - \frac{1}{c^2} v_0(v_0 \cdot E)\Big]. \quad (1)$$

This equation is readily solved for v_1 after we replace d/dt by $j\omega_b$

$$v_1 = \frac{\omega_b \omega_p{}^2 \epsilon_0}{j(\omega_b{}^2 - \omega_c{}^2)\rho_0}\Big\{E - \frac{v_0{}^2}{c^2} e_z(e_z \cdot E) - \frac{\omega_c{}^2}{\omega_b{}^2}\frac{1}{K^2} e_z(e_z \cdot E) + j\frac{\omega_c}{\omega_b}(e_z \times E) + \mu_0 v_0(e_z \times H) + j\frac{\omega_c}{\omega_b}\mu_0 v_0\big[e_z(e_z \cdot H) - H\big]\Big\}. \quad (2)$$

With the use of the relations

$$J_1 = \rho_0 v_1 + v_0 \rho_1 \quad (3)$$

$$\frac{\partial \rho_1}{\partial t} = -\nabla \cdot J_1 \quad (4)$$

$$j\omega_b \rho_1 = -\rho_0 \nabla \cdot v_1 \quad (5)$$

the space-charge density is found to be given by

$$\rho_1 = \frac{\omega_p{}^2 \omega_c \epsilon_0}{(\omega_b{}^2 - \omega_c{}^2 - \omega_p{}^2/K^2)c}\Big\{-\sqrt{\frac{\mu_0}{\epsilon_0}}H_z + j\Big[\frac{\omega_c \beta_c}{\omega_b{}^2 K^2} - \frac{v_0}{c}\frac{\omega_b}{\omega_c}\Big(1 - \frac{\omega_p{}^2}{\omega_b{}^2 K^2}\Big)\Big]E_z\Big\}. \quad (6)$$

* Received by the IRE, December 27, 1960. The research reported here was supported by the Wright Air Dev. Div., Wright-Patterson AFB, Dayton, Ohio, under Contract AF 33(616)-6139.

[1] See, for instance, R. G. E. Hutter, "Beam and Wave Electronics in Microwave Tubes," D. Van Nostrand Co., Inc., Princeton, N. J., ch. 9; 1960.

[2] A. W. Trivelpiece and R. W. Gould, "Space charge waves in cylindrical plasma columns," *J. Appl. Phys.*, vol. 30, pp. 1784–1793; 1959.

[3] W. C. Hahn, "Small signal theory of velocity modulated electron beams," *GE Rev.*, vol. 42, pp. 258–270; June, 1939.

[4] H. Suhl and L. R. Walker, "Topics in guided wave propagation through gyromagnetic media," *Bell Sys. Tech. J.*, vol. 33, pp. 579–659; 1954.

[5] See, for instance, L. Landau and E. Lifshitz, "Theory of Fields," Addison-Wesley Co., Reading, Mass., p. 46; 1959.

Obviously, for $\omega_r \rightarrow \infty$ the expression for ρ_1 of (6) becomes the familiar one which is obtained with an infinite magnetic field.

It is noted that the contribution of the high-frequency magnetic field to the space-charge density ρ_1 is not negligible in general. Calculations[6] for a beam in a drift tube, as well as for a waveguide filled with nonmoving plasma, show that in the cyclotron modes and some waveguide modes which are predominantly transverse electric at values of phase velocity greater than the velocity of light, the major contribution to the space-charge density ρ_1 is due to the axial component of the high-frequency magnetic field.

Moreover, it is apparent from (6) that near metallic walls tangential to E_z, the latter tends to vanish, and there the space-charge density ρ_1 is due almost entirely to high-frequency magnetic field H_z.

V. Bevc
Dept. of Elec. Engrg.
University of California
Berkeley, Calif.

[6] V. Bevc and T. E. Everhart, "Fast Waves in Plasma Filled Waveguides," Electronics Res. Lab., Univ. of Calif., Berkeley, Calif., Tech. Rept. under Wright Air Dev. Div. Contract AF 33(616)-6139; to be published.

The External Electromagnetic Fields of Shielded Transmission Lines*

In order to reduce the amount of interference caused by the transmission network of an electronic system, it is often expedient to shield the individual transmission lines. The most commonly used type of shielded line is the ordinary coaxial cable (Fig. 1). A second type not infrequently used is the parallel pair of wires enclosed in a circular shield—the shielded pair (Fig. 2). The problem of calculating the external fields or predicting the "shielding effectiveness" of these lines has been investigated.[1]

In the analysis, the transmission lines are assumed to be sinusoidally excited and operating in the steady state. Only lines of infinite length are considered, which restrict the results to describing the near fields of actual lines. Filamentary inner conductors and solid shields are also assumed.

The analytical method used is a direct extension of the classical perturbation technique employed to calculate the attenuation factor for high-frequency transmission lines and waveguides. Since a well-designed transmission line operates in a "nearly" TEM mode, the transverse field pattern in the line dielectric is substantially the static configuration, and only a relatively small component of axial electric intensity exists. Because of this, it is feasible to consider initially an ideal TEM mode to calculate the interior transverse fields; on this basis, the imperfect TEM mode is subsequently analyzed.

The results achieved, (1) and (2), show that the external field components of the coaxial line, E_{r3} and $H_{\theta 3}$, and the shielded pair, E_{r3}, $H_{\theta 3}$, $E_{\theta 3}$, and H_{r3}, depend on the shield properties as well as the line dielectric constant. The external longitudinal electric intensity, E_{z3}, essentially depends on only the shield properties. All field components are inverse functions of radius, and the shielded-pair fields are harmonic functions of angular displacement. For typical shielded lines, the transverse electric intensity may be several hundred times larger than the axial intensity at the outside of the shield. Using the derived external field equations, it is possible to calculate the shielding effectiveness of a shielded transmission line.

Coaxial Line

$$H_{\theta 3} = \frac{j\omega\epsilon_3}{k_3} SI \frac{1}{k_3 r \ln 2/k_3 b}$$

$$E_{r3} = \frac{\gamma}{k_3} SI \frac{1}{k_3 r \ln 2/k_3 b}$$

$$E_{z3} = SI \frac{\ln 2/k_3 r}{\ln 2/k_3 b}. \tag{1}$$

Shielded Pair

$$H_{\theta 3} = \sum_{n=1}^{\infty} 2 \frac{j\omega\epsilon_3}{k_3} SI \left(\frac{c}{a}\right)^{2n-1} \frac{2n-1}{k_3 r} \left(\frac{b}{r}\right)^{2n-1} \cos (2n-1)\theta$$

$$E_{r3} = \sum_{n=1}^{\infty} 2 \frac{\gamma}{k_3} SI \left(\frac{c}{a}\right)^{2n-1} \frac{2n-1}{k_3 r} \left(\frac{b}{r}\right)^{2n-1} \cos (2n-1)\theta$$

$$E_{z3} = \sum_{n=1}^{\infty} 2 SI \left(\frac{c}{a}\right)^{2n-1} \left(\frac{b}{r}\right)^{2n-1} \cos (2n-1)\theta \tag{2}$$

$$E_{\theta 3} = \sum_{n=1}^{\infty} 2 \frac{\gamma}{k_3} SI \left(\frac{c}{a}\right)^{2n-1} \frac{2n-1}{k_3 r} \left(\frac{b}{r}\right)^{2n-1} \sin (2n-1)\theta$$

$$H_{r3} = \sum_{n=1}^{\infty} -2 \frac{j\omega\epsilon_3}{k_3} SI \left(\frac{c}{a}\right)^{2n-1} \frac{2n-1}{k_3 r} \left(\frac{b}{r}\right)^{2n-1} \sin (2n-1)\theta$$

$$S = \left[\frac{k_2}{\sigma_2} \frac{1}{\pi a}\right]\left[\sqrt{\frac{a}{b}} \frac{j}{\epsilon^{-jk_2(b-a)}}\right], \qquad j = \sqrt{-1}$$

$$k_2^2 = -j\omega\sigma_2\mu_2, \qquad k_3^2 = -\omega^2(\mu_1\epsilon_1 - \mu_3\epsilon_3)$$

$$\gamma^2 = -\omega^2\mu_1\epsilon_1.$$

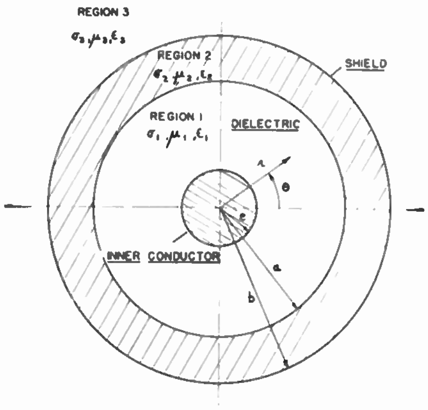

Fig. 1—The coaxial line.

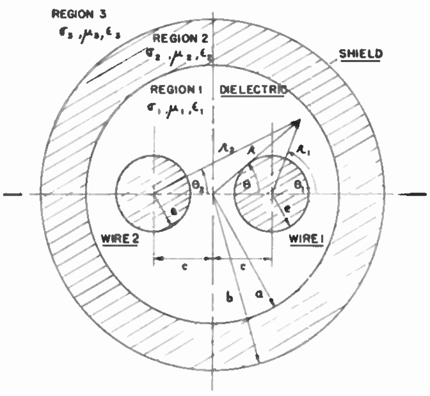

Fig. 2—The shielded pair.

J. D. Meindl
USASRDL
Fort Monmouth, N.J.
Formerly at Carnegie Inst. Tech.
Pittsburgh, Pa.
E. R. Schatz
Carnegie Inst. Tech.
Pittsburgh, Pa.

* Received by the IRE, November 21, 1960. The authors gratefully acknowledge the support of Signal Corps Contract No. DA 35-039, SC 72308.

[1] Final report on Contract No. DA 36-039, SC 72308, USASRDL Fort Monmouth, N. J., by the Dept. of Elec. Engrg., Carnegie Inst. Tech., Pittsburgh, Pa.; July, 1938.

Duality as Applied to Transformers*

The principle of duality as applied to a circuit with transformers has been generally avoided by most authors except under certain special conditions which will be briefly reviewed. The purpose of this lettter is to show that a topological dual-like circuit can always be obtained for a planar network whether or not the original circuit has transformers. By the utilization of the ideal transformer as a circuit element, it is possible to derive the topological dual circuit for any planar network. Of course, in the realization of the dual circuit, a transformer will have to be used instead of an ideal transformer; however, there are many situations where this substitution is permissible.

* Received by the IRE, November 1, 1960; revised manuscript received December 16, 1960.

The argument with respect to duality as considered by most authors simply states that duality does not apply if a negative capacitor is necessary in the dual circuit. The necessity of a negative capacitor in the dual of a transformer is a result of the use of the T-equivalent circuit as a model to represent the transformer. Assuming that a common connection can exist, a dual network is permitted if all of the capacitors in the dual circuit are positive, which constrains the T-equivalent circuit to have all positive inductors.

Let us digress for a moment to show that an ideal transformer is the dual of itself when turned end for end, and then, we will return to the original argument to show that a transformer has a dual with all positive elements if an ideal transformer is permitted in the dual circuit. In order to show that an ideal transformer is the dual of itself when turned end for end, we need to compare Fig. 1(a) and Fig. 1(b) with respect to voltages and currents, together with the hybrid h and g parameters which are themselves dual systems. The following dual comparisons can be made:

Original System	*Dual System*
[*Fig. 1(a)*]	[*Fig. 1(b)*]
i_1, i_2, v_1, v_2	v_1, v_2, i_1, i_2 (*respectively*)

$$h_{11} = \left.\frac{v_1}{i_1}\right|_{(v_2=0)} = 0 \qquad g_{11} = \left.\frac{i_1}{v_1}\right|_{(i_2=0)} = 0$$

$$h_{12} = \left.\frac{v_1}{v_2}\right|_{(i_1=0)} = 1/n \qquad g_{12} = \left.\frac{i_1}{i_2}\right|_{(v_1=0)} = 1/n$$

$$h_{21} = \left.\frac{i_2}{i_1}\right|_{(v_2=0)} = 1/n \qquad g_{21} = \left.\frac{v_2}{v_1}\right|_{(i_2=0)} = 1/n$$

$$h_{22} = \left.\frac{i_2}{v_2}\right|_{(i_1=0)} = 0 \qquad g_{22} = \left.\frac{v_2}{i_2}\right|_{(v_1=0)} = 0$$

Thus, an ideal transformer is the dual of itself when turned end for end.

Returning to the original problem of obtaining the dual of a transformer, let us define a different model, given in Fig. 2(b), to represent the transformer. The parameters of Fig. 2(b) can be identified with the parameters of Fig. 2(a) by the following equations

$$L_P = M^2/L_2, \tag{1}$$

$$L_S = L_1 - M^2/L_2, \tag{2}$$

and

$$n = L_2/M. \tag{3}$$

From these equations, it follows that L_S is always positive since the mutual inductance M must be less than $\sqrt{L_1L_2}$; however, the voltage-turns ratio n can be either positive or negative depending on the sign of M. The sign of n will be indicated by the familiar "dot rule" where a dot is located on each winding of the ideal transformer as illustrated by Fig. 3. Having defined a model for a transformer that can absorb any negative inductance by the turns ratio n, it is possible to derive the topological dual circuit for this model as given by Fig. 2(c).

From these results, it is now possible to set forth the rules for obtaining the topological dual of a planar network which contains transformers. In addition to the usual

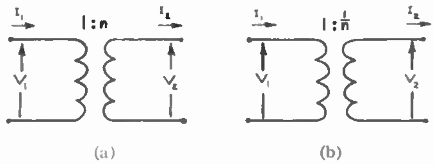

Fig. 1—The ideal transformer and its dual.

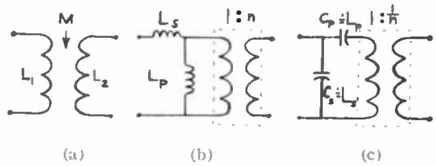

Fig. 2—A transformer and its dual as defined by a different model.

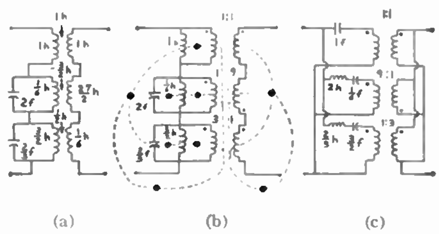

Fig. 3—A network with two separate parts and its dual.

rules for obtaining the topological dual of a given network, the following additional rules should be included:

1) Each transformer in the circuit is replaced by its model.
2) The dual network will have as many separate parts as the original network; therefore, a reference node is assigned to each separate part.
3) The dual of the primary winding is the secondary winding and conversely.
4) After the dual of each separate part of the network is obtained, the primary and secondary windings of each ideal transformer should be grouped together as in the original circuit.

These ideas will be illustrated by an example. In this example, we will derive the dual of a network which has two separate parts where the driving-point and transfer impedances are given by the equations

$$Z_{11} = \frac{(3/2)s}{s^2+1} + \frac{(1/2)s}{s^2+3} + s, \tag{4}$$

$$Z_{12} = Z_{21} = \frac{(1/2)s}{s^2+1} - \frac{(9/2)s}{s^2+3} + s, \tag{5}$$

and

$$Z_{22} = \frac{(1/6)s}{s^2+1} + \frac{(81/2)s}{s^2+3} + s. \tag{6}$$

Comparing Fig. 3(b) and Fig. 3(c), it follows that the driving-point and transfer admittances of the dual circuit are equal to the driving-point and transfer impedances given by (4), (5), and (6).

Paul G. Griffith
Dept. of Elec. Engrg.
University of Arizona
Tucson, Ariz.

Transient Behavior of Aperture Antennas*

A recent article by Polk[1] appears to contain several typographical and/or calculation errors.

Eq. (3) should read,

$$R(\bar{r}, \omega) \approx \frac{i}{2\lambda R} e^{-ikr}(\cos\theta + i_z\cdot\bar{s}) \cdot \int_A P_0(\xi,\eta) e^{ik\sin\theta(\xi\cos\phi+\eta\sin\phi)} d\xi d\eta. \tag{3}$$

Eq. (6) should read,

$$F(\omega) = \frac{1}{\sqrt{2\pi}} \frac{\omega_1}{\omega_1^2 - \omega^2}. \tag{6}$$

Eq. (7) should read,

$$R(\bar{r}, \omega) = \frac{iAe^{-i(\omega R/c)}\sin\omega x}{2\pi c R x} \tag{7}$$

Eq. (7) is based on the assumption that

$$(\cos\theta + \bar{i}_z\cdot\bar{s}) = 2, \tag{a}$$

and thus is correct for small values of θ but is off by a factor of two for large values of θ.

Eqs. (10)–(12) should read,

$$M = \frac{A\omega_1}{2\pi c R} \tag{10}$$

$$\psi_0 = 0, \qquad q < -x \tag{b}$$

$$\psi_0 = \frac{1}{2} M\left[\frac{\cos x\omega_1}{x\omega_1}\sin q\omega_1 + \frac{\sin x\omega_1}{x\omega_1}\cos q\omega_1\right], \quad -x < q < x \tag{11}$$

$$\psi_0 = M\frac{\sin x\omega_1}{x\omega_1}\cos q\omega_1, \qquad x < q \tag{12}$$

where

$$x = \frac{a}{2c}\sin\theta. \tag{8}$$

θ must be restricted to the first quadrant or (8) redefined to be

$$x = \left|\frac{a}{2c}\sin\theta\right|, \tag{c}$$

or a complementary set of equations to (a), (11), and (12) written for the case of negative x.

Eq. (13),

$$q_1 = x = \frac{a}{2c}\sin\theta \tag{13}$$

gives the time, measured on the q axis, required for the steady-state condition to be reached. However, it should be pointed out that the origin of the q axis lies at the midpoint of the transient. Thus, the transient duration, T_t, is

$$T_t = 2|x| = \left|\frac{a}{c}\sin\theta\right|. \tag{d}$$

Fig. 1 shows these relationships graphically.

Similarly the transient duration, T_t', within the θ region corresponding to the

* Received by the IRE, September 15, 1960.

[1] C. Polk, "Transient behavior of aperture antennas," Proc. IRE, vol. 48, pp. 1281–1288; July, 1960.

steady-state main beam is given by

$$T_t' \leq \tau, \qquad 0 \leq |\theta| \leq \sin^{-1}\frac{\lambda}{a} \qquad \text{(e)}$$

where τ is the period of the carrier frequency.

The transient has its maximum duration at $\theta = 90°$. This is,

$$T_t \max = \frac{\tau}{\theta_0}, \qquad \text{(f)}$$

where θ_0 is the half-beamwidth between first nulls for the steady-state pattern.

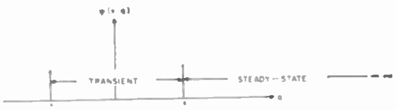

Fig. 1—Transient region for uniformly illuminated aperture.

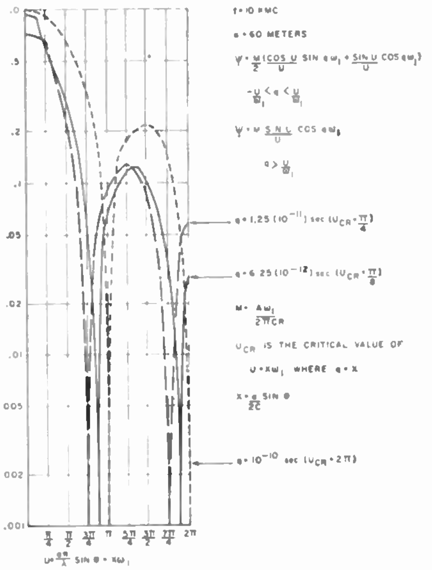

Fig. 2—Transient patterns of uniformly illuminated aperture.

Polk's Fig. 2 is in error, since it is based on incorrect versions of (11) and (12). A corrected version of Fig. 2 is included in this letter. The behavior of the curves in our Fig. 2 can best be understood by rewriting (11) and (12) to obtain

$$\psi_0 = \frac{1}{2} M \frac{\sin (U + q\omega_1)}{U}, \quad -\frac{U}{\omega_1} < q < \frac{U}{\omega_1} \qquad \text{(g)}$$

where $U = x\omega_1$, and

$$\psi_0 = M \frac{\sin U}{U} \cos q\omega_1, \qquad q > \frac{U}{\omega_1}. \qquad \text{(h)}$$

In Fig. 2, q is assumed to be a fixed parameter and ψ_0 is plotted as a function of U. For a sufficiently large value of q, the steady-state pattern will result for all values of U. As q is decreased, portions of the pattern near the U axis origin are steady-state, and portions of the pattern removed from the U axis origin are transient. For $q = 0$, the entire pattern is transient, except for the point $U = 0$, and has the same shape as the steady-state pattern, but with an amplitude one half the amplitude of the steady-state pattern when $\cos q\omega_1 = 1$. It is seen that the nulls of the transient patterns are shifted $q\omega_1$ units toward the U axis origin from the nulls of the steady-state pattern. Fig. 2 is a plot of the instantaneous field for three specific times. From (g) it is seen that the magnitude of the transient side lobes varies as $1/U$.

For small values of $(U + q\omega_1)$, (g) becomes

$$\psi_0 \approx \frac{1}{2} M \left(1 + \frac{q\omega_1}{U}\right), \quad -\frac{U}{\omega_1} < q < \frac{U}{\omega_1}, \qquad \text{(i)}$$

which, for finite $q\omega_1$, approaches infinity as U approaches zero. This accounts for the change of sign in the slope of the transient portion of the pattern for small $q\omega_1$ in the region where $U = U_{CR}$. From (g) and (i), it is evident that the magnitude of the transient sidelobes are equal to one half the magnitude of the steady-state sidelobes whenever $U \gg U_{CR}$.

Eq. (20) should read

$$R(\bar{r}, \omega) = \frac{i2\pi A e^{-i(\omega R/c)}}{\lambda R} \frac{\cos \omega x}{\pi^2 - 4\omega^2 x^2}, \qquad (20)$$

where the assumption has been made that (a) applies

Eqs. (21)–(23) should read,

$$M' = \frac{iA\omega_1}{cR} \qquad (21)$$

$$\psi_1 = 0, \qquad q < -x \qquad \text{(j)}$$

$$\psi_1 = \frac{1}{2} M' \frac{1}{\pi^2 - 4\omega_1^2 x^2} \left[\sin (q + x)\omega_1 - \frac{2x\omega_1}{\pi} \cos \frac{q\pi}{2x}\right], \quad -x < q < x, \qquad (22)$$

$$\psi_1 = M' \left[\frac{\cos x\omega_1}{\pi^2 - 4\omega_1^2 x^2}\right] \sin q\omega_1 \quad q > x, \qquad (23)$$

where again it has been assumed that θ is restricted to the first quadrant or x redefined according to (e).

Eqs. (28) and (29) should read

$$\psi_2 = \frac{1}{2} M \left[\frac{\cos x\omega_1}{x\omega_1} \sin q\omega_1 + \frac{\sin x\omega_1}{x\omega_1} \cos q\omega_1\right],$$
$$-x < (q - w) < x, \qquad (28)$$

$$\psi_2 = M \frac{\sin x\omega_1}{x\omega_1} \cos q\omega_1 \qquad (q - w) > x. \qquad (29)$$

where, by (10),

$$M = \frac{A\omega_1}{2\pi cR}, \qquad (10)$$

and θ is restricted to the first quadrant or redefined according to (e).

The RF field for the case of a continuous aperture uniformly illuminated by a square sinusoidal pulse of length W is given by (27) to be

$$\bar{\psi} = \psi_0 - \psi_2. \qquad (27)$$

It is perhaps more illuminating to present $\bar{\psi}$ in a slightly different form. If ψ_0 and ψ_2 are combined, then $\bar{x}$ has one form when $W < 2x$ and another form when $W° > 2x$.

Case I: $2x < W$ (small values of θ).

$$\bar{\psi}(x, q) = 0 \qquad q < -x \qquad \text{(k)}$$

$$\bar{\psi}(x, q) = \frac{1}{2} M \frac{\sin (q + x)\omega_1}{x\omega_1} \qquad -x < q < x \ \text{(m)}$$

$$\bar{\psi}(x, q) = M \frac{\sin x\omega_1}{x\omega_1} \cos q\omega_1$$
$$x < q < -x + w \qquad \text{(n)}$$

$$\bar{\psi}(x, q) = -\frac{1}{2} M \frac{\sin (q - x)\omega_1}{x\omega_1}$$
$$-x + w < q < x + w \qquad \text{(p)}$$

$$\bar{\psi}(x, q) = 0 \qquad q > x + w \qquad \text{(q)}$$

Fig. 3 shows the transient and steady-state regions on the q axis for this case.

Case II: $2x > w$ (large values of θ).

$$\bar{\psi}(x, q) = 0 \qquad q < -x \qquad \text{(r)}$$

$$\bar{\psi}(x, q) = \frac{1}{2} M \frac{\sin (q + x)\omega_1}{x\omega_1}$$
$$-x < q < -x + w \qquad \text{(s)}$$

$$\bar{\psi}(x, q) = 0 \qquad -x + w < q < x \qquad \text{(t)}$$

$$\bar{\psi}(x, q) = -\frac{1}{2} M \frac{\sin (q - x)\omega_1}{x\omega_1}$$
$$x < q < x + w \qquad \text{(u)}$$

$$\bar{\psi}(x, q) = 0 \qquad x + w < q \qquad \text{(v)}$$

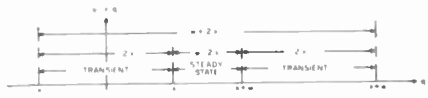

Fig. 3—Transient regions for uniformly pulse-illuminated aperture, $2x < w$.

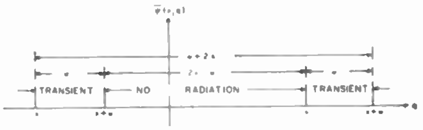

Fig. 4—Transient regions for uniformly pulse-illuminated aperture, $2x > w$.

Fig. 4 shows the transient regions on the q axis for this case. There is no steady-state region.

From the above two cases we can draw the following conclusions for the continuous aperture uniformly illuminated by a square sinusoidal pulse of time duration W:

1) The radiated energy is spread over a time interval of $W + 2x$, where $2x$ is the projected time depth of the antenna.
2) For azimuth angles for which the projected time depth of the antenna, $2x$, is less than the illuminating pulse length, W, the radiated pulse consists of an initial transient period equal in length to the projected time depth of the antenna, followed by a steady-state period equal in length to the difference between the illuminating pulse length and the projected time depth of the antenna, followed by a final transient equal in length to the projected time depth of the antenna.

3) For azimuth angles for which the projected time depth of the antenna, $2x$, is greater than the illuminating pulse length, W, the radiated pulse consists of an initial transient equal in length to the length of the illuminating pulse, followed by a period of zero radiation equal in length to the difference between the projected time depth of the antenna and the length of the illuminating pulse, followed by a final transient equal in length to the illuminating pulse.

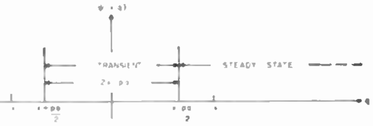

Fig. 5—Transient region for aperture uniformly illuminated by linearly time-delayed unit-stepped sinusoid.

Eq. (36) should read

$$R(\bar{r}, \omega) = \frac{iA}{4\pi c R}\left[\cos\theta + \frac{1}{\sqrt{(pc)^2+1}}\right] \cdot \frac{1}{\left(x - \frac{pa}{2}\right)} e^{-i(\omega R/c)} \sin\omega\left(x - \frac{pa}{2}\right). \tag{36}$$

Eqs. (39)–(41) should read

$$M'' = \frac{A\omega_1}{4\pi c R}\left(\cos\theta + \frac{1}{\sqrt{(pc)^2+1}}\right), \tag{39}$$

$$\psi = 0, \qquad q < -x + \frac{pa}{2}. \tag{x}$$

$$\psi = \frac{1}{2}M''\left[\frac{\cos\omega_1\left(x - \frac{pa}{2}\right)}{\omega_1\left(x - \frac{pa}{2}\right)}\sin q\omega_1 + \frac{\sin\omega_1\left(x - \frac{pa}{2}\right)}{\omega_1\left(x - \frac{pa}{2}\right)}\cos q\omega_1\right],$$

$$-x + \frac{pa}{2} < q < x - \frac{pa}{2}. \tag{40}$$

$$\psi = M''\frac{\sin\omega_1\left(x - \frac{pa}{2}\right)}{\omega_1\left(x - \frac{pa}{2}\right)}\cos q\omega_1$$

$$q > x - \frac{pa}{2}. \tag{41}$$

where $x - pa/2 \geq 0$. A complementary set of equations to (39), (x), (40), and (41) can be written for those azimuth angles for which $x - pa/2 \leq 0$, or, alternately, magnitude signs properly placed about the quantity $(x - pa/2)$. The main lobe maximum occurs for

$$x - \frac{pa}{x} = 0.$$

Fig. 5 shows the transient region on the q axis for this case.

It is seen that when $p=0$, (39), (x), (40), and (41) reduce to (10), (b), (11), and (12) if

$$(\cos\theta + 1) = 2,$$

as was assumed in those equations.

Bruce R. Mayo
Advance Engrg. Subsection
Heavy Military Elect. Dept.
General Electric Company
DeWitt, N. Y.

Author's Comment[2]

I agree substantially with the comments made by Dr. Mayo. It should be pointed out, however, that (20) is correct as given in my paper. Eq. (21) should be

$$M' = \frac{-i2A\omega_1}{\pi c R}. \tag{21}$$

Eq. (22) should be

$$\psi_1 = \frac{1}{2}M'\frac{1}{\pi^2 - 4\omega_1^2 x^2}\left[\sin(q + x)\omega_1 - \cos\frac{q\pi}{2x}\right], \qquad -x < q < x. \tag{22}$$

Eq. (36) is correct as given in my paper, provided 2π in the denominator is replaced by 4π; likewise, (39) and (41) are correct as given originally. Furthermore, the statement that the main lobe maximum occurs for

$$x - \frac{pa}{2} = 0$$

is equivalent to (37.)

None of the corrections affect the conclusions given on page 1285 of the July Proceedings.

C. Polk
College of Engineering
University of Rhode Island
Kingston, R.I.

Letter from Dr. Mayo[3]

I agree with the letter of Dr. Polk, except to the extent of the following comments.

1) Eq. (20) of the article is correct for a cosine taper in both the ξ and η planes. Eq. (20) of my first letter is correct for a cosine taper in only the ξ plane. If (20) of the article is to be accepted as correct, perhaps a better form for (19) of the article is

$$K_0(\xi, \eta) = \cos\frac{\pi\xi}{2}\cos\frac{\pi\eta}{2},$$

$$|\xi| < 1, \ |\eta| < 1. \tag{19}$$

2) Eqs. (21) and (22) are incorrect in the original paper, in my first letter, and in Dr. Polk's letter. Assuming (20) of the article to be correct, (20)–(22), (j), and (23) should read,

$$R(\bar{r}, \omega) = \frac{i4Ae^{-i(\omega R/c)}}{\lambda R}\frac{\cos\omega x}{\pi^2 - 4\omega^2 x^2} \tag{20}$$

$$M' = \frac{2A\omega_1}{\pi c R} \tag{21}$$

$$\psi_1 = \frac{1}{2}M'\frac{1}{\pi^2 - 4\omega_1^2 x^2}\left[\cos(q + x)\omega_1 + \sin\frac{q\pi}{2x}\right], -x < q < x \tag{22}$$

$$\psi_1 = 0, \qquad q < -x \tag{j}$$

$$\psi_1 = M'\frac{\cos x\omega_1}{\pi^2 - 4\omega_1^2 x^2}\cos q\omega_1, \ q > x. \tag{23}$$

For a cosine taper in only the ξ plane, (20) and (21) should be multiplied by $\pi/2$.

As a check, (21)–(23) of this letter have been obtained by two different methods. First, the signal spectrum was multiplied by the frequency-domain impulse response of the antenna and the time waveform of the resulting spectrum then found. Second, the time waveform of the signal was convolved with the time-domain impulse response of the antenna.

3) Eq. (36) is correct as given in the original paper provided 2π in the denominator is replaced by 4π, an i is inserted in the exponential term, and a ω is deleted from the denominator to give,

$$R(\bar{r}, \omega) = \frac{iAe^{-i(\omega R/c)}(\cos\theta + \sqrt{1 - p^2c^2})}{4\pi c R} \cdot \frac{\sin\omega\left(x - \frac{pa}{2}\right)}{\left(x - \frac{pa}{2}\right)}. \tag{36}$$

Eqs. (36) and (39) in my first letter should have the quantity $1/\sqrt{(pc)^2+1}$ replaced by $\sqrt{1-p^2c^2}$.

Bruce R. Mayo
Advance Engrg. Subsection
Heavy Military Electronics Dept.
General Electric Company
Dewitt, N. Y.

[2] Received by the IRE, November 3, 1960.
[3] Received by the IRE, November, 21, 1960.

RF Focusing of an Electron Stream*

A recent letter[1] discussed the possibility of focusing a stream of charged particles with electromagnetic waves. We had already formed a theory and performed verifying experiments for this type of focusing, using slow ($v_p < c$), traveling (not standing) waves on a helix.[2] However, our best results were obtained exactly in the region (wave velocity greater than that of the electron stream) where Sugata, *et al.*, said that defocusing should occur! This letter is to point out what we believe is the error in their letter.

* Received by the IRE, November 4, 1960.

[1] E. Sugata, M. Terada, K. Ura, and Y. Ikebuchi, "Beam focusing by RF electric fields," Proc. IRE (Correspondence), vol. 48, pp. 1169–1170; June, 1960.

[2] C. K. Birdsall and G. W. Rayfield, "Focusing of an Electron Stream Solely by the Radio Frequency Fields on a Slow-Wave Circuit," presented at the Internatl. Congress on Microwave Tubes, Munich, Ger., June 10, 1960. (Work supported by Wright Air Dev. Div. under Contract AF 33(616)-6139.)

The authors' argument that defocusing occurs if the wave velocity is larger than the stream velocity is as follows: as the wave accelerating (axial) field passes by an electron, the wave accelerates the electron; then, the radially inward (focusing) force of the wave acts on this electron. Similarly, after the wave decelerates an electron, the radially outward (defocusing) force acts on this electron. Thus, it appears that the electron will spend less time in the focusing field and more time in the defocusing field, resulting in net defocusing. However, we wish to point out that the opposite is true and that net focusing occurs.

The accelerated electron tends to catch up with the wave and spends more time in the focusing field than in the defocusing field that follows deceleration, where the electron tends to drop further behind the wave. Or, one may observe the action from the wave coordinate system, as follows: an electron drifting through the decelerating phase is decelerated, to be sure, as viewed by a laboratory observer, but this electron is accelerated away from this region as seen by the wave; similarly, the electron drifting through the accelerating phase is accelerated in the laboratory frame, but is decelerated in the wave frame. Thus, just as with periodic electrostatic focusing, net focusing occurs.

C. K. Birdsall
G. W. Rayfield
Dept. of Elec. Engrg.
University of California
Berkeley, Calif.

Authors' Comment[3]

Birdsall and Rayfield have pointed out that even the forward wave traveling faster than the electron can focus the beam. Although their report[2] has not yet come to our hands, we have found that the analytical procedure in our letter[1] includes the fatal mistake which led to erroneous results. It is hoped that the following will help to clarify the matters.

We consider, at first, the problem in the case of E_{01} mode in the parallel plane waveguide. We assume RF field exists in the region of $z \geqq 0$. If an electron velocity u is much smaller than the light velocity c and wave velocity is not so much larger than the light velocity (operating frequency is not near the cutoff), the force due to magnetic field can be neglected. The equations of motion are written as

$$\frac{d^2y}{dt^2} = f(y)\cos(\omega t - \beta z) + h,$$

$$\frac{d^2z}{dt^2} = g(y)\sin(\omega t - \beta z) \tag{1}$$

where

$$f(y) = \eta\beta A \sin k_y y, \quad g(y) = \eta k_y A \cos k_y y,$$

$$k_y = \pi/2a.$$

[3] Received by the IRE, December 28, 1960.

h is the space-charge term. We put

$$z = vt + \zeta \tag{2}$$

where v is wave velocity. This transformation is purely mathematical but physically fictitious. Substituting (2) into (1), one gets

$$\frac{d^2y}{dt^2} = f(y)\cos\phi + h,$$

$$\frac{d^2\zeta}{dt^2} = -g(y)\sin\phi, \quad \phi = \beta\zeta. \tag{3}$$

We assume the solution as $y = b + y_1$, and $|y_1| \ll b$. From (3) one gets

$$\left(\frac{d\zeta}{dt}\right)^2 - w_0^2 = 2\frac{g}{\beta}(\cos\phi - \cos\phi_0)$$

$$-2\frac{g'}{\beta}\int_{-\phi_0}^{\phi} y_1 \sin\phi d\phi + \text{higher-order terms} \tag{4}$$

where

$$w_0 = u_0 - v, \qquad g' = \left(\frac{dg}{dy}\right)_{y=b}.$$

$\phi_0 = \omega\tau$ is the injection phase angle. On the other hand,

$$\frac{d^2y}{dt^2} = \frac{d^2y}{d\phi^2}\left(\frac{d\phi}{dt}\right)^2 + \frac{dy}{d\phi}\frac{d^2\phi}{dt^2}. \tag{5}$$

Substituting (4) and (5) into (3), taking y_1, g and f as the first-order perturbation, and h as the second-order, and neglecting the higher-order terms, (3) reduces to the apparent "path" equation which is analogous to the path equation in the case of periodic electrostatic field.

$$y_1''[w_0^2\beta^2 + 2g\beta(\cos\phi - \cos\phi_0)] - y_1'\beta g\sin\phi$$
$$- y_1 f'\cos\phi = f\cos\phi + h, \tag{6}$$

where

$$y_1' = \frac{dy_1}{d\phi}.$$

The particular solution of (6) is written as

$$\sum_{n=1}^{\infty} p_n \cos n\phi + q_n \sin n\phi.$$

Substituting this into (6) and comparing the constant term and $n=1$ terms, one gets

$$q_1 = 0, \quad p_1 = -f[\beta^2 w_0^2 - 2g\beta\cos\phi_0]^{-1} \tag{7}$$

$$(f' + \beta g)f = 2\beta^2 w_0^2 h. \tag{8}$$

The assumption that h is the second-order perturbation is consistent with (8). h is expressed in the first approximation as follows,

$$h = \frac{\eta I_0}{2\epsilon_0 u_0}. \tag{9}$$

Eq. (8) may be expressed explicitly,

$$P = 1.01 \times 10^7 \frac{I_0}{\sqrt{V_0}}[(\omega_c/\omega)^2\sqrt{1 - (\omega_c/\omega^2)}]^{-1}$$

$$\cdot\left(\sin\frac{b}{a}\pi\right)^{-1} \text{(watts/meter)} \tag{10}$$

where P is the RF power necessary to focus beams.

If $|\beta w_0^2| \gg |g|$, p_n and q_n are of the order of $|g/\beta w_0^2|^n$.

This particular solution is equal to $p_1 \cos\phi$ to the first order. This means that the beam perturbation can be very small if an electron is injected to RF field with displacement $p_1 \cos\phi_0$ and with appropriate slope. If an electron beam is continuously injected into the RF field parallel to the axis and with the beamwidth $2b$, the perturbation cannot be expressed by $p_1 \cos\phi_0$ only, and it is expected that the perturbation will become considerably large. To estimate this, one must find the general solution of (6) or the one of the homogeneous equation which is obtained by putting the zero on the right-hand side. This latter homogeneous equation may be transformed into the standard form

$$\frac{d^2Y}{d\phi^2} + [Q_0 + Q_1\cos\phi + Q_2\cos 2\phi]Y = 0 \tag{11}$$

where

$$Y = y_1[\beta^2 w_0^2 + 2g\beta(\cos\phi - \cos\phi_0)]^{1/4}.$$

Q_0, Q_1, and Q_2 are of the second, the first and the second order, respectively. In order to investigate the stability of the solution, one must know Q_0 up to the second order at least. But (11) is exact up to the second order of Y, g and f, because (6) is so. It is not self-consistent to discuss the stability of the solution directly from the above "path" equation. However, the order of $|y_1|_{max}$ is obtained roughly as follows. The dominant terms of the general solution of (6) are given as

$$y_1 = p_1\cos\phi + D\cos\left(\frac{\mu}{2}\phi + \delta\right). \tag{12}$$

μ is the characteristic number of (11) and of the first order. Here we impose the following injection condition

$$y_1 = 0 \quad \text{and} \quad \frac{dy_1}{d\phi} = 0 \quad \text{for } \phi = \phi_0. \tag{13}$$

Then

$$D = p_1\left[\cos^2\phi_0 + \frac{4}{\mu^2}\sin^2\phi_0\right]^{1/2}.$$

That is,

$$|y_1|_{max}/b \approx \frac{p_1}{b}\frac{2}{\mu}$$

is of the zeroth order. If the condition $|y_1| \ll b$ fails to hold, the above analysis is not self-consistent. It might be expected, however, that the beam perturbation should be considerably large if electrons are injected in the above manner.

The above analysis can be extended to the case of E_{01} mode of the symmetric waveguide and the lowest mode of helix under the assumption that $u \ll c$, $v \ll c$, and γb are not so small (neglecting the forces due to magnetic field and E_θ). The above results may be applicable also to this case when we put

$$\left.\begin{array}{ll} y = r & \begin{array}{l} f(y) = \eta A(\beta/\gamma)I_1(\gamma y) \\ g(y) = \eta A I_0(\gamma y) \end{array} \\ h = \dfrac{\eta}{2\pi\epsilon_0}\cdot\dfrac{I_0}{u_0} & \end{array}\right\} \tag{14}$$

$$P = 3.03 \times 10^4 \frac{V_0}{K} I_0\left(1 - \frac{v}{u_0}\right)^2 F(B), \tag{15}$$

$$F(B) = BI_0(B)I_1(B) - \tfrac{1}{2}I_1^2(B), \quad B = \gamma b$$

where K is the coupling impedance. The necessary power P decreases as u_0 tends to v.

because the coupling between waves and electrons becomes stronger. But the "path" equation is correct when $|\beta w_0^2| \gg |g|$, or explicitly

$$1.23 \times 10^2 \sqrt{\frac{I_0}{V_0^{3/2}}} \frac{I_0(B)\sqrt{F(B)}}{|1 - v/u_0|} \ll 1. \quad (16)$$

It should be noted that the necessary power to focus the beam in the case of slow waves is much smaller compared with the one in the case of fast waves.

We made two serious (and primitive) mistakes in our previous letter. One must eliminate t in (1) in order to derive the "path" equation (6). Instead of (2), we had assumed

$$t = \frac{z}{u_0} + \tau$$

$$\tau\text{: injection time of an electron.} \quad (17)$$

Eq. (17) might be plausible as the first approximation. This assumption, however, is not self-consistent. Under (17), one may get

$$t - \tau = \frac{z}{u_0} - \frac{g}{2\alpha u_0^2} \cos \phi_0 \cdot z - \frac{g}{2\alpha^2 u_0^2} (\sin \phi - \sin \phi_0)$$

$$\alpha = \frac{\omega}{u_0} - \beta, \qquad \phi = \alpha z. \quad (18)$$

That is, $t - \tau - z/u_0$ is not small compared with the period of RF (although small compared with $\tau + z/u_0$). Secondly, in the discussion of physical meanings, we overlooked the fact that the focusing action of the periodic electrostatic field and the RF field is due not only to the lens action but also to the field *periodicity itself.*

E. Sugata
M. Terada
K. Ura
Dept. of Electronic Engrg.
Osaka University
Higashinoda, Osaka
Japan

A Wide-Band Single-Diode Parametric Amplifier Using Filter Techniques*

The application of filter techniques to achieve broad-band operation of a single-diode parametric amplifier has been suggested by Seidel and Hermann[1] and others. For example, the addition of reactive elements to a single-tuned circuit can result in flat band-pass characteristics over an increased frequency range. As far as is known, however, no descriptions of amplifiers of this type have so far appeared in the literature, and it is the purpose of this note to report the successful operation of such an amplifier recently constructed at Stanford University.

The amplifier operates in the degenerate mode at a center frequency of 3.3 kMc. The construction is shown in Fig. 1. A strip-line stepped transformer converts the 50-ohm input impedance to about 10 ohms at the input to the diode, which together with a short length of line is made to appear as a series resonant circuit at this point. A filter composed of two 80-pf capacitors at each end of a quarter-wave line, allows a dc bias to be applied while still maintaining an RF ground over the frequency band of interest.

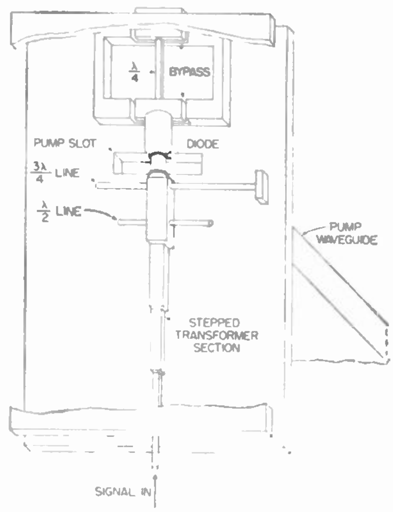

Fig. 1—General view showing arrangement of diode circuit, filter sections and dc bias connection.

To widen the bandwidth, filter sections made up of parallel-tuned circuits are placed at appropriate points along the signal line. As shown in Fig. 1, one circuit is placed at the input to the series diode circuit and consists of a shorted line at right angles to the main line, while a second parallel circuit can be placed a quarter of a wavelength closer to the signal input to form a three-section filter. The required Q's for the parallel circuits are obtained by selection of the tapping points to these lines.

The pump is fed in through resonant slots cut opposite the diode in each wall of the line as in Fig. 1. The effect of these slots on the signal circuit has been reduced by shorts provided by quarter-wavelength parallel-plate lines extending into the waveguide. Since these lines are half a wavelength at the pump frequency (6.6 kMc), they do not appreciably affect the pump circuit. The pump is fed in through the waveguide in one wall and a variable short circuit in the opposite waveguide allows a high electric field to be placed at the diode.

Tests have been carried out with a three-port circulator of bandwidth 200 Mc and insertion loss 0.2 db. The isolation exceeded 22 db.

As the number of filter sections is increased, the bandwidth changes as in Fig. 2, which shows the equivalent circuits of the amplifier for three cases alongside the corresponding frequency response. The gain in each case was 16 db while the bandwidth was 27 Mc for the diode circuit alone, 102 Mc for one added parallel circuit and 130 Mc for two parallel circuits. It is to be noted, however, that during these tests, the load connected to the circulator was slightly mismatched and this contributed an extra ripple to the pass band which was removed by matching. The ripples amounted to no more than $\pm\frac{1}{2}$ db.

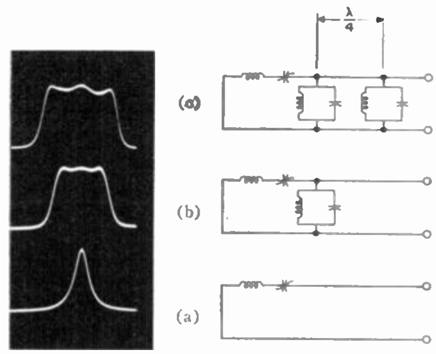

Fig. 2—Effect on bandwidth of changing the number of filter sections in (a) diode circuit alone, (b) one parallel circuit added, and (c) two parallel circuits added.

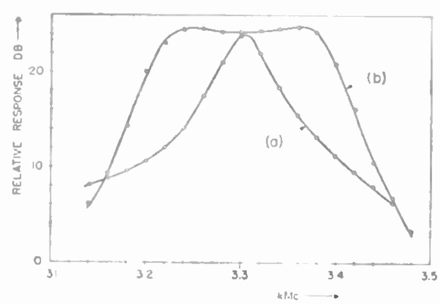

Fig. 3—Improved frequency response of amplifier in (a) diode circuit alone, and (b) one parallel circuit.

Following these tests, the amplifier was readjusted with a subsequent improvement in performance. At a gain of 16.5 db, the diode circuit alone yielded a bandwidth of 50 Mc with a double-channel noise figure of 1.7 db. Addition of one parallel-tuned circuit improved the bandwidth to 190 Mc for the same gain, while the noise figure was degraded slightly to 1.8 db. The frequency response is shown for the two cases in Fig. 3. It is to be noted that in the two-section case, the ripples amount to no more than ± 0.4 db over 150 Mc and are consistent in shape with those expected from a two-section filter. It was not possible to extend the bandwidth by the addition of a further section because of the limited bandwidth of the circulator.

The diode used in all these tests was a Microwave Associates Pill varactor with a zero bias capacitance of 1.16 pf and a cutoff frequency of 130 kMc. It was operated at a reverse bias of 1.25 volts, and about 100 mw of pump power were required at the amplifier for a gain of 16 db. More gain could be

* Received by the IRE, November 18, 1960; revised manuscript received, December 22, 1960. The development was initiated under the sponsorship of contract Nonr 225(24) as an amplifier study and has been brought to the final stages under contract AF 19(603)-53 for application to the Stanford Radio Telescope.

[1] H. Seidel and G. F. Hermann, "Circuit aspects of parametric amplifiers," 1959 IRE WESCON Convention Record, pt. 2, pp. 83–90.

obtained, indicating that the performance may be improved by utilizing more of the available capacitance swing of the diode.

In conclusion, these results support the promise of wide bandwidth offered by the filter technique, and it is expected that even greater bandwidths than that reported here can be obtained.

The work was greatly assisted by the several reports on this subject privately communicated by G. L. Matthei to the author and which it is understood will be material for a forthcoming paper. The author also wishes to acknowledge the advice and encouragement of Dr. H. Heffner and the assistance of K. Yngvesson during the initial stages of the development.

A. G. LITTLE
Radioscience Lab.
Stanford University
Stanford, Calif.

Dynamic Response of Rihaczek's Constant Phase Nonlinear Filter*

I read Dr. Rihaczek's[1] interesting paper describing a nonlinear constant phase high-selectivity filter. The nonlinear constant phase filter does perform the job for which it was designed—to provide high selectivity and maintain constant phase difference between the input phase and output phase of a slowly phase-modulated signal—it does not, however, share the principal advantages of a constant phase linear filter. As pointed out by Rihaczek, a band-pass linear constant phase filter is not physically realizable for the reason that such a transfer impedance corresponds to an impulse response different from zero before application of the impulse. This is unfortunate, since, for example, a zero phase linear filter could smooth noisy signals without time delay and could undoubtedly be used to solve many difficult servomechanism problems.

After reading Rihaczek's paper, I considered the response of his high-selectivity filter to a single-tone amplitude-modulated carrier. The argument followed was that since the filter adds zero phase (or constant phase) to both sidebands and carrier, the phase of the envelope is not altered by the filter regardless of the modulation frequency. The same argument was repeated for a single-tone frequency-modulated signal with the same conclusion of zero modulation phase-delay regardless of modulation frequency, in agreement with Rihaczek's statement. These results were baffling as they suggest zero over-all time delay, despite the definite time delay in the linear selective filters. The actual fact, however, is that modulation phase delay is a function of modulation frequency, and application of superposition to Mixer II of Fig. 1[1] is the source of error in the above argument. Mixer II is nonlinear because both its inputs are functions of the filter input. Mixers I and III, of course, can be approximated as linear time-varying networks. The following is a simple analysis which brings out some of the important characteristics of this filter.

Fig. 1 is a block diagram of a constant phase nonlinear filter equivalent to that of Fig. 1 in Rihaczek's paper. The second harmonic mixer has been replaced by a frequency doubler and a fundamental mixer to show that two nonlinear operations are involved. A delay line added in the local oscillator arm serves to adjust the phase shift through the filter. For mathematical simplicity, all linear filters are assumed to have constant gain and linear phase characteristics over the significant spectral width of their respective inputs. In addition, all linear filters are assumed to have zero gain at frequencies corresponding to undesired modulation products. Full-wave square law rectifiers are assumed for the balanced mixing and frequency doubling operations.

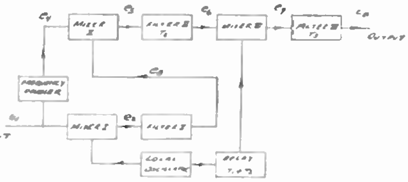

Fig. 1—Nonlinear "constant phase" filter.

The input signal is taken as a band-pass voltage with envelope and phase modulation. Accordingly, the input signal is written as

$$e_1 = a(t) \cos [W_1 t + \phi(t)]. \tag{1}$$

Keeping in mind the assumptions given above, it is a simple matter to compute the *desired* waveforms at various points in the circuits. Omitting obvious details, these waveforms are written as

$$e_2 = a(t) \cos [(W_L - W_1)t - \phi(t)] \tag{2}$$

$$e_3 = a(t + T_1) \cdot \cos [(W_L - W_1)(t + T_1) - \phi(t + T_1)] \tag{3}$$

$$e_4 = a^2(t) \cdot \cos [2W_1 t + 2\phi(t)] \tag{4}$$

$$e_5 = a^2(t) \cdot a(t + T_1) \cdot \cos [(W_L + W_1)t + (W_L - W_1)T_1 + 2\phi(t) - \phi(t + T_1)] \tag{5}$$

$$e_6 = a^2(t + T_2)a(t + T_1 + T_2) \cdot \cos [(W_L + W_1)(t + T_2) + (W_L - W_1)T_1 + 2\phi(t + T_2) - \phi(t + T_1 + T_2)] \tag{6}$$

$$e_7 = a^2(t + T_2)a(t + T_1 + T_2) \cdot \cos [W_1 t + W_1(T_2 - T_1) + 2\phi(t + T_2) - \phi(t + T_1 + T_2)] \tag{7}$$

(In writing e_7, the time delay added in the local oscillator was taken as $T_1 + T_2$; this cancels a constant phase shift in the output.)

$$e_8 = a^2(t + T_2 + T_3)a(t + T_1 + T_2) \cdot \cos [W_1 t + W_1(T_2 + T_3 - T_1) + 2\phi(t + T_2 + T_3) - \phi(t + T_1 + T_2 + T_3)]. \tag{8}$$

Letting $T_1 = T_2 + T_3$ in (8) gives the desired result as

$$e_8 = a^2(t + T_1)a(t + 2T_1) \cdot \cos [W_1 t + 2\phi(t + T_1) - \phi(t + 2T_1)]. \tag{9}$$

First consider the envelope modulation term of (9). Obviously, the distortion is quite severe, and the time delay is not zero. For example, for single-tone amplitude modulation with small modulation factor such that

$$a(t) = (1 + m \cos W_m), \quad m \ll 1, \tag{10}$$

the output envelope becomes

$$a^2(t + T_1) \cdot a(t + 2T_1) = [1 + 2m \cos W_m(t + T_1) + m \cos W_m(t + 2T_1)] \tag{11}$$

which shows an envelope phase delay between $W_m T_1$ and $2W_m T_1$ corresponding to a time delay between T_1 and $2T_1$.

The behavior of the nonlinear filter is quite different for phase modulation and, of course, more useful. The operation of the nonlinear filter on the phase modulation may be thought of as one of straight-line prediction since $2\phi(t+T_1) - \phi(t+2T_1)$ is a straight-line prediction of $\phi(t)$. This is evidenced by writing a Taylor series expansion of the phase term of (9). The result, assuming no envelope modulation, and convergence of the series, can be written as

$$e_8 = \cos \left[W_1 t + \phi(t) - \frac{d^2\phi}{dt^2} \cdot T_1^2 - \frac{d^3\phi}{dt^3} \cdot T_i^3 \cdots \right]. \tag{12}$$

Thus, if the frequency of the input signal is constant, $d^2\phi/dt^2$ and higher derivatives must be zero, and it follows that the filter exhibits no phase shift. If the input frequency changes at a rate b, there is a constand phase error of $-bT_1^2$ and no error in in instantaneous frequency. If the input is of the form

$$e_1 = \cos (W_1 t + e \cos W_m t), \tag{13}$$

the output can be approximated by

$$e_8 = \cos [(W_1 t + e \cos W_m t + eW_m^2 T_1^2 \cos W_m t + eW_m^3 T_1^3 \sin W_m t)]$$
$$W_m T_1 < 0.5 \tag{14}$$

which shows an increase in the modulation index and a phase shift of the modulating signal. It follows that the nonlinear filter, as it operates on phase modulation, has a phase modulation delay given approximately by

$$(W_m T_1)^3$$

for small values of $W_m T_1$.

The effect of moderate (matched) distortion in Filters I, II, and III was examined for a few simple cases using Wheeler's paired echo theory. The result is that any one echo does not result in output phase errors if $\phi(t)$ is well approximated by $2\phi(t+T) - \phi(t+2T)$, T being the time delay of the echo. This behavior was the object of Rihaczek's design.

The results of the above analysis may be summarized as follows: the constant phase filter exhibits constant phase only when the frequency of the input is constant. The phase error due to the phase modulation $\phi(t)$ can be approximated by the formula

* Received by the IRE, November 15, 1960.

[1] A. W. Rihaczek, "High selectivity with constant phase over the pass band," PROC. IRE, vol. 48, pp. 1756–1760; October, 1960.

Phase Error

$$= \phi(t) - 2\phi(t - T) + \phi(t + 2T_1), \quad (15)$$

$$= \frac{d^2\phi}{dt^2}\cdot T^2 + \frac{d^3\phi}{dt^3}\cdot T^3 + \cdots, \quad (16)$$

T being the time delay in Filter I or Filters II and III in cascade. If the impulse response of Filter I (or Filters II and III in cascade) is so smeared in time that T cannot be evaluated, (15) and (16) do not apply.

Rihaczek has suggested the application of this phase compensation scheme to parametric amplifiers in those cases where the input is a single angle modulated carrier. For practical reasons, it is often desirable (sometimes unavoidable) to keep the bandwidth of the parametric amplifier several times wider than the final predetection bandwidth. An important consideration in this connection is the small signal suppression effect in some nonlinear devices.[2] As a result of this effect the signal-to-noise ratio at the output of the constant phase filter will decrease very rapidly when the *desired* signal-to-noise ratio at the input to the frequency doubler and Mixer II falls below about unity.

M. G. Pelchat
Radiation Inc.
Melbourne, Fla.

Author's Comment[3]

In principle, I agree with Mr. Pelchat's analysis of the constant phase filter. In conceiving the method of phase compensation, I almost abandoned the idea because I went through the same reasoning concerning the delay of a modulating signal. If the results from linear filter theory were applicable, not only could we design a filter with delay time zero but, by overcompensating the phase, the delay time could be made negative such that the circuit would act as a predictor. These concepts of modulation delay are not valid for the nonlinear filter. Indeed, such a filter does not retain all advantages of a linear filter, but then, of course, we cannot build a selective linear filter with constant output phase.

As Pelchat confirms, the principal application for the nonlinear, phase-constant filter appears to be for signals of slowly changing frequency (or phase). However, to be more precise we have to determine how slow is "slow" for variations in frequency. To do this, we can use the results of Pelchat's analysis. For signals whose frequency changes at a constant rate, the phase "error" was shown to be *constant;* hence, this phase delay adds to the output phase, and the phase-constant filter has no error for such an input signal. For a sinusoidal phase modulation with frequency f_m, the phase delay was found to be $(\omega_m T)^3$, where T is the delay of a linear filter. For a parallel-tuned circuit, T is of the order of $Q/\pi f_r$ (Q the quality factor, f_r the resonance frequency). For a phase delay of $\Delta\phi$, the modulation frequency then becomes $f_m = (f_r/2Q)\Delta\phi^{1/3}$. Tolerating a phase delay of, say, 1 degree and using a $Q = 50$, the highest usable modulation frequency is $f_{m_{\max}} = 0.26 \times 10^{-2} f_r$. This shows that "slow" means that the ratio f_m/f_r must be small but, for practical systems, a value of $f_m/f_r = 0.26$ per cent is not so small. Under the above conditions, a center frequency of 1 Mc would permit a maximum f_m of 2.6 kc, while 100 Mc would give a value of $f_{m_{\max}} = 260$ kc. The requirement that the frequency variations be slow thus leaves a large class of signals which satisfy this condition and for which the phase compensation method is useful and practical. The exact phase constancy achievable with signals of linearly varying frequency may not be obtained, theoretically, for signals of other characteristics, but the above data prove that the suggestion that the compensation method may also be applicable for special problems in FM systems using higher modulation frequencies is justified.

August W. Rihaczek
Aerospace Corp.
Los Angeles, Calif.

[2] D. Middleton, "Introduction to Statistical Communication Theory," McGraw-Hill Book Co., Inc., New York, N. Y., p. 553; 1960.

[3] Received by the IRE, December 23, 1960.

D'Alembert's Method for Nonuniform Transmission Lines*

The present trend, found in many of the newly introduced books on mathematics for the undergraduate level, is to treat slightly the "classical" techniques developed for linear and nonlinear differential equations, while there is active interest in nonlinear differential equations.[1-3] Among those relatively neglected methods is the one developed by D'Alembert[4] for the solution of two, coupled first-order linear differential equations with variable coefficients. This note outlines his method and applies it for an approximate analytical solution of general nonuniform transmission lines. The usefulness of this analytical approximate method provides 1) checks for numerical solutions of general nonuniform line problems by high-speed digital computers, 2) a needed mesh size based on the numerical values obtained at check points preceding detailed computations, and 3) simple means to evaluate practical nonuniform problems approximately without using any digital computer if two parameters of the line $Y(x)$ and $Z(x)$ are independent of each other but $Z'(x) - Z(x) + Z^2(x)Y(x)$ is close to zero.

* Received by the IRE, December 27, 1960.

[1] R. Kalaba, "On nonlinear differential equations, the maximum operation, and monotone covergence," *J. Math. and Mechanics*, vol. 8, pp. 519–574; July, 1959.

[2] M. A. Abdelkader, "Solutions by quadrature of Riccati and second-order linear differential equations," *Amer. Math. Monthly*, vol. 66, pp. 886–889; December, 1959.

[3] I. Sugai, "Approximate solutions for a first order nonlinear ordinary differential equation," to be published in *Amer. Math. Monthly*.

[4] S. Fujita, *et al.*, "Sugaku-Koshiki" (Mathematical Formulas), Sankaido, Tokyo, Japan, 54th ed., pp. 412–413; 1950. (In Japanese.)

D'Alembert's Method[4]

Letting $y(x)$ and $z(x)$ be two unknowns and $P(x)$, $Q(x)$, $R(x)$, $S(x)$, $T(x)$ and $U(x)$ be continuous and arbitrary functions of x, we have

$$y' + Py + Qz = U, \quad (1)$$

$$z' + Ry + Sz = T, \quad (2)$$

where primes are used for derivatives with respect to x throughout this note. Let $\lambda(x)$ be an undetermined continuous function of x. Multiply $\lambda(x)$ onto (2) and add this result to (1), giving

$$t' + (P + \lambda R)t$$
$$- z(\lambda' + (P - S)\lambda + R\lambda^2 - Q) = U + \lambda T, \quad (3)$$

where

$$t(x) = y(x) + \lambda(x)z(x). \quad (4)$$

Require that the coefficient of z in (3) be zero at all times,

$$\lambda' + (P - S)\lambda + R\lambda^2 = Q. \quad (5)$$

Let λ_i $(i = 1, 2)$ be any two particular solutions of (5), then $y(x)$ and $z(x)$ are uniquely determined through

$$t_i = y + \lambda_i z, \quad (i = 1, 2), \quad (6)$$

where t_i should be obtained from

$$t_i' + (P + \lambda_i R)t_i = U + \lambda_i T, \quad (i = 1, 2). \quad (7)$$

An apparent disadvantage of D'Alembert's Method is that it depends on the solution of the generalized Riccati's nonlinear differential equation, (5). As is well known, Riccati's nonlinear differential equation has not been solved exactly with general coefficients. This could have been the chief reason why D'Aembert's Method has been almost totally forgotten. Renewed interests in nonuniform transmission lines and nonlinear differential equations should result in more careful reconsideration of his method. Operate an operator $(d/dx + S)/Q$ onto (1) and subtract (2), giving

$$y'' + (P + S)y' + (P' + PS - QR)y$$
$$= U' + SU - QT. \quad (8)$$

Similar operations give an equation for $z(x)$ as,

$$z'' + (P + S)z' + (S' + PS - QR)z$$
$$= T' + PT - RU. \quad (9)$$

Require that the coefficient of y is identically vanished, *i.e.*,

$$P \exp\left(\int S dx\right)$$
$$= a_1 + \int QR \exp\left(\int S dx\right) dx, \quad (10)$$

for (8) [or a similar one for (9)], where a_1 is any constant of integration. In this exceptional case, (4) and (2) are exactly solved for $y(x)$ and $z(x)$.

Analytical Approximate Method

A practical application of D'Alembert's Method lies in solutions of nonuniform transmission line problems. Change y, z, Q and R into more familiar symbols of $V(x)$, $I(x)$, $Z(x)$ and $Y(x)$ and assign zero to the rest of the symbols in (1) and (2). Riccati's nonlinear differential equation is expressed by

$$\lambda'(x) + Y(x)\lambda^2(x) = Z(x), \qquad (11)$$

where line parameters of nonuniform lines, $Y(x)$ and $Z(x)$, are arbitrary continuous functions of x. As it stands, (11) has no exact solution. The approximation proposed is to introduce an "accompanying" differential equation for (11), such as

$$\lambda'(x) + Y(x)\lambda^2(x) = Z'(x) + Z^2(x)Y(x). \quad (12)$$

Use a linearizing transform,

$$\lambda(x) = (YZu + u')/(Yu), \qquad (13)$$

where $u(x)$ is any arbitrary continuous function of x. Now (12) is reduced to an exactly solvable differential equation,

$$u'' + (2YZ - (Y'/Y))u' = 0. \qquad (14)$$

This technique to convert a specialized Riccati's nonlinear differential equation into a first-order linear differential equation has been reported.[5] Therefore, λ_i is given by

$$\lambda_i = Z + \exp\left(-\int 2YZdx\right) \Big/ \left(C_i + \int Y\exp\left(-\int 2YZdx\right)dx\right), \quad (15)$$

where $C_i (i=1, 2)$ is any arbitrary constant of integration. The final answers for voltage and current are given by

$$V(x) = \left(D_2\lambda_1 \exp\left(-\int \lambda_2 Ydx\right) - D_1\lambda_2 \exp\left(-\int \lambda_1 Ydx\right)\right) \Big/ (\lambda_1 - \lambda_2), \quad (16)$$

and

$$I(x) = \left(D_1 \exp\left(-\int \lambda_1 Ydx\right) - D_2 \exp\left(-\int \lambda_2 Ydx\right)\right) \Big/ (\lambda_1 - \lambda_2), \quad (17)$$

where D_1 and D_2 are constants of integrations.

This analytical approximate method becomes the exact method if $Y(x)$ is interrelated to $Z(x)$ via

$$Y(x) = (Z(x) - Z'(x))/(Z^2(x)). \quad (18)$$

where $Z(x)$ is any function of x. The previous note[6] had the sole purpose of obtaining this interrelationship. The practical use of the present note is that if

$$Z'(x) - Z(x) + Z^2(x)Y(x) \approx 0 \qquad (19)$$

is obtained when $Y(x)$ and $Z(x)$ are given *independently*, combinations of (15), (16) and (17) give approximate analytical solutions for nonuniform transmission line problems.

IWAO SUGAI
Electron Tube Lab.
ITT Federal Labs.
Nutley, N. J.

[5] I. Sugai, "A class of solved Riccati's equations," submitted to *Electrical Commun.*

[6] I. Sugai, "The solutions of nonuniform transmission line problems," PROC. IRE, (Correspondence), vol. 48, pp. 1489–1490; August, 1960.

A Broad-Band Spherical Satellite Antenna*

In a recent paper with the above title, Riblet reported on an interesting application of the equiangular spiral antenna.[1] This consisted of projecting the planar equiangular spiral antenna upon the spherical surface of the TRANSIT satellite to meet a particular pattern requirement.

Since this application is based upon the equiangular spiral antenna conceived at the University of Illinois in 1954, it is unfortunate that the author of the above paper did not reference the original work on the planar and conical antennas.[2–4]

JOHN D. DYSON
Antenna Lab.
University of Illinois
Urbana, Ill.

* Received by the IRE, April 25, 1960; revised manuscript received, January 9, 1961.

[1] H. B. Riblet, "A broad-band spherical satellite antenna," PROC. IRE, vol. 48, pp. 631–635; April, 1960.

[2] V. H. Rumsey, "Frequency independent antennas," 1957 IRE NATIONAL CONVENTION RECORD, pt. 1, pp. 114–118.

[3] J. D. Dyson, "The equiangular spiral antenna," IRE TRANS. ON ANTENNAS AND PROPAGATION, vol. AP-7, pp. 181–187; April, 1959.

[4] J. D. Dyson, "The unidirectional equiangular spiral antenna," IRE TRANS. ON ANTENNAS AND PROPAGATION, vol. AP-7, pp. 329–334; October, 1959.

A Nondegenerate *S*-Band Parametric Amplifier with Wide Bandwidth*

This correspondence discusses a practical single-diode, *S*-band parametric amplifier, operating in the nondegenerate mode, with a large gain-bandwidth product. Specifically, bandwidths up to 80 Mc have been measured at a center frequency of 2.5 kMc, with voltage gain-bandwidth products of 500 Mc and noise figures of 2.0 db. To the best knowledge of the authors, this is the highest gain-bandwidth product reported in the literature for a single-diode nondegenerate *S*-band parametric amplifier.

The amplifier utilizes band-pass filters in the input and idler circuits in a manner similar to that suggested by Seidel and Herrmann[1] for degenerate mode configurations. Applying broad-band filters to the signal and idler circuits increased the bandwidth from 20 Mc for the single-tuned case to 80 Mc. Also utilized, for convenience in tuning and obtaining a wide bandwidth, is a separate tuning adjustment for the pump and an external idler load. A unique feature of this amplifier is that it can be operated in the following modes: 1) wide-band with the idler termination at room temperature, 2) wide-band with a cooled idler termination for lower noise figures, 3) narrow-band without the external idler termination for minimum noise figure, and 4) regenerative upconverter with an *X*-band output, thereby yielding a low-noise two-port device with increased gain over the equivalent one-port device having the same regeneration.

The amplifier, shown in Fig. 1, has low-loss, low-noise tuners constructed for minimum back lash and susceptibility to vibration. Diode bias is applied via the fourth port

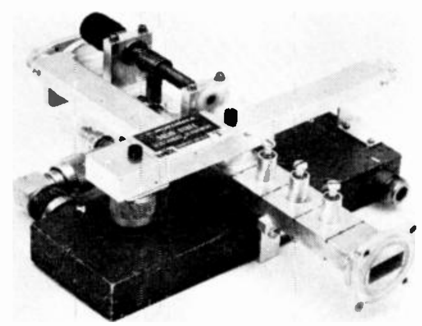

Fig. 1—*S*-band parametric amplifier.

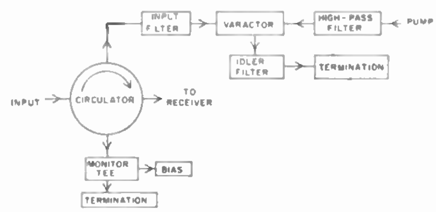

Fig. 2—Block diagram, *S*-band parametric amplifier, model SPA01.

of a four-port circulator, thereby decreasing the radiation problems normally encountered in conventional diode biasing circuits. Fig. 2 is a block diagram representation of the parametric amplifier. The input filter consists of two quarter-wavelength stub tuners (noncontacting) in strip line, and the idler filter consists of three direct coupled cavities in RG52/U waveguide. The position of the idler cavities is important, and in the first models this position was adjustable. However, an optimum position for the first idler cavity was found which has proven satisfactory on subsequent models. The high-pass filter located on the pump side of the varactor is a short section of waveguide beyond cutoff which slides inside the RG52/U waveguide. The cutoff frequency of this filter is 10.5 kMc; therefore, the filter acts as an adjustable short for the 9.0-kMc idler circuit, while passing uneffected the 11.5-kMc pump.

Typical results for this amplifier are as follows:

$f_0 = 2500$ Mc,
$BW_{3db} = 70$ Mc,
$BW_{0.5db} = 65$ Mc,
Band-pass ripple $= < 0.75$ db,
Gain $= 17.0$ db
Noise figure (less circulator) $= 2.0$ db,
$G^{1/2}BW_{3db} = 495$ Mc.

* Received by the IRE, January 3, 1961. This work was sponsored under contract with AF Cambridge Res. Lab., Cambridge, Mass.

[1] H. Seidel and G. F. Herrmann, "Circuit aspects of parametric amplifiers," 1959 IRE WESCON CONVENTION RECORD, pt. 2, pp. 83–90.

The basic concept of individual signal, idler, and pump tuning appears applicable for other frequency parametric amplifiers. Such amplifiers are presently under development at the Solid State Devices Laboratory of Motorola, Inc.

G. Schaffner
F. Voorhaar
Solid State Electronics Dept.
Motorola Inc.
Scottsdale, Ariz.

Waveguide Harmonic Generators*

The traveling-wave harmonic generator suggested by Hedderley[1] can be regarded as a multiphase rectifier circuit. The use of such circuits is feasible in waveguides, and the simplest form, the two-phase circuit, has been shown to have useful properties.[2] The essential feature of such circuits is the in-phase property of the nth harmonic outputs of rectifiers, which are excited by the possible phases of an n-phase system. This is easily demonstrated. If the fundamental current in a rectifier is

$$i = I_1 \cos \omega t,$$

the voltage developed across the crystal will be of the form

$$v = \sum_m V_m \cos (m\omega t + \phi_m).$$

Suppose that individual rectifiers are excited by the different phases of an n-phase circuit. Then, the current for rectifier r will be:

$$i_r = I_1 \cos \left(\omega t + \frac{2\pi r}{n} \right),$$

and the voltage developed will be:

$$v_r = \sum_m V_m \cos \left(m\omega t + \frac{2\pi mr}{n} + \phi \right).$$

The nth harmonic for each rectifier is therefore $V_n \cos (n\omega t + 2\pi r + \phi_n)$; *i.e.*, the nth harmonic outputs of the rectifiers are in phase.

A two-phase circuit is easily constructed using a magic T. Identical rectifiers are connected at equal distances on the side arms, and the fundamental signal is supplied via the E-plane arm. The crystal currents are therefore in antiphase, and the reflected fundamental signals, which are also in antiphase, couple only to the E-plane arm. The generated second harmonic signals are in phase, however, and so couple only to the H-plane arm. The second harmonic output is thus isolated from the input and the circuit can easily be matched to the fundamental input. The isolation depends only on the geometrical properties of the magic T, and it is thus possible to use the circuit over a wide range of frequencies.

A corresponding technique can be applied to other values of n by using the geometrical properties of modes in waveguides. Once again, this leads to a circuit which is sensibly independent of frequency and should, therefore, be much easier to adjust than circuits which rely on frequency filters to extract the wanted harmonic. A possible arrangement is indicated in Fig. 1. A circular waveguide is used and is excited by an H_{11} circularly polarized fundamental mode. The rectifiers are coupled to side arms positioned at equal angular intervals around the circumference of the guide. Fig. 2 shows the arrangement for a six-phase system. The sixth harmonics in this case give equal amplitude, in-phase signals at the coupling holes C_1, C_2, etc., and thus excite the H_{01} mode in the circular guide. The other harmonics have different phase relations at the coupling holes and so excite other H_n modes, as n is not equal to zero. Isolation is thus effected between the harmonics since they give rise to different mode types. Mode filters F_1 and F_2 may be inserted to allow the wanted harmonic to be extracted from one end of the guide. The properties required from these filters are shown in Fig. 1, and their positions are selected to maximize the harmonic output. Suitable mode transducers can be added so that the input couples only to the H_{11} circularly polarized wave and the output couples only to the H_{01} mode. The other harmonics will be restricted to the region between the transducers and thus behave as though the circuit were terminated in reactances.

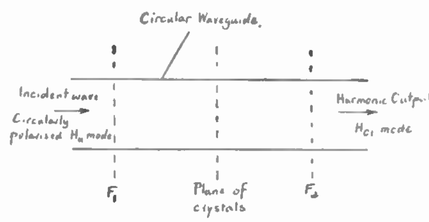

Fig. 1—F_1 transmits the H_{11} mode and reflects the H_{01} mode; F_2 transmits the H_{01} mode and reflects the H_{11} mode.

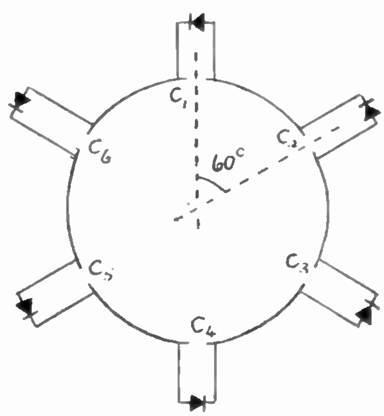

Fig. 2.

John Brown
Dept. of Elec. Engrg.
University College,
London, Eng.

* Received by the IRE, January 3, 1961.

[1] D. L. Hedderley, "A traveling wave harmonic generator," Proc. IRE, (Correspondence), vol. 48, p. 1658; September, 1960.

[2] A. Anderson, "A New Technique for Using Crystal Frequency Doubles at Millimeter Wavelengths," Ph.D. dissertation, University of London, London, Eng.; 1959.

A Complete Transistor Equivalent Circuit*

It is desired to present here, for those who might find it useful, a very simple "complete transistor equivalent circuit," which has, perhaps, often been tacitly assumed, but which, to the writer's knowledge, has not been used as such.

The circuit, shown in Fig. 1, is implicit in, though not given by, Ebers and Moll.[1] This is seen most easily by the fact that the following equations from the above paper immediately result from it:

$$-\alpha_N I_E = I_C + I_{CO}[e^{q\phi_C/KT} - 1]$$

$$-\alpha_I I_C = I_E + I_{EO}[e^{q\phi_E/KT} - 1].$$

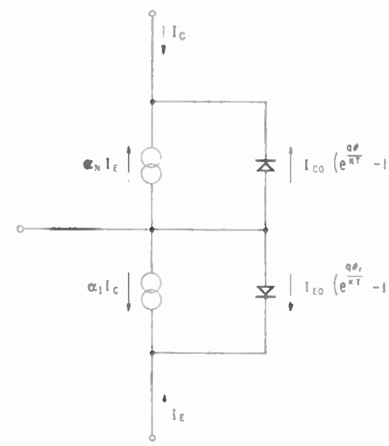

Fig. 1.

Together with the above equations, the circuit is valid in all three regions (I, II and III) and in either the forward or the reverse direction. In addition, all other equivalent large and small signal circuits, shown in the above-mentioned paper, can be derived from it. These are the reasons for calling it a "complete equivalent" circuit.

The usefulness of this circuit shows up in its application to a problem such as the following:

> It is desired to know the voltage drop across the transistor chopper shown in Fig 2(a); its equivalent circuit is shown in Fig. 2(b), where equivalent resistances have also been added to the circuit. If we make $I_B \gg I$, the circuit reduces to that of Fig. 3. Then we can write the following equation:

$$V \simeq I_B(R_{C1} - R_{C2}) + \frac{KT}{q}\left[\ln\left(\frac{I_B}{I_{CO1}} - 1\right) - \ln\left(\frac{I_B}{I_{CO2}} - 1\right) + \ln\left(\frac{\alpha_{I2} I_B}{I_{EO2}} - 1\right) - \ln\left(\frac{\alpha_{I1} I_B}{I_{EO1}} - 1\right)\right].$$

If we now assume that $I_B \gg I_{CO}$ and I_{EO}, then we have:

$$V \simeq I_B(R_{c_1} - R_{c_2}) + \frac{KT}{q} \ln \left[\frac{\alpha_{I2} I_{EO1} I_{CO2}}{\alpha_{I1} I_{EO2} I_{CO1}}\right]$$

* Received by the IRE, December 5, 1960.

[1] J. J. Ebers and J. L. Moll, "Large-signal behavior of junction transistors," Proc. IRE, vol. 42, pp. 1761–1772; December, 1954.

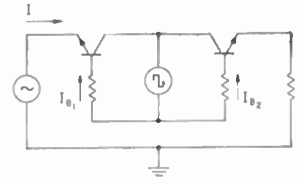

(a)

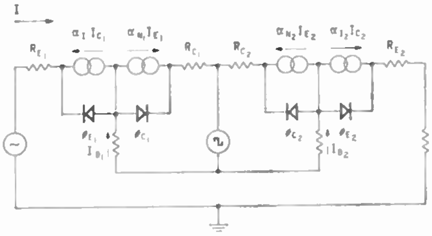

(b)

Fig. 2.

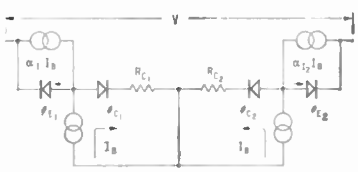

Fig. 3.

but if we assume that

$$\alpha_I I_{CO} = \alpha_N I_{EO},$$

then,

$$V \simeq I_B(R_{c_1} - R_{c_2}) + \frac{KT}{q} \ln \left[\frac{\alpha_{N2}}{\alpha_{N1}} \right].$$

R. H. Beeson
Fairchild Semiconductor Corp.
Mountain View, Calif.

The Tunnel Diode as a Highly Sensitive Microwave Detector*

A recent letter[1] described the use of the tunnel diode in a super-regenerative receiver. We have found in similar experiments that our receivers showed maximum sensitivity with minimum quenching voltage; in fact, good receiver sensitivity has been achieved with no quenching at all. In this case the diode is biased near oscillation and is operated as a square-law detector.

Fig. 1 shows the equivalent circuit of the detector at radio frequencies. V_g and R_g comprise the source, L is the external resonating inductance, and $-R$, C, and R_s make up the usual diode equivalent circuit. We define the short-circuit current sensitivity, $\beta = I_{sc}/P_a$, where I_{sc} is the short-circuit rectified current and P_a is the available power from the source.

Using the various circuit parameters shown in Fig. 1, and utilizing the above definition, we find

$$\beta = \frac{2K_2 G_g R^2}{[R_s + R_g + \omega^2 LCR - R]^2 + \omega^2[L - CR(R_s + R_g)]^2},$$

where ω is the signal carrier frequency and K_2 is the constant of proportionality between the rectified current and square of the RF voltage across the diode. The form of this relation is shown in Fig. 2 where β is plotted against frequency with R appearing as a parameter. The values of K_2, R, and C are measured, and the values of L and $R_g + R_s$ are calculated. R is normalized against R_0, the magnitude of the negative resistance necessary for oscillation, and ω is normalized against ω_0, the natural frequency of oscillation. The value of R is controlled by the choice of operating point.

The short-circuit current sensitivity measurements were made in a straightforward manner, and although the resonant circuit of the diode was crude, reasonably good results were obtained. The input signal was square-wave modulated at 1 kc or 400 cycles, but the choice of modulation frequency made little difference in the behavior of the detector. The open-circuit detected output voltage was measured by using an amplifier with a 3-db response from 20 cps to 150 kc to drive a wide-band voltmeter. The RF input of the detector was stub tuned to match the generator.

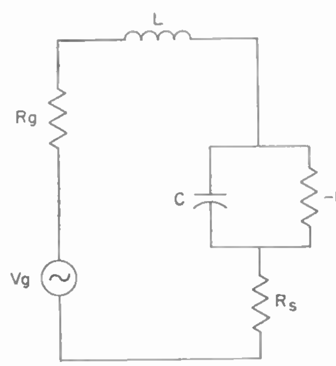

Fig. 1—Detector RF equivalent circuit.

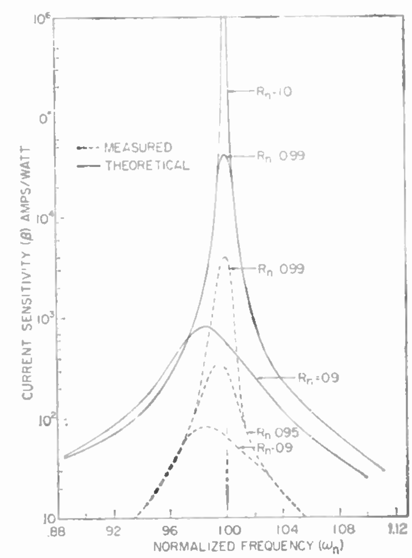

Fig. 2—Short-circuit current sensitivity as a function of normalized frequency and negative resistance.

The input signal frequency was 980 Mc, and the best short-circuit current sensitivity obtained was 10^5 ampere/watt giving a minimum detectable power of -110 dbm. This figure for minimum detectable power is somewhat pessimistic because the video bandwidth was much larger than the frequency spectrum occupied by the 1-kc square wave. The dynamic characteristic for this run is shown in Fig. 3. The RF bandwidth was 500 kc, and the video output level was extremely sensitive to crystal bias. The extremely narrow bandwidth and poor stability are to be expected when operating close to a singular point on the I-V characteristic.

Several measurements of β were made using different biases on the diode, and the results are plotted with the calculated curves of Fig. 2 for comparison. It should be noted that the experimental and theoretical curves agree in general shape, but show an order of magnitude discrepancy in sensitivity. Some of this discrepancy was due to poor RF coupling between generator and receiver as slight changes in coupling resulted in large changes in optimum sensitivity, and some discrepancy could have been due to errors in measurement of parameters. The circuit was composed of lumped elements and was coupled to the source with a one-turn loop of wire.

As expected, the diode showed square-law response to quite large input signals. The only limiting factor to the dynamic range was the tendency for large signals to start the diode oscillating.

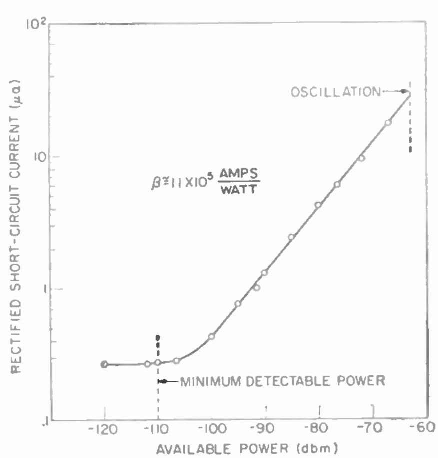

Fig. 3—Dynamic characteristic.

* Received by the IRE, December 29, 1960; revised manuscript received, January 11, 1961.

[1] A. G. Jordan, "Esaki diodes as super-regenerative detectors," Proc. IRE, (Correspondence), vol. 48, p. 1902; November, 1960.

The video noise temperature of the diode was not measured, but observations with a variable band-pass amplifier indicate a nearly flat noise spectrum down to about 500 cps. This is in agreement with studies of $1/f$ noise associated with tunnel diodes biased in the negative-resistance portion of their characteristic.[2]

The diode used in these experiments was a GE gallium arsenide diode ZJ61-10. Other diodes have been tried at various frequencies up to 1 kMc, and the results were similar. The diodes, of course, will be sensitive only when the signal frequency is equal to or below the maximum frequency of oscillation. Good sensitivities ($\beta = 5 \times 10^2$) with a minimum detectable power of -90 dbm have been obtained under quite stable conditions with a bandwidth approaching 2 per cent.

M. D. MONTGOMERY
U. S. Naval Res. Lab.
Washington, D. C.

[2] L. Esaki and T. Yajima, "Excess noise in narrow germanium p-n junctions," *J. Phys. Soc. Japan*, vol. 13, pp. 1281–1287; November, 1958.

Comments on "An Analysis of Cryotron Ring Oscillators"*

In a recent paper, Cohen[1] analyzed a film cryotron ring oscillator as an R-L circuit with variable R. In the linear amplifier analysis, the gate resistance is considered to increase linearly with the total control current $i = i_c + i_g/\mu$:

$$R_g = m\left(i_c + \frac{i_g}{\mu} - I_{\text{crit}}\right). \tag{1}$$

In the switching analysis, the assumption is made that gate resistance is a discontinuous function of current i,

$$R_g = O \quad \text{for } i < I_{\text{crit}}$$
$$R_g = R \quad \text{for } i > I_{\text{crit}}.$$

The gate current i_g then constitutes simple exponential functions of time.

When (1) is used for switching analysis, the circuit equation becomes

$$m\left(i_c + \frac{i_g}{\mu} - I_{\text{crit}}\right) i_g + L\frac{di_g}{dt} = O. \tag{2}$$

By making the substitution $y = 1/i_g$, (2) can be reduced to a first-order linear differential equation:

$$\frac{dy}{dt} - \frac{m}{L}(i_c - I_{\text{crit}})y = \frac{m}{L\mu}. \tag{3}$$

The general solution of (3) is

$$y = \exp\left[\frac{m}{L}\int (i_c - I_{\text{crit}})dt\right]\left\{C + \frac{m}{L\mu} \cdot \int \exp\left[-\frac{m}{L}\int (i_c - I_{\text{crit}})dt\right]dt\right\}, \tag{4}$$

where C is to be determined by the initial condition.

The integral is impossible to evaluate for i_c in general. However, i_c can usually be approximated by piecewise straight line segments. Then i_c takes the form

$$i_c = kt + a,$$

or

$$i_c - I_{\text{crit}}\ kt - b,$$

and

$$\int \exp\left[-\frac{m}{L}\int (i_c - I_{\text{crit}})dt\right]dt$$
$$= \int \exp\left[-\frac{m}{L}\left(\frac{k}{2}t^2 - bt\right)\right]dt$$
$$= -\sqrt{\frac{2L}{mk}}\exp\left[\frac{mb^2}{2kL}\right]\int \exp[-z^2]dz, \tag{5}$$

where

$$z = \sqrt{\frac{mk}{2L}}\left(\frac{b}{k} - t\right).$$

The value of the probability integral

$$\int \exp[-z^2]dz = P(z)$$

can be found from mathematical tables.

Substitute (5) into (4); then

$$y = \frac{1}{i_g} = \exp\left[\frac{m}{L}\left(\frac{k}{2}t^2 - bt\right)\right] \cdot \left\{C - \frac{1}{\mu}\sqrt{\frac{2m}{Lk}}\exp\left[\frac{mb^2}{2kL}\right]P(z)\right\}.$$

With the initial conditions $t = 0$, $i_g = I_{g0}$, this gives

$$i_g = \frac{I_{g0}\exp\left[-\frac{m}{L}\left(\frac{k}{2}t - b\right)t\right]}{1 + \frac{I_{g0}}{\mu}\sqrt{\frac{2m}{Lk}}\exp\left[\frac{mb^2}{2kL}\right]\left\{P\left(\sqrt{\frac{m}{2kL}}\,b\right) - P(z)\right\}}. \tag{6}$$

The denominator of (6) seems to imply that i_g decreases faster for smaller μ, even though the feedback effect of i_g/μ is to reduce the gate resistance. This is because the comparison is not made at the same region of gate resistance. If I_{crit} is adjusted (through bias control current) to compensate for the change of I_{g0}/μ as μ is varied (less b for larger μ), one would find that i_g decreases faster for larger μ.

T. H. CHENG
IBM Corp.
Research Center
Yorktown Heights, N. Y.

* Received by the IRE, January 10, 1961.

[1] M. L. Cohen, "An analysis of cryotron ring oscillators," PROC. IRE, vol. 48, pp. 1576–1582; September, 1960.

Discussion of "Fourier Series Derivation"*

I feel that I must take exception to Gadsden's article.[1] It is questionable whether his treatment constitutes a derivation of the Fourier series. In the usual order of events, the Laplace transformation integrals are developed from the exponential form of the Fourier series through a succession of limiting processes. Derivation of the Laplace transformation integrals in this manner is presented in many reference works.[2] One does not usually reverse the process, since the meromorphic functions involved are generally rather difficult to handle mathematically.

Now, so far as derivations and proofs of validity of the Fourier series are concerned, several exist. Early proofs of validity of Fourier series representation were formulated by Cauchy and Poisson. One of Cauchy's proofs has been shown to be invalid in its original form. The other employs functions of a complex variable. Poisson attempted proof by means of[3]

$$\int_{-\pi}^{\pi}(1 - h^2)f(x')[1 - 2h\cos(x - x') + h^2]^{-1}dx'$$
$$= (1/2\pi)\int_{-\pi}^{\pi} f(x')dx' + (1/\pi)\sum_{n=1}^{\infty} h^n \int_{-\pi}^{\pi} f(x')\cos n(x - x')dx'$$
$$\text{for } -1 < h < 1.$$

Further proofs of validity are provided by Dirichlet's approach, perhaps the most rigorous, and minimization of the square error.[4,5] Dirichlet's proof is based upon a sketch provided by Fourier.

The derivation of the Fourier series is not a derivation in the usual sense. Certain relations are stated from which the Fourier series representation for a piecewise continuous periodic function can be developed. This is perhaps the factor that has disturbed Gadsden. One derivation of the Fourier series may be developed from an approach employing orthogonal functions. Following is a sketch of this derivation.

The Fourier series is one of a class of general trigonometrical series which may be represented in the form[6]

$$f(t) = (a_0/2) + \sum_{k=0}^{\infty}[a_k \cos kt + b_k \sin kt]. \tag{1}$$

* Received by the IRE, November 3, 1960.

[1] C. P. Gadsden, "Fourier series derivation," PROC. IRE, (Correspondence), vol. 48, p. 1652; September, 1960.

[2] M. F. Gardner and J. L. Barnes, "Transients in Linear Systems," John Wiley and Sons, Inc., New York, N. Y., vol. 1; 1942.

C. R. Wylie, "Advanced Engineering Mathematics," McGraw-Hill Book Co., Inc., New York, N. Y.; 1960.

[3] S. D. Poisson, "Sommation des Séries des Quantités Périodique," Paris École Polytechnique, *Journal*, Tome 12, cahier 19, (1st series), 1823; "Suite du Mémoire sur les Intégrals Définies et sur la Sommation des Séries," p. 404 ff.

S. D. Poisson, "Théorie Mathématique de la Chaleur," Bachelier, Paris, France, 1837.

[4] E. W. Hobson, "The Theory of Functions of a Real Variable," Dover Publications, Inc., New York, N.Y., vol. 2; 1957.

[5] W. Kaplan, "Advanced Calculus," Addison Wesley Publishers, Cambridge, Mass.; 1953.

[6] A. Zygmund, "Trigonometrical Series," Dover Publications, Inc., New York, N. Y.; 1955.

Provided that a_0, a_k, and b_k are correctly determined, the expression on the right-hand side of (1) is a Fourier series representation for $f(t)$. The function $f(t)$ is a piecewise continuous periodic function.

As a starting point, we examine the set of orthonormal functions, $\phi_n(t)$, investigated by Fourier:

$$\phi_0(t) = 1/\sqrt{2\pi},\ \phi_1(t) = (1/\sqrt{\pi}) \sin t,$$

$$\phi_2(t) = (1/\sqrt{\pi}) \cos t,$$

$$\phi_3(t) = (1/\sqrt{\pi}) \sin 2t,$$

$$\phi_4(t) = (1/\sqrt{\pi}) \cos 2t, \cdots$$

$$\phi_{2n-1}(t) = (1/\sqrt{\pi}) \sin nt.$$

$$\phi_{2n}(t) = (1/\sqrt{\pi}) \cos nt. \tag{2}$$

Let us suppose that our piecewise continuous function $f(t)$ can be represented by the infinite series:

$$f(t) = c_0\phi_0(t) + c_1\phi_1(t) + c_2\phi_2(t) + \cdots + c_k\phi_k(t) + \cdots = \sum_{k=0}^{\infty} c_k\phi_k(t). \tag{3}$$

Now, to evaluate the constants c_k, we use the property of sets of orthonormal functions that:

$$\int_{-\pi}^{\pi} \phi_k(t)\phi_k(t)dt = 1;$$

$$\int_{-\pi}^{\pi} \phi_k(t)\phi_j(t) = 0, \quad k \neq j. \tag{4}$$

(In this case the range of definition of one period is $-\pi$ to $+\pi$.) We now form the expression

$$\int_{-\pi}^{\pi} f(t)\phi_n(t)dt$$

$$= \int_{-\pi}^{\pi} [c_0\phi_0(t) + c_1\phi_1(t) + \cdots + c_k\phi_k(t) + \cdots]\phi_n(t)dt$$

$$= \int_{-\pi}^{\pi} c_0\phi_0(t)\phi_0(t)dt + \int_{-\pi}^{\pi} c_1\phi_1(r)\phi_1(t)dt + \cdots + \int_{-\pi}^{\pi} c_k\phi_k(t)\phi_k(t)dt + \cdots$$

$$= \sum_{k=0}^{\infty} c_k \int_{-\pi}^{\pi} \phi_k(t)\phi_k(t)dt = \sum_{k=0}^{\infty} c_k. \tag{5}$$

Hence

$$\int_{-\pi}^{\pi} f(t)\phi_n(t)dt$$

$$= \sum_{k=0}^{\infty} c_k = c_0 + c_1 + c_2 + \cdots + c_k + \cdots. \tag{6}$$

Or

$$\int_{-\pi}^{\pi} f(t)\phi_0(t)dt = c_0;$$

$$\int_{-\pi}^{\pi} f(t)\phi_1(t)dt = c_1; \cdots;$$

$$\int_{-\pi}^{\pi} f(t)\phi_k(t)dt = c_k. \tag{7}$$

Substituting from (2) into (7), we find

$$c_0 = (1/\sqrt{2\pi}) \int_{-\pi}^{\pi} f(t)dt;$$

$$c_1 = (1/\sqrt{\pi}) \int_{-\pi}^{\pi} f(t) \sin tdt;$$

$$c_2 = (1/\sqrt{\pi}) \int_{-\pi}^{\pi} f(t) \cos tdt; \cdots;$$

$$c_{2n-1} = (1/\sqrt{\pi}) \int_{-\pi}^{\pi} f(t) \sin ntdt;$$

$$c_{2n} = (1/\sqrt{\pi}) \int_{-\pi}^{\pi} f(t) \cos ntdt. \tag{8}$$

Substitution of (2) and (8) into (3) produces

$$f(t) = c_0\phi_0(t) + c_1\phi_1(t) + \cdots + c_k\phi_k(t) + \cdots + c_n\phi_n(t) + \cdots$$

$$= \sum_{k=0}^{\infty} c_k\phi_k(t)$$

$$= \Big\{(1/2\pi) \int_{-\pi}^{\pi} f(t)dt + \left[(1/\pi) \int_{-\pi}^{\pi} f(t) \sin tdt\right] \sin t + \left[(1/\pi) \int_{-\pi}^{\pi} f(t) \cos tdt\right] \cos t + \cdots\Big\}$$

$$= (1/2\pi) \int_{-\pi}^{\pi} f(t)dt + \sum_{k=1}^{\infty} \Big\{\left[(1/\pi) \int_{-\pi}^{\pi} f(t) \cos ktdt\right] \cos kt + \left[(1/\pi) \int_{-\pi}^{\pi} f(t) \sin ktdt\right] \sin kt\Big\}. \tag{9}$$

Comparison of (9) with (1) yields

$$f(t) = (a_0/2) + \sum_{k=1}^{\infty} [a_k \cos kt + b_k \sin kt \tag{1}$$

$$a_0 = (1/\pi) \int_{-\pi}^{\pi} f(t)dt;$$

$$a_k = (1/\pi) \int_{-\pi}^{\pi} f(t) \cos ktdt;$$

$$b_k = (1/\pi) \int_{-\pi}^{\pi} f(t) \sin ktdt,$$

$$k = 1, 2, 3, \cdots. \tag{10}$$

The function $f(t)$, to be expressed as a Fourier series, must satisfy the Dirichlet conditions: 1) $f(t)$ may have a finite number of discontinuities only over the range of one period; 2) the integral shown must be absolutely convergent.

$$\int_a^b |f(t)| dt < \infty,$$

where a–b is the range of definition of $f(t)$; and 3) any infinite discontinuities of $f(t)$ must be integrable.

A complete discussion of the Fourier series derivation and proof of validity would include examination of the Gibbs Phenomenon and the convergence properties of the series. The sketch presented above should provide some insight into one method of deriving the Fourier series.

Clifford D. Ferris
Dept. of Elec. Engrg.
The George Washington University
Washington, D. C.

Author's Comment[7]

My brief letter was not meant to furnish a rigorous derivation of the Fourier series. It is well known that restrictions must be put on a function for it to be representable in such a series. The purpose of the note was to indicate how the general form of the series, as well as the standard formula for the Fourier coefficients, could be deduced from Laplace-transform theory. The development outlined above, which is very well known indeed, is merely a procedure for obtaining the coefficients; the form of the series is assumed.[8]

After receiving a copy of Ferris' remarks I was, however, able to expand the formal derivation of my letter into a rigorous proof, assuming that the given periodic function $p(t)$ satisfies Dirichlet's original conditions,[9] by using a general method[10] for inverting its transform:[11]

$$P(s) = (1 - e^{-Ts})^{-1} \int_0^T e^{-st}p(t)dt, \tag{1}$$

where T = the period and $\mathrm{Re}\,[s] > 0$. Soon afterward, I found an almost identical discussion in a recent book;[12] it is therefore unnecessary to repeat it here.

Still, the point can be raised whether $P(s)$ may first be expanded into its partial-fraction series

$$P(s) = \sum_{-\infty}^{\infty} k_n(s - s_n)^{-1}, \tag{2}$$

where

$$k_n = T^{-1} \int_0^T e^{-s_nt}p(t)dt, \qquad s_n = j2\pi nT^{-1},$$

$$n = 0, \pm 1, \pm 2, \cdots,$$

and then this series inverted term by term to recover $p(t)$ in its Fourier representation

$$p(t) = \sum_{-\infty}^{\infty} k_ne^{s_nt}. \tag{3}$$

[7] Received by the IRE, January 10, 1961.

[8] *Note added in proof:* In Ferris's letter, there is an error in (5) and (6). The right-hand sides should be C_n, not an infinite sum.

[9] See Hobson, *op. cit.*, pp. 502–509. These conditions are that the function be sectionally continuous, and of bounded variation in its period. The conditions listed by Ferris are presumably meant to refer to Dirichlet's later weakened conditions, and, if so, are incompletely stated; the latter conditions allow a finite number of infinite discontinuities in the period, but the function must still be of bounded variation when arbitrarily small neighborhoods of these discontinuities are excluded; the condition 3) is unnecessary as it follows from 2).

[10] R. V. Churchill, "Operational Mathematics," McGraw-Hill Book Co., Inc., New York, N. Y., 2nd ed., pp. 186–193; 1958.

[11] A proof of this formula, simpler than the usual one, is as follows. Let $p(t) = 0$, $t < 0$; $p(t) = p(t+T)$, $t > 0$. Transforming $q(t) = p(t) - p(t-T)$ we have

$$\int_0^{\infty} \exp(-st)q(t)dt = P(s) - P(s) \exp(-sT)$$

by the shifting rule. Then (1) follows since $q(t) = p(t)$, $0 < t < T$; and $= 0$ otherwise. It is not hard to see that the Lebesgue integrability of $q(t)$ is sufficient for validity, and that the abscissa of absolute convergence is 0, or $-\infty$ if $q(t)$ is null.

[12] S. Seshu and N. Balabanian, "Linear Network Analysis," John Wiley and Sons, Inc., New York, N. Y., sect. 5.5 and Problem 5.13; 1959. The inverting of (1) by residues has also been treated by N. W. McLachlan, "Fourier expansions obtained operationally," *Phil. Mag.*, vol. 24, p. 1055, 1937, and discussed by Gardner and Barnes, *op. cit.*, p. 243. However, the idea seems to have originated in O. Heaviside, "Electromagnetic Theory," Dover Publications, Inc., New York, N. Y., 1950 (see especially sect. 265, "Conversion of operational solutions to Fourier series by special ways," and sect. 275, "How to find the meaning of a Fourier series operationally").

Now, the expansion (2) can be verified rigorously by a method of Cauchy:[13] from residue theory we have

$$P(z) = \sum_{-N}^{N} k_n(z - s_n)^{-1} + \int_{C_N} (z - s)^{-1}P(s)ds, \qquad (4)$$

where C_N is the square in the s plane with corners at $\pm\sigma_N \pm j\sigma_N$, $\sigma_N = (2N+1)\pi T^{-1}$ and $z \neq s_n$ is inside C_N. We now show that the line integral of $(z-s)^{-1}P(s)$ along each side of this square $\to 0$ as $N \to \infty$. Let $s = \sigma + j\omega$, $z = x + jy$, and note the relations

$$|1 - e^{-Ts}|^2 = 1 - 2e^{-T\sigma}\cos\omega T + e^{-2T\sigma} \geq (1 - e^{-T\sigma})^2,$$

$|z - s| \geq \sigma_N - m$, where $m = \max\{|x|, |y|\}$, s on C_N and z within C_N, and

$$b = \text{l.u.b.}\ |p(t)|, \qquad 0 < t < T,$$

which is finite because $p(t)$ is sectionally continuous. First let I = the line integral along the left or right side of C_N. Then,

$$I = j\int_{\pm\sigma_N}^{\mp\sigma_N}\int_0^T (z - s)^{-1}(1 - e^{\pm\sigma_N T}e^{-j\omega T})^{-1}p(t) \cdot e^{-st}dtd\omega;$$

therefore,

$$|I| \leq b(\sigma_N - m)^{-1}|1 - e^{\pm\sigma_N T}|^{-1} \cdot \int_{-\sigma_N}^{\sigma_N}\int_0^T e^{\pm\sigma_N t}dtd\omega = 2b(\sigma_N - m)^{-1} \to 0 \text{ as } N \to \infty.$$

Now let I' = the line integral along the top or bottom of C_N. Since $\cos\omega T = -1$,

$$|I'| \leq b(\sigma_N - m)^{-1}\int_{-\sigma_N}^{\sigma_N}\int_0^T (1 + e^{-\sigma T})^{-1}e^{-\sigma t}dtd\sigma = b(\sigma_N - m)^{-1}\int_{-\sigma_N}^{\sigma_N}\sigma^{-1}\tanh(\sigma T/2)d\sigma.$$

As $N \to \infty$, the last integral diverges to $-\infty$ since the integrand is asymptotic to σ^{-1}; by L'Hospital's rule the limit of the entire expression can be evaluated as $2b \cdot \lim \sigma_N^{-1} \tanh(\sigma_N T/2) = 0$. Hence (2) is valid as the limit of (4) as $N \to \infty$. Unfortunately the rigorous term by term inversion of (2) into (3) appears to be difficult; the only general theorem on inversion of an infinite series of transforms that is given in standard works on the Laplace transform is much too restrictive for the broad conditions assumed here.[14] Of course, the valid result of inversion of $P(s)$ from the closed form (1) shows indirectly that term-by-term inversion must also be valid. If any reader can supply me with a direct proof, I would appreciate it.

Finally, in contradiction to what Ferris cites as the "usual" order of events, it may be noted that the Laplace transform predated the Fourier transform by some 30 years in its original development.[15] The approach of starting with the Fourier series is only a pedagogical device, as Gardner and Barnes clearly state.[16]

Christopher P. Gadsden
Dept. of Elec. Engrg.
Tulane University
New Orleans, La.

[13] E. T. Copson, "Theory of Functions of a Complex Variable," Oxford University Press, Oxford, England, pp. 144–145; 1935.

[14] G. Doetsch, "Laplace-Transformation," Dover Publications, Inc., New York, N. Y., p. 139, theorem 1; 1943.

[15] Gardner and Barnes, *op. cit.*, p. 104 and Appendix C.

[16] *Ibid.*, pp. 94–95.

Microwave Bistable Circuits Using Varactor Diodes*

Fast microwave switching circuits, with switching times of the order of a few nanoseconds, have been built using varactor diodes. The circuits use the nonlinear capacitance and rectification properties of the varactor to generate a negative resistance. Similar negative resistance phenomena have been reported recently, but they have been attributed to new high-frequency semiconductor phenomena.[1–3]

The basic circuit consists of a varactor diode mounted in a tunable waveguide or coaxial diode mount, and a high-frequency voltage applied to the circuit. When the tuner and the power level are properly adjusted, the voltage-current characteristic that is observed at the bias terminal has a negative resistance region and sometimes has hysteresis, as shown in Fig. 1.

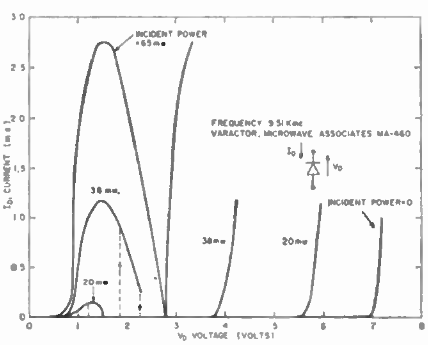

Fig. 1—Current-voltage characteristics of the varactor negative-resistance circuit for various microwave power levels.

* Received by the IRE, December 6, 1960; revised manuscript received, January 6, 1961.

[1] I. Hefni, "Effect of minority-carriers on the dynamic characteristic of parametric diodes," *Electronic Engrg.*, vol. 32, pp. 226–227; April, 1960.

[2] K. Siegel, "Anomalous reverse current in varactor diodes," Proc. IRE, vol. 48, pp. 1159–1160; June, 1960.

[3] H. C. Torrey, and C. A. Whitmer, "Crystal Rectifiers," McGraw-Hill Book Co., Inc., New York, N. Y., ch. 13; 1948. Here it was realized that the phenomena were due to the nonlinear resistance and capacitance of the diode, but the explanation was not very detailed and the diodes at that time did not show enough negative resistance and were not uniform enough to be useful.

The explanation for the operation of the circuit is as follows: at one value of bias voltage the circuit is resonant, thus causing the ac voltage across the varactor to be large and to extend into the reverse conduction region. This causes a large rectified current to flow at the bias terminal. When the bias voltage is increased or decreased from this value, the circuit is no longer resonant and the rectified current is smaller, thus giving the negative-resistance characteristic. This explanation is substantiated by the fact that the voltage at which the peak current occurs decreases as the frequency is decreased. The hysteresis occurs because the resonance can be a nonlinear resonance (ferroresonance) and occurs only for a certain range of circuit parameters. Experiments with low-frequency versions of the circuit substantiated this explanation.

The best negative resistance characteristics obtained so far have been with diffused silicon varactors with sharp breakdown characteristics and with breakdown voltages of 5 to 7 volts. Negative resistances of less than 10 ohms with a peak current of 3 ma have been observed. The cutoff frequencies of the varactors were about 25 kMc at zero bias, and the capacitances ranged from 0.5 pf to 1.6 pf.

This phenomenon is very fast, *i.e.*, the negative resistance is observed at all frequencies that are low compared to the carrier frequency. To get an indication of the speed of the phenomenon, an oscillator was made by connecting a resonant circuit across the bias terminals. Using a 10-kMc carrier, the circuit could be made to oscillate at any frequency up to at least 900 Mc.

A bistable circuit was constructed by biasing the negative resistance through the proper load resistance. The circuit could be switched between states with speeds of less than 10 nsec when the carrier frequency was 10 kMc. The circuit used had much more energy storage than necessary, due to the long length of the circuit and the high inductance of the varactor, and therefore, it is expected that the switching time would be reduced if the circuit were miniaturized and the varactor package improved. Experiments with the low-frequency circuit showed that the switching time could be made to be as short as 6 cycles of the carrier frequency. Another type of low-frequency carrier-energized varactor bistable circuit was reported by Keizer several years ago.[4]

A microwave bistable switch was made by connecting the basic circuit in shunt with a transmission line as shown in Fig. 2. The impedance presented to the main transmission line by the bistable circuit depends on the state of the circuit. In one state the circuit is resonant, and the length of the shunt line can be chosen so that the impedance is high, therefore permitting a large amount of power to be transmitted to the load, while in the other state, the impedance is low, therefore reflecting most of the incident power. Typical curves of transmitted power vs bias voltage and incident power are shown in Fig. 3.

[4] E. O. Keizer, "A carrier-energized bistable circuit using variable capacitance diodes," *RCA Rev.*, vol. 18, pp. 475–485; December, 1957.

Threshold logic circuits with power gain can be made as shown in Fig. 2. The bias power is adjusted as in Fig. 3(b), so that a certain number of inputs is required to cause the circuit to switch. The length of the shunt line can be chosen so that the transmission characteristic is as shown in either Fig. 3(b) or Fig. 3(c). In the latter case, the output is inverted.

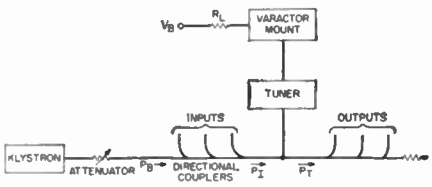

Fig. 2—Microwave bistable switch. P_B, P_I, and P_T are the microwave power levels in the circuit.

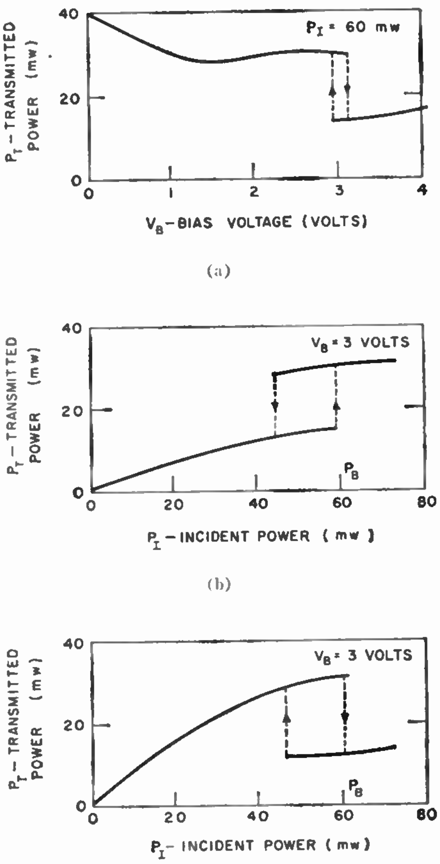

Fig. 3—Characteristics of the microwave bistable switch of Fig. 2.

The experiments indicate that the performance of the circuit in high-speed switching applications would be improved by using higher carrier frequencies, low-energy storage circuits, and better varactors.

C. L. HEIZMAN
IBM Corp.
Res. Center
Yorktown Heights, N. Y.

Mismatched Interconnection of Transistor Feedback Amplifiers*

One of the difficulties in the design of transistor feedback amplifiers is the interaction between successive stages. Consider the following example:

The voltage gain of a series feedback amplifier, Fig. 1(a), is given by

$$A_v \approx R_L/R_E. \quad (1)$$

In a cascade of series feedback stages, Fig. 2, the effective load R_L for each transistor is the parallel combination of its own collector resistor R_C and the input resistance r_i of the following stage:

$$R_L = (R_C r_i)/(R_C + r_i) \quad (2)$$

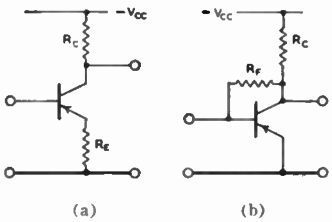

Fig. 1—Single-stage transistor feedback amplifiers: (a) series feedback, (b) shunt feedback.

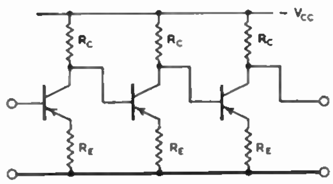

Fig. 2—Cascaded series feedback stages.

Now r_i is relatively unknown, being (roughly) proportional to β_N:

$$r_i \approx \beta_N R_E. \quad (3)$$

Therefore, if the gain of a cascade of series feedback stages is to be accurately stabilized, R_C must be very much smaller than the unknown r_i, so that R_L is known accurately. A typical value for R_C would be

$$R_C = 0.1\,\beta_{NA} R_E, \quad (4)$$

where β_{NA} is the value of β_N expected for an "average" transistor. Therefore,

$$R_L \approx R_C$$

$$= 0.1\,\beta_{NA} R_E \quad (5)$$

and, from (1), the voltage gain per stage is

$$A_v \approx 0.1\,\beta_{NA}. \quad (6)$$

Thus, the gain per stage of a cascade of series feedback amplifiers must be small if this gain is to be accurately stabilized.

A dual argument may be applied to show that the gain per stage of a cascade of shunt feedback amplifiers must be small if this gain is to be accurately stabilized.

It may be shown that a series feedback amplifier has a stable transconductance. Its input and output resistance are increased by the feedback, but are not stabilized. Further, such an amplifier should work into a low load resistance, and there is no feedback when such an amplifier is fed from a current source. Its transconductance is given by

$$\frac{i_0}{v_i} = \frac{\alpha_N}{r_B/\beta_N + r_E + R_E} \approx \frac{1}{R_E}. \quad (7)$$

The shunt feedback amplifier, Fig. 1(b), is the dual of the series feedback amplifier. It has a stable transresistance, it has low input and output resistances, it should work into a high load resistance, and there is no feedback when it is fed from a voltage source. Its transresistance is given by

$$\frac{v_0}{i_i} = \frac{R_F}{1 + (R_F + R_L)/\beta_N R_L} \approx R_F. \quad (8)$$

In view of these facts, the obvious method for cascading transistor feedback stages is the use of alternate series and shunt feedback stages. With this method of interconnection, each stage operates under very nearly the ideal conditions for which its transmittance is stabilized. The low input resistance of a shunt feedback stage forms an ideal load for a series feedback stage, and the high input resistance of a series feedback stage forms an ideal load for a shunt stage. Similarly, the high output resistance of a series stage forms an ideal source for a shunt stage, and the low output resistance of a shunt stage forms an ideal source for a series stage. For the same uncertainty in gain, more than twice the gain per stage can be realized with this method of interconnection than can be realized with either of the cascades of similar stages. Basically, what is done is to introduce a gross impedance mismatch between stages, so that the transmittance of each stage depends only on that stage. The over-all gain is closely the product of the individual stage transconductances and transresistances.

This method of interconnection of feedback stages is particularly useful in the design of transistor video amplifiers, where the use of single stage feedback circuits is almost essential for the production of designable circuits with satisfactory transient response. It also has application to audio amplifiers, and to cascades of feedback pairs, as is discussed in a paper to be published shortly.[1]

E. M. CHERRY
Dept. of Elec. Engrg.
University of Melbourne
Melbourne, Australia

* Received by the IRE, January 16, 1961.

[1] E. M. Cherry, "An engineering approach to the design of transistor feedback amplifiers," *Proc. IRE (Australia)*, vol. 22; 1961. To be published.

General Matched-Filter Analysis of Linear FM Pulse Compression*

A previous paper[1] discussed the basic concepts of linear FM pulse compression. The following discussion presents a matched-filter derivation of the pulse-compression waveform that includes the effect of a frequency shift of the received waveform (*i.e.*, Doppler shift approximation).

The transmitted waveform for the linear FM pulse compression is

$$f(t) = \cos\left(\omega_0 t + \frac{\mu t^2}{2}\right), \quad -\frac{T}{2} \leq t \leq \frac{T}{2}. \tag{1}$$

The matched filter required in the receiver has an impulse response $h(t)$ that is the time inverse of the signal at the receiver input. Thus,

$$h(t) = \sqrt{\frac{2\mu}{\pi}} \cos\left(\omega_0 t - \frac{\mu t^2}{2}\right), \quad -\frac{T}{2} \leq t \leq \frac{T}{2}, \tag{2}$$

where $\sqrt{2\mu/\pi}$ is the factor that gives the filter unity gain.

The output of the matched filter is obtained by convolving $f(t)$ and $h(t)$, yielding

$$g(\tau) = \int_{-\infty}^{\infty} f(t)h(\tau - t)dt. \tag{3}$$

When $f(t)$ and $h(t)$ are "matched," $g(\tau)$ represents the autocorrelation function of the input signal. If the signal and the filter are not matched, then $g(\tau)$ represents the cross-correlation of the two functions. In pulse-compression systems, the case of general interest lies in the effect of a moving target that causes, by virtue of the Doppler signal shift, the received signal to be mismatched to the pulse-compression filter. For the linear FM function we may take the Doppler-shifted signal as

$$f(t) = \cos\left[(\omega_0 - \omega_d)t + \frac{\mu t^2}{2}\right]. \tag{4}$$

This ignores the second-order effect produced by the frequency deviation of the signal, a valid assumption if the total signal bandwidth is very much smaller than the transmitted frequency, $\omega_0 + \omega_{rf}$.

The most general output of the linear FM matched filter is obtained by evaluating:

$$g(\tau, \omega_d) = \sqrt{\frac{2\mu}{\pi}} \int_a^b \cos\left[(\omega_0 + \omega_d)t + \frac{\mu t^2}{2}\right] \cdot \cos\left[\omega_0(\tau - t) - \frac{\mu}{2}(\tau - t)^2\right] dt, \tag{5}$$

where

$$\left.\begin{aligned} a &= -\frac{T}{2} + \tau \\ b &= \frac{T}{2} \end{aligned}\right\}, \quad \tau > 0$$

and

$$\left.\begin{aligned} a &= -\frac{T}{2} \\ b &= \frac{T}{2} + \tau \end{aligned}\right\}, \quad \tau < 0.$$

Utilizing the proper trigonometric identities and dropping higher frequency terms, the matched filter output is

$$g(\tau, \omega_d) = 1/2\sqrt{\frac{2\mu}{\pi}} \int_a^b \cos\left[\omega_0\tau + \omega_d t + \mu\tau t - \frac{\mu\tau^2}{2}\right] dt \tag{6}$$

$$= 1/2\sqrt{\frac{2\mu}{\pi}} \left[\frac{\sin\left(\omega_0\tau + \omega_d t + \mu\tau t - (\mu\tau/2)^2\right)}{\omega_d + \mu\tau}\right]_{t=a}^{t=b}. \tag{7}$$

Imposing the limits for $\tau > 0$, the above becomes

$$g(\tau, \omega_d) = 1/2\sqrt{\frac{2\mu}{\pi}} \left[\frac{\sin\left[\omega_0\tau + \frac{\omega_d T}{2} + \frac{\mu\tau}{2}(T - \tau)\right]}{\omega_d + \mu\tau} - \frac{\sin\left[\omega_0\tau + \omega_d\tau - \frac{\omega_d T}{2} - \frac{\mu\tau}{2}(T - \tau)\right]}{\omega_d + \mu\tau}\right]. \tag{8}$$

If $\omega_d\tau/2$ is appropriately added and subtracted in the argument of the first term, we obtain

$$g(\tau, \omega_d) = 1/2\sqrt{\frac{2\mu}{\pi}} \left[\frac{\sin\left[\left(\omega_0 + \frac{\omega_d}{2}\right)\tau + \frac{\omega_d}{2}(T - \tau) + \frac{\mu\tau}{2}(T - \tau)\right]}{\omega_d + \mu\tau} - \frac{\sin\left[\left(\omega_0 t + \frac{\omega_d}{2}\right)\tau - \frac{\omega_d}{2}(T - \tau) - \frac{\mu\tau}{2}(T - \tau)\right]}{\omega_d + \mu\tau}\right]. \tag{9}$$

This has the form:

$$\sin(\alpha + \beta) - \sin(\alpha - \beta) = 2\cos\alpha\sin\beta,$$

where

$$\alpha = \left(\omega_0 + \frac{\omega_d}{2}\right)\tau$$

$$\beta = \frac{\omega_d + \mu\tau}{2}(T - \tau).$$

Thus, combining with the similar result for $\tau < 0$, the final expression is obtained:

$$g(\tau, \omega_d) = \sqrt{\frac{2\mu}{\pi}} \cos\left[\left(\omega_0 + \frac{\omega_d}{2}\right)\tau\right] \frac{\sin\left[\frac{\omega_d + \mu\tau}{2}(T - |\tau|)\right]}{\omega_d + \mu\tau}, \quad -T \leq \tau \leq T. \tag{10}$$

It is interesting to note that the carrier frequency term contains no frequency modulation for the nonmatched situation. In addition, the output frequency is shifted by $\omega_d/2$, not ω_d, an expected result when considering the bandwidth-limiting effects of the matched filter. For the special case of $\omega_d = 0$, the usual autocorrelation function is obtained,

$$g(\tau) = \sqrt{\frac{2\mu}{\pi}} \cos\omega_0\tau \frac{\sin\frac{\mu\tau}{2}(T - |\tau|)}{\mu\tau}, \quad -T \leq \tau \leq T \tag{11}$$

which compares to previously derived results[1] that assume a matched filter approximation of linear time delay vs frequency, and no bandwidth limitation:

$$g(t) = \sqrt{\frac{2\mu}{\pi}} \cos\left(\omega_0 t - \frac{\mu t^2}{2}\right) \frac{\sin\frac{\mu t}{2}T}{\mu t}, \quad -\infty < t < \infty. \tag{12}$$

As the compression ratio increases (*i.e.*, T is larger for a fixed compressed pulse width) the above two functions become nearly identical except for large values of τ. In the case of the filter for the linear time delay only, there is a linear displacement with time of the compressed pulse as a function of shift in frequency, but no waveform distortion as in the matched filter solution. In actual practice, (10) presents a more realistic appraisal. It should be pointed out that this analysis does not include the case of the reduction of the signal sidelobes by additional nonmatched filtering techniques.

The writer is grateful for helpful discussions with R. F. Schreitmueller and J. E. Chin of the Sperry Gyroscope Company.

CHARLES E. COOK
Air Armament Div.
Sperry Gyroscope Co.
Div. of Sperry Rand Corp.
Great Neck, L. I., N.Y.

* Received by the IRE, January 17, 1961.

[1] C. E. Cook, "Pulse compression—key to more efficient radar transmission," PROC. IRE, vol. 48, pp. 310–316; March, 1960.

Gain vs Bandwidth Limits for Esaki Diode Amplifiers*

Calculations have been made of the theoretical limits on gain vs bandwidth for Esaki diode linear amplifiers in three different configurations. These limitations are an interesting measure of performance for such amplifiers and are not widely publicized at present.

A scattering matrix description was used for amplifiers of the transmission type, reflection type, and reflection type with circulator.[1] An absolute stability requirement was expressed in terms of the reflection coefficient of the network seen by the negative resistance. This stability requirement, together with conditions of physical realizability of passive lossless coupling networks, leads to integral restrictions of the transducer gain (output power/available source power) along the $j\omega$ axis. These integrals are as follows:[2]

1) Transmission-type amplifier:

$$\frac{1}{2}\int_0^\infty \ln\left[1 + G_T\left(\frac{G_D - G_G}{G_G}\right)\right] d\omega \leqq \frac{\pi(G_D - G_G)}{C_D}.$$

2) Reflection-type amplifier:

$$\frac{1}{2}\int_0^\infty \ln\left[G_T\frac{(G_G + G_L)^2}{G_G G_L}\right] d\omega \leqq \frac{\pi G_D}{C_D}\left(\text{approximately for } G_T\frac{(G_G+G_L)}{G_G G_L} \gg 1 \text{ or } = 1\right).$$

3) Reflection-type amplifier with circulator:

$$\frac{1}{2}\int_0^\infty \ln G_T d\omega \leqq \frac{\pi G_D}{C_D};$$

$G_T \equiv$ output power/available source power
$G_G \equiv$ generator conductance
$G_L \equiv$ load conductance
$G_G \equiv$ diode conductance (magnitude)
$C_D \equiv$ diode capacitance.

In deriving the integrals, series resistance and inductance have been neglected since careful packaging and fabrication techniques can make these effects small.

In order to demonstrate the meaning of these integrals in a general way, it was assumed that G_T is constant over a band of frequencies B_r, outside of which G_T drops to zero or to some appropriate constant value which is less than or equal to unity. This idealized response gives an estimate of the limiting gain achievable for a specified bandwidth, without restriction to a specified pole pattern. The results are plotted in Fig. 1, together with points representing a number of

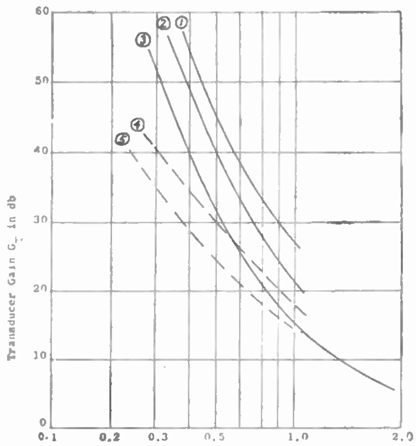

Normalized bandwidth $(\omega_2-\omega_1)\, C_D/G_D = B_r C_D/G_D$.

Fig. 1.

Curve 1 = Maximum flat gain for reflection-type amplifier with circulator.
Curve 2 = Maximum flat gain for reflection-type amplifier.
Curve 3 = Maximum flat gain for transmission-type amplifier.
Curve 4 = Maximum gain for equal-ripple response in a reflection-type amplifier with 3 db of ripple.
Curve 5 = Maximum gain for equal-ripple response in a reflection-type amplifier with 0.5 db of ripple.

realizable designs. It is seen that the reflection types are superior to transmission types, thus supporting Sard's conclusion[1] for maximally flat amplifiers.

J. S. Logan
14 Highpoint Drive, R.D. 2
Poughkeepsie, N. Y.

* Received by the IRE, January 9, 1961.

[1] Different types of amplifiers have been described by E. W. Sard, in "Tunnel (Esaki) diode amplifiers with unusually large bandwidth," Proc. IRE, (Correspondence), vol. 48, pp. 357–358; March, 1960.

[2] A detailed derivation of the integral restrictions is given by J. S. Logan, "Theoretical Limitations of Gain and Bandwidth in Wide-Band Transistor and Esaki Diode Amplifiers," Solid-State Electronics Lab., Stanford Univ., Stanford, Calif., Tech. Rept. No. 1753-1; September 20, 1960.

Some Electron Trajectories in a Nonuniform Magnetic Field*

A theoretical investigation[1] has been given to the ray paths of electrons deflected by electrostatic fields in both horizontal and vertical directions of a thin cathode-ray tube.[2] Since magnetic fields may also be used for deflections, this letter reports a magnetic method of scanning an electron beam in one direction only. The electron trajectories in the midplane of a nonuniform magnetic field are first treated as a two-dimensional problem. By including a second component of the magnetic field, trajectory calculations are then extended to the region close to the midplane.

The equation of motion of an electron in magnetic fields takes the form

$$\frac{d}{dt}(mv) = eB \times V, \tag{1}$$

where t is the time variable, m and e are the mass and the magnitude of the charge of the electron, and v is its velocity. For the region close to the x-y plane in rectangular coordinates x, y, and z, the magnetic field $\boldsymbol{B}$ can be expressed by

$$B_x = 0, \tag{2}$$
$$B_y = -\alpha z B_0[\exp \alpha y], \tag{3}$$
$$B_z = -B_0[\exp \alpha y], \tag{4}$$

where B_0 and α are parameters for the case in consideration.

Trajectories in x-y Plane

After substituting (4) into (1) and integrating with respect to t, the x, y components of (1) become

$$\frac{dx}{dt} = \frac{\omega}{\alpha}(e^{\alpha y} - 1), \tag{5}$$

and

$$\frac{dy}{dt} = \pm\sqrt{\frac{2eV}{m} - \left[\frac{\omega}{\alpha}(1 - e^{\alpha y})\right]^2}, \tag{6}$$

where $\omega = eB_0/m$ is known as the Larmor frequency. If the time variable is eliminated in these equations, the electron path in the x-y plane may be described by

$$\frac{dy}{dx} = \mp\sqrt{1 - \left(\frac{1 - e^{\alpha y}}{\alpha R}\right)^2} \Big/ \frac{1 - e^{\alpha y}}{\alpha R}, \tag{7}$$

where

$$R = \frac{1}{\omega}\sqrt{\frac{2eV}{m}}. \tag{8}$$

Eq. (7) indicates that the path will be normal to the x axis wherever it crosses the x axis. Since the slope of the curve is a function of y alone, the magnitude of the slope for the same y must be equal, but the sign may be different. If the curve is continuous, the trajectory is symmetrical about a line parallel to the y axis. The results for various values of αR are shown in Fig. 1.

Trajectories in y-z Plane

After determining the principal trajectories in the x-y plane, it is helpful to examine the focusing action in the y-z plane. Since the magnetic field has no x component, the z component of (1) becomes

$$\frac{d^2z}{dt^2} = \omega\alpha z e^{\alpha y}\left(\frac{dx}{dt}\right). \tag{9}$$

With the aid of (5) and (6), the above equation can be written as

$$\frac{d^2z}{dy^2} + \frac{\left(\frac{1 - e^{\alpha y}}{\alpha}\right)e^{\alpha y}}{R^2 - \left(\frac{1 - e^{\alpha y}}{\alpha}\right)^2}\frac{dz}{dy} + \frac{(1 - e^{\alpha y})e^{\alpha y}}{R^2 - \left(\frac{1 - e^{\alpha y}}{\alpha}\right)^2} z = 0. \tag{10}$$

The initial conditions are that the electrons having the same velocity are now injected from points off the origin, *i.e.*, $x = y = 0$ and $z = z_0$. In Fig. 2 the y-z trajectories are plotted for six values of αR.

* Received by the IRE, December 30, 1960.

[1] E. G. Ramberg, "Electron-optical properties of a flat television picture tube," Proc. IRE, vol. 48, pp. 1952–1960; December, 1960.

[2] W. R. Aiken, "A thin cathode-ray tube," Proc. IRE, vol. 45, pp. 1599–1604; December, 1957.

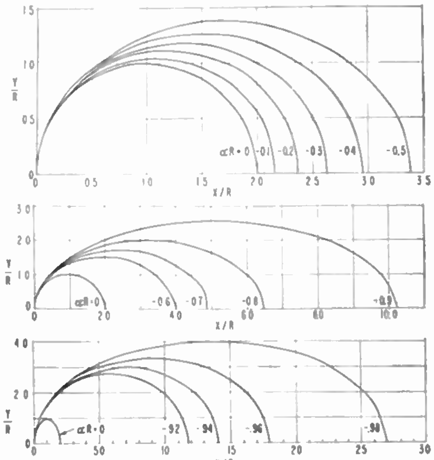

Fig. 1—Trajectories in the x-y plane for different values of αR.

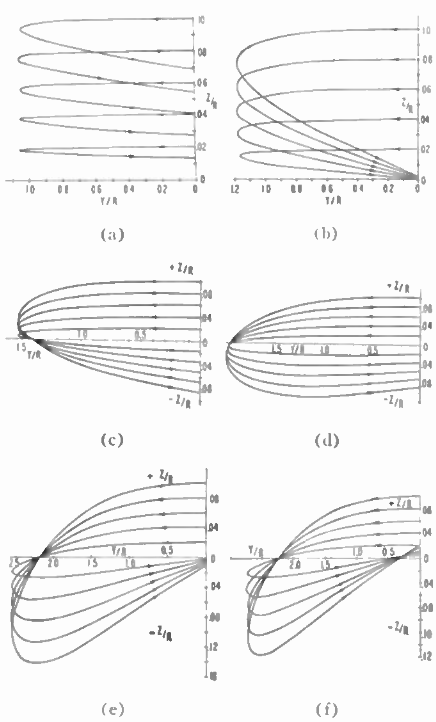

Fig. 2—y-z plot of the electrons entering perpendicular to the x-z plane at five values of z/R ranging from 0.02 to 0.1.

As compared with a uniform magnetic field, the nonuniformity is introduced here to improve the deflection sensitivity and to reduce the width of the electromagnet for a definite scanning size. Since the exit angle of the beam can be made perpendicular to the scanning direction, this scanning method may be useful in a thin picture tube.

ACKNOWLEDGMENT

The writer is indebted to Dr. E. G. Ramberg for many helpful discussions and would like to acknowledge the help of our Computer Laboratory in this work.

T. N. CHIN
RCA Labs.
Princeton, N. J.

On the Fourier Transform Constants*

The problem considered in a recent note [1] on how to divide the $1/2\pi$ between the members of the Fourier transform pair, can be resolved also as follows: absorb this factor into the $d\omega$ as $df=d(\omega/2\pi)$, and consider the cycle frequency f as the basic frequency variable instead of the radian frequency ω. Then the pair becomes symmetrical:

$$G(f) = \int_{-\infty}^{\infty} g(t)e^{-j2\pi ft}dt,$$

$$g(t) = \int_{-\infty}^{\infty} G(f)e^{j2\pi tf}df,$$

and the Parseval relation for the energy spectrum becomes simply

$$\int_{-\infty}^{\infty} |g(t)|^2 dt = \int_{-\infty}^{\infty} |G(f)|^2 df.$$

CHRISTOPHER P. GADSDEN
Dept. of Elec. Engrg.
Tulane Univ.
New Orleans, La.

* Received by the IRE, January 16, 1961.

[1] R. S. Johnson and J. L. Hammond, "On the choice of constants in the Fourier transform pair," PROC. IRE, (Correspondence), vol. 49, pp. 375–376; January, 1961.

A Nearly Optimum Wide-Band Degenerate Parametric Amplifier*

Seidel and Herrmann[1] treated the case of multiple-resonator degenerate parametric amplifiers from the viewpoint of setting frequency derivatives of the gain function equal to zero, and they showed that use of multiple resonators can increase the bandwidth. More recently, Matthaei[2,3] has treated the cases of degenerate and nondegenerate parametric amplifiers, and also the case of up-converters from the viewpoint of filter theory. This work showed that considerable improvement in bandwidth is possible by incorporation of multiple-resonator filter structures in the design of any of these three types of devices. The degenerate amplifier described in this note was constructed to verify experimentally the practicality of part of the design theory described by Matthaei.[2,3]

* Received by the IRE, January 3, 1961; revised manuscript received, January 16, 1961. This research was sponsored by the Wright Air Dev. Div., Wright-Patterson Air Force Base, Ohio, under contract AF 33(616)-5803.

[1] H. Seidel and G. F. Herrmann, "Circuit aspects of parametric amplifiers," 1959 IRE WESCON CONVENTION RECORD, pt. 2, pp. 83–90.

[2] C. W. Barnes, G. L. Matthaei, and R. C. Honey, "Application of New Techniques to Low Noise Reception," Stanford Res. Inst., Menlo Park, Calif., Quart. Progr. Rept. 7, Sec. III-A SRI Project 2550, Contract No. AF 33(616)-5803; March, 1960. See also, Quart. Progr. Rept. 8 for same contract.

[3] G. L. Matthaei, "A study of the optimum design of wide-band parametric amplifiers and up-converters," IRE TRANS. ON MICROWAVE THEORY AND TECHNIQUES, vol. MTT-9, pp. 23–38; January, 1961.

A two-resonator single-diode degenerate parametric amplifier was designed in which the first resonator, including the diode, was a series circuit and the second resonator was a shunt circuit. Fig. 1 shows a drawing of the stripline realization of the circuit using a Hughes 1N896 diode which has a computer-type package. The high-characteristic-impedance wire leads provide the additional series inductance required to bring the diode to series resonance at the 1-kMc midband frequency. The shunt resonator is formed using a small, short-circuited stub to provide the inductance, and a metal block insulated with dielectric material to form the capacitance. The capacitor block was designed so that it would become resonant at the 2-kMc pump frequency and thus provide a short circuit across the input-output line at that frequency. The pump resonator consists of a nominally quarter-wavelength resonator which has loose inductive coupling to the diode resonator and loose capacitive coupling to the pump generator line. DC bias is applied to the diode using an external battery.

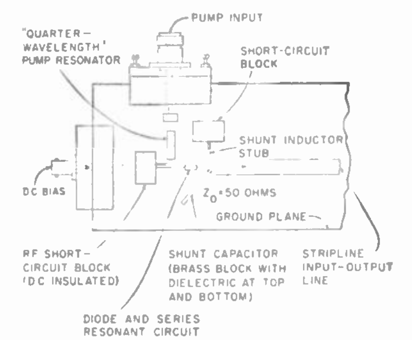

Fig. 1—Construction details of double-resonator degenerate parametric amplifier.

The single-diode degenerate amplifier described herein has a number of features which result in characteristics close to the theoretical optimum. The diode was resonated in series so that the internal inductance merely contributed part of the inductance required for resonance (when the diode was used below self-resonance). In contrast, if the diode had been resonated in shunt, the internal inductance could place a serious limitation on the bandwidth if the self-resonant frequency were at all near the operating frequency. The obtainable bandwidth could also be seriously limited by the multiple resonances which occur in any distributed element used to resonate the diode.[2,3] Therefore, the inductive elements introduced in the circuit were made as nearly lumped as possible so that their self-resonances would be far removed from the operating band of the amplifier. The loose coupling to the pump resonator was used to preclude any appreciable bandwidth narrowing as a result of the resonance introduced by the pump circuit. By making the distance from the RF short-circuit block (see Fig. 1) to the diode somewhat less than one-quarter wavelength at the 3-kMc upper-sideband frequency, the diode was made to see a large reactance at that frequency, and also at the 4-kMc second harmonic of the pump. In this manner, dissipation of power at these frequencies was prevented, and associated effects on the response and noise figure were reduced.

A negative-resistance amplifier such as this requires a circulator for best performance.[4] Since no circulators with adequate bandwidth appear to be available, separate input and output ports were obtained with a broad-band, low-VSWR, 3-db directional coupler. This was fabricated using an interleaving, printed-circuit construction developed at SRI. By use of this coupler, it was possible to make frequency response and noise-figure measurements from which the performance of the device as operated with an ideal circulator could be derived.

Fig. 2 shows the measured and computed theoretical response of the amplifier, with and without the shunt resonator. Since the amplifier is degenerate, the gain includes both signal and idler output. The agreement between the computed and the measured results gives very encouraging verification of the previously developed theory.[2,3] Note that the computed 3-db bandwidth of the single-resonator design is 81 Mc, while the measured bandwidth is practically the same. The 3-db bandwidth of the computed double resonator response is about 220 Mc, while the corresponding measured bandwidth is about 210 Mc (*i.e.*, 21 per cent bandwidth).

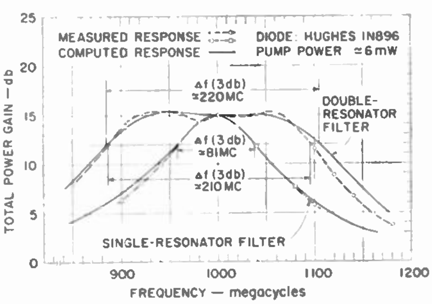

Fig. 2—Frequency response of the single- and the double-resonator parametric amplifier.

The noise figure measurements were made using a pulsed, coaxial noise source, a superheterodyne receiver, and an automatic noise figure meter. Using various precautions to make the measurements as reliable as possible, it was possible to make noise figure measurements at only the center frequency. The measured values ranged closely about 1.0 db (double-sideband). This is in acceptable agreement with the theoretical value of 0.5 db since the estimated possible error is in excess of 0.5 db when equipment accuracy and experimental errors are taken into account.

M. Gilden
G. L. Matthaei
Stanford Res. Inst.
Menlo Park, Calif.

[4] Of course, use of two identical amplifiers as a balanced pair along with a 3-db coupler can give equivalent performance. See S. H. Autler, "Proposal for a maser-amplifier system without nonreciprocal elements," Proc. IRE, (Correspondence), vol. 46, pp. 1880–1881; November, 1958.

Measurement of the Number of Impurities in the Base Layer of a Transistor*

The number of impurity atoms per unit area in the base region of a transistor is an important design parameter.[1] In diffused-base transistors, the impurity distribution in the base is frequently calculated from measurements on the diffusion depth and the sheet resistivity of the diffused layer. If one then also knows the depth to which the emitter is diffused or alloyed, one can calculate the number of impurity atoms per unit area between emitter and collector.

We wish to point out that the latter quantity can be measured directly and very easily. The method consists of measuring the collector current as a function of emitter-to-base voltage. Diodes usually show deviations from the simple exponential law[2]

$$I = I_0 \exp\left(\frac{qV}{kT} - 1\right) \tag{1}$$

because of space charge generation and recombination,[3] conductivity modulation,[4] series resistance or other processes; however, in transistors having reasonable current gain, an exponential law of the form

$$I_c = I_1 \exp\frac{qV_e}{kT} + I_2 \tag{2}$$

is very closely obeyed at currents low enough so that the voltage drop of base current flowing through the base resistance is negligible. In the above equation, I_c is the collector current, I_2 a saturation current, q the electronic charge, and kT the Boltzmann energy. If the base width is small compared to the diffusion length, *i.e.*, if recombination in the base is negligible, as is usually the case for high frequency transistors, I_1 is given by[1]

$$I_1 = \frac{qADn_i^2}{\int N(x)dx} = \frac{qADn_i^2}{N_B}. \tag{3}$$

Here A is the emitter area (or collector area if it should be smaller), D the diffusion constant of the minority carriers in the base, n_i the intrinsic carrier concentration, $N(x)$ the base inpurity concentration at a distance x from the emitter junction. The integral extends from the emitter junction to the collector junction and represents the number of impurities per unit area in the base, N_B, that we wish to find. Eq. (3) was derived for a diffusion constant D that does not vary over the base width, wheras D actually depends to some extent on the impurity concentration. Eq. (3) still applies if we interpret D as a properly averaged value.

The constant I_1 can be obtained with good accuracy by subtracting the saturation current I_2 from the measured collector current and plotting the difference in a semilog plot vs the emitter-to-base voltage. This plot results in a straight line whose intercept is I_1.

Eq. (3) can now be solved for N_B and yields:

$$N_B = \frac{q}{I_1} ADn_i^2. \tag{4}$$

If the junction area is measured microscopically, then all quantities on the right side of (4) are known. The greatest uncertainty is due to D, whose value at high impurity concentration is not known accurately. Subject to that uncertainty, this method should provide accurate measurements of N_B.

H. K. Gummel
Bell Telephone Labs., Inc.,
Murray Hill, N. J.

* Received by the IRE, January 12, 1961.

[1] J. L. Moll and I. M. Ross, "The dependence of transistor parameters on the distribution of base layer resistivity," Proc. IRE, vol. 44, pp. 72–78; January, 1956.

[2] W. Shockley, "The theory of *p-n* junctions in semiconductors and *p-n* junction transistors," *Bell Sys. Tech. J.*, vol. 28, pp. 435–489; July, 1949.

[3] C. T. Sah, R. N. Noyce, and W. Shockley, "Carrier generation and recombination in *p-n* junctions and *p-n* junction characteristics," Proc. IRE, vol. 45, pp. 1228–1243; September, 1957.

[4] R. N. Hall, "Power rectifiers and transistors," Proc. IRE, vol. 40, pp. 1512–1518; November, 1952.

Elimination of Crossover Distortion in Class-B Transistor Amplifiers*

Crossover distortion in a Class-B complementary-symmetry emitter-follower power amplifier can be virtually eliminated by use of a very-high-impedance source to drive the output stage. A practical method of doing this is shown in Fig. 1. To obtain the high source impedance, the output stage is driven from the junction of the collectors of Q2 and Q3. At each zero crossing of the signal, the voltage at the bases of Q4 and Q5 jumps from the turn-off bias of one transistor to the turn-on bias of the other. This voltage is maintained at the proper dc level by feedback to the input transistor Q1. Although the base voltage jumps as described above, the current waveforms are not distorted. The resistance-voltage divider R1 and R2 in the feedback network is chosen to give the desired ac voltage gain from input to output. The capacitor C1 is included so that full voltage feedback is effective at dc. Two positive and two negative power supplies are used. The higher-voltage supplies permit biasing Q2 and Q3 so that the output-transistor bases can be driven right up to the lower supply voltage, for maximum power output and maximum efficiency. With the circuit arrangement shown, it is unnecessary to remove ripple completely from the power supplies.

This circuit affords good protection against thermal runaway. The bases and emitters of the output transistors are tied together; thus, when one is biased on, the other is biased off by the same voltage. This virtually precludes a runaway current through the two output transistors. The "off" bias is supplied from a relatively low-impedance source (the "on" base-emitter junction of the other transistor). This fact effectively reduces the turn-off time of the power transistors, and prevents a large increase in power consumption and dissipation at high audio frequencies.

* Received by the IRE, August 1, 1960.

The average current through Q2 and Q3 must be at least as great as the peak base drive current required by the output transistors. To limit the dissipation in Q2 and Q3 (which must operate Class A), one can add driver transistors that operate Class B, as shown in Fig. 2. The average current in Q2 and Q3 can then be reduced in proportion to the current gain of the drivers, Q6 and Q7. This extensive feedback loop can be stabilized by the use of high-frequency transistors for Q1 and Q3, and by the addition of a phase-correcting capacitor C2 to the feedback divider. High-frequency instability caused by parasitic inductance in series with the load can be eliminated by addition of a series RC combination in parallel with the load.

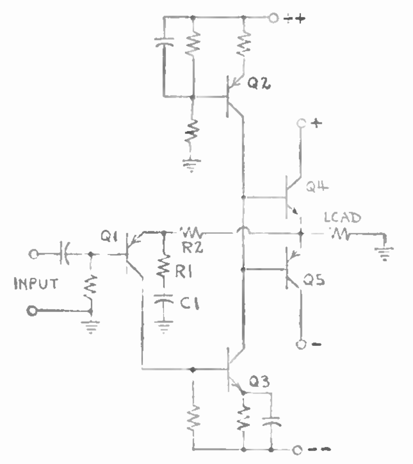

Fig. 1.

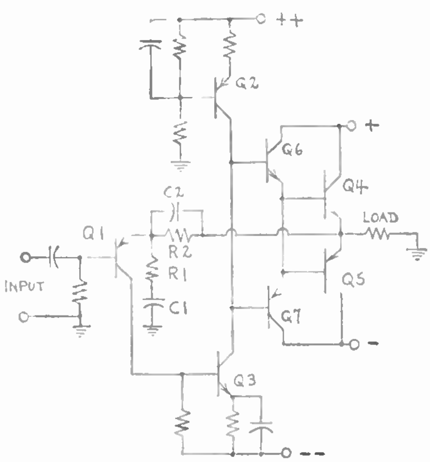

Fig. 2.

Twenty-five-volt transistors can be used with an 8-ohm load to produce a sine-wave output up to about 9 watts. Higher power would subject all transistors except Q1 to peaks greater than 25 volts. A lower load impedance would, of course, permit greater power output with transistors of the same voltage rating. However, if an output transformer is used, the dc resistance of the primary might be much less than the nominal load impedance. Here a capacitor should be added in series with the transformer primary to prevent high currents from flowing, in the event of dc unbalance at the output. This circuit is therefore best suited for direct connection to substantially resistive loads, such as loudspeaker voice coils. For higher power outputs with 25-volt transistors, the voice coil impedance must be lower than the conventional 8 ohms.

The highly satisfactory results obtained with circuits of this type lead us to hope that economically-priced power transistors of both polarities will soon be available.

JAMES J. FARAN, JR.
General Radio Co.
West Concord, Mass.

A Broad-Band Tunnel-Diode Amplifier*

A first-order theory of operation for an amplifier using tunnel diodes as active elements will be presented. The series resistance and inductance of the tunnel diodes will be neglected, except for stability consideration. The amplifier exhibits significant gain over a broad bandwidth.

Consider a lossless transmission line of characteristic resistance R_{01} terminated in a negative resistance $-R_n$ and a load resistance R_{02} as shown in Fig. 1. The line is matched if

$$R_{02} = \frac{R_{01}R_n}{R_{01} + R_n}.$$

and hence, R_{02} is less than R_{01}. Considering the capacity C_n associated with the negative resistance, the load can still be matched to the generator if a lossless, lumped transmission line is used as shown in Fig. 2. The line-terminating capacity $C/2$ is furnished by the tunnel-diode capacity C_n. The cutoff frequency of the line f_c, and the capacity C_n determine the characteristic resistance R_{01} thus:

$$R_{01} = \sqrt{\frac{L}{C}},\ f_c = \frac{1}{\pi\sqrt{LC}} \quad \therefore\ R_{01} = \frac{1}{\pi f_c C}.$$

Here L and C are the inductance and capacitance of the lumped line (see Fig. 2).

The load resistance R_{02} can be furnished by a second stage similar to the one just described, and in a similar manner a number of subsequent stages can be added. The last stage is then terminated in a load resistance R_L. The capacity associated with the negative resistance now supplies all or part of the capacity at the junction of any two lumped lines.

An N stage amplifier of the type described is shown in Fig. 3. Assuming that all negative resistances are similar, the Nth stage is terminated in its characteristic resistance if

$$\frac{1}{R_L} = \frac{1}{R_{01}} + \frac{N}{R_n}.$$

Since the lines are matched within the pass band, the voltage gain of the amplifier is 1. A power gain is, however, realized due to reduction in resistance level and is given by

$$G = \frac{R_{01}}{R_L} = 1 + \frac{NR_{01}}{R_n}.$$

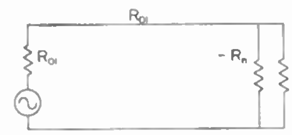

Fig. 1.

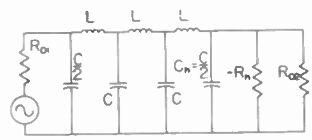

Fig. 2.

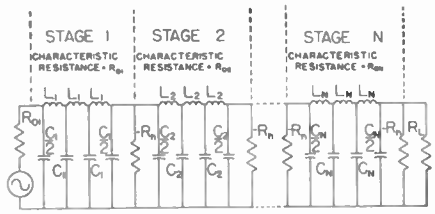

Fig. 3—$f_c = \frac{1}{\pi\sqrt{L_1C_1}} = \frac{1}{\pi\sqrt{L_2C_2}} \cdots = \frac{1}{\pi\sqrt{L_NC_N}}$

A rigorous mathematical treatment of stability will not be given; the following argument should, however, suffice. Within the pass band, the amplifier should be stable since the lines are purely resistive. Outside the pass band, the lines are purely reactive and the possibility of oscillation exists. Now a tunnel diode cannot oscillate above its resistive cutoff frequency f_{r0}; hence, if $f_c \gtrsim f_{r0}$, the amplifier should be stable outside the pass band as well. If practical considerations dictate that $f_c < f_{r0}$, then oscillations will occur. A small resistance inserted in series with the tunnel diode would be one method of preventing these oscillations, as this in effect limits the cutoff frequency of the tunnel diode.

In practice, the amplifier would be constructed using strip or coaxial line techniques. More sophisticated types of lumped lines (filters) could be used to provide a better match in the pass band. It should be pointed out that it may be possible to utilize the tunnel-diode series inductance to advantage in this respect.

N. F. MOODY
A. G. WACKER
Dept. of Elec. Engrg.
Univ. of Saskatchewan
Saskatoon, Sask., Can.

* Received by the IRE, February 2, 1961.

Self-Setting Cross-Correlator*

A method of automatically tapping a balanced delay line to provide cross-correlation of one function of time with another has been proposed by Golay.[1] With this method, the tapping function is first inserted as a signal in the delay-line input, and when the first portion of the signal reaches the end of the delay line, a special signal causes each or every other delay-line section to be tapped in accordance with the sign of the tapping function. This self-setting cross-correlator has been operated experimentally, and this note is a report on the circuits and of the results obtained.

The test system, as shown in Fig. 1, is driven by timing pulses originating in the frequency standard. These pulses occur at a rate of four megabits per second. The code derived from the shift register utilized for this test is 15 bits long; therefore, it has a 3.75-μsec duration.

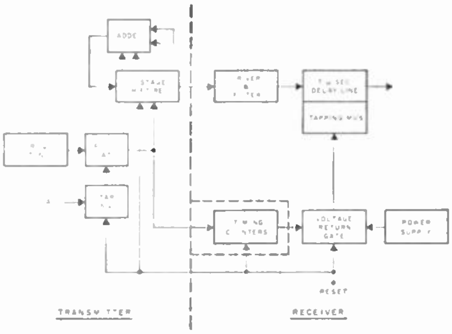

Fig. 1—Self-setting cross-correlator block diagram.

A pulse applied to the start multivibrator allows the pulse gate to open. The 4-Mc pulses are passed to the shift register and the timing counters. As the shift register generates the code, the timing counters establish the frame reference for that particular code. The instant the code is fully present in the delay line, the timing counters open the voltage return gate and power is applied to the tapping multivibrators. The tapping multivibrators assume the condition dictated by the code in the line and retain this setting. From this time on, a correlation peak will occur in the tapping buss whenever the same code is again fully present in the delay line. The application of a reset pulse destroys the memory of the tapping multivibrators by collapsing their voltages. This enables the self-setting procedure to be repeated on a new code.

The tapping multivibrator (Fig. 2) is set to a definite condition as dictated by the voltages sensed through the diodes $D1$ and $D11$, which are connected to the two tap points of alternate sections of the balanced delay line. At any given instant, diodes $D1$ and $D11$ will sense voltages of opposite polarity. Initially, voltages $V1$ and $V2$ are zero. At the precise instant that the tapping function occupies exactly the full length of the delay line, the voltages are applied to the tapping multivibrators (see Fig. 3 for waveforms). Depending on the polarity of the instantaneous voltage on the particular section tapped, $D1$ or $D11$ will conduct for a very short time. The instantaneous current drawn at a base of one of the two transistors of the bistable multivibrator will determine its state. As the voltages $V1$ and $V2$ increase to their normal values, diodes $D1$ and $D11$ become negatively biased. The tapping multivibrators will remain in the condition assumed until the voltages $V1$ and $V2$ are collapsed and the procedure is repeated.

Diodes $D2$ and $D22$ are used as the tapping capacitors. Both diodes are negatively biased at all times by the voltage $V3$. However, one diode of a given pair will be more negatively biased than the other, as determined by the voltage appearing at the collectors of the multivibrator. The least negatively biased diode exhibits the largest capacity and will become the effective tapping capacitor.

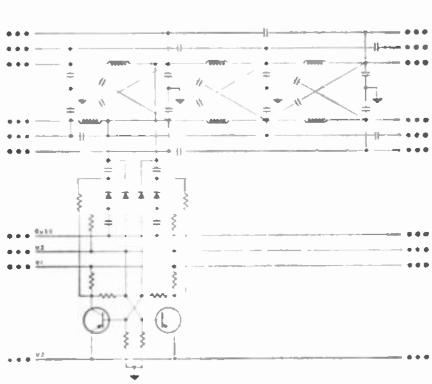

Fig. 2—Tapping multivibrator schematic diagram.

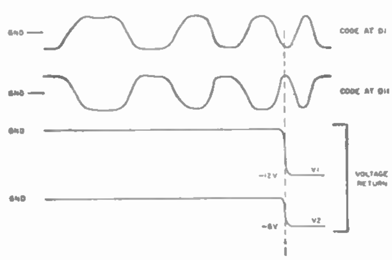

Fig. 3—Voltage return timing diagram.

(a)

(b)

(c)

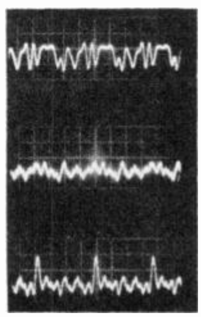

Fig. 4—(a) Oscillogram 1. Scale: vertical, 1 v/cm; horizontal, 1 μsec/cm. (b) Oscillogram 2. Scale: vertical, 100 mv/cm; horizontal, 1 μsec/cm. (c) Oscillogram 3. Scale: vertical, 100 mv/cm; horizontal, 1 μsec cm.

A 3.75-μsec code recorded from the last tap point of the delay line is shown in oscillogram 1 of Fig. 4. When this code traverses the delay line with the tapping multivibrators set up at random, a noncorrelated signal appears at the tapping buss (oscillogram 2). After the tapping multivibrators are set accoring to the code in the delay line, a correlation peak appears at the tapping buss (oscillogram 3).

J. A. Jurenko, Jr.
F. L. Burson
Philco Corp.
Philadelphia, Pa.

* Received by the IRE, January 11, 1961.

[1] M. J. E. Golay, "Self-setting cross-correlators," Proc. IRE (Correspondence), vol. 48, pp. 2037–2038; December, 1960.

A Technique for the Development of Permanent Visual Images on Magnetic Tape*

It has been found that visual images of magnetization patterns can be permanently fixed on magnetic tape if a suitable additive is combined with the carbonyl iron suspension typically used in producing such images. The well-known technique[1] remains unchanged, but greater care is required if best results are to be obtained as there is no chance to rework a messy job. On the other hand, "underdeveloped" images have been intensified by running the tape through the bath a second time.

Both carbon tetrachloride (CCl_4) and chloroform ($CHCl_3$) have been used as the additive, but it is likely that other strong clorinated solvents may also be used. It is theorized that the highly diluted solvents soften the oxide layer as the tape is immersed, allowing the carbonyl iron particles to become permanently imbedded. Upon evaporation, the layer appears to reassume its original physical characteristics. After extended use the suspension becomes discolored, indicating that part of the resinous binders is leached from the tape.

The concentration of solvent depends on the type of tape employed. Our experience has been principally with Reeves Type A Instrumentation Tape for which the following solution has been found satisfactory; $CHCl_3$—5 cc, Vehicle[2]—95 cc, and carbonyl iron—5 gms.

Unbroken lengths of tape in excess of 100 feet have been continuously developed by drawing through an agitated solution at about one inch per second. Uniform drawing and rapid dry-off appear to be the secrets for run- and streak-free images. Digital pulse separations of 0.005 inch have been consistently resolved.

Howard R. Padgitt
Cook Research Laboratory
Morton Grove, Ill.

* Received by the IRE, January 19, 1961. The work reported here was supported under Contract AF 30(602)-1913, USAF, RADC.

[1] "Visible Tracks on Magnetic Tape" Minnesota Mining & Mfg. Co., St. Paul, Minn., *Sound Talk* (Bulletin No. 5).

[2] This may be Freon-MF or Freon-TF.

Effect of Fluctuations in Density on the Esaki Effect*

The author once proposed[1] that statistical fluctuations in density of donors and acceptors might be sufficient to affect the characteristic curve of an Esaki diode. Since the tunneling probability is a very strong function of the doping density, the relatively small fluctuations in local density might give rise to large spatial fluctuations in tunnel current, and perhaps even a change in the form of the characteristic over that which would be predicted on the basis of a model using a uniformly distributed charge. It is the purpose of this communication to investigate this concept quantitatively and evaluate its relevance to our knowledge of the Esaki effect.

To approximate the diode, it will be considered to be composed of a great many cells. Each cell has a depletion region with an average of n_0 donors and n_0 acceptors. There will be a fluctuation in this number which, if there are no correlation effects, would be given by the Poisson distribution

$$P(n) = \frac{e^{-n_0}}{n!}(n_0)^n. \tag{1}$$

For mathematical convenience, this will be replaced by the Gauss distribution which it approaches for sufficiently large n_0.

$$P(n) \approx \frac{1}{2\pi\sqrt{n_0}} e^{-(n-n_0)^2/2n_0}. \tag{2}$$

It is now necessary to estimate the cell size, and thus, n_0, which is limited by the more significant of two factors, 1) the extent of influence of a charge distribution on the potential, and 2) the uncertainty in transverse position due to a well-defined transverse momentum. The latter leads to

$$n_0 \approx (\Delta x)^2 d_n N_d, \tag{3}$$

where d_n is the width of the n-type portion of the depletion layer, N_d is the donor density, and Δx is approximated by $\pi\hbar/(\overline{p^2})^{1/2}$. Using the relationships for indirect tunneling as given by Kane,[2] this value of n_0 can be expressed as

$$n_0 = \frac{\pi}{2}\left[\frac{E_g}{2E_0}\frac{\epsilon_r^2(m_{rx}/m_e)}{(m_{rt}/m_e)^2}\right]^{1/2}, \tag{4}$$

where

$$E_0 = \frac{m_e e^4}{32\pi^2\epsilon_0^2\hbar^2}$$

is 13.58 ev, the energy of the lowest level in a hydrogen atom; m_{rx} is the reduced longitudinal mass; m_{rt} is the reduced transverse mass; ϵ_r is the relative dielectric constant; and E_g is the energy gap.

In case the transverse position can be very accurately defined, it is still reasonable to restrict n_0 to not less than

$$n_0 \approx d^2 d_n N_d, \tag{5}$$

where d is the total depletion layer thickness. Again using Kane's result, plus the approximate form for the depletion layer thickness, one obtains

$$n_0 = \left(\frac{2\epsilon V}{e}\right)^{3/2}\left(\frac{N_a + N_d}{N_a N_d}\right)^{1/2}, \tag{6}$$

where V is the sum of built-in and applied voltages. The value given by (4) is generally larger and is tabulated in Table I for common tunnel diode materials. Also given is the value of

$$N_{re} = \frac{N_a N_d}{N_a + N_d}.$$

at which (6) equals (4).

TABLE I

Material	m_{rt}/m_e	m_{rx}/m_e	E_g	ϵ_r	N_{re}(cm^{-3})	n_0
Ge	0.0286	0.043	0.66	15.8	1.9×10^{18}	28
Si	0.099	0.099	1.12	11.5	8.9×10^{18}	12
InSb	0.012	(0.012)	0.16	15.8	1.7×10^{16}	18
GaAs	0.043	(0.043)	1.35	11.1	1.25×10^{19}	19

To calculate the effect of fluctuations on the tunneling current, we assume a form which is correct to the first order for the current as governed by an exponential tunneling probability

$$I(n) = Be^{-\alpha\sqrt{n}}, \tag{7}$$

n being a statistical variable related to $N_a N_d/(N_a+N_d)$.

For mathematical simplicity, it is assumed that one of the N's is much greater than the other, and the tunneling probability is dictated by this density only. The parameter α is given by

$$\alpha = \frac{8E_g}{3\hbar e}\left[\frac{E_g \epsilon n_0 (N_a + N_d) m_{rx}}{eV N_a N_d}\right]^{1/2}. \tag{8}$$

The total device current can now be written, using (2) and (7), as

$$\begin{aligned} I &= \int_0^\infty P(n) I(n) dn \\ &= \frac{B_1}{\sqrt{2\pi n_0}}\int_0^\infty \exp\left[-\frac{(n-n_0)^2}{2n_0} - \frac{\alpha}{n^{1/2}}\right] dn. \end{aligned} \tag{9}$$

Since the Gaussian portion of this expression dominates except near $n = n_0$, and we have assumed n_0 fairly large, the term $\alpha/n^{1/2}$ will be expanded about n_0 as follows:

$$\frac{\alpha}{n^{1/2}} \approx \frac{\alpha}{n_0^{1/2}}\left(1 - \frac{1}{2}\frac{(n-n_0)}{n_0}\right). \tag{10}$$

Eq. (9) can then be integrated.

$$I = B_1 e^{-\alpha/\sqrt{n_0}+\alpha^2/8n_0^2}. \tag{11}$$

Since $B_1 e^{-\alpha/\sqrt{n_0}}$ is the current which would be predicted by a model using uniform charge density, the effect of the statistical fluctuations is to multiply the total device current by $e^{\alpha^2/8n_0^2}$. $\alpha^2/8n_0^2$ is given by (6) and (8), and can be written numerically as

$$\frac{\alpha^2}{8n_0^2} = 1.5\times10^{21}\frac{E_g}{eV}\left(\frac{E_g}{e}\right)^{3/2} \cdot \left(\frac{m_{rt}}{m_e}\right)\left(\frac{m_{rx}}{m_e}\right)^{1/2}\frac{N_a + N_d}{N_a N_d}. \tag{12}$$

In this last expression, the N's are in cm^{-3} to conform with the current literature.

Table II gives values resulting from (12)

TABLE II

Material	m_{rt}/m_c	m_{rx}/m_t	E_g/e	$\frac{\alpha^2}{8n_0^2}\frac{N_a N_d}{N_a+N_d}$
Ge	0.0286	0.043	0.66	6.85×10^{18}
Si	0.099	0.099	1.12	7.7×10^{19}
InSb	0.013	0.013	0.16	1.75×10^{17}
GaAs	0.043	0.043	1.35	3.0×10^{19}

for the four common materials. The numbers in the right-hand column can be interpreted approximately as the densities of the less dense dopant which would give an e-fold increase in current over that predicted by the uniform theory. Note that these densities are generally lower than those normally used in Esaki junctions, so one might state as a general rule that the effect of statistical variations on the tunneling current will be less than e-fold.

These calculations were concerned with changes in the tunneling probability only and did not consider the changes in Fermi level due to statistical fluctuations. Neither did they take account of the possibility of "clumping," in which impurities might have an affinity for each other or the opposite repulsive effect. The latter might well be related to the excess current problem, and the effect on the Fermi level might also have some effect on excess current.

Shockley[3] has considered a model similar to the one used here and has suggested that local changes in the Fermi level would contribute to the excess current. However, if the density fluctuations in the depletion layer are uncorrelated with those adjacent, the effect will be small. Since his presentation, Chynoweth and his co-workers[4] have presented a very convincing case for deep states as the excess current mechanism. It appears that fluctuations do not influence it appreciably.

The author wishes to thank E. O. Kane for his cooperation in providing a preprint of his work, and H. S. Sommers for his suggestion regarding the effect of transverse momentum.

D. G. Dow
Dept. of Elec. Engrg.
California Inst. Tech.
Pasadena, Calif.

* Received by the IRE, January 25, 1961. The work reported here was supported by the Office of Naval Research.

[1] D. G. Dow, "The Effect of Fluctuations in Density on the Esaki Effect," presented at the IRE-AIEE Solid State Device Res. Conf., Pittsburgh, Pa.; June 14, 1960.

[2] E. O. Kane, "Theory of tunneling," *J. Appl. Phys.*, vol. 32, pp. 83–91; January, 1961.

[3] W. Shockley, "Statistical fluctuations of donors and acceptors in p-n junctions," *Bull. Am. Phys. Soc.*, vol. 5, ser. II, p. 161; March 21, 1960.

[4] A. G. Chynoweth, W. L. Feldmann, and R. A. Logan, "Excess tunnel current in silicon Esaki junctions," to be published.

Contributors

Richard B. Adler (A'44–SM'53–F'60) was born in New York, N. Y., on May 9, 1922. He received the B.S. and Sc.D. degrees in electrical engineering from the Massachusetts Institute of Technology, Cambridge, in 1943 and 1949, respectively.

R. B. Adler

From 1944 to 1946, he served in the United States Naval Reserve as an instructor at the M.I.T. Radar School. After his discharge, he became a part-time staff member at the Research Laboratory of Electronics, M.I.T., both in a teaching and a research capacity. His major interests have been in circuit theory, electromagnetic theory, and semiconductor electronics. From 1951 to 1953, he was group leader of the M.I.T. Lincoln Laboratory Solid State and Transistor Group. He subsequently continued in the same field at the M.I.T. Research Laboratory of Electronics and also at the Energy Conversion Group of the M.I.T. Electronic Systems Laboratory. At present, he is professor of electrical engineering at M.I.T.

Dr. Adler is a member of Sigma Xi and Eta Kappa Nu.

❖

James B. Angell (S'45–A'47–M'55–SM'57) was born in Staten Island, New York, N. Y., on December 25, 1924. He received the S.B. and S.M. degrees of the cooperative course in electrical engineering in 1946, and the Sc.D. degree in electrical engineering in 1952, all at the Massachusetts Institute of Technology, Cambridge.

J. B. Angell

From 1946 to 1951, he worked at the Research Laboratory of Electronics at M.I.T., studying noise in tracking radars. From 1951 to 1960, he was with the Research Division of Philco Corporation, Philadelphia, Pa., where he led a group studying the basic circuit application and evaluation of transistors and other solid-state devices, particularly for computers and high-frequency functions. He became associate professor of electrical engineering at Stanford University, Stanford, Calif., in September, 1960.

Dr. Angell is organizer and present chairman of the IRE Subcommittee on Masers and Variable Reactance Transducers, and a member of Tau Beta Pi, Eta Kappa Nu, Sigma Xi, AIEE, and the Franklin Institute.

❖

Max E. Bair (S'58–M'61) was born in Morenci, Mich., on March 12, 1932. He received the B.S.E.E. degree from the University of Michigan, Ann Arbor, in 1960.

M. E. Bair

From 1951 to 1955 he served with the U. S. Air Force as an electronics and radar instructor. In 1955 he was employed by the RCA Service Company as a contract instructor. He joined Willow Run Laboratories at the University of Michigan, as an electronics technician in 1956. He is currently an assistant in research with the Solid State Physics Group at Willow Run, and is actively engaged in the basic and applied research of maser devices.

❖

Jerald J. Cook was born in West Frankfort, Ill., on August 9, 1933. He received the B.S. degree in physics from Western Michigan University, Kalamazoo, in 1956, and the B.S.E.E. degree from the University of Michigan, Ann Arbor, in 1957.

J. J. Cook

From 1957 to 1958 he was a research assistant with the Upjohn Company, Kalamazoo, working in instrumentation. In 1958 he returned to the University of Michigan to pursue a graduate curriculum in engineering mechanics, working in the fields of solid state physics and radio astronomy at Willow Run Laboratories. He is presently a research associate at Willow Run, and a member of the teaching staff of the Department of Engineering Mechanics at the University of Michigan.

Mr. Cook is a member of Tau Beta Pi, Eta Kappa Nu, and Sigma Xi.

❖

J. S. Cook (S'52–A'53) was born in Flint, Mich., on May 30, 1927. He received the B.E.E. and M.S. degrees from The Ohio State University, Columbus, in 1952.

From 1950 to 1952, he was associated with The Ohio State University Research Foundation. Between 1952 and 1959, he was engaged in microwave tube research with Bell Telephone Laboratories, Murray Hill, N. J. In 1960 he moved to the Military Electronics Research Department at the Whippany branch of the Laboratories.

J. S. Cook

Mr. Cook is a member of Eta Kappa Nu and Tau Beta Pi.

❖

Lloyd G. Cross was born in Flint, Mich., on October 7, 1934. He received the B.S. degree in physics in 1957 and the M.S. degree in 1960, both from the University of Michigan, Ann Arbor where he is currently working toward the Ph.D. degree in physics.

L. G. Cross

From 1956 to 1958 he was an assistant in research at Willow Run Laboratories, the University of Michigan, working in the field of infrared physics. In 1958 he transferred to the Solid State Physics Group of the same laboratory, and began work on masers. He is presently a research associate at Willow Run Laboratories.

❖

James M. Early (A'48–SM'54–F'59) was born in Syracuse, N. Y., on July 25, 1922. He received the B.Sc. degree cum laude in forestry from the New York State College of Forestry, Syracuse, in 1943. After two and a half years of military service, he attended The Ohio State University, where he received the M.Sc. degree in 1948, and the Ph.D. degree in 1951, both in electrical engineering.

J. M. Early

He joined the Bell Telephone Laboratories, Inc., Murray Hill, N. J., in 1951, where he has worked on junction transistor analysis and experiment, transistor design, and the development of high-frequency germanium transistors. He is currently in charge of a subdepartment responsible for development of very-high-frequency transistors.

Dr. Early is a Fellow of the AAAS and a member of the American Physical Society, Sigma Xi, and Eta Kappa Nu.

❖

L. A. FINZI

Leo A. Finzi was born in Padova, Italy, on December 16, 1904. He received the M. El. Eng. degree from the University of Naples, Italy, in 1921, and the "Doktor-Ingenieur" degree, summa cum laude, from the Institute of Technology, Aachen, Germany, in 1932.

He has done research and development work with the Hochspannungs Ges. m.b.H. of Cologne, Germany, erection and operation of power stations and transmission systems for the Volturno Power Company of Naples, Italy, and teaching at the Electrical Institute of the University of Naples. From 1939, he was Senior Laboratory Engineer in charge of the Impulse Laboratory of Westinghouse Electric Company, Pittsburgh, Pa. In 1946, he joined the faculty of the Carnegie Institute of Technology, Pittsburgh, Pa., where he is presently Buhl Professor of Electrical Engineering. He is the author of numerous papers in European and American Journals, his main field of interest in recent years being that of nonlinear magnetic devices.

Dr. Finzi is a Fellow of the AIEE and a member of EKN, Sigma Xi and the ASEE.

❖

W. W. GÄRTNER

Wolfgang W. Gärtner (M'54–SM'60) was born in Vienna, Austria, on July 5, 1929. He received the Ph.D. degree in physics from the University of Vienna in 1951, and the Dipl.Ing. degree from the Technische Hochschule, Vienna, in 1955.

He was engaged in electron tube and semiconductor research with Siemens and Halske A.G., Vienna, and Munich, Germany. He became associated with the U. S. Army Signal Research and Development Laboratory, Fort Monmouth, N. J., in 1953, where in 1959 he advanced to the position of Chief Scientist, Solid State Devices Division. In 1960, he joined CBS Laboratories, Stanford, Conn., as Manager of the Electronic Semiconductor Department.

Dr. Gärtner is the author of papers on semiconductor properties, transistor design, circuit theory, and ultrasonics. His book, "Transistors: Principles, Design, and Applications," was published in 1960. He is a member of the American Physical Society, the Division of Solid State Physics in the American Physical Society, and the Armed Forces Communication and Electronics Association.

❖

R. U. F. HOPKINS

Robert U. F. Hopkins (S'40–A'43–M'50) was born in Long Beach, Calif., on June 18, 1918. He received the B.S.E.E. degree from the University of California, Berkeley, in 1941.

He joined the U. S. Navy Electronics Laboratory, San Diego, Calif., in 1941 (then the U. S. Navy Radio and Sound Laboratory), where he was engaged in studies of anomalous radar propagation effects. During the war years his work was concerned with experimental studies of tropospheric ducting and technical radar assistance to the fleet. He participated in the 1946–1947 Byrd Antarctic expedition conducting radar propagation and meteorological measurements. During the early 1950's he was engaged in numerous microwave communication site surveys in the U. S. and abroad for naval activities. Since 1955 he has been the head of the Tropospheric Propagation Section at the U. S. Navy Electronics Laboratory which has been engaged in theoretical and experimental studies of tropospheric scatter propagation. Recently he has been involved in experiments concerning UHF propagation by ducting between the U. S. west coast and Hawaii. At present he is primarily interested in the construction of a 60-foot X-band radio telescope.

❖

A. LAVI

Abrahim Lavi (M'57) was born in Khorramshahr, Iran, on January 12, 1934. He attended Robert College, Istanbul, Turkey, from 1953–1955, later transferring to Purdue University, Lafayette, Ind., where he received the B.S.E.E. degree with Highest Distinction in 1957. He then entered Carnegie Institute of Technology, Pittsburgh, Pa., where he obtained the M.S. and Ph.D. degrees in 1958 and 1960, respectively.

He held summer employment at Whirlpool-Seeger Research and Development Laboratory at St. Joseph, Michigan; Westinghouse Electric Corp., Pittsburgh, Pa.; and RCA Research Laboratories, Princeton, N. J. His work involved switching circuits, magnetic amplifiers, parametric and other nonlinear devices, as well as the study of hysteresis properties in ferromagnetic materials. Since 1959, he is an assistant professor of electrical engineering at Carnegie Institute of Technology.

Dr. Lavi is an Associate Member of the AIEE, and a member of Sigma Xi.

❖

D. E. NELSON

Donald E. Nelson (S'41–A'41–M'49) was born in Taylorville, Ill., on February 1, 1919. He received the B.S.E.E. and M.S. degrees from the University of Illinois, Urbana, in 1941 and 1948, respectively.

From 1941 to 1945 he worked as a development engineer at Westinghouse Electric Corporation, Bloomfield, N. J., where he worked on pulsed magnetrons. From 1945 to 1949 he was Research Assistant and Research Associate at the University of Illinois Tube Laboratory working on CW magnetrons and millimeter-wave devices. Since 1949 he has been with the RCA Tube Division in Harrision and Princeton, N. J. From 1949 to 1959 he was concerned with magnetron development. Since 1959 he has worked on development of oscillators and amplifiers employing tunnel diodes.

Mr. Nelson is a member of Eta Kappa Nu and Tau Beta Pi.

❖

N. R. ORTWEIN

N. R. Ortwein was born in Longview, Wash., on February 14, 1934. He received the B.S. degree in physics from the University of Washington, Seattle, in 1956.

Since 1956 he has been with the U. S. Navy Electronics Laboratory, San Diego, Calif., where he has been concerned with the data reduction problems of the tropospheric scatter propagation studies of the Signal Propagation Division. He has recently been involved with extreme-range overwater propagation in the microwave region.

Mr. Ortwein is a member of the San Diego Chapter of the American Meteorological Society.

❖

James E. Pohl was born in Georgetown, Ohio, on September 21, 1927. He received the B.E.E. degree from The Ohio State University, Columbus, in 1952.

Since 1952 he has been with the U. S.

Navy Electronics Laboratory, San Diego, Calif., where he has been concerned mainly with microwave scatter system instrumentation, along with related data acquisition and data handling problems in the Signal Propagation Division. He has participated in some VLF studies in the Arctic regions. His current work is connected with instrumenting a large, steerable antenna.

J. E. Pohl

Robert L. Pritchard (S'45–A'51–SM'55–F'60) was born in Irvington, N. J., on September 8, 1924. He received the B.S.E. degree from Brown University, Providence, R. I., in 1946, and the Ph.D. degree in acoustics from Harvard University, Cambridge, Mass., in 1950.

R. L. Pritchard

From 1950 to 1957 he worked at the General Electric Research Laboratory, Schenectady, N. Y., engaged in research on the transistor from an electric-circuit point of view. In 1957, he joined Texas Instruments, Inc., Dallas, where he is now manager of the Device-Electronics Branch of the Research and Engineering Department, engaged in exploratory development and electric-circuit analysis of semiconductor devices.

Dr. Pritchard is a member of the Acoustical Society of America, Sigma Xi, and Tau Beta Pi.

Max J. Schuller (M'60) was born in Schwandorf, Germany, on October 26, 1932. He received the Dipl.Ing. degree in physics in 1957 from the Technische Hochschule, Munich, Germany.

M. J. Schuller

In 1957, he joined the European subsidiary of Beckman Instruments, Munich, working in the field of infrared and ultraviolet spectroscopy. He became associated with the U.S. Army Signal Research and Development Laboratory, Fort Monmouth, N. J., in 1958, where he specialized in semiconductor device design and circuit theory. In 1960, he joined the Electronic Semiconductor Department of CBS Laboratories, Stamford, Conn., where he is Director of the Theory and Design Section.

Fred Sterzer (M'56) was born in Vienna, Austria, on November 18, 1929. He received the B.S. degree in physics from the College of the City of New York in 1951, and the M.S. and Ph.D. degrees from New York University in 1952 and 1955, respectively.

F. Sterzer

From 1952 to 1953 he was employed by the Allied Control Corporation, New York, N. Y. During 1953 and 1954 he was an instructor in physics at the Newark College of Engineering, Newark, N. J., and a research assistant at New York University. He joined the RCA Tube Division in Harrison, N. J., in October, 1954, and transferred to the Princeton, N. J., branch in 1956, where he is now group leader in microwave physics. His work has been in the field of microwave spectroscopy, traveling-wave tubes, backward-wave oscillators, solid-state microwave amplifiers and oscillators, and microwave computing circuits.

Dr. Sterzer is a member of Phi Beta Kappa, Sigma Xi, and the American Physical Society.

Robert W. Terhune was born on February 7, 1926, in Detroit, Mich. He received the B.S. degree from the University of Michigan, Ann Arbor, in 1947, the M.A. degree from Dartmouth College, Hanover, N. H., in 1948, and the Ph.D. degree in physics from the University of Michigan in 1957.

R. W. Terhune

He was head of the Solid State Physics Laboratory, Willow-Run Laboratories, the University of Michigan, Ann Arbor, where from 1951, he was engaged in work on masers, spin resonance, infrared detectors and spectroscopy, systems analysis, and design of digital data handling systems. Recently he joined the staff of the Scientific Laboratory at the Ford Motor Company.

Dr. Terhune is a member of the American Physical Society and Sigma Xi.

William M. Webster (A'48–SM'54) was born in Warsaw, N. Y., on June 13, 1925. He received the B.S. degree in physics from Union College, Schenectady, N. Y., in 1945, and the Ph.D. degree from Princeton University, Princeton, N. J., in 1951.

W. M. Webster

He joined the staff of the RCA Laboratories in 1946, as a specialist in vacuum and solid-state electronics. In 1954 he was transferred to the RCA Electron Tube Division, Harrision, N. J., and subsequently to the newly-formed Semiconductor and Materials Division, Somerville, N. J., as manager of Advanced Development. In June, 1959, he was named administrative engineer on the staff of the vice president, RCA Laboratories, Princeton, N. J., with the responsibility for special assignments relating to various aspects of the overall RCA research program. He was appointed Director of the Electronic Research Laboratory in August, 1959.

Dr. Webster is a member of Sigma Xi.

Amnon Yariv (S'56–M'59) was born in Tel Aviv, Israel, on April 13, 1930. He served in the Israeli army from 1948 to 1950, and came to the U. S. in 1951. He received the B.S.E.E. degree, with highest honors, and the M.S. and Ph.D. degrees in 1954, 1956, and 1958, respectively, from the University of California, Berkeley. His graduate research included a study of electron beam dynamics and of "Adiabatic Fast Passage" effects in paramagnetic resonance. During his graduate studies he was an IBM pre-doctoral fellow and a research assistant in the Department of Electrical Engineering. He joined the Bell Telephone Laboratories, Murray Hill, N. J., in January, 1959, where he has been working in the general field of microwave properties of solids.

A. Yariv

Dr. Yariv is a member of the American Physical Society and Phi Beta Kappa.

IRE Awards, 1961

Founders Award

RALPH BOWN

For outstanding service to the IRE and for outstanding contributions to the radio engineering profession through wise and courageous leadership in the planning and administration of technical developments which have greatly increased the impact of electronics on the public welfare.

Medal of Honor Award

ERNST A. GUILLEMIN

For outstanding scientific and engineering achievements.

Memorial Prize Award in Memory of Morris N. Liebmann

LEO ESAKI

For important contributions to the theory and technology of solid state devices, particularly as embodied in the tunnel diode.

Memorial Prize Award in Memory of Browder J. Thompson

EIICHI GOTO

For his paper entitled "The Parametron, a Digital Computing Element which Utilizes Parametric Oscillation," which appeared in the August, 1959, issue of the PROCEEDINGS OF THE IRE.

Prize Award by W. R. G. Baker

MANFRED CLYNES

For his paper entitled "Respiratory Control of Heart Rate: Laws Derived from Analog Computer Simulation," which appeared in the January, 1960, issue of the IRE TRANSACTIONS ON MEDICAL ELECTRONICS.

Prize Award by Vladimir K. Zworykin

PETER C. GOLDMARK

For important contributions to the development and utilization of electronic television in military reconnaissance and in medical education.

Memorial Prize Award in Memory of Harry Diamond

HELMUT L. BRUECKMANN

For outstanding contributions to the theory and technology of antennas.

Professional Group on Bio-Medical Electronics Prize Award in Memory of William J. Morlock

BRITTON CHANCE

For the application of a variety of advanced electronic techniques in a long-term program of fundamental biological research.

New Fellows

P. R. Adams

For contributions in the development of radio aids to navigation.

R. J. Adams

For contributions to the design of radar antennas, and for direction of research and development of naval radar systems.

Paul Adorian

For development of electronic distribution networks used in broadcasting and television.

Pierre Aigrain

For contributions to the theory and application of solid-state devices.

S. S. Attwood

For contributions to the understanding of electromagnetic field theory.

G. S. Axelby

For achievements in electronics and automatic control systems; and for promoting progress of the IRE Professional Groups at the local and national levels.

Samuel Bagno

For creative contributions in the fields of instrumentation, medical electronics, and electronic aids to law enforcement.

Vitold Belevitch

For contributions to the general theory of lumped networks.

F. B. Berger

For fundamental contributions to the theory and development of Doppler navigation.

New Fellows

G. A. Blake

For leadership in military electronics and communications.

R. N. Bracewell

For contributions to radio astronomy.

F. B. Bramhall

For contributions to the theory and practices of electrical communications.

W. B. Bruene

For advancing single-sideband radio communications.

J. W. Christensen

For contributions to photo transmission and color television systems.

J. W. Clark

For contributions to research on the effects of radiation.

P. S. Darnell

For contributions to the field of component engineering.

S. H. Dike

For contributions in the analysis and development of electronic systems.

W. J. Dodds

For technical contributions and leadership in the development of microwave tubes.

New Fellows

M. L. Doelz

For contributions to mechanical radio-frequency filter development and predicted-wave digital data communication.

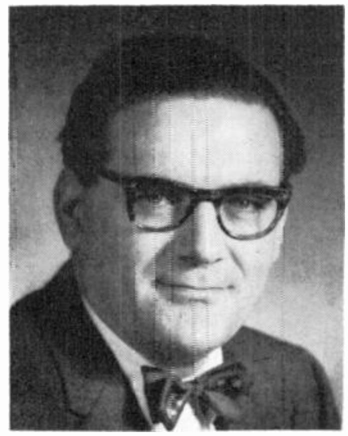

W. C. Dunlap, Jr.

For contributions to semiconductor research and transistor production techniques.

R. S. Elliott

For contributions in the field of electromagnetic waves.

Michael Ference, Jr.

For technical contributions and leadership in military communication and space electronics.

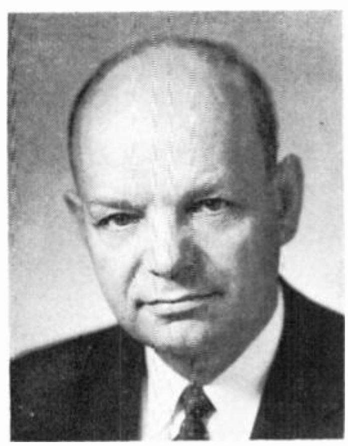

Richard Filipowsky

For contributions in the application of information theory to communication systems.

J. F. Fisher

For contributions to color television.

H. L. Flowers

For contributions to radar and guidance control systems.

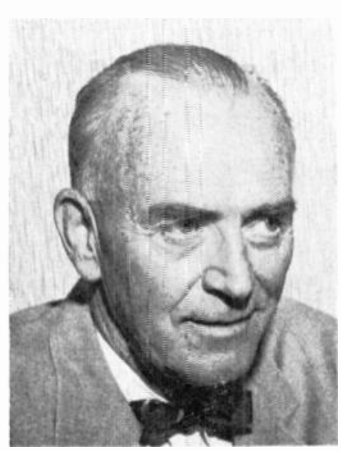

P. F. Godley

For pioneering in the short wave art.

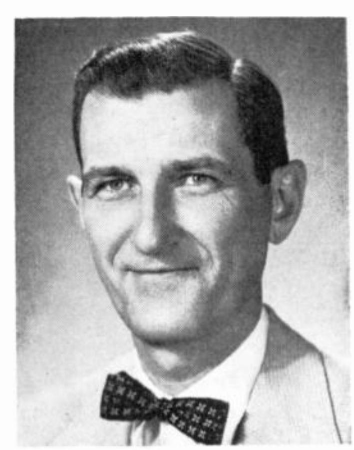

W. E. Gordon

For contributions to the understanding of radio scattering.

New Fellows

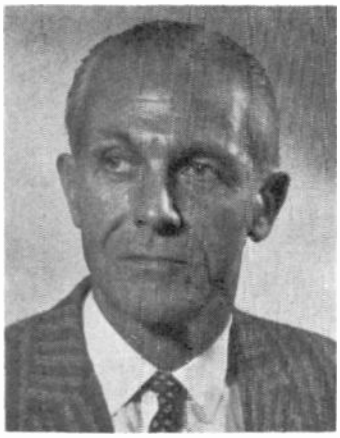

A. R. Gray

For contributions to reliability.

E. H. Greibach

For contributions to high sensitivity measuring instruments.

D. D. Grieg

For contributions to pulse modulation systems

C. M. Harris

For contributions to the science of acoustics.

C. E. Hastings

For contributions to radio surveying and navigation.

L. G. Hector

For contributions in the field of electronic devices.

J. W. Heyd

For contributions to the applications of atomic energy.

R. W. Hickman

For contributions to electronics education.

C. L. Jeffers

For contributions to domestic and foreign broadcasting and to antenna development.

New Fellows

A. S. Jensen

For contributions to the development of electronic storage tubes and special electron devices.

A. C. Keller

For contributions to the recording and reproduction of stereophonic sound and to telephone switching.

Y. H. Ku

For contributions to nonlinear circuit analysis.

A. H. LaGrone

For contributions to the theory and application of tropospheric radio wave propagation.

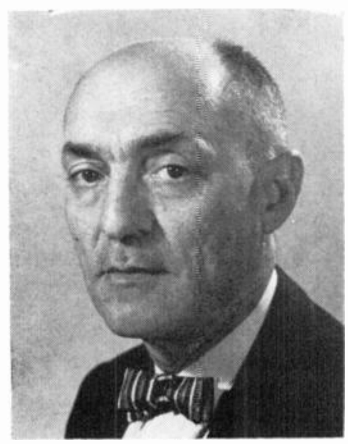

Emory Lakatos

For contributions in communications and weapon systems design.

Y. W. Lee

For contributions to communication theory and engineering education.

H. A. Leedy

For contributions to electronic research management.

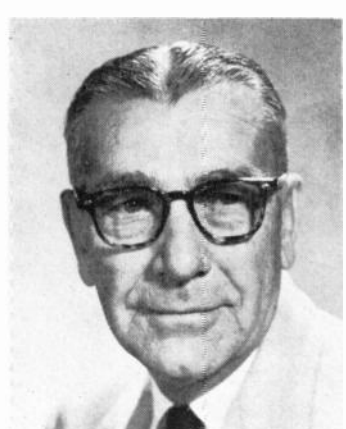

Emil Lenzner

For leadership in military communication-electronics.

Samuel Lubkin

For applications of digital computers to airborne systems.

New Fellows

D. E. MAXWELL

For contributions to radio-television broadcasting and standardization.

G. D. MCCANN

For contributions to electrical engineering literature and education.

R. L. MCFARLAN

For contributions to systems applications of electronic computers and for effective administrative activities during formative periods of technical administration.

M. E. MOHR

For contributions to military electronic systems.

F. H. NICOLL

For contributions in electron optics and electroluminescence.

H. M. O'BRYAN

For contributions to the administration of scientific research.

A. A. OLINER

For contributions to network representations of microwave structures.

R. D. O'NEAL

For leadership and technical administration in systems engineering.

D. C. PORTS

For contributions to research in electromagnetic propagation.

New Fellows

E. A. Post

For contributions to aeronautical electronics.

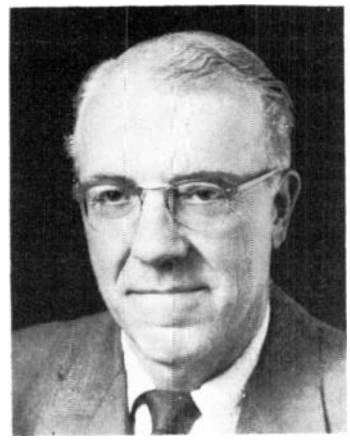

M. B. Reed

For contributions to the understanding of electrical networks.

Donald Richman

For contributions to color television.

S. D. Robertson

For contributions to engineering in the microwave field.

H. I. Romnes

For contributions in the field of communication engineering and management.

V. L. Ronci

For contributions to the development of electron devices.

Paul Rosenberg

For contributions in the field of electron physics.

R. C. Sanders, Jr.

For contributions to the art of continuous-wave radar systems.

L. S. Schwartz

For applications of information and decision theory to communication systems.

New Fellows

R. W. Sears

For contributions in the field of coding and storage electron tubes.

Gustave Shapiro

For contributions to the development of electronic miniaturization techniques and components.

T. A. Smith

For contributions in many fields of radio engineering.

R. M. Somers

For contributions to phonographic recording and dictating machines.

E. K. Stodola

For contributions to the development of extended-range radar systems.

M. E. Strieby

For pioneering in the development of the coaxial cable system.

T. E. Tice

For contributions to radome theory and techniques.

Miyaji Tomota

For development of electronic measuring instruments and automatic control devices.

H. C. A. van Duuren

For contributions toward the reliability of radio communication.

New Fellows

G. S. Wickizer

For contributions to experimental wave propagation research.

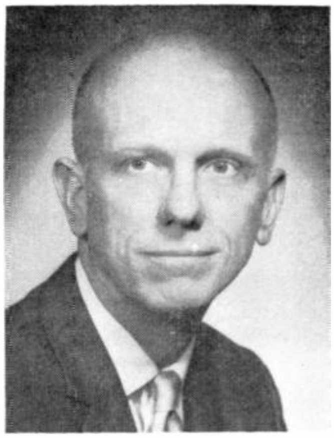

C. R. Wischmeyer

For contributions to engineering education and instrumentation.

A. M. Zarem

For contributions in the application of millimicrosecond electronic instrumentation techniques.

H. K. Ziegler

For guidance and leadership in military electronics.

Books

Solid State Physics in Electronics and Telecommunications, Vol. 4, Magnetic and Optical Properties, Part 2, M. Desirant and J. L. Michiels, Eds.

Published (1960) by Academic Press, Inc., 111 Fifth Ave., N. Y. 3, N. Y. 404 pages+xvi pages. Illus. 6¾×10. $16.00.

This is the fourth volume of the Proceedings of the International Conference on Solid State Physics in Electronics and Telecommunications, sponsored by the International Union of Pure and Applied Physics, and held in Brussels in June, 1958. It is the second of two parts dealing with the magnetic and optical properties of solids and their applications. The book is divided into six parts. It contains four papers on masers, eleven papers on electroluminescence, six papers on phosphors, five papers on the application of photosensitive materials, five papers on radiation damage, and seventeen papers on miscellaneous problems.

In the section on masers, both the cavity and the traveling-wave types are treated. The effects of radiation upon the properties of semiconductors and ferrites are covered by several papers. There are also several papers on ferroelectrics such as barium titanates. The theory of electroluminescence and its experimental interpretations are the topics of a number of papers. Methods of measurement of radiant flux, pressure effects on luminescence, and activators for phosphors are discussed in the section on phosphors. Infra-red phosphors, solid state image transducers, etc. are discussed in the section on application of photosensitive materials.

The contents of the papers contained in this book are of high quality and represent results of research of scientists and engineers from many countries. There are a number of papers in French and German in addition to the majority of papers in English. The book contains a wide range of topics in several growing fields of research in solids.

The quality of the printing and illustrations is excellent. It is recommended for researchers in the field of the magnetic and optical properties of solids and for institutional libraries.

RONALD F. SOOHOO
MIT Lincoln Lab.
Lexington

Transistors—Principles, Design and Applications, by Wolfgang W. Gärtner

Published (1960) by D. Van Nostrand Co., Inc., 120 Alexander St., Princeton, N. J. 637 pages+21 index pages+xii pages+bibliography by chapter+14 appendix pages. Illus. 6¼×9¼. $12.50.

Most of the new recruits into the broad, young field of transistor technology must still be trained on the job. This is partly due to the lack, up to now, of a clear, substantially pertinent and comprehensive textbook covering transistor principles, design and applications. Dr. Gärtner's book has, in the opinion of this reviewer, successfully filled this void. The book can also serve the full-fledged technologist as a permanent store of basic ideas and typical design examples. It can also be useful as a guide to the literature written on the subject of transistors until about two years ago.

Beginning with a fine, up-to-date introduction, the book proceeds to build a foundation of basic concepts of semiconductor physics and the properties of junction transistors, as is both logical and customary. The treatment of parameter dependence on temperature and operating point given here is more detailed and useful than any seen before under one cover by this reviewer. The author then bridges over to a survey of transistor applications with a discussion of the characterization of the transistor as an electrical network. Among the applications discussed are low-drift stages, push-pull stages, low- and high-frequency amplifiers, wide-band amplifiers, oscillators and pulse circuits. The writing style throughout the book is concise and very clear, such as to be readily readable by senior undergraduate physics or electrical engineering students.

If any part of this book must be adjudged weak, it is the applications section. The reviewer feels that the treatment here falls somewhat short of imparting the intuitive grasp needed for innovative circuit design. It is rather sketchy and occasionally overlooks highly pertinent material which would not have added many pages, such as the application of avalanche diodes in the biasing of some dc amplifiers. A more regrettably abbreviated topic is the use and stabilization of external negative feedback in transistory circuitry.

This book bears the mark of careful preparation and accuracy—an over-all impression enhanced by the many fine illustrations and the small number of typographical errors. Every technical person seriously interested in transistors should certainly examine it.

V. R. SAARI
Bell Telephone Labs.
Murray Hill, N. J.

La Modulation de Fréquence, by Jean Marcus

Published (1960) by Editions Eyrolles, 61 boulebard Saint-Germain, Paris V^e. 307 pages+3 bibliography pages. Illus. 6¼×9¾. 43,65 NF.

The subtitle of the book is, "Theory and Industrial Applications." As mentioned in the preface, the volume is intended primarily for the engineer interested in the fundamentals of the various techniques of frequency modulation. Because of the clear and concise treatment of the subject matter, this book will also be valuable to students and technicians.

In Chapter 1, the basic principles of frequency modulation and phase modulation are discussed: fundamental definitions, frequency spectrum of a frequency-modulated carrier wave, double modulation FM-FM, frequency multiplication and frequency division, response of a band-pass filter to an FM wave. In five appendixes the author gives a clear and brief mathematical development of the formula used in the text.

Chapter 2 describes the various systems used to produce frequency modulation (reactance tubes or saturated cores) or phase modulation (Armstrong's modulator, or Serrasoid modulator). In each case, the distortions produced are carefully analyzed. Modulators using delay lines or reflex klystrons are also considered, together with variable capacitances and variable inductances. Formulas relative to tuned circuits with variable elements or to reactance tubes are derived in two appendixes.

Chapter 3 discusses limiters and discriminators: Travis, Foster-Seeley, Rate Discriminators. After an analysis of the various circuits, some practical examples are described. An application to frequency control is given. The effect of noise in the limiters is described in the appendix.

Chapter 4 is devoted to the effect of noise in FM systems. With a minimum of mathematical development, it gives the fundamental formula of signal-to-noise ratio, FM improvement, the effect of distortions produced by multipath transmission, and the use of feedback to reduce the effect of interferences. The necessary mathematical analysis is very clearly given in four appendixes. Although the author has mentioned here the phase-lock demodulator, a more detailed discussion of phase-lock systems would have done more justice to this important application.

Chapter 5 discusses the frequency modulation receivers (HF and IF amplifiers mostly, since limiters and discriminators were already described in Chapter 3).

Chapter 6 gives a general outlook on multiplex FM links with an analysis of various phenomena producing distortions: nonlinearities in modulators, demodulators and limiters, or variable delays in filters and amplifiers, multiple reflections in transmission lines, or multipath transmissions in radio links. A comparison of various FM multiplex systems and conventional amplitude modulation is given for AM-PM, FM-AM, FM-PM, etc.

Chapter 7 presents some examples of industrial realizations. It gives the detailed computations for an FM telemetering project together with the characteristics of an industrial realization. The characteristics of a radio relay at 400 Mc are also given as an example of an FM multiplex system.

This book is very commendable for its clear treatment of the subject. Throughout the text are numerous references to papers and books for the reader interested in greater details in any particular subject. The book will be of value to the technicians who need the basic elements to analyze and formulate various frequency-modulated systems.

M. ARDITI
ITT Federal Labs.
Nutley, N. J.

An Introduction to Statistical Communication Theory, by David Middleton

Published (1960) by McGraw-Hill Book Co., Inc., 330 W. 42 St., N. Y. 36, N. Y. 1070 pages+20 index pages+xix pages+7 bibliography pages+32 appendix pages+9 glossary pages. Illus. 6¼×9¼. $25.00.

Some years back, an English statesman on a tour of the United States visited, among other places, Mount Rushmore National Monument. He is said to have stared at the four presidential faces carved out of the mountains for some time. Finally, he turned to his companions and exclaimed, "Marvelous—but is it art?" I feel that we are in somewhat the same sort of predicament in trying to categorize Middleton's mountainous treatise. There have been technical books with more pages than this one (though not many). There have certainly been technical books covering a wider range of topics (though few have been at such an advanced level). Few technical books, however, can claim to be packed with such a weight of material as this one.

Middleton's work, like Mount Rushmore, is divided into four parts. The first—"An Introduction to Statistical Communication Theory"—is certainly the weakest. This part consists of a good deal of introductory material of an expository nature. The basic concepts involved in random variables, random processes, expectations, linear and nonlinear systems, spectra, correlation, sampling and signal-to-noise ratio are treated. In addition, the last chapter of Part I includes a superficial introduction to information measure and channel capacity. Middleton is not at his best when explaining fundamental ideas, and most of Part I is treated in a more illuminating fashion in other books. Part I is valuable primarily for the wealth of problems and examples treated.

Part II—"Random Noise Processes"—starts with a discussion of the normal random process and processes derived from the normal. After this, the Langevin, Fokker-Planck and Boltzmann equations are examined. Finally, models of thermal, shot and even impulse noise are formulated, and various properties of these models are obtained.

Part III—"Applications to Special Systems"—is devoted to modulation, demodulation and Wiener theory. Middleton provides an extensive treatment of the second order statistics of amplitude modulated and frequency modulated signals. He also discusses in astounding detail the detection of such signals in the presence of noise. A large number of interesting results dealing with the spectra of various modulated signals and the detection of such signals are presented. Part III concludes with a chapter on Wiener filtering and a chapter devoted to some distribution problems.

Part IV—"A Statistical Theory of Reception"—is concerned with the application of statistical decision theory to communication problems. After an unnecessarily involved chapter on the elements of statistical decision theory, Middleton devotes two chapters to binary detection systems and one chapter to estimation theory. A good deal of the material in these three chapters deals with the block diagram structure of the various systems obtained. A brief and unsatisfactory chapter deals with information measures in reception and a final chapter mentioning some "Generalizations and Extensions" concludes the main body of the book. But that's not all!

After the 23 chapters outlined above, Middleton has provided 70 pages consisting of 1) an appendix on "Special Functions and Integrals," 2) an appendix on "Solutions of Selected Integral Equations," 3) "Supplementary References and Bibliography," 4) an *eight page* "Glossary of Principal Symbols," 5) a "Name Index," and 6) a remarkably complete and well-organized "Subject Index."

There is a lot to criticize in this book. There is, I think, even more to be learned from it. The book is of little use as an introduction to statistical communication theory; it is hopeless as a text. As a source book of problems, and solutions, and of methods of solving problems, it has no peers.

NORMAN ABRAMSON
Stanford University
Stanford, Calif.

The Control of Multivariable Systems, by Mihajlo D. Mesarović

Published (1960) by The Technology Press, Mass. Inst. Tech., Cambridge, and John Wiley and Sons, Inc., 440 Fourth Ave., N. Y. 16, N. Y. 106 pages+2 index pages+xi pages+2 bibliography pages. Illus. 6×9. $3.50.

A first book on any topic always leaves the reviewer with mixed feelings. Because this is the first book (at least, in English) on multivariable systems, it is a welcome addition to the control engineer's library. Since there is no other like book to compare it with (and it is not fair to compare a book with periodical literature), it must be reviewed in its own context.

Professor Mesarović has written here a remarkable book. In the space of a hundred-odd pages he defines, analyzes and synthesizes multivariable control systems. In the definition of such systems the author used three canonical structures to classify the systems. (Only one has appeared in most of the other published work in this subject.) Using matrix methods, the author then analyzes these three structures.

The first part of this book is devoted to a study of the interrelations which exist in multivariable systems. An interesting feature here is the determination of what the author calls "the strength of the interrelations," which serves to categorize the various interrelations on the basis of their ultimate effect on the outputs of the system.

The second part is concerned with the problems of synthesis. The interesting feature here is the question of the existence and uniqueness of the synthesis. The author obtains the conditions for these in terms of a binary representation of the system. He introduces the concept of "R and D numbers," thus: If r is the total number of inputs to be synthesized, and if only a subset, r_d, of these is needed to satisfy some optimum performance criterion, he defines the number of free inputs to be $R=r-r_d$. If n is the number of outputs, he defines a number $D=r_d-n$. He then arrives at the necessary conditions for optimal synthesis by showing that it is required that $D\geq 0$ and $R=0$. The R and D numbers are then obtained for linear and nonlinear deterministic systems and for stochastic systems.

This book is one of a series whose aim is the "systematic publication of research studies larger in scope than a journal article but less ambitious than a finished book." Thus, this is certainly not a book for beginners. It requires some knowledge of control system theory and of the associated mathematics. It could easily be used as a text for a one-semester course at the graduate level, supplemented by the teacher's knowledge of the pertinent literature; the lack of problems or examples can easily be made up by such a teacher.

The book is set up in typewritten lithograph form. This seems to be a departure in format from some of the other earlier books in this series, and in the opinion of the reviewer, not a happy departure. There are a number of typographic errors both in the text and in some of the figures.

Over-all opinion: By all means, get it.

N. H. CHOKSY
Applied Physics Lab.
The Johns Hopkins Univ.
Silver Spring, Md.

Information Retrieval and Machine Translation, Part I, Allen Kent, Ed.; Advances in Documentation and Library Science Series, Vol. 3, Jesse H. Shera, General Editor

Published (1960) by Interscience Publishers, Inc., 250 Fifth Ave., N. Y. 1, N. Y. 667 pages+18 index pages+xv pages. Illus. 6¼×9¼. $23.00.

This book contains twenty-one papers originally presented in Cleveland in September, 1959, at the International Conference for Standards on a Common Language for Machine Searching and Translation. Another set of thirty-eight papers from the same conference is published as Part II in a second volume which is not under review.

It must be said at the outset that this volume has all the faults of the usual conference proceedings. The papers are not grouped in any apparent manner to bring together related material, and there is no editorial comment to guide the reader. Instead, each paper is labeled as a separate "chapter" of the book, and is made to stand completely on its own, frequently surrounded by totally different material. Furthermore, the title of the book is somewhat misleading in that, with the possible exception of Chapter 1, the subject of machine translation is not covered at all.

The specific aims of the conference, as stated in the preface, were in part as follows:

> to encourage an environment for working toward a common machine language, or a series of compatible machine languages . . . .
> to characterize equipment requirements for use with common language systems . . . ,
> to promote cooperative research programs . . . , and
> to review interrelationships between machine literature searching and machine translation. . . .

The contents of this volume would seem to indicate that nothing of the kind was actually done; and the discussions at the conference, included as Chapter 22, bear testimony to the fact that the stated aims were far too ambitious. Some questions were, in fact, raised as to the wisdom of pursuing these goals, and this reviewer tends to agree with Don Andrews who, in Chapter 8, states that "until a mature and satisfactory solution (to the problem of encoding and searching) is discovered, we should, indeed, be rash to talk of, or attempt, standardization of machine language."

The book includes papers by American authors and authors from six foreign countries. All papers are printed in English with the exception of Chapter 18, by Gerard Cordonnier, which is in French. An introduction by Senator Hubert Humphrey is followed by a survey of work in the areas of linguistic analysis and machine translation by Allen Kent. This survey, encompassing almost a third of the entire book, consists largely of a set of tables, arranged in alphabetical order by organization, or by name of the principal investigator, and lists the several research activities undertaken by various groups active in the field. While these tables are evidence of a great deal of work, the material is compressed into long, narrow columns, making perusal uncomfortable. Moreover, material of this kind requires continuous updating, and would seem to be available more readily, and at less expense, in other publications.[1,2]

Chapters 10, 14, and 18 by Robert Hayes, Otto Nacke, and Gerard Cordonnier, respectively, deal with the requirements and organization of various types of documentation systems. Mr. Cordonnier makes some challenging suggestions concerning the preparation of standardized "analytical summaries" for all published material; he also underlines the need for his own research by the astonishing assertion that it is necessary "to safeguard French achievements threatened by 'European' or 'international' projects. . . ."

Various aspects of the many-faceted classification originated by S. R. Ranganathan are mentioned in Chapters 3 and 4. Chapter 5 by Kinzo Tanabe describes a classification system based on the universal decimal classification. Chapter 2 by John O'Connor presents a thorough discussion of the use of document grouping to save storage space and search time in retrieval systems. Automatic abstracting techniques are mentioned in Chapter 11 by Leslie Clark. Various types of encoding techniques and notational schemes are described in Chapters 7, 8, and 13. Chapter 12 by S. C. Rome and B. K. Rome presents a notation for the representation of behavioral system, and Chapter 15 by H. M. Semarne makes a plea for the use of symbolic logic in documentation; in both cases, the specific applications to problems in information retrieval are not made clear. The important question of determining and representing relationships between index terms is treated in Chapter 6 by Don Andrews and in the interesting paper by V. P. Cherenin *et al.*, in Chapter 9. Finally, Chapters 19 to 21 deal with equipment, describing respectively the much neglected Magnacard system, the Minicard film system, and the G.E. 250, now defunct.

To summarize, the book can be recommended only to institutional libraries, and to experts with substantial cash reserves on hand who are willing to spend the time to extract a few interesting ideas from a large mass of routine matter. The presentation is generally good, with the exception of many typographical errors still included, and a lack of editing, particularly in some of the articles translated from foreign languages.

GERARD SALTON
Harvard University
Cambridge, Mass.

[1] Series of reports on "Current Research in Scientific Documentation," National Science Foundation, Washington, D. C. Rept. No. 7; November, 1960.

[2] A. G. Oettinger, "A survey of Soviet work on machine translation," *Mech. Trans.*, vol. 5, no. 3; December, 1958.

Linear Systems Analysis, by Paul E. Pfeiffer

Published (1961) by McGraw-Hill Book Co., Inc., 330 W. 42 St., N. Y. 36, N. Y. 520 pages+8 index pages+xvii pages+2 bibliography pages+8 appendix pages. Illus. $6\frac{1}{4}\times9\frac{1}{4}$. $12.50.

To quote from the jacket, "This book is intended to supply an adequate understanding of theory as applied to passive linear circuits, linear electronic circuits, linear servomechanisms, and mechanical vibrating systems." The arrangement of the material follows a logical sequence consistent with this objective. Chapter headings begin with "A Mathematical Miscellany," "Linearized Dynamic Equations," "Steady-State Response to Periodic Driving Functions," through "Some Mathematical Properties of the Laplace Transformation," "The Transfer Function," "Matrices and Linear Algebraic Equations," "Signal-Flow Graphs and Linear Algebraic Equations," and "Some Theorems on Feedback."

There is no doubt that this text is an excellent one for a formal course directed to discrete parameter time variant linear systems. It is interesting to note that the author frequently attempts to establish a motivation for studying a new technique before developing the details of theory. In this way the student has an end goal to keep in view while immersed in learning the rules of the game. As an example, the application of the Laplace transformation is studied first; and subsequently, the mathematical bounds of the technique are discovered.

It is rather difficult to appraise the value of a formal textbook to the practicing engineer who wishes to sit down and "learn" something from it. This book seems to be above average in this respect since the author relies extensively on physical examples which are usually close enough to the world of practical engineering to be meaningful. This reviewer has "learned" from this book about subjects in which he was either behind the door or behind the times at school. Others are sure to be similarly successful.

R. P. BURR
Circuit Research Co.
Glen Cove, N. Y.

Principles of Semiconductor Device Operation, by A. K. Jonscher

Published (1960) by John Wiley and Sons, Inc., 440 Fourth Ave., N. Y. 16, N. Y. 163 pages+4 index pages+viii pages+problems and bibliography by chapter. Illus. $5\frac{3}{4}\times8\frac{3}{4}$. $5.00.

This book is a real bargain, and a real contribution to those students who want to know more about semiconductor devices than is usually presented in introductory texts. The author has provided a very readable and thorough treatment of the physical principles of semiconductor device action. To use his own words, "The specific subject of injection, decay, and transport of excess carrier densities in semiconductors has not received sufficient attention. . . . Theoretical texts stop short of discussing it, the more applied works tend to take it for granted." The author has attempted to fill the need he describes.

His method is addressed to the engineer who desires a physical description of what is going on, followed by a reasonably complete mathematical treatment that rarely, if ever, loses sight of the physics of the problem. Substantial attention is given to the departures of actual devices from the simple theory.

The least successful part of the book deals with the transistor as such. The more successful earlier parts deal with semiconductor theory, non-equilibrium carrier densities, transport of excess carrier densities, and the theory of *p-n* junctions and junction diodes. Indeed, the transistor chapter seems almost an afterthought.

All in all, however, a valuable little book.

HOWARD E. TOMPKINS
University of New Mexico
Albuquerque

Scanning the Transactions

Pigeon-guided missiles is the subject of one of the most unusual cover photographs to appear on an IRE publication in recent years. Equally unusual is the fact that the picture was not published by one of the Professional Groups that deals with military or space electronics, as one might expect, but rather by the PG on Engineering Writing and Speech (January, 1961 issue). The cover photograph shows a demonstration model of a three-pigeon guidance system for use in the nose cone of a missile. The pigeons used for this purpose had been taught to peck persistently at a given visual target on a ground-glass screen. The chosen target might be a submarine at sea or a military site on the ground. The optical image of the target is projected simultaneously on three glass screens inside the nose cone by a system of lenses and mirrors. In this proposed system the missile stays on course as the pigeons peck precisely at the image on the screens, which tilt according to the pigeons' responses. Ballistic valves at the edges of the three screens were designed to operate the missile steering system, as reported in detail by B. F. Skinner in *The American Psychologist*, vol. 15, p. 28 (January, 1960). Thus, the experimental system is a servomechanism which actually uses the majority vote of three trained pigeons as its sensing element! Training pigeons to peck at visual targets has turned out to be part of the groundwork for the development of modern teaching machines. As Professor Skinner of Harvard points out, "The scrap of wisdom we imparted to each pigeon was indeed small, but the required changes in behavior were similar to those which must be brought about in vaster quantities in human students." What has this to do with Engineering Writing and Speech? Modern teaching machines can be used in a wide variety of instruction in areas from grade school material to college physics, as pointed out in the article in the issue by Dr. G. Rath, "A New Task for the Technical Writer: Programming Teaching Machines." Dr. Rath suggests that the technical writer can have an important role in preparing programs for the teaching machines of the future.

The rapid evolution of radio astronomy can probably best be seen by observing the advances that are being made in the instrumentalities of this blossoming field. IRE members, from their reading of the January, 1958 Radio Astronomy Issue of the PROCEEDINGS, are already acquainted with the advanced nature of the equipment and techniques which radio technology has provided in the recent past. That this field has continued to blossom in the last three years, and at an even greater rate, can now be seen from a new Radio Astronomy Issue, published by the IRE TRANS. ON ANTENNAS AND PROPAGATION in January, 1961. Among the many interesting developments described in the issue are: Ohio State's 360-foot standing-parabola radio telescope with a tiltable reflector; the University of Illinois' parabolic cylinder whose aperture is 400 by 600 feet; Cornell University's ionospheric radar installation in Puerto Rico with its 1000-foot-diameter spherical-bowl antenna; Stanford University's interferometer employing 32 10-foot paraboloids arranged in two arrays; and Cal Tech's 2-element interferometer consisting of twin 90-foot steerable paraboloids. The variety of antenna configurations that are emerging in the radio astronomy field is indeed impressive. Impressive, too, are the substantial improvements which have recently been made in low-noise receivers, measurement techniques, and signal processing methods. These technical advances are providing astronomers and astrophysicists with the means of obtaining new information about the composition, dimensions and dynamics of the universe. But these advances are also advancing radio technology itself, and already have found important applications in radar, space technology and communications.

Pattern recognition problems are of widespread interest today. Although they arise in many different guises, they all have in common the fact that their solution requires the ability to recognize membership in classes and, more important, the automatic establishment of how to measure membership in each class. In word recognition, for example, the "class" is a specific word and "members" of the class are different utterances of the word by different speakers. If membership in a class could be recognized, then the word could be identified regardless of who uttered it. The same requirement applies to many other recognition problems, such as recognition of a speaker regardless of what he speaks, medical diagnosis, threat evaluation, and recognizing a person from his handwriting. A geometrical approach to the problem of class recognition was recently published which has yielded some interesting results. The point of view taken was that events can be described by points or vectors in N-dimensional space and that by formulating and applying the proper measuring methods, those events belonging to the same class will be found to lie close to each other. An experimental program, consisting of machine recognition of spoken numerals, was devised to verify the technique. The numerals "zero" through "nine" were spoken a number of times by ten persons. Each utterance was converted into a vector by means of an 18-channel vocoder. The machine was first given 3 examples of each of the ten classes of digits and then asked to identify the spoken numerals. The number of examples was later increased for succeeding experiments. The machine's error rate proved to be 45 per cent with only 3 examples per class, but improved to 30 per cent for 4 examples, 10 per cent for 7 examples, and reached 0 per cent for 9 examples. (G. S. Sebestyen, "Recognition of membership in classes," IRE TRANS. ON INFORMATION THEORY, January, 1961.)

Packaging techniques have recently become a subject of first-order importance, especially in the semiconductor device field. In pushing the operating frequencies of transistors and other semiconductor devices into the microwave region, a point has been reached where in many cases the high-frequency performance is no longer limited by the internal characteristics of the device itself but rather by its external connections to the circuit. Packaging has therefore become an intimately related and vitally important consideration in the performance of microwave devices. In this connection, a micro-alloy diffused-base transistor has been developed with a power gain of 11 db at 1000 Mc and a maximum frequency of oscillation of 3000 Mc. While the excellent high-frequency performance was due in part to fabrication improvements, it is interesting to note that the use of a new coaxial packaging technique also played an important role in the success of this development. (J. D. McCotter, *et al.*, "A coaxially packaged MADT for microwave applications," IRE TRANS. ON ELECTRON DEVICES, January, 1961.)

A novel radiation tracking device has been developed which utilizes a lesser-known effect of illuminating a semiconductor. As is well known, exposing a semiconductor junction to light will produce a photovoltage across the junction. In addition, however, a voltage will also appear parallel to the junction if the illumination is localized or nonuniform. This lateral photoeffect has been embodied in a device which is capable of detecting the angular position of a light- or radiation-emitting target, and to do it without the need for a scanning device. It appears that there will be many applications for this development, especially in the realms of tracking and guidance, computers, system instrumentation and control automation. (D. Allen, *et al.*, "Radiation tracking transducer," IRE TRANS. ON INSTRUMENTATION, December, 1960.)

Abstracts of IRE Transactions

The following issues of TRANSACTIONS have recently been published, and are now available from The Institute of Radio Engineers, Inc., 1 East 79th Street, New York 21, N. Y. at the following prices. The contents of each issue and, where available, abstracts of technical papers are given below.

Sponsoring Group	Publication	IRE Members	Libraries and Colleges	Non Members
Antennas and Propagation	AP-9, No. 1	$2.25	$ 3.25	$ 4.50
Bio-Medical Electronics	BME-8, No. 1	2.25	3.25	4.50
Circuit Theory	CT-7, No. 4	5.00	11.25	15.00
Electron Devices	ED-8, No. 1	2.25	3.25	4.50
Engineering Management	EM-7, No. 4	2.25	3.25	4.50
Engineering Writing and Speech	EWS-4, No. 1	2.25	3.25	4.50
Information Theory	IT-7, No. 1	2.25	3.25	4.50
Instrumentation	I-9, No. 3	2.25	3.25	4.50
Military Electronics	MIL-5, No. 1	2.25	3.25	4.50
Space Electronics and Telemetry	SET-6, No. 3-4	2.25	3.25	4.50

Antennas and Propagation

Vol. AP-9, No. 1, January, 1961

Radio Astronomy and Radio Science—Lloyd V. Berkner (p. 2)

Some Characteristics of The Ohio State University 360-Foot Radio Telescope—J. D. Kraus, R. T. Nash, and H. C. Ko (p. 4)

Design considerations and performance characteristics of The Ohio State University 360-foot radio telescope are discussed. The telescope is well suited for precision position and intensity measurements at frequencies from 30 to 2000 Mc. The beamwidths expected at 2000 Mc are about 11 by 30 minutes of arc. Factors involved in determining the antenna temperature are considered, and an estimate is made of the expected temperature.

The University of Illinois Radio Telescope—G. W. Swenson, Jr., and Y. T. Lo (p. 9)

The University of Illinois radio telescope is a reflector in the shape of a parabolic cylinder whose aperture is 400 feet × 600 feet. A 425-foot-long phase-adjustable array of receiving antennas lies along the focal line and produces a pencil beam one-third degree in width, steerable in the meridian plane up to 30 degrees in either direction from the zenith. The array was designed by means of a novel procedure using both variable spacing and variable excitaton to produce a prescribed beamwidth. The reflector is built of earth, utilizing a natural ravine. The purpose of the instrument is to compile a catalog of faint extragalactic radio sources.

The Design and Capabilities of an Ionospheric Radar Probe—W. E. Gordon and L. M. LaLonde (p. 17)

Staff members of the Cornell University Center for Radiophysics and Space Research have designed an ionospheric radar probe to be located near Arecibo, Puerto Rico. The radar will have the following general specifications:

1) Antenna reflector, 1000-foot-diameter spherical bowl, illuminated by a 430-Mc dual-polarized feed.
2) Transmitter of 2.5 Mw peak, 150 kw average power, or 100 kw CW power.
3) Dual-channel receiver, capable of measuring total power, polarization and received spectrum.

The radar will initially be used to measure the variation of electron density with height, the fluctuations of electron density at fixed heights and electron temperatures and magnetic field strengths at various heights. Ionospheric drifts may also be measured.

The radar will also be able to obtain echoes from planets, information of the moon's surface and possibly echoes from the sun. Hydromagnetic shocks may also be detected and a study of cislunar ionization can be made.

The passive system with the large antenna may be used as an instrument in radio astronomy to observe radio emission from planets and from true stars, and to make a survey of radio sources. With addditional facilities, many radio astronomy measurements can be made taking advantage of the large antenna aperture and resulting high resolving power.

The Stanford Microwave Spectroheliograph Antenna, a Microsteradian Pencil Beam Interferometer—R. N. Bracewell and G. Swarup (p. 22)

A pencil beam interferometer has been constructed at Stanford, Calif., with multiple beams of 3.1 minutes of arc width to half power (0.8 microsteradian). It is composed of two equatorially-mounted, 16-element, Christiansen arrays of 3-m paraboloids, each 375 feet long (1255 wavelengths at a wavelength of 9.1 cm). The half power beamwidth of the fan beam of a single array is 2.3 minutes of arc. To form the pencil beam, the two arrays are switched together as in a Mills cross. Frequency range is from 2700 to 3350 Mc. Phase adjustment and monitoring are handled by a new technique of modulated, weakly reflecting gas-discharges maintained at the focus of the paraboloids. Television-type scanning yields maps of the sun (spectroheliograms) revealing fine details of the microwave source regions in the chromosphere and corona. All the transient bursts and a large fraction of the steady solar emission at 9.1 cm prove to originate in a small number of highly compact centers, whose brightness temperatures may exceed 5×10^{6}°K. The sensitivity of the instrument also allows the thermal emission from the moon (250°K) and a number of galactic and extragalactic sources to be studied with high angular resolution. Illumination of the moon by terrestrial radar can be detected. The pencil beam interferometer furnishes the finest beams currently available from pencil beam antennas of any type. Examination of the fundamentals of extracting high resolution details of a source from its radiation field indicates the fitness of pencil beam interferometers, incorporating steerable multielement arrays for future development to higher resolving power. Adequate technique of phase preservation over wide spacings is available.

Two-Element Interferometer for Accurate Position Determinations at 960 Mc—Richard B. Read (p. 31)

A 960-Mc two-element interferometer using the twin 90-foot steerable paraboloids of the California Institute of Technology Radio Observatory is described. The response of the associated receiving equipment as it applies to interferometric position measurements is analyzed in some detail, and an advantage of not rejecting the image response of the receiver is mentioned. Finally, a brief account is given of the various ways the interferometer may be used to measure right ascensions and declinations with both an east-west and a north-south baseline.

A 2–4 kMc Sweep-Frequency Receiver—D. W. Casey, II, and J. W. Kuiper (p. 36)

To study another octave of the solar radio-frequency spectrum, a new superheterodyne receiver using a video-frequency IF was developed. This receiver scans the 2000- or 4000-Mc octave in 0.1 sec by using a backward-wave oscillator as the local oscillator. A careful designed balance mixer converts the incoming signal directly into the video signal, where it is amplified and displayed as an intensity-modulated trace on a high-resolution cathode-ray tube. The receiver has an average noise figure of 13.0 db, and a total gain variation of ±2 db over this octave. The receiver features power output stabilization of the local oscillator, a 2000- to 4000-Mc noise source, and highly stable video amplifiers.

Recent Developments and Observations with a Ruby Maser Radiometer—M. E. Bair, J. J. Cook, L. G. Cross, and C. B. Arnold (p. 43)

An X-band ruby maser radiometer is discussed. In particular, recent developments in the equipment design are detailed. Observations of radio sources are discussed, and response curves with and without the maser preamplifier are given. The detection of 3.45 cm radiation from the planet Saturn is reported, and the equivalent blackbody disk temperature calculated. The future of the maser amplifier in radio astronomy is considered.

Tolerance Theory of Large Antennas—R. N. Bracewell (p. 49)

The design of an antenna calls for definite amplitudes and phases of the currents, but when the antenna has been constructed and adjusted, there will be departures from the design currents because of several factors. The customary procedure of taking radiation patterns and making the final adjustments semi-empirically has usually been satisfactory, but two difficulties have been setting in with the trend towards large antennas of high gain. First, it is impossible to measure the radiation pattern of the largest existing antennas; even the determination of single sections through the pattern or the gain in one direction presents difficulty. Second, the adjustments themselves are more laborious on larger antennas. It is therefore very desirable that the theory of antenna tolerances should be pursued so that the effect of departures can be taken into account, statistically or otherwise, during the design.

This paper considers the effects of systematic and random errors on the radiation pattern of antennas representable by a field distribution over an aperture, such as paraboloidal reflectors and large arrays of small elements. In the case of paraboloids, the deterioration in directivity is found to depend on the mean square departure of the surface from the paraboloid of best weighted least-squares fit and on the two-dimensional autocorrelation function of the departure. The variation of directivity with wavelength of a particular paraboloid is deduced by leaving out of account those two-dimensional Fourier components of the departure with spatial periods less than a wavelength.

Practical steps are considered for unifying testing, adjusting, and design so as to lead to the greatest relaxation of the mechanical tolerances imposed on construction.

Interferometry and the Spectral Sensitivity Island Diagram—R. N. Bracewell (p. 59)

Basic principles of radio interferometry are expounded and a special diagram is established which helps with problems on interferometers, especially those with phase switching or other complications.

The information on a record, or interferogram, made by scanning a compact source or target with an interferometer comprising an antenna with two well-spaced parts, is all in one complex number, the *complex visibility* of the interference fringes. Under appropriate conditions, the complex visibility observed is equal to the *complex coherence* of the field produced by the source between the points occupied by the two elements of the interferometer. (If the elements are not infinitesimal in extent, the complex visibility is equal, instead, to a weighted mean of the values of complex coherence between the pairs of points embraced by the elements.) Furthermore, this quality gives the strength of one *spatial Fourier component* of the source distribution in amplitude and phase. To know all Fourier components would require the use of all spacings—two dimensions, this means all vector spacings.

Measurements at a finite number of spacings yield the *principal solution;* if the source is finite in extent, only certain discrete spacings need be used. *Spectral sensitivity* of antennas depends on the *complex autocorrelation function* of the antenna aperture distribution. For interferometers, the spectral sensitivity is confined to islands in the spatial frequency plane whose shorelines may be delineated by a simple graphical procedure. The *spectral sensitivity island diagram* offers an alternative approach to interferometer problems. In an application of the diagram, it is explained how the resolving power of a Mills cross is not impaired by deleting half of one arm.

Stepped Cylindrical Antennas for Radio Astronomy—L. Ronchi, V. Russo, and G. Toraldo di Francia (p. 68)

In this paper a stepped cylindrical mirror is described which satisfies the following requirements: 1) it is free from spherical aberration for a point source at infinity on the axis, 2) both off-axis spherical aberration and coma vanish for fixed values of the field angle, Ω, and the aperture, $\bar{\alpha}$.

The analysis has been carried out, in the approximation of parageometrical optics, by considering a diffraction grating of the generalized type, equivalent to the stepped mirror.

Three interesting results are obtained, and precisely: 1) independently of the values of Ω and $\bar{\alpha}$, the equivalent diffraction grating has a quasi-parabolic cross section, 2) the off-axis spherical aberration turns out to be negligible over the whole aperture $0-\bar{\alpha}$, for fields angles up to at least 20 degrees, 3) the residual coma turns out to be well corrected, too.

Phase Adjustment of Large Antennas—G. Swarup and K. S. Yang (p. 75)

A technique is described for adjustment of phase paths within large antenna arrays or paraboloidal surfaces which are now in use, or are planned, for radio astronomy. After large paraboloids have been constructed, they suffer distortions which are very difficult to investigate and for which photogrammetry, millimeterwave radar and optical survey have been suggested. A new suggestion, based on experiment at Stanford with phase measurement of long paths, is to place modulated gas discharge tubes, acting as scatterers, at various points on the paraboloidal surface and to monitor the phase path from a signal generator through the feed at the focus to each discharge tube in turn, and back. By means of a second probe, say a dipole situated at the vertex of the paraboloid, it is possible to triangulate on deflections. The feasibility of this scheme has been established in connection with the large Stanford cross antenna which has an aperture of 1339 wavelengths at 9.1 cm. The phase of the modulated reflected wave produced by the discharge tube is determined by adding it to a reference continuous wave of large amplitude and applying the resultant to a receiver sensitive to the modulating frequency. A null is obtained when the two waves are in quadrature. The coherent detection system allows measurement of the phase of the modulated reflection even when its amplitude is below −130 dbm. Using a 10-mw *S*-band signal generator, no difficulty was found in detecting the reflection from a small discharge tube placed 100 feet away from a 3 by 4 inch horn, which is sufficient range for applying the method to large paraboloids.

Centimeter-Wave Solar Bursts and Associated Effects—M. R. Kundu and F. T. Haddock (p. 82)

Most of our knowledge of solar bursts in the meter-wave region has been derived from dynamic spectral observations. Systematic spectral observations have led to the classification of meter-wave bursts into distinct spectral types. No such classification exists for cm-wave bursts because spectral observations are only just beginning. However, recent interferometric measurements have enabled the cm-wave burst to be classified into a number of distinct types. The properties of such different types of cm-wave bursts are discussed in relation to their associated effects.

Dynamic spectral observations of cm-wave bursts obtained at the University of Michigan show that cm-wave burst emission is a broadband continuum, similar in nature to meter-wave type-IV and type-V emission.

Radio Star Scintillation and Multiple Scattering in the Ionosphere—Dimitri S. Bugnolo (p. 89)

Recent experimental evidence of radio star scintillation indicates that multiple scattering effects are of importance in the ionosphere. It is therefore of interest to apply the transport equation for the expectation of the photon density function to this problem. The solution of the transport equation is used to predict the mean-squared scattering angle and corresponding size of the ionospheric irregularities as measured on the earth. The particular example discussed in detail is based on a Gallet model for turbulence in the underside of the *F* layer under night-time conditions. However, it should be noted that the general theoretical results can be applied to any other model as well.

Communications (p. 97)

Contributors (p. 120)

Bio-Medical Electronics

Vol. BME-8, No. 1, January, 1961

Papers from the 12th Southwestern IRE and National PGBME Conference:

An Active Low-Pass Filter for Biological Potential Amplifiers—Gifford White (p. 2)

An active RC filter with an m-derived low-pass response is described. With a cutoff of 45 cps and a sharp attenuation peak at 60 cps, it is particularly suitable for eliminating power-frequency interference from EKG, EEG, or other biological potential amplifiers. It is small in size and requires only one 12AX7 or its transistor equivalent for the active elements. Typical design data and performance curves are given.

A Three-Channel Electromyograph with Synchronized Slow-Motion Photography—R. W. Vreeland, D. H. Sutherland, M.D., J. J. Dorsa, L. A. Williams, C. C. Collins, and E. R. Schottsteadt, M.D. (p. 4)

Muscle transplants are performed to strengthen knee extension in polio patients. The time of contraction of muscles in relationship to gait is under investigation.

Relative activity is evaluated by electromyographic recording of muscle action potentials. Voltages are recorded from three pairs of flexible wire electrodes implainted in the working muscles.

The electromyograph incorporates three commercial preamplifiers, a three-channel electronic switch, a dc amplifier, and a long persistent cathode-ray tube with 3-second sweep.

An image of the cathode ray screen is projected optically via a half-silvered mirror into the lens of a 16-mm movie camera. The camera shoots through the mirror to photograph the walking patient on the same frame with the three muscle traces. Recording speed is 64 frames per second. Frame-by-frame analysis is accomplished by means of a hand-crank projector. This system of recording thus provides simultaneous visualization of muscle electrical activity and the mechanical aspects of gait.

Signal Theory Applied to the Analysis of Electroencephalograms—E. C. Lowenberg (p. 7)

Considered as a special problem in signal analysis, the representation of electroencephalograms (EEG's) involves the problem of determining a unique number for each degree of freedom. A method of representation is usually chosen because of the convenience of making the empirical measurements. One particular method of representation is discussed with emphasis on the problem of making the desired measurements using electronic equipment.

The statistical characteristics of EEG signals do not necessarily include all the significant information. This suggests that the goal of EEG signal analysis should be to represent as uniquely as possible the intervals of interest so that the significant information is not discarded in an averaging process.

A Rational Framework for Interpreting the Behavioral Effects of Atmospheric Ions—Allan H. Frey (p. 12)

Air ionization is a normal phenomenon in the vicinity of electrical equipment. These atmospheric ions apparently have a significant effect upon man's performance. In general, the behavioral observations of past studies indicate that negative ions normalize subjects under some stress and positive ions have debilitating effects.

The experimental studies done to date, however, have been deficient in instrumentation and control of interacting variables, and lacked a rational framework. A first approximation of a rational framework for interpreting previous experiments is offered, and it is hoped it will generate a systematic series of experiments.

The hypothesis offered is concerned with ion effects on adrenocortical secretion and a number of pertinent studies are considered from this standpoint.

A Rapidly Responding Narrow-Band Infrared Gaseous CO_2 Analyzer for Physiological Studies—Lee E. Baker (p. 16)

The rapid determination of CO_2 in expired air is one of the more important measurements in respiratory physiology. Of the CO_2 transducers currently employed, the condenser microphone and thermal conductivity types have several disadvantages. The former is sensitive to mechanical and acoustical vibrations. The latter is sensitive to other gases and lacks response time. In most cases the over-all reliability leaves something to be desired.

The CO_2 transducer developed to alleviate these difficulties employs a Fabry-Perot type interference filter and a lead selenide photoconductive infrared detector. The resulting device has rapid response time, is stable mechanically, and is simple electronically.

Digital Printout System for Whole Body Scanner—J. W. Beattie and G. Bradt (p. 24)

A scintillation scanner has been developed for large-area mapping of high-energy gamma emitting radioisotope distributions in a patient undergoing metabolic studies. An unusual method of operation uses a solenoid-operated electric typewriter as a digital plotter. A three-figure entry of the count observed at each position of the stepwise scan pattern is typed with a decimal point locator to allow five-figure dynamic range. Three numeric type alphabets are incorporated to print each entry without carriage advance. The platen and carriage are synchro motor driven by the scanner. Scan index spacing down to 3/16 inch are possible over 24-inch maximum scan widths. The complete scan is a full-scale quantitative planar map in the form of a matrix through which isocount contours may be located by inspection. The electronic system necessary to accomplish this is described in detail.

An Analog Computer Model for the Study of Water and Electrolyte Flows in the Extracellular and Intracellular Fluids—Walter H. Pace, Jr. (p. 29)

A model has been designed that considers water flow as well as electrolyte flow in the two-compartment system consisting of the extracellular and intracellular fluids. The electrolyte flows are assumed to depend only on the electrolyte concentrations, and the flow water is assumed to depend on the electrolyte concentrations as welt as the relative and absolute quantities of water. The intake rates are arbitrary and the coefficients can be varied to simulate diseased conditions. So far, however, there is not sufficient information available to be sure of the normal values. The model does not claim to explain any of the mechanics of the various flows, but only to give the same effects.

The Center for Vital Studies—A New Laboratory for the Study of Bodily Functions in Man—L. A. Geddes, H. E. Hoff, and W. A. Spencer (p. 33)

A clinical laboratory for monitoring a variety of physiological variables has been developed and is described in the following paper. The faculty was designed around a system of modular interchangeable functional units. From past experience, the flexibility provided by such a system is essential for efficient operation, because frequently it is necessary to change the physiological event being recorded on short notice during a routine diagnostic run. A detailed description of the various transducers, amplifiers and reproducers is presented.

Contributions:

The Average Response Computer (ARC): a Digital Device for Computing Averages and Amplitude and Time Histograms of Electrophysiological Response—W. A. Clark, R. M. Brown, M. H. Goldstein, Jr., C. E. Molnars, D. F. O'Brien, and H. E. Zieman (p. 46)

The Average Response Computer has proved a valuable tool for measuring statistics of neuroelectric activity, particularly of evoked responses. One of the most important aspects of the instrument is its ability to operate "on line," thus enabling the experimenter to observe and modify on the basis of the calculated results while the experiment is in progress. Although the ARC was designed to operate in fixed modes, it has demonstrated a gratifying flexibility in the face of new experimental requirements. With respect to future developments, we feel that greater speed of operation and extension to multiple channels would further extend the range of applications and increase the versatility of the device.

An Electronic Coordinate Transformer for Electrocardiography—R. McFee, A. Parungao, and W. Mueller (p. 52)

A considerable variation exists in the orientation of the hearts of different subjects. These variations make the interpretations of electrocardiograms substantially more difficult. They can be eliminated by a transformation of the "coordinates" of the three components of the heart's dipole moment to a new frame of reference which is rotated with respect to the original one. An electronic instrument for accomplishing this end is described in this article.

A Preamplifier for an Electrocardiograph Monitoring System—James B. Tommerdahl (p. 55)

An approach to a simple, dependable ECG preamplifier designed primarily for use in the operating room is presented. The 60-cps interference is analyzed and a method of reducing this intereference by utilizing the isolation offered by transformer coupling is described. A prototype unit is constructed and tested, and operational characteristics of this unit are presented.

Pulse Modulation in Physiological Systems, Phenomenological Aspects—R. W. Jones, C. C. Li, A. U. Meyer, and R. B. Pinter (p. 59)

In the development of a quantitative understanding of physiological reflex arcs it becomes apparent that the concept of pulse-frequency modulation is bound to play an important part. Not only does the discrete nature of these signals introduce some effects of itself, but possibly more significant in the total picture are the dynamical factors introduced by the modulator and demodulator. There is good reason for feeling that in the iris reflex, for instance, a large share of the dynamic behavior is intimately related to the photoreceptors themselves, and possibly a minor role is taken by the synaptic delays.

Isolated Flying Spot Detection of Radiodensity Discontinuities—Displaying the Internal Structural Pattern of a Complex Object—W. H. Oldendorf, M.D. (p. 68)

A system is described which monitors a point in space and displays discontinuities of radiodensity as the point is moved in a scanning fashion through a plane. A high degree of isolation of this point from other points in the plane is achieved by putting these changes in radiodensity of the moving point into an electrical form which allows them to be separated from all other discontinuities within the plane.

Physics and Physicians—Paul L. McLain, M.D. (p. 73)

The physician of tomorrow will almost certainly have to be a more sophisticated physicist than his predecessors of today or of yesterday. The physician is, perhaps unconsciously and perhaps reluctantly, a physicist to a very significant degree. Students anticipating a career in medicine need to be told and sold this idea since it affects their interest in physics courses during premedical training.

Abstracts of Current Bio-Medical Electronic Research Projects (p. 76)

Announcements (p. 78)

PGBME Affiliates (p. 79)

Circuit Theory

Vol. CT-7, No. 4, December, 1960

Special Issue in Memory of Dr. Balth. van der Pol

In Memoriam (p. 361)

A Tribute—N. DeClaris and L. A. Zadeh (p. 362)

Abstracts (p. 363)

Balth. van der Pol's Work on Nonlinear Circuits—F. L. H. M. Stumpers (p. 366)

Theoretical Aspects of Nonlinear Oscillations—N. Minorsky (p. 368)

This review gives an outline of the modern theory of nonlinear oscillations. This field, originated about four decades ago by the late Prof. B. van der Pol, acquired a considerable momentum in recent years with a gradually increasing number of ramifications, some of which are still in a state of development.

For this reason the selection of topics for this review is narrowed down to matters which have reached a state of a reasonable codification.

It has been assumed that a certain amount of familiarity with these topics is available on the part of the reader so that only essential points are emphasized. Topological methods and analytical methods are written in a condensed manner, while special attention is given to the stroboscopic method, which is probably less known, and which is used extensively later.

A survey of the principal nonlinear phenomena investigated under the assumption of near linearity is given. Phenomena of parametric excitation, subharmonic resonance and synchronization are outlined with some detail, but those of the so-called asynchronous actions are treated less completely as their detailed presentation would lengthen the paper unduly.

The final section of this review deals with the so-called "piece-wise linear phenomena;" it transcends already purely analytic methods and belongs to recent developments concerning nonlinear and nonanalytic oscillations often encountered in the theory of automatic regulation and control.

Periodic Solutions of van der Pol's Equation with Damping Coefficient $\lambda = 0 \sim 10$—Minoru Urabe (p. 382)

A method of computing a periodic solution of van der Pol's equation is devised reducing the problem to the solution of a certain equation by means of Newton's method. For computing the value of the derivative necessary to apply Newton's method, the properties of variation of the orbit in the phase plane are used and, for step-by-step numerical integration of differential equations, a somewhat new method based on Stirling's interpolation formula combined with an ordinary Adams' extrapolating integration formula is used. The periodic solutions are actually computed for $\lambda = 0 \sim 10$ and *the minute but important change of the amplitude described by van der Pol's equation is found.*

Two-Stroke Oscillators—P. LeCorbeiller (p. 387)

A four-stroke oscillator, whether symmetrical or moderately dissymmetrical, is one in which the linear, conservative elements receive energy from the source two times per period; such are typically a Class A vacuum tube oscillator, a Class C push-pull oscillator, or a clock with anchor escapement. This paper presents a number of nonlinear, second-order differential equations which correspond to two-stroke oscillators in which the source is active or strongly active only once per period; such as a Class C oscillator. It is hoped that this second type will lead to a better understanding of a number of oscillations which it has not been possible to interpret so far by means of the four-stroke model.

A Method of Analysis in the Theory of Sinusoidal Self-Oscillations—R. V. Khokhlov (p. 398)

The article is devoted to the theory of weak resonance action on self-oscillating systems. The theory is based on the method of secondary-simplification of "shortened" equations for amplitudes and phases of the self-oscillating process. A series of new results is obtained. These results are taken as a basis for the creation of new radiotechnical devices.

Frequency Entrainment in a Self-Oscillatory System with External Force—C. Hayashi, H. Shibayama, and Y. Nishikawa (p. 413)

This paper deals with forced oscillations in a self-oscillatory system of the negative-resistance type. When no external force is applied, the system produces a self-excited oscillation. Under the impression of a periodic force, the frequency of the self-excited oscillation falls in synchronism with the driving frequency within a certain band of frequencies. This phenomenon of frequency entrainment also occurs when the ratio of the two frequencies is in the neighborhood of an integer (different from unity) or a fraction. Under this condition, the natural frequency of the system is entrained by a frequency which is an integral multiple or submultiple of the driving frequency. In this paper, special attention is directed toward the study of periodic oscillations as caused by frequency entrainment. The amplitude characteristics of the entrained oscillations are obtained by the method of harmonic balance, and the stability of these oscillations is investigated by making use of Hill's equation as a stability criterion. The regions in which different types of entrained oscillation, as well as beat oscillation, occur are sought by varying the amplitude and frequency of the external force. The theoretical results are compared with the solutions obtained by analog-computer analysis and found to be in satisfactory agreement with them.

Periodic Solutions of Forced Systems Having Hysteresis—H. D. Block (p. 423)

In Section I, the motion of a mass on a material rod is discussed. The stress-strain law exhibits a hysteresis effect, so that the stress at any time is a function of the whole strain history. A "rupture restriction" which limits the magnitudes of the admissible displacements, velocities, and accelerations is also discussed. It is shown that the appropriate formulation of the phenomenon is in terms of function spaces and mappings of function spaces. The system is forced with a periodic forcing function of period Ω and the problem we set ourselves is to find solutions of period Ω.

In Section II, there is presented first a brief elementary introduction to "Banach Space for Engineers." Then, a purely mathematical theorem is proved concerning the convergence and the speed of convergence of an iterative method for solving a problem in mappings of a Banach Space, and the existence and uniqueness of solutions to that problem.

In Section III, the problem posed in Section I is identified with the various concepts introduced in Section II, thus furnishing rigorous proof of the existence and uniqueness of the periodic solution sought in Section I, a computational method for numerically evaluating the solution, and bounds on the errors of approximation. The problem dealt with is quite general, including, in addition to the hysteresis effects, as special cases, the equations of Hill, Mathieu, Duffing, van der Pol (with a forcing term), and a quite general class of nonlinear ordinary differential equations. The method is also applicable to partial differential equations.

Multistable Circuits Using Nonlinear Reactances—S. Kumagai and S. Kawamoto (p. 432)

This paper presents some results in the asymmetric resonant circuit, which is constructed by applying a dc voltage E_0 and a sinusoidal voltage $E_1 \sin \omega t$ to a series resonant circuit containing a nonlinear capacitance. The circuit is analyzed using the Ritz-Galerkin method. Assuming that the first approximation for the charge q takes on the form $Q_0+Q_1 \sin(\omega t+\theta)$, the curves $\omega-Q_1$, E_1-Q_1 and E_0-Q_1 are obtained. It is shown that the asymmetric circuit is a tristable circuit with respect to these parameters, while the usual ferroresonant circuit is a bistable circuit. The influence of the dc voltage E_0 upon the circuit is studied in particular, and an interesting phenomenon, called "residual jump phenomenon," may occur in the circuit only when E_0 is changed and others fixed.

Furthermore, the study shows how to construct a multistable circuit using nonlinear reactances. Combining some nonlinear reactances with suitable bias voltages, circuits having two, three, four or five stable solutions are obtained.

Amplification in Nonlinear Reactance Networks—W. R. Bennett (p. 440)

Sufficient conditions for validity of the Manley-Rowe equations in a classical nonlinear reactive network are shown to be conservation of energy and proportionality of average power with frequency. It is shown by counter example that conservation of energy alone is insufficient. A sufficient condition for a quantum mechanical maser model is found to be equilibrium of state populations. In this case conservation of energy follows as a consequence from the equilibrium condition, but proportionality of power with frequency is not required.

The Transient Behavior of Nonlinear Systems—Francis H. Clauser (p. 446)

It is shown that the classical perturbation procedure for treating nonlinear systems leads to solutions expressed as Fourier-like series with slowly varying coefficients. These slowly varying coefficients contain the information about the long term behavior of the system. Inconsistently, the classical perturbation procedure expresses these coefficients as power series, a mode of expression which has notoriously poor long term validity.

An operational procedure is presented for treating oscillations having slowly variable amplitudes and frequencies. An extension of the usual impedance concepts is presented for expressing the frequency characteristics of both linear and nonlinear elements when oscillations with many frequencies are present simultaneously and when these oscillations vary in both frequency and amplitude. From these methods, a perturbation procedure is devised which permits the behavior of systems to be computed with any order of accuracy, using only the algebraic processes which are characteristics of operational procedures. This procedure avoids expressing its results in terms of the local time. Instead, it expresses them in terms of the fundamental characteristics of the oscillations which are present. As a consequence, the final solutions have the much desired long term validity and they may be used to obtain asymptotic estimates of the behavior of the system. The method is able to treat systems containing nonlinear perturbing elements and elements which we have described as moderately nonlinear.

By means of examples it is shown that it is a straightforward process to treat systems to second order accuracy. This level of accuracy covers a large number of the intercoupling effects that characterize the more sophisticated nonlinear phenomena.

Analysis and Synthesis of Nonlinear Systems—Henri B. Smets (p. 459)

The input-output relation of linear systems (convolution integral) is generalized to a class of nonlinear systems. This class is represented by analytic functionals as studied by Volterra and Fréchet.

The analysis can be performed by measuring the response of nonlinear systems to series of impulse functions. The synthesis involves linear systems, zero-memory nonlinear systems and multiple multipliers in the general case, noninteracting linear and zero-memory nonlinear systems in many practical cases.

Physically, the class of analytical functionals describes systems obtained by cascading noninteracting linear and zero-memory nonlinear systems in open or closed loop configuration.

Orthogonal representations of nonlinear systems are considered; for bounded signals and in particular for sinusoidal signals, the Tchebycheff polynomials representation is shown to be especially convenient.

The Problem of Quality for Nonlinear Self-Regulating Systems with Quadratic Metric—A. M. Letov (p. 469)

The systems considered in this paper are characterized by differential equations of the form

$$\dot{x}_k = \sum_{\alpha} b_{k\alpha} x_\alpha + f_k(x_1, \cdots, x_n, t) \qquad (k = 1, \cdots, n),$$

which are defined over a region X of Euclidean space E_n with metric $R^2 = \sum_{i=1} x_i^2$, and with t ranging over some interval T. The $f_k(k+1, \cdots, n)$ are assumed to be such that 1) $f(0, \cdots, 0, t) \equiv 0$ and 2) there exist positive constants L_k such that

$$|f_k(x_1, \cdots, x_n, t)| \leq L_k R$$

for all points in X and all t in T.

The problem of quality means the problem of determining the values of m adjustable parameters $p_i, \cdots, p_m$ in the b_{k_α} and f_k in such a way as to result in a rapid return to equilibrium of the representative point in phase-space subject to a limitation on the amount of overshoot. This problem is formulated in precise terms, and a method of solution for it is indicated. As an illustration, the method is applied to a problem in regulation which was formulated by Bulgakov.

On Automatic Controls—Solomon Lefschetz (p. 474)

The problem of automatic controls has been treated more or less linearly by a number of Soviet authors (Lurye, Letov, Yacubovich). Here a treatment is presented taking into account the nonlinearity of the regulated system. Certain consequences of this nonlinearity are also made clear.

Some Remarks on Oscillators Driven by a Random Force—Mark Kac (p. 476)

A brief and partly heuristic discussion of the problem of spacing of zeros of the displacement of an oscillator driven by a random force is given. Although no explicit results have been obtained, the problem is reduced to a study of a certain integral equation and equivalently, of a partial differential equation with a peculiar boundary condition. The boundary condition has previously been conjectured by Uhlenbeck and Wang.

On Nonlinear Networks with Random Inputs—Y. H. Ku (p. 479)

The paper attempts to combine the Wiener-Bose method for characterizing and synthesizing nonlinear systems with the Ku-Wolf method for analyzing nonlinear systems with random inputs.

A simple partition theory is first presented. It is shown that a general nonlinear system can be partitioned into two portions: one linear portion with memory or storage, and one nonlinear portion which may also include linear elements. The partition method, the Taylor-Cauchy transform method, and the transform-ensemble method are developed, and illustrated by an example. It is shown that the output of a nonlinear system to a random input can be expressed as the summation of $a_n q_n(t)$, for $n=0, 1, 2$, and so on, where $q_n(t)$ depends upon the form of the functional representation of the modified forcing function or the actuating signal, and a_n denotes a set of random variables which are related to the statistics of the random input.

Wiener's theory of nonlinear systems is then reviewed. The Wiener-Bose method is outlined as follows. Let the output of a shot-noise generator be the standard probe for the study of nonlinear systems. The standard random input is fed to a Laguerre network giving Laguere coefficients $u_1, u_2, \cdots$. The output of the overall system is then expressed as Hermite function expansions of the Laguerre coefficients. By the ergodic hypothesis it is then possible to express the output as the summation of $A_\alpha V(\alpha) \cdot e^{-\mu^2 2}$. By taking the time average of $c(t) V(\alpha)$, where $c(t)$ represents either the actual output or the desired output, we get the coefficients A_α, which characterize the actual system or the system to be designed. Knowing A_α, the synthesis procedure is obtained from the summation of $A_\alpha V(\alpha)$.

By combining the output $c(t)$, obtained from the Ku-Wolf analysis, with the output $V(\alpha)$ from the Laguerre network, and Hermite function generator, we can get the characterizing coefficients $A\alpha$. It is suggested that the correlation of a_n, a set of random variables related to the random input, and A_α, the characterizing coefficients, may shed light on a unified approach for the analysis and synthesis of nonlinear systems with random inputs.

The Method of Determining Optimum Systems Using General Bayes Criterion—V. S. Pugachev (p. 491)

A method for obtaining an optimum system using general Bayes criterion is developed. This method is applicable to the cases in which a signal to be estimated depends on certain finite-dimensional vector U, and where the input is the sum of a function depending on the vector U and a normally distributed noise which is independent of the vector, or may be reduced to this form by some nonlinear transform. The method is also applicable to some problems in which U is a vector with countably infinite number of components. As a special case the method yields the solution previously given in which the input is a linear function of U. The method affords effective determination of optimum systems designed for the detection and estimation of signals in the presence of noise using various practically adequate criteria under rather general conditions. The optimum system given by the method is in general nonlinear, but in some special cases it may be linear. In particular, the optimum system is linear if the signal and the input are linear functions of components of the vector U, which is also normally distributed or is an unknown nonrandom vector which may assume any value, and the loss function is any function or functional of the difference between the signal and its estimate (*i.e.*, of the system error). The application of the method to the problem of signal detection and to certain problems of signal estimation are given.

Statistical Theory of Systems Reducible to Linear—V. S. Pugachev (p. 506)

A statistical theory for nonlinear systems, whose operators are reducible to linear, is given. The analysis as well as the synthesis problems of such systems are considered.

On Coding Theorems for Simultaneous Channels—J. Wolfowitz (p. 513)

This paper deals with the lengths of codes for several simultaneous channels in a general formulation. The paper is almost self-contained, and requires for its reading no prior knowledge of information theory.

On the Method of Averaging—Jack K. Hale (p. 517)

The method of averaging of van der Pol was devised to obtain periodic and almost periodic solutions of quasi-linear systems of differential equations. A theorem is stated for a particular case where this method has been justified mathematically and an example is given to illustrate the results.

Some Extensions of Liapunov's Second Method—J. P. LaSalle (p. 520)

In the study of the stability of a system, it is never completely satisfactory to know only that an equilibrium state is asymptotically stable. As a practical matter, it is necessary to have some idea of the size of the perturbations the system can undergo and still return to the equilibrium state. It is never possible to do this by examining only the linear approximation. The effect of the nonlinearities must be taken into account. Liapunov's second method provides a means of doing this. Mathematical theorems underlying methods for determining the region of asymptotic stability are given, and the methods are illustrated by a number of examples.

Differential Equations with a Small Parameter Attached to the Higher Derivatives and Some Problems in the Theory of Oscillation—E. F. Mischenko and L. S. Pontryagin (p. 527)

This paper presents a brief review, for the most part, of the author's results concerning systems of differential equations of the form

$$\epsilon \dot{x}^i = f^i(x^1, \cdots, x^k, y^1, \cdots, y^l) \qquad i = 1, 2, \cdots, k$$

$$y^j = g^j(x^1, \cdots, x^k, y^1, \cdots, y^l) \qquad j = 1, 2, \cdots,$$

where ϵ is a small positive parameter. The emphasis is on periodic solutions of such systems which are close to discontinuous solutions. Such periodic solut ons are mathematical representations of relaxation oscillations which are encountered in various mechanical, electrical and radio systems.

On the Number of Stable Periods of a Differential Equation of the van der Pol Type—J. E. Littlewood (p. 535)

Van der Pol's differential equation with forcing term can, for some values of the parameter b, have stable periodic solutions of two distinct periods. The paper examines whether, with a generalization of the equation not too unlike the original, there can be more than two distinct periods. The answer is affirmative. The example (with three periods—in principle, there can be many), while within the permissible limits, is very sophisticated of its kind. But if the phenomenon can happen at all, it may be presumed to happen in much simpler cases.

Directions of Mathematical Research in Nonlinear Circuit Theory—Richard Bellman (p. 542)

In this paper we wish to present a potpourri of problems of some interest and difficulty arising in the field of nonlinear circuit theory. Perhaps the only sensible way to catalog scientific problems is in terms of "solved or unsolved." Yet this classification is itself a very subjective one, dependent upon the times and the fashions. Recall the dictum of Poincaré that the solutions of one generation are the problems of the next.

In this paper, we have attempted, for the sake of convenience, to group categories of problems under the headings of "descriptive," "control," "stochastic," and so forth. Convenient as some of this nomenclature is, it should be regarded with a certain amount of suspicion. Most significant problems blithely cut across these artificial boundaries within fields of specialization, and within science itself.

In these days of rapidly and dramatically changing technology it would be rather brash to attempt to predict the type of mathematics that will be most urgently required even ten years from now. It is, however, fairly safe to look about and note the requirements of the present and of five years back. The difficulties that abound render a certain time lag inevitable, and it may well be that new scientific developments may render fields obsolete and mathematical solutions for problems within those fields unnecessary before they are even obtained.

Reviews of Current Literature (p. 554)

Annual Index (follows p. 555)

Electron Devices

Vol. ED-8, No. 1, January, 1961

Hollow-Beam Focusing with Electrostatic and Periodic Magnetic Fields—Y. Hiramatsu, G. Wade, and C. B. Crumly (p. 1)

A new method of focusing a hollow cylindrical electron beam is presented. The focusing system consists of a cylindrical center conductor inside the beam, a cylindrical outer conductor enclosing the beam, and a series of periodic magnets outside the tube. A radial electrostatic field between the conductors provides an outward force on the electrons. The periodic magnetic field produces an inward force on the electrons. The inward and outward forces can be adjusted to provide a balance of all the forces acting on the electrons at both boundaries of the beam by choosing the electric and magnetic fields properly.

An approximate analysis has been made and is presented which gives necessary design information. A number of curves are presented which are useful in designing focusing systems of this type.

Experimental results on a beam tester show that current transmission of over 90 per cent for perveance up to 11 micropervs can be obtained readily. The adjustments are not critical and the performance is very stable.

A Coaxially Packaged MADT for Microwave Applications—J. D. McCotter, M. J. Walker, and M. M. Fortini (p. 8)

A coaxially packaged transistor capable of delivering greater than 11 db of power gain at 1000 Mc, with a resultant maximum frequency of oscillation of 3500 Mc, has been developed. This device is a p-n-p micro-alloy diffused-base transistor (MADT). The principal difference between this device and a standard high-frequency MADT amplifier is the reduction of electrode size and use of a coaxial construction. The parasitic elements, r_b', and emitter and collector transition capacities, have very striking effects. Also, the excess phase of alpha at alpha cutoff, as described by Thomas and Moll, can be very large (150° on this device); for this reason, f_T rather than f_{c_α} should be used as the figure of merit for graded-base transistors. Because of this excess phase, the value of K (0.85 for homogeneous-base transistors), which is used to relate f_T to f_{c_α}, can be as low as 0.43 in graded-base transistors of this type.

Correction to "A Small-Signal Field Theory Analysis of Crossed-Field Amplifiers Applicable to Thick Beams"—Bernard Hershenov (p. 12)

Theoretic Curves of Drift Transistor Current Gain—George E. Terner (p. 13)

Intrinsic common-base, short-circuit current gain analysis of drift transistors may be aided by means of a simplified approximation equation. The accuracy of the equation may be controlled by the investigator. A graphic solution for determining this parameter of moderate drift field transistors may be obtained by using the arcs of circles. The interrelation between the graphic analysis and the theoretic approximation provides a flexible yet accurate method of analyzing this parameter.

Determination of Physical Parameters of Diffusion and Drift Transistors—M. B. Das and A. R. Boothroyd (p. 15)

The dynamic properties of drift and diffusion transistors are studied under both low- and high-level injection conditions in terms of the excess carrier charge in the base region. Subject to the assumptions of effectively one-dimensional device geometry with exponential impurity grading and collector conductivity much greater than that of the base, methods of determination of the main physical and high-frequency equivalent-circuit parameters of transistors are presented, utilizing the bias dependence of excess carrier charge in the base and space charge in the collector-depletion region. It is shown that measurement of the base transit time and the junction capacitances under low-level injection conditions enables the following physical parameters to be determined: base field parameter $m = \Delta V/(kT/q)$, base width, base impurity distribution, emitter area, collector-depletion layer width. All the measurements are carried out at relatively low frequencies.

Solutions for the base charge distribution, and hence charge-defined transit time, have been derived for the cases of exponential and erfc impurity grading under high-level injection conditions, assuming one-dimensional device geometry, constant base cross-sectional area, and D and μ independent of injection level. Experimental results have been found to differ greatly from the theoretical expectations based on these assumptions, the drift transistor showing greater and the diffusion transistor less than the predicted dependence on injection level. Explanations for the observed effects have been put forward in terms of reduction of emitter area and of D and μ at high injection levels.

Start-Oscillation Conditions in Modulated and Unmodulated O-Type Oscillators—J. E. Rowe and H. Sobol (p. 30)

The starting conditions for the O-type backward-wave oscillator are computed for large values of C, QC and d, using both digital and analog methods. A general method of solving complex polynomials called the "downhill" method is applied both to the secular equation and then to the RF voltage equation to obtain starting conditions. The analog computer is used to solve simultaneously, by trial and error method, the linear circuit and ballistic differential equations. The analog method is applied to the modulated BWO in order to determine the effects of modulations on the starting conditions. Extensive calculations of BWO starting conditions have been made for a wide range of C, QC and d.

Electrostatic Electron Beam Couplers—R. H. Pantell (p. 39)

Electrostatic electron beam couplers can be used in conjunction with a parametric amplifier to produce low-noise electron beam amplification. The characteristics and design of both traveling-wave and resonant couplers are considered. The latter are broader-band and shorter than the traveling-wave version; however, the traveling-wave coupler does not require critical load adjustment and is electrically tunable.

An important advantage of the electrostatic fast-wave coupler over the magnetic version considered by Cuccia is the elimination of the magnetic field.

A High-Efficiency Klystron with Distributed Interaction—M. Chodorow and T. Wessel-Berg (p. 44)

This paper describes a theoretical and experimental investigation of a special form of a three-cavity klystron amplifier having shorted sections of a slow-wave structure as resonators. Although the behavior basically is similar to that of a narrow-gap klystron, improved performance is obtained due to distributed interaction and higher cavity characteristic impedance. Higher efficiency and larger gain-bandwidth product, as predicted by theory, were observed experimentally with a pulsed S-band distributed klystron operated at a maximum beam voltage of 22 kv and a beam current of 3.5 amperes. Saturation efficiencies of approximately 50 per cent at 18 db gain and 2 per cent half-power bandwidth, and small-signal gain of 40 db at 0.5 per cent bandwidth, were measured.

Small-signal behavior is in good agreement with the space-charge-wave theory. At large-signal levels, experimental results and simplified kinematic theories agree qualitatively.

The Thermal Emissivity of Some Materials Used in Thermionic Valve Manufacture—C. M. Cade (p. 56)

The laws governing thermal radiation are briefly reviewed and methods of measuring emissivity are described. The apparatus used by the author is described and an account of possible sources of error is given. Results of other workers are quoted wherever available, and the thermal emissivity over the useful working temperature range is given for the following materials.

Metals	Alloys	Other Surfaces
Iron	Nichrome	BaO-SrO on Nickel
Molybdenum	Nimonic	Carbonized Nickel
Nickel	Moly-Tungsten	Titania on Nickel
Tantalum		Titania on Iron
Tungsten		Aluminized Iron
Gold		Titanium Hydride on Molybdenum
Silver		Zirconium Preparations on Ni, Mo and Fe
Platinum		Alumina
		Carbon

Magnetic-Field Pickup for Low-Frequency Radio-Interference Measuring Sets—M. Epstein and R. B. Schulz (p. 70)

A magnetic-field pickup has been developed utilizing the Hall effect in intermetallic semiconductors. Unlike a loop pickup, the sensor responds to magnetic flux density and thus is independent of frequency. Due to its extremely small size, it makes possible the measurement of magnetic fields in constricted regions. When used in conjunction with ferrite flux collectors, its sensitivity is 10^{-7} gauss in the range of 30 cps to 15 kc. Details of design and construction are given.

Transformation of Fluctuations Along Accelerating Crossed-Field Beams—T. Van Duzer (p. 78)

Equations are derived to express the ac potential difference and the transformation of fluctuations of velocity and current between two arbitrary planes along an accelerating crossed-field electron stream. The system of equations, after being simplified by the assumption of zero total ac current, is applied to the special cases of the temperature-limited diode, the space-charge-limited diode, and a diode in which the beam enters with appreciable average velocity. Finally, the open-circuit equations are applied to an approximate model of a beam in a crossed-field electron gun.

A new mechanism of growth, peculiar to the crossed-field beam, is discussed as a possible explanation of the observed large sole current in beam-type magnetron amplifiers and related devices.

An Analysis and Representation of Junction Transistors in the Saturation State—Z. Wiencek (p. 87)

Three diffusion processes are used to analyze the transistor behavior in Region III. This leads to a new equivalent circuit representation which is a superposition of the active-state and saturation-state models. Saturation state of the transistor is understood here as a state in which both emitter and collector junctions are so biased to obtain a uniform distribution of the minority carriers in the base. Saturation can be treated separately and be represented by a new independent model. Transient analysis made on these models, representing saturation and active states, leads us to the storage and decay phenomena, and storage and decay times agree with those calculated by others.

Contributors (p. 96)

Engineering Management

Vol. EM-7, No. 4, December, 1960

About This Issue—The Editor (p. 123)

Engineering Program Planning and Control Through the Use of PERT—Jerome Pearlman (p. 125)

An application of the recently-developed PERT system is described. Techniques for use in planning technical objectives for a project are discussed. The concept of design review is related to the setting of objectives. Time and cost estimating for program planning and control are discussed. The experience of one organization with the initiation and development of the PERT system is described. The need for gaining acceptance by the working engineer is stressed.

Product Assurance—E. S. Winlund (p. 134)

Product assurance is concerned with economy, performance, and reliability. It provides the tools and techniques with which the project engineer may design economically optimal systems and equipment, and with which he may allocate his own efforts economically. Product assurance puts "reliability" into a realistic economic perspective. This report outlines the problems of growing product complexity, earlier obsolescence, and design immaturity, and recommends specific feedback loops to maximize maturity at each design phase. A centralized Assurance group digests and organizes data from all sources and develops design "tools," providing a broad service to design engineers. Management is provided a Product Assurance Report showing progressive cost reduction and reliability improvement, both in terms of annual savings to the product user.

The Management of Research Services—Jerome Kurshan (p. 141)

The organization and function of a Research Services Laboratory are described. This laboratory groups together service functions that require research caliber personnel and centralizes major items of capital research equipment. Advantages to both the Research Services Laboratory and to the rest of the research function are obtained by having this activity report to the Director of Research. By means of a project order numbering system, accounting for these services can be handled very simply from the user's point of view while adequate accountability and control are maintained. Service groups do well to avoid a primary responsibility for administering government contracts since this would limit the availability of services to the research staff. Good administration in a research service group calls for striking the proper balance between overload and idleness, between short- and long-range jobs and between requested and self-generated research. Personnel relations differ from those in nonservice groups and the recruiting problem is greater. At the same time, Research Services is an excellent assignement for developing management talent. It is important that a Research Services Laboratory grow with the activities it supports, and there are a number of ways in which expansion into new service roles might occur with profit.

Studies of Education for Science and Engineering: Student Values and Curriculum Choice—G. K. Krulee and E. B. Nadler (p. 146)

The findings discussed in this report are drawn from a study of student backgrounds and values at a school of science and engineering. The results indicate many similarities in background for students in either science or engineering and some interesting differences when comparisons are made to certain liberal arts colleges. Aspirations and expectations that lie behind an initial commitment to a career in science and engineering are discussed, and contrasts among the values held by students in the various curricula are emphasized.

Role Adaptation of Scientists in Industrial Research—Simon Marcson (p. 159)

An interview study was made in the central research laboratory of a large electronics company on problems in recruiting and integrating scientists into the laboratory. The recruiting procedure is described. The mutual expectations of recruit and organization are discussed. Several patterns of career development are traced, including: dedication to scientific research; initial orientation toward administration within the company; later interest in administration after a successful scientific career due to 1) financial and prestige attractions, or 2) competitive pressure in research.

Research on a Research Department: An Analysis of Economic Decisions on Projects—Carl R. Gloskey (p. 166)

A case study was made of the way in which economic analyses were carried out on research and development projects in a medium-sized company. The flow diagram for a typical research project is presented. Interviews with key executives in the company and the analysis of a number of discontinued or unsuccessful projects provided data on who made what economic decisions during the life of a project. Several gaps were found in the decision-making procedure and recommendations were made for improvement. A number of new management control forms were developed and adopted by the company.

About the Authors (p. 173)

PGEM Affiliates (p. 175)

Annual Index (follows p. 175)

Engineering Writing and Speech

Vol. EWS-4, No. 1, January, 1961

A New Task for the Technical Writer—Programming Teaching Machines—Gustave J. Rath (p. 3)

Teaching machines are described and basic psychological principles behind them are discussed. The implications of programming teaching machines to the technical writer are outlined.

Human Responses—A Vital Link in Communications Progress. Part I—Beverly Dudley (p. 5)

An interpretation of the communications process is given in terms of stimulus and response. Part I deals with communications in the physical and behavioral sciences and with the nature of stimulus/sensation under various sensory conditions. Part II, to be published in the next issue of the Transactions, will deal further with the basic processes of communication and will cite an example of underwater communication between submarines.

The Rightful Role of Management in Technical Communications—Irving J. Fong (p. 14)

How long conference audiences will tolerate poor oral communication will probably depend on how much management is willing to participate. Today, technical competence alone is not enough in a conference presentation. This paper describes the inception of a PGEWS program that provides for a direct approach to this problem in which management plays a major role. It is a program that enlists the cooperation of various departments, provides suggestions for in-plant training sessions, offers pointers for initiating dry-runs of papers, and describes aids for the pre-evaluation of speakers and how to prepare potential authors for paper presentations.

The Role and Duty of the Engineer-Writer—E. R. Hagemann (p. 17)

For efficient written communication, an engineer or scientist must avoid gobbledygook, argot, useless repetition and Chinese-box constructions. Another common but basic fault is lack of transitional devices.

Proposed System of Periodic Reports to Government Agencies—Charles Süsskind (p. 19)

A new scheme is proposed for simplifying the preparation, submission, and distribution of quarterly and other periodic reports required under most technical and scientific government contracts. Each organization would submit a single report each quarter covering work under all contracts in a given field, with suitable acknowledgments of the support of each sponsor, standardized distribution, and time-saving elimination of contradictory reporting practices.

Information Theory!—Gilbert Kelton (p. 21)

A theoretical and experimental study was conducted to determine the factors affecting internal communications in fifty large organizations. The interrelationships between the various factors were also determined, and correlations between echelon and dissemination time and between echelon and reliability were established. Experimental results confirm the standard equations for data dissemination.

A Comment on "Information Theory!"—B. Dudley (p. 25)

Comment on Dudley's Comment—G. Kelton (p. 26)

Book Reviews (p. 27)

Index, Volumes 1 to 3 (p. 28)

The Authors (p. 30)

Information Theory

Vol. IT-7, No. 1, January, 1961

Single Error-Correcting Codes for Nonbinary Balanced Channels—C. W. Helstrom (p. 2)

Close-packed, single error-correcting codes are studied, the letters of which are N-tuples of M-ary digits, where M is the power of a prime. The length N of the letters must be given by $N=(M^k-1)/(M-1)$, where k is an integer. A balanced communication channel, for which all errors in a transmitted digit are equally likely, is defined and a physical model given. The probability of correct reception of the code letters and the rate with which they transmit information in a balanced channel are calculated. This involves deriving formulas for the numbers of code letters having various numbers of 0's. Numerical results are given for a quaternary code and are extended to the case where the quaternary channel has a null zone, so that erasures as well as errors may occur. For the type of signals and noise assumed, the balanced channel without a null zone is found to yield the better performance.

Linear-Recurrent Binary Error-Correcting Codes for Memoryless Channels—William L. Kilmer (p. 7)

This paper concerns the analysis of recurrent-type, parity-check, error-correcting codes for memoryless, binary symmetric channels. These codes are defined to consist of message sequences augmented by insertions of r successive parity digits every b successive message digits. An analysis framework is established for the codes which consists mainly of a parity check matrix [M] and a message difference vector (N). Within this framework, a decoding scheme is developed which renders the codes capable of correcting any set of $\overline{\leq}e$ errors in m/b successive $(b+r)$-digit blocks of coded message sequence, where e is maximized over all parity-check codes having the same redundancy ratios and maximal lengths of dependence among their digits. An example is given of a linear-recurrent code which has a lower probability of error than the best comparable block code, and several outstanding problems are discussed.

Probability Density Functions for Correlators with Noisy Reference Signals—G. M. Roe and G. M. White (p. 13)

Recently, correlation functions have had to be considered where both the reference waveform, which is usually the desired signal, and the input waveform are masked by different samples of additive noise. In this article we derive the probability density function for the random variable β where

$$\beta = \sum_{i=1}^{k} (As_{i,x} + N_{i,x})(Bs_{i,y} + N_{i,y}).$$

The $s_{i,x}$ and $s_{i,y}$ are the signal components, and $N_{i,x}$ and $N_{i,y}$ are samples of Gaussian noise.

Exact expressions involving Bessel and Whittaker functions are given for several cases. Asymptotic expressions allow $W(\beta)$ to be plotted when these exact expressions cannot be obtained or conveniently evaluated.

Demodulation of a Phase-Modulated Noise Carrier—Phillip Bello (p. 19)

In this paper, an analysis is made of a communication system in which the information-bearing signal phase modulates a Gaussian noise carrier. The effect of additive Gaussian noise and linear filtering on the first-order statistics of the receiver output noise and on the character of the output signal are determined. It is shown that with regard to determining the distortion of the output signal, the system may be replaced by a single linear filter whose input is the modulated signal impressed on a sinusoidal rather than noise carrier. In this way, conventional FM techniques may be used for the determination of signal distortion.

Minimum-Redundancy Coding for the Discrete Noiseless Channel—Richard M. Karp (p. 27)

This paper gives a method for constructing minimum-redundancy prefix codes for the general discrete noiseless channel without constraints. The costs of code letters need not be equal, and the symbols encoded are not assumed to be equally probable. A solution had previously been given by Huffman in 1952 for the special case in which all code letters are of equal cost. The present development is algebraic. First, structure functions are defined, in terms of which necessary and sufficient conditions for the existence of prefix codes may be stated. From these conditions, linear inequalities are derived which may be used to characterize prefix codes. Gomory's integer programming algorithm is then used to construct optimum codes subject to these inequalities; computational experience is presented to demonstrate the practicability of the method. Finally, some additional coding problems are discussed and a problem of classification is treated.

A Note on Signal-to-Noise Ratio in Band-Pass Limiters—Charles R. Cahn (p. 39)

A simplified analysis is presented to explain physically the change of signal-to-interference ratio which occurs in a band-pass limiter. The analysis utilizes the concept of sideband resolution into symmetric and anti-symmetric parts and considers only the asymptotic case where the signal-to-interference ratio is small in comparison with unity. Wide-band correlation-detection systems are discussed, as well as ordinary band-pass systems.

The important conclusion is reached that the degradation is highly dependent on the statistics of the interference amplitude fluctuations. However, when the signal is weak compared to the interference, the maximum possible degradation is 6 db and occurs for constant-amplitude interference.

Degradation with noise interference in a wide-band correlation-detection system has been obtained for arbitrary signal and noise bandwidths. It is found that the degradation ranges between 0.6 db and 1.0 db, the latter figure being for the case where the signal bandwidth is greater than approximately three times the noise bandwidth.

Recognition of Membership in Classes—George S. Sebestyen (p. 44)

This paper presents an approach to the general problem of recognition of membership in classes which are known only from a set of their examples. A geometrical approach is taken where membership in classes is regarded measurable by metrics with which a set of points, representing different members of the same class, may be brought "close" to one another. For the case where classes are Gaussian processes, the method described herein and that of decision theory are found to agree. A practical application of the method to the automatically "learned" recognition of spoken numerals is described.

Correction to "Correlation Detection of Signals Perturbed by a Random Channel"—Thomas Kailath (p. 50)

Correspondence (p. 51)

Contributors (p. 55)

Abstracts (p. 56)

Book Reviews (p. 57)

Instrumentation

Vol. I-9, No. 3, December, 1960

Abstracts (p. 308)

Switching Levels in Transistor Schmitt Circuits—T. J. Galvin, R. A. Greiner, and W. B. Swift (p. 309)

The operation of a Schmitt trigger circuit using transistors is briefly reviewed. A graphical method of calculating switching levels is presented which converges rapidly. Sensitivity of switching levels to changes in element values is analyzed by an approximate analytical method and by experiment.

A Simple Comparator for the Intercomparison of Unsaturated Standard Cells—Richard C. Bean (p. 313)

A solution to one of the contemporary problems of standards laboratories in industry is presented in the form of a simple standard cell comparator that can be constructed from easily obtained components. The details of the construction and the method of calibration as well as some information on the recommended accessories are described. The major limitations and some possible methods of overcoming them are also given.

Sferics Monitoring System—E. G. Goddard (p. 315)

A sferics monitoring system was developed for use at three arctic sites to study sferic population; the diurnal, seasonal, and auroral effects on VLF propagation; and the locations of sferic sources.

The system is an integrated assembly of electronic, photographic, and electromechanical equipment capable of being operated in several different modes to gather the following data:

1) number of sferics occurring in four 20-db-intensity levels in four 6-hour time blocks,
2) bearing of individual sferics,
3) waveform of individual sferics,
4) time-integrated bearing patterns,
5) noise level and signals in the 12- to 30-kc range.

A secondary frequency standard at each site is checked against WWV or WWVH daily, and provides a common time reference for the records from all sites. A modified Watson-Watt direction-finder system with a crossed-loop antenna provides instantaneous bearing. Instantaneous sense is achieved by combining the crossed-loop signals with the signal from an omnidirectional antenna. In addition to the sense function, the latter antenna also provides signal energy to a scanning receiver, a multi-threshold-time-block events counter, and a signal waveform channel.

A Simple Method of Measuring Fractional Millimicrosecond Pulse Characteristics—Oscar L. Gaddy (p. 326)

A method of measuring fractional millimicrosecond pulse characteristics is described which is in some respects similar to the sampling oscilloscope. The pulse that is being measured is split into two transmission paths and applied to the two inputs of a wide-band coincidence circuit. One of the applied pulses is delayed in time and the output voltage of the coincidence circuit is measured with a low bandwidth oscilloscope and plotted vs delay. From this curve, the pulse characteristics can be determined, even though the pulse shape is not explicitly shown. The operation of the system is analyzed for a trapezoidal input pulse, and it is shown that all of the pulse characteristics can be determined if a diode with a nonlinear forward characteristic is used in the coincidence circuit. Results of experimental measurements of approximately trapezoidal pulses generated by a mercury switch pulser are shown which indicate that the system measures the pulse characteristics to a fairly high degree of accuracy. The bandwidth of the system is estimated to be in the neighborhood of 4000 or 5000 Mc, and pulses with rise times of the order of 0.1 mμsec have been measured.

A 1500-Volt, Center-Tapped Regulated Power Supply—N. W. Bell (p. 334)

Many ion-optical devices—mass spectrometers, linear accelerators, etc.—employ a radial electric field for deflection and/or focusing of a stream of charged particles. In a high-resolution double focusing spectrograph, precisely regulated deflecting voltages which are symmetrical with respect to ground are needed. This paper describes a 1500-volt supply with stability better than 50 ppm and ripple less than 10 ppm. This is accomplished with six tubes and no choppers.

Radiation Tracking Transducer—D. Allen, I. Weiman, and J. Winslow (p. 336)

The photovoltages which result when a semiconductor junction is illuminated by a spot of radiation are used to produce a radiation tracking transducer capable of detecting the angular position of a light- or radiation-emitting target. The theory is presented, together with results on experimental models, and suggestions for possible uses are given.

Measurement and Elimination of Flutter Associated with Periodic Pulses—P. A. Harding (p. 342)

A new method of characterizing wow or flutter has been proposed. This method is based upon measurement of time separation between consecutive pulses of a pulse train rather than measurement of frequency variations of a sine wave. As an extension of these characteristics, a system for flutter elimination has been investigated theoretically. Preliminary experimental tests indicate that the system is feasible. Circuits, for measurement and elimination of flutter, are described in detail.

Phase-Sensitive Detection with Multiple Frequencies—B. O. Pedersen (p. 349)

The multiple-frequency type of phase-sensitive detector differs from the conventional detector in that the signal frequency is a multiple of the reference frequency. Conventional phase-sensitive detectors may be readily adapted for multiple-frequency operation. Two detector circuits employing diodes are analyzed and discussed in detail. The circuit configuration required for even harmonic signals differs slightly from that required for odd harmonic signals. The multiple-frequency phase-sensitive detector may be designed to discriminate against higher-order harmonics contained in the signal. As a practical application, the use of a second harmonic phase-sensitive detector in a flux-gate magnetometer, which leads to a simplification of the magnetometer circuit, is described.

The Livermore Multibeam Cathode-Ray Tube—Lloyd Mancebo (p. 355)

The Livermore multibeam cathode-ray tube displays a raster of thirty-nine traces; each trace originates from a different electron injector. These grid-controlled injectors are only 0.110 inch in diameter and $\frac{1}{2}$ inch in length. Focusing is done with a spherical lens common to all of the beams. In this system a unipotential, spherical field is reconstructed within a cylindrical envelope by a cascade of three field-shaping electrodes between the cathode dish and the concentric anode. The lens has an extremely good depth of focus and produces an image with small aberrations. A single pair of deflection plates located at the lens crossover provides horizontal sweep for all of the beams. The tube has a time resolution of one part in a thousand and excels in one-shot, fast-transient, diagnostic work such as analysis of explosive or shock wave fronts.

An Improved Sing-Around System for Ultrasonic Velocity Measurements—Robert L. Forgacs (p. 359)

A sing-around system was developed for making measurements of very small changes (few parts in 10^7), in the velocity of ultrasound in samples. Fast precision-gating circuitry is employed to select a particular cycle of a particular echo to trigger the transmitter. The time required for precisely 10^3, 10^4, 10^5 or 10^6 sing-around cycles is measured by a unique electronic counting and timing system, with a few parts in 10^8. Short-term stability of the average cycling time of one part in 10^7 has been observed. The primary limitation to detecting minute velocity changes is expected to be the accuracy with which compensation may be effected for environmentally induced variation in indicated transit time, other than that due to sample velocity changes. For instance, a sample temperature change of a few ten-thousandths degree K produces detectable velocity changes under some conditions.

PGI News (p. 368)

Contributors (p. 369)

Annual Index (follows p. 370)

Military Electronics

Vol. MIL-5, No. 1, January, 1961

Editorial—Donald R. Rhodes (p. 1)

The Breakthrough of the "Scharnhorst"—Some Radio-Technical Details—Capt. Helmuth Giessler (p. 2)

This is a sequel to the paper by Sir Robert Watson-Watt that appeared in these Transactions in March, 1957. In response to an invitation from the Editor, Captain Giessler describes the historic escape of the German battleships *Scharnhorst*, *Gneisenau*, and *Prinz Eugen* through the British radar fence along the English Channel in World War II.

Jamming of Communication Systems Using FM, AM, and SSB Modulation—Henry Magnuski (p. 8)

Jamming of voice communication systems is a very ungrateful task and "brute force" jammers have to be used, while other systems, such as radar, can be jammed effectively using low power but sophisticated jammers. Geographical situation is very much against the jammer, particularly in ground-based mobile communications systems. The propagation of ground wave is such that a rapid increase of jamming power is required, as the ratio of distances of the jammer to the desired transmitter increases. The jammer is never certain whether or not the communication network is jammed and is never actually able to jam the communications completely. It can only limit the operating range of the system.

Different modulation systems are considered and the necessary power density for jamming of each system is discussed. It is concluded that effective jamming of FM systems and other systems with threshold systems is easier than that of AM, and particularly, the SSB systems. However, for nuisance jamming, the opposite is true. Finally, the jamming of the SSB systems is considered in more detail and it is proven that the so-called reduced-carrier SSB systems are not easier to jam than systems with a completely suppressed carrier.

Improving Electronic Reliability—Morris Halio (p. 11)

Each piece of military electronic equipment passes through various phases in its normal life cycle. These are: planning, design and development, pilot production, manufacture, transportation, storage, operation, and maintenance. Each of these stages is replete with opportunities for the introduction of unreliabilities. This paper points out the pitfalls which may be encountered and makes specific recommendations to avoid them, so that total potential reliability may be realized in the final equipment.

Re-Entry Radiation from an IRBM—W. N. Arnquist and D. D. Woodbridge (p. 19)

The radiation emitted when a high-speed body reenters the atmosphere is an important source of information concerning the physical processes taking place. Missile firings may be utilized to obtain some of this information. For about two years the Army Ballistic Missile Agency has conducted a measurement program known as Project Gaslight which has utilized Jupiter firings and, to a limited extent, both Thor and Polaris firings also. An account is given of the instrumentation employed and of some of the results that have been obtained. These include radiometric data in several wavelength bands from the ultraviolet to the infrared, and spectra in the visible. Motion pictures provide a record of the spatial relationships of the re-entry bodies, and these results are interpreted in terms of the impulse causing the initial separation. In the case of the Jupiter missile, there are two separations resulting in three bodies, the thrust unit, the nose cone, and an intermediate section or instrument compartment. Selected frames of the motion picture records show these bodies and give a qualitative understanding of the relative radiation from each source, of the disintegration and burning up of the thrust unit and the instrument compartment, and of the markedly lower drag-to-weight ratio of the nose cone. Forward scattering, presumably by high cirrus clouds, is shown to increase considerably the size of the very bright images. Most of the measurements have been made from ships, although some instrumentation has been airborne and photographs have been made from a distant island. Some of the difficulties in operations and in interpretations are mentioned. A more extensive evaluation of the data is in progress and plans are being made for future tests.

Contributors (p. 26)

Space Electronics and Telemetry

Vol. SET-6, No. 3–4, September–December, 1960

Considerations on Synchronization for PCM Telemetry—Lawrence L. Rauch (p. 95)

This is a tutorial presentation of various considerations involved in the synchronization problem for PCM time-division multiplex telemetry. Information rates required for establishing and maintaining synchronization are noted. The great difference between real-time synchronization and synchronization in post-time data reduction is emphasized. Several synchronization schemes are discussed.

Re-entry Guidance and Flight Path Control—James E. Vaeth (p. 99)

The capabilities and limitations of a specific flight path control law for range maneuvering during the atmospheric phase of re-entry from orbit, as determined by a digital computer study, are presented. Results of this study demonstrate that a relatively simple guidance and flight path control loop, utilizing a preprogrammed normalized trajectory plus vehicle velocity and range-to-go measurements, is very effective; range dispersions of more than ± 100 nautical miles, caused by initial conditions or to uncertainties in lift-to-drag ratio, are reduced to less than one nautical mile. Variations in terminal accuracy are evolved as functions of control law gain, velocity measurement errors (via inertial guidance or ground radar tracking) and severe head winds.

A Secure Digital Command Link—Richard Lowrie (p. 103)

The command link described was developed for use with a radar tracked, surface-to-surface guided missile. However, it has features which are applicable to a variety of other uses, wherever communications must be disguised and coded to prevent undesired interference, and to insure secrecy.

The command link is of the time division variety, utilizing a pseudorandom command code, which code pulses are interspersed among a completely random set of pulses. A large variation is possible in the time between successive command pulses, in the time between complete commands, in the time of a complete command, in the time between random pulses (maximum and minimum values), and in the nature of the pseudorandomness.

Automatic and continuous synchronism between transmitter and receiver is maintained by transmitting at intervals (not necessarily periodic) a single synchronizing pulse which is a part of the pseudorandom code. The synchronizing action can also be obtained from any or all of the other commands without the need for a separate synchronizing pulse, if desired. Note that the synchronizing pulses are nonperiodic, and are fully encoded.

The synchronizing process in the receiver is unique in that a single pulse received does the job. The circuit utilizes 3-stage counter, operated continually in a counting mode from an internal oscillator, with the received synchronizing pulse resetting the counter to a fixed count. This reset serves to introduce a fixed time delay between the received pulse and the output of the third stage. This fixed delay is equivalent to an adjustment in phase in the conventional analog synchronizing circuit. No attempt is made to adjust the oscillator output frequency in the receiver, other than by the introduction, at random intervals, of a delay time which is automatically determined by the counter circuit to be necessary to insure adequate synchronism. The circuit will, with a 3-stage counter, correct for a drift in phase of ± 4 microseconds. The ground and missile oscillators are crystal controlled, both at 1 mc, and have a nominal stability of 1 part in 10^6. Depending on the missile speed, synchronizing pulses must be sent from once every 3 seconds to once every 0.8 second.

The method of generating the pseudorandom code utilizes a binary counter with variable feedback between stages. The feedback pulses serve to reset that stage to a state that it would not otherwise be in. The stages to which the reset pulses are applied are varied during flight by means of a diode matrix operating from the highest order counters. The wiring of the matrix is variable, manually, over a wide range. Herein lies the security of the system. Over 1000 different codes are possible in the system shown; many more are potentially available with one or two more counter stages.

Each command has an assigned time slot which corresponds to a certain count of the binary counter. A diode matrix recognizes a received pulse occurring during one of these time slots and passes it on to an integrator circuit and from there, to the actuators. The sync pulse also has an assigned time slot, although any one, or a combination of the other command pulses, could also be used for synchronizing.

A reacquisition method is described which enables synchronization to be re-established once lost, or enables a remote control station to acquire and control the missile, if desired. The inherent ECM immunity of the system is fully utilized in the reacquisition mode.

The Pioneer I, Explorer VI and Pioneer V High-Sensitivity Transistorized Search Coil Magnetometer—D. L. Judge, M. G. McLeod, and A. R. Sims (p. 114)

The magnetometer described in this paper was designed for the purpose of measuring the distant geomagnetic and interplanetary magnetic fields. The sensing element is a coil fixed in the frame of a spinning vehicle. The associated nonlinear amplifier has a dynamic range of approximately three decades and an equivalent noise threshold of 6.0 microgauss. This system has been flown in the Pioneer I, Explorer VI and Pioneer V payloads to detect both absolute magnitude and directional changes in the magnetic field intensity at great distances. The complete unit enclosed in an RF shielded container weighs one pound.

The Data Systems for Explorer VI and Pioneer V—Eugene W. Greenstadt (p. 122)

The systems for acquisition and reduction of telemetry data for 1959 Delta (Explorer VI) and 1960 Alpha (Pioneer V) are described. These include an analog and a digital system in Explorer VI and a digital system in Pioneer V. The discussion covers digitization of data in the payloads, methods of handling and recording data on the ground, reduction techniques, and the procedures used to disengage signal from noise during periods when the SNR was low

PCM/FM Telemetry Signal Analysis and Bandwidth Effects—Joseph F. A. Ormsby (p. 130)

The spectra of FM signals corresponding to various pulse shapes (or relevance in PCM work) are determined. The corresponding demodulated output pulse shapes in a limiter-discriminator receiving system have also been obtained. Both analytical and graphical results are given.

Widely Separated Clocks with Microsecond Synchronization and Independent Distribution Systems—T. L. Davis and R. H. Doherty (p. 138)

In a majority of timing applications, a problem exists in setting two or more clocks to agree with one another. Present techniques using WWV or other HF broadcasts allow clocks to be synchronized within 1 msec. This paper describes a method which offers an improvement in synchronization of three orders of magnitude.

Microsecond synchronization is obtained by use of the Loran-C navigation system as the link between a master clock at Boulder, Colorado and any slaved clock anywhere in the Loran-C service area.

The time system also includes a unique method for distribution of several time code formats on a single UHF channel.

Geometric Aspects of Satellite Communication—F. W. Sinden and W. L. Mammel (p. 146)

If a system of communications satellites is uncontrolled after launching, service interruptions are inevitable. The amount of interruption depends on the number of satellites, their altitude, the orbit inclinations, the distance between ground stations, the acceptable signal-to-noise ratio, and other parameters. Various relations between these quantities are presented in tables and graphs, and are illustrated by examples.

True RMS Voltage Discriminator—F. A. Galindo (p. 157)

This paper discusses the circuitry, the electrical specifications, the environmental specifications, and the method of calibration of a completely transistorized true root-mean-square voltage discriminator.

The circuitry is broken into four separate operational circuits, each of which is discussed in relation to what it does and what its relationship to the other configurations is.

The specifications of the discriminator are discussed along with a detailed explanation of the method employed in calibration of the module with nonsinusoidal waveforms.

Contributors (p. 160)

Annual Index (follows p. 161)

Abstracts and References

Compiled by the Radio Research Organization of the Department of Scientific and Industrial Research, London, England, and Published by Arrangement with that Department and the *Electronic Technology* (incorporating *Wireless Engineer* and *Electronic and Radio Engineer*), London, England

NOTE: The Institute of Radio Engineers does not have available copies of the publications mentioned in these pages, nor does it have reprints of the articles abstracted. Correspondence regarding these articles and requests for their procurement should be addressed to the individual publications, not to the IRE.

The Index to the Abstracts and References published in the PROC. IRE from February, 1959 through January, 1960 is published by the PROC. IRE, May, 1960, Part II. It is also published by *Electronic Technology* (incorporating *Wireless Engineer* and *Electronic and Radio Engineer*) and included in the April, 1960, issue of that Journal. Included with the Index is a selected list of journals scanned for abstracting with publishers' addresses.

The number in heavy type at the upper left of each Abstract is its Universal Decimal Classification number. The number in heavy type at the top right is the serial number of the Abstract. DC numbers marked with a dagger (†) must be regarded as provisional.

UDC NUMBERS

Certain changes and extensions in UDC numbers, as published in PE Notes up to and including PE 666, will be introduced in this and subsequent issues. The main changes are:

Artificial satellites:	551.507.362.2	(PE 657)
Semiconductor devices:	621.382	(PE 657)
Velocity-control tubes, klystrons, etc.:	621.385.6	(PE 634)
Quality of received signal, propagation conditions, etc.:	621.391.8	(PE 651)
Color television:	621.397.132	(PE 650)

The "Extensions and Corrections to the UDC," Ser. 3, No. 6, August, 1959, contains details of PE Notes 598–658. This and other UDC publications, including individual PE Notes, are obtainable from The International Federation for Documentation, Willem Witsenplein 6, The Hague, Netherlands, or from The British Standards Institution, 2 Park Street, London, W.1, England.

ACOUSTICS AND AUDIO FREQUENCIES

534.22–14:546.211 **766**

Determination of the Velocity of Sound in Distilled Water—R. Brooks. (*J. Acoust. Soc. Am.*, vol. 32, pp. 1422–1425; November, 1960.) The velocity of sound has been determined to an accuracy of ±1 foot per second from measurements in range 22–25°C of the time of transit along two sound paths of different lengths between the crystal faces of two $BaTiO_3$ transducers. Results are in close agreement with those of Greenspan and Tschiegg (1296 of 1958).

A list of organizations which have available English translations of Russian journals in the electronics and allied fields appears each June and December at the end of the Abstracts and References' section.

534.26–8 **767**

Empirical Study of the Effect of Diffraction on Velocity of Propagation of High-Frequency Ultrasonic Waves—H. J. McSkimin. (*J. Acoust. Soc. Am.*, vol. 32, pp. 1401–1404; November, 1960.) The effect of diffraction in increasing the velocity of propagation over the plane-wave value is determined experimentally by phase comparison of reflected longitudinal waves in fused silica blocks.

534.283–8:538.6 **768**

Ultrasonic Absorption in Metals in a Magnetic Field: Part 2—V. L. Gurevich. (*Zh. Eksp. Teor. Fiz.*, vol. 37, pp. 1680–1691; December, 1959.) The absorption coefficient is calculated by solving simultaneously the kinetic and Maxwell's equations. Two types of absorption mechanism are identified: 1) deformation, and 2) induction. (Part 1: 1843 of 1960.)

534.41–8:537.32 **769**

Thermoelectric Microphone for Modulated Ultrasonic Waves—R. A. Hanel. (*J. Acoust. Soc. Am.*, vol. 32, pp. 1436–1442; November, 1960.) A description is given of a small omnidirectional drift-free microphone for measuring the periodic change of temperature generated by an AM sound wave. Temperature changes of the order of 3×10 °C have been detected by a constantan-manganin couple and recorded by means of a narrow-band amplifier tuned to the modulation frequency.

534.614 **770**

The Effect of Attenuation on the Acoustic Resonant Frequencies of Gases in Tubes—H. J. Wintle. (*Proc. Phys. Soc.*, vol. 76, pp. 772–775; November 1, 1960.) "The change in the resonant frequencies of a sound tube due to the dependence of attenuation on frequency is worked out for two cases of practical interest. The effect on measured values of the velocity of sound is shown to be significant in accurate work."

534.614–8:621.3.018.75 **771**

Precision Ultrasonic Velocity Measurements—R. L. Forgacs. (*Electronics*, vol. 33, pp. 98–100; November 18, 1960.) Circuit details are given of an improved "sing-around" system incorporating modifications suggested by Myers, *et al.* (249 of 1959).

ANTENNAS AND TRANSMISSION LINES

621.315.212:621.391.822 **772**

Noise Generation by Coaxial Cables when Subjected to Vibration—R. D. Hole. (*Electronic Engrg.*, vol. 32, pp. 770–771; December, 1960.) A brief summary of factors governing noise generation is given, and two techniques are suggested for minimizing it.

621.315.212.018.75 **773**

The High-Frequency Properties of a Coaxial Cable and the Distortion of Fast Pulses—G. Fidecaro. (*Nuovo Cim.*, vol. 15, Suppl. No. 2, pp. 254–263; 1960. In English.) The high-frequency properties of a coaxial cable are discussed theoretically, and an accurate method is described for determining the delay.

621.372.2:621.372.51 **774**

Two-Path Transmission-Line Network—C. S. Gledhill. (*Electronic Tech.*, vol. 38, pp. 22–26; January, 1961.) An analysis is given in terms of the normalized terminating impedance, and is applied to the design of a two-path network for impedance transformation and for a rejection filter.

621.372.821:621.396.677.7 **775**

Printed-Circuit Waveguides and their Application to Microwave Antennas—J. C. Parr. (*Brit. Commun. Electronics*, vol. 8, pp. 20–24; January, 1961.) The principles of construction of open-line and closed-line systems are given. A comparison analysis illustrates the superior performance of high-Q closed lines.

621.372.824:537.56 **776**

On Microwave Propagation in a Plasma-Filled Coaxial Line—B. Enander. (*Ericsson Tech.*, vol. 16, no. 1, pp. 59–75; 1960.) Experimental results show that a signal passing through a glow-discharge is attenuated if the signal frequency lies within a certain band, the lower limit of which is the gyromagnetic frequency. The attenuation is caused by absorption of the signal in the discharge.

621.372.852.2:621.317.77.088 **777**

Error Analysis of a Standard Microwave Phase Shifter—G. E. Schafer and R. W. Beatty. (*J. Res. NBS*, vol. 64C, pp. 261–265; October–December, 1960.) The standard phase shifter proposed by Magid (IRE TRANS. ON INFORMATION THEORY, vol. 1–7, pp. 321–331; December, 1958) is a tunable three-arm waveguide junction with an adjustable short-circuit. Graphs are given for use in estimating the limits of tuning error from observations of amplitude changes during tuning.

621.372.852.323 778
Applications for Ferrite Resonance Isolators—E. F. Schelisch. (*Point to Point Telecommun.*, vol. 4, pp. 4–10; June, 1960.) Applications at frequencies above 2 Gc and with isolation factors of the order of 20 db, with 10 per cent bandwidth, are briefly described.

621.396.67.08:621.317.7:621.373.42.029.5 779
A Portable H.F. Spectrum Generator for Antenna Calibration—Burtnyk. (*See* 1002.)

621.396.67.095 780
Transient Electromagnetic Waves around a Cylindrical Transmitting Antenna—P. O. Brundell. (*Ericsson Tech.*, vol. 16, pp. 137–162; 1960.) The EM field generated by a cylindrical radiator fed by an arbitrary nonsinusoidal voltage is determined theoretically. The representation of the field in terms of an infinite set of elementary travelling waves reflected from the ends of the radiator is discussed with reference to Hallén's theory.

621.396.677.089.6:621.396.96:523.164.32 781
Aerial Calibration by Solar Noise using Polar Display—M. H. Cufflin. (*Marconi Rev.*, vol. 23, pp. 33–44; 1st Quarter, 1960.) Experimental equipment for the measurement of antenna polar diagrams using solar noise is described, and some records are given. (*See also* 897 *and* 898.)

621.396.679.4:621.397.62 782
Television Downleads: a Survey—R. J. Slaughter. (*J. Telev. Soc.*, vol. 9, pp. 288–293; July–September, 1960.)

621.396.677.4 783
Nonresonant End-Fed Antennas—V. L. Talekar. (*Electronic Technol.*, vol. 38, pp. 13–15; January, 1961.) The directions of maximum radiation for antennas of different length are obtained by a graphical method.

621.396.677.833.2 784
Screened Wide-Band Helical Antenna as Primary Antenna for Paraboloidal Reflectors in the 800-Mc/s Range—W. Krank. (*Telefunken Ztg.*, vol. 33, pp. 47–57; March, 1960. English summary, p. 74.) The design is described of a screened helical antenna for operation in the frequency range 635–960 Mc and particularly suitable for large-aperture reflectors. Performance data are given for reflectors of 1.75 and 3 m diameter; results are better than those achieved with ordinary helical antennas.

AUTOMATIC COMPUTERS

681.142 785
Development of Japanese Digital Computers—S. Takahashi. (*Computer J.*, vol. 2, pp. 122–129; October, 1959.) Parametron and transistor circuit techniques widely used in Japanese computers are described, and the general characteristics of 20 types of computer are tabulated.

681.142:621–526 786
A V.L.F. Function Generator—L. Whitlow. (*Electronic Engrg.*, vol. 32, pp. 750–752; December, 1960.) An electromechanical device producing a readily variable function is described.

CIRCUITS AND CIRCUIT ELEMENTS

621.3.049.7 787
Microminiaturization—M. M. Perugini and N. Lindgren. (*Electronics*, vol. 33, pp. 77–108; November 25, 1960.) An illustrated review of current achievements is given.

621.372.5 788
Calculation of the Parameters of a Quadripole by means of Signal Flow Graphs—E. Cassignol and Y. Chow. (*Onde Élect.*, vol. 40, pp. 617–623; September, 1960.)

621.372.5 789
A Modified Synthesis Procedure for Two-Terminal-Pair Networks—S. S. Forte. (*Marconi Rev.*, vol. 23, pp. 59–64; 2nd Quarter, 1960.) A general theorem given previously (2146 of 1959) is extended for a particular case of a network with one pair of terminals open-circuited.

621.372.54 790
Design of Optimum Filters—N. K. Sinha. (*J. Inst. Telecommun. Engrs., India*, vol. 6, pp. 217–222; August, 1960.) The design of low-pass filters using easily computed rational functions instead of elliptic functions permits more accurate location of the poles of the transfer function when the number of poles exceeds four, and computation is less laborious.

621.373.4 791
General Principles of Polyphase Vacuum-Tube Oscillator—T. Takagi and K. Mano. (*Sci. Rep. Inst. Tohoku Univ., Ser. B*, vol. 11, Nos. 3/4, pp. 179–190; 1960.)

621.373.4:621.376.32:621–526 792
Synchronization of Frequency-Modulated Free-Running Oscillators investigated by Servomechanism Methods—H. H. Erynei. (*Onde Élect.*, vol. 40, pp. 602–616; September, 1960.) Application of a servo system to the control of a free-running oscillator. A method is described for determining the frequency response of the closed loop from measurements of open-loop characteristics. Quadripole correctors for improving the response will also widen the frequency range over which control may be exercised. [See also 3029 of 1960 (Freeman).]

621.373.421.11 793
Pass-Band and Selective A.F. Amplification of a H.F. Oscillator—H. Hasenjäger. (*Onde Élect.*, vol. 38, pp. 838–841; December, 1958.) The bandwidth of a high-frequency oscillator has been investigated theoretically and experimentally by studying the behavior of the oscillator as a selective AF amplifier.

621.373.431.1:621.382.3 794
Analysis of a Semiconductor Multivibrator with Emitter Capacitance—E. F. Doronkin. (*Izv. Vyssh. Uch. Zav., Radiotekhnika*, vol. 3, pp. 106–111; January/February, 1960.) An analysis of an emitter-coupled transistor multivibrator showing the effect of emitter capacitance in increasing the thermal stability of the pulse-duration parameters.

621.374.3:621.387.4 795
Fast Transistorized Time-to-Pulse-Height Converter—G. Culligan and N. H. Lipman. (*Rev. Sci. Instr.*, vol. 31, pp. 1209–1214; November, 1960.) A converter of simple design is described having a 0–15 nsec timebase and giving a resolution of 10^{-9}s using conventional scintillation counters. It was used to analyze particle beams by time-of-flight measurements.

621.374.32:621.387 796
A Reversible Dekatron Circuit—A. J. Oxley. (*Electronic Engrg.*, vol. 32, pp. 746–749; December, 1960.) A description is given of the unit, with a discussion of its limitations.

621.374.43 797
Regenerative Fractional Frequency Generators—S. Plotkin and O. Lumpkin. (PROC. IRE, vol. 48, pp. 1988–1997; December, 1960.) A self-starting regenerative frequency divider circuit is described which has the advantages of simplicity and of "lock-in" stability over a wide range of frequencies. An approximate analysis is given which shows the dependence of performance on diode characteristics and transistor input impedance.

621.375.2.024 798
Simple Logarithmic D.C. Amplifier—L. V. East and W. E. Parker. (*Rev. Sci. Instr.*, vol. 31, pp. 1222–1225; November, 1960.) A simple double-triode amplifier is described. It has an accuracy within 2 per cent for input voltages from 5 to 500 v and is easily adjusted for differing tube characteristics.

621.375.23 799
The Bootstrap Amplifier—W. Tusting. (*Electronic Tech.*, vol. 38, pp. 27–31; January, 1961.) An analysis of a RC-coupled pentode amplifier with the anode decoupling capacitor returned to the cathode of a cathode follower. The effects of the coupling and decoupling capacitors on the low-frequency response characteristics are calculated.

621.375.3 800
Analysis of Half-Wave Magnetic Amplifier Circuits with A.C. Bias Voltage—T. Kikuchi. (*Sci. Rep. Res. Inst. Tohoku Univ., Ser. B*, vol. 11, nos. 3/4, pp. 133–154; 1960.) Detailed analysis with special reference to the elimination of the rectifier from the control circuit of Ramey's half-wave magnetic amplifier. (See 3507 of 1953.)

621.375.432 801
A Nonlinear Effect in Transistor Amplifiers with Feedback—I. Gumowski. (*C.R. Acad. Sci., Paris*, vol. 250, pp. 822–824; February 1, 1960.) The nonlinear effect described in an earlier paper (4150 of 1960) is analyzed. It is attributed to variations of carrier transit-time with transistor collector voltage.

621.375.9:538.569.4 802
Use of Slow Molecules in Molecular Generators—N. G. Basov and A. N. Oraevskiĭ. (*Zh. Eksp. Teor. Fiz.*, vol. 37, pp. 1068–1071; October, 1959.) Methods of improving the absolute frequency stability of a beam-type maser are considered, based on the use of molecular beams with mean velocities much less than the thermal velocity at room temperature. Three techniques are described: 1) removal of high-velocity molecules from the beam; 2) retardation of the molecules by an external field; 3) reduction of the temperature of the molecular beam.

621.375.9:538.569.4 803
Systems Applications of Solid-State Masers—J. W. Meyer. (*Electronics*, vol. 33, pp. 58–63; November 4, 1960.) Progress in solid-state maser technique is surveyed. Operating principles and circuit design are outlined.

621.375.9:538.569.4 804
The Optimum Line Width for a Reflection Cavity Maser—G. J. Troup. (*Aust. J. Phys.*, vol. 13, pp. 615–616; September, 1960.) An extension is given of previous work (2665 of 1960) to show that the maximum gain × bandwidth product is achieved.

621.375.9:538.569.4 805
Electronically Tunable Travelling-Wave Masers at *L* and *S* Bands—S. Okwit, F. R. Arams, and J. G. Smith. (PROC. IRE, vol. 48, pp. 2025–2026; December, 1960.) Tuning ranges of 250 Mc and greater have been obtained by varying only the applied magnetic field and the pump frequency. Test data are given.

621.375.9:621.372.44 806
Coupled-Cavity Travelling-Wave Parametric Amplifiers: Part 1—Analysis—M. R.

Currie and R. W. Gould. (Proc. IRE, vol. 48, pp. 1960–1973; December, 1960.) Detailed information is given on operating characteristics of a travelling-wave circuit consisting of a chain of inductively coupled cavities loaded by diodes in the capacitive region. Calculations show that unilateral gains of 12–15 db over relatively wide bandwidths are attainable with 4–6 diodes.

621.375.9:621.372.44 807

Coupled-Cavity Travelling-Wave Parametric Amplifiers: Part 2—Experiments—K. P. Grabowski and R. D. Weglein. (Proc. IRE, vol. 48, pp. 1973–1987; December, 1950.) Gain-bandwidth products of 2 Gc with a 350-Mc bandwidth have been obtained at *S*-band frequencies using commercially available diodes. Noise temperatures of 130°K have been measured. Methods for achieving short-circuit stability are investigated. These include the use of ferrite-loaded coupling irises and of upper-frequency passbands.

621.375.9:621.372.44 808

Gain of a Travelling-Wave Parametric Amplifier using Nonlinear Lossy Capacitors—W. Jasinski. (Proc. IRE, vol. 48, pp. 2018–2019; December, 1960.) An analysis of a traveling-wave parametric amplifier, considering reverse-biased diodes as lossy capacitors.

621.375.9:621.372.44 809

Aspects on Wide-Band Parametric Travelling-Wave Amplifiers—B. T. Henoch. (*Ericsson Tech.*, vol. 16, no. 1, pp. 77–135; 1960.) Methods are described for calculating amplification, bandwidth, phase conditions, and noise figure.

621.375.9:621.372.44:621.372.632 810

Gain Optimization in Low-Frequency Parametric Up-Converters by Multidiode Operation—A. K. Kamal and M. Subramanian. (Proc. IRE, vol. 48, pp. 2020–2021; December, 1960.) A method is proposed for optimizing the gain of an up-converter using more than one variable-capacitance diode at the same point. Results of a first-order analysis made with two diodes are given.

621.375.9:621.372.44:621.391.822 811

Idler Noise in Parametric Amplifiers—G. Herrmann. (Proc. IRE, vol. 48, pp. 2021–2022; December, 1960.)

621.382.23:621.375.9 812

Esaki-Diode Amplifiers at 7, 11 and 26 kMc/s—R. F. Trambarulo. (Proc. IRE, vol. 48, pp. 2022–2023; December, 1960.) Stable gains of up to 38 db at 7 and 11 Gc and 36 db at 26 Gc have been obtained with the GaAs diode in a cylindrical reflection cavity which has been described earlier. [359 of January, 1961 (Trambarulo and Burrus).]

GENERAL PHYSICS

535.13 813

Criterion of Uniqueness for the Solutions of Maxwell's Equations—P. Poincelot. (*Ann. Télécommun.*, vol. 15, pp. 77–83; March/April, 1960.) (See 3628 of 1959.)

537.122 814

The Dirac Electron in Rectilinear Fields—D. V. A. S. Amarasekera. (*Ceylon J. Sci., Phys. Sci.*, vol. 1, pp. 37–40; June, 1958.) Dirac's equations for an electron in a rectilinear field are first reduced to a single equation of simple form, suitable for the solution of problems. An explicit solution is then obtained for an electron in a constant electric field.

537.311.1 815

Variational Treatment of Warm Electrons in Nonpolar Crystals—I. Adawi. (*Phys. Rev.*, vol. 120, pp. 118–127; October 1, 1960.) Deviations from Ohm's law in nonpolar crystals are treated by the variational method for the case of weak fields. The second-order term in the electrical conductivity is calculated.

537.311.3 816

Effect of Random Inhomogeneities on Electrical and Galvanomagnetic Measurements—C. Herring. (*J. Appl. Phys.*, vol. 31, pp. 1939–1953; November, 1960.) A theoretical treatment is given in which the scale of inhomogeneities is supposed small compared with the specimen size but large compared with the mean free path and Debye length. Comparison with exactly soluble cases shows the derived formulas to be valid for sizable fluctuations.

537.331.32 817

The Validity of the Concept of Specific Surface Resistance and its Measurement—R. Lacoste and P. Paillère. (*C. R. Acad. Sci., Paris*, vol. 250, pp. 816–818; February 1, 1960.) Earlier work by Lacoste is extended (3252 of 1959) to show that the criterion for surface conduction is independent of the electrode-system configuration. The influence of the configuration on accuracy of measurement is considered.

537.311.33:535.215 818

Steady-State Distribution Function in Dilute Electron Gases—D. C. Mattis. (*Phys. Rev.*, vol. 120, pp. 52–57; October 1, 1960.) The effects determining the distribution function of optically liberated carriers are investigated. For a simple model semiconductor, significant deviations from the Boltzmann distribution are possible at temperatures below a few degrees K.

537.311.62:535.137 819

On the Possible Influence of Electron Interaction on the Reflectivity of Metals—C. W. Benthem. (*Appl. Sci. Res.*, vol. B7, No. 4, pp. 275–292; 1958.) A continuation is given of the work by Benthem and Kronig (3523 of 1954) on the influence of electron viscosity on the absorption factor of metals in the infrared region.

537.525 820

Sustained, Localized, Pulsed-Microwave Discharge in Air—C. W. Hamilton. (*Nature, Lond.*, vol. 188, pp. 1098–1099; December 24, 1960.) Details are given of a small localized discharge obtained in low-pressure air, using a pulsed *X*-band radar transmitter as the microwave source.

537.533.7:539.23 821

Transmission of Slow Electrons through Thin Films—O. Klemperer and A. Thetford: F. Lenz. (*Proc. Phys. Soc.*, vol. 76, pp. 705–720; November 1, 1960.)

537.56 822

Investigation of a Plasma Column Continuously Fed and Subjected to a Magnetic Field: First-Order Approximations for the Diffusion Velocities; Manifestation of a Frontier Zone—J. M. Dolique and M. Y. Bernard. (*C. R. Acad. Sci., Paris*, vol. 250, pp. 1458–1459; February 22, 1960.) [See 496 of February (Dolique).

537.56 823

Free-Path Formulas for the Coefficient of Diffusion *D* and Velocity of Drift *W* of Ions and Electrons in Gases—L. G. H. Huxley. (*Aust. J. Phys.*, vol. 13, pp. 578–583; September, 1960.) (See also 94 of 1958.)

537.56 824

Ion Resonance in a Multicomponent Plasma—S. J. Buchsbaum. (*Phys. Rev. Lett.*, vol. 5, pp. 495–497; December 1, 1960.) Interactions between different types of ion produce additional resonances.

537.56:538.56 825

Oscillations of an Electron-Ion Plasma—L. M. Kovrizhnykh. (*Zh. Eksp. Teor. Fiz.*, vol. 37, pp. 1692–1696; December, 1959.) Investigation of the spectrum of longitudinal oscillations for the case of low temperature (Fermi distribution) and high temperature (Maxwell distribution). For low values of the wave vector, the dispersion equation has two branches, corresponding to optical and acoustic modes.

538.114 826

Direct Exchange in Ferromagnets—R. Stuart and W. Marshall. (*Phys. Rev.*, vol. 120, pp. 353–357; October 15, 1960.) Evaluation for all internuclear spacings of the direct-exchange integral occurring in the Heisenberg theory of ferromagnetism leads to the conclusion that direct exchange is not responsible for ferromagnetism in ferromagnetic metals.

538.114 827

Collective Excitations of Electrons in Degenerate Bands: Part 1—Spin Waves in Stoner's Model of Ferromagnetism—T. Izuyama. (*Progr. Theor. Phys.*, vol. 23, pp. 969–983; June, 1960.) Spin waves in the collective electron model of ferromagnetism are derived.

538.114 828

Anisotropic Superexchange Interaction and Weak Ferromagnetism—T. Moriya. (*Phys. Rev.*, vol. 120, pp. 91–98; October 1, 1960.) A theory is developed by extending the Anderson theory of super-exchange (*Phys. Rev.*, vol. 115, pp. 2–13; July 1, 1959) to include spin-orbit coupling.

538.3 829

Determining the Dielectric Permittivity and Magnetic Permeability Tensors of a Medium—G. S. Krinchik and M. V. Chetkin. (*Zh. Eksp. Teor. Fiz.*, vol. 36, pp. 1924–1925; June, 1959.) An analytical note is given on the separation of gyroelectric and gyromagnetic effects.

538.561:537.533.7 830

Transition Radiation in a Waveguide—K. A. Barsukov. (*Zh. Eksp. Teor. Fiz.*, vol. 37, pp. 1106–1109; October, 1959.) Investigation is made of the radiation which arises in a waveguide by the passage of a charged particle through the boundary between two media. At ultrarelativistic charge velocities the radiation is mainly in the forward direction and its magnitude is proportional to the particle energy. Formulas for the total energy of the radiation and its spectral distribution are derived.

538.566 831

Some Absorbent Materials at U.H.F.—H. G. Stubbs and J. Peyssou. (*Onde Élect.*, vol. 38, pp. 809–818; December, 1958.) The characteristics of two types of absorbent material are described: 1) a plastic or rubber sheet impregnated with carbon powder, applicable over a wide band of frequencies, and 2) a similar material $\lambda/4$ thick, impregnated with carbonyl-iron or carbon powder and backed with a thin metallic sheet, applicable over a narrow band.

538.566:535.42 832

Contribution to the Study of Diffraction of Electromagnetic Waves by Spheres—J. Mével. (*Ann. Phys., Paris*, vol. 5, pp. 265–320; March/April, 1960.) A thesis is given, describing theoretical and experimental methods of obtaining the diffraction field of both a single sphere and a pair of spheres. (For a report of experimental apparatus, see 1393 of 1958.)

538.566:535.42 833

Diffraction of a Plane Electromagnetic Wave by Cylinders with Anisotropic Conductivity—R. E. Kelly and A. Russek. (*Nuovo Cim.*, vol. 16, pp. 593–610; May 16, 1960. In English.)

538.560:535.43 834

A Study of Surface Roughness and its Effect on the Back-Scattering Cross-Section of Spheres—R. E. Hiatt, T. B. A. Senior, and V. H. Weston. (PROC. IRE, vol. 48, pp. 2008–2016; December, 1960.) Experimental data obtained by measuring the back-scattering cross section of a large rough sphere at three frequencies in the *S*, *X*, and *K* bands, are presented. Even for a sphere whose depth of roughness is as large as 10^{-2} λ, the measured change in cross section is no more than 0.1 db; this is in good agreement with the theoretical prediction.

538.569.4 835

Line Breadths in the Ammonia Spectrum—J. A. Fulford. (*Nature, Lond.*, vol. 188, pp. 1097–1098; December 24, 1960.) Measurements have been made of the NH_3 inversion spectrum ($J=K$, 1 to 6). From the results a value of 25.7 ±0.2 Mc per mm Mg at 27°C has been obtained.

538.569.4:535.853 836

Line Structure in Paramagnetic Resonance and Direct Measurement of the Moments—J. Hervé. (*Ann. Phys., Paris*, vol. 5, pp. 321–364; March/April, 1960.)

538.569.4:535.853 837

The Influence of Modulation on the Recording of Resonance Phenomena—F. Bruin and D. van Ladesteyn. (*Appl. Sci. Res.*, vol. B7, No. 4, pp. 270–274; 1958.) Curves based on the standard resonance curve, $y=1/(1+X^2)$, of a simple harmonic oscillator are given as an aid to the construction of spectrographs and the analysis of recorded spectra.

538.569.4:538.221:621.318.134 838

Nonlinear Effects of Crystalline Anisotropy on Ferrimagnetic Resonance—P. Gottlieb. (*J. Appl. Phys.*, vol. 31, pp. 2059–2062; November, 1960.) Analysis shows that the magnetic resonance frequency depends quadratically upon the precession amplitude, to lowest order; this can cause a fold-over of the resonance line.

538.569.4:538.222 839

Cross-Relaxation in Dilute Paramagnetic Systems—A. Kiel. (*Phys. Rev.*, vol. 120, pp. 137–140; October 1, 1960.)

538.652:548.0 840

The Direction Dependence of Magnetostriction—W. Döring and G. Simon. (*Ann. Phys., Lpz.*, vol. 5, pp. 373–387; March 29, 1960.) Tensor methods are used to describe the lattice distortion caused by magnetostriction. For similar calculations of the direction dependence of crystal energy see *Ann. Phys., Lpz.*, vol. 1, pp. 102–109; December 12, 1957 (Döring).

539.2 841

Proceedings of the International Congress on Many-Particle Problems—(*Physica*, vol. 26, Suppl., pp. S1–S217; December, 1960.) The texts are given of invited papers read at a conference held in Utrecht, June 13–18, 1960.

541.135:621.319.4 842

Ion Size Effect and Mechanism of Electrolytic Rectification—P. F. Schmidt, F. Huber, and R. F. Schwarz. (*J. Phys. Chem. Solids*, vol. 15, pp. 270–290; October, 1960.) Previous theories of electrolytic rectification are shown to be inadequate. Extensive experimental work is presented which shows the importance of the size of the cation in solution, and the existence of an extremely thin (~250Å) surface barrier of height about 1 v.

GEOPHYSICAL AND EXTRATERRESTRIAL PHENOMENA

523.14:538.69 843

Note on the Transference of Angular Momentum within the Galaxy through the Agency of a Magnetic Field—F. Hoyle and J. G. Ireland. (*Monthly Notices Roy. Astron. Soc.*, vol. 121, no. 3, pp. 253–259; 1960.) (Extension of 2322 of 1960.)

523.164:523.45 844

Magnetic Field of Jupiter—C. H. Barrow. (*Nature, Lond.*, vol. 188, pp. 924–925; December 10, 1960.) A review is presented of theoretical and experimental evidence in support of the hypothesis of an ionosphere and magnetic field associated with Jupiter.

523.164:551.594.5 845

The Correlation of Radio Source Scintillation in the Southern and Northern Hemispheres—P. M. Brenan. (*J. Atmos. Terrest. Phys.*, vol. 19, pp. 287–289; December, 1960.) Observations of radio source scintillation made simultaneously at Halley Bay and Jodrell Bank show a significant correlation. This is relevant to theories which associate high-latitude scintillation with auroral activity.

523.164:551.594.5 846

The Magnetic Storm-Time Variation of Radio Star Scintillations and Auroral Radio Echoes—C. D. Watkins. (*J. Atmos. Terrest. Phys.*, vol. 19, pp. 289–292; December, 1960.) The variations of scintillation rate and auroral echo incidence, during periods following magnetic sudden commencements, resemble the variation of magnetic *K* index.

523.164.3 847

A 21-cm Determination of the Principal Plane of the Galaxy—C. S. Gum, F. J. Kerr, and G. Westerhout. (*Monthly Notices Roy. Astron. Soc.*, vol. 121, no. 2, pp. 132–149; 1960.) Data from the Leiden and Sydney surveys of the Milky Way have been used to determine the position of the plane of the neutral hydrogen layer which is found to be exceedingly flat over the galaxy within 7 kiloparsecs from the center.

523.164.3 848

Radio Data Relevant to the Choice of a Galactic Coordinate System—C. S. Gum and J. L. Pawsey. (*Monthly Notices Roy. Astron. Soc.*, vol. 121, no. 2, pp. 150–163; 1960.) Because of the large-scale association found between sources of the radio continuum and the distribution of the 21-cm-λ hydrogen-line radiation, the coordinate system may be defined by the HI principal plane and by a center situated in Sagittarius A.

523.164.32:523.745 849

Some Statistics of Solar Radio Bursts at Sunspot Maximum—A. Maxwell, W. E. Howard III, and G. Garmire. (*J. Geophys. Res.*, vol. 65, pp. 3581–3588; November, 1960.) Bursts at 125 and 200 Mc are mainly of spectral type I and occur more frequently than bursts at 425 and 500 Mc, which are of a greater intensity and of spectral type IV.

523.164.4 850

On the Identification of Extragalactic Radio Sources—B. Y. Mills. (*Aust. J. Phys.*, vol. 13, pp. 550–557; September, 1960.) Radio data from Sydney and Cambridge have been compared with a catalog of galaxies in a limited region of the sky. Forty-six possible identifications of RF sources with galaxies have been made, and fifty-five with clusters of galaxies.

523.165 851

Solar Modulation of Primary Cosmic Rays—Y. Terashima. (*Progr. Theor. Phys.*, vol. 23, pp. 1138–1150; June, 1960.) The observed solar modulation of cosmic rays may be explained, assuming the existence of two solar magnetic fields, one uniform and the other irregular, and two solar streams, one continuously ejected and the other produced by solar eruptions.

523.5 852

Southern-Hemisphere Meteor Shower Activity in July and August—A. A. Weiss. (*Aust. J. Phys.*, vol. 13, pp. 522–531; September, 1960.) Observations for 1957–1959 are described, and measurements of the radiant coordinates and echo rates for the δ Aquarids and three other minor showers are summarized.

523.5 853

Meteor Height Distributions and the Fragmentation Hypothesis—A. A. Weiss. (*Aust. J. Phys.*, vol. 13, pp. 532–549; September, 1960.) A comparative study is made of fragmentation amongst bright and faint meteors.

523.5 854

The Variation of Meteor Heights with Velocity and Magnitude—J. S. Greenhow and J. E. Hall. (*Monthly Notices Roy. Astron. Soc.*, vol. 121, no. 2, pp. 174–182; 1960.) Radio echo observations of meteors of +6 magnitude show marked departures from the theoretically predicted heights. Possible explanations for these departures are considered. (*See* 856.)

523.5:621.391.812.5 855

Volume Density of Radio Echoes from Meteor Trails—Carrara, Checcacci, and Ronchi. (*See* 1016.)

523.5:621.396.96 856

The Importance of Initial Trail Radius on the Apparent Height and Number Distributions of Meteor Echoes—J. S. Greenhow and J. E. Hall. (*Monthly Notices Roy. Astron. Soc.*, vol. 121, pp. 183–196; 1960.) Fewer echoes from faint meteors of +6 magnitude are observed at 8 mλ than at 17 mλ. This effect is attributed to an attenuation in echo amplitude due to the large initial radii of the ionized trails.

523.5:621.396.96 857

The Determination of the Incident Flux of Radio-Meteors—T. R. Kaiser. (*Monthly Notices Roy. Astron. Soc.*, vol. 121, no. 3, pp. 284–298; 1960.) Simple formulas are derived which allow the incident flux of shower meteors to be deduced from the observed rate after allowing for the antenna characteristics and the geometry of reflection. The limitations of the method are discussed.

550.38:523.75 858

The Interaction of the Terrestrial Magnetic Field with the Solar Corpuscular Radiation—D. B. Beard. (*J. Geophys. Res.*, vol. 65, pp. 3559–3568; November, 1960.) The shape of the cavity between the earth and a neutral solar stream differs by only 7–11 per cent from a hemisphere of radius 7 earth radii on the incident side, but is elongated on the other side to a distance of the order of 100 earth radii. The cavity is indented at the polar latitudes where the current layer reverses.

550.385.4 859

The Cause of Magnetic Storms and Bays—R. A. Duncan. (*J. Geophys. Res.*, vol. 65, pp. 3589–3592; November, 1960.) Circulating currents set up around regions of proton and electron precipitation by the Hall effect are suggested as the cause of magnetic bays and storms.

550.385.4 860

Daytime Enhancement of the Amplitude of Geomagnetic Sudden Impulses in the Equa-

torial Region—H. Maeda and M. Yamamoto. (*J. Atmos. Terrest. Phys.*, vol. 19, pp. 284–287; December, 1960.) IGY data from equatorial stations provide some evidence that sudden impulses and sudden commencements are caused by similar mechanisms.

550.385.4:539.16 861

Evidence of Quasi-perpendicular Propagation of Hydromagnetic Waves caused by Nuclear Explosions over Johnston Island—H. Maeda and T. Ondoh. (*Nature, Lond.*, vol. 188, pp. 1018–1019; December 17, 1960.)

551.507.362.2 862

Verification of Earth's "Pear Shape" Gravitational Harmonic—C. J. Cohen and R. J. Anderle. (*Science*, vol. 132, pp. 807–808; September 23, 1960.) Errors in the predictions of the orbit of the Transit 1B satellite (1960γ) are accounted for by a third-order gravitational harmonic previously evaluated by O'Keefe, *et al.* (2236 of 1959).

551.507.362.2:523.165:621.391.812.6 863

The Relation of the Satellite Ionization Phenomenon to the Radiation Belts—J. D. Kraus and R. C. Higgy. (PROC. IRE, vol. 48, pp. 2027–2028; December, 1960.) During March and April, 1960, when telemetry transmissions from Explorer VII were monitored, the strongest enhancements of WWV signals received at Columbus, Ohio, occurred at times of peak counting rate aboard the satellite. Many of these events were accompanied by a partial or complete fade-out of the satellite signal. [See also 1603 of 1960 (Kraus, *et al.*).]

551.507.362.2:621.391.812.63 864

Some Characteristics of the Signal Received from 1958 δ2—F. de Mendonca, O. G. Villard, Jr., and O. K. Garriott. (PROC. IRE, vol. 48, pp. 2028–2030; December, 1960.) The correlation between scintillation effects and the occurrence of spread F is noted, and skip-distance phenomena observed in ordinary- and extraordinary-wave propagation are discussed.

551.507.362.2:621.396.96 865

Electromagnetic Waves and Satellites; Echoes from Ionized Trails of Satellites at High Frequency—A. Flambard and M. Reyssat. (*Onde Élect.*, vol. 38, pp. 830–837; December, 1958.) Ionized trails from 1957β and 1958ϵ were detected at 25 Mc, using a pulsed 75-kw transmitter and a receiver with 20-kc bandwidth. The results are discussed and the most favorable conditions for detecting echoes are examined.

551.510.535 866

On the Lunar Semidiurnal Variation of the D and F_2 Layers—M. Bossolasco and A. Elena. (*Geofis. Pura Appl.*, vol. 46, pp. 167–172; May–August, 1960. In English.) The variations at Freiburg, Genoa, and Léopoldville are compared with those obtained by other authors. Magnetic dip rather than geomagnetic latitude controls the variation in the F_2 layer. The amplitude of the f_0F_2 variation is plotted against magnetic dip.

551.510.535 867

On Some Disturbances in the E Region—B. J. Robinson. (*J. Atmos. Terrest. Phys.*, vol. 19, pp. 160–171; December, 1960.) *E*-layer stratifications and complex phenomena observed on ionograms are discussed in relation to computed electron $N(h)$ distributions. The passage of transient cusps on $h'(f)$ curves is found to be due to redistribution of E-layer ionization. Factors influencing the identification of E-layer penetration frequencies are discussed.

551.510.535 868

Investigation of the Transparency of the Ionospheric E_s Layer—K. Rawer. (*C. R. Acad. Sci., Paris*, vol. 250, pp. 1517–1519; February 22, 1960.) A report is presented of an analysis of world-wide observations of diurnal changes in E_s. Results are discussed and tabulated in the form of an index called the "degree of occultation" which is defined as the ratio f_b/f_t, where f_b is the blanketing frequency for reflections from the *F* layer and f_t the highest frequency at which reflections from the E_s layer are detected.

551.510.535 869

Mechanism of Ionization of the Sporadic-E Layer—K. Bibl. (*Ann. Géophys.*, vol. 16, pp. 148–151; January–March, 1960.) Observations made using a technique based on that introduced by Nakata, *et al.* (see 3297 of 1953, and 2937 of 1954) have shown that the height of E_s varies in a systematic way during the lifetime of an E_s event; if the intensity of ionization increases, the layer height decreases.

551.510.535 870

Horizontal Drift in the Ionosphere over Delhi—S. N. Mitra, K. K. Vij, and P. Dasgupta. (*J. Atmos. Terrest. Phys.*, vol. 19, pp. 172–183; December, 1960.) The drift was measured using spaced-receiver techniques and both E- and F-layer reflections analyzed for the period April, 1958 to March, 1959. Velocity histograms of the north-south and east-west components and plots of the seasonal variations in velocity and drift direction are given.

551.510.535 871

On the Observational Results of f_{min} at Yamagawa—S. Ishikawa and K. Muramatsu. (*J. Radio Res. Labs., Japan*, vol. 7, pp. 405–408; July, 1960.) Measurements of f_{min}F and f_{min}E made between August, 1959, and February, 1960, showed the presence of the winter anomaly in absorption at night.

551.510.535 872

On the Electron and Ion Density Distributions from the Lower up to the Uppermost Part of the F Region—T. Yonezawa and H. Takahashi. (*J. Radio Res. Labs., Japan*, vol. 7, pp. 335–378; July, 1960.) The thesis that the main ionizing radiations in the F region are the helium resonance lines at 304 and 584 Å and the Lyman continuum leads to the following results: 1) the calculated electron density distribution in the lower F region is in good agreement with experimental electron density profiles, 2) the observed and calculated relative abundances of the ions O^+, O_2^+ and NO^+ are not in good agreement unless their charge exchange reactions are assumed to be a few orders of magnitude slower than expected on simple theory, and 3) if a scale height gradient of 0.2 is assumed, then the calculated and experimental electron densities are in agreement up to 100 km above the F region maximum. [See also 4222 of 1960 (Yonezawa).]

551.510.535 873

On the F_2 Region of the Ionosphere—S. Datta. (*Indian J. Phys.*, vol. 34, pp. 66–75; February, 1960.) A continuation of earlier work (800 of 1959) to include calculations of diurnal variations of production rate for March, 1950, using the attachment-coefficient model suggested by Ratcliffe, *et al.* (2724 of 1956). Results are compared with those for January, 1950, given in the earlier paper, and are found to be consistent with Bradbury's hypothesis for the formation of the F_2 layer.

551.510.535 874

World-Wide Daily Variations in the Height of the Maximum Electron Density in the Ionospheric F_2 Layer—J. W. Wright and R. E. McDuffie: T. Shimazaki. (*J. Radio Res. Labs, Japan*, vol. 7, pp. 409–420; July, 1960.) The heights given by the method of Shimazaki (419 of 1956), which related $(M3000)F_2$ and the height of a parabolic F layer, have been compared with the more correct values derived from corresponding $N(h)$ profiles. The agreement between the two methods is quite good during the night in middle and low latitudes, but during the day in these latitudes and for all hours at high latitudes Shimazaki's relation overestimates the height by about 20 km.

551.510.535 875

Investigation of the Formation of the Ionospheric F_2 Layer at Léopoldville-Binza—P. Herrinck. (*Ann. Géophys.*, vol. 16, pp. 77–87; January–March, 1960.) Data for the period 1952–1958 are analyzed. Photoionization and drift are insufficient to explain the variations of maximum electron density; additional ionization due to corpuscles accelerated in a region near the earth is suggested.

551.510.535 876

Bifurcation and other Irregularities of the Ionospheric F_2 Layer—E. Woyk (Chvojková). (*Nature, Lond.*, vol. 188, pp. 906–907; December 10, 1960.) Splitting is considered to occur when the excess of energy of each ionizing photon over the ionizing potential is transformed into heat. On account of the quasi-neutrality, the rarefaction of the gas at the maximum of ionization can create a small secondary minimum of electron density which separates the F layer into F_1 and F_2. This secondary minimum of electron density appears just at the maximum of electron production.

551.510.535 877

Effects of Diffusion of Electrons near the Magnetic Equator—V. C. A. Ferraro, J. E. C. Gliddon, and P. C. Kendall. (*Nature, Lond.*, vol. 188, pp. 1017–1018; December 17, 1960.) If it is assumed that ionization in the F_2 layer is produced according to Chapman's law, then, as the magnetic equator is approached, the rate of increase in ionization will exceed any decrease due to the effects of vertical diffusion described by Schmerling (4224 of 1960). The hypothesis of vertical diffusion does not therefore account for the "geomagnetic anomaly."

551.510.535 878

The Geomorphology of Spread-F—D. G. Singleton. (*J. Geophys. Res.*, vol. 65, pp. 3615–3624; November, 1960.) The occurrence of spread F is roughly symmetrical about the geomagnetic equator, and is greatest in the equatorial and auroral regions. It occurs mainly during the night, and is greatest in winter in the auroral region, and at equinox in the equatorial region.

551.510.535 879

The Belt of Equatorial Spread-F—A. J. Lyon, N. J. Skinner, and R. W. H. Wright. (*J. Atmos. Terrest. Phys.*, vol. 19, pp. 145–159; December, 1960.) IGY data are used to discuss the morphology of nocturnal spread-*F* incidence in the equatorial belt, and this is compared with the morphology of the post-sunset increase of F-layer virtual height. Between magnetic latitudes $\pm 30°$, the incidence of spread F is high, but decreases during periods of magnetic disturbance. Existing theories are inadequate to explain the observations.

551.510.535:523.745 880

M.U.F. Factor and Solar Activity—C. S. R. Rao and J. C. Bhargava. (*Indian J. Phys.*, vol. 34, pp. 85–91; February, 1960.) An analysis of ionospheric data for Delhi and Ahmedabad indicates that a linear relation exists between $(M3000)F_2$ and the sunspot number for both places.

551.510.535:550.385.4 881
Hydromagnetic Waves in the Ionosphere—W. E. Francis and R. Karplus. (*J. Geophys. Res.*, vol. 65, pp. 3593–3600; November, 1960.) The results of numerical integration of the hydromagnetic wave equations in the ionosphere are presented. Earlier estimates of ionospheric heating by hydromagnetic waves are confirmed.

551.510.535:550.507.362.1 882
Electron Densities in the *F* Region of the Ionosphere from Rocket Measurements: Parts 1 & 2—J. S. Nisbet and S. A. Bowhill. (*J. Geophys. Res.*, vol. 65, pp. 3601–3614; November, 1960.) The recording and analysis of Faraday-rotation and range-error measurements on radio waves from long-range military and satellite-launching rockets are described. Corrections for horizontal gradients and refraction are included. The results from seven launchings show that the vertical electron-density gradient is greatest near sunrise and lowest after sunset, suggesting a time lag before diffusive equilibrium is reached.

551.510.535:621.391.812.63 883
The D_1, D_2 Layers and the Absorption of Radio Waves—G. C. Rumi. (*J. Geophys. Res.*, vol. 65, pp. 3625–3630; November, 1960.) The possibility of separating absorption at different levels in the lower ionosphere is discussed theoretically with experimental examples.

551.510.535:621.391.812.63.029.45 884
The Sunrise in the Ionosphere and its Repercussions on Long-Wave Propagation—J. Rieker. (*Geofis. Pura Appl.*, vol. 46, pp. 241–328; May–August, 1960. In French.) The basic data are the records made at Zurich of the variations in number and direction of arrival of atmospherics at a frequency of 27 kc. The sudden fall in number of received atmospherics near dawn is attributed to the sunrise at a height of 75 km at a point on the wave trajectory. The height of the ozone layer is found to be 28 km. The transitory "nose effect" in recordings of atmospherics is attributed to the transition from D-layer to E-layer propagation.

551.510.536 885
Physical Parameters of the Atmospheric Escape Layer—J. J. Gilvarry. (*Nature, Lond.*, vol. 188, pp. 804–805; December 3, 1960.) The height of the atmospheric escape layer is approximately 670 km in the daytime, dropping to 480 km at night. The temperature of the layer is too low to cause the dissipation of helium-4 from the atmosphere and it is suggested that this process occurs during solar disturbances.

551.510.62:551.508.8 886
Adaptation of the Radiosonde for Direct Measurement of Radio Refractive Index—A. H. Clinger and A. W. Straiton. (*Bull. Am. Met. Soc.*, vol. 41, pp. 250–252; May, 1960.) The system described is based on standard meteorological sensing devices and provides an accuracy sufficient for many radio-propagation applications.

551.594.5 887
On the Magnetic Time Dependence of the Auroral Zone Currents—B. Hultqvist and G. Gustafsson. (*J. Atmos. Terrest. Phys.*, vol. 19, pp. 246–259; December, 1960.) The geomagnetic time for the evening passage of the geomagnetic component *H* through the zero-disturbance level was measured at Kiruna and College on 386 days. A time difference of 42 min was found, only part of which can be explained by means of higher spherical harmonic terms of the geomagnetic field.

551.594.5:550.385.4 888
A Dynamo Theory of the Aurora and Magnetic Disturbance—K. D. Cole (*Aust. J. Phys.*, vol. 13, pp. 484–497; September, 1960.) A model of the aurora is examined in which a slab of ionized air exists parallel to the geomagnetic field. A wind of neutral molecules causes movement of the aurora and certain features of auroral and magnetic disturbances are explained.

551.594.6 889
Radiation from Protons of Auroral Energy in the Vicinity of the Earth—W. B. Murcray and J. H. Pope. (*J. Geophys. Res.*, vol. 65, pp. 3569–3574; November, 1960.) Cyclotron radiation of protons in the earth's magnetic field could be one source of dawn chorus.

551.594.6 890
Choice of a Parameter Characterizing Radio Whistlers—Y. Corcuff. (*Ann. Géophys.*, vol. 16, pp. 128–139; January–March, 1960.) The dispersion *D* is proposed as a character-figure for whistlers. It is also proposed that, as long as whistlers have a dispersion which is dependent on frequency, the frequency should be stated; zero frequency is considered optimum for this purpose.

551.594.6 891
Travelling-Wave Amplification of Whistlers—N. M. Brice. (*J. Geophys. Res.*, vol. 65, pp. 3840–3842; November, 1960.) Theory of the travelling-wave tube is applied to AF waves in the ionosphere to explain the generation of whistlers.

551.594.6:551.594.5 892
Auroral Noise at H.F.—R. D. Egan and A. M. Peterson. (*J. Geophys. Res.*, vol. 65, pp. 3830–3832; November, 1960.) Observations made with fixed-frequency back-scatter equipment and riometers are discussed.

551.594.6:621.391.821 893
On the Theory of Amplitude Distribution of Impulsive Random Noise and its Application to the Atmospheric Noise—K. Furutsu and T. Ishida. (*J. Radio Res. Labs., Japan*, vol. 7, pp. 279–307; July, 1960. Charts.) Atmospheric noise is considered to be a superposition of sources of independent randomly occurring Poisson noise wave packets. Theoretical amplitude distributions from both discrete and continuous spatial distributions of sources are compared with actual noise measurements with considerable agreement.

551.510.535 894
Physics of the Upper Atmosphere. [Book Review]—J. A. Ratcliffe, Ed. Publishers: Academic Press, New York, N. Y., 586 pp., 1960. (*J. Atmos. Terrest. Phys.*, vol. 19, p. 295; December, 1960.)

LOCATION AND AIDS TO NAVIGATION

621.396.933 895
Doppler Navigation and Tracking—B. R. Gardner. (PROC. IRE, vol. 48, pp. 2016–2017; December, 1960.) An airborne Doppler CW mapping system operating on 9.25 Gc is briefly described and some results are given.

621.396.96:621.396.677.089.6:523.164.32 896
Aerial Calibration by Solar Noise using Polar Display—Cufflin. (*See* 781.)

621.396.96.089.6:523.164.32 897
Aerial Investigations using Natural Noise Sources—E. Eastwood. (*Marconi Rev.*, vol. 23, pp. 2–20; 1st Quarter, 1960.) Experiments are described using radiation from the quiet sun as a means of measuring the polar diagrams of 1.5-m-λ and microwave radar systems. A moon-reflected solar noise signal is also reported.

621.396.96.089.6:523.264.32 898
Some Measurements on Radar Aerials, using Stellar Noise—M. J. B. Scanlan. (*Marconi Rev.*, vol. 23, pp. 21–32; 1st Quarter, 1960.) Some measurements of the vertical polar diagrams of radar antennas, using the sun as the source of radiation, are presented. Other celestial objects are considered as possible radiators for the calibration of antennas.

621.396.969.36 899
Far-Field Scattering from Bodies of Revolution—K. M. Siegel. (*Appl. Sci. Res.*, vol. B7, no. 4, pp. 293–328; 1958.) By the use of approximations based on physical reasoning, radar cross sections for bodies of revolution are determined. [See also 4073 of 1959 (Brysk, *et al.*) and *Appl. Sci. Res.*, vol. B8, no. 1, pp. 8–12; 1959 (Siegel, *et al.*).]

621.396.969.36 900
Effects of the Dielectric Coatings with Non-uniform Thickness on the Radar Cross-Section of the Perfectly Conducting Sphere—A. Komata and Y. Mushiake. (*Sci. Rep. Res. Inst. Tohoku Univ., Ser. B*, vol. 11, nos. 3/4, pp. 191–201; 1960.)

MATERIALS AND SUBSIDIARY TECHNIQUES

535.215:539.23 901
On High-Voltage Photoelectromotive Forces in Thin Semiconductor Layers—V. M. Lyubin and G. A. Fedorova. (*Dokl. Akad. Nauk SSSR*, vol. 135, pp. 833–836, December 1, 1960.) Measurements have been made of the photo-EMF in CdTe, Sb_2Se_3, and $Sb_2S_3 \cdot BiS_3$ films. Results are shown graphically. In some samples photovoltages of 150–180 v/cm were obtained at room temperature.

535.215:546.47'221:539.23 902
Hole Mobility and Crystal Size in Lead Sulphide Photoconductive Films—H. E. Spencer and J. V. Morgan. (*J. Appl. Phys.*, vol. 31, pp. 2024–2027; November, 1960.)

535.215+535.37]:546.48'221 903
The Temperature Dependence of the Absorption Edge in CdS Crystals—H. Radelt. (*Z. Naturforsch.*, vol. 15a, pp. 269–270; March, 1960.) A preliminary report is presented on measurements of the spectral distribution of transmission in the range from 5500 Å to the absorption edge at temperatures down to 21°K. This is an extension of earlier measurements, and results agree with those of other authors. [*E.g.*, 1208 of 1959 (Dutton).]

535.215:546.48'221 904
Further Experimental Evidence on Majority-Carrier Injection in CdS Single Crystals—I. T. Steinberger. (*J. Phys. Chem. Solids*, vol. 15, pp. 354–355; October, 1960.) The work of Smith and Rose (2666 of 1955) and of Böer and Kümmel (2749 of 1958) is discussed; further experiments are described which show that the results of Smith and Rose can be explained only on the assumption of majority-carrier injection, and cannot be accounted for by bulk liberation of carriers.

535.215:546.48'221 905
Direct Observation of Exciton Motion in CdS—D. G. Thomas and J. J. Hopfield. (*Phys. Rev. Lett.*, vol. 5, pp. 505–507; December 1, 1960.)

535.37 906
Excitation Spectra of Vanadium-Activated Zinc and Cadmium Sulphide and Selenide Phosphors—G. Meijer and M. Avinor. (*Philips Res. Rept.*, vol. 15, pp. 225–237; June, 1960.) The emission in the 2-μ fluorescence band is

excited by absorption in two composite bands due to vanadium at 1.1 and 1.6 ev, by absorption in an auxiliary impurity center, such as copper or silver, if present, and by fundamental excitation. [See also 3121 of 1960 (Avinor and Meijer).]

535.37:[546.47'221+546.48'221 907

Polarization of Fluorescence in CdS and ZnS Single Crystals—J. L. Birman. (*J. Electrochem. Soc.*, vol. 107, pp. 409–417; May, 1960.) A number of models are proposed in which the energy-level structure of centers is consistent with observations of polarization. The Lambe-Klick model is preferred for its simplicity, but conclusive data are at present lacking.

535.37:[546.47'221+546.48'221 908

Polarization of Luminescence in ZnS and CdS Single Crystals—A. Lempicki. (*J. Electrochem. Soc.*, vol. 107, pp. 404–409; May, 1960.) The fluorescent emission from hexagonal ZnS and CdS single crystals is found to be polarized preferentially perpendicular to the *c* axis for both polarized and unpolarized excitation. Cubic ZnS crystals emit unpolarized radiation.

535.37:546.47'221 909

Fluorescence of some Activated ZnS Phosphors—W. van Gool, A. P. Cleiren, and H. J. M. Heijligers. (*Philips Res. Rept.*, vol. 15, pp. 254–274; June, 1960.) The effects of different activators (Ag, Cu, Au) and co-activators (Al, Sc, Ga, In) are studied, in all combinations and at room temperature and −196°C.

535.37:546.47'221 910

Self-Activated and Cu-Activated Fluorescence of ZnS—W. van Gool and A. P. Cleiren. (*Philips Res. Rept.*, vol. 15, pp. 238–253; June, 1960.) Krgöer's theory of these emissions [see 2228 of 1950 (Kröger and Dikhoff)] is reviewed, and further experimental data are presented, especially regarding the temperature dependence of the fluorescence bands.

535.37:546.47'48'221 911

Effect of CdS Addition in ZnS:Cu,In and ZnS:Ag,In Phosphors—E. F. Apple. (*J. Electrochem. Soc.*, vol. 107, pp. 418–422; May, 1960.) "ZnS:Cu,In and ZnS:Ag,In phosphors each can show two emission bands under 3650 Å excitation, namely, in the green (short) and orange (long) with Cu and in the blue and yellow with Ag activator. Addition of CdS causes the ratio of intensities of the short to long wavelength emission to increase. This observation is interpreted using the donor-acceptor associated pair model proposed recently for the long wavelength emission process [187 of 1960 (Apple and Williams)]."

535.376 912

A Note on Electroluminescence due to Carrier Accumulation—H. K. Henisch and B. R. Marathe. (*Proc. Phys. Soc.*, vol. 76, pp. 782–783; November 1, 1960.) Some observations of electroluminescence, at present attributed to injection, could be due to recombination of accumulated carriers.

535.376 913

Apparatus for the Study of Luminescent Substances under the Action of Cathodic Bombardment—F. Gans. (*C.R. Acad. Sci., Paris*, vol. 250, pp. 1821–1823; March 7, 1960.) In the apparatus described, the screen is magnetically coupled to a motor rotating at a speed of 2800 rpm. Results obtained with screens of CdS are briefly reported.

535.376 914

The Light Waveforms Emitted from Electroluminescent Cells Energized by Square Waves and Pulses of Voltage—G. R. Hoffman and D. H. Smith. (*J. Electronics Control*, vol. 9, pp. 161–216; September, 1960.) Light pulses which rise to a maximum in less than 0.2 μs can be obtained from electroluminescent cells under square-wave excitation. The pulses decay more slowly, taking from 2 to 3 μs to decay to one-third of their maximum amplitude at a repetition frequency of 50 kc, and about 100 μs at 200 cps. A proposed model of a phosphor crystal is discussed and the predicted effects on the light waveforms of variations in frequency, pulsewidth, and temperature are correlated with observations.

535.376:546.41'221 915

CaS:Cu, Eu Electroluminescent Phosphors—A. Wachtel. (*J. Electrochem. Soc.*, vol. 107, pp. 199–206; March, 1960.)

535.376+535.215]:546.681'18 916

***P-N* Luminescence and Photovoltaic Effects in GaP**—H. G. Grimmeiss and H. Koelmans. (*Philips Res. Rept.*, vol. 15, pp. 290–304; June, 1960.) Depending on the method of preparation, GaP crystals show either *p*- or *n*-type conductivity. Nondoped crystals show electroluminescence, point-contact rectification, and photovoltaic effects. A level scheme for GaP is proposed. The wavelength dependence of the photovoltage has been found, and an explanation in terms of optical and thermal effects is given.

537.227 917

Some Properties of Ferroelectrics at a Frequency of 3000 Mc/s—V. M. Petrov. (*Fiz. Tverdogo Tela*, vol. 2, pp. 997–1001; May, 1960.) The small-signal UHF permittivity ϵ and loss tangent tan δ of single-crystal and ceramic $BaTiO_3$ and of VK1 materials have been measured as a function of an applied dc field in the range 0–22 kv/cm. Both ϵ and tan δ decrease on application of the dc field. Hysteresis and aging effects are observed.

537.227 918

Ferroelectric Domain Delineation in Triglycine Sulphate and Domain Arrays Produced by Thermal Shocks—A. G. Chynoweth and W. L. Feldmann. (*J. Phys. Chem. Solids*, vol. 15, pp. 225–233; October, 1960.)

537.227 919

Kinematic Theory of Ferroelectric Domain Growth—T. Nakamura. (*J. Phys. Soc. Japan*, vol. 15, pp. 1379–1386; August, 1960.)

537.227 920

Switching Properties of Tetramethylammonium-trichloromercurate—E. Fatuzzo. (*Proc. Phys. Soc.*, vol. 76, pp. 797–799; November 1, 1960.)

537.227:546.431'824'28–31 921

The Problem of Replacement of a Titanium Ion by a Silicon Ion in Polycrystalline Barium Titanate—L. N. Kamysheva. (*Fiz. Tverdogo Tela*, vol. 2, pp. 1002–1003; May, 1960.) A note is made of measurements on $Ba(Ti, Si)O_3$ samples in weak 1-kc fields showing the variation of permittivity with temperature in the range 80°–160°C.

537.227:546.431'824–31 922

An Investigation of the Cubic-Hexagonal Transition in Barium Titanate—R. M. Glaister and H. F. Kay. (*Proc. Phys. Soc.*, vol. 76, pp. 763–771; November 1, 1960.)

537.311.33 923

Resonance Transfer of Ionization Energy in Semiconductors—S. Koshino and T. Ando. (*J. Phys. Soc. Japan.*, vol. 15, p. 1538; August, 1960.) An interpretation of anomalous thermal conductivity is given which involves dependence on the impurity concentration.

537.311.33 924

Integral Equations for Determining the Mobility in Semiconductors—W. Franz. (*Z. Naturforsch.*, vol. 15a, pp. 366–368; April, 1960.) Equations are given for use in the iteration method of calculating the mobility tensor for strong-field conditions.

537.311.33 925

Free-Carrier Absorption due to Polar Modes in the III–V Compound Semiconductors—S. Visvanathan. (*Phys. Rev.*, vol. 120, pp. 376–378; October 15, 1960.) A quantum-mechanical calculation gives an absorption varying as $\lambda^{2.5}$ and such behavior is observed experimentally in InP and GaP. The calculated value of the absorption coefficient in InP agrees with experiment.

537.311.33 926

Free-Carrier Absorption arising from Impurities in Semiconductors—S. Visvanathan. (*Phys. Rev.*, vol. 120, pp. 379–380; October 15, 1960.) Available data for bremsstrahlung have been used to calculate the absorption coefficient. Results agree with calculations by other methods. The inadequacy of the Born approximation is brought out.

537.311.33 927

Phenomenology of Impurity Conduction in Semiconductors—E. C. McIrvine. (*J. Phys. Chem. Solids*, vol. 15, pp. 356–358; October, 1960.) A simple empirical relation is deduced between the critical impurity concentration above which temperature-independent impurity conduction is observed, and the static dielectric constant, using data on Ge, Si, InSb, SiC, CdS, and Mg_2Sn.

537.311.33 928

Measurement of Decay Times of Excess Carriers in Semiconductors, Excited by X-Ray Pulses—J. A. W. van der Does de Bye. (*Philips Res. Rept.*, vol. 15, pp. 275–289; June, 1960.) The experimental method is described. The decay times found are of the order of 3 μs, and are similar to those for excess carriers excited by pulses of light.

537.311.33:535.215:538.63 929

The Photomagnetic Effect in Isotropic Semiconductors and its Use in Measuring the Lifetime of Minority Current Carriers—A. A Grinberg. (*Fiz. Tverdogo Tela*, vol. 2, pp. 836–847; May, 1960.) A convenient form of the kinetic equation is derived for current in the case of two types of carrier with the same sign. This is used to determine the photocurrent and photomagnetic emf in an arbitrary magnetic field. The photomagnetic method of measuring carrier lifetime is discussed and formulas are derived for determining the lifetime in strong fields.

537.311.33:537.32 930

Thermal Conductivity of Semiconductor Solid Solutions—A. V. Ioffe and A. F. Ioffe. (*Fiz. Tverdogo Tela*, vol. 2, pp. 781–792; May, 1960.) The mechanism of thermal conduction is discussed with special reference to the scattering of phonons by impurities. Results of an experimental investigation of a wide range of semiconductors are tabulated and shown graphically.

537.311.33:538.569.4 931

Magneto-Plasma Resonance in Semiconductors: Part 1—M. Date. (*J. Phys. Soc. Japan*, vol. 15, pp. 1488–1492; August 1960.) Theory developed for the general case where several kinds of free carriers are moving under a static magnetic field shows that, under certain conditions, the resultant plasma frequency can be determined as though there were only one kind of carrier with the reduced mass of all the carriers concerned.

537.311.33:538.63 932

Theory of the Ettingshausen Effect in Semiconductors—B. V. Paranjape and J. S. Levinger. (*Phys. Rev.*, vol. 120, pp. 437–441; October 15, 1960.) The Ettingshausen coefficient P is calculated and discussed for intrinsic p-type and n-type semiconductors. Results agree reasonably well with experimental data for P as a function of temperature for different samples of Ge and Si.

537.311.33:538.63 933

Theory of the Absorption Edge in Semiconductors in a High Magnetic Field—R. J. Elliott and R. Loudon. (*J. Phys. Chem. Solids*, vol. 15, pp. 196–207; October, 1960.) An extension of previous theory [see 501 of 1959 (Elliott, *et al.*)] to include the effect of the Coulomb interaction of the hole-electron pair.

537.311.33:538.63 934

Magneto-electrical Field-Effect Measurements—E. Aerts. (*J. Electronics Control*, vol. 9, pp. 217–228; September, 1960.) Further experimental results are given on the influence of combined orthogonal transverse electric and magnetic fields on the mobility of the carriers in the space-charge layer at the surface of a semiconductor. In particular, it is shown that the Hall field could change the type of surface layer. [See 3154 of 1960 (Aerts, *et al.*).]

537.311.33:546.23:537.226.2/.3 935

Dielectric Investigations on Polycrystalline Selenium—W. Ludwig. (*Z. Naturforsch.*, vol. 15a, pp. 285–286; March, 1960.) Report on measurements of the dispersion characteristics of dielectric constant and loss angle of high-purity Se in the frequency range 0.5–1000 kc between $+40°$ and $-160°$C.

537.311.33:546.28 936

Optical Constants of Silicon in the Region 1 to 10 eV—H. R. Philipp and E. A. Taft. (*Phys. Rev.*, vol. 120, pp. 37–38; October 1, 1960.)

537.311.33:546.28 937

Scattering Anisotropies in n-Type Silicon—D. Long and J. Myers. (*Phys. Rev.*, vol. 120, pp. 39–44; October 1, 1960.) Magnetoresistance measurements show that the main features of the scattering anisotropies can be represented by the relaxation time ratio $\tau_1/\tau_2 \approx \frac{2}{3}$ for acoustic lattice scattering, and $\tau_1/\tau_2 > 1$ for ionized-impurity scattering, where τ_1 and τ_2 are the relaxation times parallel and perpendicular to the constant-energy spheroid axes.

537.311.33:546.28 938

A Note on the Method of Determining Ionization Coefficients for Electrons and Holes in Silicon—R. J. McIntyre. (*J. Electronics Control*, vol. 9, pp. 229–231; September, 1960.) This is an analytical note showing that ionization coefficients need not be equal for symmetrical pairs to have equal breakdown voltages, contrary to the analysis of Shields (2625 of 1959).

537.311.33:546.28 939

On the Determination of Diffusion Coefficient of Boron in Silicon—J. Yamaguchi, S. Horiuchi, K. Matsumura, and Y. Ogino. (*J. Phys. Soc. Japan*, vol. 15, pp. 1541–1542; August, 1960.) This is a note of measurements made in terms of the conductivity of the diffused layer.

537.311.33:546.28 940

Long-Term Variations of the Field Effect in Silicon—V. G. Litovchenko and O. V. Snitko. (*Fiz. Tverdogo Tela*, vol. 2, pp. 815–822; May, 1960.) The main cause of long-term variations is the presence of water vapor in the atmosphere. Measurements in air and in vacuum are reported and a critical field is defined, above which an additional surface conductivity is observed. This conductivity persists for long periods after the field is removed.

537.311.33:546.289 941

Impurity Conductivity of Germanium at Low Temperature—B. M. Vul, É. I. Zavaritskaya, and L. V. Keldysh. (*Dokl. Akad. Nauk SSSR*, vol. 135, pp. 1361–1363; December 21, 1960.) Graphs show the variation of the current density and the drift velocity of holes with field strength at temperatures of 4.2°, 14° and 20.4° K.

537.311.33:546.289 942

Concerning the Properties of Germanium in a Strong Electric Field—G. M. Avak'yants. (*Fiz. Tverdogo Tela*, vol. 2, pp. 810–814; May, 1960.) A brief analysis is presented showing that Paranjape's theory (3513 of 1957) does not explain the hole mobility in p-type Ge. An interpretation is suggested which is based on interaction of holes with acoustic- and optical-mode lattice vibrations.

537.311.33:546.289 943

Scattering of Hot Carriers in Germanium—E. M. Conwell and A. L. Brown (*J. Phys. Chem. Solids*, vol. 15, pp. 208–217; October, 1960.) A theoretical study is presented of the dependence of lattice mobility of hot carriers on their "temperature," for lattice temperatures of 300°, 78°, and 20.4°K. The effects of impurity scattering are briefly considered.

537.311.33:546.289 944

Orientation-Dependent Dissolution of Germanium—F. C. Frank and M. B. Ives. (*J. Appl. Phys.*, vol. 31, pp 1996–1999, November, 1960.) The dissolution of single crystals of undoped Ge is shown to be almost completely dependent on orientation.

537.311.33:546.289 945

Exciton and Magneto-optical Effect in Strained and Unstrained Germanium—D. F. Edwards and V. J. Lazazzera. (*Phys. Rev.*, vol. 120, pp. 420–426; October 15, 1960). Measurements indicate that the absorption peaks correspond to transitions to exciton levels associated with each Landau level in qualitative agreement with calculations of others. A definitive experiment is suggested to test this theory.

537.311.33:546.289 946

Surface States on High-Purity Germanium—K. Schuegraf and K. Seiler. (*Z. Naturforsch.*, vol. 15a, pp. 368–369; April, 1960.) Results are discussed of measurements on Ge with impurity concentration $<10^{10}$/cm^2, and an interpretation is given of the surface states resulting from exposure to various gases.

537.311.33:546.289 947

A Controlled Diffusion Process for Indium in n-Type Germanium—F. Barson, M. J. Dyett, C. Karan, and W. E. Mutter. (*J. Electrochem. Soc.*, vol. 107, pp. 459–461; May, 1960.) Experimental results are given to show that molten In in contact with Ge can be used both as a getter to prevent thermal conversion and simultaneously as a source of In vapor for diffusion into Ge. The surface concentration of In can be reduced by dilution with Sn.

537.311.33:546.289:538.24 948

Magnetic Susceptibility of p-Type Ge—R. Bowers and Y. Yafet. (*Phys. Rev.*, vol. 120, pp. 62–66; October 1, 1960.) Measured carrier susceptibility is compared with theoretical expectations to obtain information concerning the band structure.

537.311.33:546.289:538.569.4 949

Additional Spin Resonance Spectrum in Antimony-Doped Germanium—R. W. Keyes and P. J. Price. (*Phys. Rev. Lett.*, vol. 5, pp. 473–474; November 15, 1960.)

537.311.33:546.289:538.639 950

The Phonon Component of the Transverse Thermo-magnetic Nernst Effect in p-Type Germanium—Yu. N. Obraztsov, I. V. Mocham, and T. V. Smirnova. (*Fiz. Tverdogo Tela*, vol. 2, pp. 830–835; May, 1960.) Results of calculations are compared with experimental data for the temperature range 96°–143°K and magnetic fields up to 5500 G.

537.311.33:546.289:621.382.23 951

Solvent Evaporation Technique for the Growth of Arsenic-Doped Germanium Single Crystals for Esaki Diodes.—F. A. Trumbore and E. M. Porbansky. (*J. Appl. Phys.*, vol. 31, p. 2068; November, 1960.)

537.311.33:546.47–31 952

Reactions of Lithium as a Donor and an Acceptor in ZnO.—J. J. Lander. (*J. Phys. Chem. Solids*, vol. 15, pp. 324–334; October, 1960.) The conditions for production of donors and acceptors by Li in ZnO are described. Solubilities and diffusion coefficients are given as well as some results for the kinetics and equilibria of the displacement reaction.

537.311.33:546.47'221:537.32 953

Thermoelectricity and Thermal Conductivity in the Lead Sulphide Group of Semiconductors—D. Greig. (*Phys. Rev.*, vol. 120, pp. 358–365; October 15, 1960.) Results of measurements from 4° to 100°K are given and discussed.

537.311.33:[546.49'241+546.49'241] 954

Band Structures and Scattering Mechanisms in Single-Crystal Mercury Telluride and Selenide—M. Rodot and H. Rodot. (*C.R. Acad. Sci., Paris*, vol. 250, pp. 1447–1449; February 22, 1960.) Measurements show that the conduction band is probably isotropic in HgTe and formed of ellipsoids in HgSe. In both materials scattering by acoustic phonons is predominant. For thermomagnetic properties of HgTe see 3779 of 1959 (Fumeron-Rodot and Rodot).

537.311.33:546.57'86'241 955

A Structural Study of the Compound $AgSbTe_2$—R. W. Armstrong, J. W. Faust, Jr., and W. A. Tiller. (*J. Appl. Phys.*, vol. 31, pp. 1954–1959; November, 1960.)

537.311.33:546.57'86'241 956

Anomalous Hall Effect in $AgSbTe_2$—R. Wolfe, J. H. Wernick, and S. E. Haszko. (*J. Appl. Phys.*, vol. 31, pp. 1959–1964; November, 1960.) The measurement of both positive and negative Hall coefficients in different samples is attributed to the presence of a second phase of Ag_2Te. [See also 3146 of 1960 (Rodot).]

537.311.33:546.623'682'86 957

Some Electrical Properties of the AlSb-InSb System—Ya. Agaev and D. N. Nasledov. (*Fiz. Tverdogo Tela*, vol. 2, pp. 826–829; May, 1960.) Investigation of the Hall effect and conductivity over a wide range of temperatures.

537.311.33:546.681'18 958

Carrier Concentration and Hole Mobility in p-Type Gallium Phosphide—G. F. Alfrey and C. S. Wiggins. (*Z. Naturforsch.*, vol. 15a, pp. 267–268; March, 1960. In English.) Results of measurements on polycrystalline material in the temperature range 100–500°K are given and compared with values predicted by other authors.

537.311.33:546.681'19 959
Influence of Arsenic Pressure on the Doping of Gallium Arsenide with Germanium—J. O. McCaldin and R. Harada. (*J. Appl. Phys.*, vol. 31, pp. 2065–2066; November, 1960.)

537.311.33:546.681.19 960
Diffusion of Cadmium into Gallium Arsenide—F. A. Cunnell and C. H. Gooch. (*Nature, Lond.*, vol. 188, p. 1906; December 24, 1960.) [See also 3945 of 1960 (Goldstein).]

537.311.33:546.682'86 961
Influence of the Electric Field on the Electrical Conductivity, Hall Coefficient, and Magnetoresistance of *n*-Type InSb at Low Temperature—Lyan Chzi-chao and D. N. Nasledov. (*Fiz. Tverdogo Tela*, vol. 2, pp. 793–798; May, 1960.) Observed deviations from Ohm's law may be be explained by assuming that electrons in the impurity band are excited into the conduction band under the influence of the applied electric field.

537.311.33:546.682'86 962
Calculation of Transport Effects for a Relaxation Time almost Independent of the Energy. Case of Indium Antimonide—M. Rodot. (*C.R. Acad. Sci., Paris*, vol. 250, pp. 1621–1623; February 29, 1960.)

537.311.33:546.682'86:535.215 963
Impurity Photoconductivity in *n*-Type InSb—E. H. Putley. (*Proc. Phys. Soc.*, vol. 76, pp. 802–805; November 1, 1960.) Photoconductivity is reported in InSb containing about 10^{14} impurities/cm³ when irradiated at mmλ in magnetic fields of 4–9 kG, at temperatures of the order of 1.5°K.

537.311.33:546.812'221 964
The Preparation and the Electrical and Optical Properties of SnS Crystals—W. Albers, C. Haas, and F. van der Maesen. (*J. Phys. Chem. Solids*, vol. 15, pp. 306–310; October, 1960.) Single crystals were prepared by heating the components to 900°C, and zone refining. The crystals were of *p* type with a hole density of $10^{17}-10^{18}$ cm^{-3} and mobility of 65 cm²/volt-second at room temperature.

537.311.33:546.817'231 965
Hall Coefficient and Electrical Conductivity Measurements on Lead Selenide Single Crystals Grown from the Vapour—R. H. Jones. (*Proc. Phys. Soc.*, vol. 76, pp. 783–787; November 1, 1960.)

537.311.33:547.491 966
Electronic Conduction and Exchange Interaction in a New Class of Conductive Organic Solids—R. G. Kepler, P. E. Bierstedt, and R. E. Merrifield. (*Phys. Rev. Lett.*, vol. 5, pp. 503–504; December 1, 1960.) The salts of a radical-anion formed by the addition of an electron to tetracyanoguinodimethane show a high electrical conductivity. The electric and magnetic properties of two such salts are described briefly.

537.312.62 967
Direct Measurement of the Superconducting Energy Gap—J. Nicol, S. Shapiro, and P. H. Smith. (*Phys. Rev. Lett.*, vol. 5, pp. 461–464; November 15, 1960.) The tunnelling *I/V* characteristic of an Al-Al_2O_3-Pb sandwich shows a negative-resistance region when both metals are superconducting. From this characteristic the energy gap for each metal is derived.

537.312.62 968
Electron Tunnelling between Two Superconductors—I. Giaever. (*Phys. Rev. Lett.*, vol. 5, pp. 464–466; November 15, 1960.) The energy gaps of Pb, In, and Al are found from the tunnelling *I/V* characteristics of sandwiches of these metals with Al and Al_2O_3.

537.312.62:538.63 969
Critical Fields of Superconducting Tin, Indium and Tantalum—R. W. Show, D. E. Mapother, and D. C. Hopkins. (*Phys. Rev.*, vol. 120, pp. 88–91; October 1, 1960.)

538.22 970
Model of Exchange Inversion Magnetization—C. Kittel. (*Phys. Rev.*, vol. 120, pp. 335–342; October 15, 1960.) A thermodynamic theory is given of a class of magnetic crystals which transform from ferromagnetic to antiferromagnetic states as the temperature is varied. Applications are suggested.

538.221 971
Thermally Activated Ferromagnetic Domain Wall Motion—F. D. Stacey. (*Aust. J. Phys.*, vol. 13, pp. 599–601; September, 1960.) An elementary theory is presented which is in close agreement with the results of Olmen and Mitchell (*J. Appl. Phys.*, vol. 30, Suppl., pp. 258S-259S; April, 1959.)

538.221 972
Theory of Stability of the Magnetic States of Ferromagnetic Substances during Magnetization—E. I. Kondorskiĭ. (*Zh. Eksp. Teor. Fiz.*, vol. 37, pp. 1110–1115; October, 1959.) An examination is made of the factors affecting stability of the magnetic states of a ferromagnetic single crystal with respect to external magnetic fields and elastic strains. An expression is derived giving the minimum value of the magnetic field and stress for which irreversible changes of the magnetization are observed.

538.221 973
Contribution of the Fermi Contact Term to the Magnetic Field at the Nucleus in Ferromagnets—A. J. Freeman and R. E. Watson. (*Phys. Rev. Lett.*, vol. 5, pp. 498–500; December 1, 1960.)

538.221 974
Contribution to the Theory of the Temperature Dependence of Ferromagnetic Anisotropy—E. A. Turov and A. I. Mitsek. (*Zh. Eksp. Teor. Fiz.*, vol. 37, pp. 1127–1132; October, 1959.) Mathematical analysis based on the phenomenological theory of spin waves is given.

538.221 975
Domain Patterns on "Cube-Textured" Silicon-Iron Sheet—L. F. Bates and R. Carey. (*Proc. Phys. Soc.*, vol. 76, pp. 754–758; November, 1, 1960.)

538.221 976
On the Effect of Heat Treatment in a Magnetic Field on Magnetic Properties of Iron-Aluminum Alloys—M. Sugihara. (*J. Phys. Soc. Japan*, vol. 15, pp. 1456–1460; August, 1960.)

538.221:537.312:62 977
On the Intermediate State in Ferromagnetic Superconductors—G. F. Zharkov. (*Zh. Eksp. Teor. Fiz.*, vol. 37, pp. 1784–1788; December, 1959.) A calculation is given of the range of external magnetic field values for which a single-domain ferromagnetic ellipsoid can exist in the intermediate state. [See 1556 of 1960 (Matthias and Suhl).]

538.221:538.569.4 978
Ferromagnetic Resonance and the Theory of Phases—A. Coumes. (*C.R. Acad. Sci., Paris*, vol. 250, pp. 819–821; February 1, 1960.) The two maximums in the absorption curve for a single-crystal disk of Fe-Si measured at a frequency of 9375 Mc are explained in terms of the "theory of phases" of Néel (*J. Phys. Radium*, vol. 5, nos. 11, 12, pp. 241–251, 265–276; November/December, 1944.)

538.221:538.65 979
Anomalies in Internal Friction and the Elasticity Modulus in Ferromagnetic Substances near the Curie Point—K. P. Belov, G. I. Kataev, and R. Z. Levitin. (*Zh. Eksp. Teor. Fiz.*, vol. 37, pp. 938–943; October, 1959.)

538.221:539.12.04 980
Effect of Neutron Bombardment on the Magnetic Properties of Very-High Permeability Iron—G. Biorci, A. Ferro, and G. Montalenti. (*J. Appl. Phys.*, vol. 31, pp. 2046–2047; November, 1960.) Samples show lower permeability and higher coercive force.

538.221:539.23 981
Magnetic Properties of Epitaxially Grown Films—O. S. Heavens. (*Research, Lond.*, vol. 13, pp. 404–410; October, 1960.) A review is given of methods used and results achieved in the measurement of magnetic properties of epitaxially grown ferromagnetic films.

538.221:621.318.124 982
Origin ov the Magnetic Anisotropy Energy of Cobalt Ferrite—M. Tachiki. (*Progr. Theor. Phys.*, vol. 23, pp. 1055–1072; June, 1960.) The magnetic anisotropy of Co ferrite is considered to arise from the Co^{2+} ions in the crystalline field of low symmetry.

538.221:621.318.124 983
Magnetic Anisotropy of Iron-Cobalt Ferrite Measured by Ferromagnetic Resonance—Y. Sugiura. (*J. Phys. Soc. Japan*, vol. 15, pp. 1461–1468; August, 1960.) The cubic magnetic anisotropy and the uniaxial magnetic anisotropy induced by heat treatment in a magnetic field are measured in the temperature range 70–250°C.

538.221:621.318.124:538.65 984
Origin of Magnetoelastic Effects in Cobalt-Iron Ferrite—J. C. Slonczewski. (*J. Phys. Chem. Solids*, vol. 15, pp. 335–353; October, 1960.) The influence of orbitally degenerate ions on the magnetostrictive strain and elastic energy of a ferrimagnetic crystal are calculated for a trigonal crystal field and cubic structure. Some comparisons are made with experimental data for Co-Fe ferrite.

538.221:621.318.134 985
Kinetics of Magnetic Annealing in Cobalt-Substituted Magnetite—W. Palmer. (*Phys. Rev.*, vol. 120, pp. 342–352; October 15, 1960.)

538.221:621.318.134 986
Ferrite Materials with Very Low Temperature Coefficient for High Frequencies—R. Sibille. (*Onde Élect.*, vol. 40, pp. 586–589; September, 1960.) Characteristic curves are given for a range of Ni-Zn ferrites with variations of permeability $\gg$0.02 per cent per °C over the range −60°C to +250°C.

538.221:621.318.134 987
On the Magnetic Properties of Gadolinium Oxides—K. P. Belov, M. A. Zaitseva, and A. V. Ped'ko. (*Zh. Eksp. Teor. Fiz.*, vol. 36, pp. 1672–1679; June, 1959.) Report and discussion of measurements of the variation of magnetization, coercive force and magnetostriction with temperative in Gd oxides of garnet and perovskite structure.

538.221:621.318.134:538.569.4 988
Influence of the Porosity on the Width of the Absorption Curve of Pure and Cr- and Al-Substituted Yttrium Garnet—R. Vautier and A. J. Berteaud. (*C. R. Acad. Sci., Paris*, vol. 250, pp. 1812–1814; March 7, 1960.)

538.221:621.318.134:538.569.4 989
Ferrimagnetic Resonance in Rare-Earth-Doped Yttrium Iron Garnet: Part 1—Field for Resonance—J. F. Dillon Jr., and J. W. Nielsen

(*Phys. Rev.*, vol. 120, pp. 105–113; October 1, 1960.) A description is given of experiments on single-crystal spheres of doped Y-Fe garnet in the temperature range 1.5–25°K to determine the field required for ferrimagnetic resonance as a function of crystal direction.

538.221:621.318.134:548.0 990

Dislocations, Stacking Faults and Twins in the Spinel Structure—J. Hornstra. (*J. Phys. Chem. Solids*, vol. 15, pp. 311–323; October, 1960.)

538.222 991

Etching Patterns on (100) Planes of the Single Crystal $K_3Co(CN)_3$—H. Iwasaki. (*J. Radio Res. Labs., Japan*, vol. 7, pp. 389–403; July, 1960.) Two types of pattern are observed: 1) a "pyramidal" form predominating on the $(100)^+$ plane and attributed to dislocation lines, 2) a "hill-like" form predominating on the $(100)^-$ plane and attributed to point defects. Both patterns are attributed to impurities.

538.222:528.569.4 992

Spin Lattice Relaxation Times in Ruby at 34.6 Gc/s—J. H. Pace, D. F. Sampson, and J. S. Thorp. (*Proc. Phys. Soc.*, vol. 76, pp. 697–704; November 1, 1960.) The measured relaxation times show dependence on temperature, transition order, and Cr concentration. Maser action should be possible at relatively high temperatures. Preliminary results were noted earlier (2107 to 1960).

538.222:538.569.4 993

Rotational Properties of Paramegnetic Resonance Spectra of Noncubic Crystals—M. Sachs. (*J. Phys. Chem. Solids*, vol. 15, pp. 291–305, October, 1960.)

MATHEMATICS

517.918 994

Laurent-Cauchy Transforms for Analysis of Linear Systems Described by Differential-Difference and Sum Equations—E. I. Jury: Y. H. Ku and A. A. Wolf. (PROC. IRE, vol. 48, pp. 2026–2027; December, 1960.) Comment on 2854 of 1960 and the author's reply are given.

519.271 995

Generalized Padé Approximation—J. L. Stewart. (PROC. IRE, vol. 48, pp. 2003–2008; December, 1960.) Approximation by minimizing the magnitude of the complex error vector in the steady state is considered, and its relation to conventional approximations for magnitude alone and phase alone is discussed.

MEASUREMENTS AND TEST GEAR

621.018.41(083.74):621.373.421.13 996

Atomic-Clock Accuracy for Crystal Oscillators—K. Nygaard. (*Electronics*, vol. 33, pp. 82–83; November, 1960.) A servo-system for locking crystal oscillators to a standard-frequency signal such as WWV is described.

621.317.3:537.311.33 997

An Analysis of the Circuit of Dauphinee and Mooser for Measuring Resistivity and Hall Constant—L. J. v. d. Pauw. (*Rev. Sci. Instr.*, vol. 31, pp. 1189–1192; November, 1960.) Switch capacitance is shown to introduce systematic errors whose magnitude is estimated; they can be eliminated by suitably placed trimming capacitors and a definite switching sequence. [See 201 of 1956 (Dauphinee and Mooser).]

621.317.35.029.4 998

Using Digital Techniques in L.F. Spectrum Analysis—B. Grand, L. Packer, and J. L. West. (*Electronics*, vol. 33, pp. 78–81; November, 1960.) Spectrum analysis over the range 0.0025 cps to 1 kc is made using a change-of-time-scale principle. Components of transient as well as harmonic content are measured.

621.317.412:537.311.33 999

A Sensitive Magnetic Balance for Determining Small Differences in Susceptibility—D. Geist. (*Z. Phys.*, vol. 158, pp. 359–366; March 14, 1960.) A torsion pendulum is described for measuring the susceptibility difference between semiconductor specimens with differing doping. For measurements carried out with this balance see 618 of February and back references.

621.317.444:550.380.8 1000

Terrestrial-Field Magnetometer using Nuclear Paramagnetic Resonance with Dynamic Polarization ot Nuclei—(*Onde Élect.*, vol. 40, pp. 590–601, September, 1960.)

Part 1. Theoretical Considerations—J. Freycenon and I. Solomon (pp. 590–595).

Part 2. Design and Construction—J. Freycenon (pp. 596–601).

621.317.444:621.385.832.032.26 1001

Investigation of Focusing Magnets—M. Arnaud and O. Cahen. (*Rev. Tech. Comp. franç. Thomson-Houston*, pp. 41–58; February, 1960.) Descript'on of a turbine magnetometer for recording fields of 1–10^4 oersteds. The measuring probes have a diameter of 6 or 9 mm and consist of a compressed-air-driven copper vane in which a current is induced under the influence of the magnetic field and which in turn induces current in a fixed coil connected to the recording amplifier. The magnetometer is used in conjunction with an electrolyte tank to design focusing systems for O-type tubes.

621.317.7:621.373.42.029.5:621.396.67.08 1002

A Portable H.F. Spectrum Generator for Antenna Calibration—N. Burtnyk. (*Electronics Engrg.*, vol. 32, pp. 767–769; December, 1960.) Description of a pulsed harmonic generator providing signals at 200-kc intervals from 200 kc to 30 Mc with a high order of stability, which is attained by use of a crystal.

621.317.725 1003

An Electronic Digital Voltmeter—J. L. J. van Vroonhoven and A. M. Muhlbaum. (*Instr. Practice*, vo . 14, pp. 1317–1319; December, 1960.) The experimental voltmeter is described with a range of Q-1V and operating at a rate of 100 measurements per second; it incorporates secondary-emission distributor tubes as stepping switches. [See *Instr. Practice*, vol. 14, pp. 1313–1316; December, 1960. (van Vroonhoven).]

621.317.733 1004

A Method of Controlling the Effect of Resistance in the Link Circuit of the Thomson or Kelvin Double Bridge—D. Ramaley. (*J. Res. NBS*, vol. 64C, pp. 267–270; October–December, 1960.) Simple modifications to minimize the potential difference in the link circuit include a supplementary power source and an auxiliary galvanometer. A step-by-step procedure is outlined for making measurements with bridges incorporating these modifications.

621.317.737.029.65 1005

High-*Q* Wavemeter Design—E. F. Goodenough. (*Marconi Rev.*, vol. 23, pp. 85–98; 2nd Quarter, 1960.) The principles and comprehensive design details are given for a cavity-resonator type of wavemeter. For a particular wavemeter covering the frequency range 33–36 Gc, a *Q* of over 70,000 is claimed.

621.317.77.088:621.372.852.2 1006

Error Analysis of a Standard Microwave Phase Shifter—Schafter and Beatty. (*See* 777.)

OTHER APPLICATIONS OF RADIO AND ELECTRONICS

531.7:538.682 1007

Mechanical Measurement—M. Nałęcz. *Electronic Technol.*, vol. 38, pp. 15–17; January, 1961.) A method of measuring small displacements utilizing the Hall effect in semiconductors is described.

531.719.33:621.3.087.4 1008

Water-Level Surge Recorder—E. G. Sandels. (*Electronic Technol.*, vol. 38, pp. 2–10; January, 1961.) The circuits, including a two-stage active RC-network low-pass filter with a cutoff frequency of 0.07 cps, are fully described.

621.362:621.387 1009

Effect of Magnetic Fields on Thermionic Power Generators—A. Schock. (*J. Appl. Phys.*, vol. 31, pp. 1978–1987; November, 1960.) The high currents present in large thermionic power generators produce magnetic fields which reduce efficiency. An applied magnetic field parallel to the current flow will correct this. The possibility of generating alternating current by using a modulated field coil current is noted. [See also 4353 of 1960 (Garvin, *et al.*)]

621.362:621.387 1010

Effect of Interelectrode Spacing on Cesium Thermionic Converter Performance—R. L. Hirsch. (*J. Appl. Phys.*, vol. 31, pp. 2064–2065; November, 1960.) The graphs presented show that efficiency is very dependent upon electrode spacing for medium-temperature devices, where Cs is used to modify emitter work function and space charge.

621.383:535.24 1011

Double-Modulation Photometer—H. P. Kalmus. (*Rev. Sci. Instr.*, vol. 31, pp. 828–832; August, 1960.) Details are given of a bridge instrument in which the photocurrent is modulated by an RF signal of 1 Mc chopped at 75 cps. A signal/noise ratio of 100 may be obtained at a bandwidth of 1 c/s; the maximum sensitivity is 4×10^{-9} lu.

621.383:681.6 1012

Nonscanning Character Reader uses Coded Wafer—L. R. Brown. (*Electronics*, vol. 33, pp. 115–117; November 25, 1960.) A description is given of a lenticular-array/photocell system for recognizing characters or patterns.

621.385.833 1013

Fifth-Order Spherical Aberration of Magnetic Lenses—G. D. Archard. (*Brit. J. Appl. Phys.*, vol. 11, pp. 521–522; November, 1960.) For moderate-strength lenses of the bell-shaped-field type, third- and fifth-order coefficients are numerically very similar.

621.387.464 1014

Performance of Large-Area Scintillation Counters—C. F. Barnaby and J. C. Barton. (*Proc. Phys. Soc.*, vol. 76, pp. 745–753; November, 1960.) The light collection efficiency is shown to be greater if the photomultiplier is in optical contact with the phosphor. Counters with and without this advantage are compared with an experimental design described.

621.398.621.387.4 1015

Telemetering Radiation Data by Frequency Variation—H. K. Richards. (*Electronics*, vol. 33, pp. 84–87; November 11, 1960.) The relative advantages of three types of radiation monitor are discussed.

PROPAGATION OF WAVES

621.391.812.5:523.5 1016

Volume Density of Radio Echoes from Meteor Trails—N. Carrara, P. F. Checcacci, and L. Ronchi. (Proc. IRE, vol. 48, pp. 2031–2032; December, 1960.) A method is described for determining the number of echoes received per unit time as a function of the region of the sky where the receiver beam crosses the transmitter beam.

621.391.812.5:523.5 1017

The Fading of Radio Waves Reflected Obliquely from Meteor Trails—G. S. Kent. (*J. Atmos. Terrest. Phys.*, vol. 19, pp. 272–283; December, 1960.) Bursts of signal received over a distance of 500 km on a frequency of 53 Mc in England have been studied. Spaced antennas allowed the structure of the diffraction pattern to be estimated. The reasons for the observed fading of the signals have been deduced.

621.391.812.62 1018

Some Thoughts on the Propagation of Radio Waves Through the Troposphere—J. A. Saxton. (*Onde Élect.*, vol. 40, pp. 505–514; July/August, 1960.) A survey of developments in the field of tropospheric propagation and a review of current theories advance to explain propagation beyond the horizon are given; the most satisfactory model is considered to be one based on a layered troposphere. 58 references.

621.391.812.62 1019

Radio Wave Propagation and Attenuation in the Troposphere—E. M. Hickin. (*Research, Lond.*, vol. 13, pp. 503–506; December, 1960.) The attenuation of microwaves due to meteorological phenomena is discussed. Contours are given of constant path length for equal "out-of-service" time for 11-Gc radio links in Europe; these contours are based on published rainfall data.

621.391.812.621 1020

The Equivalent Gradient: Direct Measurement and Theoretical Calculation—P. Misme. (*Ann. Télécommun.*, vol. 15, pp. 92–99; March/April, 1960.) If variations in the gradient of the refractive index as a function of height are ignored, the path between transmitter and receiver may be drawn as an arc of a circle, defined by the positions of both ends of the link and the transmission angle. This corresponds to a constant refractive-index gradient called the "equivalent gradient." Experimental values of this gradient have been obtained from radar measurements between Corsica and Southern France, and theoretical values are calculated for Niamey in West Africa. [See also IRE Trans. on Antennas and Propagation, vol. AP-6, pp. 289–292; July, 1958.)

621.391.812.63 1021

Scattering of Electromagnetic Waves from a Nondegenerate Ionized Gas—J. Renau. (*J. Geophys. Res.*, vol. 65, pp. 3631–3640; November, 1960.) The scattering cross section for an ionized gas in thermal equilibrium is derived and compared with ionospheric experimental observations. The cross section of turbulent irregularities is also discussed, and the relative importance of the two kinds of scattering at different wavelengths is considered.

621.391.812.63 1022

Flutter Fading of Short-Wave Radio Signals in Equatorial Regions and its Connection with Spread Echoes, Magnetic Storms and the Radiation Belt—C. Lal. (*J. Inst. Telecommun. Engrs., India*, vol. 6, pp. 223–230; August, 1960.) The effect of the flutter fading on the broadcasting services of all India Radio broadcasting services is summarized. The cause is assumed to be the turbulence created by interaction between high-energy particles of the inner Van Allen belt and the upper edge of the F region when it rises soon after local sunset.

621.391.812.63:551.510.535 1023

The D_1, D_2 Layers and the Absorption of Radio Waves—Ruini. (*See* 883.)

RECEPTION

621.391.822:551.578.1 1024

The Effect of Rain on the Noise Level of a Microwave Receiving System—D. C. Hogg and R. A. Semplak. (Proc. IRE, vol. 48, pp. 2024–2025; December, 1960.) A note is given on the noise levels observed using a low-noise receiving system [1379 of 1960 (DeGrasse, *et al.*)], which are much higher when rain occurs or is imminent at the receiver location.

621.396.62.001.4 1025

The Monitoring of Receiver Performance under Operational Conditions—O. E. Kealle. (*Marconi Rev.*, vol. 23, pp. 53–58; 2nd Quarter, 1960.) Techniques for checking receiver performance using a gas-discharge noise source to provide a constant signal are discussed. Block schematic diagrams are given for suggested daily and semi-automatic checks and for continuous monitoring.

STATIONS AND COMMUNICATION SYSTEMS

621.396.215 1026

A Comparison between Alternative H.F. Telegraph Systems—J. V. Beard and A. J. Wheeldon. (*Point to Point Telecommun.*, vol. 4, pp. 20–48; June, 1960.) The comparison is in terms of an ideal detector. In high-frequency propagation, a two-tone system gives substantially the best performance for multichannel telegraphy, and is slightly superior to FSK for simple-channel telegraphy.

621.396.215 1027

An Improved Decision Technique for Frequency-Shift Communications Systems—E. Thomas. (Proc. IRE, vol. 48, pp. 1998–2003; December, 1960.) A description is given of a variable-decision-threshold device which enables a frequency-shift signaling system to use information in mark and space channels independently, resulting in an improvement in circuit quality where fading exists between mark and space frequencies. Results of tests over several ionospheric scatter circuits show improvements in signal detectability of 10–16 db.

621.396.4 1028

Interstitial Channels for Doubling TD-2 Radio System Capacity—H. E. Curtis, T. R. D. Collins, and B. C. Jamison. (*Bell Sys. Tech. J.*, vol. 39, pp. 1505–1527; November, 1960.) Laboratory and field measurements show that by using cross-polarization antenna systems and IF filters, the interstitial channels can be operated without detriment to the existing channels.

621.396.43:551.507.362.2 1029

A Possible Long-Range Communications Link between Ground and Low-Orbiting Satellites—M. S. Macrakis. (*J. Atmos. Terrest. Phys.*, vol. 19, pp. 260–271; December, 1960.) Under certain restrictive conditions, a ray properly injected into the ionosphere can travel long distances without entering the upper atmosphere. A possible method of injection is discussed.

621.396.97:534.76 1030

Engineering Performance of Six Proposed Stereo Systems—A. P. Walker. (*Electronics*, vol. 33, pp. 85–89; November 18, 1960.) Field information is presented relevant to the evaluation undertaken by Panel 5 of the NSRC. The methods used to obtain the data are briefly described.

SUBSIDIARY APPARATUS

621.3.087.4:621.395.625.3 1031

Instrumentation Wide-Band Magnetic Tape Recording—J. P. Pritchard. (*Electronic Engrg.*, vol. 32, pp. 762–766; December, 1960.) The development of a recorder with a bandwidth from dc to 4 Mc is described.

621.3.087.4:621.395.625.3 1032

The Mechanical Considerations of Magnetic Recording Heads—M. B. Martin. (*J. Brit. IRE*, vol. 20, pp. 877–883; November, 1960.) Manufacturing problems associated with multitrack heads are discussed in relation to the effects of mechanical variations on head performance. Performance criteria are listed.

621.3.087.4:621.395.625.3:681.142 1033

Some Engineering Aspects of Magnetic Tape System Design—D. W. Willis and P. Skinner. (*J. Brit. IRE*, vol. 20, pp. 867–876; November, 1960.) A system is described for the evaluation of random and transient effects in terms of specific measurements on waveforms generated by standard tapes rather than in terms of dimensional tolerances.

621.3.087.4:621.395.3:681.142 1034

A Fast Start/Stop Machine for Handling Magnetic Tape—W. C. R. Withers. (*J. Brit. IRE*, vol. 20, pp. 857–866; November, 1960. Discussion, pp. 884–885.) The ½-inch-wide tape is handled at a speed of 100 inches per second with start/stop times of 3 msec (referred to 90 per cent of the final speed). The tape loop length is controlled by phototransistors driving an error-correcting servomechanism.

621.3.087.4:621.395.625.3:681.142 1035

The Development of a High-Performance Tape Handler—H. M. Harrison. (*J. Brit. IRE*, vol. 20, pp. 841–856; November, 1960. Discussion, pp. 884–885.) Magnetic tape 1 inch wide is handled completely "out of contact" at 200 inches per second by means of vacuum techniques. Start, stop, and reverse times are better than 5 msec.

621.314.5:621.382.3 1036

Stabilized Voltage Supplies using Transistors—J. S. Bell and P. G. Wright. (*Electronic Engrg.*, vol. 32, pp. 758–731; December, 1960.) Two completely transistorized circuits are described which produce ±300 v dc from a 28 v dc supply.

621.314.63 1037

Reverse Characteristics with Surface Breakdown of Silicon p-s_p-n Rectifiers—O. Jäntsch. (*Z. Naturforsch.*, vol. 15a, pp. 302–307; April, 1960.) The influence of surface recombination on the reverse and breakdown characteristics is investigated. Measurements were made on Si rectifiers with weakly doped diffusion region, which had been exposed to dry nitrogen and oxygen with or without ozone for different lengths of time, with or without heat treatment. For measurements in moist gases see *J. Naturforsch.*, vol. 15a, pp. 141–149, February, 1960.)

621.316.721.078.3:621.318.381 1038

Stabilization of a Magnetic Field by means of a Galvanometer/Photocell Assembly—R. Stefant. (*C. R. Acad. Sci., Paris*, vol. 250, pp. 1453–1455; February 22, 1960.) A note is given on the application of a galvanometer/amplifier system [3571 of 1958 (Sauzade)] for magnetic-field stabilization.

TELEVISION AND PHOTOTELEGRAPHY

621.397.13(43) 1039

Television in Germany—R. Möller. (*J. Telev. Soc.*, vol. 9, pp. pp. 247–259; July-September, 1960. Discussion, pp. 259–262.)

A survey is presented of the history and present state of the German television network, the studios used, and their technical equipment.

621.397.132.001.4 1040
Equipment for the Generation of Colour Bars for the N.T.S.C. Standard—G. Bolle. (*Elektron. Rundschau*, vol. 14, pp. 85–86; March, 1960.) (See 345 of January, 1961.)

621.397.331.24 1041
Electron-Optical Properties of a Flat Television Picture Tube—E. G. Ramberg. (Proc. IRE, vol. 48, pp. 1952–1960; December, 1960.) Ray paths and cocusing properties are calculated for the deflection and ecceleration fields of a flat picture tube with lateral injection similar to that described by Aiken (977 of 1958).

621.397.331.24 1042
High-Slope Television Picture Tubes for Low Modulation Voltages—E. Gundert and H. Lotsch. (*Telefunken Ztg.*, vol. 33, pp. 58–65; March, 1960. English summary, pp. 74–75.) The design principles of high-transconductance tubes are reviewed. 39 references.

621.397.331.24:621.385.832.032.269.1 1043
Focus Reflex Modulation of Electron Guns—Schlesinger. (*See* 1052.)

621.397.334:621.397.621 1044
Beam Indexing Tubes—I. Macwhirter. (*Wireless World*, vol. 67, pp. 2–7, 92–98; January/February, 1961.) The single-gun picture tube described has none of the deficiencies of the shadow-mask type of tube. The necessary modification of the NTSC signal is discussed, and details are given of a suitable television display unit providing the requisite indexing and synchronization facilities.

621.397.6(204) 1045
Equipment for Underwater Television—K. Schultz. (*VDI Z.*, vol. 102, pp. 339–346; March 21, 1960.) A review is given of international developments in this field with a description of an underwater trailing unit capable of carrying up to three television cameras and lighting equipment. The depth of submersion is remotely controlled from the ship which tows the equipment.

621.397.62:621.396.679.4 1046
Television Downleads: a Survey—R. J. Slaughter. (*J. Telev. Soc.*, vol. 9, pp. 288–293; July–September, 1960.)

TRANSMISSION

621.396.61.026:621.391.812.44 1047
The Influence of Sunspot Number on Transmitter Power Requirements for H.F. Ionospheric Circuits—F. T. Koide. (Proc. IRE, vol. 48, pp. 2033–2035; December, 1960.) Formulas are derived for calculating the change in radiated power, as a function of sunspot number, necessary to maintain a constant field strength at a receiver.

TUBES AND THERMIONICS

621.382.23 1048
Avalanche Breakdown in a Diode with a Limited Space-Charge Layer—Z. S. Gribnikov. (*Fiz. Tverdogo Tela*, vol. 2, pp. 854–856; May, 1960.) An estimation is given of the lowering of the breakdown voltage in a diode with closely spaced rectifying and ohmic contacts, assuming that the ionization coefficients of carriers depend strongly on the field.

621.382.23:621.373.029.65 1049
Millimetre-Wave Esaki-Diode Oscillators—C. A. Burrus. (Proc. IRE, vol. 48, p. 2024; December, 1960.) Performance data are given for Esaki diodes made by electrically "forming" a point contact between Zn and heavily doped *n*-type GaAs. Maximum power obtained was 25 μW at 50 Gc, falling to 2 μW at 90 Gc. [See also 359 of January, 1961 (Trambarulo and Burrus).]

621.382.23:621.375.9:621.372.44 1050
Noise-Figure Measurements Relating the Static and Dynamic Cut-Off Frequencies of Parametric Diodes—C. R. Boyd. (Proc. IRE, vol. 48, pp. 2019–2020; December, 1960.) Measurements have been made at about 8.2 Gc with a number of Ge and Si diffused-junction mesa-type diodes. A quantitative correspondence between experimental and analytical behavior is evident and a static-to-dynamic cutoff frequency ratio of 10 is indicated.

621.385.832.032.26:621.317.444 1051
Investigation of Focusing Magnets—Arnaud and Cahen. (See 1001.)

621.385.832.032.269.1:621.397.331.24 1052
Focus Reflex Modulation of Electron Guns—K. Schlesinger. (*J. Telev. Soc.*, vol. 9, pp. 263–271; July–September, 1960.) Source focusing by electron lens, and modulation from low drive signals by electron reflection, are incorporated in an advanced CR-tube gun design. [See also 3128 of 1959.]

621.387:621.362 1053
Effect of Magnetic Fields on Thermionic Power Generators—Schock. (*See* 1009.)

621.387:621.362 1054
Effect of Interelectrode Spacing on Cesium Thermionic Converter Performance—Hirsch. (*See* 1010.)

TRANSACTIONS OF THE IRE

1960 INDEX

Contents of TRANSACTIONS — PAGE

The Institute of Radio Engineers, Inc.
1 East 79 Street, New York 21, N.Y.

Vol. AU-8, No. 5, September–October, 1960

Vol. AU-8, No. 6, November–December, 1960

Automatic Control

Vol. AC-5, No. 1, January, 1960

Vol. AC-5, No. 2, June, 1960

Vol. AC-5, No. 3, August, 1960

Vol. AC-5, No. 4, September, 1960

Broadcast and Television Receivers

Vol. BTR-6, No. 1, May, 1960

Broadcasting

Circuit Theory

Vol. CT-7, Special Suppl., August, 1960

Vol. CT-7, No. 3, September, 1960

Vol. CT-7, No. 4, December, 1960

Communications Systems

Vol. CS-8, No. 1, March, 1960

Vol. CS-8, No. 2, June, 1960

Vol. CS-8, No. 3, September, 1960

Component Parts

Education

Electron Devices

Vol. ED-7, No. 3, July, 1960

Vol. ED-7, No. 4, October, 1960

Electronic Computers

Vol. EC-9, No. 1, March, 1960

Vol. EC-9, No. 2, June, 1960

Vol. EC-9, No. 3, September, 1960

Vol. EC-9, No. 4, December, 1960

Engineering Management

Vol. EM-7, No. 1, March, 1960

Vol. EM-7, No. 2, June, 1960

Vol. EM-7, No. 3, September, 1960

Vol. EM-7, No. 4, December, 1960

Engineering Writing and Speech

Vol. EWS-3, No. 1, April, 1960

Vol. EWS-3, No. 2, July, 1960

Human Factors in Electronics

Vol. HFE-1, No. 1, March, 1960

Vol. HFE-1, No. 2, September, 1960

Industrial Electronics

Vol. IE-7, No. 1, March, 1960

Follows Vol. P61E-11

Vol. IE-7, No. 2, July, 1960

Vol. IE-7, No. 3, December, 1960

Information Theory

Vol. IT-6, No. 1, March, 1960

Vol. IT-6, No. 2, Special Monograph Issue, April, 1960

Vol. IT-6, No. 3, June, 1960

Vol. IT-6, No. 4, September, 1960

Vol. IT-6, No. 5, December, 1960

Instrumentation

Vol. I-9, No. 1, June, 1960

The Economics of Test Packages, *M. A. Dean* 19
Problems Associated with Precise Determination of the Index of Refraction of the Earth's Atmosphere, *A. M. Bush* 23

Vol. I-9, No. 2, September, 1960

Vol. I-9, No. 3, December, 1960

Medical Electronics

Vol. ME-7, No. 1, January, 1960

Vol. ME-7, No. 2, April, 1960

Vol. ME-7, No. 3, July, 1960

Twelfth Annual Conference on Electrical Techniques in Medicine and Biology

Vol. ME-7, No. 4, October, 1960

Proceedings of Conference on Diagnostic Data Processing

Microwave Theory and Techniques

Vol. MTT-8, No. 1, January, 1960

Vol. MTT-8, No. 2, March, 1960

Vol. MTT-8, No. 3, May, 1960

Vol. MTT-8, No. 4, July, 1960

Vol. MTT-8, No. 5, September, 1960

Vol. MTT-8, No. 6, November, 1960

Military Electronics

Vol. MIL-4, No. 1, January, 1960

Vol. MIL-4, Nos. 2–3, April–July, 1960

Part I—Army Project Juno I and II

Part II—Army Communication Satellite Activities

Part III—Army Role in Other Space Activities

Part IV—Army Satellite and Space Probe Tracking

Vol. MIL-4, No. 4, October, 1960

Nuclear Science

Vol. NS-7, No. 1, March, 1960

Vol. NS-7, No. 2, June–September, 1960

Proceedings of the Seventh Scintillation Counter Symposium, Washington, D. C., February 25–26, 1960

Vol. NS-7, No. 4, December, 1960

Radio Frequency Interference

Vol. RFI-1, No. 2, May, 1960

Reliability and Quality Control

Vol. RQC-9, No. 1, April, 1960

Follows Vol. PGRQC-16

Space Electronics and Telemetry

Ultrasonics Engineering

Vehicular Communications

COMBINED INDEX TO SUBJECTS

B

C

Q

R

S

T

This four-cryotron flip-flop can be switched in *two billionths of a second.* It was developed by an IBM team investigating the possibilities of low-temperature devices for basic binary storage in digital computers.

IBM scientists and engineers designed the flip-flop around a primary law of low-temperature physics: A superconductive metal loses its superconductivity in the presence of a magnetic field. In the IBM device, a small control current is used to destroy the superconductivity of one of two parallel lines. This sets up a resistance in the first line and causes current to switch to the second.

The new flip-flop offers another advantage in addition to speed. Its eight layers of thin metallic and insulation films operate in a temperature range where chemical deterioration is nonexistent. As a result, the device should have an unusually high degree of reliability.

Creative careers start here. A good deal of this project's success came from the creative interplay of different technical areas. IBM physicists and mechanical and electrical engineers worked together to develop new films, improved vacuum equipment and more reliable test circuits.

Perhaps you'd like to work . . . and grow . . . in a professionally stimulating atmosphere like this. You may be interested in the progress IBM is making in such areas as solid state, magnetics or IBM Tele-Processing.* If you have a degree in engineering, mathematics, or one of the physical sciences, plus experience in your field, write, briefly describing your background, to:

Manager of Technical Employment
IBM Corporation, Dept. 645D
590 Madison Avenue
New York 22, New York

IBM ®

*Trademark

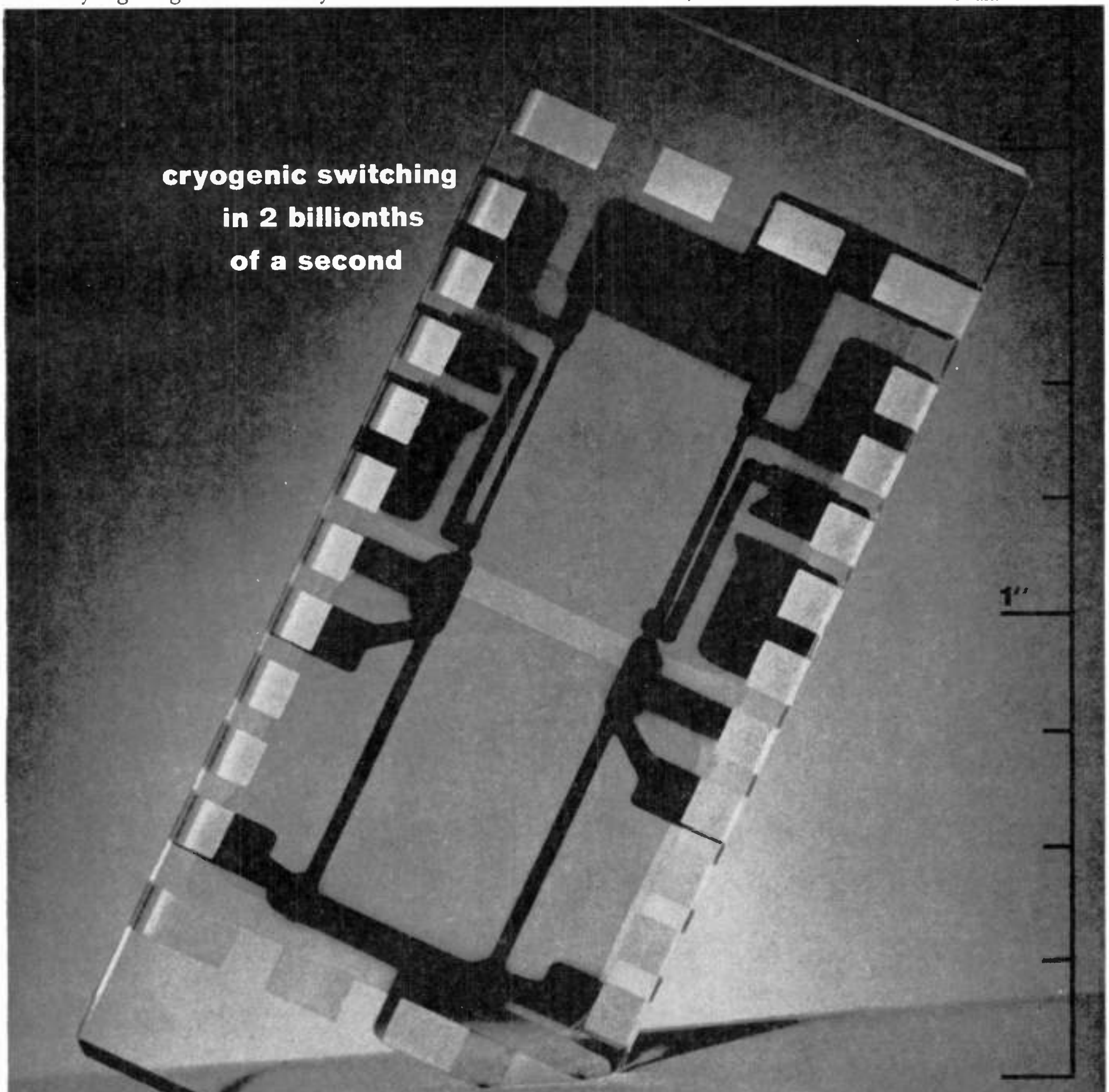

IRE People

(Continued from page 96A)

Dr. Victor Twersky (S'47–A'48–M'55) head of research at the Electronic Defense Laboratories of Sylvania Electric Products Inc., Mountain View, Calif., has been promoted to senior scientist, it was recently announced by J. R. Lien, director of the laboratories.

In making the announcement, Mr. Lien said that Dr. Twersky is the first person on the west coast and one of three in the nation to achieve this position within GT&E. He added that "the appointment was made in recognition of Dr. Twersky's outstanding scientific contributions." He said the senior scientist role is "similar to that of a professor at large in our leading universities—where an outstanding individual's work is recognized as transcending the interests of a particular part of the organization."

Dr. Twersky is internationally known for his work in the fields of electromagnetic wave scattering and propagation. He joined Sylvania in 1953 as EDL's first engineering specialist; since then he has been senior engineering specialist, laboratory consultant, and will continue as head of research at the Electronic Defense Laboratories.

Before joining Sylvania, he spent more than three years as a staff member at the Institute of Mathematical Sciences, New York University, New York, N. Y., and as a consultant in wave propagation at the Nuclear Development Associates, New York, N. Y. He has also held appointments as a lecturer in the mathematics department of Stanford University, Stanford, Calif., and has served as Palo Alto and bay area coordinator and chairman for University of California lecture series.

His earlier work included development of electroacoustic and mechanical guidance devices to aid the blind in foot travel and obstacle avoidance, and studies on the physical basis of obstacle perception by audition.

He received a bachelor's degree in physics from City College of New York, New York, N. Y., a master's degree from Columbia University, New York, N. Y., and the Ph.D. degree from New York University, New York, N. Y.

Dr. Twersky is a Fellow of the American Physical Society, a member of the New York Academy of Sciences, and of Commission VI of the International Scientific Radio Union (URSI). He was also a National Academy of Sciences-National Research Council delegate to the General Assemblies of URSI in 1954, 1957 and 1960.

❖

Robert M. Walker (A'37–M'40–SM'43) recently joined the staff of the IBM Research Laboratory, San Jose, Calif., as manager of magnetic recording research. He was previously manager of reliability research at IBM's Watson Laboratory in New York, N. Y., which he joined in 1946. Prior to this, he spent four years (1942–1945) as a staff member of the MIT Radiation Laboratory, working on display techniques for radar. Before 1942, he was in broadcast engineering work with KOMO in Seattle.

R. M. Walker

While at the Watson Laboratory, he also served as Adjunct Assistant Professor (1953–1955) and Adjunct Associate Professor (1957–1958), in the department of electrical engineering, Columbia University, New York, N. Y.

Holder of 10 patents, Mr. Walker is a member of the American Physical Society, the AAAS, and is a registered professional engineer.

❖

Conductron Corporation, New York, N. Y., has announced the appointment of **Artemus W. Wren, Jr.** (A'51–M'56) as head of the Plasma Engineering Department. He received the B.S. degree in physics in 1950 and the M.S. degree in electrical engineering in 1956, both from Georgia Institute of Technology, Atlanta. From 1951 to 1956, he was a research physicist for the Engineering Experiment Station at Georgia Institute of Technology; from 1956 to 1959 he was group leader of the Range Instrumentation Group of the Space Technology Laboratories at Patrick Air Force Base, Fla. He was a research engineer with the Radiation Laboratory of the University of Michigan, Ann Arbor, 1959–1960, where he was Project Engineer for studies involving tropospheric scattering and VLF detection techniques. During this period he was also a lecturer in electrical engineering at the University of Michigan.

A. W. Wren, Jr.

Mr. Wren is a member of the American Physical Society, and Sigma Pi Sigma.

❖

Allen Avionics, Inc. of Mineola, L. I., N. Y., has announced the appointment of **Norman E. Wunderlich** (M'49) as Vice President and Marketing Director. He will be primarily concerned with sales and marketing of Allen Avionics' line of electromagnetic delay lines, precision coils, transformers, filters and temperature compensated capacitors.

N. E. Wunderlich

He has been associated with the electronics industry since its infancy. Prior to joining Allen Avionics, he was associated with Intercontinental Electronics Corporation of Westbury and Compagnie Generale de Telegraphie Sans Fil of Paris, France, Vice President of Link Radio Corporation, Executive Director of Federal Tel. & Radio Corporation IT & T, National Sales Director of Motorola Communications & Electronics, Inc., Vice President of the Rauland Corporation, Vice President of Lear, Inc., and owner of Wunderlich Radio Co., engineering consultants.

❖

Robert C. Sprague (SM'53), Chairman of the Board and Treasurer of the Sprague Electric Company of North Adams, Mass., has been elected a Director of the First National Bank of Boston. He retired in January, 1961, as Chairman and Fiscal Agent of the Federal Reserve Bank of Boston, terminating his service under the Bank's five-year-limit rule.

R. C. Sprague

❖

Dr. Jerrold R. Zacharias (SM'57), nationally-known nuclear scientist, was recently elected to the board of directors of the Sprague Electric Company, North Adams, Mass. He succeeds Dr. Jerome B. Wiesner. Formerly a consultant to this company, he is professor of physics and director of the Laboratory for Nuclear Science at the Massachusetts Institute of Technology, Cambridge, Mass. Dr. Zacharias has directed numerous Government projects on radar, nuclear weapons, and defense.

❖

STRETCH YOUR IMAGINATION

Beckman Systems . . . a world-famous name that stands for the most advanced developments in Electronic Data Processing. Beckman research, study and engineering groups were the first to develop many of today's realistic answers to the ever-increasing demands for reliable, high performance data processing systems. Among them... Multiple Channel Recording, High-Speed Digital Processing, Solid-State Circuitry, and Floating, Low-Level Amplification. Systems applications include space vehicle guidance, automatic plant control, missile ground support and nuclear research.

At Beckman, the difficult problems are our business. Here, the selection of qualified engineers and scientists is as equally important as the problem at hand. In an atmosphere where initiative is encouraged and where achievement is well recognized, top men in the field are your associates in meeting the challenges of tomorrow. Both you and your family will heartily endorse Southern California living. World-renowned Disneyland, beach communities, desert resorts, and mountain areas all are minutes away.

If you have a background in Systems Management, Telemetry, Timing and Translation, Research and Study, Systems Engineering, or Advanced Circuits Development, why not contact Mr. James R. Abell. He will arrange for an interview in your area to discuss opportunities with Beckman Systems in Northern or Southern California.

Beckman® / *Systems*

a division of Beckman Instruments, Inc.
325 North Muller Avenue
Anaheim, California : PRospect 4-5430

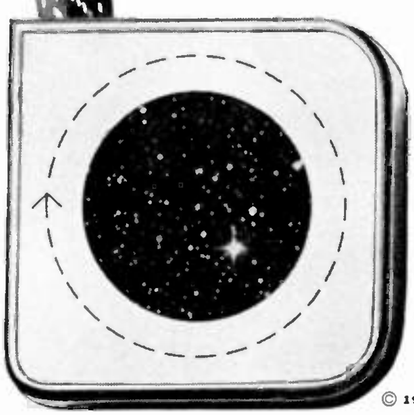

Positions Open

The following positions of interest to IRE members have been reported as open. Apply in writing, addressing reply to company mentioned or to Box No. ....

The Institute reserves the right to refuse any announcement without giving a reason for the refusal.

Proceedings of the IRE
1 East 79th St., New York 21, N.Y.

MICROWAVE SPECIALISTS

Microwave engineers needed for research and engineering in precision measurement. This work is in connection with the expanding Ordnance Calibration Program for which Frankford Arsenal has world-wide responsibility. Engineers are needed to evaluate and apply newest microwave techniques to attenuation, power and impedance measurements both pulse and cw. Development of specialized equipments in a modern, fully equipped microwave lab. is offered. Salaries to $10,635. Federal Civil Service benefits and requirements. Apply Recruitment Office, Frankford Arsenal, Bridge and Tacony Sts., Phila. 37, Penna. Refer to ad by Mr. A. Bruno.

EE'S, PHYSICISTS

Expanding electronics concern has prestige position for qualified patent attorney to join its legal staff. LL.B. preferred but will consider minimum 2 years of law study. Ability to work closely with scientific and management people essential. Salary to $15,000. Northeast location. Please forward complete resume to Box 2041.

PROFESSOR OR ASSOCIATE PROFESSOR

Professor or Associate Professor with salary to $11,000 for session of two semesters. This fully accredited well equipped E.E. Dept. needs one or two senior-level staff members with high qualifications. Ph.D. essential, to ensure full participation in graduate program and research activities. Prefer experience in electron devices, solid state or computer electronics, but other specialties considered. Medium size engineering college (700 undergraduate students) in brand new building. Exceptionally good retirement plan. Numerous sources of extra income. Pleasant living and working conditions in attractive uncrowded city. Address inquiries to Robert A. Chipman, Chairman, E.E. Dept., University of Toledo, Toledo 6, Ohio.

TEACHING AND RESEARCH

Opening for Electrical Engineer with Ph.D. to supervise graduate research and do some teaching. Research experience in microwave or semiconductors desirable. Private research or consultation encouraged. Excellent salary and rank arrangements. Department offers work leading to Ph.D. Position available Sept. 1961 or sooner. Apply Chairman, E.E. Dept., Vanderbilt University, Nashville 5, Tenn.

NOISE RESEARCH ENGINEERS

As a result of recent rapid expansion, Quan-Tech Laboratories—a leading manufacturer of equipment for the measurement and analysis of component noise—has openings for imaginative E.E.'s interested in this important new field. Address replies to Chief Engineer, Noise Research Div. Quan-Tech Labs. Inc., 60 Parsippany Blvd., P.O. Box 187, Boonton, New Jersey. Tel. DEerfield 4-8500.

(Continued on page 104A)

ELECTROMAGNETIC COMPATIBILITY ANALYSIS

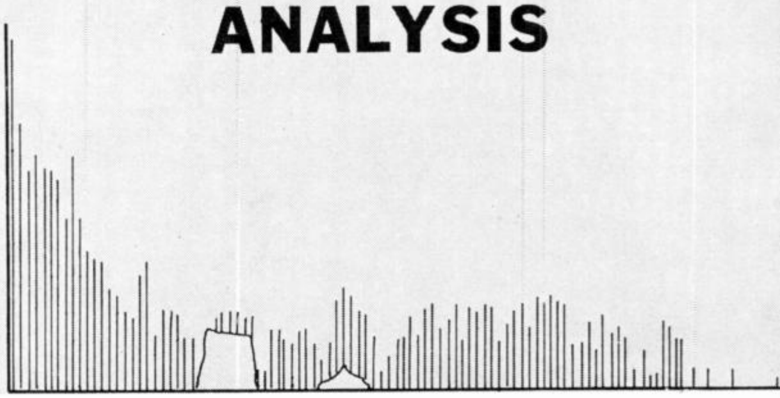

Here is your opportunity for professional growth in a challenging and extremely interesting field, as a member of an outstanding and stimulating scientific team. Armour Research Foundation, specialist in electronic interference evaluation, is now expanding its facilities and staff requirements in the area of Electromagnetic Compatibility Analysis. We are looking for qualified electronic engineers at all levels (B.S. through Ph.D.) for research and applied studies concerned with system analysis and performance prediction. Immediate openings are available at either our *Chicago* or *Washington, D. C.* area facilities for individuals with experience in one or more of the following fields . . .

RADAR	**PROPAGATION**
MICROWAVES	**CIRCUIT ANALYSIS**
ANTENNAS	**MEASUREMENT AND ANALYSIS**
COMMUNICATION	**TACTICAL EVALUATION**

In addition to the cited professional status, staff members receive attractive salaries, up to four weeks vacation, generous insurance and retirement benefits, and tuition paid graduate study. If you are interested in one of these professional opportunities, please reply in confidence to Mr. R. B. Martin.

ARF

ARMOUR RESEARCH FOUNDATION

OF ILLINOIS INSTITUTE OF TECHNOLOGY
TECHNOLOGY CENTER • CHICAGO 16, ILL.

Positions Open

(Continued from page 103A)

STATISTICAL COMMUNICATION THEORIST

Senior Staff opportunity to initiate and direct advanced research programs in such areas as statistical communication and information theory; automatic pattern recognition and processing; adaptive, self-organizing learning systems; bionics; advanced computer theory. Contact J. R. Campbell, Chief Scientist, Chance Vought Electronics Div. P.O. Box 1500, Arlington, Texas.

OPERATIONS RESEARCH SPECIALIST

Establish and direct operations research activity. Analyses and recommendations must be provided for both (a) operational application of present products, and requirements for potential future products, and (b) intra- and inter-departmental operations. Contact J. R. Campbell, Chief Scientist, Chance Vought Electronics Div., P.O. Box 1500, Arlington, Texas.

ASSISTANT OR ASSOCIATE PROFESSOR

Assistant or Associate Professor with Ph.D. in Electrical Engineering or Physics. Interest in electronics, microwaves, solid state or circuit theory. Active research and graduate program with opportunities for outside consulting. Send resume to W. P. Smith, Chairman E.E. Dept., University of Kansas, Lawrence, Kansas.

TEACHING POSITIONS

PROFESSORS all levels. Ph.D. required. Solid-state, electromagnetics, and engineering analysis especially. Income with research, competitive with industry. Graduate program as large as undergraduate. Mile high, dry climate.

INSTRUCTORS, Associates, Assistants for teaching and research part-time positions while working for M.S. and S.Sc. Large graduate program assures variety of offerings. Apply Chairman, E.E. Dept., University of New Mexico, Albuquerque, New Mexico.

BROADCAST ENGINEER

Long term European assignment with private organization engaged in construction and operation of large high-powered shortwave radio stations. Top qualifications, experience and executive ability desired. Good salary plus overseas benefits. Inquiries treated in confidence. Reply to Box 2043.

ASSOCIATE PROFESSOR

Electrical Engineering faculty being expanded in relatively new and rapidly growing department, with positions available to rank of Associate Professor with initial salary range to $6000 for base year of 9 months, depending upon education and experience. Further opportunity for research and other programs in this industrial area. Preferred background emphasis in field and circuit theory, electronic systems and control. Address full background to Chairman, E.E., University of Bridgeport, Bridgeport 4, Conn.

ELECTRONICS SECTION HEAD

Cornell Aeronautical Lab. has an attractive opening as technical supervisor of a section involved in the solution of complex problems associated with the electronics field, especially in the areas of weapon systems, reconnaissance and surveillance, and guidance and control. Position holds outstanding opportunities for growth from an already well established research program, both by way of personnel and highly successful technical

(Continued on page 107A)

Nowhere is this closeness more apparent than at Lockheed. Here, with each passing day, new technological advances help bring nearer the exploration of Mars, the Moon, Venus.

As the time grows shorter, the pace grows faster. New designs in Spacecraft and Aircraft are rapidly being developed—and the number continues to mount. Included are: Missiles; satellites; hypersonic and supersonic aircraft; V/STOL; manned spacecraft.

For Lockheed, this accelerated program creates pressing need for additional Scientists and Engineers. For those who qualify, it spells unprecedented opportunity. Notable among current openings are: Aerodynamics engineers; thermodynamics engineers; dynamics engineers; electronic research engineers; servosystem engineers; electronic systems engineers; theoretical physicists; infrared physicists; hydrodynamicists; ocean systems scientists; physio-psychological research specialists; electrical—electronic design engineers; stress engineers; and instrumentation engineers.

Scientists and Engineers are cordially invited to write: Mr. E. W. Des Lauriers, Manager Professional Placement Staff, Dept. 1804, 2402 N. Hollywood Way, Burbank, California.

LOCKHEED

CALIFORNIA DIVISION

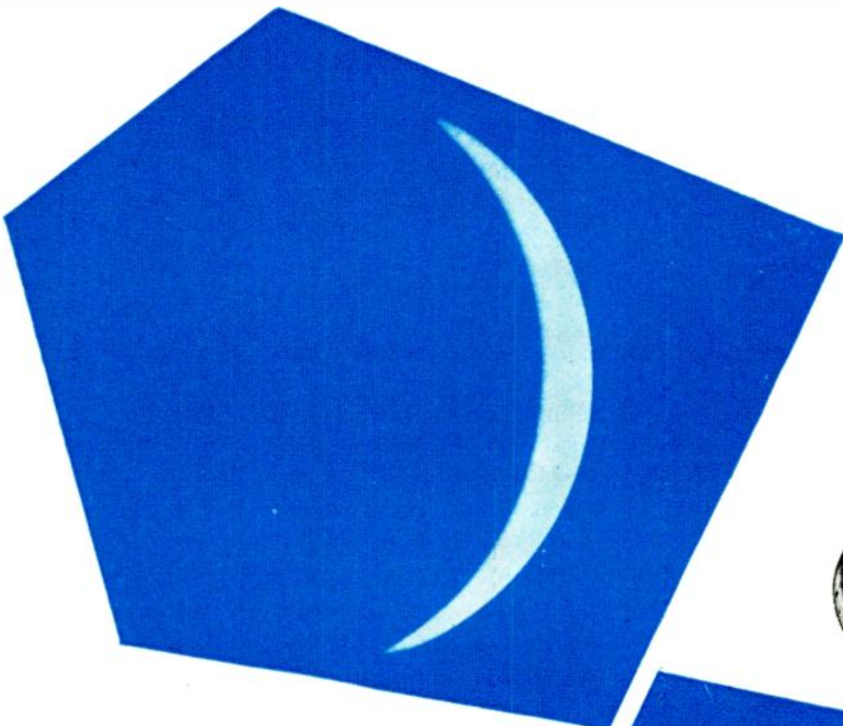

WE'RE CLOSER THAN YOU THINK...

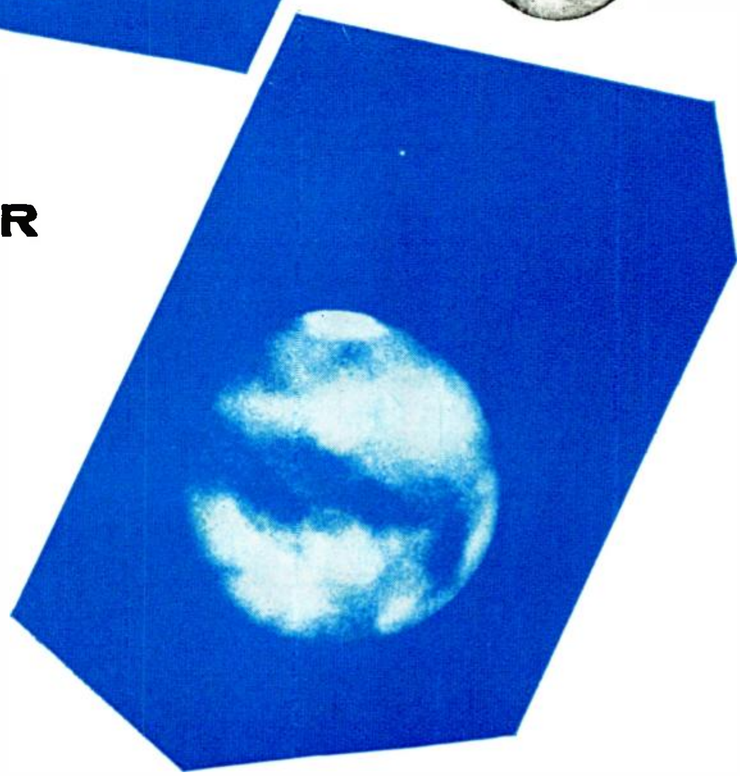

Reading clockwise: Venus, Moon, Mars. Approximate distance from Venus to Earth, 25,000,000 miles; from Moon, 240,000 miles; from Mars, 50,000,000 miles.

Photos courtesy of Mount Wilson and Palomar Observatories.

Positions Open

(Continued from page 104A)

projects. Horizons not limited by marketing and sales. The Laboratory provides a desirable combination of the best features of industry as to financial and equipment resources coupled with a university associated atmosphere for constructive R&D activity at the highest level. Salary range starts at $13,500 depending on qualifications and experience. Send complete resume to F. L. Rentschler, Cornell Aeronautical Lab. Inc., 445 Genesee St., Buffalo 21, N.Y.

ELECTRONIC ENGINEER

Electronic engineer to teach lecture and laboratory courses. Up to date knowledge of the field required. Working and living conditions excellent: salary and opportunity good. Write to Dean of Engineering, California State Polytechnic College, San Luis Obispo, Calif.

ASSOCIATE DIRECTOR AND DIRECTOR

Associate Professor and Director of Research in Electrical Engineering. To have the responsibility for developing a research program including the securing of research contracts and the directing of research activity. Salary depending on experience and academic background. Write to Head, E.E. Dept., South Dakota School of Mines and Technology, Rapid City, South Dakota.

TWO ELECTRONIC ENGINEERS

Good theoretical background, one with at least 7 years' experience, and the other with at least 2 years' in research and/or development. Excellent career possibilities in rapidly expanding industry. Congenial atmosphere. Call Personnel Dept. RIver view 9-4800, Massa Div. Cohu Electronics, Inc. 280 Lincoln St., Hingham, Mass.

PROFESSOR

The University of Alaska has an opening for an Assistant Professor of Electrical Engineering to teach and to do research on the ionosphere, the aurora, or on Northern problems in communications or power. Industrial experience or Masters' degree required, or for an instructor with less preparation. This is a pioneer university in a new state. We work and live in conventional surroundings, but beyond us is wilderness. Write Air Mail to Dept. of E.E., University of Alaska, Box 97, College, Alaska.

COMMUNICATION ENGINEER

College graduate with several years' experience and good technical background, including r-f system application or installation. Consulting engineering firm in New York City. Box 2044.

ASSOCIATE PROFESSOR OF E.E.

Ph.D. required and special competence in electromagnetic theory desirable. Should have some teaching and research experience. Position available Sept., 1961. Write Head of E.E. Dept., State University of Iowa, Iowa City, Iowa.

ELECTRONIC ENGINEER

Inductive Devices. Well established and growing company located in Culver City, Calif., has an excellent opportunity for a capable engineer to organize and manage the design and manufacture of low pass, high pass and band pass filters and electro magnetic delay lines. Salary will be commensurate with training, experience and ability to manage. Liberal company benefits. Box 2047.

(Continued on page 108A)

Positions Open

(Continued from page 107A)

ELECTRICAL ENGINEERING TEACHING POSITIONS

Ph.D. degree required. Teaching experience desirable but not necessary. Excellent opportunity for young man interested in teaching electronics, network theory, control systems and computers at undergraduate and graduate level. Appointment effective Sept. 1961. Write, Chairman, E.E. Dept., University of Houston, Houston 4, Texas.

ASSISTANT & ASSOCIATE PROFESSOR

Applications are invited for Assistant and Associate Professor of E.E. Candidates should be well qualified academically, preferably to the doctorate level, and should have some research, design or teaching experience in control systems. Duties include teaching at undergraduate and graduate levels, organization and direction of laboratory classes, conducting research and supervising research students. Salary scales are open and competitive with those of industrial and research establishments. Additional stipends are offered to professors who remain on the campus for 11 months of the year and carry out research during this period. Write to Chairman, Dept. of E.E., McMaster University, Hamilton, Ontario.

DESIGN ENGINEER

Design Engineer for low noise and wide band UHF and VHF amplifiers. Outstanding opportunity. Chief Engineer potential. Small, vigorous firm, located in beautiful central Pennsylvania. Educational opportunities across the street at Penn State. Stock option. Send resume to Community Engineering Corp., P.O. Box 824, State College, Pa.

TEACHING POSITIONS

The E.E. Dept. of the City College of New York has several positions available on the teaching staff beginning Sept. 1961. Rank and salary commensurate with qualifications and experience. Opportunity for graduate study. Applicants must be present residents of the U.S. Address inquiry to Prof. H. Taub, Dept. of E.E., The City College, Convent Ave. at 139th St., New York 31, N.Y.

SENIOR ELECTRONIC ENGINEERS

Electronic Engineers are needed for development of new types of Power Supplies and other electronic instruments. Experience is desired in the fields of power supplies, AC line regulators, electronic instruments and magnetic amplifier and transistorized circuits. Salary is open and is commensurate with applicant's background and ability. Company benefits. Apply Perkin Electronics Corp. 345 Kansas St., El Segundo, Calif.

ENGINEERS

Openings for Electrical Engineering Dept. Chairman and for Assistant or Associate Professor. Must have Doctorate. Opportunity for research in Bio medical Electronics. Excellent salary and environment. Send resume to Chairman, Dept. of E.E., University of Vermont, Burlington, Vermont.

A WORD OF WARNING ABOUT THE NEW ALLUREMENTS OF RECOMP II [and a modest word about price]

Could you be enticed by a computer? Surprisingly, there *are* businessmen and scientists who have allowed their emotions to get quite out of control regarding Recomp II.

And now there is more reason than ever for becoming enamored with this amazing computer. *Three* reasons, to be exact, and all of them new. Hence, our warning to you.

The first reason is, in itself, enough to steal your heart away: it is Recomp II's new reduced lease price. Always the darling of the medium-scale computer user, Recomp II has been so well accepted that it can now be offered at significantly lower terms. And it *still* provides the identical quality, solid-state performance, and features that can't be found on computers costing three times what Recomp II *used* to cost.

This is heady stuff—but even more enticements lie in wait. You can now add an optional modification to your Recomp II to enlarge its capacity by using magnetic tape. Here you see the new Recomp Magnetic Tape Transport unit.

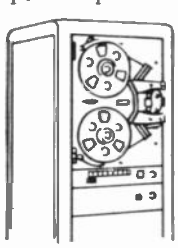

Naturally it's superbly designed, solid state throughout. But don't let its quietly well-bred air fool you; it has a memory that would stagger an elephant—over 600,000 words. And up to eight of the Transport units can be connected to Recomp II, giving you a computer with a total memory capacity of over 5,000,000 words. Steady there, Mr. Simpson!

The speed of this new magnetic tape control is something to applaud, too: read and write speed is 1850 characters a second; bidirectional search speed is 55 inches per second. Do you begin to see why we warned you about these new allurements of Recomp?

Below you see another new optional feature for your Recomp II: the Facitape tape punch and reader console. It punches 150 characters a second, reads 600 characters a second, and stops on a character. It adjusts to read and punch from 5

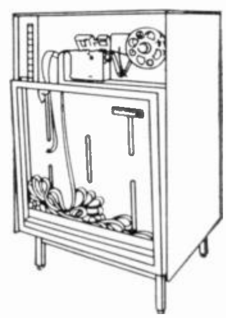

through 8 channels. It is versatile, accurate, fast, simple-to-operate, economical, reliable. And it has perfect manners: the mechanical components are completely enclosed in a soundproof housing.

But lest we harp too much on the *new* features of Recomp II, perhaps we had better remind you of some of the extraordinary features that Recomp II *already had*. Features that have always made it the finest computer in the low-priced field.

1] Recomp II is the *only* compact computer with built-in floating point arithmetic. It defies being hemmed in on a problem. With its large capacity it obviates computer-claustrophobia.

2] Recomp II was the first solid-state computer on the market. As you can see by the new features above, Recomp II's scrupulous engineers have seen to it that it remains the *finest* solid-state computer on the market.

3] Recomp II seems to have more built-in features than a dream home kitchen. It has built-in square root command. Built-in automatic conversion from decimal to binary.

Here you see Recomp II's distinctive keyboard. It looks easy enough to operate—and it *is!* And because Recomp II

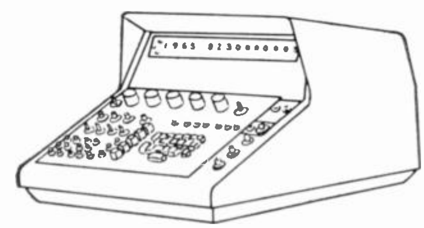

requires no specialized talents, anyone with computer problems can be taught to use it.

One look at Recomp II leaves little wonder that even practical people have allowed their hearts to influence them in choosing Recomp II. Without being showy, it is an object of beauty that reflects its supreme precision of performance. Its distinguished exterior bespeaks the ultimate of excellence; *c'est sans pareil.*

But if you want to avoid being captivated by a computer you should know how strong your emotions will run. May we suggest a *test?* Expose yourself to Recomp II. See it in action. Touch it. Feed problems into it. This is the only way to know how you will react to this extraordinary computer. Make a date to see Recomp II right away.

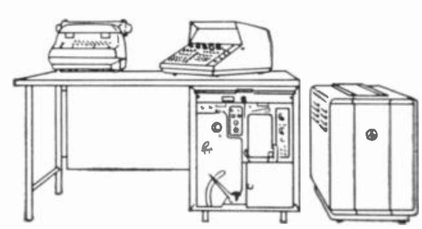

Write AUTONETICS INDUSTRIAL PRODUCTS, Dept. 048, 3400 E. 70th St., Long Beach, Calif.
The Autonetics Division of North American Aviation, Inc.

Positions Wanted

By Armed Forces Veterans

In order to give a reasonably equal opportunity to all applicants and to avoid overcrowding of the corresponding column, the following rules have been adopted:

The IRE publishes free of charge notices of positions wanted by IRE members who are now in the Service or have received an honorable discharge. Such notices should not have more than five lines. They may be inserted only after a lapse of one month or more following a previous insertion and the maximum number of insertions is three per year. The IRE necessarily reserves the right to decline any announcement without assignment of reason.

Address replies to box number indicated, c/o IRE, 1 East 79th St., New York 21, N.Y.

ENGINEERING MANAGER

Washington D.C. situation desired with military electronics firm engaged in R & D and production. Experienced in project and contract technical administration, customer service and liaison, market analysis, and operational evaluation planning. BSEE, plus USN special schools; age 41; married, 2 children. Will relocate from New York area. Resume upon request. Box 3012 W.

ENGINEER

Ph.D., summer 1961. 5 years college teaching experience. 1 year industrial experience. Interested in teaching and research progressive E.E. department. Prefer western U. S. Box 3013 W.

ENGINEER

Expects to receive MEE. degree from the University of Tokyo, January 1961. BEE. Cornell 1953. U. S. citizen. Experience in transistor circuits, electronic test equipment design and fabrication, technical writing, and technical translating. Military experience includes teaching and technical intelligence. Good knowledge of written and spoken Japanese. Desires position in Japan requiring professional competence. Box 3014 W.

BIOPHYSICIST—ENGINEER

Ph.D., MSEE., wishes faculty appointment teaching and research. Publications and author of two books. Can develop biomedical instrumentation program. Equivalent industrial positions considered. Box 3020 W.

TEACHING

Naval officer, aged 38. B.S. in Engineering Electronics plus 35 graduate hours. Retiring in July 1961. 5 years teaching experience, both graduate and undergraduate. Desires teaching position at university in West or Southwest. Textbook author. Resume upon request. Box 3021 W.

R & D MANAGER

Desires assignment in industry or university. 20 years experience in industry, government and universities in R & D teaching, and management, encompassing broad fields of physics, electronics, earth sciences, education and administration. Box 3022 W.

SENIOR ENGINEER

MSEE. Age 30. Presently employed in practical network synthesis in time and frequency domains from audio to .5 Kmc. Desires position involving more network research challenges and responsibilities. Salary secondary. Will relocate. Box 3023 W.

PATENT ATTORNEY

BEE., B.Aero E., LLB; 4 years corporate and law office experience writing and prosecuting applications, interferences, infringement studies and licensing. 6 years diversified engineering experience including transistor circuitry and aircraft instruments. Interested in position in New York City area. Box 3024 W.

PUBLIC RELATIONS EXECUTIVE

Desires opportunity to help put medium or large company and its management on map with small to medium budget; strong with financial community, press, educators; electronics, wire service background. Now with a "top ten" company. Box 3025 W.

TECHNICAL WRITER

Electronics Technician Chief would like to ghost or write under a dual byline with electronics engineers. If you have ideas which you feel fit the popular market but do not have the time to develop and write a practical do-it-yourself article we could probably work to our mutual advantage. Would also like technical writing assignments. Box 3026 W.

INTERNATIONAL OPERATIONS

Former Lieutenant-Colonel Marine Corps with strong civilian background for executive or liaison responsibilities heavy experience South America and Europe. Technically trained to assist manufacturing, sales or field engineering management overseas. Box 3027 W.

(Continued on page 114A)

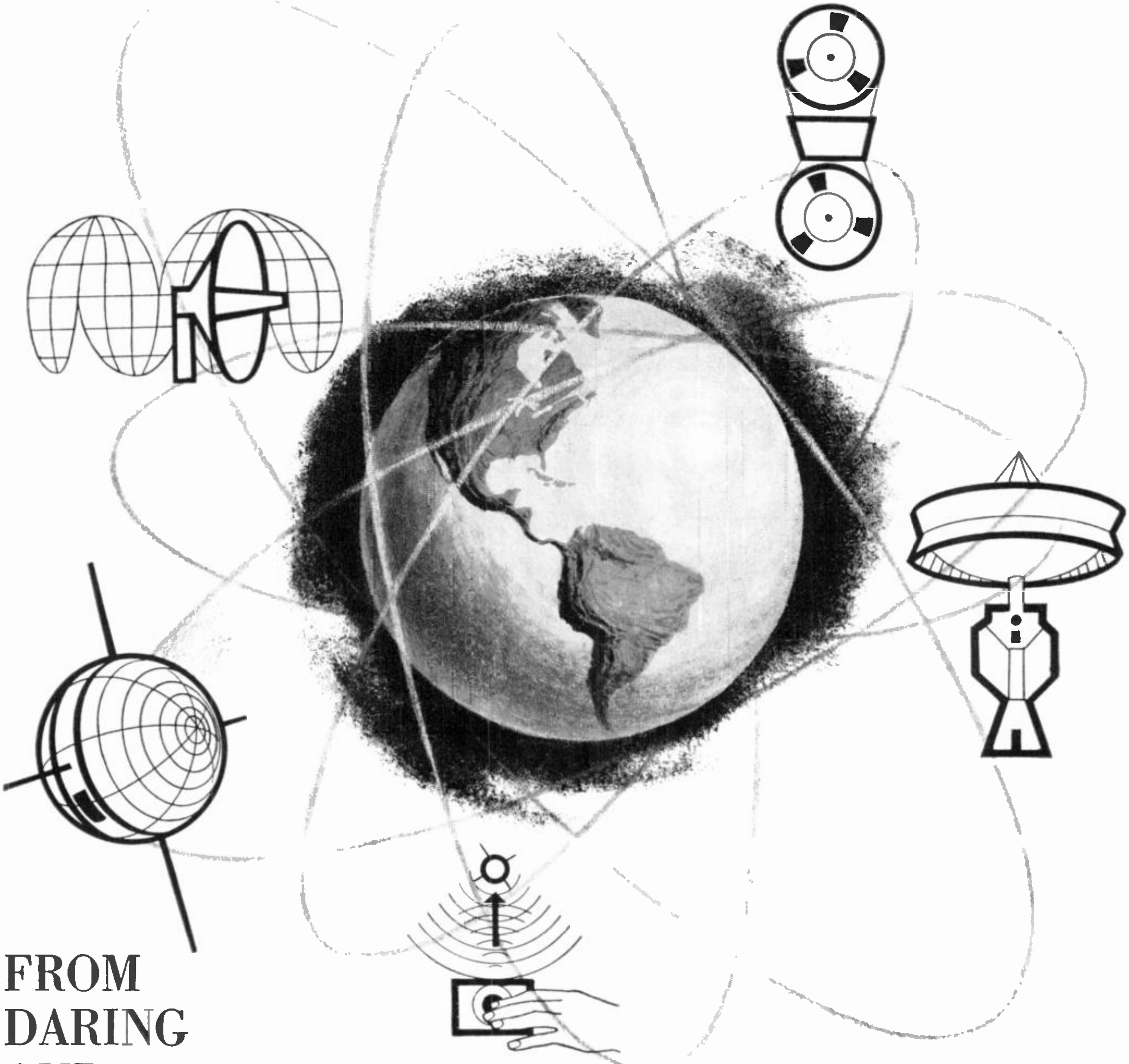

NEEDED: more Electronics Engineers qualified to work on advanced missile detection systems

Complexity of, for example, the BMEWS project, indicates the need for experience, competence... highlights the kind of opportunities open with General Electric's Missile Detection Systems Section.

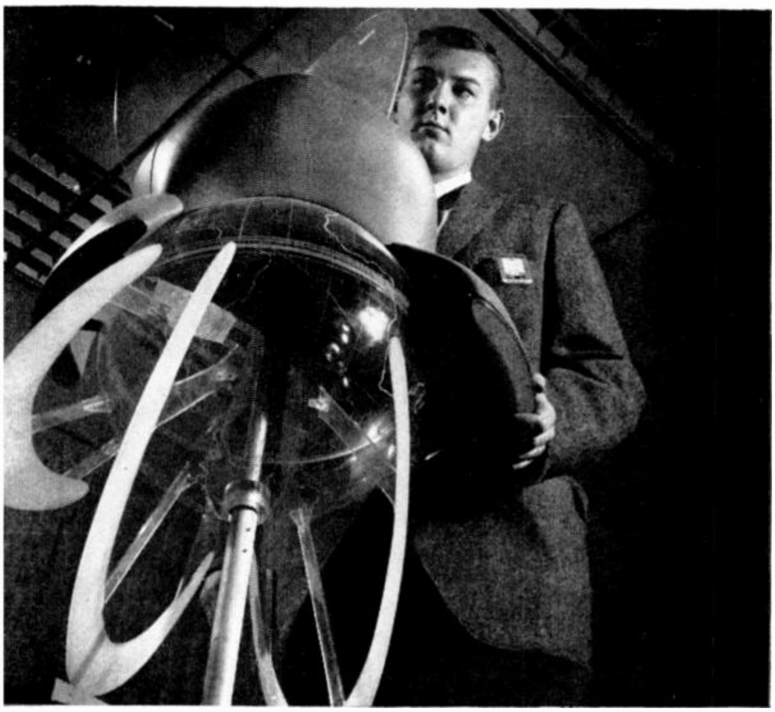

FUTURE DEFENSE, SPACE PROBLEMS

Future-generation space vehicles will necessitate even more sophisticated detection systems. The creation of such systems is the job of the Advanced Radar Systems Development Engineer. Qualifications are high . . . but the rewards are in keeping—the opportunities for advancement excellent.

Within the next ten years the need for qualified engineers and scientists will quadruple in the field of missile, space-probe and satellite detection. This prediction is made by General Electric's Missile Detection Systems Section, based on present and anticipated space vehicle state-of-the-art.

And because of this, there is a possibility that a technical manpower "vacuum" may develop in what many consider to be one of the most vital, fast-growing technologies of the space age. What's needed are more engineers who can meet the strict requirements. For example . . .

It takes a unique kind of engineer to work in the field of detection. An Advanced Systems Engineer must be extremely competent technically. Yet, he must also be something of a "dreamer"—able to anticipate and define future *problems* as well as conceive practical systems *solutions*. To do this, he must keep abreast of virtually every significant advancement, not only in his own, but in other fields.

The same holds true for Equipment Specialists who must meet exacting detection-system specifications. Yet, there are relatively few related fields where this kind of specialized experience can be obtained.

BMEWS is a good example of the magnitude of system and equipment requirements. Its 66,000 square-foot antenna reflectors had to be engineered to hold a ¾ of an inch tolerance over a 150° tem-

PROVIDING 15-MINUTE WARNING

BMEWS' massive radar reflectors are indicative of the system's complexity. According to MDSS four electronics engineers will be needed within the next decade for every one now working on such systems.

REPORTS FOR ELECTRONICS ENGINEERS

perature range . . . with a 2-inch tolerance in winds up to 185 mph. Its radar detection sub-system, designed and developed by G.E.'s Missile Detection Systems Section, transmits multi-million watt pulses . . . to receive milli-micro-microwatt echoes. And this is just one part of a complex system to detect missiles, calculate trajectory, impact area, impact time, and point of launch.

It's indicative of why the Missile Detection Systems Section can offer growth opportunities in a technology that has some of today's most unique engineering and scientific challenges.

IMMEDIATE OPENINGS FOR SYSTEMS EXPERIENCED ENGINEERS AND SCIENTISTS

General Electric's Missile Detection Systems Section has openings right now for qualified scientists and engineers anxious to broaden their experience and continue their professional careers in this exciting new technology. Although requirements are necessarily high, the opportunities for rewards and advancement are unusual.

DEFINING FUTURE SPACE PROBLEMS . . .

. . . is the job of the *Advanced Radar Systems Development Engineer*. There is an immediate need for competent men to conceive detection systems that will outpace the most advanced state-of-the-art in missiles, space-probes and satellites.

Advancement is in keeping with the highly demanding nature of this position. Your responsibilities will include determining broad parameters for—and establishing feasibility of—advanced detection systems. Basic requirements include a BSEE, an advanced degree, and five to ten years' experience in systems design and analysis.

PROVIDING HARDWARE SOLUTIONS . . .

. . . for future detection systems is the job of the Systems Analysis Engineer. A high degree of technical competence and the ability to manage are prerequisites. In this position you will specialize in evaluating missile defense systems and coordinating the tools and talents of the organization in order to obtain optimum configurations based on utility, performance, cost and delivery.

Basic requirements include a BSEE degree, Physics, or Math. You should be familiar with mathematical probability, systems simulation, operational analysis, and generalized harmonic analysis.

PROGRAMMING COMPLEX DATA . . .

. . . is the challenging job of the Senior Programmer in Computer Operations. This job requires an ability to interpret problems related to analysis of missile detection systems. As group leader, you will be responsible for computer programming and other detailed investigations.

Basic requirements include a BSEE or Math degree, with three to five years of experience on large scale scientific computers.

INSTALLATION, CHECKOUT AND INTEGRATION . . .

. . . must be successfully accomplished by the Systems Engineer working at the installation site. As such, you will be responsible for actual system installation, checkout, and integration with all other systems or subsystems. Your job will include initial operation of the system and training of operating personnel. Rewards are in keeping with the highly demanding nature of this position.

Basic requirements include a BSEE degree with five years' experience in radar, high power transmitters and/or microwave systems. 177-44

FOR MORE INFORMATION:

or for a copy of this new brochure which describes the challenging and rewarding opportunities open to you in General Electric's Missile Detection Systems Section, write today to:
Mr. Dana S. Brown
Missile Detection Systems Section T-12
General Electric Company
Court Street, Syracuse, N. Y.

GENERAL ELECTRIC

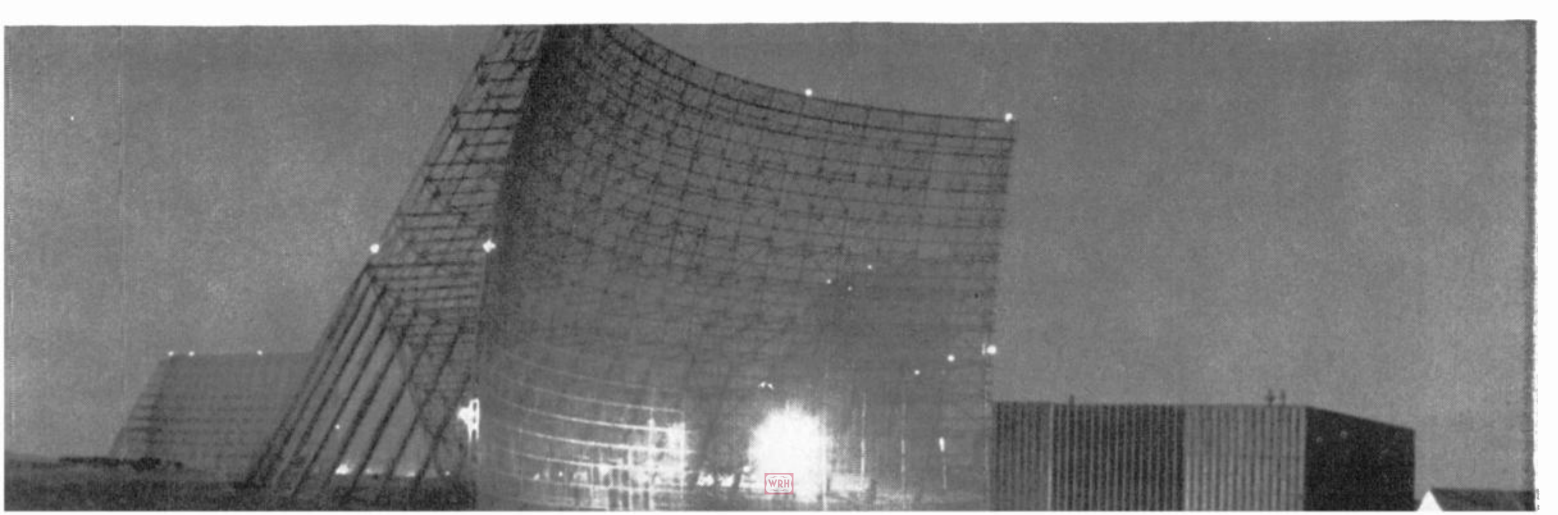

Positions Wanted

By Armed Forces Veterans

(Continued from page 110A)

REPRESENTATIVE / ENGINEERING

Engineer with electronic and executive experience; age 32; married with no family desires association with firm requiring representation western Canada or anywhere abroad. Position in engineering offering a challenge. Experience in systems planning, research and production mostly in communications VHF (FM) and SSB telemetry. Member IRE. Overseas experience. British subject. Box 3935 W.

MANUFACTURERS REPRESENTATIVE

Phila. Pa. area (Pennsylvania, New Jersey, Delaware). Well established 10 years radio, television, electronic components. Member IRE. Excellent contacts purchasing and engineering level. Seeking additional quality component line. OEM & IND. Box 3936 W.

ENGINEER—MANAGER

BSEE., PE, age 39. Can help you set up and run foreign operations. 5 years unique experience organizing and running electronics engineering consulting and liaison service between U.S. plants and foreign subsidiaries of large firm. 15 years managerial and team leader experience, consumer and military products. Box 3937 W.

ELECTRONICS ENGINEER

Naturalized citizen leaving for Europe in March or April 1961 with wife who is a mathematician. Desires offers of full, part time, or commission assignment while in Europe on a 1 year leave of absence from the Operations Research Dept. of a major missile company. Speaks fluent Polish and German with good knowledge of French. Has good technical knowledge and experience in ground communications systems, weapons systems study procedures, etc. BSEE. Oregon State College 1957. Ex-USAF Air and Airways Communications System Maintenance Chief. Box 3938 W.

COMMUNICATIONS ENGINEER

Desires position in Europe with progressive company in wire or radio communications projects. Experienced in systems operation and management and military R & D. MSEE. and advanced education; Professional Engineer; age 30; languages; highest security clearances; 7½ years military service (Signal Corps and ASA Officer). Box 3939 W.

ELECTRONICS ENGINEER

BSEE.; age 30; desires position in electronic systems engineering, marketing and management. 6 years experience in radar, communications, television and missile electronics. Foreign assignments preferred. Box 3940 W.

Membership

The following transfers and admissions have been approved and are now effective:

Transfer to Senior Member

Bacon, F. S., Jr., Marion, Mass.
Bains, R. W., Shreveport, La.
Borgese, A. L., Pittsfield, Mass.
Britton, J. R., Honolulu, Hawaii
Butler, H. L., Little Silver, N. J.
Cavenaugh, D. E., Saratoga Springs, N. Y.
Chirlian, P. M., New York, N. Y.
Ellis, T. E., Rochester, N. Y.
Feldmeier, J. R., Phiadelphia, Pa.
Ferber, D., Encino, Calif.
Francisco, G. E., Jr., Columbus, Ohio
Garceau, L., South Woodstock, Vt.
Gavsie, F. F., Montreal, Que., Canada
Ghormley, R. K., Lincoln, Neb.
Hamilton, G. H., Norfolk, Va.
Hayre, H. S., Albuquerque, N. M.
Herzog, G. B., Cambridge, England
Hummer, E. W., Sandusky, Ohio
Jackson, S. P., Columbus, Ohio
Kemp, J. C., Johnsville, Pa.
Kitsopoulos, S. C., Summit, N. J.
Lane, J. W., Prairie Village, Kan.
Liebman, P. M. Brooklyn, N. Y.
Longerich, E. P., Southfield, Mich.
Marceau, J. P., Drummondville, Que., Canada
McElwee, J. F., Jr., Glendora, Calif.
Meier, D. A., Inglewood, Calif.
Mommo, E. J., Irvington, N. J.
Morrow, A. J., Huntington Station, L. I., N. Y.
Murphy, A. T., Wichita, Kan.
Myers, P. B., Phoenix, Ariz.
Niebuhr, J. E., Los Angeles, Calif.
Novak, J. F., Chicago, Ill.
Orefice, G. T., Yonkers, N. Y.
Oslake, J. J., Costa Mesa, Calif.
Otterman, J., Whippany, N. J.,
Palandri, G. L., Milano, Italy
Randolph, A. M., Shreveport, La.
Regulinski, T. L., Wright-Patterson, AFB, Ohio
Risley, M. I., Omaha, Neb.

(Continued on page 118A)

"EUREKA" IS HARDLY THE WORD FOR IT, ARCHIMEDES!

"Astounding" is more like it, because we use your principle to buoy the "heart" of our precision gyroscopic instruments. Floatation eliminates frictional forces on pivots and thereby reduces drift rates. Consequently, we are able to develop precise gyros and pendulous accelerometers for missile guidance and ship navigation.

If you are interested in putting ancient laws to work in the missile age, and if you have a BS, MS or PhD in EE, ME, Physics or Math, contact Mr. G. F. Raasch, Director of Scientific and Professional Employment, Dept. B, 7929 S. Howell, Milwaukee 1, Wisconsin.

AC SPARK PLUG ⚛ THE ELECTRONICS DIVISION OF GENERAL MOTORS

MILWAUKEE • LOS ANGELES • BOSTON

AC

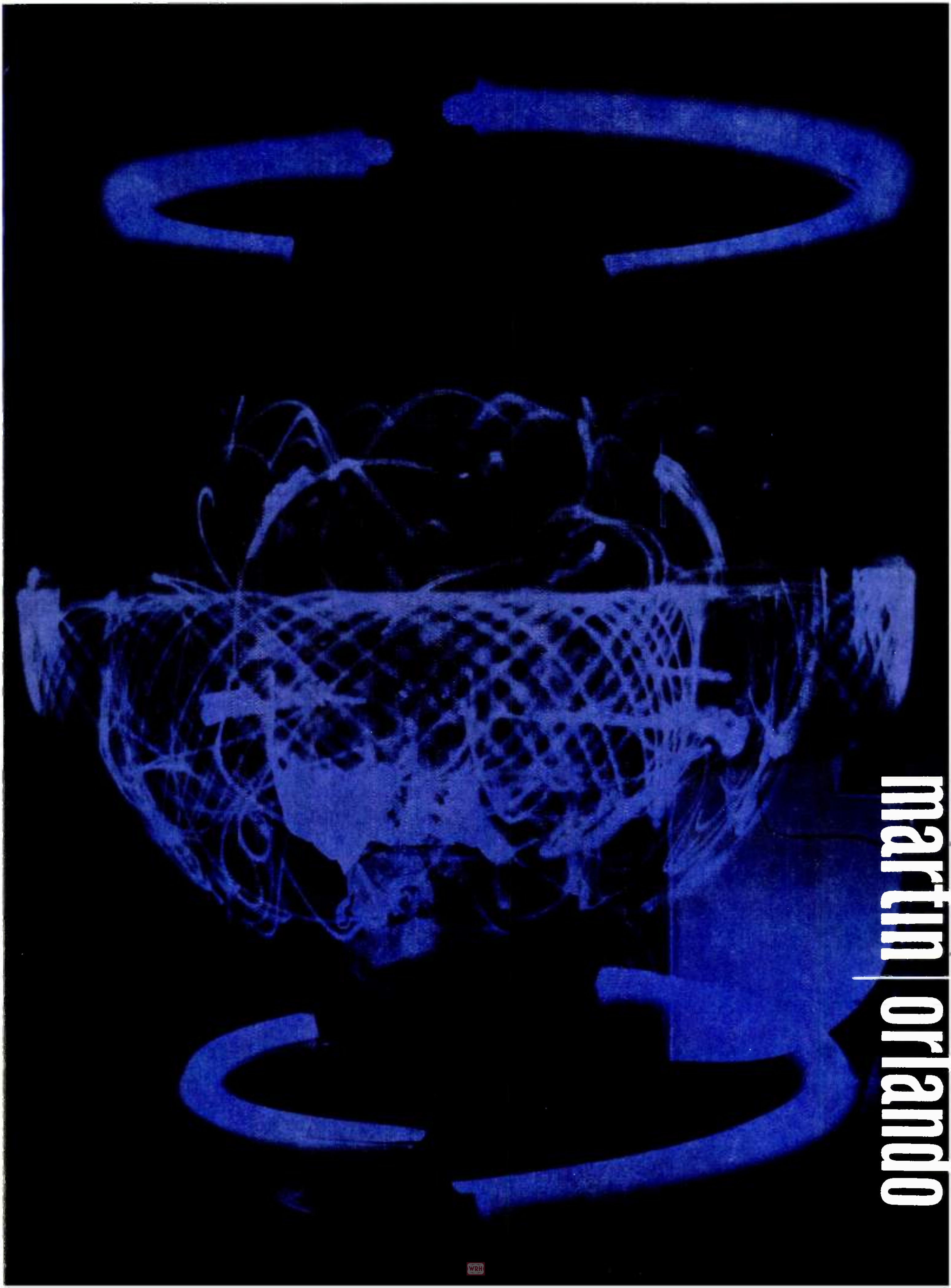
martin | orlando

Membership

(Continued from page 114A)

Schmitt, H. J., Cambridge, Mass.
Schon, F. K. K., Cote St. Luc, Mont., Que., Canada
Schreiner, K. E., Yorktown Heights, N.Y.
Sellars, R. F., Offutt AFB, Neb.
Sharki, P., Rome, N. Y.
Silleni, S. R., Padova, Italy
Smith, P. J., Norwalk, Conn.
Smith, R. T., Austin, Tex.
Soorian, D. A., Wayland, Mass.
Strohecker, J. P., Seattle, Wash.
Thompson, F. T., Verona, Pa.
Wanselow, R. D., Woodland Hills, Calif.
Weppler, H. E., Madison, N. J.
Wheeler, M. S., Balitmore, Md.
Wiggins, C. P., Northridge, Calif.
Wilson, F. J., Little Rock, Ark.
Wouk, V., New York, N. Y.
Yowell, G. M., Johnsville, Pa.
Zelinger, G., Montreal, Que., Canada
Zillger, W. H., Little Silver, N. J.

Admission to Senior Member

Alger, P. L., Schenectady, N. Y.
Amonette, E. L., Albuquerque, N. M.
Baines, E. A., Fayetteville, N. Y.
Bartlett, W. D., Washington, D. C.
Byrd, C. G., Orlando, Fla.
Carson, C. T., Philadelphia, Pa.
Carter, C. W., Jr., Brookfield Center, Conn.
Dalasta, D., West Allis, Wis.
Damon, R. W., Burlington, Mass.
Deane, J., Victoria, B. C., Canada
DeCarlo, C. J., Brooklyn, N. Y.
Eriksen, W. T., Newton, Mass.
Finzi, L. A., Pittsburgh, Pa.
Friedland, S. S., Sherman Oaks, Calif.
Gambling, W. A., Southhampton, England
Harac, S., Verona, N. J.
Hix, I. M., Endicott, N. Y.
Humme, C. W., Jr., Los Angeles, Calif.
Jones, A. F., Paramus, N. J.
Klaiber, G. S., Kenmore, N. Y.
Kraay, R. A., Allentown, Pa.
Lederberg, J., Stanford, Calif.
Leeds, B. L., East Northport, L. I., N. Y.
Long, W. H., Pacific Palisades, Calif.
Lucic, A., Garden Grove, Calif.
Maresca P. T., Elberon Park, N. J.
McLaughlin, J. W., Arlington, Va.
Menzel, W., Vesenaz (Geneva), Switzerland
Moody, N. F., Saskatoon, Sask., Canada
Oertel, E. C., La Mesa, Calif.
Parker, J. C., Sr., Memphis, Tenn.
Peterson, A. E., Dayton, Ohio
Pettit, B. L., Washington, D. C.
Rondou, J. K., Sunland, Calif.
Roos, W. B., Sacramento, Calif.
Rosenfeld, M. M., Woodside, L. I., N. Y.
Ryerson, H. R., Garfield Heights, Ohio
Savage, C. F., Scarsdale, N. Y.
Schenker, L., Murray Hill, N. J.
Shugart, A. F., San Jose, Calif.
Stuart, R. D., Boston, Mass.
Volz, P. E., Severna Park, Md.
Weiss, J. A., Burlington, Mass.
Wells, C. R., Jr., Billerica, Mass.
Wilder, H. B., Claremont, Calif.
Wylie, R. R., Springfield, Ill.
Zverev, A. I., Hanover, Md.

Transfer to Member

Baxter, J. L., Bethesda, Md.
Beardsworth, R., Syosset, L. I., N. Y.
Birsten, B. R., Douglaston, L. I., N. Y.
Bonseigneur, P. F., Jr., Offutt AFB., Neb.
Borgen, H., Hicksville, L. I., N. Y.

(Continued on page 120A)

Membership

(Continued from page 118A)

Brendle, T. A., Suffern, N. Y.
Brown, C. W., Jr., El Paso, Tex.
Buchan, J. F., Orlando, Fla.
Buhrman, H. M., Sunnyvale, Calif.
Butler, R. M. Raleigh, N. C.
Clayton, G. H., Des Peres, Mo.
Cobb, F. L., San Carlos, Calif.
Connelly, T. R., Bath, N. Y.
Corbett, T., Portland, Ore.
Dague, G. L., Winston-Salem, N. C.
Dishler, J. J., Haddonfield, N. J.
ElKashlan, E. I., Imbaba, Cairo, U. A. R.
Emslie, N. M., Yardley, Pa.
Fisher, G. F., Kansas City, Kan.
Fliegler, E., West Belmar, N. J.
Frager, A. M., University City, Mo.
Frank, E. J., Chicago, Ill.
Fuller, G. L., Council Bluffs, Iowa
Grasselli, A., Princeton, N. J.
Gumb, D. F., Mary Esther, Fla.
Guthrie, T. F., Richmond Hill, L. I., N. Y.
Hollis, T. W., Jr., Towson, Md.
Horowitz, P., Costa Mesa, Calif.
Jelinek, G., Grand Island, Neb.
Jones, A. C., Scottsdale, Ariz.
Joseph, D. L., Apalachin, N. Y.
Kampmeyer, R. A., Baltimore, Md.
Kelley, R. J., San Diego, Calif.
Kienast, D. J., North Hollywood, Calif.
Lowenstein, H. L., Watertown, Mass.
Milbrodt, P. E., Fairfax, Va.
Miller, W. A., Scranton, Pa.
Mita, Shigeru, Tokyo, Japan
Quinn, T. B., Los Angeles, Calif.
Sanders, N. D., Falls Church, Va.
Sharp, N. S., Washington, D. C.
Shipley, D. G., Rocky Point, L. I., N. Y.
Soohoo, E. L., Beverly, N. J.
Tatum, F. A., Santa Monica, Calif.
Walker, R. J., Owensboro, Ky.
Wilson, C. M., No. Vancouver, B. C., Canada

Admission to Member

Allen, W. W., Jr., Berwyn, Pa.
Amundsen, R. C., Ridgefield, Conn.
Anderson, K. R., Midland, Mich.
Andrews, W. W., Cranford, N. J.
Baker, O. R., Sunnyvale, Calif.
Baldwin, R. A., Jr., Arlington, Tex.
Becker, P. A., Brooklyn, N. Y.
Behringer, R. W., Scarsdale, N. Y.
Bennett, E. C., Manlius, N. Y.
Benson, J. J., Albuquerque, N. M.
Berkowitz, C. E., King of Prussia, Pa.
Berns, P. B., Fullerton, Calif.
Bernstein, B., Scarsdale, N. Y.
Berntsen, T. J., Montclair, N. J.
Beyer, W. G., Philadelphia, Pa.
Billings, R. D., Barstow, Calif.
Birutis, G., Richmond Hill, L. I., N. Y.
Blackie, J. C., Wakefield, Mass.
Blount, L. A., Johnsville, Pa.
Bluth, A., Philadelphia, Pa.
Booth, R. A., Glendale, Calif.
Borrello, R. P., Baltimore, Md.
Borrok, M. J., St. Louis, Mo.
Bowles, T. J., Seattle, Wash.
Bradley, R. R., Jr., Washington, D. C.
Bradley, R. W., Nutley, N. J.
Brand, B., Syracuse, N. Y.
Brennan, R. F., Riverside, Calif.
Bridge, G. W., Oklahoma City, Okla.
Britten, E. F., Lakewood, Calif.
Brookman, A. S., China Lake, Calif.
Brown, A. H., Getzville, N. Y.
Brown, J. K., Deer Park, L. I., N. Y.
Brown, S., Cleveland, Ohio
Brown, T. M., New York, N. Y.
Brownell, H. J., San Mateo, Calif.
Brunel, A., Montreal, Que., Canada
Budne, T. A., Great Neck, L. I., N. Y.
Buell, V. B., Los Altos, Calif.
Bull, E. D., Sepulveda, Calif.
Bunko, W., Calgary, Alta., Canada
Busch, A. C., Cincinnati, Ohio
Bush, W. D., Goletta, Calif.
Byars, B. R., Jr., Fort Worth, Tex.
Carver, O. T., Riverton, N. J.
Caini, V., Uppsala, Sweden
Campbell, R. B., Jr., Brookline, Mass.
Carmody, W. F., Bellevue, Wash.
Carvajal, R. L., Dallas, Tex.
Cecil, J. W., Tulsa, Okla.
Chang, D. M. Y., Haddonfield, N. J.
Childs, P. B., Jr., Irving, Tex.
Chin, B., Las Cruces, N. M.
Cittadini, J. L. G., Huntington Station, L. I., N. Y.
Clark, G. E., Rome, N. Y.
Clarke, J. M., Arlington, Mass.
Claycomb, H. E., Phoenix, N. Y.
Cobb, A. G., Winnipeg, Man., Canada
Cohen, M. R., Paterson, N. J.
Colvard, J. E., China Lake, Calif.
Conyers, W. T., Baltimore, Md.
Cornell, K. M., San Jose, Calif.
Corrihons, L. J., Washington, D. C.
Courtney, R. A., Dayton, Ohio
Craig, W. C., Baldwin Park, Calif.
Crane, J. W., Anaheim, Calif.
Crockett, I. L., Bountiful, Utah
Curry, C. T., Seattle, Wash.
Cutting, A. B., Montreal, P. Q., Canada
Czobor, S. E., Montreal, P. Q., Canada
Dachert, F., Chestnut Hill, Mass.
Davis, I. T., Washington, D. C.
DeMaria, F. C., Dearborn, Mich.
Dewland, J. F., Secaucus, N. J.
de Wolfe, G. C., Pasadena, Calif.

(Continued on page 121A)

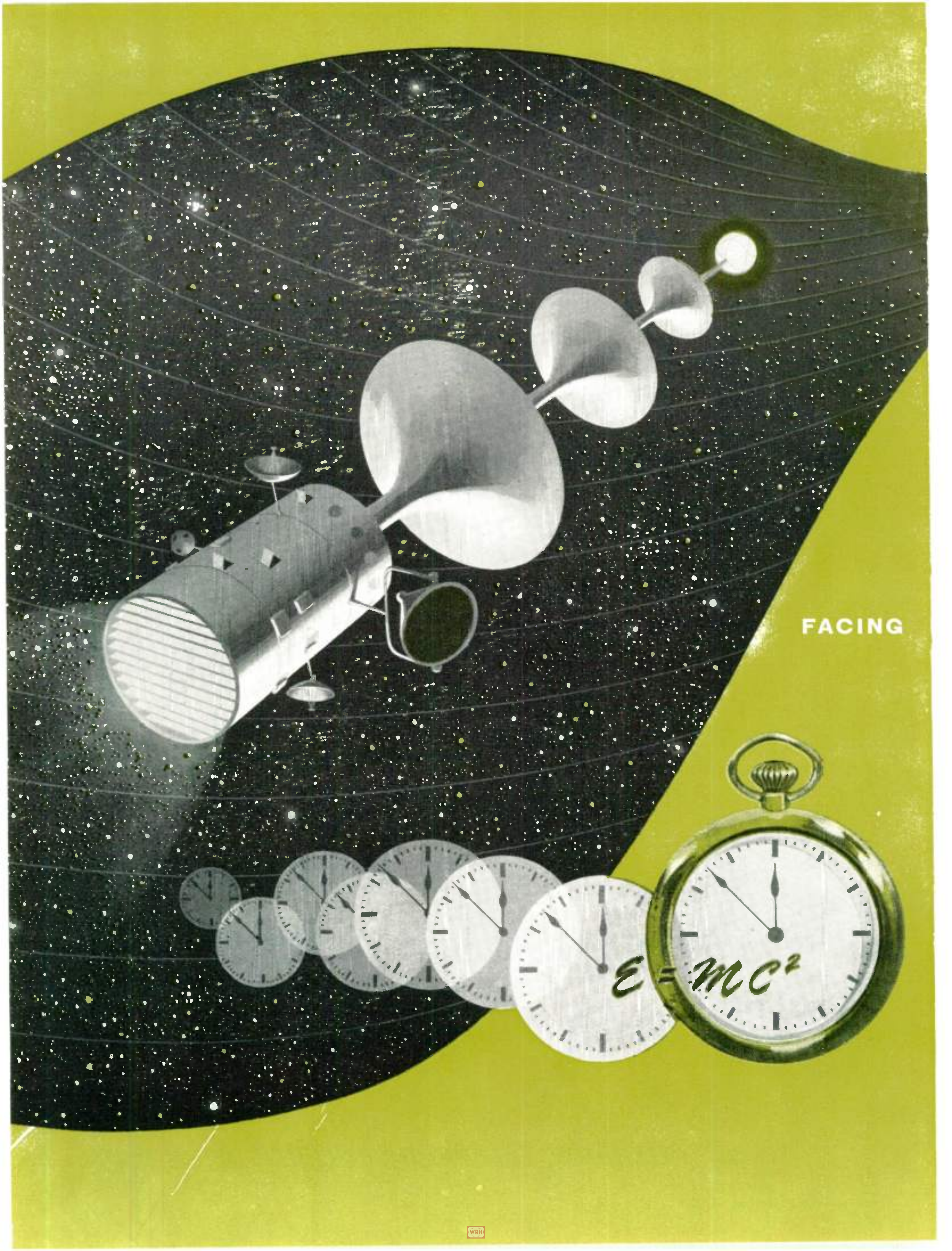
FACING
E = MC²

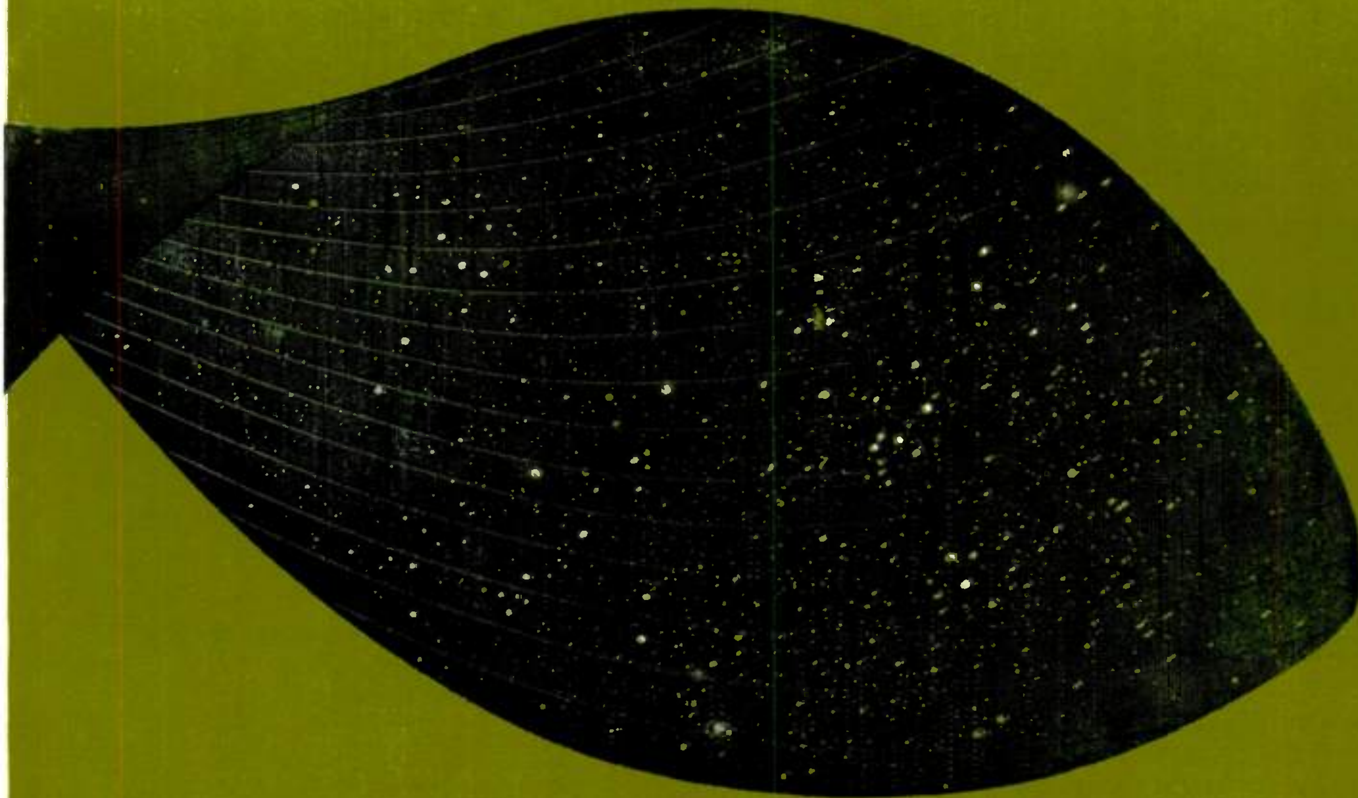

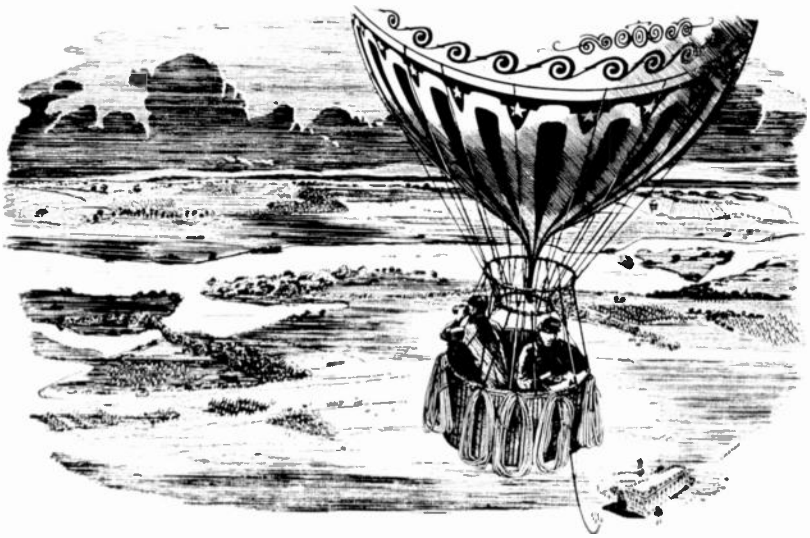

Membership

(Continued from page 120A)

Dixson, J. R., Des Plaines, Ill.
Dodson, G. A., Murray Hill, N. J.
Eckhart, E. P., Cocoa Beach, Fla.
Edwards, W. L., South River, N. J.
Eisner, H., Kensington, Md.
Elschener, H. J., New York, N. Y.
Endbinder, M., Liverpool, England
Estwick, S. M., Goderich, Ont., Canada
Everest, C. E., Sierra Madre, Calif.
Fallows, R. P., Phoenixville, Pa.
Fick, J. E., Chalfont, Pa.
Finkel, L., Haddonfield, N. J.
Fisher, J. M., Jr., Pitman, N. J.
Flanagan, J. E., Newton, Mass.
Fletcher, W. K., Dayton, Ohio
Franks, L. E., Murray Hill, N. J.
Freund, R. E., Philadelphia, Pa.
Frick, D. F., Palatine, Ill.
Friederichs, J. W., Toddville, Iowa
Friedlander, I. N., Bayside, L. I., N. Y.
Furey, R. J., Hatboro, Pa.
Gabbert, J. J., San Francisco, Calif.
Gehrke, F. H., North Olmsted, Ohio
Ghiselin, W. F., Jr., Bellaire, Tex.
Ghosh, A. K., Chandernagore, West Bengal, India
Gilbert, J. D., Melbourne, Fla.
Gille, J. C., Paris, France
Gillet, C. C., Evanston, Ill.
Gilliland, M. E., Clay, N. Y.
Giova, F. N., Philadelphia, Pa.
Gliatti, E. L., No. Babylon, L. I., N. Y.
Glowacki, R. E., Huntsville, Ala.
Graham, W. L., Cocoa Beach, Fla.
Guttmann, H. E., Minneapolis, Minn.
Haddock, R. L., Jr., Orlando, Fla.
Haffner, J. W., Elk Grove Village, Ill.
Hanlon, J. E., Jr., Pittsfield, Mass.
Hansen, V. G., Den Haag, Holland
Hardy, H. L., Monroe, Conn.
Harmon, C. R., Garland, Tex.
Harry, J. W., Phoenix, Ariz.
Haque, S. M. E., Dhanbad, Bihar, India
Hartz, R. S., Long Branch, N. J.
Hassler, K. E., Grove City, Ohio
Hearn, F. L., Palo Alto, Calif.
Hedrick, K. M., Cumberland, Md.
Henry, J. L., Catonsville, Md.
Herbert, D. E., San Diego, Calif.
Hinkle, M. L., Jr., Orishany, N. Y.
Holsborg, W., Culver City, Calif.
Holzer, W. H., Silver Spring, Md.
Hovey, H. H., Winston-Salem, N. C.
Hoyt, E. M., Ann Arbor, Mich.
Humpage, W. H., Griffiss A.F.B., New York
Huskin, J. T., Baltimore, Md.
Inami, T., Naha, Ryukyus, Okinawa
Jackson, A. M., Jr., Portsmouth, Va.
Jackson, G. E., Wakefield, Mass.
Janssen, W. W., Sparks, Nev.
Jassen, C., Haledon, N. J.
Jetton, R. P., University, Ala.
Johnson, A. B., Laval Islands, P. Q., Canada
Jungbluth, E. J., Granby, Que., Canada
Kaplan, C., Van Nuys, Calif.
Karpenko, V. A., Los Angeles, Calif.
Katz, P., New York, N. Y.
Kemp, G. K., Toronto, Ont., Canada
Kettleman, E. V. B., New York, N. Y.
Kimura, H., Tokyo, Japan
King, S. W., Los Angeles, Calif.
Klahr, C. N., Brooklyn, N. Y.
Klein, R., Rockaway, N. J.
Knight, G. T., Oklahoma City, Okla.
Koshinz, E. F., Glendora, Calif.
Kronlage, J. W., Dallas, Tex.
Kronstadt, N., Silver Spring, Md.
Kudielka, V. W., Wien, Austria

(Continued on page 126A)

Why don't you **Talk** with Westinghouse about Advanced Education

In the past 8 years, over 16,000 credit hours have been completed by employes under the company sponsored program.

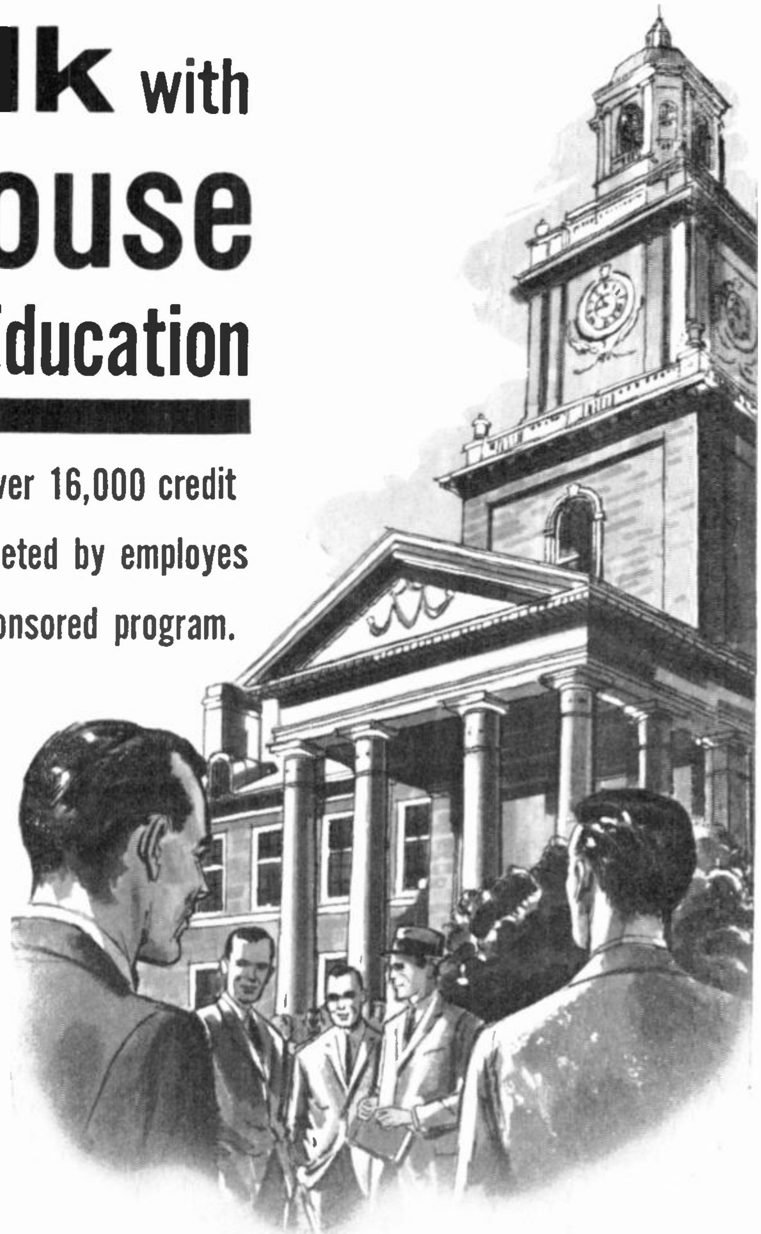

Your career potential is unlimited at Westinghouse-Baltimore. The Westinghouse Advanced Education Program will enable you to combine project work on space age electronics programs with the pursuit of graduate degrees at The Johns Hopkins University or the University of Maryland. The engineer who *wants* to advance will find it rewarding to talk with Westinghouse.

Current openings include:
Communications Systems
Digital Techniques
Solid State Systems
Microwave Theory
Systems Engineering Analysis
Transistor Circuit Design
Radiating Systems Design

Send resume to: Mr. J. F. Caldwell, Dept. 389

Westinghouse

1961 Represents 75 years of Service & Achievement by Westinghouse

BALTIMORE
P.O. BOX 746 **Baltimore 3, Maryland**
AIR ARM • ELECTRONICS • ORDNANCE

Membership

(Continued from page 124A)

Kulda, R. J., Orange, Calif.
Landolina, W. C., Jr., Winston-Salem, N. C.
Lavik, A., Harthorne, Calif.
Leach, J. F., Chicago, Ill.
Leibmann, V., Elmhurst, L. I., N. Y.
Letsch, W. L., Baltimore, Md.
Lewis, W. E., Falmouth, Mass.
Li, Y-L., Birmingham, England
Lietzau, K. E., Severna Park, Md.
Liu, C. C. Y., Ellenville, N. Y.
Lockner, J. G., Rome, N. Y.
Long, K. A., Phoenix, Ariz.
Lorden, J. R., North Hollywood, Calif.
Lorenz, R., Jr., San Jose, Calif.
Lujetic, V. J., Camden, N. J.
Macha, M., Garden City, L. I., N. Y.
Machen, J. W., Point Clear, Ala.
Mack, D. E., Rochester, N. Y.
MacLachlan, R. K., Fullerton, Calif.
MaFoy, J. H., Silver Spring, Md.
Mandis, G. A., Rochester, N. Y.
Maone, V. P., Jericho, L. I., N. Y.
Markowitz, A., Middle Village, L. I., N. Y.
Martinovitch, V. N., Springfield, N. J.
Marushak, J. B., Brooklyn, N. Y.
Mathias, R. J., Shreveport, La.
Matthews, R. E., Baltimore, Md.
Maurer, W. M., So. Lancaster, Mass.
McCarty, J. W., Linthicum, Md.
McDowell, C. L., Jr., Richardson, Tex.
Meddaugh, S. A., St. Paul, Minn.
Merow, D. W., Baltimore, Md.
Michel, W. E., Phoenix, Ariz.
Mikesell, L. G., Lubbock, Tex.
Miles, L. M., Atlanta, Ga.
Mihauskas, V., Seattle, Wash.
Montasser, S. H., Cairo, Dokkey, U. A. R.
Montgomery, H. S., Cocoa Beach, Fla.
Moore, C. J., Philadelphia, Pa.
Moore, J. P., Downey, Calif.
Moore, J. S., Jr., Tampa, Fla.
Moss, R. K., Chatsworth, Calif.
Murphy, J. T., Jr., Maitland, Fla.
Murphy, J. J., Wantagh, N. Y.
Nakamoto, T. I., Syracuse, N. Y.
Nance, V. K., El Paso, Tex.
Neill, D. E., Syracuse, N. Y.
Nelson, R. H., Jr., Denver, Colo.
Nicolet, M-A., Pasadena, Calif.
Nicosia, S. C., Roma, Italy
Nicotra, L., Pisa, Italy
Norman, H. A., Seabrook, Md.
Northrop, P. G., Dayton, Ohio
Novak, J. R., Canoga Park, Calif.
Opoku, N. K., Coventry, England
Osborne, G. G., Los Angeles, Calif.
Oswalt, H., Zurich, Switzerland
Ott, F. J., Gumligen, Berne, Switzerland
Oyler, E. M., Dayton, Ohio
Papale, L. R., Hawthorne, Calif
Paulson, R. C., Needham, Mass.
Peters, R. A., Queens Village, L. I., N. Y.
Piazza, M., Waldwick, N. J.
Picardi, J. E., Concord, Mass.
Pierce, J. T., Plano, Tex.
Piol, E., Milano, Italy
Ponnuraj, H. S., Madras, India
Popelarski, A. F., Trenton, N. J.
Porter, R., Santa Barbara, Calif.
Power, J. A., Huntsville, Ala.
Presson, B. R., Jr., Dallas, Tex.
Quade, T. E., Linthicum, Md.
Queen, P. D., Beverly Hills, Calif.
Rafuse, R. P., Cambridge, Mass.
Ragsdale, R. D., Fairfax, Va.
Reid, K. L., Midwest City, Okla.
Reigel, E. W., State College, Pa.
Reise, R. E., Glen Burnie, Md.
Retelle, J. P., Lexington, Mass.
Robertson, R. P., Newark, N. J.
Robinson, A. J., Winnipeg, Man., Canada
Roess, L. C., Beacon, N. Y.
Rogers, M. F., Olean, N. Y.
Roiter, A., Washington, D. C.
Rollett, J. M., London, England
Rome, J. E., Philadelphia, Pa.
Rose, E. G., No. Vancouver, B. C., Canada
Rosenbaum, E., Baltimore, Md.
Rotramel, W. T., Oklahoma City, Okla.
Ruetz, L., Minneapolis, Minn.
Rutsey, J. P., Livonia, Mich.
Saxena, A. N., Palo Alto, Calif.
Schubach, R., East Cleveland, Ohio
Schuette, R. K., Indianapolis, Ind.
Seelig, W., Flushing, L. I., N. Y.
Selman, V., Bayonne, N. J.
Shevel, W. L., Jr., Yorktown Heights, N. Y.
Shoobridge, M. J., Richmond, Surrey, England
Siperko, C. M., Ellicott City, Md.
Slouka, G. E., Rome, N. Y.
Small, J. W., Jr., Hampton, Va.
Smith, D. A., Hagerstown, Md.
Smith, J. S., Alfred, N. Y.
Smyth, K. A., Silver Spring, Md.
Snoderly, R. O., Anchorage, Alaska
Snow, H. E., Whippany, N. J.
Snyder, H. C., Fremont, Neb.
Soneki, J. H., Bethlehem, Pa.
Southern, P. F., Dallas, Tex.
Springall, T. L., Andover, Mass.
Squires, G. A., Upland, Calif.
Stailing, E. W., Merritt Island, Fla.
Starita, F. A., Nutley, N. J.
Starz, W. A., Liverpool, N. Y.
Steinitz, R. J., Lutherville, Md.
Stinson, L. F., Brigantine, N. J.
Stoltz, W. S., Royal Oak, Mich.
Stookey, B. H., Cornwells Heights, Pa.
Stumpt, F. M., Rome, N. Y.

(Continued on page 128A)

Membership

(Continued from page 126A)

Swirbalus, R. A., South Boston, Mass.
Szekely, G. S., Seattle, Wash.
Takacs, F., Kitchener, Ont., Canada
Tang, D. T., Yorktown Heights, N. Y.
Taylor, W. E., Santa Maria, Calif.
Terry, F. R., Downey, Calif.
Thompson, B. C., Montclair, N. J.
Thomson, C. E., Shawnee Mission, Kan.
Thorgrimson, G. N., Minneapolis, Minn.
Tiffany, J. M., Winston-Salem, N.C.
Timlin, E. S., Philadelphia, Pa.
Travland, W. W., Port Arthur, Tex.
Traxler, H. A., Calgary, Alberta, Canada
Turner, D. E., Littleton, Colo.
Tyler, J. T., Belleville, Nev.
Vahle, R. W., Kokomo, Ind.
Valitski, W. F., Philadelphia, Pa.
Van Koevering, B. D., Syracuse, N. Y.
Vinokur, M., Green Bank, W. Va.
Volpe, J. R., Jr., Ozone Park, L. I., N. Y.
Wagner, W. K., Mountain View, Calif.
Walker, P. C., Gardena, Calif.
Wallace, M. E., Clearwater, Fla.
Waltz, R. B., Philadelphia, Pa.
Wang, G. C-C., Ellenville, N. Y.
Ward, J. R., Providence, R. I.
Waring, G. W., Palo Alto, Calif.
Weber, J. W., Raleigh, N. C.
Weinstein, A. K., Hermosa Beach, Calif.
Wernikoff, R. E., Cambridge, Mass.
Whittle, H. P., South Acton, Mass.
Whitworth, W. D., Anchorage, Alaska
Wignall, J. R., Lincoln, Neb.
Wilcox, D. L., Richardson, Tex.
Wilken, A. C., Albuquerque, N. M.
Wilhelmd, G. E., Los Angeles, Calif.
Williams, F. R., Redstone Arsenal, Ala.
Williams, R. O., Chicago, Ill.
Willis, C. E., Englewood, Colo.
Winacott, E. L., Ottawa, Ont., Canada
Wiseman, D. G., Greensboro, N. C.
Wisner, D. A., North Adams, Mich.
Wojcik, M. H., Garfield, N. J.
Wootten, E. J., Thistletown, Ont., Canada
Woythal, J. M., Arlington, Va.
Yuen, R., Canoga Park, Calif.
Zimmerman, H. A., Albany, Calif.
Zmuda, E. L., Emporium, Pa.
Zuk, P., Rexdale, Ont., Canada

Admission to Associate

Austin, C. L., St. Paul, Minn.
Barnes, R. B., Lexington, Mass.
Bikis, A., Rome, N. Y.
Bixby, B. S., Waltham, Mass.
Boyce, W. E., Plainfield, N. J.
Broecker, K. M. R., Berkley, Mich.
Burr, J. K., III, Baltimore, Md.
Chester, S. R., Toronto, Ont., Canada
Coyne, B. D., Scarborough, Ont., Canada
Crocker, C. W., Houston, Tex.
Darcus, R. J., Victoria, B. C., Canada
DeVerter, W. G., Chicago, Ill.
Duell, A. N., Denham, Bucks, England
Eleovsson, K. S., Solna 1, Sweden
Evans, D. D., Stockton, Calif.
Feeney, W. R., Utica, N. Y.
Frame, W. W., Michigan City, Ind.
Granese, D. G., Garden City, L. I., N. Y.
Guiducci, G., Milan, Italy
Harris, M. E., Lewisburg, Pa.
Hayes, R., Vancouver, B. C., Canada
Heberlein, D. G., Madison Heights, Mich.
Henderson, D. E., Cleveland, Ohio
Honeycutt, J. C., Jr., Las Vegas, Nev.
Hope, J. N., San Diego, Calif.
Horvat, J. R., Wickliffe, Ohio
Hyman, S. P., Milwaukee, Wis.
Jackson, L. A., Dayton, Ohio
Jackson, O., Fort Huachuca, Ariz.
Kaufmann, P., Sao Paulo, S. P., Brazil
Keil, R. A., Flushing, L. I., N. Y.
Kemp, E. J. C., Vancouver, B. C., Canada
Lackey, M. L., APO 23, New York, N. Y.
LaGrange, D. L., Biloxi, Miss.
Lamparero, F. A., Panama, Rep. de Panama
Looram, J. J., Massapequa, L. I., N. Y.
Moffatt, J. E., Rockford, Ill.
Nicoletti, R. J., Buffalo, N. Y.
Nite, J., Orlando, Fla.
Noah, A. S., Mattapan, Mass.
Purinton, R. L., Byfield, Mass.
Reynolds, E. E., Dayton, Ohio
Riquelmy, A. H., Houston, Tex.
Rivara, L., Torino, Italy
Robison, M. M., Worthington, Ohio
Ross, F. R., Phoenixville, Pa.
Rowe, A. C., Schenectady, N. Y.
Ryan, J. F., Jr., Utica, N. Y.
Schmit, C. M., Milwaukee, Wis.
Schrager, S., Philadelphia, Pa.
Seo, W. Y., Seoul, Korea
Sicker, M., Flushing, L. I., N. Y.
Siering, W. G., Cedar Grove, N. J.
Smith, A. A., Los Angeles, Calif.
Stewart, A. G., Victoria, B. C., Canada
Storm, R. L., Chatsworth, Calif.
Suloway, N. S., Northlake, Ill.
Szymanowski, H. W., Karthaus, Pa.
Trapper, R. P., Chicago, Ill.
Utt, C. J., Jr., Lanham, Md.
Uyechi, S. T., Southgate, Calif.
Votava, J. M., Elgin, Ill.
Werner, R. G., Syracuse, N. Y.
Willey, J. A., Monrovia, Calif.
Williams, G. V., Auburn, N. Y.

Section Meetings

ALAMOGORDO-HOLLOMAN

"Optical Laser Research at Hughes Research Laboratories," I. J. D'Haenens, Hughes Res. Labs. 1/24/61.

ALBUQUERQUE-LOS ALAMOS

"Distance Measuring Equipment and Use of Satellites for Mapping," Tom Witowski, Cubic Corp. 1/24/61.

ANCHORAGE

"Radio & Radar-controlled Traffic Light System in Anchorage," Dave Fulton, City of Anchorage. Joint meeting with AIEE. 1/19/61.

ATLANTA

"Quantized Frequency Modulation," W. B. Jones, Jr., Ga. Tech. 1/27/61.

BAY OF QUINTE

"Microwave Ferrites," E. G. Spencer, Bell Tel. Lab., Inc. 1/18/61.

BUFFALO-NIAGARA

"Fundamentals of Television Tape Recording," J. W. Wentworth, RCA. 1/10/61.

"World-Wide Communications Via Artificial Earth Satellites, Passive & Active," J. D. Tebo, Bell Labs., Joint meeting IRE-AIEE. 2/2/61.

CENTRAL FLORIDA

"The Bio-Medical Dilemma of Man & Outer Space," Lt. Col. Rosa, USAF. 1/21/61.

CHINA LAKE

"Systems Applications of Masers," F. E. Goodwin, Hughes Res. Labs. 10/20/60.

(Continued on page 130A)

Programming

Customer Training

Career Opportunities in Computer Marketing

Management Seminars

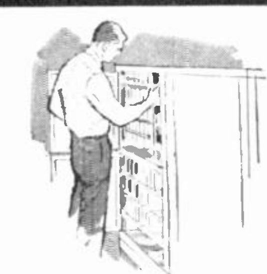

Installation and Maintenance

The widespread acceptance of the PHILCO 2000 Data Processing System continues to open up new opportunities for experienced computer marketing personnel.

Sales offices throughout the United States are now expanding. Home office staffs are being enlarged. The opportunity for experienced people has never been greater. Candidates showing managerial interest and ability will be considered for supervisory positions.

This is the time to join the nation's fastest growing computer marketing organization. There are openings for:

SALES REPRESENTATIVES who are experienced in the preparation of presentations to top management groups and who have established a record of success in data processing sales.

SYSTEMS ANALYSTS experienced in the study of customer's problems and individual data processing needs who can suggest economical and practical systems configurations for a particular application.

PROGRAMMERS experienced in scientific, business and commercial programming who can provide on-site assistance to customers.

EDUCATIONAL SPECIALISTS who can develop comprehensive courses to train personnel for the optimum performance of a data processing system.

INSTALLATION and MAINTENANCE ENGINEERS experienced in all phases of installation, start-up and continued maintenance of transistorized large scale data processing equipment.

PUBLICATIONS SPECIALISTS who can prepare technical sales bulletins, instruction manuals, reports and other material on the subject of electronic data processing.

CONTACT
Mr. John Felos
Professional Placement Mgr.
PHILCO/COMPUTER DIV.
Willow Grove, Pa.

PHILCO®

Famous for Quality the World Over

Section Meetings

(Continued from page 128A)

Cincinnati

"FM Multiplexing for Stereo," E. S. Miller, Sherwood Electronics Labs., Inc. 1/17/'61.

Cleveland

"Listening & Looking in Space," R. E. Anderson, GE Co. 1/19/61.

"Stereophonic AM Broadcasting," A.A. Goldberg, CBS Labs. 2/9/61.

Colombia

"Long Distance Telephone Communications in Colombia," S. Albornoz P., National Telecom. Co. 1/27/61.

"Communication by Tropospheric Scattering," Lt. Col. A. Ospina T., Colombian Navy. 2/6/61.

Columbus

"Plasma Dynamics," G. I. Cohn, Illinois Inst. of Tech. 1/10/61.

Dallas

"The IRE," Dr. L. V. Berkner, IRE President. 1/25/61.

"Space Communications," G. E. Mueller, Space Technology Labs. Inc. 2/2/61.

"Lightweight Irertial Navigation Systems," S. S. Kolodkin, RCA. 2/9/61.

"The New York UHF Project," E. W. Allen, FCC. 2/14/61.

"Development of An Active Communications Satellite," Don Culler, ITT Labs. 2/16/'61.

Denver

"Magneto Hydrodynamics," J. F. Young, GE Co., Joint IRE-AIEE meeting. 10/14/60.

"Frequency & Time Standards & Their Distribution," A. H. Morgan, Radio Broadcast Service, Joint meeting IRE-AIEE. 11/18/60.

"Insertion Loss & Power Measurements at Microwave Frequencies," A. L. Hedrich, Weinschel Engrg. & Mfg. Corp. 12/15/60.

"Electrical & Electronic Applications of Ceramics," Messrs. C. Hageman, R. Whiting, L. Ferreira, Coors Porcelain Co., Joint meeting IRE-AIEE. 2/10/61.

El Paso

Technical films presented by Bell Tel. Labs. & Western Elec. Co. 1/26/61.

Emporium

"Future Planning of Radio Tube Operations," R. P. Clausen, Sylvania Elec. Products Inc. 1/17/61.

Erie

"Transistorized Voltage Control Regulator for Distribution Transformers," J. J. Astleford, Jr., Westinghouse Elec. Corp. 10/19/60.

"Measurements in the 3¾ IPS Quarter Track Audio Tape Recording System," A. R. Keskinen, Astatic Corp. 12/6/60.

Evansville-Owensboro

"A Television Stereophonic System," R. B. Dome, GE Co. 11/14/60.

"Engineering Management Problems in South America," R. D. Chipp, ITT. 12/14/60.

"Nuclear Reactor Startup," A. Hurst, Argonne National Lab. 1/11/61.

Florida West Coast

"A Thermoelectric Omnibus," W. G. Evans, Westinghouse Elec. Corp., Joint meeting IRE-AIEE. 1/18/61.

Fort Huachuca

"Electronics is a Generic Art," D. E. Noble, Motorola, Inc., Presentation of Fellow Award 2/3/61.

Hawaii

"The KHVH-TV Mobile Unit," Dan Hunter, KHVH-TV. 9/14/60.

"Masers, Theory & Applications," William Pong, Univ. of Hawaii. 10/12/60.

"The Pacific Missile Range," C. H. Wehmeyer, Pacific Missile Range. 11/9/60.

"The GPL 1000-Line Closed-Circuit Television System," G. D. Brill, General Precision Labs. 1/11/61.

Houston

"Impressions of Soviet Work," R. L. Petritz, Central Res. Labs. 1/17/61.

Huntsville

Stereo Talk & Demonstration, Donald Biltucci: Hornbuckle Record Ship, Joint meeting IRE-AIEE. 12/12/60.

Indianapolis

"Trends in Automatic Missile Checkout Equipment," W. F. McWhorter, Bendix Corp. 1/26/61.

Israel

"A Transistorized Private Telephone Exchange," Israel Paz, Ministry of Defense. 12/28/60.

Ithaca

"The Perceptron—A Device for Explaining Brain Functions," H. D. Block, Cornell Univ. 12/19/60.

"Coherent Optical Computing," L. J. Cutrona, Univ. of Michigan. 2/2/61.

Kansas City

"Bionics," J. E. Steele, Wright Air Dev. Div. 1/10/61.

Kitchener-Waterloo

"Cryogenics," C. C. Lim, Univ. of Waterloo. 1/16/61.

Las Vegas

"Power System Design & Operation," C. L. Ryan, Southern Nevada Power Co. 1/16/61.

Little Rock

"Technical Operation of TV Broadcasting," L. C. Smith, KARK TV. 1/16/61.

London (Canada)

"Masterminds at Work," A. E. Smith, Bell Tel. Co. 10/25/60.

Long Island

"What is Operations Research," George Kimble, A. D. Little, Inc. 10/27/60.

"Applications to Traffic Flow Analysis," Leslie Edie, Port of N. Y. Authority. 11/3/60.

"Management Gaming Technique," C. J. Cratt, Peat-Marwick-Mitchel & Co. 11/10/60.

"Development of Mathematical Models," Joseph Fischback, Fischback & McCoach Assocs. 11/17/60.

"Probability Forecasting in Business Problems," David Hertz, Arthur Anderson Co. 12/1/60.

"Management Problems in Small Companies," S. Dubin, Telechrome Mfg. Co., R. S. Marston, Crosby Telectronics Corp., A. Dorne, Dorne & Margolin, Inc. 12/20/60.

Los Angeles

"Strategy of Conflict," T. C. Schelling, Harvard Univ. 1/17/61.

Lubbock

"Electronics in the Oil Industry," Bare Hollingsworth, Pan American Pet. Co. 1/17/61.

Miami

"The Atlantic Missile Range & Its Mission," R. A. Fox, PAA. 1/20/61.

(Continued on page 132A)

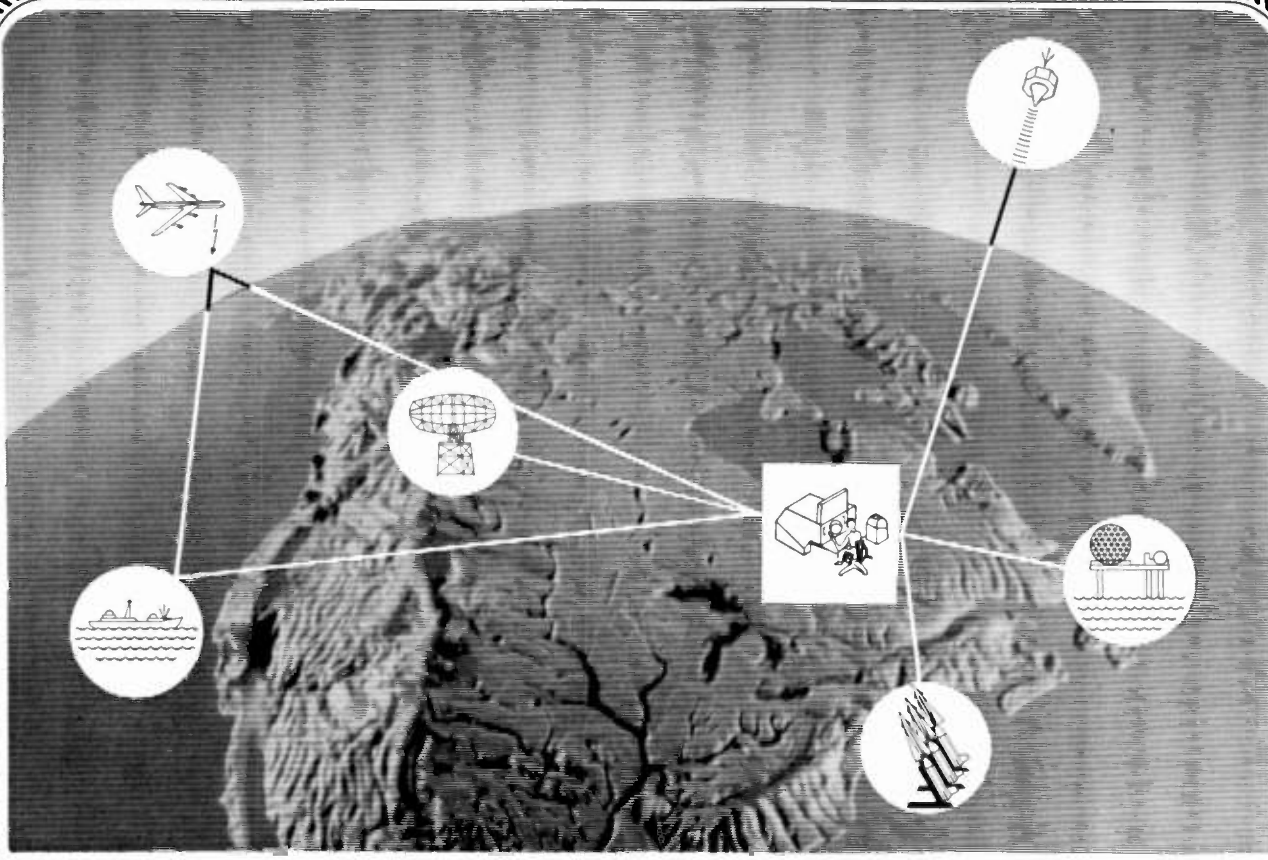

New Frontiers in System Engineering at

THE MITRE CORPORATION

"SYSTEM" has become a much-used term in engineering. It is all things to all men. It may be a simple circuit, an automatic control, a computer or a complex world-wide system such as the command and control system of the Strategic Air Command. MITRE works in all of these areas within a total system context.

- **An oversea theatre tactical air weapons control and warning system**
- **Extension of DEWline**
- **SAGE Air Defense System**
- **NORAD Combat Operations Center**
- **Weather Observation and Forecasting — a global semi-automatic electronic system**

As Technical Advisor to the United States Government – notably the Air Force Command and Control Development Division – MITRE is engaged in system analysis, broad conceptual design and inter-system integration for such command and control programs as:

- **Intelligence Data Handling System — high-speed processing of world-wide information**
- **Strategic Air Command and Control System**
- **Electromagnetic Intelligence System — a world-wide system**

In conjunction with its system work, MITRE conducts a vigorous program of electronic research and experimentation in system engineering technology. Outstanding engineers and scientists interested in working on problems vital to the nation and its security are invited to direct inquiries in confidence.

Openings are also available at MITRE's facilities in Montgomery, Alabama and Fort Walton Beach, Florida

Write to Vice President — Technical Operations

THE MITRE CORPORATION

Post Office Box 208, 4-MR—Bedford, Massachusetts

Section Meetings

(Continued from page 130A)

MILWAUKEE

"Radio Engineering In Controlled Fusion Research," W. W. Salisbury, Varo Mfg. Co. 1/16/61.

NEW YORK

"The Role of Electronics in Highways & Autos of the Future," Jerome Fine, Columbia Teachers College, George Gray, RCA Labs. 10/5/60.

"RFI Measurement Techniques," Panel Discussion by: Bernard Rosen, Leonard Milton, John Chappell, Albert Kall, Polarad Electronics, Filtron Co. 11/2/60.

"Value Engineering in Practice," Marvin Kaplan, Loral Electronics Corp.; "Yardstick Techniques for Optimum Weight Volume & Mechanical Reliability," David Ehrenpreis, Consulting Engineer. 12/7/60.

"Professional Responsibilities of the IRE," Dr. L. V. Berkner, IRE President. 1/11/61.

NORTH CAROLINA

"Nike Zeus," C. P. Smith, Western Elec. Co., Inc. 1/20/61.

NORTHERN ALBERTA

Film: "High Speed Flight." 1/17/61.

NORTHERN NEW JERSEY

"Electroluminescent Devices," I. D. Greenberg, Sylvania Elec. Products. 1/11/61.

OMAHA-LINCOLN

"Navy Missile Development at Cape Canaveral," R. F. Sellars, U. S. Navy, Joint meeting with ECO. 1/18/61.

"Fifty Years of Progress in Electronics—Tubes VS Transistors," R. E. Moe, Regional Director of Region 5; Student Award presentations. 2/6/61.

ORLANDO

"Optically Pumped Masers," R. Johnson and A. Sheppard, The Martin Co. 1/18/61.

OTTAWA

"HF Communication Network for Project Mercury," Michael Yurko, Technical Materiel Corp. 1/5/61.

PHILADELPHIA

"The Future, Static or Dynamic," Panel of Editors: Messrs. Kramer, Chilton, Cannah, Hochgesang, Miller, MacDonald, McGraw Hill Publishing Co., Joint meeting IRE-AIEE. 1/23/61.

PITTSBURGH

Two Films by Bell Labs.—"Project Echo & Passive Satellite," Joint meeting IRE-AIEE. 11/1/60.

"Moscow Automatic Control Congress," Dick Dicker, Westinghouse Elec. Corp., Tom Schuerger, U. S. Steel Applied Res. 11/14/60.

"Superconductivity, Properties & Application," D. L. Feucht, Carnegie Inst. of Tech. 12/12/60.

"Learning Theory, The Teaching Machine, & Education for the Engineering Profession," E. M. Williams, Carnegie Inst. of Tech. 1/16/61.

PRINCETON

"Communication Satellites," J. R. Pierce, Bell Tel. Labs. 1/12/61.

QUEBEC

"The Measurement of Major Atmospheric Constituent Concentrations in the 100 Km Region by a Chemical Seeding Technique," G. B. Spindler, CARDE. 1/27/61.

ROCHESTER

"Research Problems in Undersea Warfare," F. A. Parker, U. S. Dept. of Defense. 1/19/61.

ROME-UTICA

"Non-Linear Modeling," K. F. Siegel, Univ. of Michigan. 1/17/61.

SACRAMENTO

"Selection of Computers for Instruction & Engineering," William Lane, Chico State College. 1/14/61.

SALT LAKE CITY

"A Tunnel Diode Square Wave Generator," J. E. Dalley, Univ. of Utah. 1/12/61.

SAN ANTONIO-AUSTIN

"IBM Random Access Method of Accounting," Glen Countryman, IBM. 1/20/61.

Presentation of Fellow IRE Awards to C. L. Jeffers, A. H. LaGrone by A. W. Straiton, Univ. of Texas; "Contrast in Culture," W. W. Hagerty, Univ. of Texas. 2/3/61.

SAN DIEGO

"Inter-action of a Plasma With an Electro Magnetic Wave," R. S. Elliott, UCLA. 11/2/60.

"Unmanned Exploration of the Moon," Jim Burke, Jet Prop Lab.; Installation of Officers. 1/4/61.

"Automatic Drafting—A New Engineering Technique," E. F. Myers, General Dynamics Electronics. 2/1/61.

SHREVEPORT

Talks by Mrs. Almeada Dorman, Continental Baking Co. & E. D. Nuttall, United Gas Corp. 2/7/61.

SOUTHERN ALBERTA

"The Aurora," B. W. Currie, Univ. of Saskatchewan; Joint meeting IRE, Alberta Society of Petroleum Geologists & Canadian Society of Exploration Geophysicists. 10/25/60.

"The Principles & Applications of the Electron Microscope," C. E. Challice, Univ. of Alberta. 11/28/60.

SYRACUSE

"The IRE, Present and Future," Dr. L. V. Berkner, IRE President; Fellow Award Presentation. 1/17/61.

TOKYO

"Glorious Future Development of Electrical Communications," H. S. Osborne, ITT Labs. 9/22/60.

"Era of Data Communications," G. W. Gilman, Bell Telephone Lab. 11/9/60.

"Electronic Navigation in the Future," A. G. Kandolian, ITT. 11/21/60.

Talks on Recent Trips by: H. Shinkawa, S. Okamura, O. Nishino, M. Terao, T. Osatake and K. Iwama. 1/10/61.

TORONTO

"Lecture Demonstration on IBM 1620 Solid State Engineering & Scientific Computer," John Buck, IBM. 1/16/61.

Tour of the new Technology building at Ryerson Institute. 1/31/61.

Annual Students' Night (IRE-AIEE Student Branch of Univ. of Toronto and Student Associate Branch of Ryerson Inst.) 2/16/61.

TUCSON

"Sensitivity of Ranking to Waiting," R. E. Frese, USAEPG. 11/23/60.

"Television in Astronomy," Dr. Livingston, Kitt Peak National Observatory. 12/14/60.

"Epitaxial Mesa Transistors," H. C. Knowles, Motorola, Inc. 1/25/61.

(Continued on page 134A)


important openings for senior
E.E.'s and Physicists
to assume responsibility
for development of
new
infrared
search
systems

Section Meetings

(Continued from page 132A)

TULSA

Tour of FAA Facilities. 11/14/60.

"A Telemetric System for Gathering Physiological Data From Humans Under Various Stresses," M. C. Oviatt, FAA Aeromedical Res. Labs. 1/19/61.

TWIN CITIES

"Aspects of the Man in Space Program," Richard Plaisted, Minneapolis Honeywell Regulator Co. 9/7/60.

"National IRE Organization Status," R. L. McFarlan, Past IRE President; "The Need for a Technical Research Institute in the Twin Cities Area," B. C. Smith, Midwest Technical Dev. Corp. 10/20/60.

VANCOUVER

"Some Practical Aspects of Electronic Components," C. R. Williams, B. C. Tel. Co. 1/16/61.

WASHINGTON

"MOBOT—Complex of Control Functions," J. W. Clark, Hughes Aircraft Co. 1/9/61.

WILLIAMSPORT

"Air Traffic Control," K. E. Landis, FAA 11/31/60.

"Trends in Solid State Physics with Emphasis on Present, Past & Coming Decades," Carl Volts, Pa. State Univ. 2/6/61.

SUBSECTIONS

LEHIGH VALLEY

"The Application of Plasma Pinch Engines to Space Travel," Irving Granet, Republic Aviation Corp.; Presentation of Fellow Award. 1/11/61.

MERRIMACK VALLEY

"Generation, Transmission & Use of Microwave Energy for Power Purposes," W. C. Brown, Raytheon Co. 1/16/61.

"Engineering Trends & Applications Resulting From Recent Solid State Developments," H. A. Stone, Jr., Bell Labs. 2/6/61.

MONMOUTH

"Communications Engineering for BMEWS," F. J. Skinner, Western Elec. Co. 1/18/61.

NEW HAMPSHIRE

"Electronically Steered Radars," John Allen, MIT Lincoln Lab. 1/24/61.

ORANGE BELT

"Low Noise Traveling-Wave Tubes," D. A. Watkins, Watkins Johnson Co.; "Linear Phase Response in Modern Microwave Systems," Seymore Cohn, Rantec Corp. 1/26/61.

PASADENA

"The Electronic Unknowns of Chemical Engineering," G. N. Richter, Calif. Inst. of Tech. 1/19/61.

PIKES PEAK

"Space Mechanics," Robert Collier, USAF Academy. 1/11/61.

SAN FERNANDO VALLEY

"Challenge to American Management," J. R. Van de Water, UCLA. 1/10/61.

SANTA ANA

"Strategy of Conflict," T. C. Schelling, Harvard Univ. 1/17/61.

SANTA BARBARA

"Acoustics & Mechanics in HiFi," Gordon Mercer, Audio-Vision Co. 1/17/61.

WESTCHESTER

"Aspects of the Root Locus Methods," Charles Rehberg, New York Univ. 1/25/61.

"Limitations of Science," Pollykarp Kusch, Columbia Univ.; Presentation of Fellow Award. 2/10/61.

WESTERN NORTH CAROLINA

"Direct Distance Dialing," Charles Jones, Southern Bell Tel. & Tel. Co. 1/27/61.

NEWS New Products

These manufacturers have invited PROCEEDINGS readers to write for literature and further technical information. Please mention your IRE affiliation.

Computer Components

Electronic Associates, Inc., Long Branch, N. J., is now offering a transistorized, "do-it-yourself" special purpose analog computer that will perform a variety of laboratory, engineering and process control computing tasks.

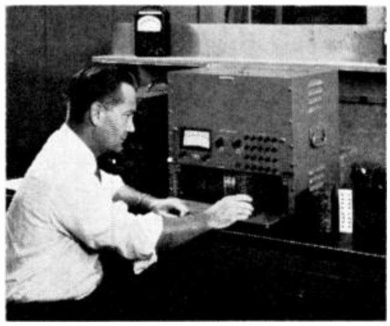

The introduction of the TR-5 Mounting Unit makes it possible for special purpose analog computers to be assembled without the problems usually associated with such a project. The PACE solid state analog computing components plug into the TR-5 mounting unit where they may be interconnected according to the computing function to be performed.

The mounting unit contains all the controls necessary to operate a 20-amplifier computer. The basic unit will house up to six computing components and a fully-transistorized power supply. It may be expanded by adding up to two expansion units to the basic rack.

One expansion unit, the TR-5-1, is prewired to accept an additional five dual transistorized amplifiers. Additional space is available, but not wired, for five more dual modules or ten single modules for the addition of assorted linear or nonlinear computing components. Both expansion units are powered from the power supply located in the basic TR-5 mounting unit.

(Continued on page 136A)

NEWS New Products

These manufacturers have invited PROCEEDINGS readers to write for literature and further technical information. Please mention your IRE affiliation.

(Continued from page 134A)

Automatic Timer

Automatic cycling between high and low temperatures with any precision series delta temperature chamber is now achieved by the new MR-1 Timer, introduced by **Delta Design, Inc.,** 7460 Girard Ave., La Jolla, Calif. Range of these chambers is −100°F to +500°F, and accuracy is ±½°F. Used with the MR-1, fast response Model 1060RF Chamber can complete a cycle in 12 minutes total time.

Individual high and low temperature timer adjustments allow independent time durations of up to 3 hours each for any pair of pre-selected high and low temperatures. A selector switch permits timed intervals to include only the constant-temperature time or to include the transition times as well. A master timer either will permit cycling indefinitely or will stop the cycling after any period up to 24 hours.

The Model MR-1 Timer is packaged for rack or bench mounting and measures $19 \times 3\frac{1}{2} \times 3\frac{1}{2}$ inches.

For further information write to the firm.

Electro-Mechanical Names Brown and Klibaner

Alan M. Brown has been named president and Bernard Klibaner vice president in charge of engineering and manufacturing of the **Electro-Mechanical Corp.,** Town Dock Rd., New Rochelle, N. Y. This firm is a manufacturer of precision electronic equipment.

KLIBANER

BROWN

(Continued on page 138A)

NEWS New Products

These manufacturers have invited PROCEEDINGS readers to write for literature and further technical information. Please mention your IRE affiliation.

(Continued from page 136A)

Brown has held various executive positions for the past nine years at Adler Electronics including Director of Purchasing, sales, and contract administration.

Klibaner was formerly supervisor of manufacturing engineering for Adler Electronics and chief mechanical engineer for C.B.S. Laboratories and C.B.S.—Columbia, Division of Columbia Broadcasting System.

In addition to their executive duties, Klibaner will be responsible for manufacturing and engineering and Mr. Brown for marketing and sales.

Ceramic-Metal Thyratron

Designed by **Edgerton, Germeshausen & Grier, Inc.,** 160 Brookline Ave., Boston 15, Mass., for radar modulator packages, the 7621/HY-2 hydrogen thyratron is equipped with a cathode flange to facilitate mounting and through-hole tabs to which filament and grid connections are made. Flexible wire leads and separate mounting sockets are eliminated.

The new thyratron is capable of switching 350 kw peak power after a 30-second filament warm-up time. Operation at 125° ambient temperature is possible without forced cooling when the tube is operated at its maximum plate dissipation factor (P_b) of 2.7×10^9. A hydrogen reservoir, connected internally across the cathode filament, increases tube life.

The 7621/HY-2 withstands shocks of 200 g at 11 ms duration and vibration from 0 to 2000 cps at 20 g. These tubes may be used as replacements for or in new applications specifying conventional 1258, 3C45 or 4C35 glass envelope tubes with considerable savings in weight and size for airborne and shipboard applications as well as ground-based equipment.

Complete specifications are available from Applications Engineering Group N.T.

Use Your IRE DIRECTORY! It's Valuable

Switches

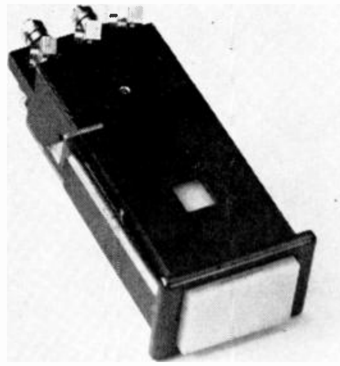

Truco Engineering Co., 289 Fairfield Ave., Hartford 6, Conn., offers a new design in snap action push button switches. They are available in both illuminated and non-illuminated versions. Of one piece construction these switches are available in either momentary or alternate action configurations. This design eliminates the need for external accessories. The mounting arrangement allows rigid mounting in virtually any panel thickness. Available configurations include 1 or 2 SPDT switches with ratings of 5 amperes at 220 volts ac and 0.25 amperes at 220 volts dc. All switches are rated at one million operations. Prices range from $7.55 to $9.00 in unit quantities.

Please refer all inquiries to the firm.

Rutherford Appoints Griggs

Charles E. Rutherford, president of **Rutherford Electronics Co.,** 8944 Lindblade St., Culver City, Calif., recently announced the addition of the new communications division.

John R. Griggs, former president and chief engineer of Transpace, Inc., San Fernando and Northridge, has been selected to supervise the engineering of this new division. Griggs' background also includes Packard Bell Electronics Corp., Enright Engineering Co., Hoffman Laboratories and Convair, San Diego.

Since 1952, the firm has been actively engaged in the field of pulse instrumentation and pulse technique. The communications division will introduce as its first product the "400," a two-way, citizens' band radiophone.

Voltage To Digital Converter

A new high-speed, multichannel voltage to digital converter is available from **the Link Division, General Precision, Inc.,** Binghamton, N. Y. This precision multiplex converter maximizes conversion ac-

(Continued on page 140A)

America's FIRST man into space will rely on a Honeywell designed and developed Attitude Stabilization and Control System for controlling his space capsule. This system automatically damps out initial launch rates, orients and maintains the capsule in proper orbital plane, and provides for the correct descent trajectory and re-entry angle. This device is just one of the many contributions being made by Honeywell scientists and engineers to our nation's space programs.

Honeywell

Military Products Group

SCIENTISTS, ENGINEERS

Increased activity in the design and development of advanced stabilization and reference systems has created these select, high-level professional openings in the Aero Division of the Honeywell Military Products Group.

Senior Development Engineer—3 to 5 years' experience in Electro-Optical Development Design of unique optical pick-offs and their application to advanced inertial instruments.

Senior Development and Analysis Engineer—Experienced and proficient in complex servo-analysis with related circuitry development. Also development engineers with supplementary experience such as transistor circuitry related to servo-mechanisms.

Gimbal Servo Design Engineers—Experience in design and development of platform type servos with gearless torque motors; familiar with transistor circuitry.

Senior Development Engineer for Gimbal Transmitters—Experienced in servo-design high-accuracy repeater systems, with specific experience on precision resolvers and inductosyns.

Senior Systems Development Engineer—Experience in electronic systems and sub-systems. Capable of translating requirements into block diagrams and block diagrams into circuits.

Senior Mechanical Development Engineer—Experienced in electromechanical design with gyro or platform design and analysis.

Send your résumé stating your areas of interest, or request for further information to: Mr. Clyde W. Hansen, Technical Director, Aeronautical Division, 2626 Ridgway Road, Minneapolis 40, Minnesota.

To explore professional opportunities in other Honeywell operations, coast to coast, send your application in confidence to: Mr. H. D. Eckstrom, Honeywell, Minneapolis 8, Minnesota.

NEWS New Products

These manufacturers have invited PROCEEDINGS readers to write for literature and further technical information. Please mention your IRE affiliation.

(Continued from page 138A)

curacy through the incorporation of advanced error and drift correction schemes.

The unit is completely transistorized, with commutation and conversion loops combined into one system for increased reliability and compactness.

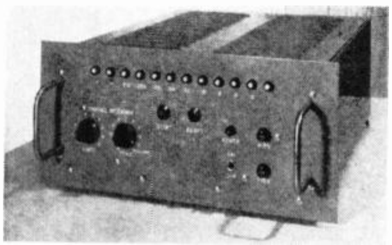

Advanced design features and integration techniques employed provide for a low cost per conversion channel, without limiting the possibilities for channel expansion or multiple operation modes. The unit is of modular design, utilizing standard printed circuit cards. This feature insures maximum flexibility and minimum maintenance costs.

The outstanding features of the converter include: automatic drift correction; integrated reference voltage supplies; incorporated visual display; no moving parts, and a minimum cost per conversion channel.

Specifications for the standard model are:

Input
- Capacity: 1 to 100 channels (500 channels optional)
- Voltage: 0 to ±10 volts

Conversion
- Format: 10 bits plus sign or 11 bits plus sign
- Code: Natural binary, binary coded decimal, or excess three
- Speed: 5 μs/bit; 60 μs/channel
- Rate: 16,667 channels/second
- Precision: 0.048%

Output
- Format: Parallel
- Voltage: −10V = "1"
  0V = "0"
- Current: 2 ma/line

Weight, 40 pounds+2 oz./channel

Size, 19 inches wide×6 31/32 inches high ×27 inches deep

Mount, Standard 19 inch relay rack or desk.

Circuit Breakers

To protect three-phase and two-phase systems, electro-magnetic circuit breakers are now available from **Airpax Electronics Inc.**, Cambridge Div., Cambridge, Md., in gang assemblies. Series 600 and Series 700 explosion proof breakers provide maximum protection in these critical applications. Units are hermetically sealed, withstand 50G shock and operate from −55°C to +100°C. All types have either a slow or fast time delay action. Instantaneous acting units can also be supplied for these gang assemblies.

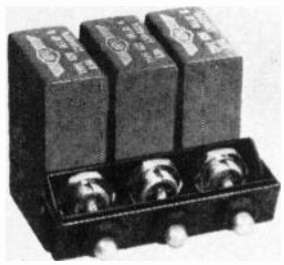

Characteristics are as follows: Continuous duty ratings from 50 milliamperes to 15 amperes. Contacts are rated for 50 dc volts or 120 rms volts at 60 or 400 cps. Operational life is at least 10,000 operations, at rated current.

Delivery is from stock. Price on request. For further information contact W. D. Heisler, sales manager.

(Continued on page 142A)

NEWS New Products

These manufacturers have invited PROCEEDINGS readers to write for literature and further technical information. Please mention your IRE affiliation.

(Continued from page 140A)

Strain Gage Plotters

A new line of Model 114 strain gage plotters, available for immediate delivery from stock, has been announced by **Gilmore Industries, Inc.,** 13015 Woodland Ave., Cleveland 20, Ohio.

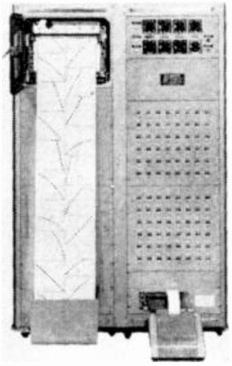

The Model 114 is a multi-channel recording and plotting instrument for strain gage use, available with 48 or 96 channels. It requires no manual plotting or reading, automatically records data in visual form for immediate evaluations. Other features include 3 zero positions per channel, individual graphs for each channel, individual channel lights and a portable motor-driven zero balance gun.

According to the manufacturer, with the 114, structural design engineers get required data while a test is in actual progress. The unit is used for static aircraft structural tests and strength tests on machinery, structures, railroads and automotive parts. A Model 114TC is also available for thermocouple or millivoltage use and the manufacturer offers custom models with speeds of up to 20 channels per second.

Computer Format Recorder

Systems Division of Epsco, Inc., 275 Massachusetts Ave., Cambridge 39, Mass., offers a comprehensive eight-page brochure on its new Model S-2010, solid-state version of the well-established vacuum-tube S-2010 Computer Format Recorder. The S-2010 is described as a universal recording unit which accepts digital data from a wide variety of sources and records it on magnetic tape in digital computer format. The brochure details how the new recorder, when used in conjunction with a digital output data gathering system, automatically processes continuous data into gapped computer format magnetic tape, thereby eliminating the need for hand coding of analog test data for computer processing. Where costly computer time will be required for reprocessing raw digital data into a form suitable for computation, the S-2010 is suited to do the job at appreciable savings in cost. Input data rates are limited only by the tape writing speed of the particular computer format, and may be as high as 30,000 characters per second. The brochure discusses features, a wide variety of available options, typical configurations, and specifications. Copies available on request.

"C" Band Oscillator

The Model 151C Miniature Triode Oscillator with a power output 65 milliwatts minimum at 4200 mc, has been designed and produced by the **John Gombos Co., Inc.,** Webro Rd., Clifton, N. J. Approximately 4½ ounces in weight, this oscillator covers the range of frequencies from 4200 mc to 6000 mc in 50 mc minimum steps. Each oscillator is designed for maximum stability having temperature stability of ±10 kc/°C, minimum size, maximum output and has a vernier (50 mc) control of frequency. Only plate voltage 200 volts nominal and 6.3 volts for filaments are required, simplifying power problems.

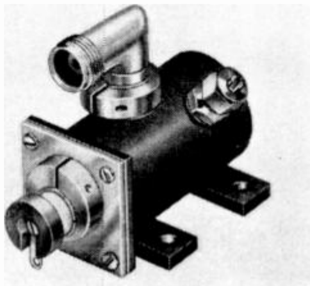

The 151C also features pre-set tuning. This tiny unit may be applied as a local oscillator, CW signal source and driver for crystal harmonic generators.

For further information write to the firm.

Logic Circuits

A basic selection of building block logic circuit packages and accessory equipment which can be used to design, test and demonstrate various logical operations is offered in kit form by **Digital Equipment Corp.,** Maynard, Mass. The new kit is suitable for educational purposes, serving both as an aid to classroom instruction and as a versatile piece of laboratory apparatus.

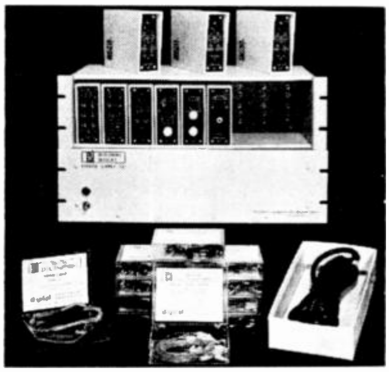

Up counters, down counters, four-bit shift registers, decimal and Gray-to-binary decoders, and two-binary-digit adders and

(Continued on page 144A)

(F101, AIR FORCE PHOTO)

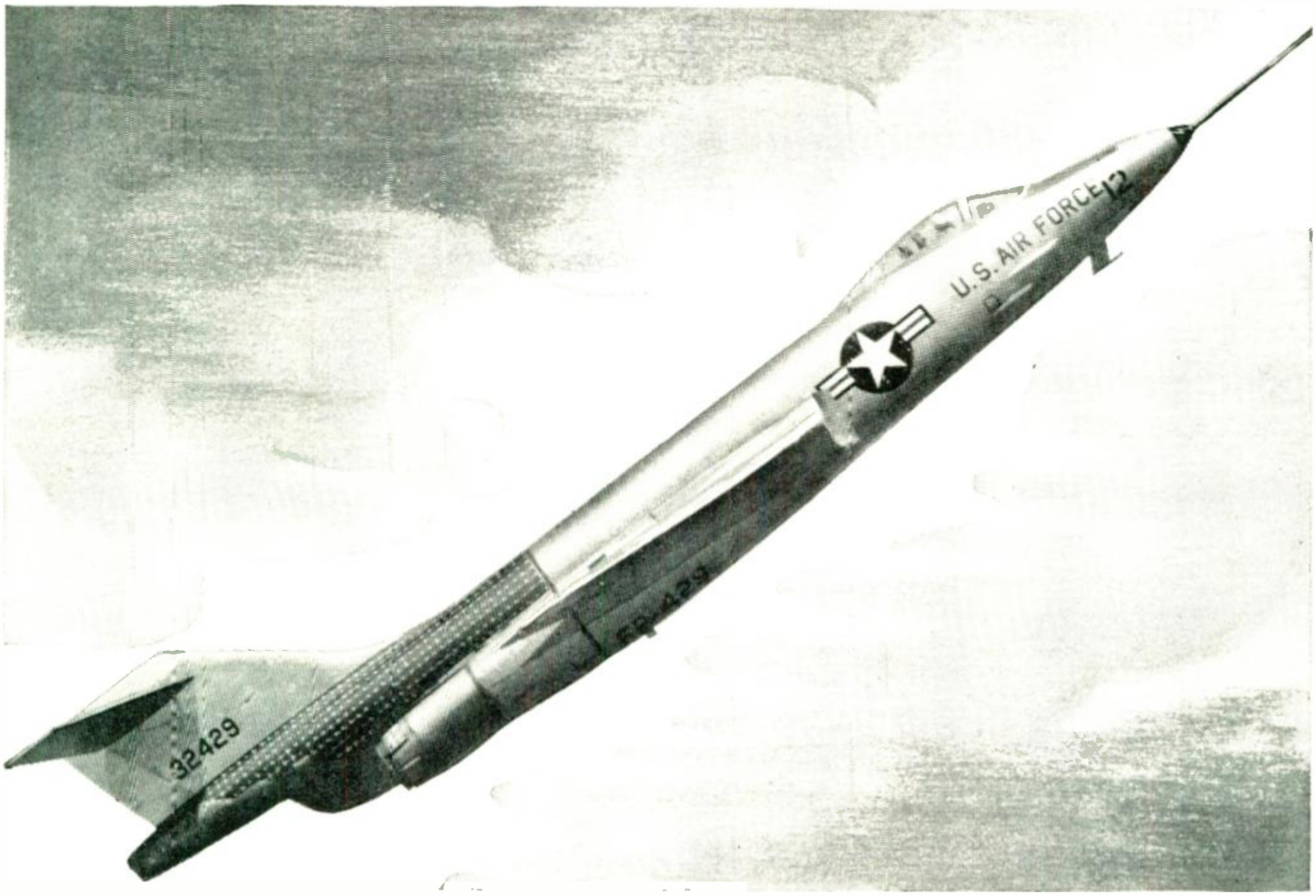

NEWS New Products

These manufacturers have invited PROCEEDINGS readers to write for literature and further technical information. Please mention your IRE affiliation.

(Continued from page 142A)

subtracters are among the numerous pieces of pulse apparatus which can be built with the interchangeable test equipment units in the logic kit. Assembly of various applications is rapid since all logical interconnections are made on the graphic front panels of the units by means of stacking banana-jack patch cords.

The logic kit consists of nine 500 kc building blocks (a logic inverter package, a dual diode nor, four flip-flops, a delay, a clock, and a pulse generator), a mounting panel, a power supply, and one hundred patch cords. It can be expanded with other units of compatible 500 kc, 5 mc and 10 mc digital test equipment.

Price of the kit is $1038, FOB Maynard, and shipments are made from stock. A technical bulletin on the kit (Bulletin E-150) and a handbook on "DEC Building Block Logic" (Bulletin A-400) are available through the sales department in Maynard, the West Coast office in Los Angeles, or representatives in major cities.

Mobile Instrument Table

The Model 73-2 instrument table, available from **Radiation Instrument Development Laboratory, Inc.,** 61 E. North Ave., Northlake, Ill., brings portability to the laboratory that uses rack mounted electronic equipment and its associated accessory instrumentation.

The mobile table has 6-inch rubber tires and will provide 24×50 inches of non-skid top space for an experimental set-up, while providing rack space for 38 vertical inches of scalers, ratemeters, assorted amplifiers and other equipment in the accessory space beneath the top.

Inside are ac service strips for plugging in as many as ten instruments. All instrument cables are tucked inside a double-doored back panel and only a power cord need be attached to a floor service or wall bracket.

Rotary Switches

Two-color, 4 page brochure from **American Solenoid Co., Inc.,** U. S. Highway 22, Union, N. J., gives detailed information on a new line of modular designed rotary switches which meet thousands of requirements at standard prices and on short deliveries. Designated as "Blue Line" switches, these units can be quickly assembled with any practical contact arrangement from modules in stock at a regional service center.

The text describes other advantages which include cam operated contacts, up to 4 isolated double-break silver-alloy contacts per stage, simple twist-to-lock bayonet principle for assembling and mounting, full insulation, and rugged construction. Switches can be supplied in current ratings from 20 to 200 amperes. Units are also HP rated for motor control.

Isolation Transformers

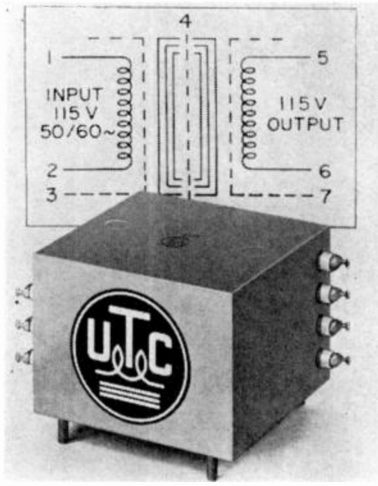

These new ultrashielded isolation transformers, a product of **United Transformer Corp.,** 150 Varick St., New York 13, N. Y., are hermetically sealed to MIL-T-27A—type TF4RX01YY—and simulate battery operation. They are designed for critical circuits requiring ultimate in isolation for power line equipment. These units are stock items and are immediately available from your local distributor. Isolation, which formerly could only be obtained from battery power, can now be realized by the use of these transformers. The effective capacity coupling between primary and secondary windings is less than 0.1 $\mu\mu$f. (Even this minute capacitance can be substantially reduced by optimum circuit design suited to the individual application.) For this purpose shields are individually terminated to allow maximum flexibility. Input and output terminals are brought out on opposite sides of a special housing in order to maintain the excellent isolation between line and load.

Silicon Diffused Junction Rectifiers

Rectified dc output currents up to 1.8 amperes per rectifier cell along with extremely low reverse leakage (500 μa at rated PRV at 150°C) are now available in a new diffused junction "top hat" rectifier series from **International Rectifier Corp.,** 1521 E. Grand Ave., El Segundo, Calif. Designated types X10B1 through X10B6,

(Continued on page 146A)

ENGINEERS, EE · ME

THE DIVERSITY OF OPPORTUNITIES OPEN AT HMED*

See where your engineering Specialty applies...

NUMBER OF OPENINGS SHOWN IN CIRCLES

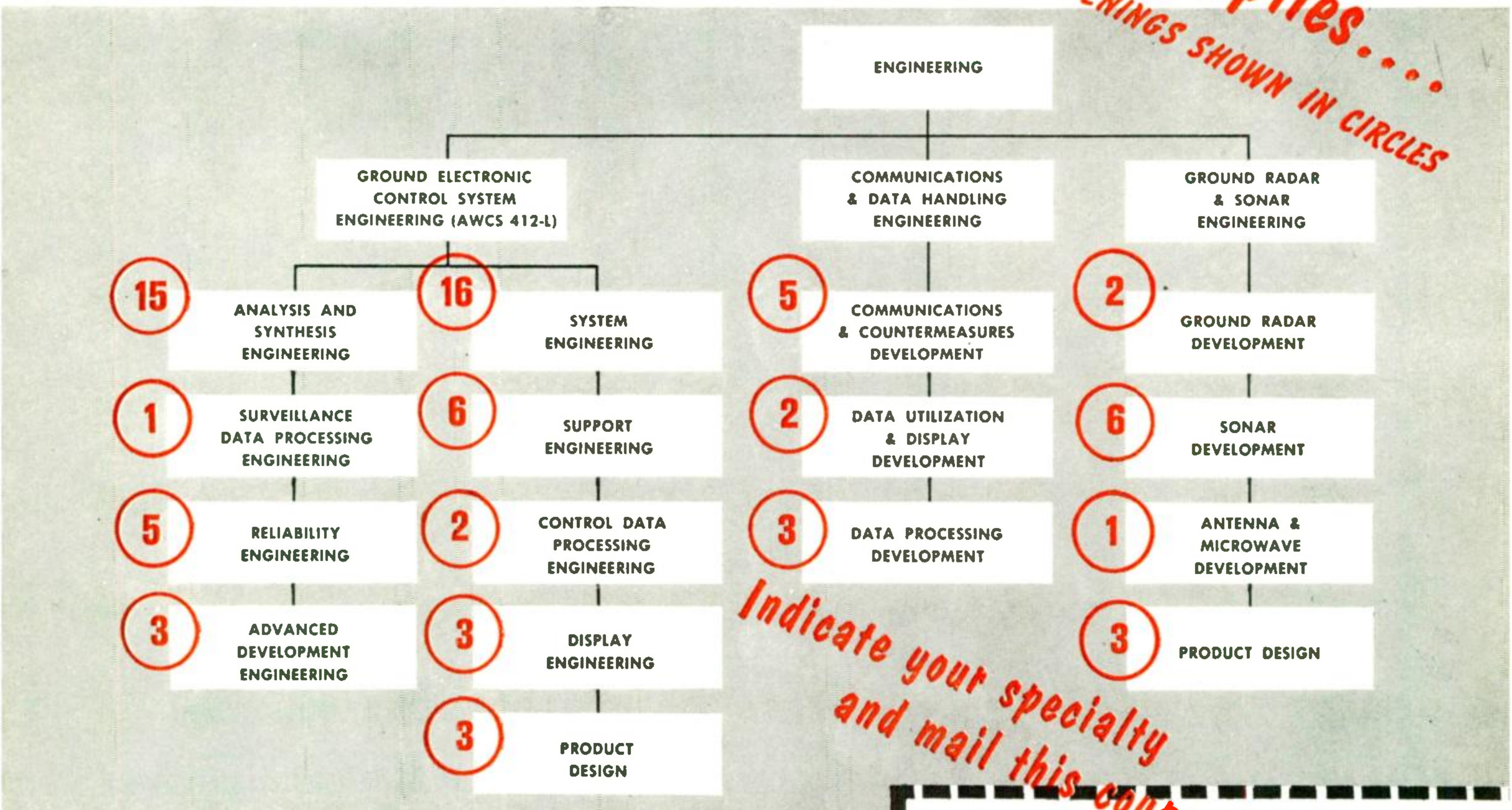

Indicate your specialty and mail this coupon!

BECAUSE OF ITS DIVERSITY OF PROJECTS, General Electric's Heavy Military Electronics Department is interested in a wide variety of engineering skills—men with many different backgrounds, specialties and talents who want to extend their technical horizons.

Primarily concerned with creating large-scale complex electronic systems, HMED currently has projects underway for all three military services—projects that range from underwater detection systems to programs in air space management and missile defense. For example, FABMDS (Field Army Ballistic Missile Defense System), the AN/SQS-26 Search Sonar System, and the 412L Air Weapons Control System.

To find out how you can further your career with HMED—an organization of growing diversity and proved stability—inquire about the excellent positions which are currently open at advanced levels of education and experience. For a fast reply, select your specialty from the chart above, and fill in the coupon at the right.

* HEAVY MILITARY ELECTRONICS DEPARTMENT

GENERAL ELECTRIC

Court Street Syracuse, N.Y.

Mr. George B. Callender, Department 53-MD
Heavy Military Electronics Department
General Electric Company
Court Street, Syracuse, New York

Please send me information about current opportunities at HMED in the area(s) of interest I have checked below.

- ☐ ANALYSIS AND SYNTHESIS ENGINEERING
- ☐ SURVEILLANCE DATA PROCESSING ENGINEERING
- ☐ RELIABILITY ENGINEERING
- ☐ ADVANCED DEVELOPMENT ENGINEERING
- ☐ SYSTEM ENGINEERING
- ☐ SUPPORT ENGINEERING
- ☐ CONTROL DATA PROCESSING ENGINEERING
- ☐ DISPLAY ENGINEERING
- ☐ PRODUCT DESIGN
- ☐ COMMUNICATIONS & COUNTERMEASURES DEVELOPMENT
- ☐ DATA UTILIZATION & DISPLAY DEVELOPMENT
- ☐ DATA PROCESSING DEVELOPMENT
- ☐ GROUND RADAR DEVELOPMENT
- ☐ SONAR DEVELOPMENT
- ☐ ANTENNA & MICROWAVE DEVELOPMENT
- ☐ PRODUCT DESIGN

Name________________________
Street________________________
City____________ State____________
Degree____________ Year____________
Experience________________________

NEWS New Products

These manufacturers have invited PROCEEDINGS readers to write for literature and further technical information. Please mention your IRE affiliation.

(Continued from page 144A)

the new series will provide forward currents up to 1.8 amperes (when mounted on heat sink) or 1.3 amperes (without heat sink in air) over a peak reverse voltage range from 100 to 600 volts.

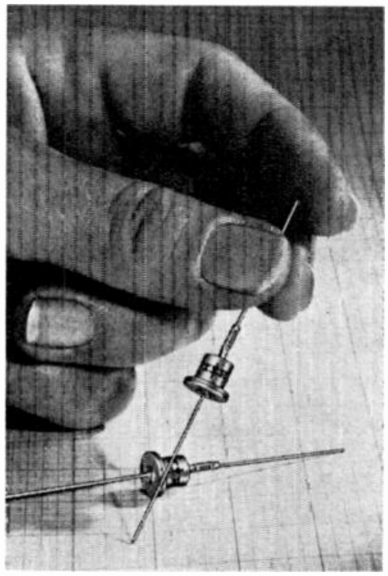

All units are suited for magnetic amplifier applications where low leakage is a design parameter. Additional characteristics include very low forward voltage drop (1.10 volts maximum at rated current at 25°C) and high surge current capabilities (40 amperes peak at 0.01 second). All types have an operating temperature range from −65°C to +175°C, and feature hermetically sealed, welded construction. Price: $.50 to $1.50 each, 1 to 99 quantity, delivery from stock. For additional data, request Bulletin XSR-217.

Custom-Made Cable Harnesses

Lowered cost, savings in weight and space are just a few of the advantages claimed for harnesses being made from MULTI-TET ribbon cables by **W. L. Gore & Associates,** 555 Paper Mill Rd., Newark, Delaware.

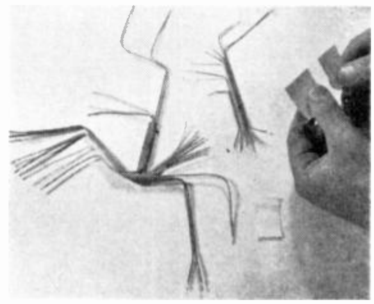

These harnesses, manufactured to customers' specifications, are insulated with

(Continued on page 148A)

These manufacturers have invited PROCEEDINGS readers to write for literature and further technical information. Please mention your IRE affiliation.

(Continued from page 146A)

Teflon. Abrasion-resistant and corona-resistant cables are also available. Since Teflon only is used in harnesses, they can be used at high temperatures and in corrosive environments. Any combination of wire sizes, conductors and color-coding is possible.

Distortion Measuring Filter

Ortho Filter Corp., a division of **Ortho Industries, Inc.,** 7 Paterson St., Paterson, N. J., manufacturers of electric wave filters, toroidal transformers, magnetic amplifiers, delay lines, equalizers and attenuators, announces that it has developed a new distortion measuring filter which, when used in conjunction with a vacuum tube voltmeter, permits accurate distortion measurement of an ac signal, eliminating the need for a distortion analyzer. The harmonic content can be viewed on an oscilloscope.

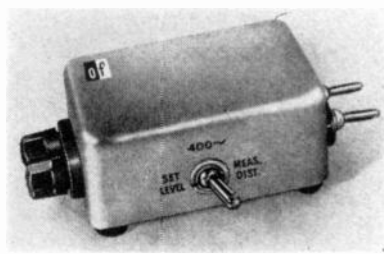

Specifications on the filter are as follows: Stock Frequencies, 400 cps, 300 cps, 1000 cps (other frequencies from 50 to 50,000 cps available custom-built to your specifications); Input impedance, 50,000 ohms; Range, 0.05 to 20% total harmonic distortion; Overall dimensions, $5\frac{3}{4} \times 3 \times 2''$. The price is $47.25. Delivery is immediate on stock models, 2 weeks for custom built units.

For complete information and engineering assistance on the filter, inquiries should be addressed to the firm.

Premium Power Pentode

The first tube to incorporate two frame grids, one a control grid, the other a screen grid, has been announced by **Amperex Electronic Corp., Semiconductor and Special Purpose Tube Div.,** 230 Duffy Ave., Hicksville, L.I., N. Y. Named the type 7534, it is an output pentode and is a Premium Quality (PQ) tube designed for 10,000 hours. It is intended for use in military and industrial applications as a wide band amplifier, cathode follower, series stabilizer in electronic power supplies, and as an output tube in Class B push-pull circuits.

(Continued on page 150A)

IS *YOUR* COMPANY ON THE *OFFENSE* FOR *DEFENSE?*

SIGNAL is your introduction to the men who control the growing $4 billion dollar government radio-electronics spending

Never before have our armed forces so badly needed the thinking and products of the electronics industry. Advertising in SIGNAL, the official journal of the *Armed Forces Communications and Electronics Association*, puts you in touch with almost 10,000 of the most successful men in the field—every one a prospect for your defense products!

Share in the defense and the profits! Company membership in the AFCEA, with SIGNAL as your spokesman, puts you in touch with government decision-makers!

SIGNAL serves liaison duty between the armed forces and industry. It informs manufacturers about the latest government projects and military needs, while it lets armed forces buyers know what *you* have to offer to contribute to our armed might. SIGNAL coordinates needs with available products and makes developments possible.

But SIGNAL is more than just a magazine. It's *part of an over-all plan!*

A concerted *offensive* to let the government, which has great faith in industry and the private individual producer, know exactly what's available to launch its far-sighted plans. Part of this offensive is the giant AFCEA National Convention and Exhibit (held this year in Washington, D.C., June 6-8). Here, you can *show* what you have to contribute directly to the important buyers. Your sales team meets fellow manufacturers and military purchasers and keeps "on top" of current government needs and market news.

Besides *advertising* in SIGNAL which affords year-round exposure by focusing your firm and products directly on the proper market . . . besides *participation* in the huge AFCEA National Convention and Exhibit . . . the over-all plan of company membership in the AFCEA *gives your firm a highly influential organization's experience and prestige to draw upon.*

As a member, you join some 175 group members who feel the chances of winning million dollar contracts are worth the relatively low investment of time and money. On a local basis, you organize your team (9 of your top men with you as manager and team captain), attend monthly chapter meetings and dinners, meet defense buyers, procurement agents and sub-contractors. Like the other 55 local chapters of the AFCEA, your team gets to know the "right" people.

In effect, company membership in the AFCEA is a "three-barrelled" offensive aimed at putting your company in the "elite" group of government contractors—the group that, for example in 1957, for less than $8,000 (for the full AFCEA plan) made an amazing total of *459.7 million dollars!*

This "three-barrelled" offensive consists of

(1) Concentrated advertising coverage in SIGNAL, the official publication of the AFCEA;

(2) Group membership in the AFCEA, a select organization specializing in all aspects of production and sales in our growing communications and electronics industry; and

(3) Attending AFCEA chapter meetings, dinners and a big annual exposition for publicizing your firm and displaying your products.

If *you're* in the field of communications and electronics . . . and want prestige, contacts and exposure . . . let SIGNAL put your company on the *offense* for *defense!* Call or write for more details—now!

SIGNAL BPA

Official Journal of AFCEA

Wm. C. Copp & Associates
72 West 45th Street, New York 36, New York
MUrray Hill 2-6606
Boston · Chicago · Minneapolis
Los Angeles · San Francisco

NEWS New Products

These manufacturers have invited PROCEEDINGS readers to write for literature and further technical information. Please mention your IRE affiliation.

(Continued from page 148A)

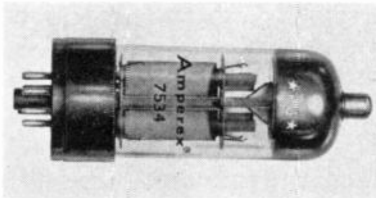

The 7534 features a high transconductance of 25,000 micromhos, low screen grid current (4 ma), and a peak voltage of 6 kv. The cathode current is 300 ma and with this high current capacity, the 7534 is suitable for passing high currents through deflection coils of CRT's.

The 7534 is characterized by very low distortion for 60 watts output in push-pull Class B circuits. The total harmonic distortion is 5% and with feedback it can be reduced to less than 1%.

The 7534 achieves its high transconductance with very low screen grid currents.

This results in lower dissipation, less noise and more economical operation.

Its internal resistance is low compared to that of the other power pentodes, which makes possible lower output impedances in cathode follower applications.

Precision Power Supply

The Industrial Test Equipment Co., 55 E. 11th St., New York 3, N. Y., has developed a precision power supply. The unit meets all military specifications for ground support equipment. Packaged in a splash proof enclosure, the power supply has the following specifications:

Output power, 25 va; Output frequency, 350–450 cps (other frequencies fixed or variable are available); Amplitude stability, 0.1%. Frequency stability, 0.1%. Regulation, 1% 0 to full load. Output voltage is variable, 0 to 130 volts.

The unit features circuit breaker overload protection. All controls are external to the equipment. The frequency and amplitude may be remotely controlled.

Delivery of standard units can be made within thirty days from receipt of an order. Price and delivery information upon request.

Micro-Miniature Transformers

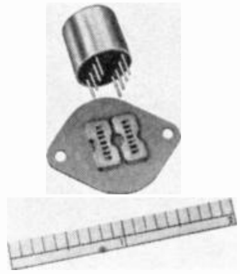

A new series of micro-miniature transformers with 0.030" diameter brass pin leads spaced 0.100" apart, to "plug-in" to a standard 5 pin subminiature socket or to facilitate "soldering-in" for permanent installations, is now available from **James Electronics, Inc.,** 4050 North Rockwell St., Chicago 18, Ill. The ½" diameter metal cases are sealed and potted to meet MIL-T-27A, grade 5. "U" Series impedance ranges are available from 10 ohms to 300 K ohms. Designs can be offered for a wide range of applications where balance, power and low distortion are required in a micro-miniature size. The units are also available in a 10 unit decade box like kit, Model C-2650.

Prices range from $5.00 to $8.00 each in sample quantities. Availability is from stock.

Resistance Element Data Sheet

CTS Corp., Elkhart, Ind., offers Interim Data Sheet 181 illustrating and giving full technical details on a new concept in high temperature, high stability, high reliability ceramic-metal resistance element for modular fixed resistors. Technical data includes resistance range, wattage, temperature rating, resistor configuration, substrate size, voltage rating and complete performance specifications.

Miniature Frame Grid Tubes

Five miniature frame grid tubes featuring high transconductance and low noise have been announced by **Raytheon Co., Industrial Components Div.,** 55 Chapel St., Newton 58, Mass.

The tubes and their transconductance are the 6939, a double tetrode with 10,500 micromhos per section; 6688, a pentode with 16,500 micromhos; 6922, a twin diode with 12,500 micromhos per section; 5842, a triode with 25,000 micromhos; and the 5847, a pentode with 13,000 micromhos.

Applications include use in RF amplifiers, IF amplifiers, driver stages, cathode followers and cathode amplifiers. Outstanding small-signal, high-gain characteristics of these tubes reduce the number of tubes required in an IF strip.

Immediately available from the factory or Raytheon distributors in sample quantities, the frame grid tubes' suggested resale and factory prices range from $2.95 to $7.90.

(Continued on page 152A)

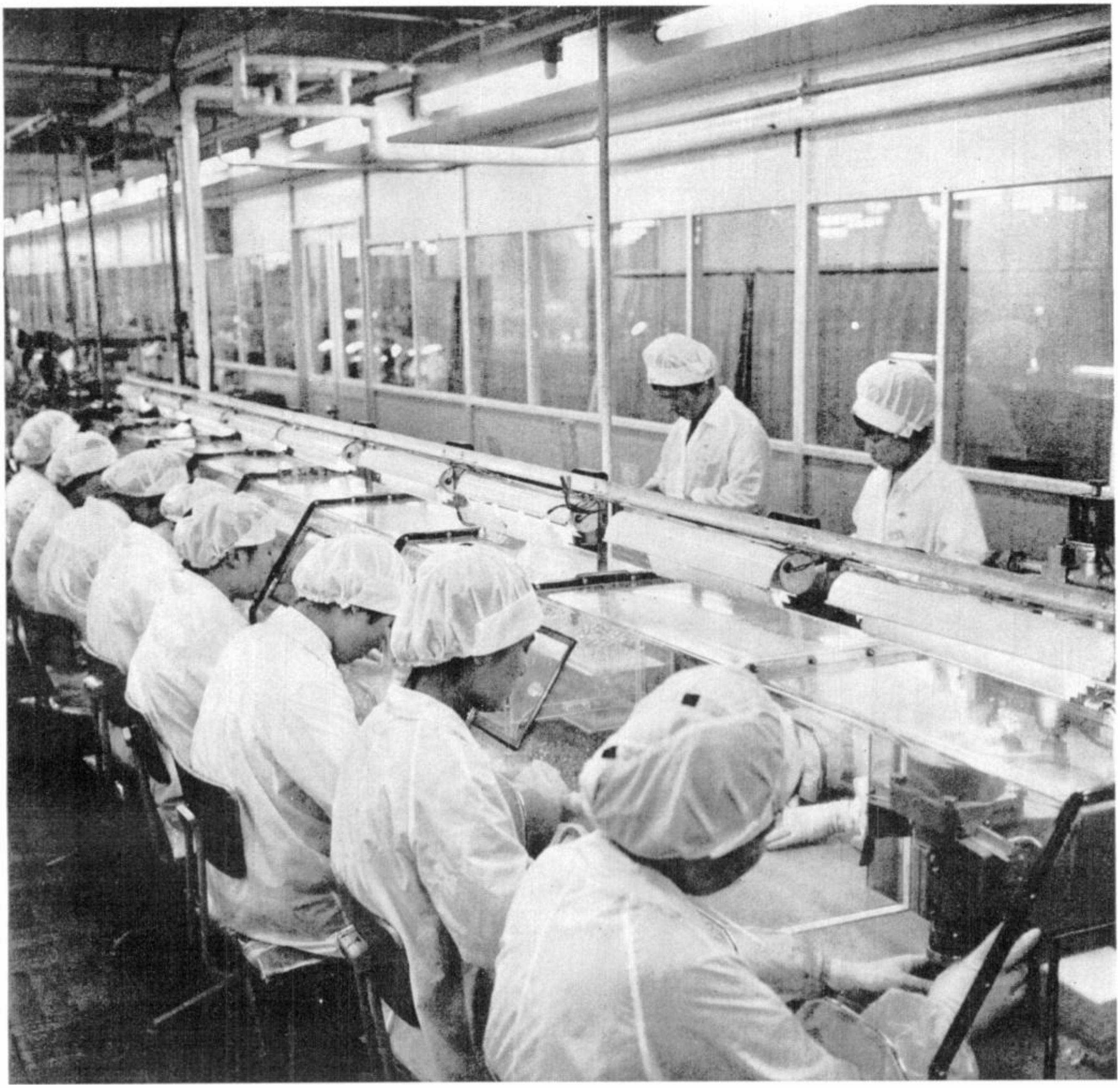

An NEC semiconductor device for every circuit application

The range of semiconductor products at NEC is perhaps the widest of any manufacturer. Entertainment or industrial, standard broadcast frequencies to microwave — NEC has a semiconductor device with the ratings and characteristics for your application. There's a wide selection of current ratings, operating temperatures, and mountings.

These are produced in NEC's new semiconductor plant where crystal surfaces are cleaned by 100 tons of hyper pure water daily. Every seal is tested in krypton isotopes, providing a failure rate suitable for the most critical applications.

A single source for semiconductors can mean a saving in time and costs. Just let NEC know your requirements and full technical data will be sent.

Types of NEC semiconductor devices

• PNP super-grown Germanium transistors • Germanium photo transistors • PNP alloy junction Germanium transistors • Silicon Mesa transistors • Germanium Mesa transistors • Germanium gold-bonded diodes • Silicon rectifiers • Silicon controlled rectifiers • Silicon capacitors • Zener diodes • Germanium point-contact mini-diodes • Silver-bonded diodes • Microwave mixer diodes • Silicon junction mini-diodes

Reliability The first NEC transistorized carrier telephone system was an NT & T installation in 1958 between Toyama and Takaoka, a distance of 15 miles. It consists of two terminal stations and a repeater station with 240 channels using 1,600 transistors.
During last 14,000 hours of operation transistor failure has caused only two channel faults. This corresponds to a failure rate of 0.009% per 1,000 hours.

Communications Systems / Electronic Components NEC *Nippon Electric Co., Ltd.* Tokyo, Japan

NEWS New Products

These manufacturers have invited PROCEEDINGS readers to write for literature and further technical information. Please mention your IRE affiliation.

(Continued from page 150A)

Global Mapping System

Cubic Corp., San Diego 11, Calif., announced detailed plans and schedules for Geodetic SECOR, which will make its debut in conjunction with the Navy's Transit IIIB satellite. Geodetic SECOR has been developed by Cubic under contract to the U. S. Army Map Service, Corps of Engineers, for use in Army Mapping projects.

SECOR (SEquential COllation of Range) is an electronic system to accurately determine geodetic positions anywhere on the surface of the earth.

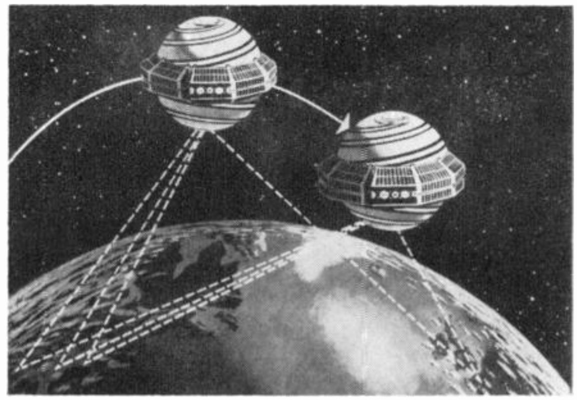

A miniature 7-pound transponder, a component of the SECOR system, is planned to be aboard the 36-inch Transit IIIB sphere to be placed in a 500-mile orbit by a THOR-ABLE-STAR vehicle. Fired downrange from Cape Canaveral, the launch vehicle will program into an orbit inclined 22.5° to the equator. The satellite ground track will cover an imaginary 2850-mile-wide belt around the earth, centered on the equator, extending from Mexico City to southern Brazil in the Western Hemisphere, from the Sahara to Mozambique in Africa, all of India, and from Formosa to central Australia. The airborne SECOR transponder will be interrogated initially by ground stations operated by U. S. Army Map Service personnel located in Costa Rica, Honduras, Haiti, and Colombia.

SECOR is expected to give geodicists more accurate data on the relative locations of continents, islands, cities and other landmarks around the globe. SECOR geodetic studies are also expected to yield more precise facts on the earth's shape and gravitational fields.

Four identical SECOR ground stations, all helicopter-transportable, are employed; they make distance measurements by sending and receiving signals through the satellite transponder. With three of the ground stations located at accurately surveyed points, the precise position of the fourth can be computed using resectioning techniques.

Each ground station determines its distance from the satellite by first transmitting a frequency-modulated, continuous-wave signal which is received and rebroadcast by the transponder. During transmission the ground station measures and records the phase shift between its transmitted signals and those received from the transponder. To permit compensation for errors introduced by ionospheric refraction of the SECOR signals, the transponder replies on two different frequencies.

The four SECOR ground stations interrogate the transponder, in sequence, for 122 milliseconds (1/80 second) apiece. Dynamic smoothing of the distance-information allows interpolation to provide the equivalent of simultaneous sightings by all stations. Cubic data handling equipment incorporated in each ground station provides real-time recording of binary range words. A by-product of SECOR geodetic measurements is an accurate predic-

(Continued on page 156A)

look into Panoramic's new SPA-4a

exclusive features for more reliable spectrum analysis 10 mc to 44,000 mc

2 to 4 TIMES THE USABLE SENSITIVITY

Lower internal noise enables analysis of even smaller signals than before (see chart) . . . accurate measurement of more highly dispersed energies, as typified by extremely narrow pulsed signals.

BAND	RF SENSITIVITY*
1- 10 — 420 MC	−100 to −110 dbm
2- 350 — 1000 MC	− 95 to −105 dbm
3- 910 — 2200 MC	−100 to −110 dbm
4- 1980 — 4500 MC	− 90 to −100 dbm
5- 4.5 — 10.88 KMC	− 90 to −100 dbm
6-10.88 — 18.0 KMC	− 85 to −100 dbm
7- 18.0 — 26.4 KMC	− 70 to − 90 dbm
8- 26.4 — 44.0 KMC	− 60 to − 85 dbm

*measured when signal and noise equal 2x noise

EXCEPTIONALLY LOW DISTORTION

Reduced threshold allows SPA-4a to operate at smaller input signal levels (and attenuated larger ones). Unretouched screen photos show how this permits virtually spurious-free measurement—over a wide dynamic range—of harmonics, in-band distortion, and other weak signals in the presence of strong ones.

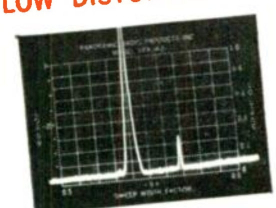

Extended dynamic range comparison of 2 signals on SPA-4a. Larger is + 15 db over full scale log. Smaller is at −28 db on scale or −43 db from larger. Note exceptional freedom from spurious. (Photo not retouched)

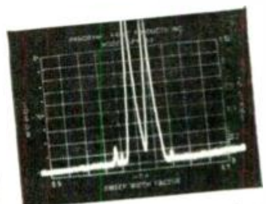

Distortion analysis illustrates SPA-4a wide range linearity. Odd-order distortion here is measured more than 50 db below level of 2 main tones (deflected 20 db above full scale). Photo unretouched.

HIGHLY RESOLVED & CALIBRATED ANALYSIS

Reduced internal hum improves resolution of closely spaced signals; also improves minimum dispersions for more highly magnified analyses. Marker modulation permits highly accurate measurements of frequency differences during high speed analysis. See photos.

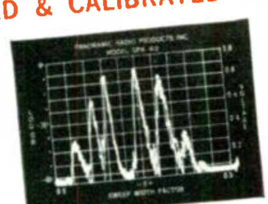

Narrow band 20 kc dispersion analysis shows unique resolution capability. Here, a 1000 mc FM signal with 2 kc modulation is seen near first carrier null. Photo unretouched.

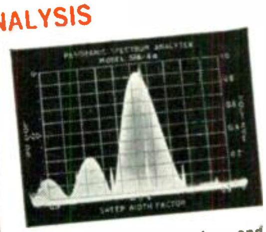

Pips of internal marker and sidebands (ext. mod. ≈ 100 kc) accurately measure pulse width in spectrum of 10μs. radar pulse. Upper lobes seen to be very small. (Unretouched)

dependable CERTIFIED SPECIFICATIONS for accurate data

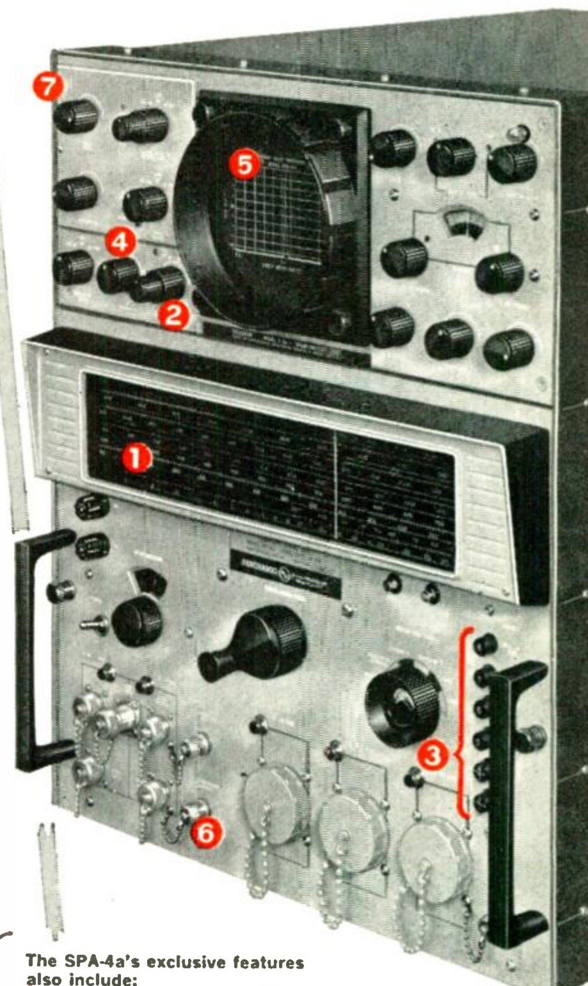

Important as these advantages are, there are many more.

The SPA-4a's exclusive features also include:

1. **ONE TUNING HEAD** — 10 mc to 44,000 mc, utilizing 3 stabilized, low hum local oscillators (1 HF triode and 2 klystrons). Fundamentals to 11 kmc. Direct reading with ± 1% accuracy.
2. **TWO INDEPENDENT FREQUENCY DISPERSION RANGES:** Continuously adjustable; 0-70 mc with exceptional flatness, stable 0-5 mc for narrow band analysis. Both swept local oscillators operate on fundamentals only for spurious-free analysis.
3. **PUSH-BUTTON FREQUENCY RANGE SELECTOR.**
4. **ADJUSTABLE IF BANDWIDTH 1 KC to 80 KC.**
5. **3 CALIBRATED AMPLITUDE SCALES** — 40 db log, 20 db lin, 10 db power.
6. **SYNCHROSCOPE OUTPUT WITH 40 DB GAIN.**
7. **SWEEP RATE ADJUSTABLE FROM 1-60 CPS.** May be set free running, synchronized to the line or to external prf. Also provisions for sweep rate calibrations.

Easy to use, too . . . human engineered for simple operation, component accessibility.

The advanced new SPA-4a is unmatched for visually analyzing FM, AM and pulsed signal systems —instabilities of oscillators —noise spectra—for detection of parasitics—studies of harmonic outputs, radar systems and other signal sources.

Write, wire, phone today for detailed SPA-4a specification bulletin and new Catalog Digest.

eem Sec. 2900

Panoramic RADIO PRODUCTS, INC.

the pioneer is the leader

PANORAMIC RADIO PRODUCTS, INC.
522 South Fulton Avenue, Mount Vernon, N. Y. • Phone: OWens 9-4600
TWX: MT-V-NY-5229 • Cables: Panoramic, Mount Vernon, N. Y. State

New LAMBDA Transistorized REGULATED POWER SUPPLIES

0 - 34 VDC 5, 10 and 20 Amp
20 - 105 VDC 2, 4 and 8 Amp
75 - 330 VDC 0.8, 1.5 and 3 Amp

CONVECTION COOLED
No Blowers or Filters
Maintenance Free

Highly efficient, radiator type heat sinks eliminate internal blowers, maintenance problems, risk of failure, moving parts, noise and magnetic fields. Units are rated for continuous duty at 50°C ambient.

SHORT CIRCUIT PROOF
All models are completely protected with magnetic circuit breakers, fuses, and thermal overload.

EASY SERVICE ACCESS
Dual-deck, swing-out back construction provides simple and fast service access without the need to remove unit from rack. All major component terminals are accessible from rear.

REMOTE SENSING
Minimizes effect of power output leads on DC regulation, output impedance and transient response.

NO VOLTAGE SPIKES OR OVERSHOOT
Lambda's design prevents output voltage overshoot on "turn on, turn off," or power failure.

MIL QUALITY
Hermetically-sealed magnetic shielded transformer designed to MIL-T-27A quality and performance. Special, high-purity foil, hermetically-sealed long life electrolytic capacitors.

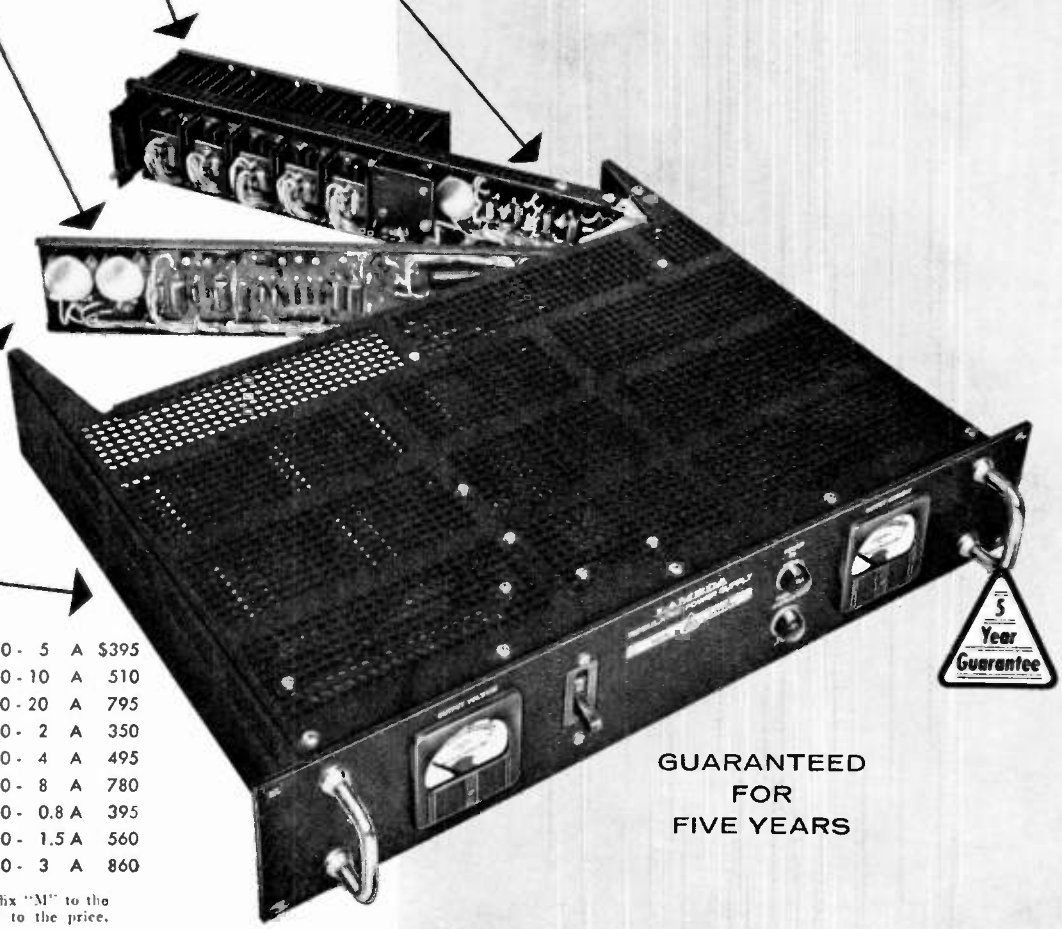

GUARANTEED FOR FIVE YEARS

LA 50 - 03A	0 - 34 VDC	0 - 5 A	$395
LA100 - 03A	0 - 34 VDC	0 - 10 A	510
LA200 - 03A	0 - 34 VDC	0 - 20 A	795
LA 20 - 05A	20 - 105 VDC	0 - 2 A	350
LA 40 - 05A	20 - 105 VDC	0 - 4 A	495
LA 80 - 05A	20 - 105 VDC	0 - 8 A	780
LA 8 - 08A	75 - 330 VDC	0 - 0.8 A	395
LA 15 - 08A	75 - 330 VDC	0 - 1.5 A	560
LA 30 - 08A	75 - 330 VDC	0 - 3 A	860

For metered models add the suffix "M" to the model number and add $30.00 to the price.

LA-117

DIMENSION DRAWINGS

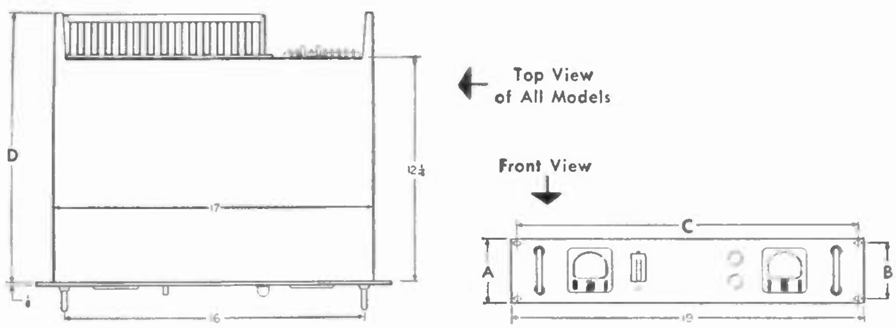

MODEL †	LA 50-03A LA 20-05A LA 8-08A	LA 100-03A LA 40-05A LA 15-08A	LA 200-03A LA 80-05A LA 30-08A
A	3½"	7"	10½"
B	3"	•4"	•7½"
C	18 5/16"	18¼"	18¼"
D	14⅜"	14⅜"	16½"

* These models notched per RETMA Standards
† Includes metered models with suffix "M"

COMPLETE SPECIFICATIONS OF LAMBDA LA SERIES

DC OUTPUT (Regulated for line and load)

Model	Voltage Range	Current Range	Minimum Voltage (1)	Voltage Steps (1)	Price(2)
LA 50-03A	0- 34 VDC	0- 5 AMP	0	2, 4, 8, 16, and 0- 4 volt vernier	$ 395
LA100-03A	0- 34 VDC	0-10 AMP	0	2, 4, 8, 16, and 0- 4 volt vernier	510
LA200-03A	0- 34 VDC	0-20 AMP	0	2, 4, 8, 16, and 0- 4 volt vernier	795
LA 20-05A	20-105 VDC	0- 2 AMP	20	5, 10, 20, 40, and 0-10 volt vernier	350
LA 40-05A	20-105 VDC	0- 4 AMP	20	5, 10, 20, 40, and 0-10 volt vernier	495
LA 80-05A	20-105 VDC	0- 8 AMP	20	5, 10, 20, 40, and 0-10 volt vernier	780
LA 8-08A	75-330 VDC	0- 0.8 AMP	75	15, 30, 60, 120, and 0-30 volt vernier	395
LA 15-08A	75-330 VDC	0- 1.5 AMP	75	15, 30, 60, 120, and 0-30 volt vernier	560
LA 30-08A	75-330 VDC	0- 3 AMP	75	15, 30, 60, 120, and 0-30 volt vernier	860

(1) The DC output voltage for each model is completely covered by four selector switches plus vernier control. The DC output voltage is the summation of the minimum voltage plus the voltage steps and the continuously variable DC vernier.

(2) Prices are for unmetered models. For metered models add the suffix "M" and add $30.00 to the price.

Regulation (line) ...... Better than 0.05 per cent or 8 millivolts (whichever is greater). For input variations from 100-130 VAC.

Regulation (load) ..... Better than 0.10 per cent or 15 millivolts (whichever is greater). For load variations from 0 to full load.

Transient Response ..... Output voltage is constant within regulation specifications for step function:

(line) .... line voltage change from 100-130 VAC or 130-100 VAC.

(load) .... load change from 0 to full load or full load to 0 within 50 microseconds after application.

Internal Impedance .... LA 50-03A less than .008 ohms
LA100-03A less than .004 ohms
LA200-03A less than .002 ohms
LA 20-05A less than .06 ohms
LA 40-05A less than .03 ohms
LA 80-05A less than .015 ohms
LA 8-08A less than .5 ohms
LA 15-08A less than .25 ohms
LA 30-08A less than .15 ohms

Ripple and Noise ...... Less than 1 millivolt rms with either terminal grounded.

Polarity .... Either positive or negative terminal may be grounded.

Temperature Coefficient .... Better than 0.025 %/°C

AC INPUT .... 100-130 VAC, 60 ± 0.3 cycle[3]
LA 50-03A....360 watts[4]
LA100-03A....680 watts[4]
LA200-03A...1225 watts[4]
LA 20-05A....390 watts[4]
LA 40-05A....710 watts[4]
LA 80-05A...1350 watts[4]
LA 8-08A....415 watts[4]
LA 15-08A....760 watts[4]
LA 30-08A...1450 watts[4]

[3]This frequency band amply covers standard commercial power lines in the United States and Canada.
[4]With output loaded to full rating and input at 130 VAC.

AMBIENT TEMPERATURE AND DUTY CYCLE Continuous duty at full load up to 50°C (122°F) ambient.

OVERLOAD PROTECTION:

Electrical .... Magnetic circuit breaker front panel mounted. Special transistor circuitry provides independent protection against transistor complement overload. Fuses provide internal failure protection. Unit cannot be injured by short circuit or overload.

Thermal .... Thermostat, manual reset, rear of chassis. Thermal overload indicator light front panel.

METERS .... Voltmeter and ammeter on metered models.

CONTROLS:

DC Output Controls ... Voltage selector switches and adjustable vernier-control rear of chassis.

Power .... Magnetic circuit breaker, front panel.

Remote DC Vernier .... Provision for remote operation of DC vernier.

Remote Sensing .... Provision is made for remote sensing to minimize effect of power output leads on DC regulation, output impedance and transient response.

PHYSICAL DATA:

Mounting .... Standard 19" Rack Mounting

Size

LA 50-03A, LA20-05A, LA 8-08A	3½" H x 19" W x 14⅜"D
LA100-03A, LA40-05A, LA15-08A	7" H x 19" W x 14⅜"D
LA200-03A, LA80-05A, LA30-08A	10½" H x 19" W x 16½"D

Weight

LA 50-03A, LA20-05A, LA 8-08A	55 lb Net	85 lb Ship. Wt.
LA100-03A, LA40-05A, LA15-08A	100 lb Net	130 lb Ship. Wt.
LA200-03A, LA80-05A, LA30-08A	140 lb Net	170 lb Ship. Wt.

Panel Finish .... Black ripple enamel (standard). Special finishes available to customers' specifications at moderate surcharge. Quotation upon request.

LAMBDA ELECTRONICS CORP.
515 BROAD HOLLOW ROAD, HUNTINGTON, L. I., NEW YORK 516 MYRTLE 4-4200

Send for complete Lambda Catalog.

These manufacturers have invited PROCEEDINGS readers to write for literature and further technical information. Please mention your IRE affiliation.

(Continued from page 152A)

tion of the ephemeris (path) of the satellite.

Cubic officials said the SECOR ground and airborne equipment will be delivered to the Army in February, after extensive tests in the San Diego area.

In these tests, three of the four ground stations will be located at Carlsbad, Ramona and Valley Center, California, with the fourth station at the Cubic plant. The satellite transponder will be flown in an Army L-23 aircraft during the calibration tests.

Illuminated "Multi-Switch"

A new "Multi-Switch," Series 21000, designed for use in computers, telephone apparatus, data systems and ground to air support equipment in the business machine, telephone, aircraft and missile and other allied industries, has been introduced by **Switchcraft, Inc.**, 5555 N. Elston Ave., Chicago 30, Ill.

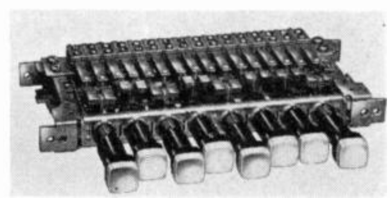

This new series features a square button design with a concave face. These buttons have side as well as front illumination and a large area for engraving identification. The buttons can be keyed in any of four planes for horizontal or vertical mounting of the switch frame.

The jewels are available in white, red, yellow, green and others.

Three different voltages are now available: 6 volts, 28 volts and Neon (115 volt ac), to give the engineer an unlimited latitude in equipment designs.

Lamps are retained in socket by knurled retaining collar. Bulbs are under spring tension assuring contact of lamp circuit when button is in or out. Lamps can be replaced from front side of panel by removing button.

Insulation Varnish

A technical bulletin on the formulation and use of insulating varnishes based on Dapon® diallyl phthalate resins is now available from **Food Machinery and Chemical Corp.**, 161 East 42nd St., New York 17, N. Y.

The 8-page bulletin covers findings recently announced which indicate a successful technique for utilizing the proper-

(Continued on page 158A)

New Broadband Klystrons

140 MEGACYCLES - (1db) BANDWIDTH AT L-BAND
10 MEGAWATTS - PEAK POWER OUTPUT

New additions to the Litton Industries Broadband Klystron family extend broadband performance to even higher power levels as shown in the typical performance curves to the right. These tubes, like all those produced by Litton Industries, are conservatively designed and rated; and rigorously processed to provide many thousands of hours of reliable operation. Using Litton developed broadbanding techniques, it is now possible to achieve wide bandwith, high peak and average rf power output and linear phase shift versus frequency characteristics simultaneously. This latter feature enables the radar equipment designer to utilize pulse compression techniques to attain improved system performance.

Litton Klystrons providing these outstanding performance characteristics can be supplied in both the L and S-bands at peak rf power levels ranging from 2 to 20 megawatts. Typical of the performance obtained with Litton Klystrons is that of the L-3035, a 2.2 megawatt L-band Klystron, whose average operating life in field service is approaching 3,000 hours. Some of these tubes are continuing to provide excellent service after having operated for more than *17,000* hours.

Should you require high power broadband amplifier tubes to satisfy your system requirements, please write to us at Litton Industries, Electron Tube Division, 960 Industrial Road, San Carlos, California. Our telephone number is LYtell 1-8411.

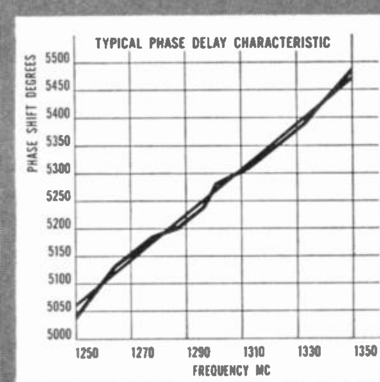

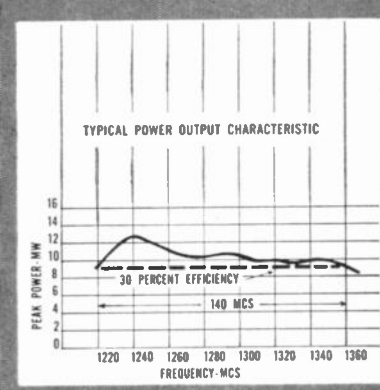

LITTON INDUSTRIES
Electron Tube Division
MICROWAVE TUBES AND DISPLAY DEVICES

"Capability that can change your planning"

These manufacturers have invited PROCEEDINGS readers to write for literature and further technical information. Please mention your IRE affiliation.

(Continued from page 156A)

ties of diallyl phthalate in coating, sealing, dip encapsulation, and laminating applications.

Formula, application, and processing data—supported by several photographs and tables—are given for Dapon varnishes, which are applied by dipping the selected part in a resin solvent solution, drying to remove solvent, and baking to cure. Cured resin properties of finished coatings are also described in detail.

Copies of the technical bulletin (No. 32) may be obtained on request from Dapon Department.

Coil Turns Analyzer

A new instrument for checking the number of turns on a variety of coils is introduced by **Deluxe Coils, Inc.**, Wabash, Ind.

Called a Model 165 Coil Turns Analyzer, the instrument compares an internal universal standard against a production coil product, and rapidly provides coil turns error information to within 0.1%.

The instrument is said to reduce rejection of end products by providing precision quality count at component stages.

Inline digital readout is provided on tabulator type pushbutton board with a maximum reading of 99,999 turns. Modification can be supplied where alternate performance requirements are indicated.

As a further aid in data reading, a galvanometer is installed, which indicates whether the coil under test is high or low in turns, so that the correct digital buttons may be depressed to determine the degree of error.

Complete details are available from the firm.

Microwave Tube Catalog

A new eight-page, two-color short form catalog has been released by the microwave tube division of **Hughes Aircraft Co.**, 11105 Anza Ave., Los Angeles 45, Calif.

The catalog features more advanced high power traveling-wave tubes now in production at this firm.

Hughes has pioneered in development of multi-kilowatt linear traveling-wave tubes with high gain and wide bandwidth, principally in S, C and X bands. This catalog also includes the company's line of backward-wave oscillators.

Copies of the catalog can be obtained by writing to the marketing department.

Microwave Components Catalog

Microlab, 570 W. Mt. Pleasant Ave., Livingston, N. J., has made available a new catalog of microwave components. This catalog consists of 72 pages and includes detailed descriptions and specifications of their line of coaxial attenuators, filters, power dividers, terminations, crystal mounts, tuners and other coaxial microwave components.

A good portion of this catalog is devoted to design sections for each product which present technical information of a general nature to assist the design engineer in the selection of the proper component. Also included is a special article on "The Application of Matrix Algebra to the Design of Microwave Networks."

This new catalog, number 10, is available from the firm.

Miniature Telemetering Accelerometer

Production of a newly developed miniature telemetering accelerometer is announced by **Giannini Controls Corp.**, 1600 S. Mountain Ave., Duarte, Calif. This new unit, Model 24155, incorporates features essential for obtaining good records along with miniature size to conserve payload and space.

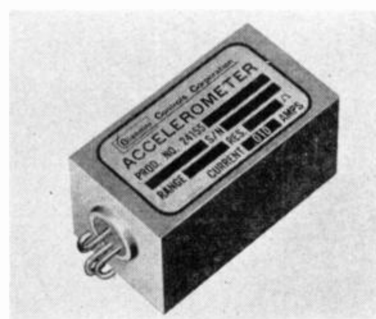

The Model 24155 weighs less than 2.5 ounces, occupies 1 cubic inch in volume, and operates with linearity and repeatability of ±1 percent and hysteresis of 1 percent. Available in resistance ranges from 2000 to 5000 ohms yielding a 0.5 percent resolution, the new accelerometer is supplied in ranges from ±2 g to ±25 g at natural frequencies from approximately 20 to 70 cps. Range can be extended to +100

(Continued on page 160A)

Professional Group on Bio-Medical Electronics

For centuries mankind has searched for a fuller knowledge of the workings of the human body and for improved means of diagnosing and curing bodily ailments. This noble task has been greatly aided in recent years by the application of electronics to medicine, biology and related fields.

Electronics has provided the physician and the biologist with the means for making better, more exact, more comprehensive measurements of countless parameters important to his work. As a result they now know a great deal more about the brain, heart, blood, respiratory system, tissue, muscle and nervous system.

Having thus increased his knowledge, the doctor has turned to electronics also for assistance in the treatment of disease. Cancer therapy, the location of tumors, diathermy, and the treatment of heart diseases are but a few examples of the uses to which electronic equipment and techniques are being put.

To provide the bio-medical field with the necessary electronic equipment, almost every branch of radio engineering has been called into play: from ultrasonics to X rays, from dc amplifiers to microwave apparatus, aids for the blind and aids for the deaf, electronic recording and mapping devices. Even television has supplied an important and useful tool, the television microscope.

However, the rapid development of medical electronic equipment has been hampered by a serious obstacle. For here was a situation which called for the combined knowledge of two highly skilled and hitherto unrelated fields. Either the doctor would have to become an engineer or vice versa, unless some common meeting ground could be provided to enable an exchange of vitally needed information.

It was to meet this urgent need that the IRE Professional Group on Bio-Medical Electronics was formed. Already over 2000 strong, the Group is actively engaged in publishing valuable technical papers and sponsoring national meetings, thereby providing the only organized activity of its kind in this vital field.

Ernst Weber

Chairman, Professional Groups Committee

NEWS New Products

These manufacturers have invited PROCEEDINGS readers to write for literature and further technical information. Please mention your IRE affiliation.

(Continued from page 158A)

g with natural frequency of 145 cps, and switch output can be provided in place of potentiometric output.

Resistant to shock of 50 g, 11 ms duration, the Model 24155 is damped 0.25 to 1 of critical over the temperature range of −18 to +71°C. It is available with functional outputs and can be supplied for practically any type mounting desired.

Switching Transistors

Texas Instruments Incorporated, P. O. Box 1079, Dallas, Texas, announces the commercial availability of two ultra-fast silicon switching transistors manufactured by the new epitaxial process.

TI announced that the devices will perform their switching function in 24 billionths of a second or more than twice as fast as any other silicon transistors manufactured for general sale.

While the new devices are expected to find their greatest immediate application in electronic computers, the firm said their potential range of usage permits them to be classified and used also as small-signal general purpose transistors.

In semiconductor device construction, the epitaxial process consists of the carefully controlled growth by vapor deposition of an extremely thin layer or zone of high-resistivity single-crystal semiconductor material upon a substrate of low-resistivity material and the addition by diffusion method of two more thin layers within the material.

By means of this process the actual transistor function is confined to these three upper layers with the substrate serving only as the platform or handling mechanism for ease of fabrication. As a result, the saturation resistance characteristics are virtually insensitive to changes in temperature in contrast to devices of conventional construction. Resulting advantages are fast performance of the transistor function and operating capability within a range of −65 to +175°C.

Subminiature Relay

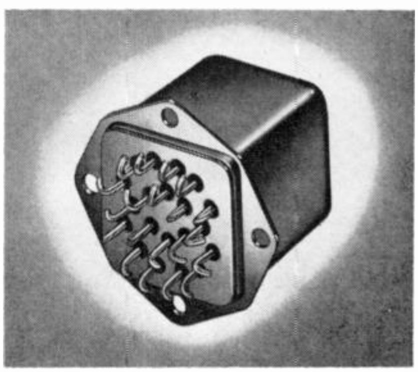

The new subminiature Series 2505 relay developed by **Guardian Electric Mfg. Co.,** Dept. 72D, 1550 W. Carroll Ave., Chicago 7, Ill., carries complete military standard approval. The contact arrangement is 6-pole, double throw. Specification requirements of 3-ampere contacts and 0.35 pounds maximum weight are more than adequately met with the Guardian rating of 5 amperes and 0.30 pounds maximum. Unit meets a vibration specification of 10 g's to 2,000 cps with certified operation at 20 g's. All contacts are staked for utmost reliability. Guardian's exclusive sealing methods eliminate the possibilities of internal contamination. Standard terminals are of the solder-hook type. For more information write to the firm.

Half-Adder Module

A new half-adder digital building block module is available from **Harvey-Wells Electronics, Inc.,** 14 Huron Drive, Natick, Mass., for use in digital system applications where it is necessary to compare the outputs of flip-flops and registers in order to perform arithmetic operations.

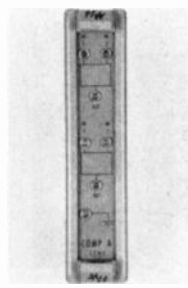

Another member of the line of high-speed logical building blocks, the Model 1281 consists of two identical circuits, each of which performs a comparison function to satisfy the Boolean equations $A\bar{B}+\bar{A}B=C$ and $AB+\bar{A}\bar{B}=\bar{C}$. Other names for this basic digital circuit are "comparator," "modulo-two-adder" and "exclusive-OR circuit."

Price of the Model 1281 DATA BLOC is $125.00 F.O.B. Natick, Mass. Delivery is from stock.

To receive complete technical data on this new product, write to the firm.

Precision Voltage Source

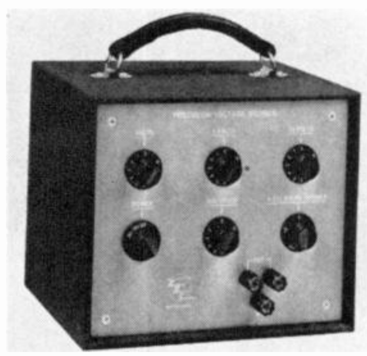

Electronic Development Corp., 432 W. Broadway, Boston 27, Mass., has introduced a new Precision Voltage Reference Source which features an increased voltage range of −111.11 to +111.11 volts dc, selectable in 10 millivolt increments. The new Model VS-111 is a 4-decade direct-reading instrument available in portable or standard rack-mounting models. Absolute accuracy is 0.025 percent and resolution is 1 part in 10,000 plus vernier resolution.

(Continued on page 162A)

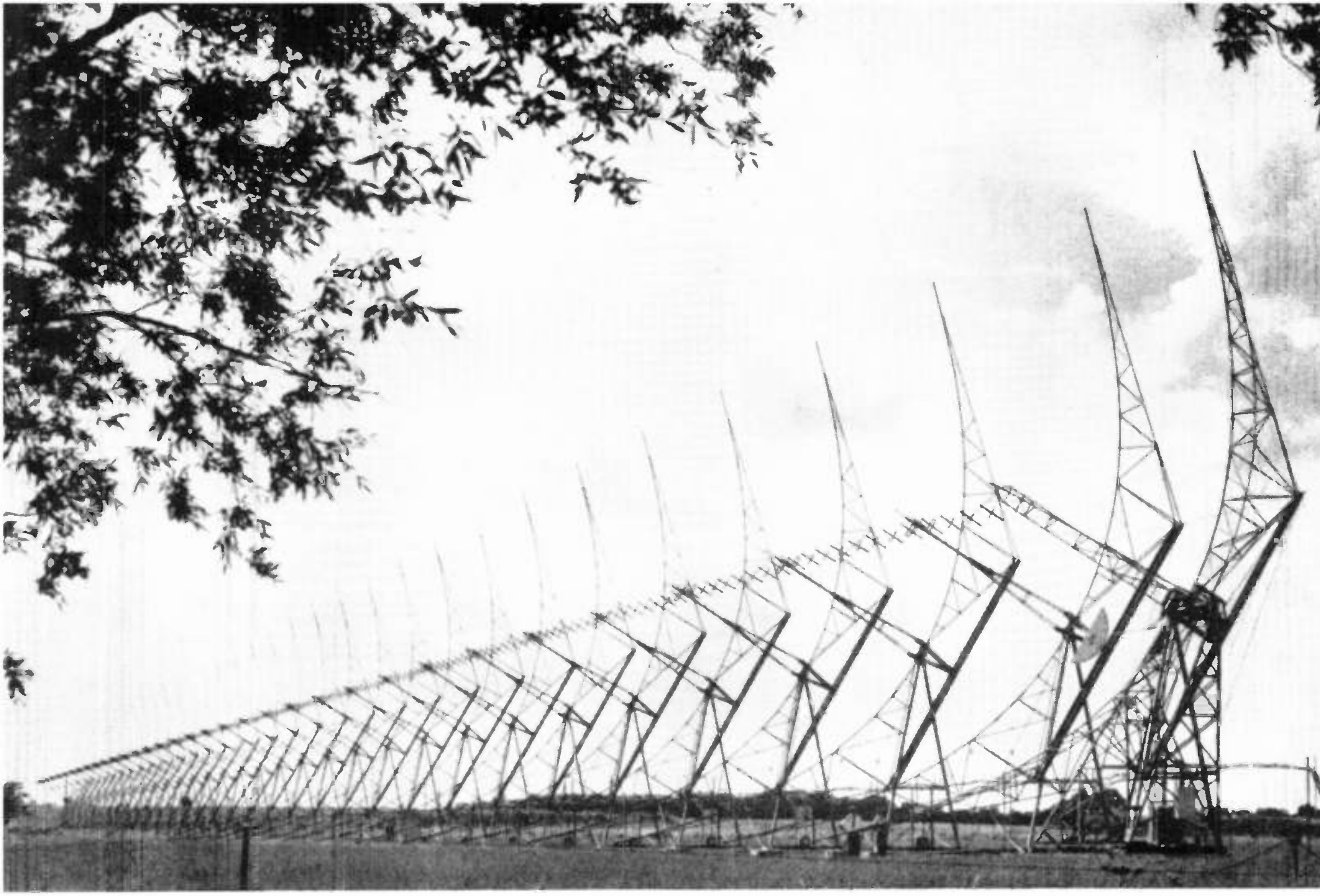

The giant radio-telescope aerial at Mullard Radio Astronomy Observatory, Cambridge

NEWS New Products

These manufacturers have invited PROCEEDINGS readers to write for literature and further technical information. Please mention your IRE affiliation.

(Continued from page 160A)

The VS-111 is an all solid-state unit designed specifically to provide an inexpensive, reliable and rugged precision voltage reference source for laboratory and industrial application.

Price of the VS-111 is $795.00 F.O.B. Boston. Delivery is from stock.

Complete technical data is available on request from the firm.

Component Marking Machine

Model RG is a conveyor-type machine available from **International Eastern Co.,** 801 Sixth Ave., New York 1, N. Y., for printing cylindrical pieces such as capacitors, resistors, tubes, and so forth. The printing rate is 3600 pieces per hour or if a double conveyor is used, twice that output is possible.

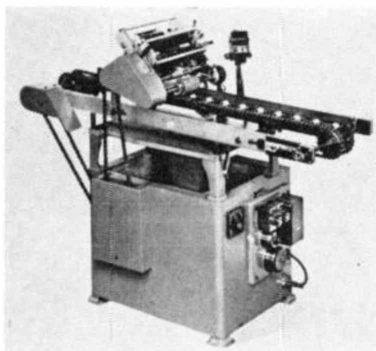

Model B3/2F is a hand-operated machine, which may be set up with a special lever action numbering head for printing serial numbers in a minimum space. The firm has been successful in printing 6 digits on the top of a transistor (¼″) diameter.

Other machines are available for printing components of all shapes, as well as Model R1 for printing meter scales, subpanels and all flat pieces.

Hydrazine Activated Core Solder

Hydrazine flux, formerly available only in liquid form, has now been incorporated into core solder by **Fairmount Chemical Co.,** Newark, N. J. Called H-32, the new core solder combines the advantages of standard hydrazine flux while providing an integrated ratio of flux to solder for proper wetting.

The H-32 core solder can be used in soldering all electrical and electronic equipment. In addition, the non-acidic flux leaves no resin residue to support fungus growth, is non-corrosive, and non-hygroscopic. It vaporizes completely at soldering temperature, eliminating cleaning and residue removal. Joints made with this flux will not corrode.

The following metal surfaces can be soft-soldered: copper, brass, hot tin dipped, hot solder dipped, tin plate, solder plate, copper plate, cadmium plate, zinc, silver plate, beryllium copper and nickel plated brass. It can be used with the following systems: common solders of tin-lead; tin lead silver; tin antimony; tin silver; certain fusible alloys containing tin, lead, cadmium, bismuth, antimony, indium; pure tin; pure lead for bonding to copper.

Technical data, as well as information on how it can be used for specific applications, is available from the company's general sales office, 136 Liberty St., New York 6, N. Y.

Plug Insulator

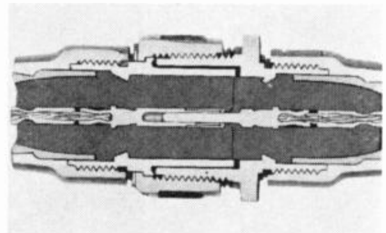

A method of molding together two sections of polychloroprene material of different hardness, to form one homogeneous piece, was recently developed by **Cannon Electric Co.,** 3208 Humboldt St., Los Angeles 31, Calif. The new molding technique provides the rear of the insulator, or the sealing end, with a low-shore hardness which enables the endbell to compress the rubber into a solid, sealing mass around the conductors; and the front, or mating end, is a high-shore hardness which is sufficient to retain the contacts firmly in place and yet is resilient enough to allow them to be removed repeatedly. This new development is used on the MS/RX and KPT/KSP type plugs.

Low Cost Digital Voltmeter

An economical digital voltmeter that owes its low price ($295) to an electromechanical-optical system that successfully combines patented stroboscopic readout techniques with the long life and high accuracy of a conductive plastic potentiometer, has been produced by **Electro-Logic Corp.,** 515 Boccoccio Ave., Venice, Calif.

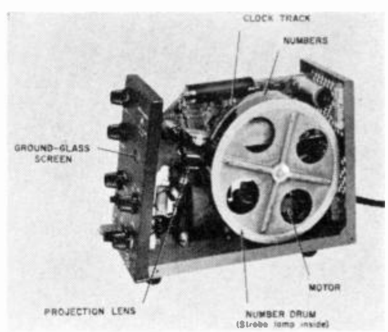

The DVM affords an accuracy of 0.4%. Heart of the instrument is a number drum, rotating continuously at high speed, which

(Continued on page 164A)

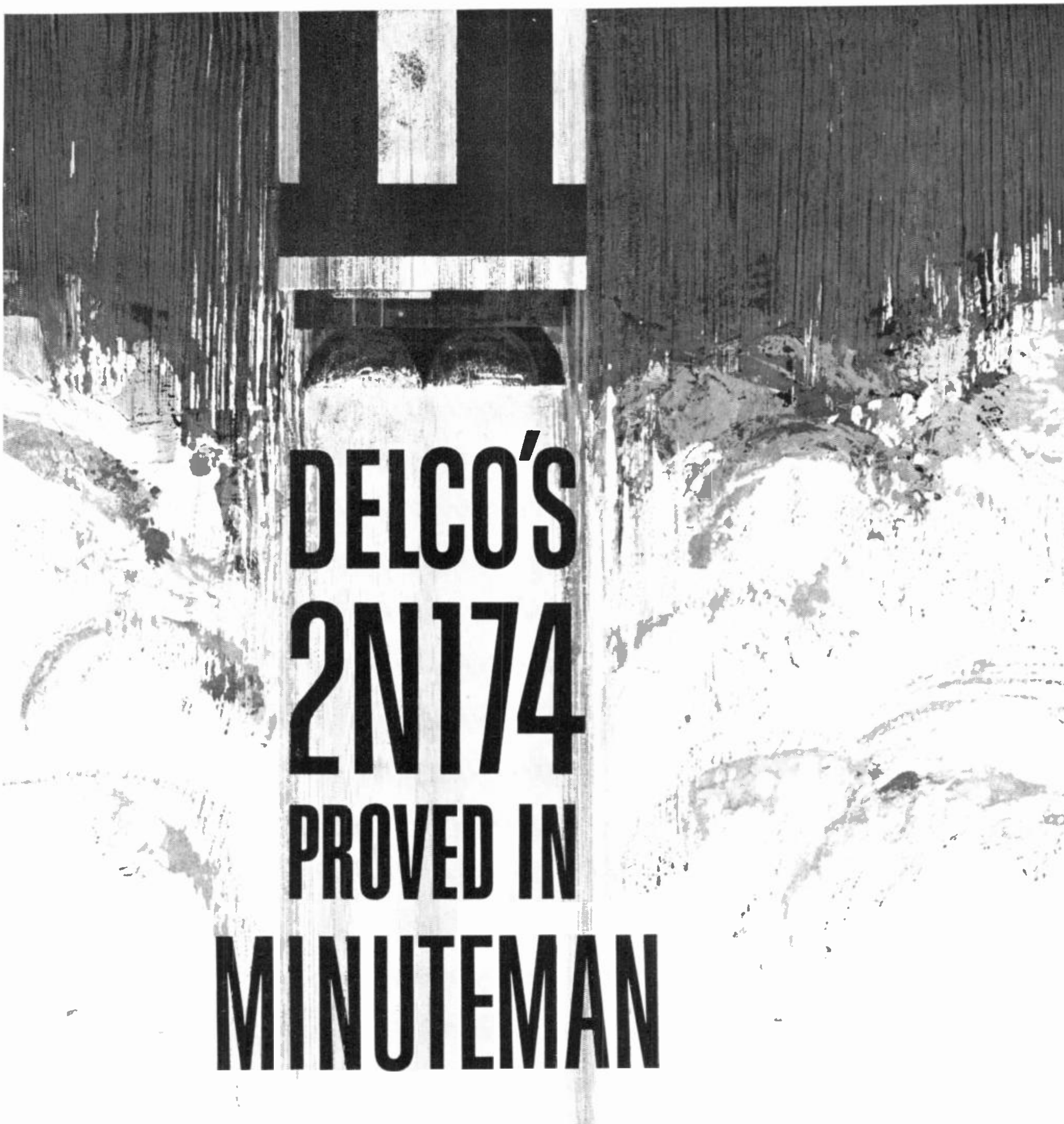

. . . and Polaris and Talos and Atlas and Jupiter and Thor and Titan and Bomarc and Zeus and Pershing and hundreds of other military and industrial applications.

For Delco Radio's highly versatile family of 2N174 power transistors meet or exceed the most rigid electrical and extreme environmental requirements.

Over the past five years since Delco first designed its 2N174, no transistor has undergone a more intensive testing program both in the laboratory and in use, in applications from mockups for commercial use to missiles for the military. And today, as always, no Delco 2N174 leaves our laboratories without passing at least a dozen electrical tests and as many environmental tests before and after aging.

This 200 per cent testing, combined with five years of refinements in the manufacturing process, enables us to mass produce these highly reliable PNP germanium transistors with consistent uniformity. And we can supply them to you quickly in any quantity at a low price.

For complete information or application assistance on the Military and Industrial 2N174's or other application-proved Delco transistors, just write or call our nearest sales office.

Union, New Jersey 324 Chestnut Street MUrdock 7-3770	Santa Monica, California 726 Santa Monica Blvd. UPton 0-8807	Chicago, Illinois 5750 West 51st Street POrtsmouth 7-3500	Detroit, Michigan 57 Harper Avenue TRinity 3-6560

DELCO RADIO
DEPENDABILITY
RELIABILITY

Division of General Motors • Kokomo, Indiana

NEWS New Products

These manufacturers have invited PROCEEDINGS readers to write for literature and further technical information. Please mention your IRE affiliation.

(Continued from page 162A)

is coupled directly to a rotary linear potentiometer that generates a sawtooth sweep voltage. This setup is expensive and said to be more reliable than an equivalent-purpose electronic sawtooth generator plus clock and counter system of the conventional all-electronic DVM.

On the surface of the drum is a film strip containing a row of small holes, each aligned with one of a sequential series of 250 numbers. Holes and numbers are placed at equal intervals of 320° of the drum periphery. The potentiometer, with electrical angle of 320°, is mounted on the same shaft as the drum—both being rotated continuously at a nominal speed of 24 revolutions per second by a small motor.

A light shines through the holes in the film, onto a photodiode which feeds a series of clock pulses to a flip-flop, pulses so timed that a strobe lamp, located inside the drum, fires only when a number and a projection lens are properly aligned.

A standard voltage is impressed across the potentiometer, generating a sawtooth or "ramp" voltage for each revolution of the potentiometer (and drum).

The unknown voltage is continually compared, by electronic means, to this sweep voltage, and at the instant the two voltages—the potentiometer-generated sweep and the unknown—are equal, the flip-flop is triggered so that the next hole coming into alignment causes the strobe lamp to flash. A film strip number is thereby projected through an enlarging lens onto a ground-glass viewing screen on the front of the instrument. Since this comparison is made once for each revolution, the strobe lamp "fixes" or stops the number which corresponds to the unknown voltage.

Because of the high rotational speed plus long life requirement, wire-wound potentiometers were ruled out by the designers who concluded that performance degradation due to wear caused linearity problems within a relatively short time.

The problem was solved by the use of a conductive plastic sweep potentiometer, manufactured by **Markite Corp.**, 155 Waverly Pl., New York City. This component had the life and wear characteristics advantages afforded by the uninterrupted surface of the conductive plastic resistance track, along which the precious metal wiper continually travels. The potentiometer was specified as equal to the accuracy of the voltmeter.

Timing and Data Handling Catalog

Electronic Engineering Co. of California, 1601 E. Chestnut Ave., Santa Ana, Calif., has published a new short form catalog, No. 2, which gives details, prices and illustrations of their time code generators, timing system auxiliary equipment, magnetic tape search and control systems, data handling equipment, punched tape programmers, adapter sockets, and relay testers.

Precision-Moldable Insulation Material

The development of SUPRAMICA 620 "BB" ceramoplastic, a precision-moldable, ultra-high temperature dielectric, is announced by **Mycalex Corporation of America**, Clifton Blvd., Clifton, N. J.

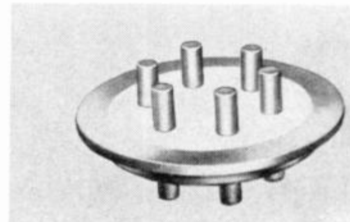

This insulation will operate at temperatures to 1200°F. This widens the range of problems ceramoplastics can solve in the area of missile and space research, and the heat generated by even the most modern high-speed and miniaturized electrical and electronic equipment will have no effect on 620 "BB" parts. This material can be molded, it is said, to the most complex geometries with gage-like tolerances.

The hermetic sealing capabilities of this insulation material are said to surpass generally accepted standards. In testing, a group of precision-molded component parts were subjected to a helium mass spectrometer leak detector sensitive enough to detect leaks as small as 2×10^{-10} cc of helium per second. They showed no sign of leakage.

SUPRAMICA 620 "BB" retains its insulation resistance at elevated temperatures. At 932°F, its volume resistivity is 1×10^{8} ohm cm.

The thermal expansion factor matches that of many metals.

Dual Coaxial Couplers

The first dual coaxial couplers specifically designed for use in coaxial reflectometer setups, featuring high directivity and a four-to-one frequency range, have been announced by **the Narda Microwave Corp.**, 118-160 Herricks Rd., Mineola, L. I., N. Y.

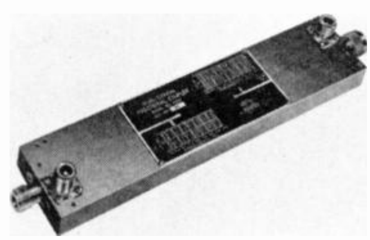

A directional coupler used as a reflectometer must exhibit extremely high directivity, since the error in VSWR introduced in the measurement is equal to the VSWR associated with the directivity of the reflected wave coupler. The directivity

(Continued on page 166A)

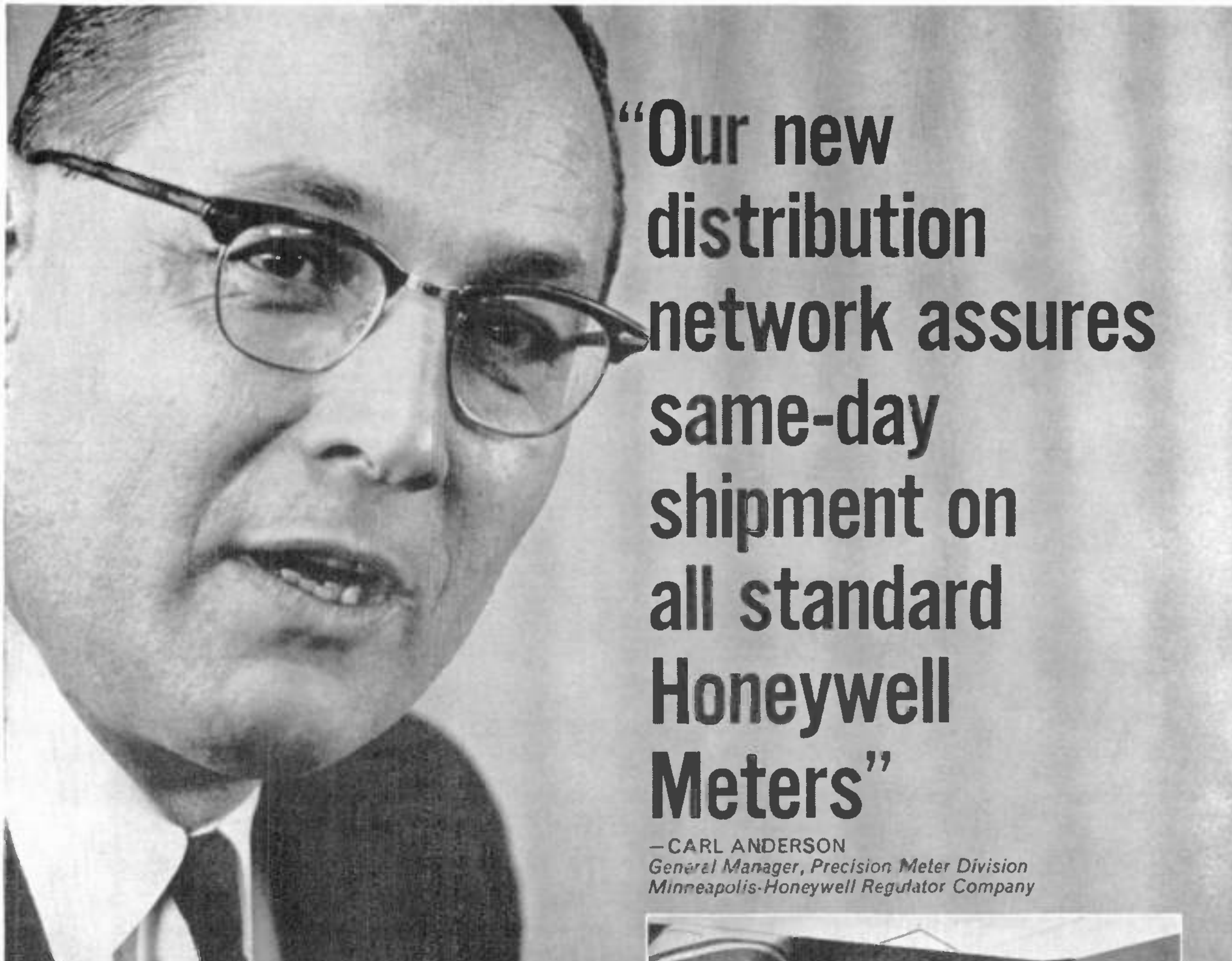

We now have distributors in 20 key cities throughout the nation. For prompt handling of all orders for our top-quality panel instruments, just get in touch with the Honeywell distributor nearest you, our sales representatives, or with us directly: Precision Meter Division, Minneapolis-Honeywell Regulator Co., Manchester, N. H., U.S.A. In Canada, Honeywell Controls Limited, Toronto 17, Ontario; and around the world, Honeywell International Division, Sales and Service Offices in all principal cities.

These are the organizations who can get Honeywell Precision Meters to you in a hurry:

CALIFORNIA: Atlas Electronics, Inc., 4618 Santa Fe St., San Diego 9, BR 4-3131; Bell Electronic Corp., 306 E. Alondra Blvd., Gardena, FL 1-5802; Fisher Switches Inc., 40 Gouch St., San Francisco, UN 1-2569; Elwyn W. Ley Co., 16514 So. Garfield Ave., Paramount, NE 6-8339; Newark Electronics Corp., 4747 W. Century Blvd., Inglewood, OR 8-0441; **CONNECTICUT:** Radio Shack Corp., 230 Crown St., New Haven, ST 7-7121; Radio Shack Corp., 29 High Ridge St., Stamford, DA 5-4371; **WASHINGTON, D.C.:** Electronic Wholesalers Inc., 2345 Sherman Ave., W., Washington 1, HU 3-5200; **ILLINOIS:** Newark Electronics Corp., 223 W. Madison St., Chicago 6, ST 2-2944; **MASSACHUSETTS:** Electrical Supply Corp., 205 Alewife Brook Pky., Cambridge, UN 4-6300; Radio Shack Corp., 730 Commonwealth Ave., Boston 17, RE 4-1000; **MICHIGAN:** Electronic Supply Co., 94 Hamelin Ave., Battle Creek, WO 4-1241; **MINNESOTA:** Stark Electronics Supply Co., 112 Third Ave., No., Minneapolis, FE 6-9220; **NEW JERSEY:** State Electronic Parts Corp., 399 Rte. 10, Whippany, TU 7-2550; **NEW YORK:** A & M Instrument Service Inc., 48-01 31st Ave., L.I. City 3, RA 6-4343; Peerless Radio Distributors Inc., 19 Wilbur St., Lynbrook, L.I., LY 3-2121; **OHIO:** Herrlinger Distributing Co., 112 East Liberty St., Cincinnati 10, GA 1-5285; **PENNSYLVANIA:** Harold H. Powell Co., 2102 Market St., Philadelphia 3, LO 7-5285; **WASHINGTON:** Branom & Leeland Instrument Co., 2137 2nd Avenue, Seattle 1, MA 2-7320.

Honeywell International Sales and Service offices in all principal cities of the world.

Honeywell

H HONEYWELL *Precision Meters*

NEWS New Products

These manufacturers have invited PROCEEDINGS readers to write for literature and further technical information. Please mention your IRE affiliation.

(Continued from page 164A)

of these couplers, Models 3020 and 3022, is held to 35 db and 30 db minimum, respectively, allowing a maximum error of 1.035 VSWR, for the Model 3020.

Both models cover two octaves in frequency; Model 3020 covers the 250 to 1000 mc range and Model 3022 covers the 1000 to 4000 mc range. Coupling of each arm is held to 20 db $\pm$1.0 db over the frequency range and the coupling of the forward and reverse arms track each other within 0.3 db total.

In addition, the couplers feature unusually low main and secondary line VSWR. Model 3020 holds the main line VSWR to 1.05 maximum; Model 3022 is 1.10 maximum.

Model 3020 is priced at $160 and is available from stock; Model 3022 is $150 and will be available from stock after April 1.

FM Signal Generator

For testing Command Receivers operating in the 400–550 mc band, **Marconi Instruments,** 111 Cedar Lane, Englewood, N. J., has produced FM Generator Model 1066B/2. With this new instrument, carrier frequency can be set precisely to any 1 mc channel and multiple tone modulation to 300 kc deviation can be applied.

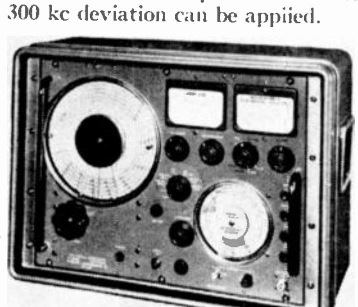

Additional features include a calibrated fine frequency control for bandwidth measurements, a modulation compression circuit for constant FM deviation and mutual inductance piston attenuator of very low VSWR for RF level control.

Advertising Index

Advertising Index

Advertising Index

IN THE MOST EXACTING APPLICATIONS

PHILCO MADT®

SWITCHING TRANSISTORS

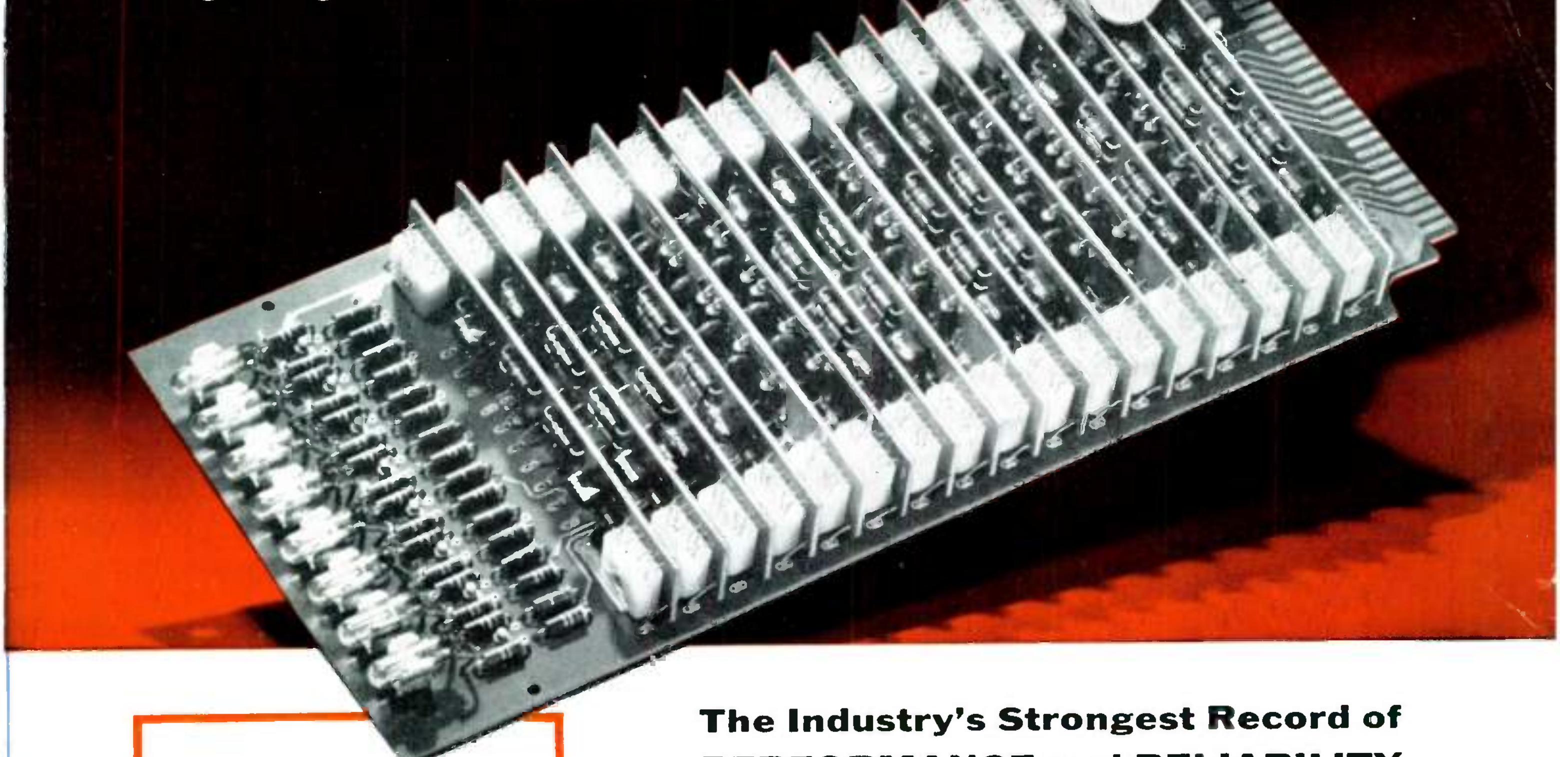

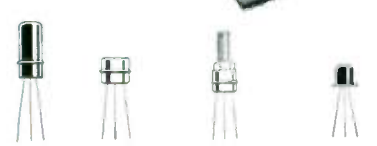

TO-1 TO-9 TO-31 TO-18

In TO-1 CASE:
2N501—Ultra high speed switch
2N501A—Military version of 2N501

In TO-9 CASE:
2N1204—Ultra high speed, high current switch
2N1495—High voltage, high speed, high current switch
2N1499A—High speed, low cost switch (MIL version available)
2N1500—Ultra high speed switch (MIL version available)
2N1754—Very low cost, high speed switch

In TO-31 CASE:
2N1494—High power version of the 2N1204

In TO-18 CASE:
2N768—Ultra high speed switch for very low power circuits
2N769—World's fastest switch
2N779A—Ultra high speed switch—very high beta
2N846A—Ultra high speed switch

Immediately available in quantities 1-999 from your Philco Industrial Semiconductor Distributor

The Industry's Strongest Record of PERFORMANCE and RELIABILITY

In high-speed computers, control systems, guidance systems and many other critical military and industrial switching applications, Philco's patented high-frequency Micro Alloy Diffused-base Transistors are used more widely than any other type. There are many reasons for this broad acceptance. Philco MADTs are available in a full range of types, each designed and produced to tight specifications for specific applications. They are manufactured by Philco's patented Precision-Etch* process on the world's first fully-automatic transistor production lines . . . under rigid quality control. Philco MADTs have proved their outstanding performance capabilities and reliability in *billions of transistor hours of actual field operation* . . . far more than any other type of transistor.

There is a Philco MADT to meet your requirements . . . offering the advantages of cadmium junctions for cooler operation . . . low collector capacitance . . . low saturation voltage . . . high beta with good linearity . . . excellent frequency response . . . low hole storage time . . . and excellent temperature stability.

Specify Philco MADTs with complete confidence. For full information on any specific type write Dept. IRE461.

*Trademark Philco Corp.

PHILCO®

Famous for Quality the World Over

LANSDALE DIVISION, LANSDALE, PENNSYLVANIA

TRANSISTOR CENTER U.S.A. ®

New! 1000-Megacycle FREQUENCY STANDARD

Any or All of These Outputs with Stability of 5 Parts in 10^{10}

60C 100C 400C 1Kc 10Kc 100Kc 1Mc 10Mc 100Mc 1000M

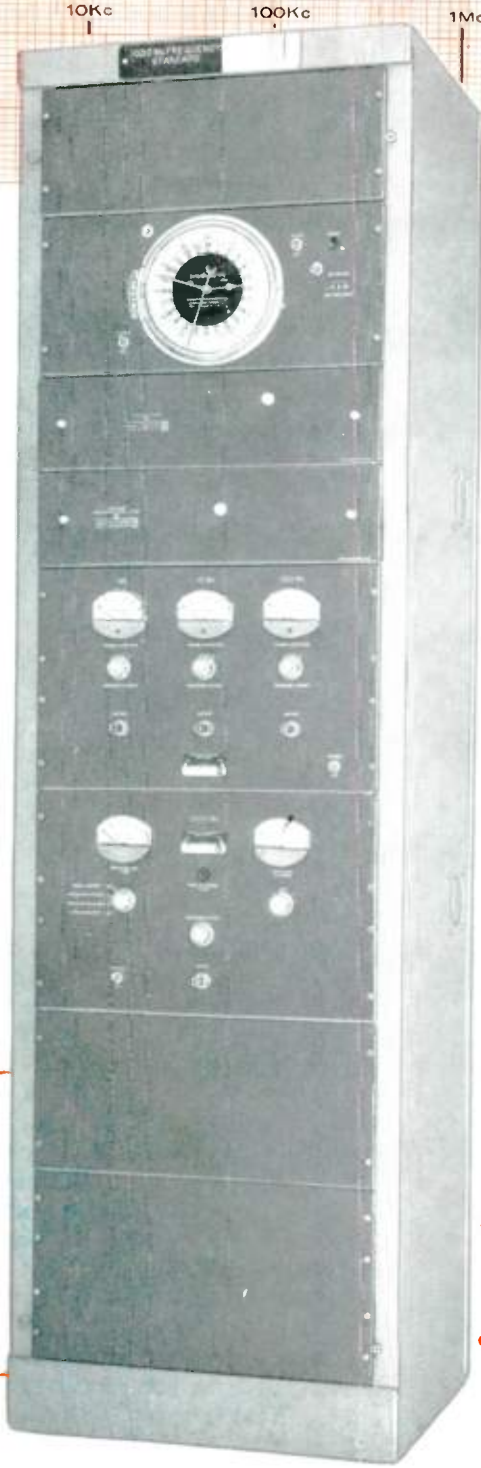

1120-AH
1000-Mc Frequency Standard

. . . $6450

A 5-Mc Crystal Oscillator with Decade Dividers to 100 cps. and Decade Multipliers to 1000 Mc.

INCLUDES:
1103-B Syncronometer
1114-A Frequency Divider
1113-A Standard-Frequency Oscillator
1112-A and -B Standard-Frequency Multipliers

1120-A
5-Mc Frequency Standard

. . . $3640

With Decade Dividers to 100 cps.

INCLUDES three top instruments only

For Use With These Standards . . .

1105-A Measuring Equipment provides high selectivity for the measurement of weak signals in the presence of noise;

1130-A Digital Time and Frequency Meter for general laboratory work.

- High performance at reasonable cost with 5-Mc fifth-overtone Warner crystal and two-stage oven.
- Short-Term Stability: 1 part in 10^{10} per min, using 1 sec samples.
- Long-Term Stability: 5 parts in 10^{10} per day, averaged over 10 days after 60 days operation.
- Low Noise: *Below 5 Mc* — pulse-type dividers provide fail-safe operation and minimize phase noise. *Above 5 Mc* — phase-locked crystal oscillators provide clean signals — f-m noise less than 1 part in 10^9.
- Syncronometer gives resolution ($\pm$0.2 msec) for time comparisons consistent with stability of sky-wave signals from WWV and other stations. Direct digital readout.
- 10-kc and 100-kc square waves for triggering purposes.
- Harmonics for measurements well beyond X-band can be produced with simple distorting and mixing diode.
- Additional Plug-In Units provide 400 cps and 60 cps; 1114-P6 $85 and 1114-P7, $115, respectively.
- Type 1116-A Emergency Power Supply available as an accessory.

Write for Complete Information

GENERAL RADIO COMPANY
WEST CONCORD, MASSACHUSETTS

The Best Instruments In Electronics

NEW YORK, WOrth 4-2722
NEW JERSEY, Ridgefield, WHitney 3-3140

CHICAGO
Oak Park
Village 8-9400

PHILADELPHIA
Abington
HAncock 4-7419

WASHINGTON, D.C.
Silver Spring
JUniper 5-1088

SAN FRANCISCO
Los Altos
WHitecliff 8-8233

LOS ANGELES
Los Angeles
HOllywood 9-6201

IN CANADA
Toronto
CHerry 6-2171